DOTTORATO DI RICERCA IN CHIMICA

Convenzione tra
UNIVERSITÀ DEGLI STUDI DI TRIESTE
e
UNIVERSITÀ CA' FOSCARI DI VENEZIA

In cotutela con
THE UNIVERSITY OF SYDNEY

School of Chemistry, PhD in Science

CICLO XXXIV

SUSTAINABLE PROCESSES FOR THE CHEMICAL UPGRADING OF RENEWABLES

Settore scientifico-disciplinare: **CHIM/06**

DOTTORANDO / A
DAVIDE RIGO

COORDINATORE
PROF. ENZO ALESSIO

SUPERVISORE DI TESI
PROF. MAURIZIO SELVA, Università Ca' Foscari
PROF. THOMAS MASCHMEYER, the University of Sydney

ANNO ACCADEMICO 2020/2021

SUSTAINABLE PROCESSES FOR THE CHEMICAL UPGRADING OF RENEWABLES

A thesis submitted in fulfilment of the requirements for the degree of

Doctor of Philosophy (Cotutelle)

by
Davide Rigo

Ciclo XXXIV
November 2021

This PhD thesis is dedicated to my mum and dad

Sustainability - Sostenibilità

Davide – Amy – Matilde - Ryan

Table of contents

1   Introduction

1.1   Efforts to sustainability: current state and perspectives

Circular chemistry and the design of new chemicals and renewable materials will play a fundamental role to achieve the global goals of sustainable development.[1] This vision has been excellently reviewed on a special section recently published by *Science*, whose opening words were *"The scientific question facing the chemical sector when designing for the future Earth is not whether products of the chemical industry will be necessary, because they surely will be. Rather, the question is, what will be the character, nature, and production processes of synthetic chemicals needed for a sustainable civilization?".*[2] In the tomorrow's view, the transition from fossil- to renewable-based chemistry will take place under a paradigm shift from linear to circular processes where not only synthetic protocols should be aimed to waste minimization, but when generated, low-value residues must be valorized to new useful products through "waste design" strategies which should be typically implemented in an advanced biorefinery. (Figure 1.1)
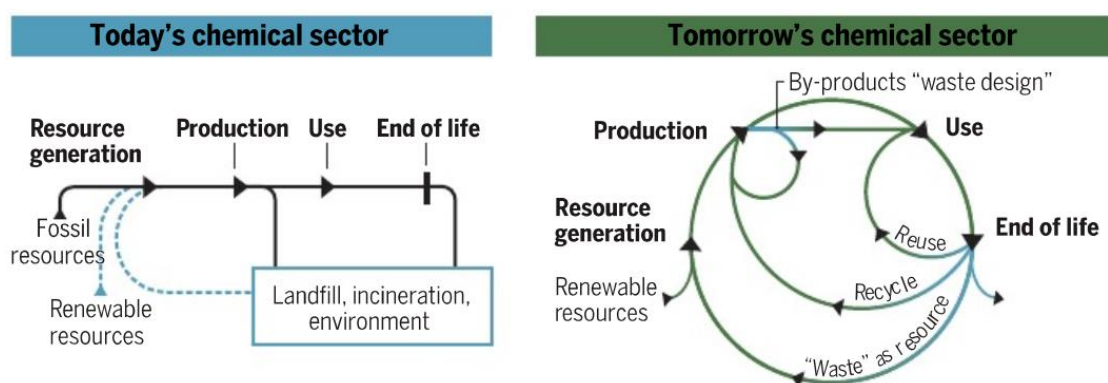
Figure 1.1. Today's and tomorrow's chemical sectors (from ref. 2)

The current situation, however, is still an open challenge. By comparison with the well-established petro-industry, which is based on mature and competitive technologies, the development of biorefineries is still in its infancy with an immense potential often lacking knowhow and tools for its full exploitation. Recent data on the European situation accounts for a total of € 542 billion chemical market which comprises only € 5,8 billion of bio-based compounds in 2016 (mostly given by Germany) with an expected growth to € 21,6 million by 2025, at a CAGR of 16.16% between 2017 and 2025.[3] From the launch of the European Bio-economy strategy defined as "the production of renewable biological resources and the conversion of these resources and waste streams into value added products", the total EU economy of the sector rose from €2.09 trillion in 2008 to €2.29 trillion in 2015.[4] In 2017, there were 224 biorefineries operating across Europe, of which 181 were 'first- generation' facilities, which used feedstocks such as sugar, starch, oils, and fats, to produce mainly biofuels and products of oleo-chemistry, and only 43 biorefineries were 'second-generation' plants where lignocellulosic feedstocks, such as non-food and non-energy crops and biowaste, were processed for obtain energy (biofuel, electricity, heat) and synthesize renewable chemicals and materials.[5] Currently, 803 biorefineries have been identified in the EU, of which 507 produce bio-based chemicals, 363 liquid biofuels and 141 bio-based composites and fibres (multi-product facilities are counted more than once).[6] Of those facilities, 177 are reported as

integrated biorefineries that combine the production of bio-based products and energy. The location of most biorefineries shows correspondence with chemical clusters and ports. Generally, the highest concentration of biorefineries is located in the central part of the EU, particularly in Belgium and the Netherlands (Figure 1.2). Agricultural resources are the feedstock source used by most biorefineries in all EU countries with the exception of Finland, Sweden and Portugal. Marine and waste resources are relevant in some countries but not yet highly exploited.

Here some examples are briefly described. Bigadan's Kalundborg Bioenergy plant in Denmark enzymatically converts biomass from pharmaceutical and other organic waste to energy,[7] where the biogas generated is purified to the same quality as the natural gas. BioWanze SA does justice to the topic of sustainability throughout converting the husks of wheat grains into a large part of the required thermal and electrical process energy.[8] Sekab E-Technology utilizes the value of residual products from forestry and agriculture with the goal to synthesize chemicals and propellants.[9] StoraEnso offers bio-based chemicals that are from renewable resources and non-food/non-land competing, like fragrances and flavors, lubricants, resins, construction, natural fertilizers, industrial and household cleaners and solvents, applications in the chemical and plastics industries, drop-in biofuels and other fuels produced from biomass sources, and biobased materials.[10]
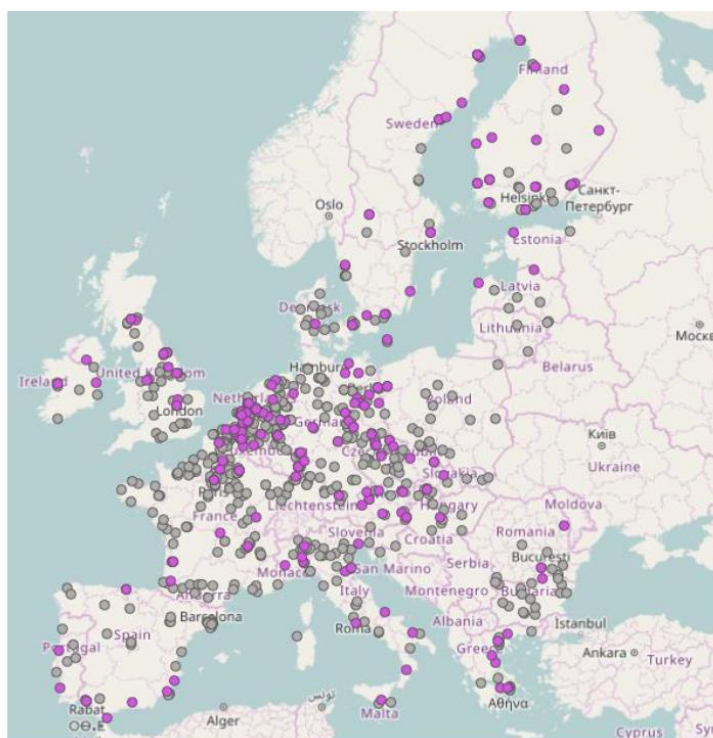
Figure 1.2. *Map of biorefineries producing bio-based chemicals, liquid biofuels and composites and fibres in the EU. (●) integrated biorefineries (chemicals and energy); (●) non-integrated biorefineries. (Taken from ref. 10)*

In this context, fast-paced regulations in the EU are continuously accelerating towards the exploitation of lignocellulosic biomass. This is witnessed by the number of projects funded within the Horizon 2020 program during the 7-year period from 2014 to 2020 (Table 1.1).[11]

Table 1.1. *Projects funded by the EU for utilizing lignocellulosic feedstocks in the biorefinery industry. (Taken from ref. 15)*

Project name	Biorefinery feedstock	Country coordinated in	Period	Total cost (€)
AgriChemWhey	Byproducts from dairy processing	Ireland	2018–2021	29 949 323
GRACE	*Miscanthus* or hemp varieties from marginal lands	Germany	2017–2022	1 500 085 121
SmartLi	Kraft lignins, lignosulfonates, and bleaching effluents	Finland	2015–2019	240 746 125
BIOSKOH	Lignocellulosic feedstock	Italy	2016–2021	3 012 231 375
BARBARA	Agri and food waste	Spain	2017–2020	2 711 375
AgriMax	Agri and food waste	Spain	2016–2020	1 554 349 456
PULP2VALUE	Sugarbeet pulp	Netherlands	2015–2019	1 142 834 750
GreenSolRes	Lignocellulosic residues or wastes	Netherlands	2016–2020	1 060 963 701
Dendromass4Europe	Dendromass on marginal land	Germany	2017–2022	2 044 231 875
SYLFEED	Wood residues	France	2017–2020	14 976 590
GreenProtein	Vegetable residues from packed salad processing	Netherlands	2016–2021	554 651 999
PROMINENT	Cereal processing side streams	Finland	2015–2018	310 389 750
FIRST2RUN	Cardoon from marginal lands	Italy	2015–2019	2 502 268 875
Zelcor	Lignocellulosic residues from ethanol production, lignins dissolved during pulping process, and lignin-like humins formed by sugar conversion	France	2016–2020	671 001 250
STAR4BBI	Lignocellulosic feedstocks from forests and agriculture	Netherlands	2016–2019	99 587 750
BIOrescue	Wheat straw and agroindustrial waste	Spain	2016–2019	376 758 750
OPTISOCHEM	Residual wheat straw	France	2017–2021	1 637 681 683
US4GREENCHEM	Lignocellulosic feedstock	Germany	2015–2019	3 803 925
FUNGUSCHAIN	Mushroom (*Agaricus bisporus*) farming residues	Netherlands	2016–2020	814 366 125
POLYBIOSKIN	Food waste	Spain	2017–2020	405 835 938
ValChem	Woody feedstock	Finland	2015–2019	1 850 270 325
LIBBIO	Andes lupin from marginal lands	Iceland	2016–2020	4 923 750
LIGNOFLAG	Straw	Germany	2017–2022	34 969 215

This scenario shows the effort that the scientific/industrial community is undertaking to shift the Society's dependence away from petroleum in favor of an innovative and economic viable use of methods and technologies to convert renewable biomass resources into clean energy and products. For instance, future steps in this direction are being carried out by linking the location of current bio-based facilities with the specific kinds of locally available biomass (with main focus on agriculture and forestry at the moment), to establish optimal locations of new biorefineries for the best exploitation of local resources. The JRC (Joint Research Centre of the EU) is also planning to make future updates of the map of bio-based facilities, depending on policy needs and available resources. Chemical industries should necessarily follow the green chemistry principles as an effective, practical, and sociological answer to all these issues. Products, feedstocks, and manufacturing processes will need to integrate the principles of green chemistry and green engineering under an expanded definition of performance that includes sustainability considerations.

Parallelly to the bio-economy program, within the vision of circularity, EU has forbidden the commercialization of single-use plastics since 3rd July 2021,[12] in favor of biobased and especially biodegradable alternatives, while any decarbonisation strategy is supported by governments via both a gradual switch to renewable or to less carbon-intensive fossil fuels and the improvement of the efficiency of transformation processes.[13] If this declining trend observed in the past decade will continue, EU electricity generation would fully decarbonize by 2050. Albeit very encouraging, this should not mislead since the global energy exploitation from renewable sources as wind, hydropower, geothermal heat, and the sun is far from being satisfactorily. To

cite only one example, in 2019 the US produced only 11% of renewable energy:[14] an oil-free world is clearly not yet competitive.[15]

1.2   The use of renewable feedstocks: biomass and biorefineries

A feedstock is renewable if it is replaced at a higher rate than the one it is consumed. Biomass typically falls in this definition as it comes up as one of the most abundant and diversified repositories of chemical products in nature including plants, animals, and microorganisms, or, from a biochemical perspective, cellulose, lignin, sugars, fats, and proteins.[16] Due to the vastity of the subject, the following discussion will be limited on specific biomass sources and it will describe protocols for the extraction of bio-based molecules and biopolymers which have been used and transformed in this thesis work. Lignocellulose and natural oils (triglycerides) have been of interest in this respect.

1.2.1. Lignocellulose: composition and treatment/biorefining

Lignocellulose is comprised of sugar-based polymers including cellulose (35-50% of dry weight) and hemicellulose (20-35%), and a complex aromatic polymeric structure as lignin (10-25%).[17] The major component, cellulose, is constituted by glucose units linked *via* β-glycosidic bonds that confer a rigid, robust and crystalline structure with chains interlinked and orientated by hydrogen bonding between them (Figure 1.3; a). Hemicellulose, instead, is a heteropolymer of different C_5 (mainly xylose and arabinose) and C_6 (galactose, glucose and mannose) saccarides,[18] with a random and amorphous structure which is relatively easy to hydrolyse by dilute acids, bases and numerous hemicellulase enzymes (Figure 1.3; b).[19]
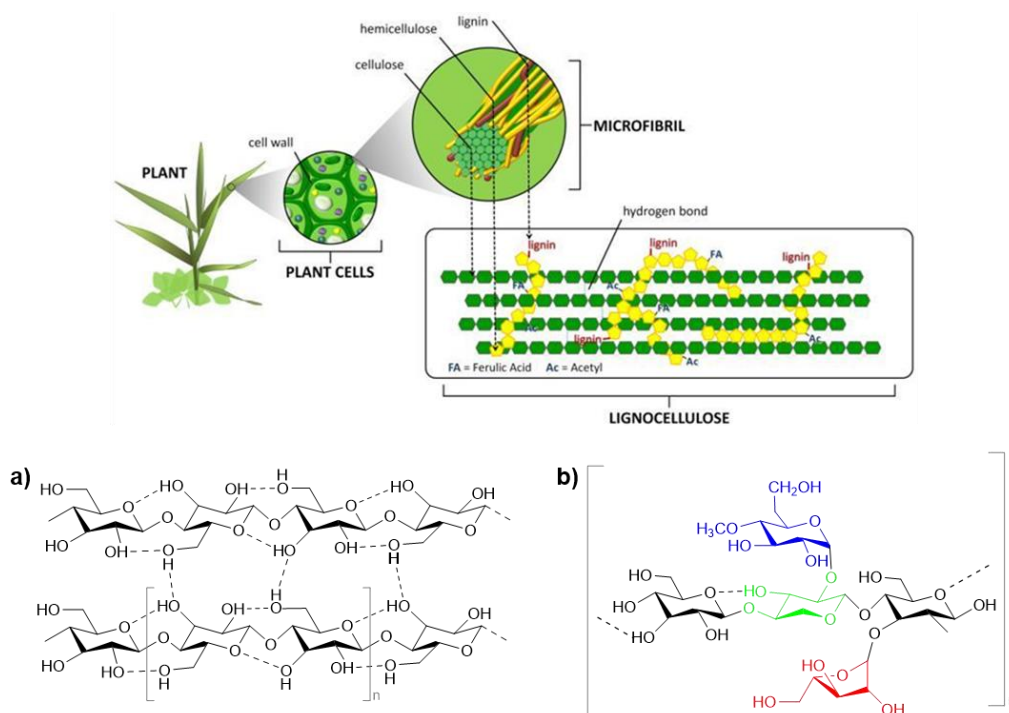
Figure 1.3. *Top: plat cell wall. Bottom, left: structure of cellulose. Bottom, right: structure of hemicellulose showing L-arabinose (**red**), D-xylose (**green**), D-glucose (**black**) and D-galactose (**blue**)*

Finally, lignin is based on the coupling of aromatic monolignols, the three main ones being *p*-cumaryl-, coniferyl-, and sinapyl-alcohols (Figure 1.4, left). The distribution of monolignols in the structure largely depends on the botanical nature of the matrix, and determines the origin

of diversified classification as hardwood, softwood, and herbaceous plants.[20] The distribution of phenolic units in plats is reported in Table 1.2.

Table 1.2. Distribution of phenolic units in plants

Source	H-unit (wt%)	G-unit (wt%)	S-unit (wt%)	Lignin (wt%)
Hardwood	0-8	25-50	45-75	16-24
Softwood	<5	>95	Traces	25-31
Herbaceous	5-33	33-80	20-54	10-25

Aromatic macromolecule in the lignin fraction, impart not only toughness to plants, but thanks to their antioxidant activity,[21] confer resistance to microbial infections and light irradiation.
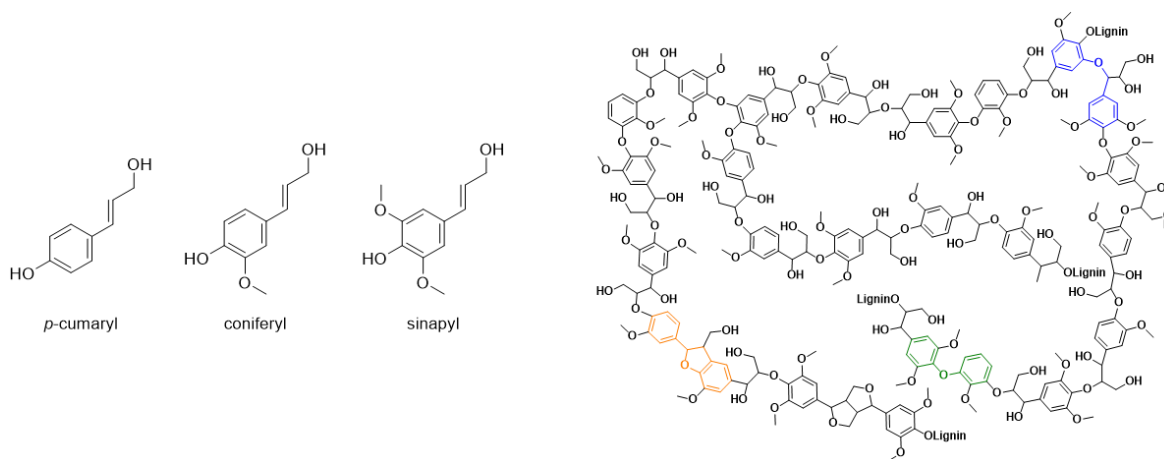
Figure 1.4. Left: structures of monolignols, namely p-coumaryl alcohol (H-unit), coniferyl alcohol (G-unit), and sinapyl alcohol (S-unit). Right: structure of lignin

The heterogeneity of such a biomass is further complicated by the fact that major components (lignin, cellulose and hemicellulose) are organised together and networked with acetyl groups, minerals and phenolic substituents.[22] This implies a number of pre-treatments and treatments necessary to break down lignocellulose, the design of which must consider both the potential products that can be achieved, and the economic feasibility and the environmental impact.[23]

Pre-treatments are generally classified into physical, chemical, thermophysical, thermochemical and biological.[24] These are highlighted in Figure 1.5 for the fractionation of lignocellulosic biomass.
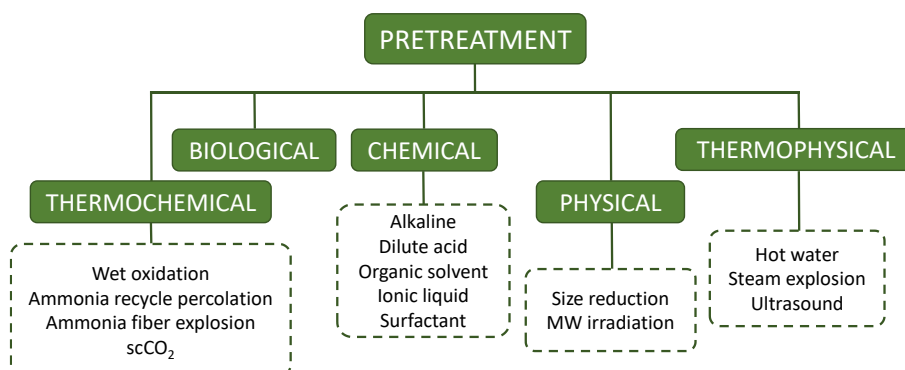
Figure 1.5. Pre-treatments commonly used for fractionating lignocellulosic biomass

For space reasons, only a few examples of such procedures can be commented in this Thesis. Among thermo-physical and thermo-chemical pre-treatments, one of the most promising

approaches is the so called liquid hot water (LHW) method which consists in treating the biomass in water at elevated temperature and pressure (T = 160-240 °C; $p > 20$ bar). Besides the low environmental impact, this technology is effective in hydrolysing the lignocellulosic biomass and, as an added advantage, it does not require any washing of the residues after the treatment. Another thermal fractionation protocol is based on steam explosion which is often combined to the use of supercritical carbon dioxide (sc-CO_2) as a nonpolar, low-viscous solvent. In this case, the breakdown of lignocellulose structures is favoured by the high diffusivity of scCO$_2$ (at T > 35 °C and p > 75 bar) which may deeply penetrate within the solid material. Ultrasound-based methods offer also potentially valuable solutions by which cavitation phenomena are exploited to enhance heat and mass transfer during the biomass breakdown. These operations consist in disorganizing lignin, cellulose and hemicellulose from other components as acetyl groups, minerals and phenolic substituents. Finally, biological pre-treatments are extensively studied for thermally labile bio-based derivatives. These methods are low energy demanding since they operate under mild conditions (T < 50 °C; pH = 4-10); however, their high cost is a severe constraint for any large-scale implementation and industrial applications.[25]

The second step in the biorefining of biomass is the secondary treatment of the primary fractionation. Cellulose and hemicellulose are converted to small oligomers and sugars, together with furans, through the partial or total cleavage of the glycosidic bonds of cellulose. The multiple interactions (hydrogen bonds and van der Waals forces) present into the cellulose/hemicellulose structures together with the reluctance of the anomeric oxygen to protonation make the depolymerization of such biopolymers not trivial. Generally, this involves high temperatures/pressure procedures. The Proesa^{TM} protocol commercialised by Beta Renewables in Crescentino, Italy[26] and the supercritical solvolysis in water or polar aprotic solvents are two examples of such processes.[27] PROESA™ belongs to the so-called "second-generation" biofuel technologies which allow the use of the sugars present in lingo-cellulosic biomass to be converted into fuel (ethanol) and other chemicals in up to 1 ton of ethanol produced per 5-6 tons of dry biomass. It comprises sequential multi-step procedure of biomass steam/water cooking, enzymatic hydrolysis, and yeast fermentation. An example of supercritical solvolysis is the hydrolysis of cellulose in supercritical water (T= 400 °C and p = 250 bar) which occurs in extremely low reaction times (t = 0.02 s) to obtain a sugar yield higher than 95 wt %, whereas the 5-hy- droxymethylfurfural (5-HMF) yield was lower than 0.01 wt%.

Of the several other strategies reported in the literature, an inventive protocol has described the use of γ-valerolactone (GVL), a well-known biomass-derived compound,[28] to solubilize cellulose and favour its subsequent acid hydrolysis.[29] In particular, soluble carbohydrates mixtures (with a recovery of 90 to 95% of soluble polysaccharides) are obtained from corn stover, hardwood, and softwood by continuously delivering a solution of GVL/water containing H_2SO_4 (0.05 wt %) into a stainless-steel flow-through reactor packed with the lignocellulosic biomass, at 157-217 °C. The final aqueous phase is separated along with 75–91% of the carbohydrates from the binary GVL/water mixture (which is then recovered) by the addition of either NaCl or liquid CO_2. An overview of the process is shown in Figure 1.6.
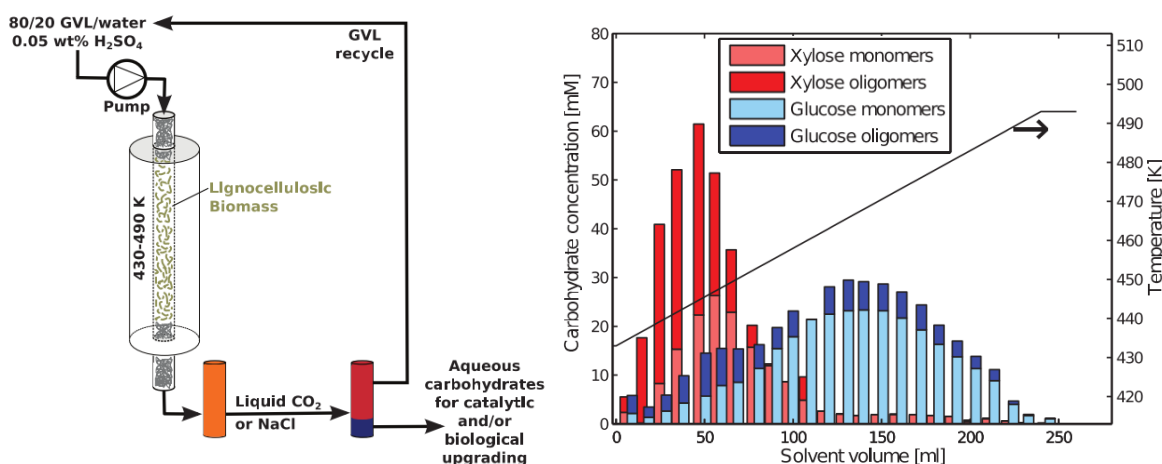
Figure 1.6. *Left: the aqueous-phase soluble-sugar production using GVL as a solvent. Right: soluble carbohydrates produced by progressive heating of corn stover in a packed-bed flow-through reactor using 5 mM H2SO4 in 80 wt % GVL and 20 wt % water*

The selective depolymerization of cellulose to low molecular weight glucans, has been reported also through non-thermal technologies (T = 25-100 °C; NTT) that offer advantages in terms of selectivity and downstream processing.[30] NTT include ionic liquids (Figure 1.7)[31] and mechanocatalysis which is based on a synergistic effect between mechanical forces and acid catalysis: in this latter case, the use of both solid layered mineral kaolinite[32] and the impregnation of cellulose with strong acid catalysts (H_2SO_4 or HCl) followed by grinding of the mixture, has been proposed.[33]
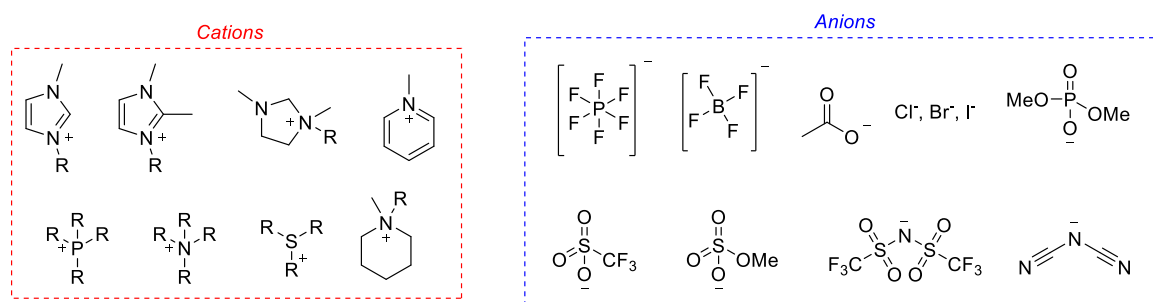
Figure 1.7. *Common ionic liquids cations and anions for NTT*

As far as the lignin fraction, this is first separated from the cellulose and hemicellulose and then it is treated with dedicated processes, which are focused to the production of either monomeric aromatic compounds or energy. For example, lignin is isolated by the pulping of lignocellulose in the paper industry.[34] Several pulping processes have been developed over the years. The three main ones are Kraft pulping,[35] sulfite pulping,[36] and organosolv pulping.[37] Since Lignin was used as a starting feedstock in this Thesis work, a more in-depth analysis of this subject is discussed here. Kraft pulping is the most extensively exploited technology in the paper industry. It allows for the selective removal of lignin and the parallel production of fibres with high strength properties. In the Kraft pulping, wood chips are impregnated with the so-called white liquor which consists of a mixture of hot water, NaOH and Na_2S. The suspension is then cooked at 140–170 °C for 1.5–4 hours to achieve a dispersion of a highly delignified solid into an alkali solution of lignin derivatives called black liquor (BL). During the process, the β-O-4' linkages are targeted and cleaved by -SH⁻ anions (Scheme 1.1). Parallelly, the high reactivity of

the cleaved target molecules leads to their immediate recombination by means of formation of new C-C bonds.
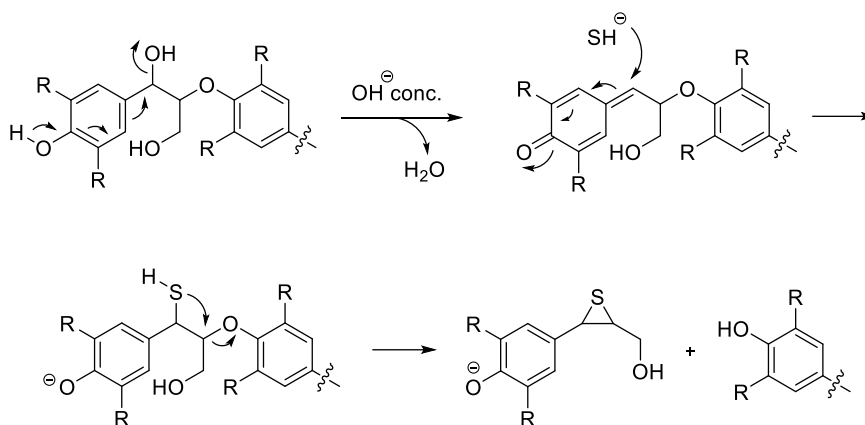
Scheme 1.1. *Cleavage of the β-O-4' linkages during Kraft process*

Heating temperature and time, together with alkali amount and sulphide ion concentration (sulfidity), are properly tuned depending on the type of raw material used. As expected, softwoods usually require harsher pulping conditions compared to hardwoods which include a higher cooking temperature, a higher alkali content (18–23% compared to 16–20% for softwood), and higher sulfidity (25–40% instead of 20–30%).[38] After the filtration of the left solid pulp, the so-called brown stock (rich in cellulose and hemicellulose) is achieved. This fraction is washed and collected. The resulting black liquor (BL), instead, is concentrated by evaporation and the lignin fraction is isolated by precipitation at a pH below 9-10. Alternatively, the BL is burned to produce energy and to recover inorganic components. A pictorial view of the Kraft process in shown in Figure 1.8.
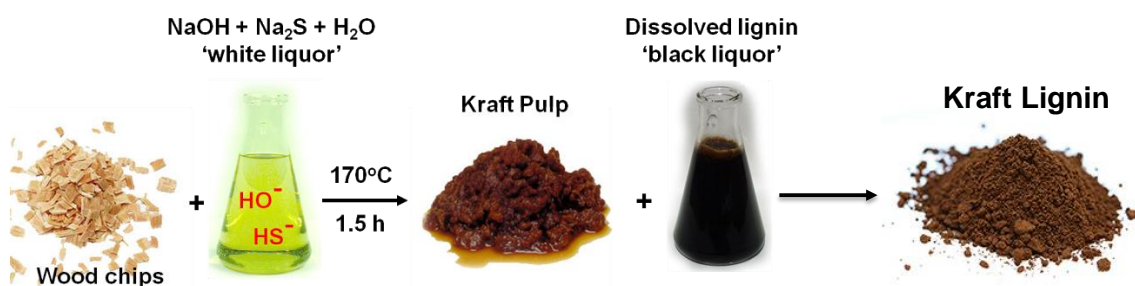
Figure 1.8. *The Kraft process main steps*

It should be noted that Kraft lignin has been mainly exploited to produce energy as illustrated in Figure 1.9. The BL is concentrated to a thick black liquid and combusted in a special furnace that works both as a steam boiler and as a chemical reactor. The process generates heat energy, steam (H_2O and CO_2) and the cooking chemicals (Na_2CO_3 and Na_2S). Curiously, the dissolution of these salts in water produces a greenish solution, known as the green liquor, the color of which is due to small amounts of iron sulphides. The last step of the Kraft pulp mill is the recausticising step, where pulping chemicals are recovered by converting the sodium carbonate back to sodium hydroxide. This reaction is performed using slaked lime (CaO) (Eq. 1.1).

$$Na_2CO_3 + CaO + H_2O \rightarrow 2NaOH + CaCO_3 \qquad \text{(Eq. 1.1)}$$
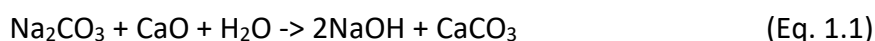
NaOH and Na_2S (white liquor) can therefore re-enter the pulp cycle and be reused.
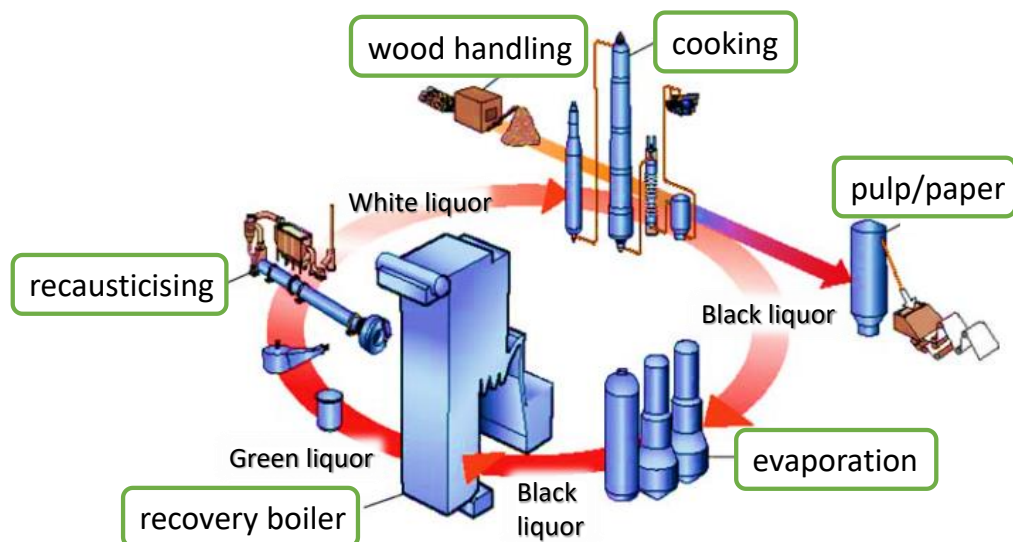
Figure 1.9. *Recovery system for a Kraft pulp mill*

Although a huge amount of Kraft lignin (≈630,000 tons/y) is produced, most of the past industrial effort has been focused on cellulose, downgrading lignin as a by-product. The focus on the valorization of lignin has emerged only recently, in the view of "*lignin-first*" approach,[39] where lignin has been considered as the sole valuable source of renewable aromatics. This scenario is currently opening a plethora of opportunities for the upgrading of lignin and lignin-derived platforms into chemicals, fuels, and materials, and studies are booming to identify catalytic systems for lignin fractionation using both noble and non-noble metals (Cu and Ni).[40] Yet, none of them can be considered an effective *lignin-first* technology. A demonstrative plant on a pilot scale has been developed for the reductive catalytic fractionation (RCF), but its implementation on a large commercial scale is yet to come.[41] It has been recently reported that the efficiency of the pulp production can be increased by extracting lignin, without heavy investments with the design of a new recovery boiler which is the typical bottleneck of a pulp mill plant. The extraction is performed by using 0.20 and 0.15 weight equivalents of CO_2 and H_2SO_4, respectively. Then, lignin undergoes an esterification process with fatty acids as benign reagents, to generate a lignin ester mixable with gas oils. This lignin ester is further hydro processed to hydrocarbons in gasoline, aviation, and diesel range.[42] The same Authors also proposed a method based on the oxidative C-C bond cleavage by which a high molecular weight lignin fraction can be exploited to isolate valuable aromatic monomers. The oxidative reaction proceeds with a high selectivity to give 2,6-dimethoxybenzoquinone (DMBQ) in a yield up to 18 wt% (Scheme 1.2), thus increasing the benchmark yield of monomers by 32%.[43] Overall, the process significantly contributes to improve the economy and competitiveness of the of the lignocellulose biorefining.
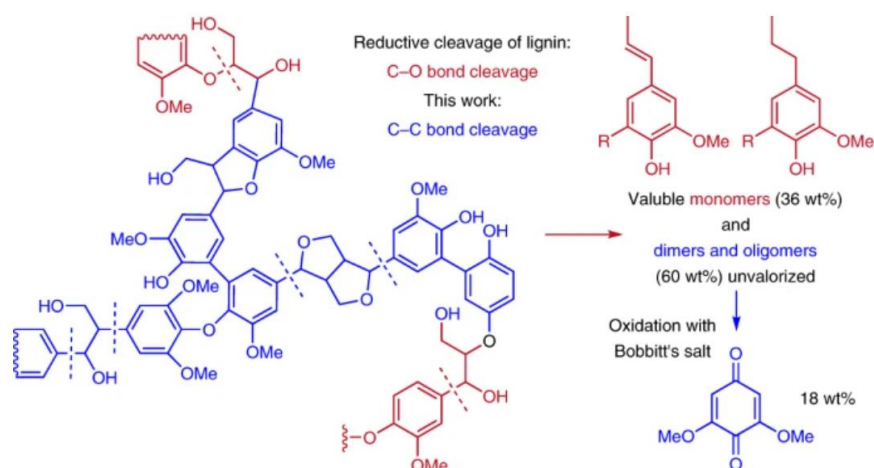
Scheme 1.2. Oxidative C-C bond cleavage of a high molecular weight fraction of lignin

1.2.2. Bio-based platform chemicals: 5-HMF and glycerol

As was mentioned above, biomass is an exceptional heterogeneous source of chemicals and the high oxygen content of bio-based feedstocks compared to fossil resources may represent an opportunity to avoid energy-intensive oxidative processes used in the petroleum industry. The complexity of biomass, however, poses a significant issue in the identification of the most promising compounds or families of compounds worth to be considered. Among the available analyses, extensive work performed by the US Department of Energy in 2004 and its revisitation in 2010 still represent cornerstones in this field.[44,45,46] For the first time, these studies offered rational criteria based on the type of raw material, the estimated processing costs, the estimated selling price, the chemical functionality, the potential use and development in the market, for the choice of the so-called "top 10" platform chemicals, that is, a small group of biobased derivatives that could be utilised as building blocks for higher-value products and materials. This approach was refined further over the years,[47] but the current top 10 lists of biomass-derived platform compounds still include most of the originally identified compounds which are mono- and dicarboxylic-functionalised acids, some furans, 3-hydroxybutyrolactone, bio-hydrocarbons derived from isoprene, glycerol and derivatives as well as other sugars such as sorbitol and xylitol (Figure 1.10). In this thesis work, the interest was focused on both 5-hydroxymethylfurfural (HMF) and glycerol (dashed box).
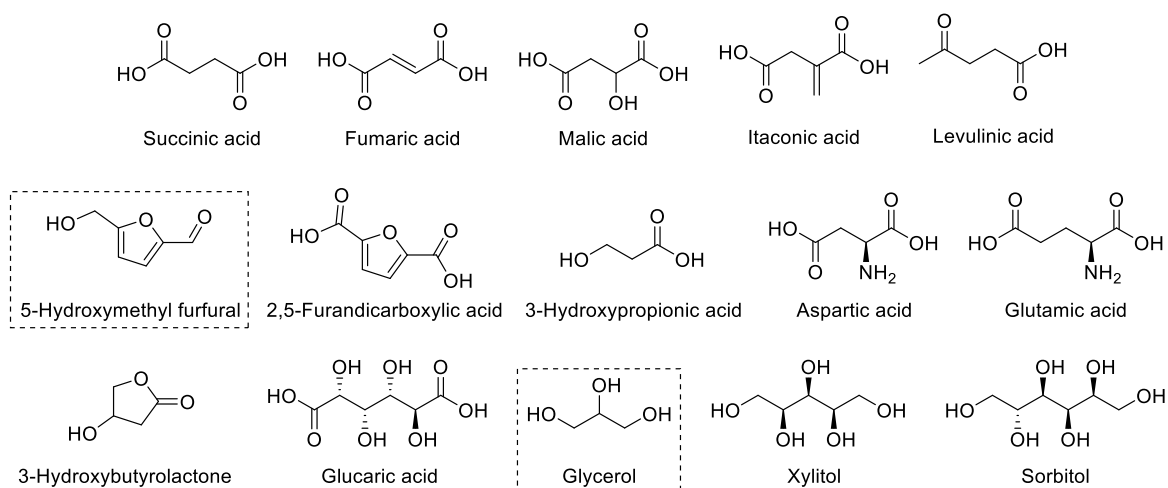
Figure 1.10. Top 10 platforms chemicals

10

1.2.2.1. 5-hydroxymethylfurfural (HMF): synthesis and reactivity

Synthesis. The majority of HMF is produced from cellulose and starch trough a strategy which includes four main steps: i) pre-treatment of biomass into cellulosic components; [48] ii) hydrolysis of the glucan polymers to form monomers of glucose; iii) isomerization of glucose into fructose by keto-enol tautomerism; [49] iv) dehydration of fructose to HMF.[50]

The pre-treatment of lignocellulose follows the destructurization procedures illustrated in Figure 1.6. Beside the already described thermo-physical and thermo-chemical methods, chemical pre-treatments should also be mentioned. Particularly, the most common are the continuous-flow acid hydrolysis (4% H_2SO_4) which is carried out at high temperature (T > 160 °C) for high solids loadings (10-40% w/w substrate/solution) or at lower T (<140 °C) for solids loadings of 5-10% w/w, the alkaline hydrolysis which is often performed close or at ambient temperature and pressure with $Ca(OH)_2$ (0.5% wt., air or N_2 atmosphere, at 25-55°C), and the enzymatic oxidation with peroxidase and H_2O_2 (2%, 30 °C) for 8h) which is efficient for the solubilization of lignin and hemicellulose.[51]

The subsequent transformations of hydrolysis of cellulose, glucose-fructose isomerisation and dehydration of fructose are mostly performed using either mineral or organic Brønsted acids as HCl, H_2SO_4 and HNO_3 or lactic acid and acetic acid, and Lewis acids based on metal salts (Scheme 1.3).[52]
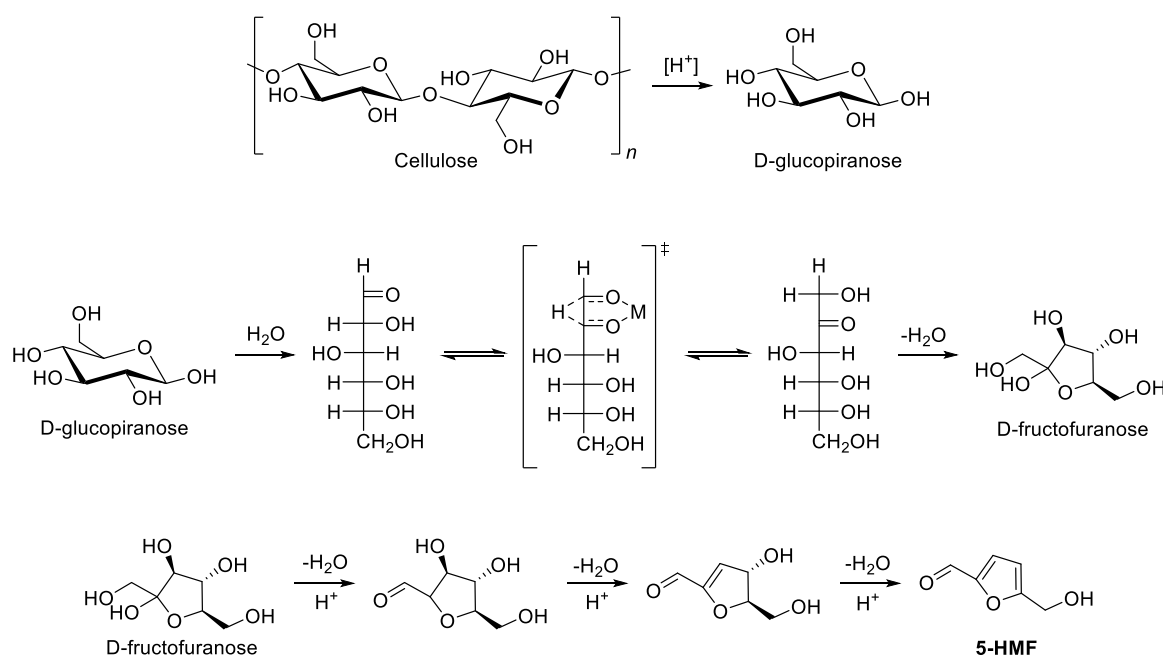
Scheme 1.3. *Top: hydrolysis of cellulose; centre: isomerization of glucose to fructose; bottom: dehydration of fructose*

It should be noted that even glucose as such can be directly dehydrated to HMF, but it has been proved that fructose is a more convenient starting substrate, leading to a higher HMF selectivity.[53] Indeed, the reported activation energies for the dehydration glucose and fructose to HMF are 36.4 and 29.4 kcal mol^{-1}, respectively.[54] Crucial to the success of the synthesis of HMF is therefore the glucose-fructose isomerisation that is a ring opening reaction promoted by the formation of complex between a metal-based catalysts and carbonyl/hydroxyl groups on C_1 and C_2, respectively, of a glucose molecule. To this scope, AlCl$_3$,[55] CrCl$_3$, [56] GaCl$_3$, and InCl$_3$ [57]

have been reported as active systems: typical yields of fructose (from glucose) are in the range of 52-54%. The metal toxicity and the non-recyclability of salts were, however, significant issues. Safer alternatives have been proposed using solids acids as Sn-Beta zeolites; though isomerization yields were lower (34%).[58] One of the most effective protocol to produce fructose is the enzymatic isomerisation of glucose which use xylose isomerase. Some Authors, however, have reported that due to the strict control of operating conditions (pH and temperature) and the enzyme deactivation, the resulting process and the cost of the final product are less convenient than the straightforward transformation of cellulose into HMF requires.[59] Whichever the situation, examples discussed here will consider either cellulose or fructose as starting materials. A comparative study carried out in [BMIM][Cl] as an ionic liquid solvent demonstrated that the acid(H_2SO_4)-catalysed conversion of fructose afforded excellent yields of HMF (80–90%) at 60°C, while the reaction of cellulose proceeded at 130 °C with $CrCl_3 \cdot 6H_2O$ as a catalyst, and it produced HMF in 43 % yield.[60] With the aim of performing a one-pot conversion of cellulose, starch, or even glucose to HMF, bifunctional catalysts comprised of combinations of $SnCl_4$ and H-ZSM-5 or Amberlyst 15 and $CrCl_3$ in [BMIM][Cl] as a solvent, have been described: the co-presence of both Brønsted and Lewis acid sites was exploited to promote simultaneously the hydrolysis/dehydration and the isomerization reactions of Scheme 1.3. Accordingly, at T≥ 110 °C, HMF was isolated with yields in the range of 21-42% starting from bread waste, glucose, and cellulose respectively.[61] Other solutions have been designed using both batch and continuous biphasic reactors. The dehydration of fructose and other sugars was explored in multiphase systems comprised of ethyl acetate and an ionic liquid (IL) synthesized from choline chloride and citric acid, or water-DMSO and methyl isobutyl ketone (MiBK)+*n*-butanol. [62,63] (Figure 1.11)
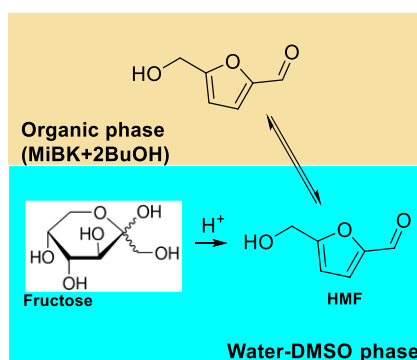
Figure 1.11. Pictorial view of a biphasic reactor for HMF production in an aqueous solution (bottom) and its concurrent extraction in an organic phase (bottom). Fructose is shown as a model sugar

Under these conditions, the reaction was favored by the continuous extraction of HMF into the organic solvent so that final yields were highly improved, typically in the range of 75-90%. In the same multiphase system, other mono-, di- and polysaccharides of C_6/C_5 sugar units including glucose, sucrose, starch, cellobiose and inulin provided HMF with variable yields of 23-75 wt%. More recently, as a further development of these studies, a continuous dehydration of fructose to HMF was described using a water/dimethyl carbonate (1:3 v/v) biphase with added HCl catalyst: in a tube reactor at 1 min residence time, a 96.5% conversion and 87.2% HMF yield were reached at 200 °C.[64] Authors proposed that a H-bonding interaction between DMC and HMF strongly limited the onset of side-reactions and improved selectivity, though part the product (ca. 18% of the total) remained in the water phase and was recovered by

further extraction at the end of the reaction. Other inventive MP-protocols for the synthesis of HMF have been developed by combining the use of ionic liquids as reactions media and compressed CO_2 as an extraction solvent, under the principle of univocal solubility, *i.e.* ILs do not dissolve in dense CO_2, but dense CO_2 is soluble in ILs.[65-66]

It should finally be noted that, regardless of the synthetic method used, the degree of purity of HMF is critical for the preservation of its structure. The product is often isolated as an oily compound with 97–99% purity which is considered high enough for several applications. However, traces of acidic impurities coming from the synthesis of HMF are responsible for a rapid aging of the product through oligomerization processes.[67] These side-reactions can be prevented only if HMF is obtained in a crystalline form (>99.9%, purity) in which the occurrence of an extended intermolecular hydrogen bonding network, restricts molecular mobility and improves stability.[68]

Reactivity. Several comprehensive reviews have reported how the multiple functionalization of HMF makes it a suitable substrate for a range of reactions, including oxidations, hydrogenations, etherifications, couplings, condensations, and others.[69,70,71,72,73,74] Regrettably, HMF is not yet available on large scale because its production and isolation steps are not yet optimized for industrial exploitation/production, but elucidating the reactivity of HMF is an extremely attractive area in view of potential future applications. The following section will briefly overview the features of some of these reactions whose most promising products are illustrated in Scheme 1.4.
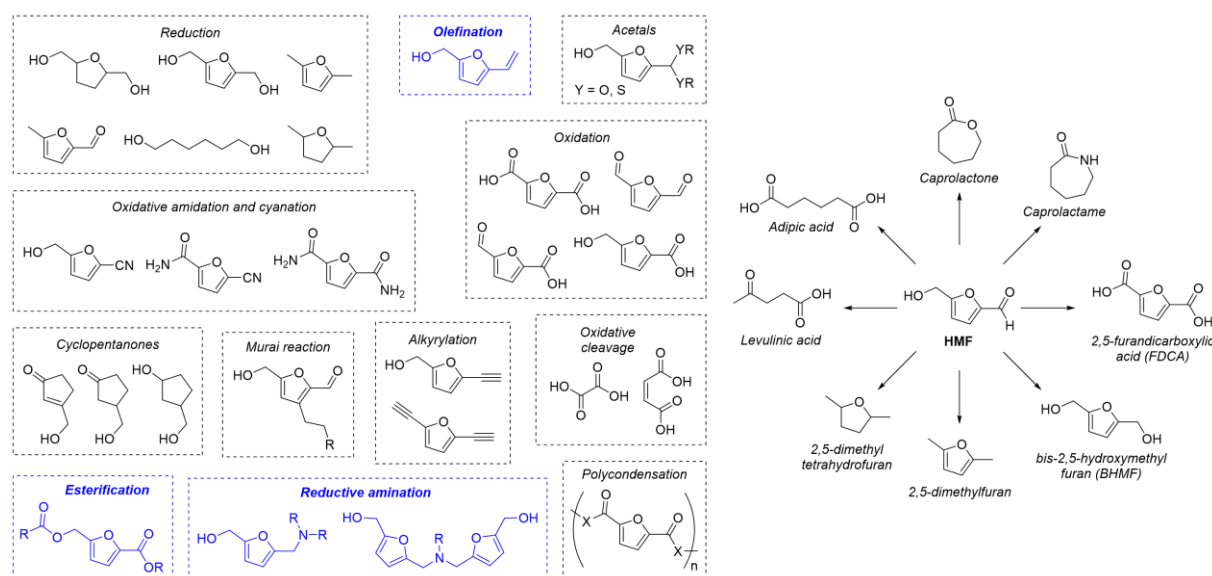
Scheme 1.4. *Left: main pathways of HMF reactivity studied since 2017 (the routes of interest for this thesis work are highlighted in* **blue***). Right: most promising HMF derivatives*

Esterification. Among the esterification processes of HMF, its acetylation to 5-formylfuran-2-yl)methyl acetate (HMF-acetate or AMF) exemplifies the most studied and interesting reaction. The AMF product, thanks to its low hydrophilicity and improved stability, has been proposed as an alternative platform to HMF (Scheme 1.5).[75] Several acetyl donors including acetic anhydride, acetic acid and even simple esters, and catalysts (pyridine, sodium acetate, I$_2$, etc.)[76,77,78]or biocatalysts (e.g. Lipase Cal-B)[79,80] have proved effective for the synthesis of AMF.
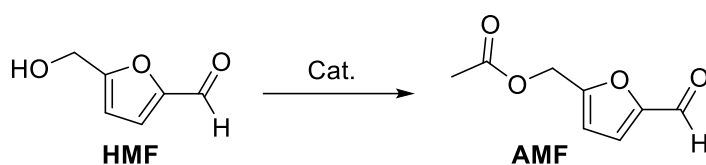
Scheme 1.5. *The acetylation of HMF to AMF*

Even more attractive is the esterification of the oxidation derivative of HMF, 2,5-furandicarboxylic acid (FDCA), which was identified as one of 12 priority chemicals. FDCA received considerable interest as a potentially renewable replacement for petro-based terephthalic acid in polymer applications. Indeed, the synthesis of the most common furan-based polyester, polyethylene 2,5- furandicarboxylate (PEF), can be carried out directly from the esterification of FDCA with ethylene glycol through a standard melt polycondensation procedure with antimony glycolate as a catalyst.[81] Noteworthy, the Coca-Cola Company's sustainable packaging journey crossed a major milestone with the unveiling of its first-ever beverage bottle made from 100% plant-based plastic. Approximately 900 of the prototype PEF bottles have been produced.[82] The same polymerization protocol has been described for the synthesis of fully bioderived polyesters based on itaconic acid (IA), FDCA, succinic acid (SA), and 1,3-propanediol (PD).[83] One-pot reaction conditions were also reported for the conversion of FDCA into furan polyesters:[84,85] in this case, the given strategy included the catalytic esterification of FDCA in the presence of at least an alcohol or a mixture of different alcohols (not specified in the Patent) with a homogeneous water-tolerant Lewis acid catalyst as a metal triflate species followed by the transesterification of the intermediate ester product with glycol. The last process was catalyzed by the same catalyst retained in the intermediate ester mixture.

Oxidation. HMF can be oxidized to a variety of products including 2,5-diformylfuran (DFF), 5-hydroxymethyl furoic acid (HFC), and 2,5-Furandicarboxylic acid (FDCA). These products are building blocks for polymers, resins, foams, sealants, pharmaceuticals, and solvents. FDCA in particular, has been extensively investigated as a monomer in the synthesis of polyethylene furanoate (PEF), a recyclable biopolymer analogous to the fossil-derived polyethylene terephthalate (PET), but with improved gas barrier, higher thermal stability and low-temperature formability. PEF can be used to produce films, fibers and mainly bottles for the packaging of soft drinks, water and fruit juice.[86] Several catalysts have been designed to control the selectivity of the multiple oxidation steps of the hydroxymethyl and aldehyde group of HMF. For example: i) the synthesis of HFC has been achieved with a 93 % yield at > 99 % HMF conversion by using both Au nanoparticles supported on acidic high surface area graphite (HSAG) and Ag_2O as a catalyst, in the presence of O_2 and H_2O_2 as oxidants;[87,88] ii) the oxidation of HMF to DFF was reported using a mesoporous cobalt oxide catalyst doped with manganese oxide (*meso*-5%-Mn-CoO$_x$-250), by which under optimized conditions, the conversion and DFF selectivity were 80 % and 96 % respectively, in dimethylformamide solvent; [89] iii) the preparation of FDCA in a 91 % yield was carried out through the direct oxidation of HMF in water over MnO_2 as a catalyst, under atmospheric pressure of O_2.[90] The latter reaction, however, has been described with many other catalysts based on Pt, Pd and Au supported on carbon, Al_2O_3 and ZrO_2.[62]

Hydrogenation/hydrogenolysis. The catalytic hydrogenation/hydrogenolysis of HMF is one of the most studied reactions for the transformation of bio-based platform chemicals (Scheme 1.6).
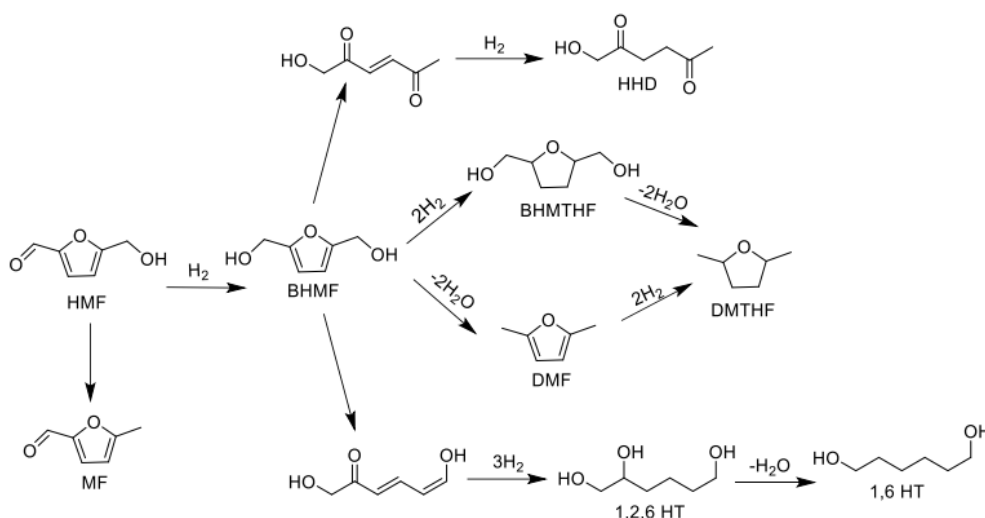
Scheme 1.6. Different pathways for HMF hydrogenation/hydrogenolysis

The process may lead to several different products whose distribution is primarily steered by the nature of catalysts, the temperature, and the pressure. Due to the vastity of the subject, this paragraph will be limited to some representative examples. The preparation of BHMF *via* the selective hydrogenation of the aldehyde group of HMF, has been accomplished with both noble metal (Ru, Pd, Ir) and non-noble metal based (mostly Cu and Ni) catalysts,[91] with operating T and p in the range of 25-80 °C and 5–50 bar. For example, a catalyst comprised of Ru clusters immobilized in nanosized mesoporous zirconia silica (Ru/MSN-Zr) allowed the almost quantitative conversion (98%) of HMF into BHMF (92 % selectivity) at T = 25 °C and *p* (H_2) = 0.5 MPa.[92] Other excellent catalysts were Ru/CeO$_x$ and Ru/Mg-Zr that at 130 °C and 30 bar of H_2, in a 2:1 bi-phase 1-butanol/water batch reactor, allowed to achieve both the partially hydrogenated derivative (BHMF) or the fully hydrogenated derivative (BHMTHF) with 94% and 91% selectivity, respectively, at complete conversion.[93] The role/benefits of oxide-based supports with high isoelectric points and of the biphasic reaction medium (with respect to water alone) was highlighted in the prevention of acid-catalyzed degradation reactions of HMF, particularly those forming linear hexane-polyols (1,2,5-HT, 1,2,5,6-HT, and 1,2,6-HT) from BHMF. However, compared to BHMF, the preparation of BHMTHF usually implies harsher reaction conditions: in the presence of Ni-Raney (10 %wt.), the quantitative HMF conversion to BHMTHF was achieved at T = 100 °C , *p*(H_2) = 9.0 MPa.[94] Hydrogenolysis processes take place competitively to hydrogenation reactions of HMF, and are favored by acidic catalysts/environment. Three major products as 2,5-dimethylfuran (DMF), 5-methylfurfural (MF), and 2,5-dimethyltetrahydrofuran (DMTHF), have been described. For example, DMF was obtained directly from HMF in 85-100% yields using either 5 wt% Pd/C under a combined atmosphere of CO_2 (100 bar) and H_2 (10 bar) at 80 °C,[95] or a bimetallic catalyst comprised of a Lewis-acidic Zn(II) and Pd/C at 150 °C and 22 bar of H2.[96] Another effective synthesis of DMF with > 95% yield was accomplished by the use of formic acid (FA) and H_2SO_4 in the presence of Pd/C.[97] An emerging product from the hydrogenolysis pathways of HMF is 1-hydroxyhexane-2,5-dione (HHD), the synthesis of which was described using Pd/Nb2O5 and Pd/C at 120-140 °C

and 10-40 bar,[98,99]and more recently with a half-sandwich [Cp*Ir(dpa)Cl]Cl (dpa = dipyridylamine) catalyst at 120 °C and 10 bar H₂.[100] The latter system allowed to isolate HHD in a 69% (isolated) yield.

Reductive amination. The reductive amination of HMF has been described with both aliphatic and aromatic amines in the presence of different reductants (Scheme 1.7).
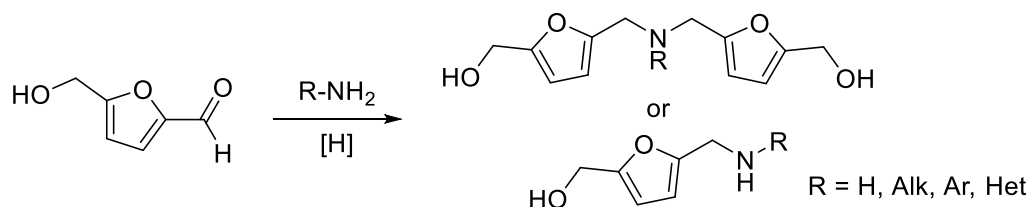
Scheme 1.7. *Reductive amination of HMF*

The reaction may take place in two-steps involving the formation of an HMF-imine intermediate followed by hydride reduction,[101] or by one-pot metal catalyzed reactions in the presence of H₂,[102,103] and carbon monoxide.[104] Catalytic procedures, however, have been preferred over hydride donors (*e.g.* NaBH₄) that generate over-stoichiometric amounts of toxic waste to be disposed of. An unsubstituted aminomethyl derivative is obtained using ammonia and heterogeneous catalysts,[105,106] or biocatalysts (enzymes) [107] via the transamination process. A Pd-functionalized MOF/polymer composite has been employed in the reductive amination of HMF under mild conditions (T = 50 °C, $p(H_2)$ = 5 bar).[108] Ni-based catalysts, as Ni-raney[109] and Ni/SBA-15[110] have been employed, too. A key challenge of these transformations remains the development of robust protocols able to operate in aqueous solutions which are more suitable for the upgrading of furanics in biorefineries.[111]

Aldol condensation. The model aldol condensation of HMF with acetone has been the object of several recent investigations (Scheme 1.8).[112]
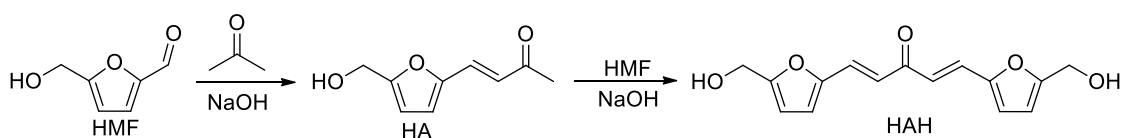
Scheme 1.8. *Aldol condensation between HMF and acetone*

In the presence of conventional base catalysts (e.g. NaOH), the products distribution of the reaction was closely related to the reactants' molar ratio (Q= Ace:HMF). At 35 °C, the mono-condensation (HA) was achieved in a 93% selectivity when the Q ratio was 9.5, while the almost exclusive formation of the bis-condensation product HAH (99%) was obtained by reducing Q to 0.5. Interestingly, the highly conjugated structure of HAH makes it suitable for light absorbtion in the visible blue region (acting as a yellow organic dye) and for the synthesis of conductive polymers. Mesoporous spinel oxides (MgAl₂O₄) were employed as heterogeneous catalysts for the HMF/Ace aldol condensation, too. In this case, HA was attained as the main product (81 % yield).[113]

Olefination. It has been reported that the carbonyl group of HMF can be selectively subjected to the Wittig reaction without any protecting groups shielding the acidity of the OH function (Scheme 1.9).[114]

69%
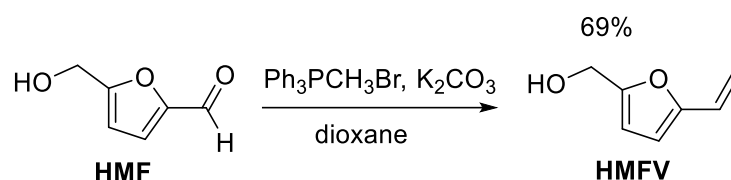
Scheme 1.9. *Wittig reaction with unprotected HMF*

Albeit only one product has described from this reaction so far, a significant potential can be envisioned for this process. The obtained 2-hydroxymethyl-5- vinylfuran (HMVF) has been polymerized giving a material with high adhesiveness to steel, copper, aluminum, and glass, and with cell-adhesive properties.

1.2.2.2. Glycerol from natural triglycerides: manufacture, applications, and reactivity

Manufacture. Lipids are comprised of a broad group of water-insoluble molecules which occur naturally in a variety of terrestrial and aquatic plants as palm, soybeans, sunflower, rapeseed and

microalgae, to name a few.[115] Lipids include fatty acids, waxes, sterols, oil-soluble vitamins, phospholipids, terpenes and others: as such, they are an excellent source of triglycerides (triacylglycerols, TGs), which are formally the products of the triple esterification of glycerol with different or identical fatty acids. The high carbon content per unit of weight makes TGs highly energy dense. For that reason, they are currently employed as source of biofuels, particularly biodiesel that chemically speaking, is prepared by a rather simple transesterification   of   TGs with light alcohols, more often methanol and ethanol, in the presence of a base (e.g. KOH, NaOH, NaOCH$_3$, etc.) or even an acid catalyst (Scheme 1.10). [116]
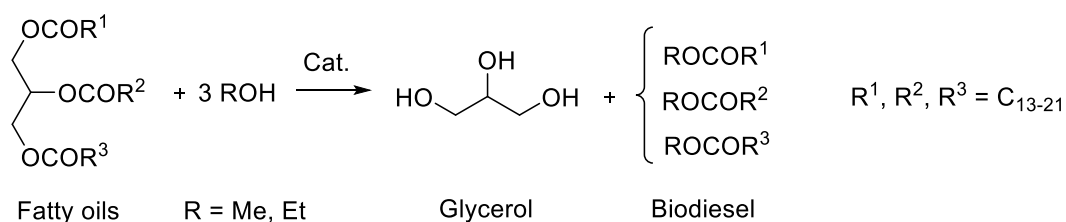
Scheme 1.10. *The transesterification of TGs in the Biodiesel production*

With a current global market size estimated at USD 41.2 billion in 2021, biodiesel is the second most abundant renewable liquid fuel (after bioethanol) whose demand has been increased at a CAGR of 3.8%, between 2016 and 2021.[117] A crucial factor driving this market is the governmental subsidies for environmentally friendly policies by which the search for fuels that reduce greenhouse gas emissions are supported. In this respect, the largest producer of biodiesel is the European Union accounting for ca 40% of all world's production in 2019 (ca 175 thousands of barrels per day, Figure 1.12).[118]
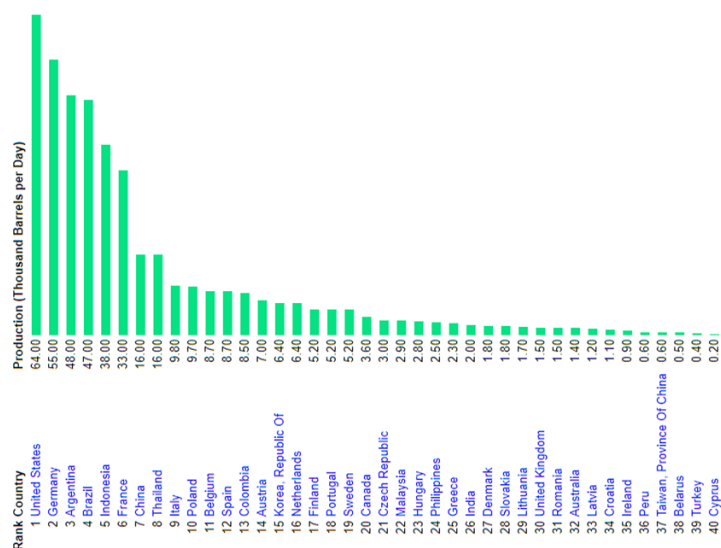
Figure 1.12. Rank country for the production of biodiesel in the World (from ref. https://www.indexmundi.com/energy/?product=biodiesel&graph=production&display=rank)

This manufacture is dominated by the use of rapeseed as a feedstock but accepted raw materials for second generation biodiesel include also jatropha and cottonseed. It should be noted that whatever the starting biomass, the stoichiometry of Scheme 1.8 implies the generation of one mole of glycerol every three moles of fatty acid ester meaning that approximately 10 wt% of the products mixture consist of glycerol. The obvious consequence is that the biodiesel market has also become the largest source of commercial glycerol at the level that all the previous technologies to synthesize glycerol are considered obsolete (Scheme 1.11). [119,120,121]
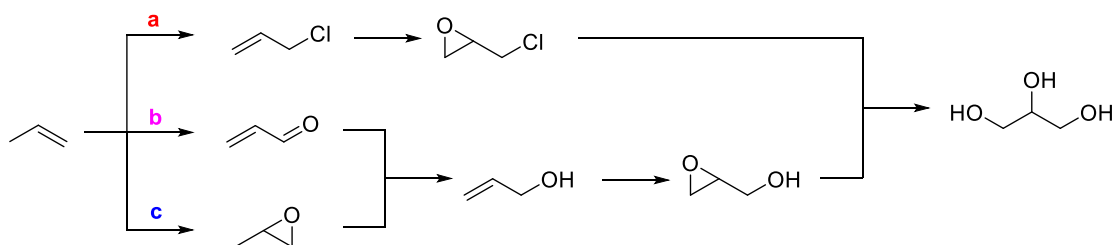
Scheme 1.11. The three most important processes (today obsolete) for the synthesis of glycerol from propene. (a) German process designed during WWII; (b) Shell process; (c) Progil process

Notably, even the current production of epichlorohydrin no longer uses propylene, but glycerol as a starting material for a catalytic hydrochlorination reaction. Dow Chemical, Solvay and Spolchemie have designed different processes based on this transformation (Scheme 1.12). [122,123]
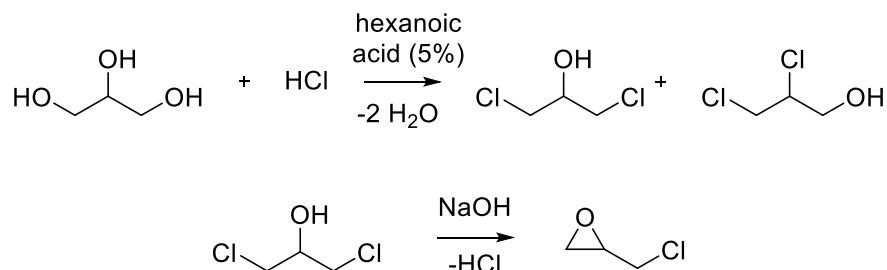
Scheme 1.12. Current routes for the manufacture of epichlorohydrin from glycerol

18

Notwithstanding the biodiesel production looks as a simple and straightforward process (Scheme 1.10), it involves several chemical/engineering issues including the soap formation, the need to separate/recycle the excess alcohol, the disposal of waste generated by the catalyst neutralization, the glycerol/biodiesel separation, and the relatively high investment and operating costs. If co-product glycerol is used for any further application/upgrading, attention should be paid to its purification. It should be noted that conventional transesterification protocols of TGs originate a low-grade glycerol (crude glycerol) that contains variable amounts of contaminants as H_2O, MeOH, NaCl and other salts, and saponified fatty acids. A typical composition includes <65 wt% glycerol, 15-50 wt% MeOH, 10-30 wt% water, 2-7 wt% salts,[124] and the corresponding refining implies energy-intensive operations (evaporation, desalting, ion exchange and distillation) which also depend on the requested purity grade for glycerol (technical: >90%; pharmaceutical: >99.7%).[125] The consequence is that most often, the chemical upgrading of glycerol is economically viable only if high-added value products are synthesised. Otherwise, alternative options for the straightforward transformation of the raw prodcuts become cheaper and simpler than refining the crude reagent and proceeding with its upgrading.[126]

Two technologies have offered a particularly efficient design. The first one was the Esterfif process patented in 2005 by the Institut Francais du Pétrole (IFP).[127] This was based on a methanol-promoted transesterification of triglicerides using a mixed Zn-Al oxide as a solid heterogeneous catalyst. The latter was filtered (and recycled) at the end of the reaction, and the excess methanol was removed by partial evaporation. Products and glycerol (>98%) were then separated in a settler. The second technology was developed in 2006 by the Gadi Rothenberg's group at the University of Amsterdam, and it was then licensed to the Yellow Diesel BV Company. [128] In this case, mixed feedstocks such as used cooking oil, low grade grease, and in general, low-quality oils, waste oils and fats are treated by combining the tranesterification reaction and the separation in a single step through a reactive distillation system. In addition, a vast literature is available to produce biodiesel based on the use of enzymatic,[129] ultrasonic[130] and supercritical [131] protocols. The latter (supercritical) conditions look particualrly promising since they allow to overcome the lack of mutual miscibility of reactants (apolar TGs and polar alcohols) and parallelly to avoid the use of either basic or acid catalysts which are often added in stoichiometric amounts.

Applications and reactivity. The biocompatibility, the non-toxicity, and the renewable origin of glycerol are unique properties that along with the simultaneous presence of three reactive -OH groups in its structure, make it a flexible substrate suitable for applications in a plethora of industrial fields.[132] Glycerol is a colorless hygroscopic and viscous compound with a wide liquid dictated by the occurrence of intra- and inter-molecular hydrogen bonds. Table 1.3 summarizes the main physical and chemical properties of pure glycerol.

Table 1.3. Major physicochemical properties of glycerol at 20 °C

Molecular mass	92.09382 g/mol
Density	1.261 g/cm^3
Viscosity	1.5 Pa·s
Melting point	18.2 °C
Boiling point	290 °C
Food energy	4.32 kcal/g

Flash point	160 °C (closed cup)
Surface tension	64.00 mN/m

Glycerol is used as such in the food, cosmetic, and polymer industry as humectant, solvent and sweetener, lubricant, hydrating agent, and monomer mostly for polyesters and polyethers materials. Moreover, it is used as an intermediate building block to produce nitro-glycerine, acrolein, diols, epichlorohydrin, ethers, and fuels (H_2 and short chain alkanes) through reforming processes. The major products of these reactions are illustrated in Figure 1.13.[133,134]
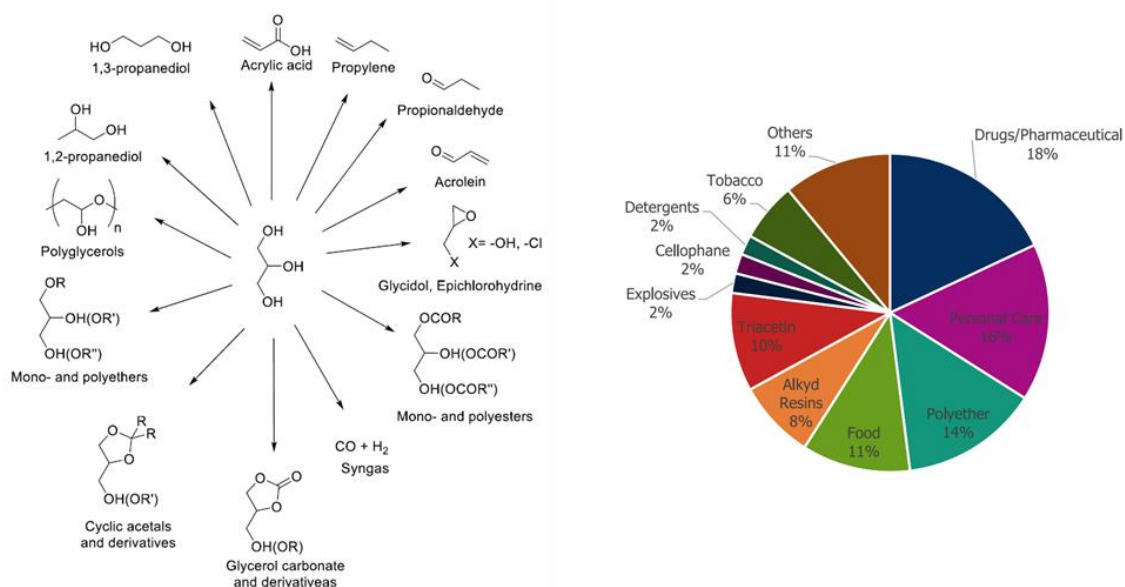
Figure 1.13. Left: value added products derived from glycerol. Right: glycerol market

A massive research effort has been addressed to explore valorization strategies of (renewable) glycerol available as a by-product of the biodiesel synthesis. Two representative examples of large scale applications are: i) the batch process for the chlorination of glycerol to epichlorohydrin, an important building block of the polymer industry, that in the early 2000's was designed by Dow and Solvay;[135,136] ii) the production of 1,2-propanediol from the hydrogenolysis of glycerol implemented in 2011, by ADM on a 100.000 tons/year capacity.[137] The latter reaction was commercialized also by Ayas Renewables and a joint venture between Oleon and BASF.[138] Other routes based on technologies with a current industrial potential are the reforming of glycerol to hydrogen,[139] and the synthesis of C_3 building blocks derivatives like propylene, acrylic acid, acrolein, propionaldehyde, and 1,3-propanediol.[140] A recent analysis has reviewed the impact of integrating different glycerol upgrading routes within a biorefinery, which is functional to evaluate the sustainability of biodiesel production from vegetable oils.[141] According to these Authors, the focus of this research is narrowing on products, such as specialty chemicals and intermediates for plastic, based on the manufacture of lactic acid, acrylic acid, glycerol carbonate, propanediols, epichlorohydrin and allyl alcohol which possess a market size comparable to the global availability of glycerol (derivatives **P1**-**P8**: Figure 1.14, top and bottom).
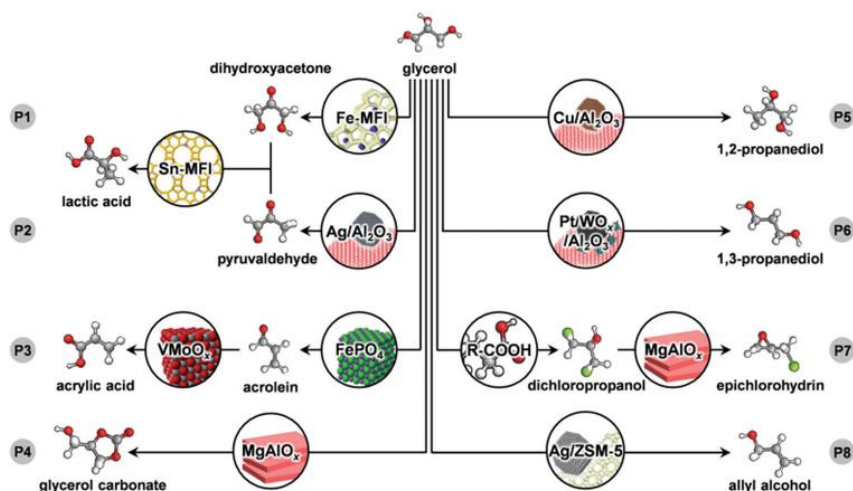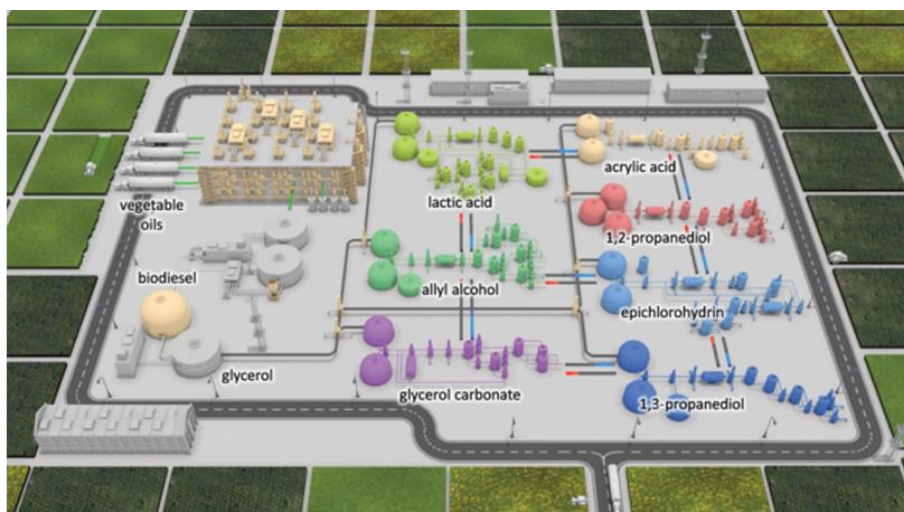
Figure 1.14. *Top: most relevant products (P1-P8) in the glycerol biorefinery; bottom: best catalysts for the upgrading of the products P1-P8 on realistic large-scale processes. From Ref. https://pubs.rsc.org/en/content/articlepdf/2018/ee/c7ee03116e*

The study quantified the advantages of a glycerol biorefinery in lowering environmental and cost-related footprints and described the best heterogenous catalysts for the upgrading of the most promising derivatives (**P1**-**P8**) on realistic large-scale processes.

For the specific interest in this Thesis work, two other families of reactions, *i.e.* the acetalizations and the acetylation of glycerol, are considered in more detail below.

Acetalization. The cyclic acetals of glycerol (GAs) obtained by the condensation of glycerol with light (up to C_4) aldehydes and ketones, are the most common derivatives of this class of compounds.[142] The acetalization of glycerol has been reported in the presence of homogeneous catalysts as mineral Bronsted acids (H_2SO_4, HCl, *p*-toluenesulphonic acid) and Lewis acids, and a variety of heterogeneous catalysts including for example, amberlyst resins, zeolites, sulfonic acid functionalized silicates, K 10 montmorillonites, and zirconia-based catalysts.[143,144,145,146,147,148,149] Notwithstanding the intrinsic activity of homogeneous systems, heterogeneous catalysts that can be recovered and reused especially under continuous flow conditions are becoming the preferred options to improve the process sustainability.[150] The reaction affords both 5- and 6-membered ring products, the ratio of which is strongly affected by the characteristics of the involved carbonyls and on the reaction conditions. As an example,

glycerol formal which come from the simplest aldehyde (formaldehyde) is commercially available as a 60:40 mixture of six- and five-membered ring isomers, while solketal which derive from acetone is obtained almost exclusively as a C_5-cyclic product (Scheme 1.13).[144,151]
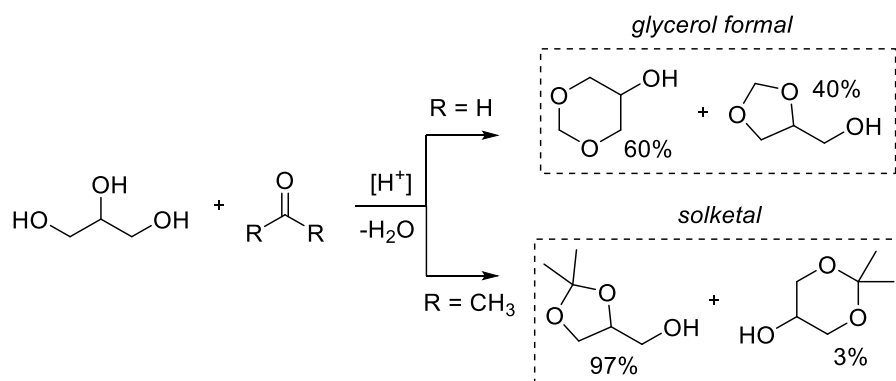
Scheme 1.13. *Left: Glycerol formal as a 60:40 mixture of six- and five-membered ring isomers. Right: solketal*

Glycerol formal and solketal have certainly received the greatest interest in this field because of their intriguing properties which impart both similarities and differences with glycerol. As glycerol, they are viscous, dense, non-toxic, and thermally stable liquids with boiling points in the proximity and over 200 °C. However, since they are obtained by the protection of two OH groups of glycerol, they display polarity, hydrophobicity, and hydrogen bonding ability comparable to those of simple aliphatic alcohols. These aspects account for applications of GAs as safe solvents in large-scale production of paint and ink formulations and in the pharmaceutical industry as additives for injectables and vehicles for drugs.[146,152] Moreover, the stability of glycerol acetals to oxidative conditions and their miscibility with biodiesel blends have made them suitable as fuel additives to improve the quality of both standard (petrochemical-based) and bio-diesels by reducing particulate emissions, viscosity, and pour point.[153,154]

Another interesting approach for the acetalization glycerol is through high-temperature (HT) transformations carried out in the absence of any catalyst: this technique which was originally thought for improving the biodiesel production, has turned out to be excellent for achieve acetals from the reaction of glycerol with enol esters.[155]

Acetylation. The product of the triple acetylation, triacetin, is undoubtedly the most appealing derivative of this specific class of esterification reactions of glycerol.[156] With a market projected to reach USD 309.9 million by 2022, the application of triacetin spans over a variety of sectors including the tobacco industry, food and beverage, pharmaceutical, adhesives and sealants, cosmetics, paints and coatings industries.[157,158] Even though the synthesis is apparently simple, the main issue is the selectivity control in the subsequent mono, double, and triple acetylation steps yielding monoacetylglycerols (MAGs), diacetinglycerols (DAGs), and triacetinglycerols (TAGs), respectively (Scheme 1.14).
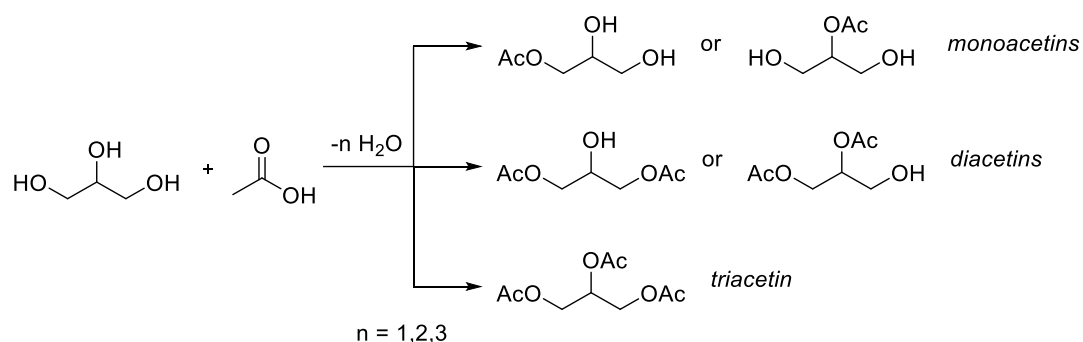
Scheme 1.14. *Mono-, di- and tri- acetilglycerols obtained from the reaction of glycerol with organic acids*

Various acetyl donors can be employed for the acetylation. While acetic acid (AcOH) is the greenest alternative, as it is renewable, non-toxic, and eco-friendly, a major drawback of such systems is posed by the formation of water as by-product during the reaction, which makes the reaction not selective.[159,160,161] To give some examples, a 56% selectivity towards triacetin was reached by Venkatesha *et al.* from the reaction of glycerol with AcOH under organic sulfonic acid-functionalized montmorillonite (T = 120 °C, t = 1h).[161] Da Silva and co-workers achieved the highest glycerol conversion (>99%) in the $Fe_4(SiW_{12}O_{40})_3$-catalyzed esterification reaction, along with the highest selectivity for *di-* and *tri*-acetyl glycerol (55 and 42%, respectively) at 60 °C for 8h.[162] A sustainable approach was adopted by Rezayat and co-workers, who investigated the CF esterification of glycerol with acetic acid in supercritical carbon dioxide: using Amberlyst-15 as a heterogeneous catalyst, they achieved 41% yield of triacetin under the best conditions.[163] Another investigation by H. S. Ghaziaskar *et al.*, reports that under the optimized conditions of an acetic acid-to-glycerol mole ratio of 7, T = 100 °C, and p = 1 bar, over 3 g of Amberlyst-36 as a catalyst, monoacetin, diacetin, and triacetin selectivity reached 43%, 44%, and 13%, respectively, with total conversion of glycerol.[164] Though these approaches were green, they were not selective.

An alternative favored route is the Ac_2O-mediated acetylation. Rajabi synthesized triacetin in >99% yield under a heterogeneous cobalt (II) Salen complex at 50 °C.[165] The results of Mota *et al.* indicate that at 60 °C, zeolite Beta and K-10 Montmorillonite showed 100% selectivity to triacetin within 20 min, with a molar ratio of 4:1 between Ac_2O and glycerol. Amberlyst-15 acid resin yielded 100% triacetin after 80 min, whereas niobium phosphate gave diacetin and triacetin in 53% and 47% selectivity, respectively.[166] Shanbhag *et al.* achieved 82% triacetin selectivity at room temperature over cesium phosphotungstate catalysis.[167] Even though the latter protocols displayed high selectivity, the high potential of explosion, the corrosivity, and the legislative restrictions related to acetic anhydride,[168,169] makes its application not suitable for large scale synthesis. Not to mention the use of acetyl chloride (AcCl) since its toxicity and the formation of stoichiometric amounts of salts (NaCl) complicates the work up procedures due to the Cl-contaminated waste disposal.

In light of all these considerations, the development of more efficient and greener routes for the synthesis of triacetin is still an opened challenge. Other aspects related to this subject will be discussed later on this thesis work.

1.3 Carbon dioxide as a building block in the synthesis of cyclic organic carbonates

The environmental compatibility and the intrinsic safety of carbon dioxide makes it the natural candidate as a C1-building block for chemical synthesis. CO_2 has been used to produce materials since the 1970s, but the interest for its applications has progressively grown over time in parallel to the climate change concerns and sustainability in the public debate.[170] Figure 1.15 shows some of the major chemicals and polymers that can be synthesized by the fixation of carbon dioxide. Albeit the use of the carbon dioxide shows several appealing features, the outcomes related to this chemistry cannot prescind from considering the energy demand of CO_2-mediated reactions and the overabundance of CO_2 generated by human activities.[171]
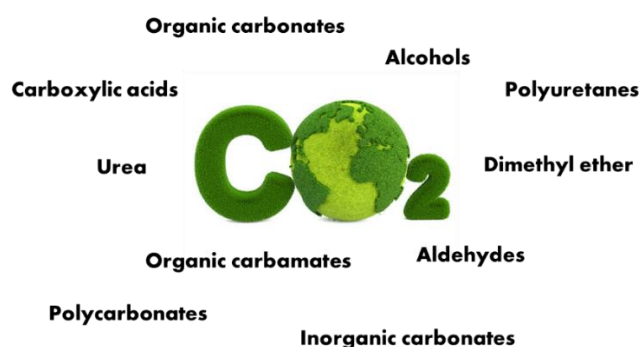
Figure 1.15. *Application of CO_2 as a building block*

A first significant issue is the high thermodynamic stability of carbon dioxide which implies that the activation/fixation of CO_2 as a reagent becomes feasible only in the presence of high-energy reaction partners: only a relatively limited number of molecules including hydrogen, unsaturated derivatives, or strained cyclic reactants have proved to be effective to steer chemical transformations of carbon dioxide toward low energy products. The success of such processes, however, can be undermined by the risk of emitting more CO_2 than that incorporated into the synthesis products.[172] Another critical concern is the lifetime of the products that derive from the conversion of CO_2: liquid fuels may exist for days or weeks, while other compounds as plastics or cements are far more persistent in the environment, for years, decades or even centuries. Quite obviously, the longer their lifetime, the longer the release of CO_2 back to the atmosphere is prevented.[173] Though, the imbalance between current emission and use of CO_2 remains impressively high. The amount of carbon dioxide fixated in chemicals and fuels is about 180 Mt and 2 Gt per year compared to a total of ca 37 Gt (in 2017) from anthropogenic emissions. This leads to conclude that the problems due to CO_2 release can be mitigated only through a strategic vision where options based on carbon capture and utilization (CCU) are integrated to other key enabling technologies, including carbon capture and storage (CCS) and exploitation of renewable (*e.g.,* solar, geothermal, wind) or decarbonated (*e.g.,* nuclear) energy sources.[174]

In this respect, part of this Thesis work has been aimed at exploring the chemical activation of carbon dioxide for the synthesis of cyclic organic carbonates (COCs) which are intermediates in the production of durable polymers as polycarbonates. This section will briefly outline the features of the preparation and properties of COCs.

Cyclic organic carbonates (COCs). COCs are used as polar aprotic solvents, lithium ion-battery electrolytes, cosmetics, plasticizers, detergents, and as mentioned above, as building blocks for polymers.[175,176,177] The main reported routes for the synthesis of COCs are based on reactions shown in Scheme 1.15.
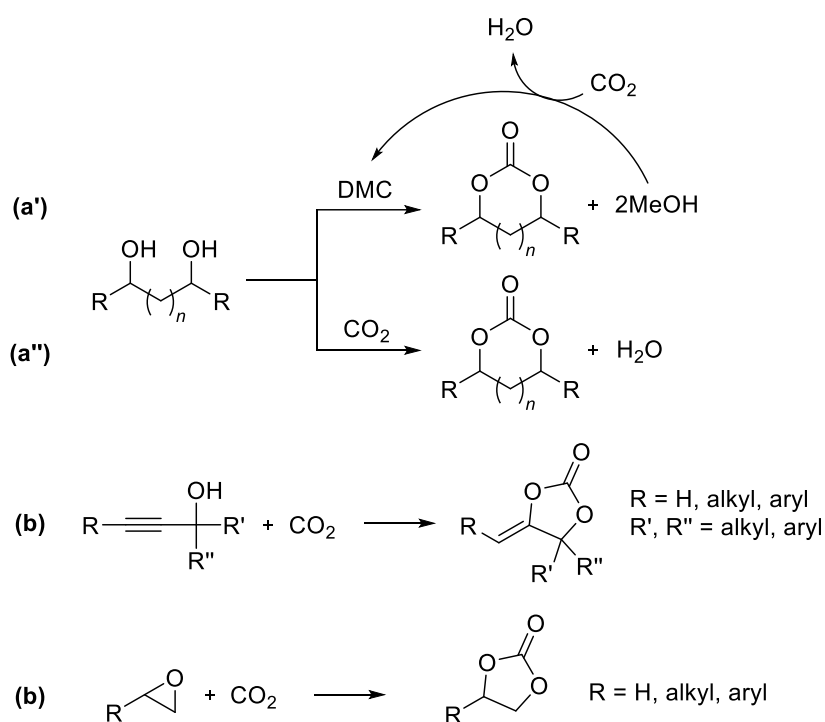
Scheme 1.15. *Major routes for the synthesis of COCs*

Starting from diols the synthesis of COCs can be performed either through the transesterification with dimethyl carbonate (DMC),[178,179] where methanol is formed as co-product, or directly by the incorporation of CO_2 with loss of water (Scheme 1.15, route a'). Both catalytic,[180,181] and catalyst-free[182] protocols have been described with the use of DMC. Pattanaik *et al.* recently reported the continuous synthesis of glycerol carbonate (GlyC) in 71% yield by transesterifcation of glycerol with DMC over Fe–La mixed oxide catalysts at 260 °C.[183] Another recent paper by Wang reports the preparation of GlyC in >90% yield over mesoporous CaO-ZrO$_2$ catalysis at 100 °C.[184] Other routes for the synthesis of five-/six-membered cyclic carbonates refer to the use of enzymes (lipases) under mild conditions (T = 50-60 °C),[185,186] and carbonate phosphonium salts at 90-120 °C.[187] Catalyst-free protocols usually request high temperature (150-260 °C) and pressure (30-50 bar) to achieve good yields of products (>90%). In the case of CO_2, however, despite the tremendous efforts made in search of effective catalysts, the results are not yet satisfactory with yields in the carbonate products which are usually moderate, though some excellent results are also present.[188] For instance, propylene glycol (PG) was obtained in >99% yield from propylene glycol and CO_2 over combined catalytic system composed by CeO$_2$ and 2-cyanopyridine as dehydrating agent at T = 150 °C in 1h.[189] Buchard and coworkers performed the synthesis of six-membered cyclic carbonates in 11-70% yields directly from various 1,3-diols and CO_2 at room temperature, 0.1 MPa of CO_2 using a DBU, tosyl chloride, and triethylamine.[190]

Another strategy is the carboxylation of highly reactive propargylic alcohols (Scheme 1.15, route b) with carbon dioxide. This process is generally carried out in the presence of Lewis

acidic catalysts based on silver and produces COCs functionalized with exocyclic double bonds.[191] Most published reports are limited to secondary and tertiary propargylic alcohols which can be easily cyclized, with the exception of one recent work that describes the conversion of primary propargylic alcohols to exovinylene carbonates with high yields (65-95%).[192] Albeit synthetically efficient, the procedure can be hardly considered sustainable since parent reagents for the preparation of propargylic alcohols are of fossil origin as for example, formaldehyde obtained from methanol and acetylene which comes from the cracking of methane.[193]

The most widely investigated reaction for the COCs preparation is the CO_2 insertion into epoxides (Scheme 1.15, route c). In the last years, studies aimed to identify bifunctional catalysts capable of contemporarily activating CO_2 and epoxides, are becoming a mainstay in this field,[194] including also tandem catalysis.[195] Recent review articles have reported a plethora of such (catalytic) systems.[196,197,198] The use of metal organic frameworks (MOFs) has been the mainstream approach. MOFs arises from different structural characteristics: i) Zn, Ni, Zr, In metal coordination sites) Lewis basic functionalized linkers can be functionalized during or after synthesis) that can act as the site of CO2fixation; (iii) presence of Lewis acidic or basic defect sites inside/-surface of the MOF, (iv) presence of accessible Brønsted acidicCOOH groups, and (v) presence of accessible Lewis and Brønstedacid bifunctional siteTypical epoxides for the reaction are ethylene and propylene oxides (EO and PO) which are available on a commercial scale of 15 and 8 million tons/year, respectively, and to a lesser extent, C_4-C_{10} linear aliphatic epoxides, isoamilene oxide, cyclohexene oxide, styrene oxide and norbornene oxide.[199,200,201] Alike the above mentioned propargylic alcohols, however, epoxides are not only fossil-derived compounds, but they are dangerous and toxic compounds whose use as chemical building-blocks is not sustainable and even less safe.[202]

A greener route for the synthesis of COCs is the direct oxidative carboxylation of olefins (Scheme 1.16).

$$R\diagup\diagdown \quad + \quad \text{Oxidant} \quad + \quad \text{Carbonyl source} \quad \longrightarrow$$

(e.g. O_2, H_2O_2, TBHP)   (e.g. CO_2)
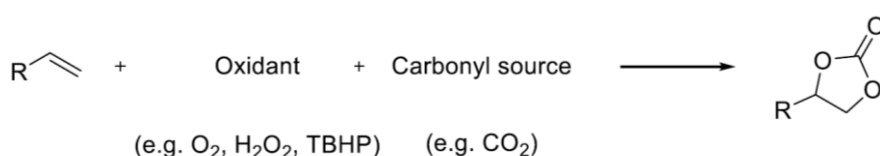
Scheme 1.16. *Direct oxidative carboxylation of olefins*

This reaction involves alkenes that are widely available on the market and in general, are far less toxic with respect to the corresponding epoxides. A variety of olefins are of natural origin [e.g. terpenes and (poly)unsaturated fatty acids] or they can be obtained by the processing of renewable feedstocks as for example, ethylene from bioethanol, C_3-C_6 olefins from MTO (alcohol or methanol to olefins) processes, and other substrates from lignin-derived molecules.[203,204] Albeit the chemistry of Scheme 1, implies the formal epoxidation of the C=C bond, the resulting epoxides are genuine intermediates that are achieved and directly transformed *in situ* without the need of isolating them. This fact obviously bypasses the main issue connected with the previously described CO_2 insertion reaction (path c, Scheme 1.15). The overall process which exemplifies a tandem catalytic transformation (epoxidation followed by CO_2 insertion) has been studied since 1962 and the commercial interest is witnessed by the filing of a several patents.[205] From both economic and environmental standpoints, the best

oxidants are either molecular oxygen or hydrogen peroxide. The latter produces only water as waste and has been more widely legitimized and thoroughly explored,[206] while molecular oxygen has proven quite unreactive towards many olefins with a mechanism often leading to lower conversions and selectivity. The design of catalysts suitable for the tandem sequence, however, is the most critical aspect to the success of the oxidative carboxylation reaction. The scope of the catalytic systems includes various i) catalysts, such as Rh, Ru, Mn complexes, Nb_2O_5, MOFs, TiO_x, ii) different halide sources (*i.e.* ionic liquids, alkaline metal halides, NBS, etc.), and iii) oxidants, like O_2, H_2O_2, tertbutyl hydroperoxide (TBHP). Typical conditions span from low to high CO_2 pressure (0.5-100 bar) and temperature in the range 50-140 °C. Considering the synthesis of styrene carbonate (SC) as a model reaction, until now yields in the range 35-95% towards the desired COC have been achieved, depending on the reactions conditions. One of the best results has been reported by Yuan *et al.*, wo developed an electro-chemical route for the synthesis of SC (94% yield) thanks to the synergistic action of I_2 and NH_3 electrochemically generated *in-situ* from NH_4I at room temperature.[207]

1.4   Green Chemistry and green chemical engineering: tools for sustainability

Green chemistry is an extraordinary tool to sustainability since, by definition, it conceives benign processes for the conversion of (preferably renewable) raw materials using nontoxic and/or non-hazardous reagents, catalysts, and solvents. Giant leaps have been made in the past 25-years towards the application of these concepts. Albeit the technological reliability of many new protocols still requires improvements compared to conventional (non-green) chemical routes, there is no doubt that the massive research effort undertaken especially for the chemical upgrading of bio-based compounds through eco-friendly methods, is paying off. Current achievements in the fields of "green chemistry"[208,209] and "green engineering"[210] have demonstrated that more performance and functionality from chemical products and processes can be realized while decreasing adverse impacts, but these successes need to be made systematic and not anecdotal. This implies that not only the conditions and circumstances by which we make and use chemical products need to be altered but the inherent nature of the chemical products and reagents themselves across the entire value chain from feedstock to application also needs to be changed. The unavoidable consequence is that the very definition of "performance" of the product from function alone to function and sustainability must be revised through thoughtful design of the starting material, the intrinsic properties of the molecules, and their transformations.

In this thesis, these considerations have been addressed from multiple perspectives which have included not only the use of bio-based molecules as glycerol and HMF (see above), but also the design of innovative continuous flow (CF) protocols with supercritical carbon dioxide (scCO2) as a solvent/carrier, and an extended investigation on the reactivity of isopropenyl acetate as a safe and innocuous reagent. The following section will offer a concise overview on CF-technologies also in the presence of $scCO_2$. The use of enol esters and particularly isopropenyl acetate will be, instead, described later on dedicated parts of chapter Two (results and discussion). This subject (enol esters) has been developed within a PhD cotutelle program in collaboration with the group led by prof. Thomas Maschmeyer at the University of Sydney (Australia). Due to the covid-19 pandemic, the experimental program originally planned for the

activity in Sydney has been converted to a project from remote consisting in the preparation of a review article.

1.4.1. Engineering and implementation of continuous flow (CF) technologies

In 2019, the International Union of Pure and Applied Chemistry (IUPAC) has nominated flow chemistry as one of the top ten emerging technologies in chemistry with potential to make our planet more sustainable.[211] Compared to batch reactors which despite being versatile, easy to operate, and able to process most chemicals, are characterized by low surface/volume ratios, flow systems (referred to *plug flow* or *continuous flow*) offer a powerful alternative to improve the reaction efficiency by enhancing the mass and heat transfers and the overall control of the reaction parameters.[212] Particularly, over the past two decades, CF technologies have evolved to become a crucial for process intensification (PI) by substantially decreasing equipment size/production capacity ratio, energy consumption, or waste production, and ultimately resulting in cheaper, sustainable technologies.[213] Flow chemistry allows chemical reactions in a continuous manner within a well-defined micro- or mesometric environment. A continuous flow reactor is typically made up of narrow channels through which streams of chemicals are pumped and set to react for a definite time at a given temperature and pressure. The dimensions of flow reactors range from sub-millimetric (microfluidic reactors) to sub-centimetric (mesofluidic reactors).[214,215] These configurations usually enable to improve the reaction rates since reagents can be easily pressurized and heated above their normal boiling point (superheating);[216] even more generally, thanks to a quick variation of reaction conditions (T, p, flow rate, molar ratio, concentration, etc.), a rapid reaction optimization and scale-up can be achieved. Also, the product(s) isolation is facilitated in the case of catalytic processes since the catalyst is usually immobilized inside the reactor where, if necessary, it can be reactivated. Another unique aspect of flow systems compared to batch ones is the option to carry out multistep syntheses by designing a set-up comprised of several flow reactors. This last subject has been exhaustively reviewed elsewhere.[217] The small size of microreactors (less than 1 mm in at least one dimension) offers additional multiple advantages in minimizing the reagent consumption and energy waste, and in improving safety during handling of hazardous chemicals and/or the conduction of exothermic reactions.[218] Moreover, a virtually instantaneous mixing can be achieved in micro-structured devices.[219]

In recent years, many conventional batch plants have been replaced by continuous flow technologies as witnessed by the fact that the top 30 petrochemicals and most of the top 300 chemicals produced in the World are obtained through flow reactions that have proved to be more efficient and sustainable than batchwise counterparts.[220,221] Figure 1.13 shows the basic features of a typical CF-apparatus.[222]
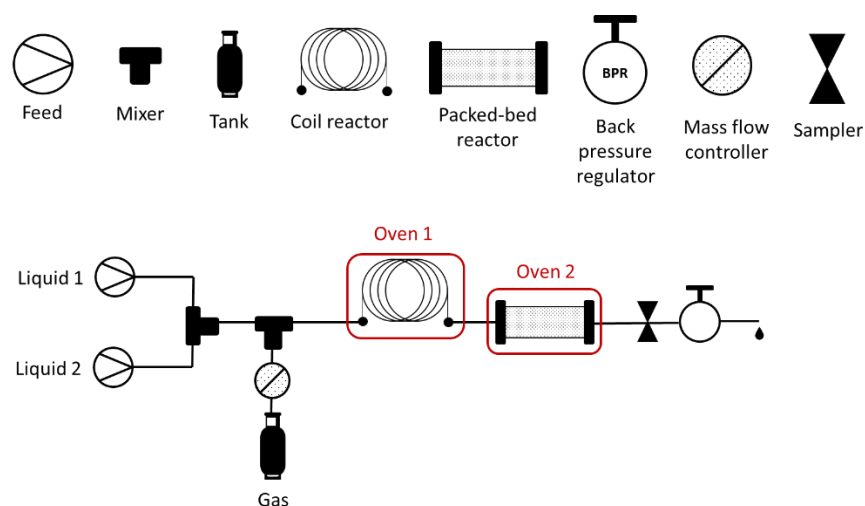
Figure 1.16. *Schematic chart of a continuous flow apparatus*

In a lab configuration, different kinds of pumps (HPLC, syringe, etc.) are used to deliver liquid reactants (or their solutions) at the desired flow rate, into the reactor. If gases are necessary, the relative amounts are set and checked by a mass-flow controller. Four main types of reactors can be employed:[212] i) continuous flow stirred tank reactors (CFSTR); ii) packed-bed reactors (PBR); iii) coil reactors (CR); and iv) chip reactors (ChR). CFSTR are the most conventional ones in which the reactants are continuously delivered and stirred at the desired conditions. A PBR is a tubular reactor filled with a catalytic bed where, very often, the active phase (metal, ionic liquid, etc.) is dispersed/grafted in/on a support (carbon, alumina, silica, etc.) or even a simple inert matrix (Raschig rings or sand).[223] CR are also tubular reactors, but in the form of coils with outer diameters of 1/8" - 1/16" and inner diameters >1mm. Microfluidic reactors belong to this subclass and they have proved to be well suited to catalyst-free high T/*p* applications, to photochemical reactions, and to processes where the catalyst is deposed at a molecular level. Finally, notwithstanding the significant cost, ChR systems offer extremely high surface-to-volume ratios and high accuracy in heat transfer. For instance, glass chip reactors are a thin pane of glass with a *micro*-channel in between, allowing for reagents to travel through. A CF-apparatus is then completed by a back-pressure regulator (BPR) which allows to operate at a constant upstream system pressure, and one or more samplers, often in the form of Rheodyne valves, to withdraw and analyze the products mixture without affecting the reactions conditions.

In this thesis, both PBR and CR reactors have been used using liquid and superheated reagents, and CO_2 in its supercritical state as a reagent/carrier.

1.4.2. Continuous reactions with supercritical CO_2 as a green solvent/carrier and reagent

The Gibbs' phase rule describes the physical state of a pure substance at thermodynamic equilibrium by three distinct phases (solid, liquid and gas) which are separated by coexistence curves and are a function of independent intensive variables. The liquid–vapor coexistence curve is not infinite, but it shows a maximum where at a certain T and p, the liquid and vapor are no longer two separate states, but becomes the extremes of the same continuum.[224] The critical point is the end of the liquid–vapor coexistence curve.[225] Above the critical point, *i.e.* at T and pressure above the critical values, the substance reaches its supercritical (sc) state. Table

1.4 compares average values of density, viscosity, and diffusivity for gases, liquids, and sc-phases.[226]

Table 1.4. Comparison of physical and transport properties of gases, SCFs and liquids

Property	Density (Kg·m⁻³)	Viscosity (cp)	Diffusivity (cm²·s⁻¹)
Gas	10^{-3}	10^{-3}-10^{-3}	10^{-1}
SCF	0.7	10^{-2}	10^{-3}
Liquid	1.0	10^{-1}	10^{-5}

A supercritical fluid (SCF) generally provides a more efficient heat and mass transfer with respect to liquids or gases, because of its intermediate values of density, viscosity and diffusivity which are higher and lower than the gas and the liquid, respectively. Moreover, the SCF properties may be modulated by small changes in the temperature and/or pressure, as well as by adding modifiers or co-solvents. A representative case is carbon dioxide that reaches its sc-state at T = 32 °C and p = 13.78 MPa. Figure 1.17 shows the dramatic variation of the density of CO_2 which, at 31 °C, is more than triplicated from ca 0.2 to above 0.6 g/mL when the pressure is slightly increased in the proximity of the sc-point. [227]
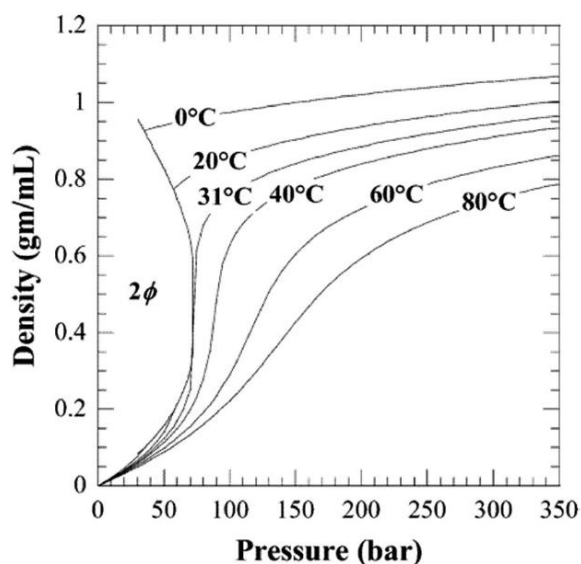
Figure 1.17. Carbon dioxide density as a function of pressure and temperature

In addition, compared to pure sc-CO_2, the presence of a co-solvent/modifier not only induces further variations of both the density and the viscosity, but also alters the dielectric constant and the solvency so that more and more polar substances can be dissolved in the sc-CO_2/modifier mixture. This effect can be observed by mixing CO_2 with a variety of hydrocarbons as *n*-hexane, heptane, pentane, toluene, and alcohols, most commonly methanol, ethanol, and isopropanol.[228]

Processes based on SCFs and particularly on scCO$_2$ are generally considered sustainable, environmentally friendly and cost efficient for a number of practically reasons: (i) CO_2 is inexpensive, abundant and easily available in pure form (food grade) worldwide; (ii) CO_2 is the simplest renewable C_1-feedstock; (iii) CO_2 is not flammable, nontoxic, and intrinsically eco-compatible; (iv) the critical point of CO_2 (7.38 MPa and 31 °C) is attained at near-ambient temperature and mild overpressures with a low energy demand. Another crucial advantage is the product separation/drying that can be achieved in a single step, simply by the

depressurization and expansion of CO_2. This last operation can be engineered to minimize the compression energy and optimize the gas recovery and recycle.

Among the most relevant continuous flow technologies based on sc-CO_2, a top position is occupied by the extraction of biomass and bio-based derived matrixes. Examples of commercial applications include the coffee bean decaffeination which was designed from the seminal work of Kurt Zosel in 1978, [229] the lycopene extraction from tomato skins which proceeds with yields up to 86% at T = 60 °C and $p(CO_2)$ = 300 bar [flow rates, $F(CO_2)$, between 0.16 and 0.41 g min^{-1}], [230] and the sc-CO_2 technology filed by KD-Pharma for the refining of fish oils and the extraction of long-chain ω-3 polyunsaturated fatty acids (PUFAs) as dietary supplements.[231]

Several other CF-applications have been reported using sc-CO_2 as a reagent or a carrier/solvent. An example described some years ago by the group with which this Thesis has been carried out, was the implementation of a CF-protocol for the metathesis of olefins. Scheme 1.17 provides a general description of the reaction by which the redistribution of substituents in reactant olefins takes place through the scission and regeneration of C-C double bonds.
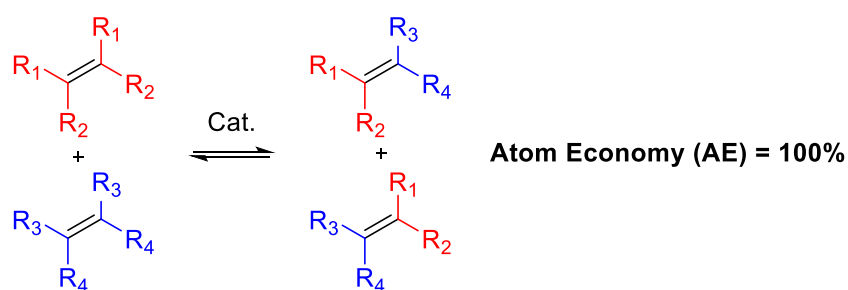
Scheme 1.17. *General reaction scheme for the metathesis of olefins*

The reaction is a powerful and elegant means of constructing complex carbon frameworks,[232] and it has become over time an established green, clean, and highly atom efficient transformation, characterized by low waste. Notably, Yves Chauvin, Robert Grubbs and Richard Schrock shared the 2005 Nobel Prize in Chemistry for their work on carbene complexes as catalysts for the olefin metathesis.[233,234,235] A comparative analysis of the self-metathesis of different α-olefins (1-hexene, 1-heptene, and 1-octene) catalysed by Re_2O_7 supported on γ-Al_2O_3 demonstrated that not only did the reaction occur efficiently and selectively in scCO_2 (90 bar, 35 °C), but it was even faster than in classic liquid media (*n*-heptane and toluene).[236] Moreover, in the CF-mode, the catalytic bed abruptly deactivated to become completely inefficient with *n*-hexane and toluene, while the reaction proceeded without changes in scCO_2. The improvement of the reaction outcome was correlated to the capability of scCO_2 to overcome the mass transfer limitations associated with heterogeneous catalysis in conventional liquid solvents.

The use of scCO_2 for continuous flow synthesis has been excellently reviewed by Poliakoff and Han who reported a variety of protocols of hydrogenation and oxidation reactions.[237] To cite some examples, Stevens *et al.* explored the potential of carrying out sequential reactions in separate but linked continuous flow reactors in scCO_2. By packing the two reactors with different catalysts and controlling the reactor temperatures separately no fewer than five different products (furfuryl and tetrahydrofurfuryl alcohols, methyl and tetrahydro methyl furan, and furan) could be obtained at T = 120-300 °C from a single feedstock (furfural) with high yields in the range 82-98%.[238] Bourne *et al.* reported γ-valerolactone product of the

hydrogenation of levulinic acid carried at 200 °C could be separated in >99% yield from the coproduced water by using the pressure of CO_2 already present inside the reactor.[239] A special case of sequential reaction was reported by Hyde *et al.*, who developed a procedure for hydrogenation reactions of several organic substrates (alkenes, ketones, and aldehydes) in which the supercritical fluid mixture (CO_2 and H_2) was generated by the catalytic decomposition of liquid formic acid, HCO_2H, over a preheated Pt catalyst bed.[240,241]

A novel and very recent method of continuous synthesis using supercritical carbon dioxide ($scCO_2$) has been introduced for the preparation of MOF (UiO-66 MOF) introduced through a custom counter-current mixer which provides enhanced heat and mass transfer.[242] The UiO-66 MOF was synthesized by continuously delivering the two precursors, $ZrOCl_2 \cdot 8H_2O$ (metal precursor) and terephthalic acid (organic precursor) dissolved in DMF, together with $scCO_2$. At T <130 °C, *p* = 100 bar with a reaction time > 3s, UiO-66 MOF was produced at a production rate of 104 g/h.

Notewprthy, Lozano *et al.* recently reported a clean chemo-enzymatic synthesis of omega-3 *mono*-acylglycerides was carried out in two consecutive catalytic steps in $scCO_2$. First, the enzymatic transesterification carried at 60 °C for 6h of raw fish or linseed oil with solketal for producing fatty acid solketal esters. Second, the hydrolysis of these solketal moieties catalysed by solid acids (*i.e.* zeolites) at 50 °C under continuous flow. By using $scCO_2$ as the reaction/extraction medium and *t*-butanol as a co-solvent, 100% *mono*-acylglyceride yield in seven days under continuous operation and without any loss in catalytic activity was achieved.[243]

1.5   Aim and summary of the thesis

This Thesis work was originally planned within a cotutelle agreement between the Università Ca' Foscari di Venezia and the University of Sydney (USyD), in the groups led by Prof. Maurizio Selva and Prof. Thomas Maschmeyer, respectively. Due to the covid-19 pandemic, the expected period abroad of the Author of this Thesis at the USyD was not possible and the related experimental work was converted in a remote collaboration finalized at the writing of a review paper on the synthesis and reactivity of enol esters, a subject of common interest of the involved groups. Part of the research activities of this PhD program, however, was carried at the Stockholm University in Sweden, under the supervision of Prof. Joseph Samec, where the chemical valorization of Kraft lignin was investigated.

Sustainable processes, the use of renewable feedstocks, continuous flow chemistry, and catalysis have been the main themes to which this work has been focused on. Particularly, the research program has been aimed to the following activities:

- The conceptualization and implementation of tandem protocols of esterification/amidation and acetalization, by exploiting the peculiar reactivity of isopropenyl esters (iPEs). Biobased substates as 1,2-diols, glycerol, and glycerol-derived aminodiols were employed for this purpose.
- A literature review on the synthesis and reactivity of isopropenyl esters (iPEs), with emphasis on the green chemistry-related aspects.
- The engineering of a lab scale microfluidic reactor for the continuous flow reaction of CO_2 insertion into terminal epoxides.

- The development of strategies of acetylation, aldol condensation, carboxymethylation, vinylation, and reductive amination for the upgrading of 5-hydroxymethyl furfural (HMF) as a furan bio-based representative substrate.
- The design of a two-step sustainable procedures for the preparation of moldable Kraft lignin-based polyesters.

1.5.1 Isopropenyl Esters (iPEs)-mediated tandem reactions

iPEs have been used to develop tandem reactions of esterification/amidation and acetalization. The iPEs-promoted transesterification reaction allows the formation of an ester and a prop-1-en-2-ol that quickly tautomerizes to the corresponding ketone (acetone), making the overall transformation irreversible. Scheme 1.18 shows the reaction of the lightest term of the iPEs series, isopropenyl acetate (iPAc), with a generic alcohol.[244]
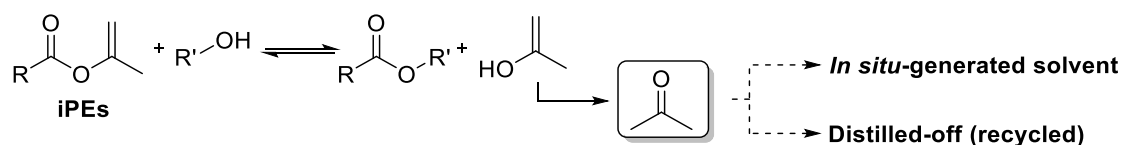
Scheme 1.18. *The reactivity of isopropenyl esters (iPEs) in esterification reactions*

Interestingly, the co-product acetone can be exploited *in-situ* to run additional reactions. This strategy has been implemented in this Thesis to design several types of tandem protocols where an esterification reaction carried out by iPAc was followed by an acetalization process promoted by the released acetone.

Tandem reactions of 1,2-diols with iPEs

An acid-catalyzed tandem sequence was investigated to upgrade renewable 1,2-diols such as propylene glycol (PG) and ethylene glycol (EG), with isopropenyl acetate. At 50 °C and in the presence of Amberlyst-15 as a catalyst, the reaction of both diols afforded a 1:1 mixture of acetates and acetal products with a 100% carbon efficiency, and the formation of water as the sole byproduct (Scheme 1.19, R=CH$_3$).
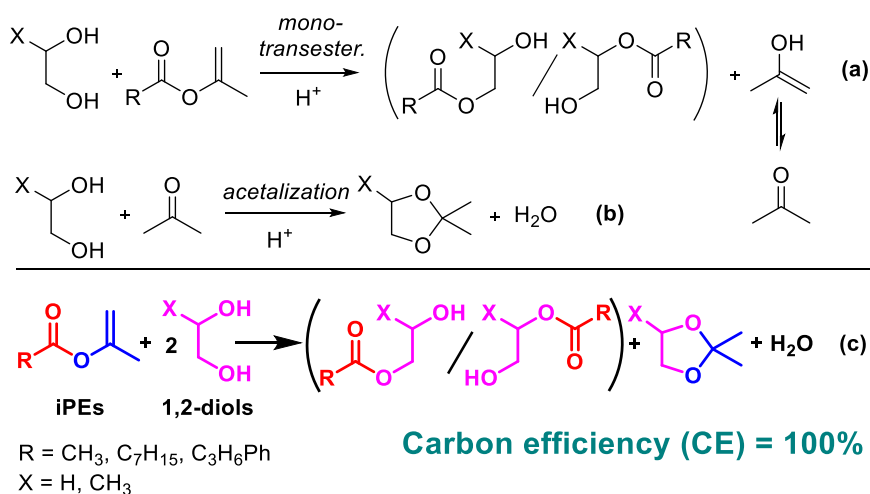
Scheme 1.19. *One-pot tandem acid catalyzed tandem transesterification/acetalization between 1,2-diols and iPEs*

The reaction scope was extended to higher homologues of enol esters as isopropenyl-octanoate and phenylbutyrate. Additionally, the tandem sequence was successfully transferred in the continuous-flow (CF) mode where the catalyst (Amberlyst-15) could be used virtually indefinitely without loss of performance, and the solvent (THF or CPME) was quantitatively recovered and reused. Under CF conditions, the reaction of PG with isopropenyl acetate could be run at 30 °C and atmospheric pressure with a productivity up to 9.7 mmol g_{cat}^{-1} h^{-1}, 3 times higher than that achieved in the batch mode. When ethylene glycol was used, a lower tandem selectivity was observed due to predominance of transesterification products, mono- and di-esters, over the acetal compound.

The results of this study have been reported in D. Rigo, G. Fiorani, A. Perosa, and M. Selva, *ACS Sustainable Chem. Eng.*, **2019**, *7*, 18810–18818.

Tandem reactions of glycerol with iPEs.

The protocol shown in Scheme 1.19 was further developed by replacing 1,2-diols with glycerol. In this case, the tandem sequence was implemented using a pool of innocuous reactants (isopropenyl acetate, acetic acid and acetone). The study provided evidence for the occurrence of multiple concomitant reactions: isopropenyl acetate acted as a transesterification agent to provide glyceryl esters, and it was concurrently subjected to an acidolysis reaction promoted by AcOH. Both these transformations co-generated acetone which converted glycerol into the corresponding acetals, while the acidolysis process sourced also acetic anhydride that acted as an acetylation reactant. Tuning the reaction conditions, mostly by changing the reactant molar ratio and optimizing the reaction time, the overall set of transformations was successfully steered towards the synthesis of either a 1 : 1 mixture of acetal acetates (97% of which was solketal acetate) and triacetin, or acetal acetates in up to 91% yield, at complete conversion of glycerol (Figure 1.18).
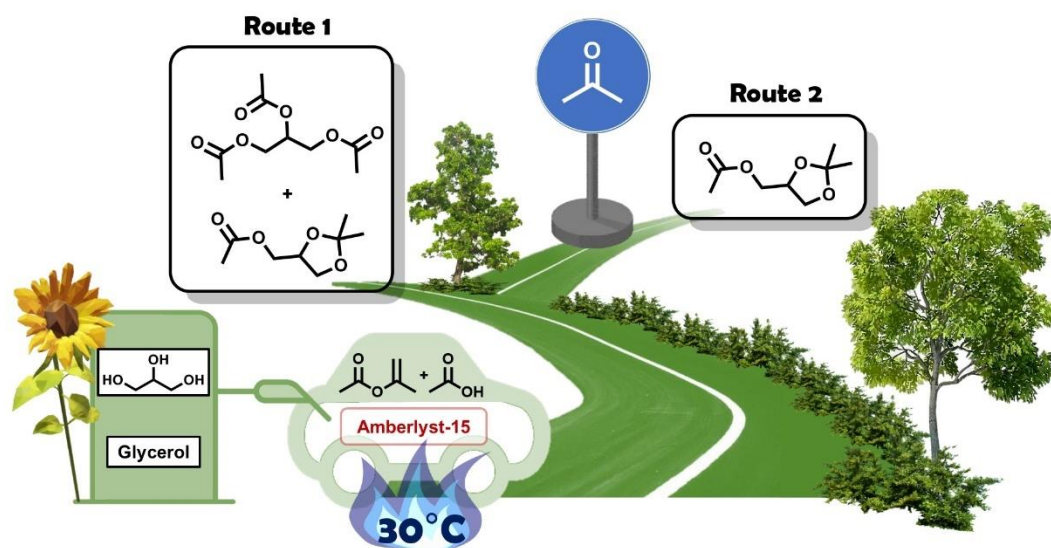
Figure 1.18. Tandem esterification/acetalization protocols for the valorization of glycerol

To the best of our knowledge, a one-pot protocol with such a degree of control on the functionalization of glycerol via transesterification and acetalization reactions had not been previously reported. The procedure was also easily reproduced on a gram scale, thereby proving its efficiency for preparative purposes. Finally, the design of experiments with

isotopically labelled reagents, particularly d_4-acetic acid and d_6-acetone, helped to estimate the contribution of different reaction partners (iPAc/AcOH/acetone) to the formation of final products.

The results of this study have been reported in D. Rigo, R. Calmanti, A. Perosa, and M. Selva, *Green Chem.*, **2020**, *22*, 5487-5496.

The upgrading of glycerol-derived aminodiols with iPEs.

An unprecedented two-step sequence was designed in this Thesis work, by combining batch and continuous flow (CF) protocols for the conversion of two aminodiol regioisomers derived from glycerol, i.e., 3-amino-1,2-propanediol and 2-amino-1,3-propanediol (serinol) using sequentially both iPAc and acetone. Under batch conditions, at 80–90 °C, both substrates were quantitatively transformed into the corresponding amides through a catalyst-free N-acetylation reaction mediated by isopropenyl acetate (iPAc). Thereafter, at 30–100 °C and 1–10 atm, the amide derivatives underwent a selective CF-acetalization in the presence of acetone and a solid acid catalyst, to afford the double-functionalized (amideacetal) products (Figure 1.19).
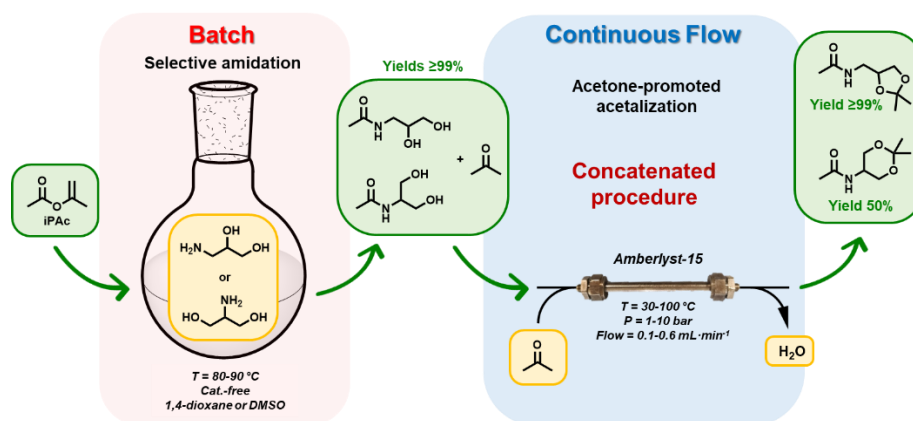
Figure 1.19. *Concatenated batch and continuous flow (CF) procedure for the upgrading of glycerol-derived aminodiols*

The results of this study have been reported in D. Rigo, N. A. C. dos Santos, A. Perosa and M. Selva, *Catalysts*, **2021**, *11*, 21-33.

1.5.2 Isopropenyl Esters (iPEs) in green organic synthesis

In (remote) collaboration with the group of Prof. Maschmeyer at the University of Sydney, the use of isopropenyl esters (IPEs) has been reviewed by focusing the attention on green synthetic applications.

iPEs are a class of enol esters (EEs), characterized by the presence of a methyl substituted vinyl group adjacent to an ester functionality (Scheme 1.20).
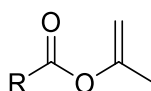
Scheme 1.20. *General iPEs structure (R= alkyl, aryl)*

These polyfunctional compounds can be used in a range of applications in both organic synthesis and material science, with a major interest as intermediates for the preparation of antibiotics and steroids,[245,246,247] building blocks for polymer synthesis in emulsion phase

coatings,[248] and acylating agents in presence of alcohols and amines.[249,250,251] Details of the review study will be discussed in the chapter 2 of this Thesis with emphasis on sustainability-related aspects of irreversible transesterification processes mediated by iPEs. A review article on this subject is currently under preparation and its submission for publication is expected by the end of this year.

1.5.3 CO_2 insertion into terminal epoxides

The insertion reaction of CO_2 on terminal epoxides (styrene oxide, 1,2-epoxyhexane and butyl glycidyl ether) to obtain the corresponding cyclic organic carbonate products (COCs), was performed in a binary homogeneous mixture comprising of NaBr as the nucleophilic catalyst and diethylene glycol (DEG) as both solvent and catalyst activator (cation coordinating agent). The reaction was studied initially under batch conditions (autoclave) at T = 100 °C and $p_0(CO_2)$ = 1 - 40 bar, and then transferred to continuous-flow (CF) mode. The effects of the reaction parameters (T, $p(CO_2)$, catalyst loading, and flow rates) were studied using microfluidic reactors of capacities variable from $7.85 \cdot 10^{-2}$ to 0.157 cm^3, by which a remarkable improvement of the productivity was achieved. For the model case of 1,2-epoxyhexane, the rate of formation of the corresponding carbonate, 4-butyl-1,3-dioxolan-2-one, was increased up to 27.6 mmol h^{-1} equiv^{-1}, a value 2.5 higher than in the batch mode. Under CF-conditions, the catalyst (NaBr/DEG) was recycled through a semi-continuous extraction procedure and reused without loss of performance for at least 4 subsequent CF-tests (Figure 1.20)
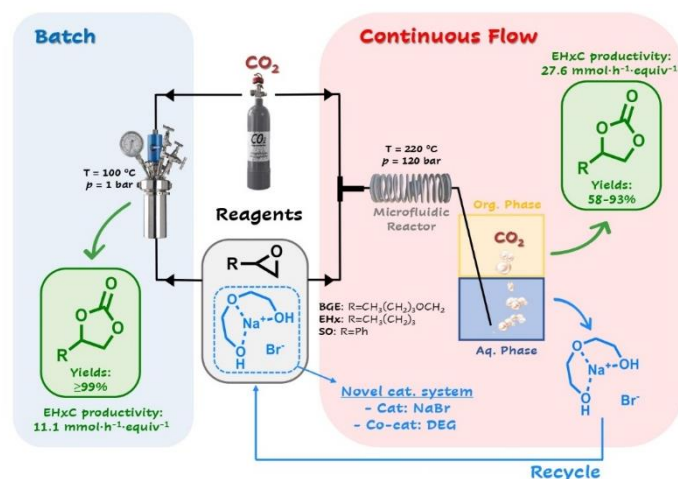
Figure 1.20. *Batch and continuous flow (CF) CO2 insertion into terminal epoxides*

The results of this study have been reported in D. Rigo, R. Calmanti, A. Perosa, M. Selva, and G. Fiorani, *ChemCatChem*, **2021**, *13*, 2005–2016.

1.5.4   Diversified routes for the chemical upgrading of 5-hydroxymethylfurfural (HMF)

Multiple sustainable methodologies were developed for the chemical upgrading of HMF: i) at 30-90 °C, highly selective base-catalyzed acetylation and carboxymethylation reactions of HMF with nontoxic reagents as isopropenyl acetate (iPAc) and dimethyl carbonate (DMC) were achieved to prepare the corresponding ester and carbonate products, (5-formylfuran-2-yl) methyl acetate (5-formylfuran-2-yl) methyl carbonate, respectively; ii) based on the combined use of iPAc with acetone or DMC, a tandem protocol of acetylation/(or transcarbonation) and aldol condensation was designed to synthesize a variety of HMF-derived α,β-unsaturated

carbonyl compounds; iii) in water as a solvent, a chemoselective Pd-catalysed reductive amination of HMF with amino-alcohols also including glycerol derivatives, was developed using H_2 at atmospheric pressure; iv) finally, both HMF and its ester and carbonate products successfully underwent Wittig vinylation reactions promoted by a methyl carbonate phosphonium salt ($[Ph_3PCH_3][CH_3OCO_2]$), to obtain the corresponding olefins. The vinylation reagent (the salt) was a DMC derivative. In all cases i-iv), not only processes occurred under mild conditions, but post-reaction procedures (work-up and purification) were optimized to isolate final products in high yields of 85-98%. Figure 1.21 summarizes the work.
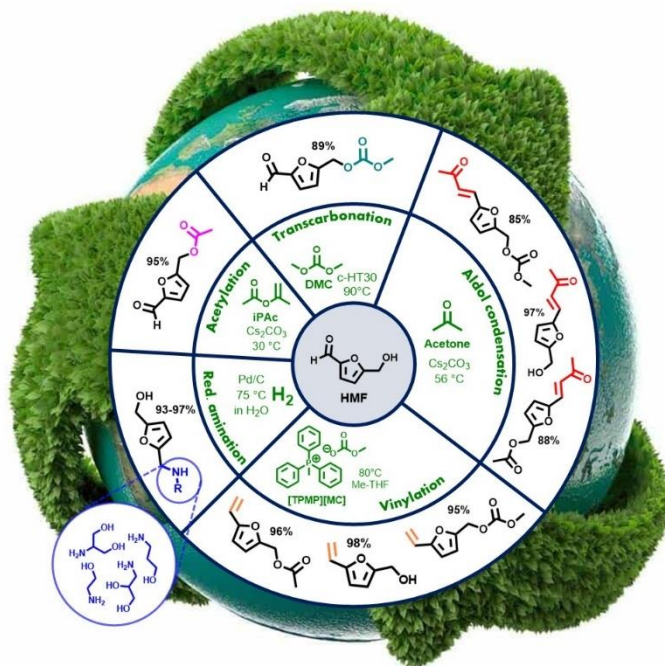
Figure 1.21. Diversified routes for the chemical upgrading of HMF

The results of this study have been reported in D. Rigo, D. Polidoro, A. Perosa, and M. Selva, *Mol. Cat.*, **2021**, *514*, 111838-111848.

1.5.5 A new family of renewable thermosets: Kraft lignin polyadipates

The last part of this PhD Thesis was carried out at the Stockholm University under the supervision of Prof. Joseph Samec.

Thermosetting polymeric materials (thermosets) have advantageous properties and are therefore used in numerous applications. In this study, we hypothesized and ultimately showed that thermosets could be derived from comparably sustainable sub-components. A two-step procedure to produce a thermoset comprising Kraft lignin (KL) and the cross-linker adipic acid (AdA) was developed. The cross-linking was activated by means of an acetylating agent comprising isopropenyl acetate (IPA) to form a crosslinking mixture (CLM). The crosslinking was confirmed by FT-IR and solid-state NMR, and the esterification reactions were further studied using model compounds. The mechanical properties of the resulting materials were evaluated. When the KL lignin powder was mixed with the CLM, partial esterification occurred to yield a homogeneous viscous liquid that could easily be poured into a mold, as the first step in the procedure. Without any additions, the mold was then heated and the material transformed into a thermoset by reaction of the two carboxylic acid derivatives of AdA and KL in the second

step. Thus, a thermoset material that merely contained KL and AdA was formed. This study shows that thermosets of KL can be made with control of the crosslinking event.
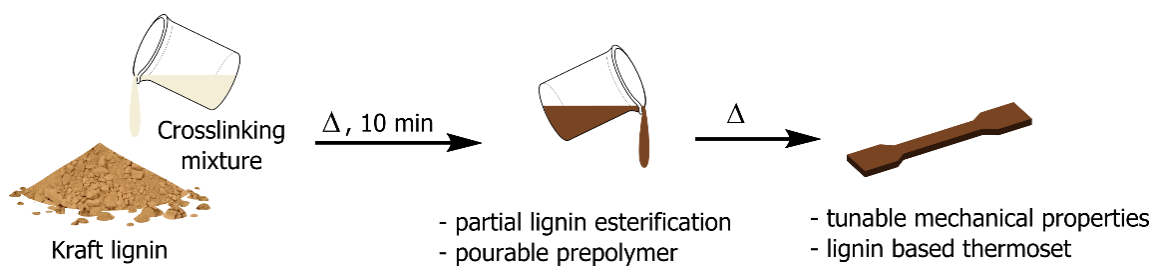

Figure 1.22. *Kraft lignin, a by-product from the paper and pulp industry is converted into a mouldable thermoplastic that can be further converted into a tunable thermoset without any additives*

The results of this study are the object of a manuscript which has been submitted for publication in *GreenChem*.

References

[1] D. Stanujkic, G. Popovic, E. K: Zavadskas, D. Karabasevic, and A. Binkyte-Veliene, Assessment of Progress towards Achieving Sustainable Development Goals of the "Agenda 2030" by Using the CoCoSo and the Shannon Entropy Methods: The Case of the EU Countries, *Sustainability,* **2020**, *12*, 5717. https://doi.org/10.3390/su12145717

[2] J. B. Zimmerman, P. T. Anastas, H. C. Erythropel, and W. Leitner, Designing for a green chemistry future, *Science*, 2020, *367*, 397. https://doi.org/10.1126/science.aay3060

[3] Global Bio-based Chemicals Market | Trends, Share, Analysis 2019-2027. Available at: https://www.inkwoodresearch.com/reports/bio-based-chemicals-market/ (accessed: 08/11/2021).

[4] S. Piotrowski, M. Carus, and D. Carrez, European bioeconomy in figures, *Ind. Biotechnol.,* **2016***, 12*, 78. https://doi.org/10.1089/ind.2016.29030.spi

[5] *Map of 224 European biorefineries published by BIC and nova-Institute* (nova-Institut GmbH; Bio-based Industries Consortium, 2017).

[6] Parisi, C., Biorefineries distribution in the EU, Publications Office of the European Union, Luxembourg, 2018, ISBN 978-92-79-94883-1, doi:10.2760/119467, JRC113216

[7] https://www.danfoss.com/en/service-and-support/case-stories/dds/full-scale-biogas-plant-in-kalundborg-ensures-the-return-of-all-nutrients-back-to-nature/ (accessed 18/08/2021)

[8] https://www.cropenergies.com/en/company/locations/wanze (accessed 18/08/2021)

[9] https://www.sekab.com/en/this-is-how-it-works/biorefinery-demo-plant/ (accessed 18/08/2021)

[10] https://www.storaenso.com/en/products (accessed 18/08/2021)

[11] Hassan, S. S., Williams, G. A. & Jaiswal, A. K., Lignocellulosic Biorefineries in Europe: Current State and Prospects, *Trends in Biotechnology,* **2019***, 37*, 231. https://doi.org/10.1016/j.tibtech.2018.07.002

[12] https://www.kvk.nl/english/ban-on-single-use-plastics/ (accessed 18/08/2021)

[13] https://www.eea.europa.eu/data-and-maps/indicators/overview-of-the-electricity-production-3/assessment-1 (accessed 18/08/2021)

[14] https://www.eia.gov/energyexplained/ (accessed 28/08/2021)

[15] https://www.ipcc.ch/report/2019-refinement-to-the-2006-ipcc-guidelines-for-national-greenhouse-gas-inventories/ (accessed 28/08/2021)

[16] R.A. Houghton, *Biomass* in Encyclopedia of Ecology, 2008.

[17] H. J. Huang, S. Ramaswamy, U. W. Tschirner, and B. V. Ramarao, A review of separation technologies in current and future biorefineries. Separation and Purification Technology, *Sep. Purif. Tech.,* **2008**, *62*, 1. https://doi.org/10.1016/j.seppur.2007.12.011

[18] I. Kogel-Knabner, The macromolecular organic composition of plant and microbial residues as inputs to soil organic matter, *Soil Biol. Biochem.*, **2002**, *34*, 139. https://doi.org/10.1016/S0038-0717(01)00158-4

[19] A. Corma, S. Iborra, and A. Velty, Chemical routes for the transformation of biomass into chemicals, *Chem. Rev.,* **2007**, *107*, 2411. https://doi.org/10.1021/cr050989d

[20] G. Koch, Raw material for pulp. In Handbook of pulp; John Wiley & Sons, Ltd, 2008; pp 21-68.

[21] Z. li, J. Zhang, L. Qin, and Y. Ge, Enhancing antioxidant performance of lignin by enzymatic treatment with laccase, *ACS Sust. Chem. Eng.*, **2018**, *6*, 2591. https://doi.org/10.1021/acssuschemeng.7b04070

[22] J. N. Putro, F. E. Soetaredjo, S.-Y. Lin, Y.-H. Ju, and S. Ismadji, Pretreatment and conversion of lignocellulose biomass into valuable chemicals, *RSC Adv.*, **2016**, *6*, 46834. https://doi.org/10.1039/C6RA09851G

[23] P. F. H. Harmsen, W. Huijgen, L. Bermudez, and R. Bakker *Literature review of physical and chemical pretreatment processes for lignocellulosic biomass*; Wageningen UR - Food & Bio-based Research: Wageningen, 2010.

[24] W. C. Lam, T. H. Kwan, V. L. Budarin, E. B. Mubofu, J. Fan, and C. S. K. Lin, Pretreatment and Thermochemical and Biological Processing of Biomass, in Introduction to Chemicals from Biomass, Second Edition (eds J. Clark and F. Deswarte), John Wiley & Sons, Ltd, Chichester, UK, 2015.

[25] L. D. Gottumukkala, K. Haigh, and J. Görgens, Trends and advances in conversion of lignocellulosic biomass to biobutanol: microbes, bioprocesses and industrial viability, *Renew. Sust. Energ. Rev.*, **2017**, *76*, 963. https://doi.org/10.1016/j.rser.2017.03.030

[26] https://www.bio.org/sites/default/files/files/beta%20renewables%20proesa%20technology%20june%202013_bio_michele_rubino.pdf (accessed 29/09/2021).

[27] (a) D. A. Cantero, M. D. Bermejo and M. J. Cocero, Governing chemistry of cellulose hydrolysis in supercritical water, *ChemSusChem*, **2015**, *8*, 1026. https://doi.org/10.1002/cssc.201403385; (b) A. Ghosh, R. C. Brown, and X. Bai, Production of solubilized carbohydrate from cellulose using non-catalytic, supercritical depolymerization in polar aprotic solvents, *Green Chem*., **2016**, *18*, 1023. https://doi.org/10.1039/C5GC02071A

[28] J. Q. Bond, D. M. Alonso, D. Wang, R. M. West, and J. A. Dumesic, Integrated catalytic conversion of γ-valerolactone to liquid alkenes for transportation fuels, *Science*, **2010**, *327*, 1110. https://doi.org/10.1126/science.1184362

[29] J. S. Luterbacher, J. M. Rand, D. M. Alonso, J. Han, J. T. Youngquist, C. T. Maravelias, B. F. Pfleger, and J. A. Dumesic, Nonenzymatic sugar production from biomass using biomass-derived γ-valerolactone, *Science*, **2014**, *343*, 277. https://doi.org/10.1126/science.1246748

[30] F. Jérôme, G. Chatel, and K. De Oliveira Vigier, Depolymerization of cellulose to processable glucans by non-thermal technologies, *Green Chem.*, **2016**, *18*, 3903. https://doi.org/10.1039/C6GC00814C

[31] (a) J. B. Binder, and R. T. Raines, Fermentable sugars by chemical hydrolysis of biomass, *Proc. Natl. Acad. Sci. U.S.A.*, **2010**, *107*, 4516. https://doi.org/10.1073/pnas.0912073107; (b) C. G. Yoo, Y. Pu, and A. J. Ragauskas, Ionic liquids: Promising green solvents for lignocellulosic biomass utilization, *Current Opinion in Green and Sustainable Chemistry*, **2017**, *5*, 5. https://doi.org/10.1016/j.cogsc.2017.03.003

[32] R. G. Blair, K. Chagoya, S. Biltek, S. Jackson, A. Sinclair, A. Taraboletti and D. Restrepo, The scalability in the mechanochemical syntheses of edge functionalized graphene materials and biomass-derived chemicals, *Faraday Discuss.*, **2014**, *170*, 223. https://doi.org/10.1039/C4FD00007B

[33] N. Meine, R. Rinaldi and F. Schüth, Solvent-free catalytic depolymerization of cellulose to water-soluble oligosaccharides, *ChemSusChem*, **2012**, *5*, 1449. https://doi.org/10.1002/cssc.201100770

[34] C. J. Biernmann, Handbook of Pulping and Papermaking, Elsevier, 1996.

[35] H. Sixta, A. Potthast and A. W. Krotschek, Chemical pulping processe: sections 4.1-4.2.5 in Handbook of Pulp, John Wiley & Sons, Ltd, 2008; pp 109-229.

[36] P. Fatehi and Y. Ni, *ACS Symposium Series*, vol. 1067, Chapter 16, pp 409-441

[37] A. Johansson, O. Aaltonen, and P. Ylinen, Organosolv pulping-methods and pulp properties, *Biomass*, **1987**, *13*, 45. https://doi.org/10.1016/0144-4565(87)90071-0

[38] M. Ragnar, G. Henriksson, M. E. Lindström, M. Wimby, J. Blechschmidt, and S. Heinemann, Pulp. In *Ullmann's Encyclopedia of Industrial Chemistry*, 2014; pp 1–92.

[39] M. M. Abu-Omar, K. Barta, G. T. Beckham, J. S. Luterbacher, J. Ralph, R. Rinaldi, Y. Román-Leshkov, J. S. M. Samec, B. F. Sels and Feng Wang, Guidelines for performing lignin-first biorefining, *Energy Environ. Sci.*, **2021**, *14*, 262. https://doi.org/10.1039/D0EE02870C

[40] M. V. Galkin and J. S. M. Samec, Selective route to 2-propenyl aryls directly from wood by a tandem organosolv and palladium-catalysed transfer hydrogenolysis, *Chemsuschem*, **2014**, *7*, 2154. https://doi.org/10.1002/cssc.201402017

[41] https://sels-group.eu/demonstration-of-lignin-first-technology-at-pilot-scale-1 (accessed 22/09/2021)

[42] D. di Francesco, C. Dahlstrand, J. Löfstedt, A. Orebom, J. Verendel, C. Carrick, Å. Håkansson, S. Eriksson, H. Rådberg, H. Wallmo, M. Wimby, F. Huber, C. Federsel, M. Backmark, and J. S. M. Samec, Debottlenecking a Pulp Mill by Producing Biofuels from Black Liquor in Three Steps, *ChemSusChem*, **2021**, *14*, 2414. https://doi.org/10.1002/cssc.202100496

[43] E. Subbotina , T. Rukkijakan, M. D. Marquez-Medina, X. Yu, M. Johnsson, and J. S. M. Samec , Oxidative cleavage of C–C bonds in lignin, *Nature Chem.*, **2021**, *13*, 1118. https://doi.org/10.1038/s41557-021-00783-2

[44] T. Werpy, and G. Petersen, Top Value Added Chemicals From Biomass Volume I: Results of Screening for Potential Candidates from Sugars and Synthesis Gas in *National Renewable Energy Lab.*, Golden, CO (US), 2004.

[45] James F. White, Top Value-Added Chemicals from Biomass Volume II—Results of Screening for Potential Candidates from Biorefinery Lignin in *Pacific Northwest National Lab. (PNNL),* Richland, WA (US), 2007.

[46] J. J. Bozell, and G. R. Petersen, Technology development for the production of biobased products from biorefinery carbohydrates—the US Department of Energy's "Top 10" revisited, *Green Chem.,* **2010***, 12*, 539. https://doi.org/10.1039/B922014C

[47] T. J. Farmer, M. Mascal in Introduction to Chemicals from Biomass, 2nd ed. (Eds.: J. Clark, F. Deswarte), Wiley, Chichester, 2015.

[48] P. Kumar, D.M. Barrett, M.J. Delwiche, and P. Stroeve, Methods for pretreatment of lignocellulosic biomass for efficient hydrolysis and biofuel production, *Ind. Eng. Chem. Res.,* **2009**, *48*, 3713. https://doi.org/10.1021/ie801542g

[49] Y. Román-Leshkov, M. Moliner, J.A. Labinger, and M.E. Davis, Mechanism of glucose isomerization using a solid Lewis acid catalyst in water, *Angew. Chem.,* **2010**, *49*, 8954. https://doi.org/10.1002/ange.201004689

[50] A.S. Amarasekara, L.D. Williams, and C.C. Ebede, Mechanism of the dehydration of d-fructose to 5-hydroxymethylfurfural in dimethyl sulfoxide at 150 C: an NMR study, *Carbohyd. Res.,* **2008**, *343*, 3021. https://doi.org/10.1016/j.carres.2008.09.008

[51] M. Azzam, Pretreatment of cane bagasse with alkaline hydrogen peroxide for enzymatic hydrolysis of cellulose and ethanol fermentation, *J. Environ. Sci. Health B,* **1989**, *24*, 421. https://doi.org/10.1080/03601238909372658

[52] P.K. Rout, A.D. Nannaware, O. Prakash, A. Kalra, and R. Rajasekharan, Synthesis of hydroxymethylfurfural from cellulose using green processes: A promising biochemical and biofuel feedstock, *Chem. Eng. Sci.,* **2016**, *142*, 318. https://doi.org/10.1016/j.ces.2015.12.002

[53] R. M. Abdilla-Santes, W. Guo, P. C. Bruijnincx, J. Yue, P. J. Deuss, and H. J. Heeres, High-Yield 5-Hydroxymethylfurfural Synthesis from Crude Sugar Beet Juice in a Biphasic Microreactor, *ChemSusChem,* **2019**, *12*, 4304. https://doi.org/10.1002/cssc.201901115

[54] R. van Putten, J. C. van der Waal, E. de Jong, C. B. Rasrendra, H. J. Heeres, and J. G. de Vries, Hydroxymethylfurfural, a versatile platform chemical made from renewable resources, *Chem. Rev.*, **2013**, *113*, 1499. https://doi.org/10.1021/cr300182k

[55] Tang, X. Guo, L. Zhu, and C. Hu, Mechanistic Study of Glucose-to-Fructose Isomerization in Water Catalyzed by [Al(OH)2(aq)], *ACS Catal.*, **2015**, *5*, 5097. https://doi.org/10.1021/acscatal.5b01237

[56] S.H. Mushrif, J.J. Varghese, and D.G. Vlachos, Insights into the Cr (III) catalyzed isomerization mechanism of glucose to fructose in the presence of water using ab initio molecular dynamics, *Phys. Chem. Chem. Phys.*, **2014**, *16*, 19564. https://doi.org/10.1039/C4CP02095B

[57] H. Nguyen, V. Nikolakis, and D.G. Vlachos, Mechanistic insights into Lewis acid metal salt-catalyzed glucose chemistry in aqueous solution, *ACS Catal.*, **2016**, *6*, 1497. https://doi.org/10.1021/acscatal.5b02698

[58] Z. Shen, L. Kong, W. Zhang, M. Gu, M. Xia, X. Zhoub, Y. Zhang, Surface amino-functionalization of Sn-Beta zeolite catalyst for lactic acid production from glucose, *RSC Adv.*, **2019**, *9*, 18989. https://doi.org/10.1039/C9RA01264H

[59] J. G. de Vries, Green syntheses of heterocycles of industrial importance. 5-hydroxymethylfurfural as a platform chemical, *Adv. Heterocycl. Chem.*, **2016**, *121,* 247. https://doi.org/10.1016/bs.aihch.2016.09.001

[60] Q. Cao, X. Guo, S. Yao, J. Guan, X. Wang, X. Mu, and D. Zhang, Conversion of hexose into 5-hydroxymethylfurfural in imidazolium ionic liquids with and without a catalyst, *Carbohydr. Res*. **2011**, *346*, 956. https://doi.org/10.1016/j.carres.2011.03.015

[61] (a) I.K.M. Yu, D.C.W. Tsang, Conversion of biomass to hydroxymethylfurfural: A review of catalytic systems and underlying mechanisms, *Bioresour. Technol.,* **2017**, *238*, 716. https://doi.org/10.1016/j.biortech.2017.04.026; (b) M. Moreno-Recio, J. Santamaría-González, P. Maireles-Torres, Brönsted and Lewis acid ZSM-5 zeolites for the catalytic dehydration of glucose into 5-hydroxymethylfurfural, *Chem. Eng. J.*, **2016**, *303*, 22. https://doi.org/10.1016/j.cej.2016.05.120; (c) K. I. Galkin, E. A. Krivodaeva, V. P. Ananikov, A catalytic system for the selective conversion of cellulose to 5-hydroxymethylfurfural under mild conditions, *Russ. Chem. Bull. Int. Ed.,* **2015**, *64*, 2954. https://doi.org/10.1007/s11172-015-1253-3

[62] S. Hu, Z. Zhang, Y. Zhou, B. Han, H. Fan, W. Li, J. Song, Y. Xie, Conversion of fructose to 5-hydroxymethylfurfural using ionic liquids prepared from renewable materials, *Green Chem*. **2008**, *10*, 1280. https://doi.org/10.1039/B810392E

[63] B. Saha, M. M. Abu-Omar, Advances in 5-hydroxymethylfurfural production from biomass in biphasic solvents, *Green Chem*. **2014**, *16*, 24. https://doi.org/10.1039/C3GC41324A

[64] M. Sayed, N. Warlin, C. Hulteberg, I. Munslow, S. Lundmark, O. Pajalic, P. Tunå, B. Zhang, S.-H. Pyo, R. Hatti-Kaul, 5-Hydroxymethylfurfural from fructose: an efficient continuous process in a water-dimethyl carbonate biphasic system with high yield product recovery, *Green Chem*., **2020**, *22*, 5402. https://doi.org/10.1039/D0GC01422B

[65] X. Sun, Z. Liu, Z. Xue, Y. Zhanga, T. Mu, Extraction of 5-HMF from the conversion of glucose in ionic liquid [Bmim] Cl by compressed carbon dioxide, *Green Chem*. **2015**, *17*, 2719. https://doi.org/10.1039/C5GC00092K

[66] C. Shi, J. Xin, X. Liu, X.-G. Lu, S. Zhang, Activated carbon-coated carbon nanotubes for energy storage in supercapacitors and capacitive water purification, *ACS Sustainable Chem. Eng.* **2016**, *4*, 557. https://doi.org/10.1021/sc500118r

[67] K.I. Galkin, E.A. Krivodaeva, L.V. Romashov, S.S. Zalesskiy, V.V. Kachala, J.V. Burykina, V.P. Ananikov, Critical influence of 5-hydroxymethylfurfural aging and decomposition on the utility of biomass conversion in organic synthesis, *Angew. Chem.*, **2016**, *55*, 8338. https://doi.org/10.1002/ange.201602883

[68] T. Shalumova, J. M. Tanski, 5-(Hydroxymethyl) furan-2-carbaldehyde, *Acta Crystallogr. Sect. E,* **2010**, *66*, 2266. https://doi.org/10.1107/S1600536810031119

[69] R. J. Van Putten, J. C. Van Der Waal, E. De Jong, C. B. Rasrendra, H. J. Heeres and J. G. De Vries, Hydroxymethylfurfural, a versatile platform chemical made from renewable resources, *Chem. Rev.*, **2013**, *113*, 1499. https://doi.org/10.1021/cr300182k

[70] A. A. Rosatella, S. P. Simeonov, R. F. M. Frade, and C. A. M. Afonso, 5-Hydroxymethylfurfural (HMF) as a building block platform: Biological properties, synthesis and synthetic applications, *Green Chem.*, **2011**, *13*, 754. https://doi.org/10.1039/C0GC00401D

[71] F. A. Kucherov, L. V. Romashov, K. I. Galkin and V. P. Ananikov, Chemical transformations of biomass-derived C6-furanic platform chemicals for sustainable energy research, materials science, and synthetic building blocks, *ACS Sustain. Chem. Eng.*, **2018**, *6*, 8064. https://doi.org/10.1021/acssuschemeng.8b00971

72 X. Zhang, K. Wilson, and A. F. Lee, Heterogeneously Catalyzed Hydrothermal Processing of C5–C6 Sugars, *Chem. Rev.*, **2016**, *116*, 12328. https://doi.org/10.1021/acs.chemrev.6b00311

73 K. Gupta, R. K. Rai, and S. K. Singh, Metal catalysts for the efficient transformation of biomass-derived HMF and furfural to value added chemicals, *ChemCatChem*, **2018**, *10*, 2326. https://doi.org/10.1002/cctc.201701754

74 V. M. Chernyshev, O. A. Kravchenko, and V. P. Ananikov, Conversion of plant biomass to furan derivatives and sustainable access to the new generation of polymers, functional materials and fuels, *Russ. Chem. Rev.* **2017**, *86* 357. https://doi.org/ 10.1070/RCR4700

75 E.S. Kang, Y.W. Hong, D.W. Chae, B. Kim, B. Kim, Y.J. Kim, J.K. Cho, Y.G. Kim, From lignocellulosic biomass to furans via 5-acetoxymethylfurfural as an alternative to 5-hydroxymethylfurfural, *ChemSusChem*, **2015**, *8*, 1179. https://doi.org/10.1002/cssc.201403252

76 J.A.S. Coelho, A.F. Trindade, V. Andr´e, M.Teresa Duarte, L.F. Veiros, C.A. M. Afonso, Trienamines derived from 5-substituted furfurals: remote ε-functionalization of 2, 4-dienals, *Org. Biomol. Chem.*, **2014**, *12*, 9324. https://doi.org/10.1039/C4OB01759E

77 D. Koszelewski, R. Ostaszewski, The studies on chemoselective promiscuous activity of hydrolases on acylals transformations, *Bioorg. Chem.*, **2019**, *93*, 102825. https://doi.org/10.1016/j.bioorg.2019.02.050

78 M. Sheykhan, H.F. Moafi, M. Abbasnia, Novel access to carbonyl and acetylated compounds: the role of the tetra-n-butylammonium bromide/sodium nitrite catalyst, *RSC Adv*, **2016**, *6*, 51347. https://doi.org/10.1039/C6RA08672A

79 M. Krystof, M. P´erez-S´anchez, P. Domínguez De María, Lipase-Catalyzed (Trans) esterification of 5-Hydroxy-methylfurfural and Separation from HMF Esters using Deep-Eutectic Solvents, *ChemSusChem,* **2013**, *6*, 630. https://doi.org/10.1002/cssc.201200931

80 L. Wiermans, S. Hofzumahaus, C. Schotten, L. Weigand, M. Schallmey, A. Schallmey, P.D. De María, Transesterifications and Peracid-Assisted Oxidations in Aqueous Media Catalyzed by Mycobacterium smegmatis Acyl Transferase, *ChemCatChem*, **2013**, *5*, 3719. https://doi.org/10.1002/cctc.201300683

81 van Berkel, J. G. Process for enhancing the molecular weight of a polyester by solid state polymerization. WO2017043974A1, 2017.

82 https://www.coca-colacompany.com/news/100-percent-plant-based-plastic-bottle (accessed 26/10/2021)

83 J. Dai, S. Ma, N. Teng, X. Dai, X. Shen, S. Wang, X. Liu, J. Zhu, 2, 5-furandicarboxylic acid-and itaconic acid-derived fully biobased unsaturated polyesters and their cross-linked networks, *Ind. Eng. Chem. Res.,* **2017**, *56*, 2650. https://doi.org/10.1021/acs.iecr.7b00049

84 Howard, S. J.; Stensrud, K. Oligomers of fdca and glycols from a one-pot esterification-transesterification process using water-tolerant metal triflate catalyst. WO2017091412A1, 2017.

85 Hagberg, E.; Howard, S. J.; Stensrud, K. Oligomerizations of fdca and glycols in a one-pot esterification-transesterification process catalyzed by homogeneous organometallic lewis acids. WO2017091435A1, 2017

86 E. de Jong, M. A. Dam, L. Sipos, J. G. Gruter, in *Biobased Monomers, Polymers*, and materials, ed. Patrick B. Smith and Richard A. Gross, American Chemical Society, Washington D. C., 1st edn, 2012, ch. 1, pp 1-13.

87 D. Zhao, D. Rodriguez-Padron, R. Luque, C. Len, Insights into the selective oxidation of 5-hydroxymethylfurfural to 5-hydroxymethyl-2-furancarboxylic acid using silver oxide, *ACS Sustainable Chem.Eng.*, **2020***, 8*, 8486. https://doi.org/10.1021/acssuschemeng.9b07170

88 B. Donoeva, N. Masoud, P. E. de Jongh, Carbon support surface effects in the gold-catalyzed oxidation of 5-hydroxymethylfurfural, *ACS Catal.*, **2017**, *7*, 4581. https://doi.org/10.1021/acscatal.7b00829

89 S. Biswas, B. Dutta, A. Mannodi-Kanakkithodi, R. Clarke, W. Song, R. Ramprasad, S. L. Suib, Heterogeneous mesoporous manganese/cobalt oxide catalysts for selective oxidation of 5-hydroxymethylfurfural to 2, 5-diformylfuran, *Chem. Commun.*, **2017**, *53*, 11751. https://doi.org/10.1039/C7CC06097A

90 E. Hayashi, T. Komanoya, K. Kamata, M. Hara, Heterogeneously-Catalyzed Aerobic Oxidation of 5-Hydroxymethylfurfural to 2,5-Furandicarboxylic Acid with MnO2, *ChemSusChem*, **2017**, *10*, 654. https://doi.org/10.1002/cssc.201601443

91 J. Wei, X. Cao, T. Wang, H. Liu, X. Tang, X. Zeng, Y. Sun, T. Lei, S. Liu, L. Lin, Catalytic transfer hydrogenation of biomass-derived 5-hydroxymethylfurfural into 2, 5-bis (hydroxymethyl) furan over tunable Zr-based bimetallic catalysts, *Catal. Sci. Technol.*, **2018**, *8*, 4474. https://doi.org/10.1039/C8CY00500A

92 J. Chen, F. Fu, J. Zhang, W. Yu, F. Wang, J. Gao, J. Xu, Immobilized Ru Clusters in Nanosized Mesoporous Zirconium Silica for the Aqueous Hydrogenation of Furan Derivatives at Room Temperature, *ChemCatChem*, **2014**, *5*, 2822. https://doi.org/10.1002/cctc.201300316

93 R. Alamillo, M. Tucker, M. Chia, Y. Pagán-Torres, J. Dumesic, The selective hydrogenation of biomass-derived 5-hydroxymethylfurfural using heterogeneous catalysts, *Green Chem.*, **2012**, *14*, 1413. https://doi.org/10.1039/C2GC35039D

[94] T. Buntara, S. Noel, P. H. Phua, I. Meliàn-Cabrera, J. G. De Vries, H. J. Heeres, Caprolactam from renewable resources: catalytic conversion of 5-hydroxymethylfurfural into caprolactone, *Angew. Chem. Int. Ed.,* **2011**, *123*, 7221. https://doi.org/10.1002/ange.201102156

[95] M. Chatterjee, T. Ishizaka, H. Kawanami, Hydrogenation of 5-hydroxymethylfurfural in supercritical carbon dioxide–water: a tunable approach to dimethylfuran selectivity, *Green Chem.*, **2014**, *16*, 1543. https://doi.org/10.1039/C3GC42145G

[96] B. Saha, C.M. Bohn, M.M. Abu-Omar, Zinc-assisted hydrodeoxygenation of biomass-derived 5-hydroxymethylfurfural to 2, 5-dimethylfuran, *ChemSusChem*, **2014**, *7,* 3095. https://doi.org/10.1002/cssc.201402530

[97] T. Thananatthanachon, T. B. Rauchfuss, Efficient production of the liquid fuel 2, 5-dimethylfuran from fructose using formic acid as a reagent, *Angew. Chem. Int. Ed.*, **2010**, *122*, 6766. https://doi.org/10.1002/ange.201002267

[98] Y. Duan, M. Zheng, D. Li, D. Deng, L.F. Ma, Y. Yang, Conversion of HMF to methyl cyclopentenolone using Pd/Nb 2 O 5 and Ca–Al catalysts via a two-step procedure, *Green Chem.*, **2017**, *19*, 5103. https://doi.org/10.1039/C7GC02310C

[99] F. Liu, M. Audemar, K. De Oliveira Vigier, J.-M. Clacens, F. De Campo, F. Jérôme, Palladium/carbon dioxide cooperative catalysis for the production of diketone derivatives from carbohydrates, *ChemSusChem*, **2014**, *7*, 2089. https://doi.org/10.1002/cssc.201402221

[100] B. Wozniak, A. Spannenberg, Y. Li, S. Hinze, J.G. de Vries, Cyclopentanone Derivatives from 5-Hydroxymethylfurfural via 1-Hydroxyhexane-2, 5-dione as Intermediate, *ChemSusChem*, **2018**, *11*, 356. https://doi.org/10.1002/cssc.201702100

[101] A. Cukalovic, C.V. Stevens, Production of biobased HMF derivatives by reductive amination, *Green Chem.*, **2010**, *12*, 1201. https://doi.org/10.1039/C002340J

[102] A. García-Ortiz, J.D. Vidal, M.J. Climent, P. Concepcion, A. Corma, S. Iborra, Chemicals from biomass: selective synthesis of N-substituted furfuryl amines by the one-pot direct reductive amination of furanic aldehydes, *ACS Sustainable Chem. Eng*., **2019**, *7* 6243. https://doi.org/10.1021/acssuschemeng.8b06631

[103] Z. Zongchao, X. Zhanwei, W. Lu, Y. Peifang, Furandiolamine compound and preparation method thereof. CN106632166, 2017.

[104] M.-M. Zhu, L. Tao, Q. Zhang, J. Dong, Y.-M. Liu, H.-Y. He, Y. Cao, Y., Versatile CO-assisted direct reductive amination of 5-hydroxymethylfurfural catalyzed by a supported gold catalyst, *Green Chem.,* **2017**, *19*, 3880. https://doi.org/10.1039/C7GC01579H

[105] R. V. Jagadeesh, K. Murugesan, A. S. Alshammari, H. Neumann, M. Pohl, J. Radnik, M. Beller, MOF-derived cobalt nanoparticles catalyze a general synthesis of amines, *Science*, **2017**, *358*, 326. https://doi.org/10.1126/science.aan6245

[106] T. Komanoya, T. Kinemura, Y. Kita, K. Kamata, M. Hara, Electronic effect of ruthenium nanoparticles on efficient reductive amination of carbonyl compounds, *J. Am. Chem. Soc.,* **2017**, *139*, 11493. https://doi.org/10.1021/jacs.7b04481

[107] A. Dunbabin, F. Subrizi, J. Ward, T. D. Sheppard, H. C. Hailes, Furfurylamines from biomass: transaminase catalysed upgrading of furfurals, *Green Chem.,* **2017**, *19*, 397. https://doi.org/10.1039/C6GC02241C

[108] V. V. Karve, D. T. Sun, O. Trukhina, S. Yang, E. Oveisi, J. Luterbacher, and L. Q. Wendy, Efficient reductive amination of HMF with well dispersed Pd nanoparticles immobilized in a porous MOF/polymer composite, *Green Chem.,* **2020**, *22*, 368. https://doi.org/10.1039/C9GC03140E

[109] K. Zhou, H. Liu, H. Shu, S. Xiao, D. Guo, Y. Liu, Z. Wei, and X. Li, A Comprehensive Study on the Reductive Amination of 5-Hydroxymethylfurfural into 2, 5-Bisaminomethylfuran over Raney Ni Through DFT Calculations, *ChemCatChem* **2019**, *11*, 2649. https://doi.org/10.1002/cctc.201900304

[110] W. Chen, Y. Sun, J. Du, Z. Si, X. Tang, X. Zeng, L. Lin, S. Liu, T. Lei, Preparation of 5-(Aminomethyl)-2-furanmethanol by direct reductive amination of 5-Hydroxymethylfurfural with aqueous ammonia over the Ni/SBA-15 catalyst, *J Chem Technol Biotechnol*, **2018**, *93*, 3028. https://doi.org/10.1002/jctb.5661

[111] H. Yuan, J.-.P. Li, F. Su, Z. Yan, B.T. Kusema, S. Streiff, Y. Huang, M. Pera-Titus, F. Shi, Reductive Amination of Furanic Aldehydes in Aqueous Solution over Versatile NiyAlOx Catalysts, *ACS Omega*, **2019**, *4*, 2510. https://doi.org/10.1021/acsomega.8b03516

[112] R. S. Malkar, H. Daly, C. Hardacre, G. D. Yadav, Aldol condensation of 5-Hydroxymethylfurfural to fuel precursor over novel aluminum exchanged-DTP@ ZIF-8, *ACS Sustainable Chem. Eng.,* **2019**, *7*, 16215. https://doi.org/10.1021/acssuschemeng.9b02939

[113] K. Pupovac, R. Palkovits, Cu/MgAl2O4 as Bifunctional Catalyst for Aldol Condensation of 5-Hydroxymethylfurfural and Selective Transfer Hydrogenation, *ChemSusChem*, **2013**, *6*, 2103. https://doi.org/10.1002/cssc.201300414

114 M. Han, X. Liu, X. Zhang, Y. Pang, P. Xu, J. Guo, Y. Liu, S. Zhang, S. Ji, 5-Hydroxymethyl-2-vinylfuran: a biomass-based solvent-free adhesive, *Green Chem*., **2017**, *19*, 722. https://doi.org/10.1039/C6GC02723G

115 D. L. Nelson and M. M. Cox, in Lehninger, Principles of biochemistry, 3rd ed., worth publishing, New York, 2000.

116 A. Behr and T. Seidensticker, in Chemistry of Renewables, Springer, 2020, pp. 89-109

117 https://www.marketsandmarkets.com/Market-Reports/Global-Biodiesel-Market-190.html (accessed 10/10/2021)

118 https://www.indexmundi.com/energy/?product=biodiesel&graph=production&display=rank (accessed 10/10/2021)

119 W. Dilla, H. Dillenburg, E. Ploenissen et al., Solvay Deutschland GmbH, US5393428, 1993.

120 Finch, H. D. V. & Benedicts, A. De. Aluminum alkoxide reduction of alpha methylidene alkanals, 1953.

121 Thizy, A., Degeorges, M. E. & Charles, E. PROGIL French Body Corporate, 1961.

122 B. M. Bell, J. R. Briggs, R. M. Campbell, Glycerin as a renewable feedstock for epichlorohydrin production. The GTE process, *CLEAN - Soil, Air, Water*, **2008**, *36*, 657. https://doi.org/10.1002/clen.200800067

123 A. Almena and M. Martín, Technoeconomic analysis of the production of epichlorohydrin from glycerol, *Ind. Eng. Chem. Res.*, **2016**, *55*, 3226. https://doi.org/10.1021/acs.iecr.5b02555

124 Y. Xiao, G. Xiao, A. Varma, A universal procedure for crude glycerol purification from different feedstocks in biodiesel production: experimental and simulation study, *Ind. Eng. Chem. Res.*, **2013**, *52,* 14291. https://doi.org/10.1021/ie402003u

125 S. Hu, X. Luo, X., C. Wan, Y. Li, Characterization of crude glycerol from biodiesel plants, *J. Agricult. Food Chem.*, **2012**, *60*, 5915. https://doi.org/10.1021/jf3008629

126 D. T. Johnson and K. A. Taconi, The glycerin glut: Options for the value-added conversion of crude glycerol resulting from biodiesel production, *Environmental Progress*, **2007**, *26*, 338. https://doi.org/10.1002/ep.10225

127 L. Bournay, D. Casanave, B. Delfort, G. Hillion, and J. A. Chodorge, New heterogeneous process for biodiesel production: A way to improve the quality and the value of the crude glycerin produced by biodiesel plants, *Catalysis Today,* **2005***, 106*, 190. https://doi.org/10.1016/j.cattod.2005.07.181

128 A. A. Kiss, A. C. Dimian and G. Rothenberg, Solid acid catalysts for biodiesel production–-towards sustainable energy, *Adv. Synth. Catal.*, **2006**, *348*, 75. https://doi.org/10.1002/adsc.200505160

129 Du, W., Xu, Y., Liu, D. & Zeng, Comparative study on lipase-catalyzed transformation of soybean oil for biodiesel production with different acyl acceptors, *J. Mol. Catal. B Enzym.,* **2004**, *30*, 125. https://doi.org/10.1016/j.molcatb.2004.04.004

130 A. K. Singh, S. D. Fernando, and R. Hernandez, Base catalyzed fast-transesterification of soybean oil using ultrasonication, *Energy and Fuels,* **2007***, 21*, 1161. https://doi.org/10.1021/ef060507g

131 K. Bunyakiat, S. Makmee, R. Sawangkeaw, and S. Ngamprasertsith, Continuous production of biodiesel via transesterification from vegetable oils in supercritical methanol, *Energy and Fuels,* **2006***, 20*, 812. https://doi.org/10.1021/ef050329b

132 A. Singhabhandhu, and T. Tezuka, A perspective on incorporation of glycerin purification process in biodiesel plants using waste cooking oil as feedstock, *Energy,* **2010***, 35*, 2493. https://doi.org/10.1016/j.energy.2010.02.047

133 B. Katryniok, S. Paul, V. Bellière-Baca, P. Rey, and F. Dumeignil, Glycerol dehydration to acrolein in the context of new uses of glycerol, *Green Chem.,* **2010***, 12*, 2079. https://doi.org/10.1039/C0GC00307G

134 R. Ciriminna, C. Della Pina, M. Rossi, M. Pagliaro, Understanding the glycerol market, *Eur. J. Lipid Sci. Technol.,* **2014**, *116*, 1432. https://doi.org/10.1002/ejlt.201400229

135 P. Kraft, P. Gilbeau, B. Gosselin, S. Claessens, Process for Producing Dichloropropanol from Glycerol, the Glycerol Coming Eventually from the Conversion of Animal Fats in the Manufacture of Biodiesel. World Pat. 2005054167, 2005.

136 B. M. Bell, J. R. Briggs, R. M. Campbell, S. M. Chambers, P. D. Gaarenstroom, J. G. Hippler, B. D. Hook, K. Kearns, J. Kenney, W. J. Kruper, D. J. Schreck, C. N. Theriault, C. P. Wolfe, *Clean,* **2008**, *36*, 657.

137 http://news.bio-based.eu/adm-announces-industry-first-biobased-propylene-glycol-usp/ (accessed 23/09/2020).

138 https://www.chemeurope.com/en/news/138616/basf-and-oleon-celebrate-grand-opening-of-propylene-glycol-production-plant.html (accessed 23/09/2021).

139 M. Slinn, K. Kendall, C. Mallon, and J. Andrews, Steam reforming of biodiesel by-product to make renewable hydrogen, *Bioresour. Technol.,* **2008***, 99*, 5851. https://doi.org/10.1016/j.biortech.2007.10.003

140 W. M. Budzianowski, High-value low-volume bioproducts coupled to bioenergies with potential to enhance business development of sustainable biorefineries, *Renew. Sust. Energ. Rev.,* **2017**, *70*, 793. https://doi.org/10.1016/j.rser.2016.11.260

[141] G. M. Lari, G. Pastore, M. Haus, Y. Ding, S. Papadokonstantakis, C. Mondelli, J. Perez-Ramırez, Environmental and economical perspectives of a glycerol biorefinery, *Energy Environ. Sci.,* **2018**, *11*, 1012. https://doi.org/10.1039/C7EE03116E

[142] A. Behr, J. Eilting, K. Irawadi, J. Leschinski, F. Lindner, Improved utilisation of renewable resources: New important derivatives of glycerol, *Green Chem.,* **2008**, *10*, 13. https://doi.org/10.1039/B710561D

[143] A. R. Trifoi, P. Ş. Agachi and T. Pap, Glycerol acetals and ketals as possible diesel additives. A review of their synthesis protocols, *Renew. Sust. Energ. Rev.*, **2016**, *62*, 804. https://doi.org/10.1016/j.rser.2016.05.013

[144] S. Guidi, M. Noè, P. Riello, A. Perosa and M. Selva, Towards a Rational Design of a Continuous-Flow Method for the Acetalization of Crude Glycerol: Scope and Limitations of Commercial Amberlyst 36 and AlF3·3H2O as Model Catalysts, *Molecules*, **2016**, *21*, 657. https://doi.org/10.3390/molecules21050657

[145] M. R. Nanda, Z. Yuan, W. Qin, H. S. Ghaziaskar, M.-A. Poirier and C. C. Xu, Thermodynamic and kinetic studies of a catalytic process to convert glycerol into solketal as an oxygenated fuel additive, *Fuel*, **2014**, *117*, 470. https://doi.org/10.1016/j.fuel.2013.09.066

[146] V. R. Ruiz, A. Velty, L. L. Santos, A. Leyva-Pérez, M. J. Sabater, S. Iborra and A. Corma, Gold catalysts and solid catalysts for biomass transformations: Valorization of glycerol and glycerol–water mixtures through formation of cyclic acetals, *J. Catal*., **2010**, *271*, 351. https://doi.org/10.1016/j.jcat.2010.02.023

[147] G. Vicente, J. A. Melero, G. Morales, M. Paniagua and E. Martín, Acetalisation of bio-glycerol with acetone to produce solketal over sulfonic mesostructured silicas, *Green Chem.*, **2010**, *12*, 899. https://doi.org/10.1039/B923681C

[148] J. Kowalska-Kus, A. Held, M. Frankowski and K. Nowinska, Solketal formation from glycerol and acetone over hierarchical zeolites of different structure as catalysts, *J. Mol. Catal. A: Chem.*, **2017**, *426*, 205. https://doi.org/10.1016/j.molcata.2016.11.018

[149] L. Li, T. I. Korányi, B. F. Sels and P. P. Pescarmona, Highly-efficient conversion of glycerol to solketal over heterogeneous Lewis acid catalysts, *Green Chem.*, **2012**, *14*, 1611. https://doi.org/10.1039/C2GC16619D

[150] R. Gérardy, D. P. Debecker, J. Estager, P. Luis and J.-C. M. Monbaliu, Continuous Flow Upgrading of Selected C2–C6 Platform Chemicals Derived from Biomass, *Chem. Rev.,* **2020**, *120*, 7219. https://doi.org/10.1021/acs.chemrev.9b00846

[151] A. Vivian, L. Soumoy, L. Fusaro, S. Fiorilli, D. P. Debecker, C. Aprile, Surface-functionalized mesoporous gallosilicate catalysts for the efficient and sustainable upgrading of glycerol to solketal, *Green Chem*., **2021**, *23*, 354. https://doi.org/10.1039/D0GC02562C

[152] J. I. García, H. García-Marín and E. Pires, Glycerol based solvents: synthesis, properties and applications, *Green Chem*., **2014**, *16*, 1007. https://doi.org/10.1039/C3GC41857J

[153] P. H. Silva, V. L. Gonçalves, C. J. Mota, Glycerol acetals as anti-freezing additives for biodiesel, *Bioresource Technol.,* **2010**, *101*, 6225. https://doi.org/10.1016/j.biortech.2010.02.101

[154] A. Cornejo, I. Barrio, M. Campoy, J. Lázaro and B. Navarrete, Oxygenated fuel additives from glycerol valorization. Main production pathways and effects on fuel properties and engine performance: A critical review, *Renew. Sust. Energ. Rev.*, **2017**, *79*, 1400. https://doi.org/10.1016/j.rser.2017.04.005

[155] R. Calmanti, M. Galvan, E. Amadio, A. Perosa, M. Selva, High-temperature batch and continuous-flow transesterification of alkyl and enol esters with glycerol and its acetal derivatives, *ACS Sustainable Chem. Eng.,* **2018**, *6*, 3964. https://doi.org/10.1021/acssuschemeng.7b04297

[156] Z. Mufrodi, A. Budiman, S. Purwono, Operation conditions in syntesize of bioaditive from glycerol as by-product biodiesel: a review, *Energy Procedia* **2018**, *145*, 434. https://doi.org/10.1016/j.egypro.2018.04.071

[157] https://www.mordorintelligence.com/industry-reports/triacetin-market (accessed 25/08/2021)

[158] https://www.marketsandmarkets.com/Market-Reports/triacetin-market-1433253.html (accessed 25/08/2021)

[159] I. Kim, J. Kim and D. Lee, Sulfonic acid functionalized deoxycellulose catalysts for glycerol acetylation to fuel additives, *Appl. Catal. A Gen.*, **2014**, *482*, 31. https://doi.org/10.1016/j.apcata.2014.05.018

[160] P. Ferreira, I. M. Fonseca, A. M. Ramos, J. Vital and J. E. Castanheiro, Acetylation of glycerol over heteropolyacids supported on activated carbon, *Catal. Commun.*, **2011**, *12*, 573. https://doi.org/10.1016/j.catcom.2010.11.022

[161] N. J. Venkatesha, Y. S. Bhat and B. S. J. Prakash, Volume accessibility of acid sites in modified montmorillonite and triacetin selectivity in acetylation of glycerol, *RSC Adv.*, **2016**, *6*, 45819. https://doi.org/10.1039/C6RA05720A

[162] M.J. Da Silva, N. Aparecida, L. Lorena, C. De Andrade, L. Ulisses, A. Pereira, Fe4 (SiW12O40) 3-catalyzed glycerol acetylation: Synthesis of bioadditives by using highly active Lewis acid catalyst, *J. Mol. Cat. A: Chem.*, **2016**, *422*, 69. https://doi.org/10.1016/j.molcata.2016.03.003

[163] M. Rezayat and H. S. Ghaziaskar, Continuous synthesis of glycerol acetates in supercritical carbon dioxide using Amberlyst 15®, *Green Chem.,* **2009**, *11*, 710. https://doi.org/10.1039/B815674C

[164] H. Rastegari, H. S. Ghaziaskar and M. Yalpani, Valorization of biodiesel derived glycerol to acetins by continuous esterification in acetic acid: focusing on high selectivity to diacetin and triacetin with no byproducts, *Ind. Eng. Chem. Res.*, **2015**, *54*, 3279. https://doi.org/10.1021/acs.iecr.5b00234

[165] F. Rajabi, A heterogeneous cobalt (II) Salen complex as an efficient and reusable catalyst for acetylation of alcohols and phenols, *Tetrahedron Lett.*, **2009**, *50*, 395. https://doi.org/10.1016/j.tetlet.2008.11.024

[166] L. N.Silva, V. L. C.Gonçalves, C. J. A. Mota, Catalytic acetylation of glycerol with acetic anhydride, *Catal. Comm.*, **2010**, *11*, 1036. https://doi.org/10.1016/j.catcom.2010.05.007

[167] S. Sandesh, P. Manjunathan, A. B. Halgeri and G. V. Shanbhag, Glycerol acetins: fuel additive synthesis by acetylation and esterification of glycerol using cesium phosphotungstate catalyst, *RSC Adv.*, **2015**, *5*, 104354. https://doi.org/10.1039/C5RA17623A

[168] P. S. Kong, M. K. Aroua and W. M. A. Wan Daud, Esterification of Glycerol With Oleic Acid Over Hydrophobic Zirconia-Silica Acid Catalyst and Commercial Acid Catalyst: Optimization and Influence of Catalyst Acidity, *Renew. Sust. Energ. Rev.*, **2016**, *63*, 533. https://doi.org/10.3389/fchem.2019.00205

[169] L. J. Konwar, A. Samikannu, P. Mäki-Arvela, D. Boström and J. P. Mikkola, Lignosulfonate-based macro/mesoporous solid protonic acids for acetalization of glycerol to bio-additives, *Appl. Catal. B Environ.*, **2018**, *220*, 314. https://doi.org/10.1016/j.apcatb.2017.08.061

[170] T. Bruhn, H. Naims and B. Olfe-Kräutlein, Separating the debate on CO2 utilisation from carbon capture and storage, *Environ. Sci. Policy*, **2016**, *60*, 38. https://doi.org/10.1016/j.envsci.2016.03.001

[171] A. Zimmermann, M. Kant, CO$_2$ utilisation Today, report 2017. https://doi.org/10.14279/ depositonce-5806.

[172] M. Selva, A. Perosa, G. Fiorani, L. Cattelan, In *CO$_2$ and Organic Carbonates for the Sustainable Valorization of Renewable Compounds*, Green Chemistry Series 61, Green Synthetic Processes and Procedures, Ed. R. Ballini, The Royal Society of Chemistry, 2019.

[173] E. A. Quadrelli, G. Centi, J.-l. duplan and S. perathoner, Carbon dioxide recycling: emerging large-scale technologies with industrial potential, *ChemSusChem*, **2011**, *4*, 1194. https://doi.org/10.1002/cssc.201100473

[174] M. Pérez-Fortes, A. Bocin-dumitriu and E. Tzimas, CO2 utilization pathways: Techno-economic assessment and market opportunities, *Energy Procedia*, **2014**, *63*, 7968. https://doi.org/10.1016/j.egypro.2014.11.834

[175] L. Maisonneuve, O.A. Lamarzelle, E. Rix, E. Grau, H. Cramail, Isocyanate-free routes to polyurethanes and poly (hydroxy urethane)s, *Chem. Rev.*, **2015**, *115*, 12407. https://doi.org/10.1021/acs.chemrev.5b00355

[176] B. Schaffner, F. Schaffner, S.P. Verevkin, A. Borner, Organic carbonates as solvents in synthesis and catalysis, *Chem. Rev.*, **2010**, *110*, 4554. https://doi.org/10.1021/cr900393d

[177] R.-S. Kühnel, N. Böckenfeld, S. Passerini, M. Winter, A. Balducci, Mixtures of ionic liquid and organic carbonate as electrolyte with improved safety and performance for rechargeable lithium batteries, *Electrochimica Acta*, **2011**, *56*, 4092. https://doi.org/10.1016/j.electacta.2011.01.116

[178] B.A. Santos, V.M. Silva, J.M. Loureiro, A.E. Rodrigues, Review for the direct synthesis of dimethyl carbonate, *ChemBioEng Reviews*, **2014**, *1*, 214. https://doi.org/10.1002/cben.201400020

[179] A.H. Tamboli, A.A. Chaugule, H. Kim, Catalytic developments in the direct dimethyl carbonate synthesis from carbon dioxide and methanol, *Chem. Eng. J.,* **2017**, *323*, 530. https://doi.org/10.1016/j.cej.2017.04.112

[180] M. Selva, A. Perosa, S. Guidi, L. Cattelan, Ionic liquids as transesterification catalysts: applications for the synthesis of linear and cyclic organic carbonates, *Beilstein J. Org. Chem.*, **2016**, *12*, 1911. https://doi.org/10.3762/bjoc.12.181

[181] W.K. Teng, G.C. Ngoh, R. Yusoff, M.K. Aroua, A review on the performance of glycerol carbonate production via catalytic transesterification: Effects of influencing parameters, *Energ. Conv. Manag.,* **2014**, *88*, 484. https://doi.org/10.1016/j.enconman.2014.08.036

[182] S. Guidi, R. Calmanti, M. Noè, A. Perosa, M. Selva, Thermal (catalyst-free) transesterification of diols and glycerol with dimethyl carbonate: A flexible reaction for batch and continuous-flow applications, *ACS Sust. Chem. Eng.*, **2016**, *4*, 6144. https://doi.org/10.1021/acssuschemeng.6b01633

[183] P. P. Pattanaik, P. M. Kumar, N. Raju, and N. Lingaiah, Continuous synthesis of glycerol carbonate by transesterification of glycerol with dimethyl carbonate over Fe–La mixed oxide catalysts, *Catal. Lett.*, **2021**, *151*, 1433. https://doi.org/10.1007/s10562-020-03397-4

[184] X. Zhang, S. Wei, X. Zhao, Z. Chen, H. Wu, P. Ronga, Y. Sun, Y. Li, H. Yu, D. Wang, Preparation of mesoporous CaO-ZrO2 catalysts without template for the continuous synthesis of glycerol carbonate in a fixed-bed reactor, *Appl. Cat. A, Gen.*, **2020**, *590*, 117313. https://doi.org/10.1016/j.apcata.2019.117313

[185] S.-H. Pyo, K. Nuszkiewicz, P. Persson, S. Lundmark, R. Hatti-Kaul, Lipase-mediated synthesis of six-membered cyclic carbonates from trimethylolpropane and dialkyl carbonates: Influence of medium engineering on reaction selectivity, *J. Mol. Cat. B: Enzym*., **2011**, *73*, 67. https://doi.org/10.1016/j.molcatb.2011.07.019

[186] S.-H. Pyo, R. Hatti-Kaul, Selective, Green synthesis of six-membered cyclic carbonates by lipase-catalyzed chemospecific transesterification of diols with dimethyl carbonate, *Adv. Synth. Catal*., *2012*, *354*, 797. https://doi.org/10.1002/adsc.201100822

[187] M. Selva, A. Caretto, M. Noè, and A. Perosa, Carbonate phosphonium salts as catalysts for the transesterification of dialkyl carbonates with diols. The competition between cyclic carbonates and linear dicarbonate products, *Org. Biomol. Chem*., **2014**, *12*, 4143. https://doi.org/10.1039/C4OB00655K

[188] N. Kindermann, T. Jose and A. W. Kleij, in Chemical Transformations of Carbon Dioxide, Springer, 2017, pp. 61–88.

[189] M. Honda, M. Tamura, K. Nakao, K. Suzuki, Y. Nakagawa, K. Tomishige, Direct Cyclic Carbonate Synthesis from CO2 and Diol over Carboxylation/Hydration Cascade Catalyst of CeO2 with 2-Cyanopyridine, *ACS Catal*, **2014**, *4*, 1893. https://doi.org/10.1021/cs500301d

[190] G. L. Gregory, M. Ulmann, A. Buchard, Synthesis of 6-membered cyclic carbonates from 1, 3-diols and low CO 2 pressure: a novel mild strategy to replace phosgene reagents, *RSC Adv*, **2015**, *5*, 39404. https://doi.org/10.1039/C5RA07290E

[191] K. Sekine, T. Yamada, Silver-catalyzed carboxylation, *Chem. Soc. Rev*., **2016**, *45*, 4524. https://doi.org/10.1039/C5CS00895F

[192] S. Dabral, B. Bayarmagnai, M. Hermsen, J. Schießl, V. Mormul, A.S.K. Hashmi, T. Schaub, Silver-Catalyzed Carboxylative Cyclization of Primary Propargyl Alcohols with CO2, *Org. Lett*., **2019**, *21*, 1422. https://doi.org/10.1021/acs.orglett.9b00156

[193] P. Pässler, W. Hefner, K. Buckl, H. Meinass, A. Meiswinkel, H.-J. Wernicke, G. Ebersberg, R. Müller, J. Bässler, H. Behringer, Acetylene Production in *Ullmann's encyclopedia of industrial chemistry*, Wiley Eds., 2012, pp. 277-326.

[194] Q.-W. Song, Z.-H. Zhou and L.-N. He, Efficient, selective and sustainable catalysis of carbon dioxide, *Green Chem.,* **2017**, *19*, 3707. https://doi.org/10.1039/C7GC00199A

[195] R. Calmanti, A. Perosa and M. selva, Tandem catalysis: one-pot synthesis of cyclic organic carbonates from olefins and carbon dioxide, *Green Chem.*, **2021**, *23*, 1921. https://doi.org/10.1039/D0GC04168H

[196] M. Selva, A. Perosa, G. Fiorani, L. Cattelan, CO2 and Organic Carbonates for the Sustainable Valorization of Renewable Compounds, in *Green Synthetic Processes and Procedures,* 2019, pp. 319-342.

[197] F. Della Monica and A. W. Kleij, Mechanistic guidelines in nonreductive conversion of CO 2: the case of cyclic carbonates, *Catal. Sci. Tech.*, **2020**, *10*, 3483. https://doi.org/10.1039/D0CY00544D

[198] T.K. Pal, D. De, P.K. Bharadwaj, Metal–organic frameworks for the chemical fixation of CO2 into cyclic carbonates, *Coord. Chem. Rev*., **2020**, *408*, 213173. https://doi.org/10.1016/j.ccr.2019.213173

[199] S. Rebsdat, D. Mayer, Ethylene Oxide in *Ullmann's Encyclopedia of Industrial Chemistry*, Wiley Eds., 2012, pp. 547-572.

[200] T.A. Nijhuis, M. Makkee, J.A. Moulijn, B.M. Weckhuysen, The production of propene oxide: catalytic processes and recent developments, *Ind. Eng. Chem. Res*., **2006**, *45*, 3447. https://doi.org/10.1021/ie0513090

[201] S.T. Oyama, Rates, kinetics, and mechanisms of epoxidation: homogeneous, heterogeneous, and biological routes, in: *Mechanisms in homogeneous and heterogeneous epoxidation catalysis*, Elsevier, 2008, pp. 3-99.

[202] L.H. Pottenger, D.R. Boverhof, J.M. Waechter Jr, *Patty's Toxicology*, Wiley Eds., 2001, pp. 425-490.

[203] A. Chieregato, J.V. Ochoa, F. Cavani, *Chemicals and Fuels from Bio-Based Building Blocks*, Wiley, 2016.

[204] A. Bazzanella, F. Ausfelder, Low carbon energy and feedstock for the European chemical industry, DECHEMA, Gesellschaft für Chemische Technik und Biotechnologie eV, 2017.

[205] (a) R. G. Austin, R. C. Michaelson and R. S. Myers, US4824969A, 1989; (b) S. E. Jacobson, US4483994A, 1984; (c) S. E. Jacobson, US4325874A, 1982; (d) J.-L. Kao, G. A. Wheaton, H. Shalit and M. N. Sheng, US4247465A, 1981; (e) C. Fumagalli, G. Caprara and P. Roffia, CA6010327A, 1977; (f) J. A. Verdol, US3025305A, 1962.

[206] B.S. Lane, K. Burgess, Metal-catalyzed epoxidations of alkenes with hydrogen peroxide, *Chem. Rev.*, **2003**, *103*, 2457. https://doi.org/10.1021/cr020471z

[207] X. Gao, G. Yuan, H. Chen, H. Jiang, Y. Li, C. Qi, Efficient conversion of CO2 with olefins into cyclic carbonates via a synergistic action of I2 and base electrochemically generated in situ, *Electrochem. Commun.*, **2013**, *34*, 242. https://doi.org/10.1016/j.elecom.2013.06.022

[208] P. T. Anastas, J. C. Warner, *Green Chemistry: Theory and Practice*, Oxford Univ. Press, 1998.

[209] H. C. Erythropel, J. B. Zimmerman, T. M. de Winter, L. Petitjean, F. Melnikov, C. Ho Lam, A. W. Lounsbury, E. Mellor, N. Z. Janković, Q. Tu, L. N. Pincus, M. M. Falinski, W. Shi, P. Coish, D. L. Plata, and P. T. Anastas, The Green ChemisTREE: 20 years after taking root with the 12 principles, *Green Chem.*, **2018**, *20*, 1929. https://doi.org/10.1039/C8GC00482J

[210] P. T. Anastas, J. B. Zimmerman, Peer reviewed: design through the 12 principles of green engineering, *Environ. Sci. Technol*., **2003**, *37*, 94. https://doi.org/10.1021/es032373g

[211] Gomollón-Bel, F. Ten, Ten Chemical Innovations That Will Change Our World: IUPAC identifies emerging technologies in Chemistry with potential to make our planet more sustainable, *Chem. Int.* **2019**, *41*, 12. https://doi.org/10.1515/ci-2019-0203

[212] M. B. Plutschack, B. Pieber, K. Gilmore, P. H. Seeberger, The hitchhiker's guide to flow chemistry, *Chem. Rev.,* **2017**, *117*, 11796. https://doi.org/10.1021/acs.chemrev.7b00183

[213] A. I. Stankiewicz and J. A. Moulijn, Process intensification: transforming chemical engineering, *Chem, Eng. Progr.*, **2000**, *96*, 22.

[214] K. F. Jensen, Flow chemistry—microreaction technology comes of age, *AIChE J.,* **2017**, *63*, 858. https://doi.org/10.1002/aic.15642

[215] R. Gérardy, N. Emmanuel, T. Toupy, V.-E. Kassin, N. N. Tshibalonza, M. Schmitz, J.-C. Monbaliu, Continuous flow organic chemistry: successes and pitfalls at the interface with current societal challenges, *Eur. J. Org. Chem.,* **2018**, *2018*, 2301. https://doi.org/10.1002/ejoc.201800149

[216] Proceedings of the Royal Society of London. Series A, Containing Papers of a Mathematical and Physical Character

Vol. 86, No. 587, 1912, pp. 330-332.

[217] J. Wegner, S. Ceylan, A. Kirschning, Flow chemistry–a key enabling technology for (multistep) organic synthesis, *Adv. Synth. Catal.*, **2012**, *354*, 17. https://doi.org/10.1002/adsc.201100584

[218] A. Tanimu, S. Jaenicke and K. Alhooshani, Heterogeneous catalysis in continuous flow microreactors: A review of methods and applications, *Chem. Eng. J.*, **2017**, *327*, 792. https://doi.org/10.1016/j.cej.2017.06.161

[219] B. Gutmann, D. Cantillo, C. O. Kappe, Continuous-flow technology—a tool for the safe manufacturing of active pharmaceutical ingredients, *Angew.Chem. Int.Ed*. **2015**, *54*, 6688. https://doi.org/10.1002/anie.201409318

[220] S. Falß, N. Kloye, M. Holtkamp, A. Prokofyeva, T. Bieringer and N. Kockmann, *Handbook of Green Chemistry*, Wiley-VCH, 2018.

[221] P. Poechlauer, J. Colberg, E. Fisher, M. Jansen, M. D. Johnson, S. G. Koenig, M. Lawler, T. Laporte, J. Manley and B. Martin, Pharmaceutical roundtable study demonstrates the value of continuous manufacturing in the design of greener processes, *Org. Proc. Res. Dev.*, **2013**, *17*, 1472. https://doi.org/10.1021/op400245s

[222] J. Britton and T. F. Jamison, The assembly and use of continuous flow systems for chemical synthesis, *Nat. Protocol.*, **2017**, *12*, 2423. https://doi.org/10.1038/nprot.2017.102

[223] D. Cantillo and C. O. Kappe, Immobilized Transition Metals as Catalysts for Cross-Couplings in Continuous Flow—A Critical Assessment of the Reaction Mechanism and Metal Leaching, *ChemCatChem*, **2014**, *6*, 3286. https://doi.org/10.1002/cctc.201402483

[224] M. Selva, G. Fiorani and D. Rigo, Chapter 10, *Supercritical Solvents*, in Sustainable Organic Synthesis: Tools and Strategies, 2021.

[225] P. Carles, A brief review of the thermophysical properties of supercritical fluids, *J. Supercrit. Fluids*, **2010**, *53*, 2. https://doi.org/10.1016/j.supflu.2010.02.017

[226] T. Yan, J. Xu, L. Wang, Y. Liu, C. Yang and T. Fang, A review of upgrading heavy oils with supercritical fluids, *RSC Adv.*, **2015**, *5,* 75129. https://doi.org/10.1039/C5RA08299D

[227] P. S. Shah, T. Hanrath, K. P. Johnston and B. A. Korgel, Nanocrystal and nanowire synthesis and dispersibility in supercritical fluids, *J. Phys. Chem. B*, **2004**, *108*, 9574. https://doi.org/10.1021/jp049827w

[228] S. D. Manjare and K. Dhingra, Supercritical fluids in separation and purification: A review, *Mater. Sci. Energy Technol.*, **2019**, *2*, 463. https://doi.org/10.1016/j.mset.2019.04.005

[229] K. Zosel, Praktische Anwendungen der Stofftrennung mit überkritischen Gasen, *Angew. Chem.*, **1978**, *90*, 748. https://doi.org/10.1002/ange.19780901005

[230] B. P. Nobre, L. Gouveia, P. G. S. Matos, A. F. Cristino, A. F. Palavra and R. L. Mendes, Supercritical extraction of lycopene from tomato industrial wastes with ethane, *Molecules*, **2012**, *17*, 8397. https://doi.org/10.3390/molecules17078397

[231] T. Maschmeyer, R. Luque and M. Selva, Upgrading of marine (fish and crustaceans) biowaste for high added-value molecules and bio (nano)-materials, *Chem. Soc. Rev.*, **2020**, *49*, 4527. https://doi.org/10.1039/C9CS00653B

[232] K. J. Ivin and J. C. Mol, *Olefin Metathesis and Metathesis Polymerization*, Academic Press, San Diego, 1997.

[233] Y. Chauvin, Olefin metathesis: The early days (Nobel lecture), *Angew. Chem., Int. Ed.*, **2006**, *45*, 3740. https://doi.org/10.1002/anie.200601234

[234] R. H. Grubbs, Olefin-metathesis catalysts for the preparation of molecules and materials (Nobel lecture), *Angew. Chem., Int. Ed.*, **2006**, *45*, 3760. https://doi.org/10.1002/anie.200600680

[235] R. R. Schrock, Multiple metal–carbon bonds for catalytic metathesis reactions (Nobel lecture), *Angew. Chem., Int. Ed.*, **2006**, *45*, 3748. https://doi.org/10.1002/anie.200600085

[236] M. Selva, A. Perosa, M. Fabris and P. Canton, The metathesis of α-olefins over supported Re-catalysts in supercritical CO_2, *Green Chem.*, **2009**, *11*, 229. https://doi.org/10.1039/B815121K

[237] X. Han and M. Poliakoff, Continuous reactions in supercritical carbon dioxide: problems, solutions and possible ways forward, *Chem. Soc. Rev.*, **2012**, *41*, 1428. https://doi.org/10.1039/C2CS15314A

[238] J. G. Stevens, R. A. Bourne, M. V. Twigg and M. Poliakoff, Real-Time Product Switching Using a Twin Catalyst System for the Hydrogenation of Furfural in Supercritical CO2, *Angew. Chem., Int. Ed.*, **2010**, *49*, 8856. https://doi.org/10.1002/anie.201005092

[239] R. A. Bourne, J. G. Stevens, J. Ke and M. Poliakoff, Maximising opportunities in supercritical chemistry: the continuous conversion of levulinic acid to γ-valerolactone in CO2, *Chem. Commun*., **2007**, 4632. https://doi.org/10.1039/B708754C

[240] J. R. Hyde and M. Poliakoff, Supercritical hydrogenation and acid-catalysed reactions "without gases", *Chem. Commun*., **2004**, 1482. https://doi.org/10.1039/B404181J

[241] J. R. Hyde, B. Walsh, J. Singh and M. Poliakoff, Continuous hydrogenation reactions in supercritical CO 2 "without gases", *Green Chem*., **2005**, *7*, 357. https://doi.org/10.1039/B419276A

[242] E. G. Rasmussen, J. Kramlich, and I. V. Novosselov, Scalable Continuous Flow Metal–Organic Framework (MOF) Synthesis Using Supercritical CO2, *ACS Sustainable Chem. Eng*., **2020**, *8*, 9680. https://doi.org/10.1021/acssuschemeng.0c01429

[243] R. Villa, E. Alvarez, S. Nieto, A. Donaire, E. Garcia-Verdugo, S. V. Luis, and P. Lozano, Chemo-enzymatic production of omega-3 monoacylglycerides using sponge-like ionic liquids and supercritical carbon dioxide, *Green Chem*., **2020**, *22*, 5701. https://doi.org/10.1039/D0GC02033H

[244] (a) Y. Ishii, M. Takeno, Y. Kawasaki, A, Muromachi, Y. Nishiyama and S. Sakaguchi, Acylation of Alcohols and Amines with Vinyl Acetates Catalyzed by Cp*2Sm(thf)2, *J. Org. Chem.*, **1996**, *61*, 3088. https://doi.org/10.1021/jo952168m; (b) X. Zhu, B. Qian, R. Wei, J-D. Huang and H. Bao, Protection of COOH and OH groups in acid, base and salt free reactions, *Green Chem.*, **2018**, *20*, 1444. https://doi.org/10.1039/C8GC00037A

[245] K. Matsumoto, C. Feng, S. Handa, T. Oguma and T. Katsuki, Asymmetric epoxidation of (Z)-enol esters catalyzed by titanium (salalen) complex with aqueous hydrogen peroxide, *Tetrahedron*, **2011**, *67*, 6474. https://doi.org/10.1016/j.tet.2011.06.022

[246] Y. Kita, H. Maeda, F. Takahashi and S. Fukui, A convenient synthesis of dicarboxylic monoesters using isopropenyl esters: synthesis of oxaunomycin derivatives, *J. Chem. Soc., Chem. Commun.*, **1993**, 410. https://doi.org/10.1039/C39930000410

[247] F. S. Crossley, E. Miller, W. H. Hartung, and M. L. Moore, Thiobarbiturates. III. Some N-substituted derivatives, *J. Org. Chem.,* **1940**, *5*, 238. https://doi.org/10.1021/jo01209a004

[248] R. E. Murray and D. M. Lincoln, New catalytic route to vinyl esters, *Catal. Today*, **1992**, *13*, 93. https://doi.org/10.1016/0920-5861(92)80189-T

[249] R. Pelagalli, I. Chiarotto, M. Feroci, and S. Vecchio, Isopropenyl acetate, a remarkable, cheap and acylating agent of amines under solvent-and catalyst-free conditions: a systematic investigation, *Green Chem.*, **2012**, *14*, 2251. https://doi.org/10.1039/C2GC35485C

[250] HJ Hagemeyer, DC Hull, Reactions of isopropenyl acetate, *Ind. Eng. Chem*., **1949**, 2920. https://doi.org/10.1021/ie50480a063

[251] N. Ahmed, J. E. van Lier, Molecular iodine in isopropenyl acetate (IPA): a highly efficient catalyst for the acetylation of alcohols, amines and phenols under solvent free conditions, *Tetrahedron Lett.*, **2006**, *47*, 5345. https://doi.org/10.1016/j.tetlet.2006.05.122

2 Isopropenyl esters (iPEs)-mediated tandem esterification-acetalization reactions

2.1 Introduction

The catalytic transesterification of esters with alcohols is of paramount importance in synthetic organic chemistry.[1,2,3,4] The reaction usually occurs under mild conditions compatible with a variety of functionalized alcohols bearing acetals, epoxides, and alkenes/alkynes groups, and it is characterized by a low environmental footprint as coproduct alcohols (often MeOH and EtOH) can be easily recovered and recycled. Transesterification, however, is a reversible process that requires over stoichiometric quantities of reactants (alcohol or ester) and/or active catalytic systems, to ensure quantitative product formation.[5] In this context, enol esters (EEs), and in particular nontoxic, commercially available, and cheap isopropenyl acetate (iPAc) and some of its higher homologues, have emerged as privileged reagents since their reactions with alcohols result in the formation of an ester and an enol that quickly converts into the corresponding ketone, thereby making the overall transformation irreversible. Scheme 2.21 depicts the case of iPAc as an acetylating agent.[6,7]
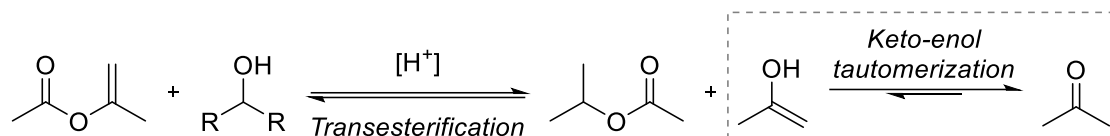
Scheme 2.21. *Acid-catalyzed transesterification between iPAc and alcohols*

iPAc-based transesterification reactions have been successfully applied to a variety of substituted alcohols, including sterically hindered ones,[8] employing catalytic systems composed of enzymes for the kinetic resolution of racemic alcohols,[9,10] Lewis acid metal complexes,[11,12] and alkylammonium salts as organocatalysts.[13] iPAc was also investigated as a chemoselective acylating agent of polyfunctional substrates such as polyols bearing primary and secondary hydroxyls and/ or phenol groups, or aminoalcohols. Accordingly, the protection of primary alcohols was achieved via catalytic and biocatalytic procedures,[14,15] and the selective N-amidation of aminoalcohols was obtained under solventless and catalyst-free conditions.

Intriguingly, acetone released as a by-product in Scheme 3.1 may be a suitable reagent to promote further reactions in situ, for example, subsequent acetalization processes with the starting alcohols in an overall tandem sequence of transesterification/acetalization.

The use of iPAc-derived acetone as a reactant for the ketalization of alcohols was first exploited in 1948 by Croxall et al.[16] who noticed that when iPAc was added to an excess alcohol containing a small amount of mercury oxide and boron trifluoride, heat was evolved and an acetal and acetic acid were obtained (4 examples, yields 32-63%). Thereafter, Hirsh and co-workers reported that the reaction of ethanol and iPAc yielded the corresponding ketal by using mercuric acetate;[17] the reaction scope was extended to different alcohols (MeOH, EtOH, BuOH, and allyl alcohol) with which the formation of 4 acetone ketals was achieved with yields in the range of 50-83%. The use of Hg based catalysts was then abandoned due to their toxicity.

In the first decade of the 2000s, Frost et al. observed the simultaneous formation of acetylated and acetalized products during the reaction between iPAc and 1-phenyl-1,2-ethanediol

catalyzed by In(ClO$_4$)$_3$ (Scheme 2.22, top),[18] while Taneja *et al.* reported that molecular iodine catalyzed the acetalization and acetylation of sugars with stoichiometric amounts of enol acetates under solvent-free conditions (14 examples; 62-91% yields; Scheme 2.22, bottom).[19]
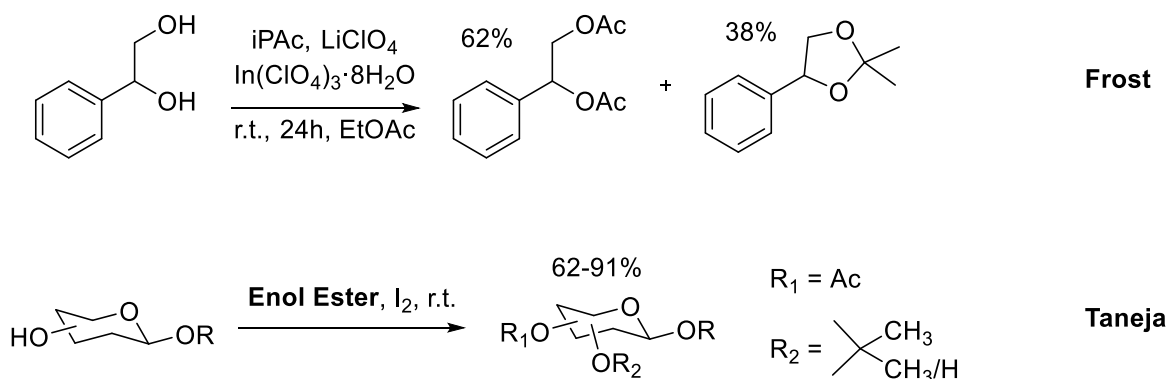
Scheme 2.22. *Reported examples of tandem iPAc-mediated acetalization/transesterification reactions*

Except for these few reports, no other papers were described on these tandem reactions until the group with which this Thesis work was developed, revisited the reactivity of enol esters, and in particular, isopropenyl acetate. As part of the long-standing interest of this research group on the chemical upgrading of biobased platform chemicals, the use of nontoxic iPAc was recently considered to investigate innovative transesterification reactions of glycerol. Intriguingly, under thermal (noncatalytic) conditions, it was noticed that the expected acetylated products were obtained along with non-neglectable quantities of cyclic acetals of glycerol (solketal and solketal acetate) that were derived from a tandem acetalization process promoted by acetone released during the transesterification step (Scheme 2.22).[20] Thermal experiments, however, clearly favored acetylation over the acetalization reaction (Scheme 2.23, top right).
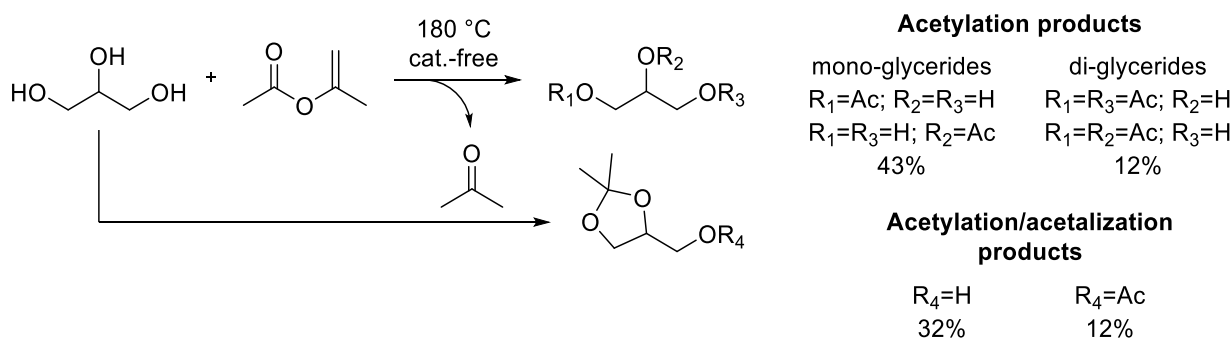
Scheme 2.23. *Thermal (non-catalytic) batch reaction of iPAc and glycerol*

These results prompted the research program of this Thesis work towards the study of new conditions by which both the involved transformations (transesterification and subsequent acetalization) of Scheme 3.3 could proceed to an equal extent in relation to each other. The tandem sequence mediated by enol esters has been thoroughly reconsidered by exploring the reactions of different isopropenyl esters (iPEs) with various types of renewable 1,2-diols as ethylene and propylene glycols, glycerol as a model triol, and glycerol-derived aminodiols, namely 3-aminopropanediol and 2-aminopropanediol. The overall strategy was to devise a 100% carbon efficient tandem process,[21] where an irreversible transesterification mediated by an isopropenyl ester released acetone which was quantitatively used in a following

acetalization step. The results of this investigation are described in the following paragraphs 3.2-3.4.

2.2 The tandem reaction of iPEs and renewable 1,2-diols: from batch to continuous flow

Abstract. Compared to Scheme 2.23, an initial study was carried out by using 1,2-diols as propylene glycol and ethylene glycol in place of glycerol, and acid catalysis rather than thermal conditions. Both 1,2-diols can be derived from glycerol,[22,23] but they are far more soluble in conventional solvents and less viscous than the parent molecule. These were key features, especially under the perspective of extending the investigation in the continuous-flow mode. It should however be noted that, albeit acetalization easily occurs under acid-catalyzed conditions,[24] very few examples of one-pot acetylation/acetalization sequences have been described for diols or polyols.[25] These involve anhydrides and acetals as reagents to promote acylation and transacetalization of sugar-derived O- and S-glycosides. To the best of our knowledge, tandem reactions triggered by enol esters have not been reported before this study. Results have demonstrated that, in the presence of a heterogeneous acid catalyst such as Amberlyst-15 and a polar aprotic solvent, not only does the reaction of propylene glycol and isopropenyl esters (acetate octanoate and phenylbutyrate) allow the desired cascade sequence, but the selectivity can also be steered toward formation of monoacetylation and acetalization products in substantially equivalent amounts, with water as the sole byproduct. The tandem sequence has been successfully transferred under continuous-flow (CF) conditions where the more accurate control of T and flow rate and process intensification have improved the reaction productivity up of 9.7 mmol of acetal gcat^{-1} h^{-1}.[26] Regardless of the enol ester, changing the diol from propylene- to ethylene-glycol has brought about a drop of the tandem selectivity due to the predominant formation of transesterification products, both mono- and diacetate compounds, at the expenses the acetal derivative.

2.2.1 Tandem reactions of propylene glycol (PG, 1) under batch conditions

The batch reaction of propylene glycol (PG, **1**) with isopropenyl acetate (iPAc, **2a**) was chosen as a model to begin the investigation. Screening of the reaction conditions was required since no studies were available in the literature. Initial control experiments pointed to the use of a nontoxic, renewable based solvent, such as cyclopentyl methyl ether (CPME) and Amberlyst-15 as a heterogeneous acid catalyst active for both transesterification and acetalization processes.[27,28] Accordingly, the effects of the temperature and the reactants' molar ratio on the reaction selectivity were investigated.

Role of the temperature. The temperature was varied between 50 and 90 °C. In this range, an equimolar solution of **1** and **2a** (1.39 mmol) in CPME as a solvent (1 mL; [**1**] = [**2a**] = 1.4 M) was set to react in the presence of Amberlyst-15 (15.8 mg, 15 wt%, 7.9·10^{-2} H$^+$ *m*eq) as a catalyst. Glass reactors were used up to 70 °C, while stainless-steel autoclaves were dedicated for tests at 90 °C to avoid loss of volatiles by evaporation (acetone and acetal products). The four observed products were PG derivatives identified as two monoacetate isomers, i.e., hydroxypropyl acetate (**3a**) and 1-hydroxypropan-2-yl acetate (**3a***), the diacetate ester propane-1,2-diyl diacetate (**3a'**), and the dimethyl acetal 2,2,4-trimethyl-1,3-dioxolane (**4**) (Figure 2.23 and Scheme 2.24). Such compounds were fully characterized by MS and NMR analyses: structural details are reported the Appendix . Figure 2.23 shows the reaction profiles at 50 and 70 °C, respectively.
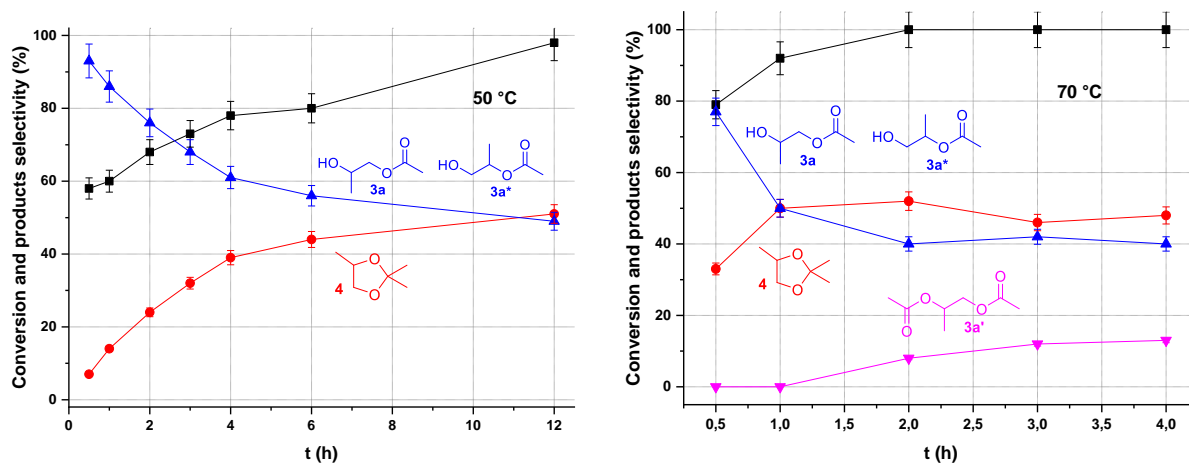
Figure 2.23. *Reaction of an equimolar solution of propylene glycol (**1**) and i-propenylacetate (**2a**) ([**1**] = [**2a**] = 1.4 M; 1.39 mmol each) in CPME solvent (1 mL) in the presence of Amberlyst-15 (15 wt %). Other conditions: T = 50 °C (left), T = 70 °C (right). (black ■) conversion of **1**; (magenta ▼) acetal (**4**) selectivity; (blue ▲) monoacetate (**3a**) selectivity; (red ●) diacetate (**3a'**) selectivity*

Conversion of **1** and the product distribution were determined by GC and GC/MS using an external standard (*vide infra*). For convenience, the total amount of monoester isomers is shown in a single curve (**blue** trace) since the relative ratio of such products remained constant over time (**3a/3a*** = 1.9). At 70 °C, full conversion of PG was achieved after 2 h, while the reaction was 6 times longer (12 h) at 50 °C (compare **black** traces).

More interesting, however, was the effect on the product distribution. At 70 °C, formation of monoesters **3a/3a*** and acetal **4** compounds was accompanied by the presence of diester **3a'** as a side coproduct in 11-13% amount (Figure 2.23, right). Moreover, additional experiments at the same T confirmed that increasing the reagents concentration from 0.6 to 2.8 M (CPME: 0.5-2.5 mL) decreased the reaction time with minor changes on the selectivity (Figure 2.24).
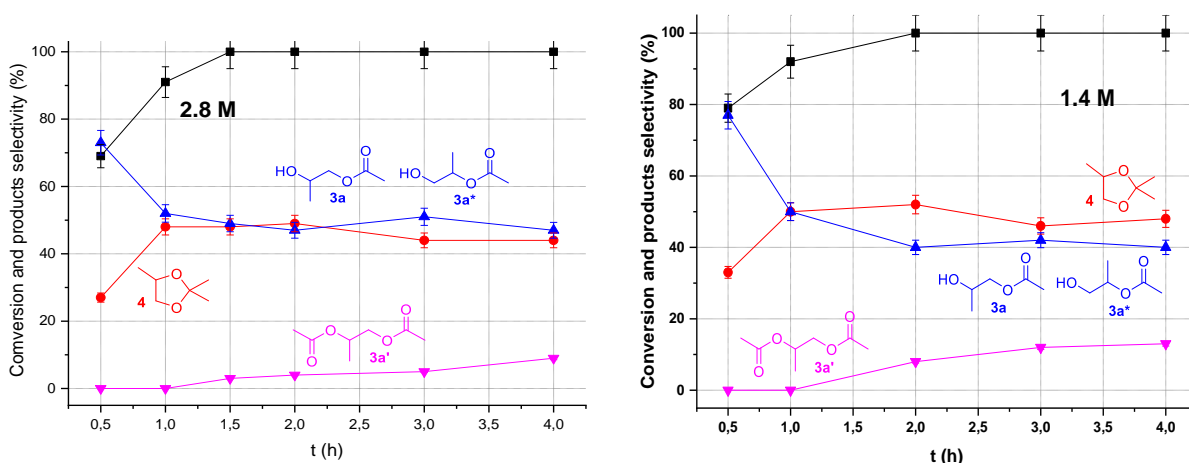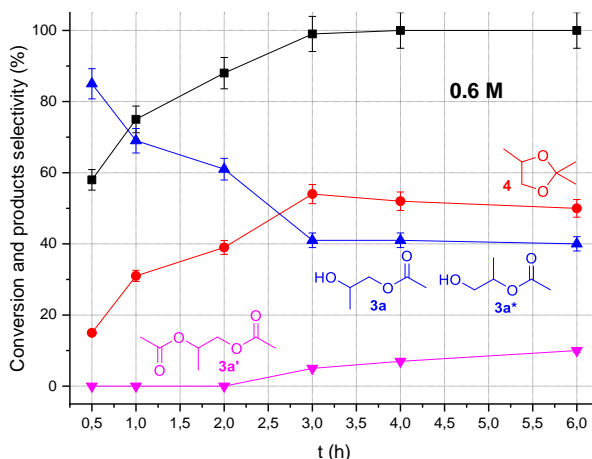
Figure 2.24. *The reaction of PG (1.39 mmol) and iPAc (1.39 mmol, 1 equiv.) using CPME as solvent. Experiments were carried out at 70 °C, starting from 2.8 M (top left), 1.4 M (top right) and 0.6 M (bottom) solutions. (-■-) conversion of **1**; (-●-) acetal (**4**) selectivity; (-▲-) mono-acetate (**3a**) selectivity; (-▼-) di-acetate (**3a'**) selectivity. Top, right is illustrated also in Figure 2.23*

At 50 °C, instead, the transesterification and the subsequent acetalization processes proceeded affording only the desired monoester isomers and acetal in comparable amounts (Figure 2.23, left). This behavior was consistent with paths illustrated in Scheme 2.24. Initial transesterification of PG produced isomers **3a/3a*** and prop-1-en-2-ol as a leaving group from iPAc (Scheme 2.24, equation **a**). The observed ratio **3a/3a*** = 1.9 reflected the higher reactivity of primary vs secondary OH functionalities of the diol. Next, enol tautomerization made the transesterification process irreversible by releasing acetone which, as soon as formed, triggered the acetalization of **1** (Scheme 2.24, equation **b**). This was evident from the increase of compound **4** as the reaction proceeded (Figure 2.23, left: **red** profile). Once all PG was consumed, *mono*-esterification compounds (as the sum of **3a** and **3a***) and **4** were achieved in substantially equivalent amounts (ca. 50% each), thereby indicating that acetone was quantitatively formed and consumed.
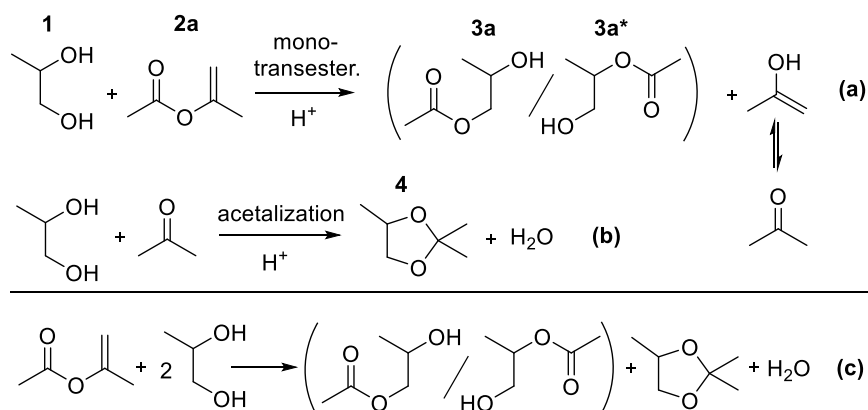
Scheme 2.24. *One-pot tandem acid-catalyzed sequential transesterification/acetalization between PG (1) and iPAc (2a)*

The acid catalyst enhanced the electrophilic reactivity of both the enol ester and acetone and facilitated the release of water as a leaving group in the acetalization step. At 50 °C, not only did the desired tandem sequence take place, but the relative kinetics of transesterification and acetalization also steered the two reactions to proceed with the maximum allowed extent. The

55

overall transformation occurred with 100% carbon efficiency (CE) and high atom economy, forming water as the sole byproduct (Scheme 2.24, equation **c**).[29] Finally, increasing the temperature to 90 °C mostly affected the reaction time: conversion of PG was complete after at 1 h, while the product distribution was similar to that achieved at 70 °C, with a selectivity for compounds **3a/3a***, **3a'**, and **4** of 39%, 50%, and 11%, respectively.

Effect of the reactants molar ratio. The trend of Figure 2.23 (right, at 50 °C) showed that although iPAc was present in a large excess compared to acetone throughout the tandem process, the acetylated derivatives and the acetal product were achieved in almost identical amounts. This seemed consistent with the well-known electrophilic reactivity of carbonyl compounds, higher to that of esters, towards any nucleophilic partner.[30] To gain insights on this aspect, additional experiments were carried out in which PG was set to react competitively with an equimolar mixture of acetone and isopropenyl acetate. Results are summarized in Table 2.5. Experiments were carried out mixing equimolar amounts of acetone, iPAc and PG (11.3 mmol each) using CPME as solvent (8 mL, 1.4 M) (Figure 2.25, top). After three evacuation/back-fill cycles with N$_2$, the mixture was set to react at different temperatures (T = 50, 70 and 90 °C), in presence of Amberlyst-15 as catalyst (129 mg, 15 wt %). Figure 2.25 (bottom) reports the conversion of PG (**1**) and products distribution as function of time.

Table 2.5. *Competitive reactions of propylene glycol with acetone and isopropenyl acetate*

Entry 1	1:2a:acetone (molar ratio)	T (°C)	t (h)	Conv. (%)[a]	Selectivity (%)[b]		
					3a/3a*[c]	3a'	4
1		50	4	75	1		99
2	1	70	4	100	31	4	65
3		90[d]	4	100	48	9	43

All reactions were carried out using an equimolar mixture of **1a**, **2a**, and acetone (11.3 mmol each) dissolved in CPME (8 mL; 1.4 M) as solvent. Amberlyst-15 (129 mg, 15 wt%) [a] Conversion of propylene glycol (**1**). [b] Selectivity towards products **3a**, **3a'** and **4**. [c] Total amount of monoester isomers **3a** and **3a***. [d] The reaction was carried out in a closed vessel (autoclave) to minimize the evaporation of acetone.
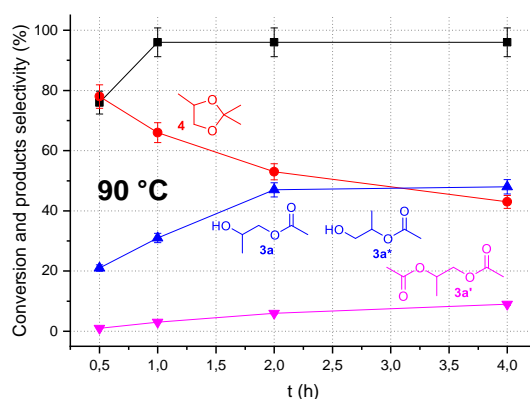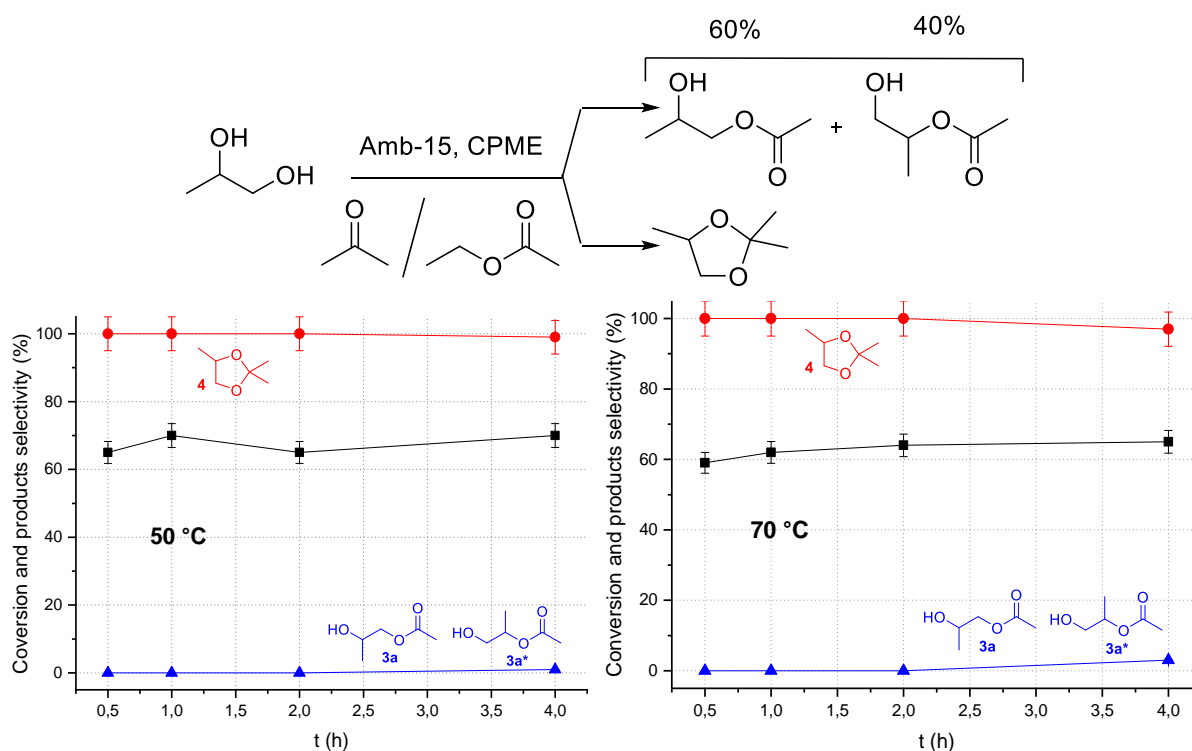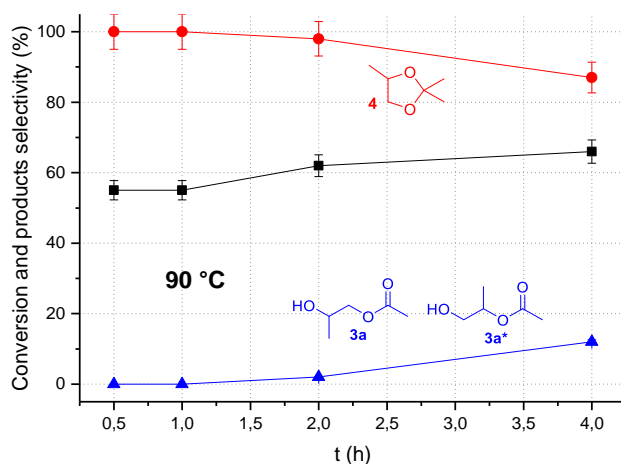

56
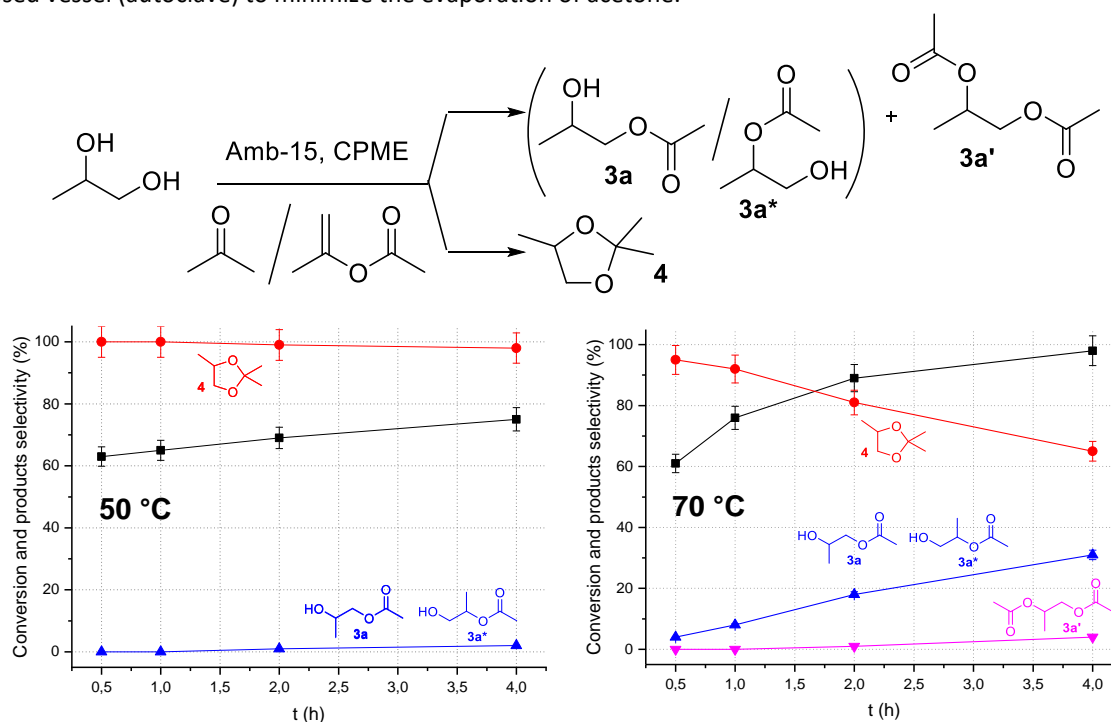
Figure 2.25. *The reaction of an equimolar mixture of acetone, isopropenyl acetate and 1,2-propanediol (11.3 mmol each) in CPME as a solvent (8 mL, 1.4 M). Experiments carried out at 50, 70, and 90 °C are shown at the top left, top right, and bottom, respectively. (-■-) conversion of 1; (-●-) acetal (4) selectivity; (-▲-) mono-acetate (3a) selectivity; (-▼-) di-acetate (3a') selectivity*

At 50 °C, in the presence of Amberlyst-15 as a catalyst, the selectivity ratio of products **4** and **3a/3a*** was 99:1 (entry 1), highlighting a far superior reactivity of acetone with respect to isopropenyl acetate, and thus explaining why the tandem sequence of Scheme 2.24 occurred despite the different concentration of the two reactants. In analogy to results of Figure 2.23, an increase of the temperature progressively favored the transesterification that became the predominant reaction at 90 °C, producing both **3a/3a*** and **3a'** in a 57% selectivity (entry 3). This trend was further confirmed by other competitive experiments carried out under the conditions of Table 2.5 but replacing isopropenyl acetate with ethyl acetate (Figure 2.26). Experiments corroborated the results of Figure 2.25; though, the amount of the ester products was considerably lower than that obtained with iPAc. This was ascribed to the higher propensity of enol esters towards nucleophilic attacks with respect to conventional esters.[20]

Figure 2.26. *The reaction of an equimolar mixture of acetone, ethyl acetate and 1,2-propanediol (11.3 mmol each) in CPME as a solvent (8 mL, 1.4 M). Experiments carried out at 50, 70, and 90 °C are shown at the top left, top right, and bottom, respectively. (-■-) conversion of **1**; (-●-) acetal (**4**) selectivity; (-▲-) mono-acetate (**3a**) selectivity*

This behavior prompted us to study the tandem sequence at 50 °C using propylene glycol and isopropenyl acetate in the stoichiometric ratio of Scheme 2.24 (**1:2a** = 2, equation **c**; other conditions were those of Figure 2.23). However, decreasing the relative concentration of **2a** resulted in an unsatisfactory outcome: the corresponding selectivity leveled off to 55-60% and 40-45% for monoester isomers **3a/3a*** and acetal **4** products, respectively (Figure 2.27). This was likely due to an insufficient availability of acetone as a reactant in solution.
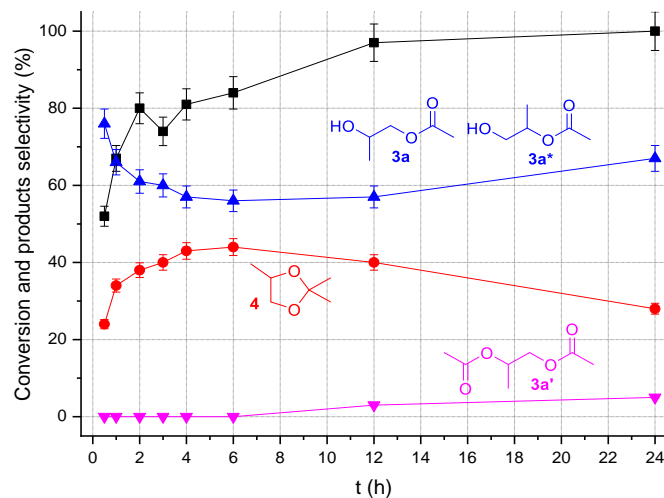
Figure 2.27. *The reaction of 1,2-propylene glycol (1.39 mmol) and isopropenyl acetate in a 1:05 molar ratio, respectively (stoichiometric ratio, Scheme 1), in CPME solvent (1 mL), at 50 °C. (-■-) conversion of **1**; (-●-) acetal (**4**) selectivity; (-▲-) mono-acetate (**3a**) selectivity; (-▼-) di-acetate (**3a'**) selectivity*

Choice of the solvent and the catalyst. Further experiments were carried out to compare the tandem reaction under solventless conditions and with different solvents and catalysts.

The reaction of PG and iPAc was first explored by replacing CPME with THF. Conditions were those of Figure 2.23: PG/iPAc = 1:1 mol/mol, T = 65 °C (reflux THF), Reactants concentration in the range of 0.6 and 2.8 M. In all cases, conversion and products distribution in THF were similar to those achieved in CPME (cfr. Figure 2.23 right and Figure 2.24). Variations, on average, were within ±3 %. In both solvents, the tandem sequence was observed by helping the

58

acetalization process plausibly through solubilization and confinement of (volatile) acetone in the liquid phase of reagents. By contrast, a non-negligible drop in the formation of the acetal product was noticed when performing the reaction under solventless conditions: mixing equimolar amounts of **1** and **2a** in presence of Amberlyst-15 (15 wt %) as catalyst at T = 50 °C resulted in a quantitative conversion of **2a** in t = 6 h, but the diol transesterification largely over its acetalization. Products **3a/3a*** and **4** were obtained in 56 and 44% yield, respectively. Common protic solvents as light alcohols were obviously ruled out due to their competitive reactivity with PG, while other commonly employed polar aprotic solvents, such as DMF and DMSO, were not tested because of their high boiling points, difficult separation and/or toxicity.

The catalytic performance of heterogeneous Amberlyst-15 was compared to that of two homogeneous Brønsted acid catalysts: H_2SO_4, a commonly employed as transesterification catalyst, and an organocatalyst, the ionic liquid BSMIMHSO$_4$. Control experiments were carried out under the following conditions: at T = 50 °C: equimolar amounts of **1** and **2a** (1.39 mmol) were dissolved in CPME (1 mL; 1.4 M) and set to react in presence of the chosen acid catalyst. The amount of homogeneous catalyst employed was calculated based on acid sites available for the reaction catalyzed by Amberlyst-15 (15.8 mg, 15 wt %, $7.9 \cdot 10^{-2}$ H$^+$ *m*eq). A blank test without catalyst was also performed, confirming that neither the transesterification nor the acetalization of **1** took place. Results are reported in Table 2.6, which summarizes conversion and products distribution after t = 4 h. For the Reader convenience, results obtained with Amberlyst-15 are also included (Entry 2, Table 2.6).

Table 2.6. *The reaction of 1,2-propylene glycol with iPAc in the presence of different acid catalysts*[a]

| Entry	Catalyst (amount, mg)	Conv. (%)[b]	Selectivity[b]		
			3a/3a*[c]	4	3a'
1	None	< 1			
2	Amb-15 (15.8)	78	62	38	
3	H_2SO_4 (3.63)	62	59	36	5
4	BSMIMHSO$_4$ (22.4)	71	61	35	4

[a]All reactions were carried out at 50°C for 4 h, using an equimolar solution of 1,2-propylene glycol and isopropenyl acetate (1.39 mmol) in CPME (1 mL, 1.4 M). [b] Conversion and selectivity were determined by GC with responses corrected by calibration curves. Products were mono-acetate isomers **3a/3a***, dimethyl acetal **4**, and di-acetate **3a'** as defined in Scheme 4. [c] Total amount of isomers **3a** and **3a***

At comparable products distributions, the higher conversion was obtained with the acid resin (entry 1). Overall, results highlighted that the presence of the solvent was crucial to the success of the tandem sequence, while the choice of the catalysts mostly affected the diol conversion: the best combination was observed with a polar aprotic ether as CPME and THF, and Amberlyst-15 rather than homogeneous systems as H_2SO_4 and BSMIMHSO$_4$, to improve both conversion and selectivity of the process.

Other isopropenyl esters (iPEs). The scope of the tandem sequence between PG and iPAc (**2a**) was extended to higher ester homologues such as isopropenyl phenylbutyrate (**2b**) and

isopropenyl octanoate (**2c**). The effect of the temperature on the reactivity of **2b** and **2c** was explored in the range 50-110 °C, under the same conditions of Figure 2.23.

As observed for iPAc, reproducible tandem transesterification/acetalization was feasible also for enol esters **2b** and **2c**. However, clear reactivity differences emerged. Results are summarized in Scheme 2.25 which shows the observed products, and Figure 2.28 which illustrates conversion profiles and selectivity against time obtained at 70 and 90 °C, respectively, for the reaction of **2b** and **2c**, respectively.
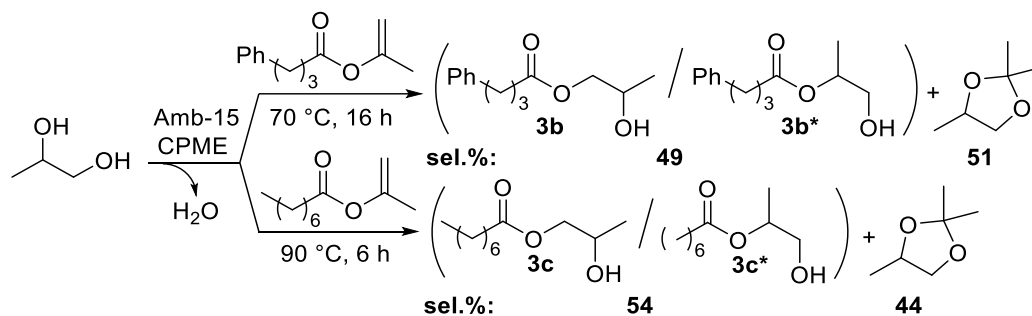
Scheme 2.25. *Tandem transesterification/acetalization between PG and isopropenyl phenylbutyrate (top) or isopropenyl octanoate (bottom)*
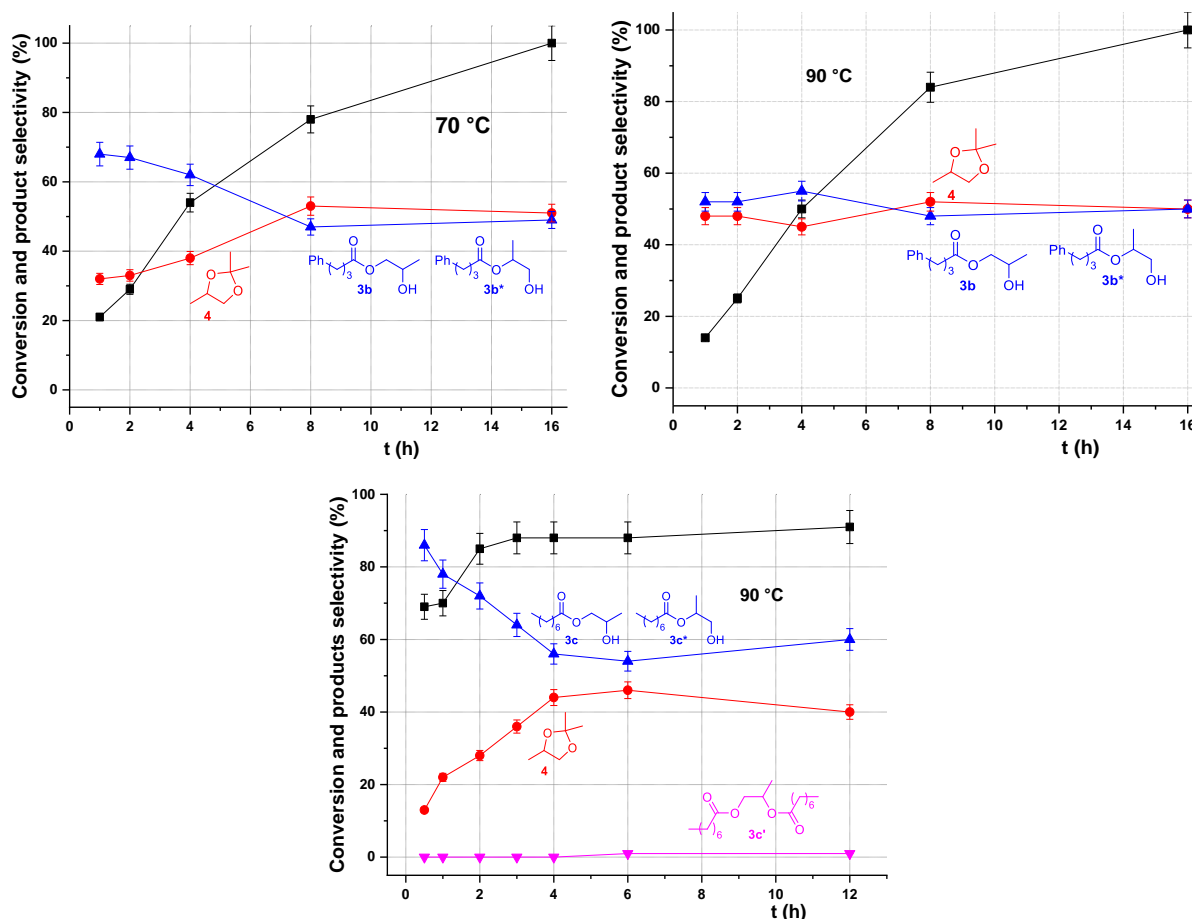
Figure 2.28. *The reaction of an equimolar solution of 1,2-propylene glycol (**1**, 1.39 mmol) with: **a**) i-propenyl phenylbutyrate (**2b**) at 70 °C, top-left; **b**) i-propenyl phenylbutyrate (**2b**) at 90 °C, top, right. **c**) i-propenyl octanoate (**2c**) at 90 °C, bottom; Other conditions: CPME solvent (1 mL) and Amberlyst-15 (15 wt%). The reaction of **2c** was carried out in a closed vessel (autoclave). (-■-) conversion of **1a**; (-●-) acetal (**4**) selectivity; (-▲-) mono-ester product (**3b**, left; **3c**, right) selectivity; (-▼-) di-ester product (**3c'**, right) selectivity*

The reaction of PG with isopropenyl phenylbutyrate **2b** showed quantitative conversion of the diol at 70 °C after 16 h, with 49% and 51% selectivity toward tandem products **3b/3b*** and **4**, respectively (Figure 2.28, **a**). Increasing the temperature to 90 °C accelerated equilibration between the tandem reactions without any substantial change of the product distribution and, surprisingly, of the conversion rate of PG (Figure 2.28, **c**). By contrast, at 50 °C, the reaction was extremely slow, with more than 50% of unreacted **1** after 8 h (the profile is not reported in Figure 2.6). The ratio of two monoester isomers **3b** and **3b*** was rather constant (1.5:1) regardless of conditions, while the diester product [propane-1,2-diyl bis(4-phenylbutanoate) **3b'**] was never observed. The reaction of PG with isopropenyl octanoate **2c** showed high conversion (90%) only at 90 °C, though the tandem selectivity was slightly below that of other enol esters. Products of *mono*-transesterification **3c/3c*** (in a 1.5:1 ratio) and acetalization **4** were obtained in 54% and 44% amounts, respectively, with traces (≤2%) of diester **3c'** (Figure 2.28, **b**). Increasing T to 110 °C allowed a quantitative process but was detrimental for selectivity due to the formation of a significant amount (37%) of caprylic (octanoic) anhydride. The mass balance of tandem sequences was further validated with additional experiments where reactions of **1** with **2a**, **2b**, and **2c** were scaled up by a factor of 10 (13.2 mmol of each reagent; [**1**] = [**2a**] or [**2b**] or [**2c**] = 1.4 M in CPME). Other conditions were those of Figure 2.23 and Figure 2.24. Mixtures of monoester isomers **3a/3a***, **3b/3b***, and **3c/3c*** were thus isolated in 0.78, 1.32, and 1.17 g yields (89%, 92%, and 81% based on quantitative conversion of **1** and 51%, 49%, and 54% selectivity, respectively).

The comparison of Figure 2.23 and Figure 2.28 highlighted the influence of the nature of the enol ester on the reaction outcome and indicated the need of a case-by-case optimization of conditions. In particular, the observed reactivity order, i.e., acetate > phenylbutyrate > octanoate, suggested an effect of the alkyl chain length in the α position at the ester function. In this respect, Goodwin Jr. et al. reported that, in the presence of a Nafion/silica acid catalyst, esterification rates of C_3-C_8 linear carboxylic acids systematically decreased with growth of the alkyl chain.[31] This led to the conclusion that the reactivity was controlled by steric factors, but through restrictions of the conformational freedom of reagents adsorbed on the solid surface of the catalyst that gave rise to a "conformational leveling" effect.[32] An analogous reasoning was plausible for reactions of enol esters **2a**-**2c** in which the Amberlyst resin catalyst bears sulfonic acid sites anchored to an organic matrix as in the Nafion polymer.

2.2.2   Tandem Reactions of PG (1) under Continuous-Flow

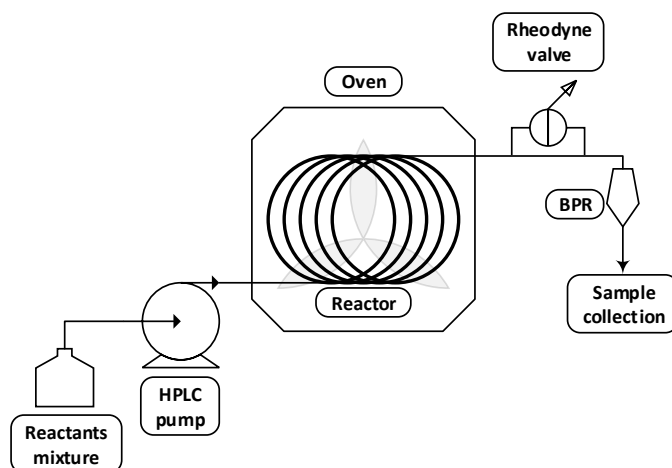*Conditions.* The reaction of PG and iPAc was explored in the continuous flow (CF) using the apparatus of Figure 2.29.

Figure 2.29. *Experimental setup used for continuous-flow reactions*

The apparatus was in-house assembled. An HPLC pump was used to send the reactants solution (diol, enol ester, and the solvent) to a stainless-steel tubular reactor (l = 12 cm, i.d. = ¼", inner volume = 1.16 cm^3) filled with the solid catalyst. At the outlet of the reactor, a manual Swagelok KPB1N0G412 back pressure regulator (BPR), equipped with an electronic pressure sensor, was used to control the system pressure. Reactions were all carried out at a pressure slightly above ambient conditions to overcome the pressure drop within the continuous-flow system. The reaction mixture was sampled by a Rheodyne valve (7725i) with a 100 μL loop, placed between the reactor and the BPR.

Effect of T and flow rate. Experiments were performed by continuously delivering an equimolar solution of **1** and **2a** ([**1**] = [**2a**] = 1.2 M) in THF solvent, to a catalytic bed of Amberlyst-15 (0.8 g). Because of the large solvent volumes required in the CF mode, initial tests were run with THF, more affordable than CPME. Reactions were run at p = 1.3-1.5 bar, varying T and flow rates (F) in the range 30-70 °C and 0.1-0.6 mL min^{-1}, respectively. Results are described both in Figure 2.30, which shows the composition of reaction mixtures after 3 h, as a function of T and F, and in Table 2.7, which reports the reaction productivity.
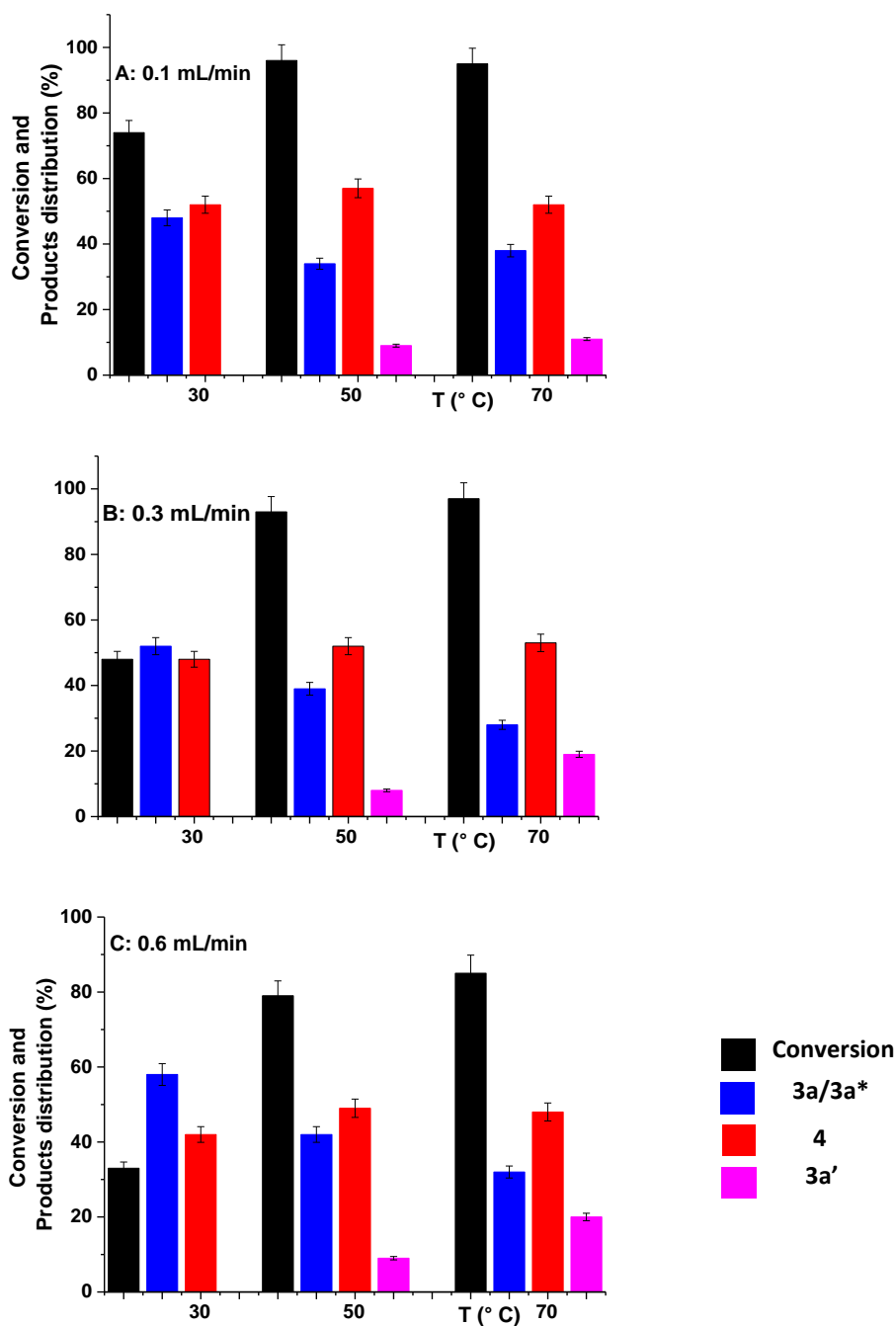
Figure 2.30. *The continuous-flow reaction of an equimolar solution of PG (**1**) and iPAc (**2a**) ([**1**]=[**2a**]=1.2 M) in THF solvent using Amberlyst-15 (0.8 g) as a catalyst. The flow rate (F) was set at 0.1, 0.3, and 0.6 mL/min at T of 30, 50, and 70 °C. The reaction time was 3 h in all cases. (-■-) conversion of **1**; (-■-) acetal (**4**) selectivity; (-■-) mono-acetate isomers (**3a/3a***) selectivity; (-■-) di-acetate (**3a'**) selectivity*

Table 2.7. *Comparison of the productivity of tandem reaction of 1,2-propanediol and isopropenyl acetate in batch and continuous-flow mode*

Entry	Reaction mode	Conc. (M)[c]	T (°C)	Flow rate (mL min⁻¹)	Conv (%)[d]	Product selectivity (%)		Productivity [e] [mmol 4 (g_{cat} h)⁻¹]
						3a/3a*	4	
1	Batch [a]	1.4	50	-	100	49	51	3.5
2	CF [b]	1.2	30	0.1	74	48	52	3.1

3	CF [b]	1.2	30	0.3	48	51	49	6.2
4	CF [b]	1.2	30	0.6	33	58	42	6.9
5	CF	4.8	30	0.1	52	48	52	9.7

[a] Conditions of Figure 1 (right). [b] Conditions of Figure 4. [c] Concentration (M) of reactants solution. [d] Conversion of 1,2-propanediol. [e] Productivity calculated on the acetal derivative **4**.

The selected time (3 h) was sufficient to achieve steady conversion and product selectivity over time. Additional control tests demonstrated that no changes were appreciable even after prolonged runs up to 12 h. Experiments proved the feasibility of the tandem reaction in the CF mode in a relatively narrow window of conditions. The best outcome was achieved at 30 °C and F = 0.3 mL min^{-1} (Figure 2.30, top left): the products of *mono*-transesterification **3a/3a*** (in 1.9:1 ratio) and acetalization **4** formed in a selectivity of 51% and 49%, respectively, very close to the theoretical expected value, and the productivity was 6.2 mmol **4** (gcat h)$^{-1}$, almost twice higher than that of the best batch reaction occurring at 50 °C (compare Figure 2.23 and entries 1-3 of Table 2.7). The mixture at the reactor outlet was recovered in a substantially quantitative amount (53 mL, >98% after 3 h), and its distillation afforded monoester isomers **3a/3a*** in an isolated yield of 1.8 g (94% based on conversion and selectivity of entry 3), and pure solvent (THF) in up to 95% of its initial volume. The acetal **4** was also isolated: its purity, however, did not exceed 85% (by GC) due to a residual amount of solvent. At the same T (30 °C), increasing F at 0.6 mL min^{-1} resulted in a lower conversion (33%), consistent with a shorter contact time (τ = 1.9 min), but still with a slight increase, up to 6.9 mmol (gcat h)$^{-1}$, of productivity (Figure 2.30, bottom; entry 4, Table 2.7). The latter was remarkably improved with more concentrated reaction mixtures. Operating at 0.1 mL min^{-1}, a test carried out by quadrupling [**1**] and [**2a**] from 1.2 to 4.8 M yielded a conversion of 52% and a selectivity for tandem products **3a/3a*** and **4** of 48% and 52%, respectively, with a productivity enhanced to 9.7 mmol **4** (gcat h)$^{-1}$ (entry 5, Table 2.7). Temperatures above 30 °C were always detrimental for the product distribution. At both 50 and 70 °C, the conversion of **1** increased up to quantitative values, but the *di*-esterification reaction could not be ruled out as product **3a'** formed in amounts of 9-19% (Figure 2.30: right, magenta bars), nor was the tandem selectivity improved by varying the flow rate. An additional experiment proved that at 30 °C the catalyst could be used almost indefinitely. The activity of Amberlyst-15 was not altered even after 4 weeks (ca. 40 h week^{-1}) of time on-stream as shown in Figure 2.31 reporting the conversion of **1** and the selectivity toward products **4** and **3a/3a*** with time.
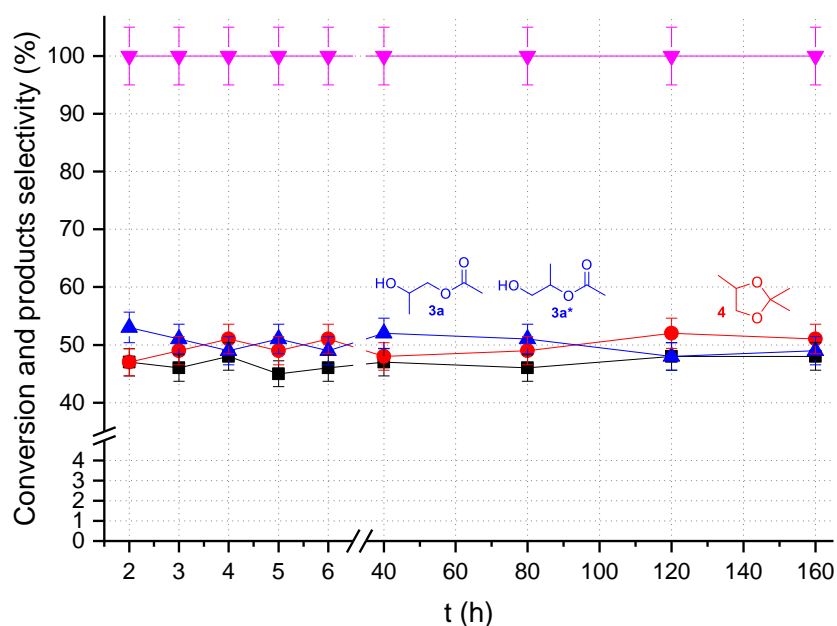
Figure 2.31. *Reaction of an equimolar solution of 1,2-propylene glycol (**1**) and iPAc (**2a**) (1.2 M) in CPME solvent at 30 °C, under continuous-flow conditions (flow rate: 0.3 mL min^{-1}). (black ■) Conversion of **1**; (red ●) acetal (**4**) selectivity; (blue ▲) monoacetate (**3a/3a***) selectivity; (magenta ▼) total tandem selectivity (sum of the selectivity toward acetal and monoacetate products)*

Profiles were substantially steady with values oscillating in the range 46-48% for conversion (**black** curve), and 49-53% and 47-52% for selectivity on products **3a/3a*** (both monoester isomers) and **4**, respectively (**red** and **blue** curves). The total selectivity of the tandem process was always 100% (**magenta** trace) since not even traces of other derivatives were observed during the reaction. Once recovered after 160 h of usage, the Amberlyst solid did not show appreciable changes of its acid titer and weight with respect to the fresh catalyst (Table 2.8). Moreover, NMR analyses of the reaction mixture did not display any aromatic signal, thereby offering further indications that the resin was stable under the investigated conditions, and no leaching occurred during the tandem reaction. Mild reaction conditions (30 °C, 1 atm, nonaggressive reactants) most plausibly accounted for such behavior.

Table 2.8. *Weight and acid titre of Amberlyst-15 before and after use in the continuous flow apparatus*

Entry	Sample	Weight (g)	Concentration of active sites (eq/Kg)[c]			
			T_1	T_2	T_3	Average[d]
1	*Fresh*[a]	0.807	2.7	2.7	2.7	2.7
2	*Used*[b]	0.817	2.8	2.8	2.8	2.8

[a]Fresh catalyst loaded in the CF-reactor; [b]Catalyst after 160 h of time-on-stream, in the reaction of 1,2-propanediol and isopropenyl acetate (conditions of Figure 2.31). [c] Equivalents of H$^+$ acid sites per Kg of wet resin determined in three independent titration tests (T_1, T_2, and T_3, respectively). [d]Average acid titre of the resin.

Reactant molar ratio. An interesting difference between CF and batch reactions was observed when PG and iPAc were employed in a 2:1 molar ratio in THF solvent.
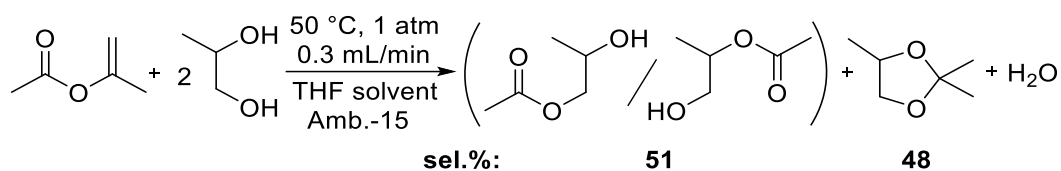
Scheme 2.26. *CF-tandem sequence using stoichiometric reagents*

Control experiments proved that, at 50 °C and F = 0.3 mL min^{-1}, a 68% conversion of PG was reached, with products **3a/ 3a*** and **4** being formed in a 51% and 48% selectivity (Scheme 2.26), demonstrating that CF conditions could optimize the kinetics of *mono*-transesterification and acetalization processes even when reactants were used in the stoichiometry ratio (Figure 2.32).
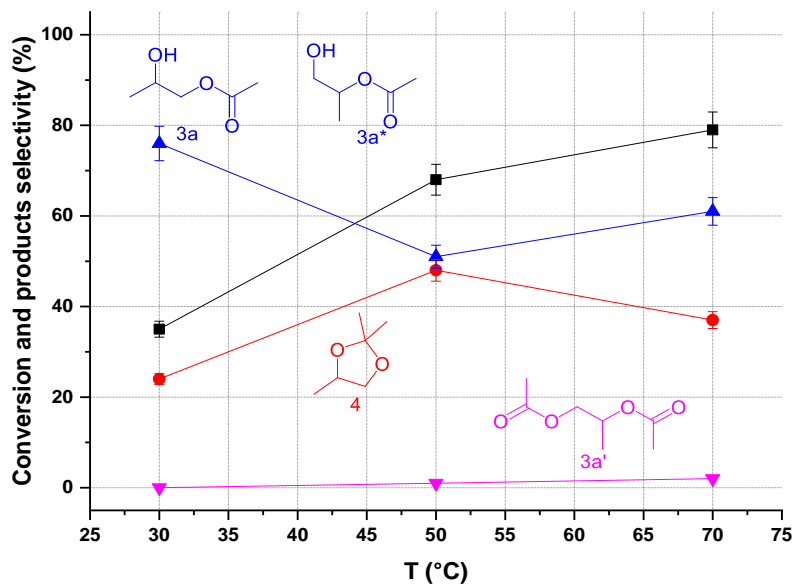

Figure 2.32. *The continuous-flow reaction of 1,2-propylene glycol and i-propenylacetate in a 2:1 molar ratio. Reactants concentration was 1 and 0.5 M in THF solvent. Other conditions: Amberlyst-15 (0.8 g); flow rate = 0.3 mL/min; T =30, 50, and 70 °C. The reaction time was 3 h in all cases. (-■-) conversion of 1; (-■-) acetal (4) selectivity; (-■-) mono-acetate (3a/3a*) selectivity; (-■-) di-acetate (3a') selectivity*

At 30 °C, the monoester isomers **3a/3a*** were the largely predominant product suggesting that the concentration of acetone released by *i*-propenyl acetate (in a stoichiometric amount) was not enough to impart a sufficient acetalization rate. However, increasing the temperature at 50 °C brought about an increase of conversion to 68% and improved the kinetics of the acetal formation so that the two tandem products formed in comparable selectivity (51 and 48%). A further rise of T to 70 °C unbalanced the products distribution once again in favour of transesterification derivatives as shown either by the increase of products **3a/3a*** and by the onset of *di*-esterification reaction yielding compound **3a'**.

Additional CF experiments were carried out also by using CPME solvent. An equimolar solution of **1** and **2a** ([**1**] = [**2a**] = 1.2 M) in CPME, was fed continuously to a tubular stainless-steel reactor filled with the catalyst (Amberlyst-15, 0.8 g). Tests were carried out at atmospheric pressure by varying T and flow rate (F) between 30-50 °C and 0.1-0.6 mL·min^{-1}, respectively. Reaction mixtures were collected at the outlet of the CF-reactor and analyzed by GC and GC/MS. Conversion of **1** and products distribution were determined as previously described for batch reactions. The results are summarized in Figure 2.33: a 3D-view was chosen to report composition of reaction mixtures after t = 3 h as a function of the operating temperature and flow rates. Minor effects on conversion were noticed, though; compared to THF, the

transesterification process was moderately favored over acetalization. This was noticed when performing the tandem reaction at T = 30 °C, observing formation of the corresponding transesterification (**3a/3a***) and acetalization (**4**) products in selectivity of 56 and 44 % at F = 0.3 mL·min^{-1}, and 71 % and 29 % at F = 0.6 mL·min^{-1}, respectively. Although this behavior is still unclear, short contact times of CF-reactions likely emphasized the differences in boiling points and dielectric constants of THF (66 °C and 7.58) and CPME (106 °C and 4.76). Other properties as η, ρ and surface tension are indeed very similar from one solvent to another.[33]
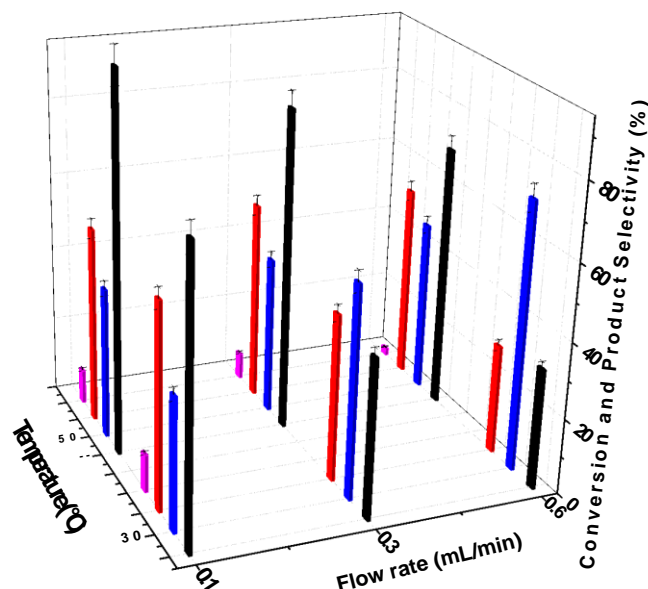
Figure 2.33. *The continuous-flow reaction of an equimolar solution of 1,2-propylene glycol (**1**) and i-propenylacetate (**2a**) (1.2 M in each reagent) in CPME solvent in the presence of Amberlyst-15 (0.8 g). The flow rate was set at 0.1, 0.3, and 0.6 mL/min at T of 30 and 50 °C. The reaction time was 3 h in all cases. (-■-) conversion of **1**; (-■-) acetal (**4**) selectivity; (-■-) mono-acetate (**3a**) selectivity; (-■-) di-acetate (**3a'**) selectivity*

*Enol Esters (EEs) **2b** and **2c** in the CF mode.* Both **2b** and **2c** were not commercially available compounds and needed to be synthesized on a relatively large scale to run CF reactions requiring up to 4.5-5 g(EE) h^{-1}. Therefore, only few CF reactions of PG with **2b** and **2c** were carried out. Experiments confirmed the reactivity order observed under batch conditions, **2a** > **2b** > **2c**, but the tandem selectivity was not optimized. At 50-70 °C and F = 0.3 mL min^{-1}, conversions of 83-88% were achieved, with a ratio between isomer products of monotransesterification and the acetal **4** in the variable range 2.2-3. Details are reported in Table 2.9.

Table 2.9. *The reaction of 1,2-propanediol with i-propenyl esters **2b** and **2c** in the continuous-flow mode*

Entry	EE	T (°C)	F (mL/min)	Conv (%)^a	Product selectivity (%)^a			
					3b/3b*	3c/3c*	3c'	4
1	2b	50	0.3	88	75			25
2	2c	70	0.3	83		68	1	31

Reactions were carried using an equimolar (1.4 M) solution of 1,2-propanediol and enol ester, **2b** or **2c**, in THF as the solvent. ^{a}Conversion of 1,2-propanediol, products distribution, and mass balance were validated and determined by an external standard (see experimental). Data refer to 4 h runs. Mono-ester isomers **3b**-**3b*** and **3c**-**3c*** formed in a 1.5:1 ratio.
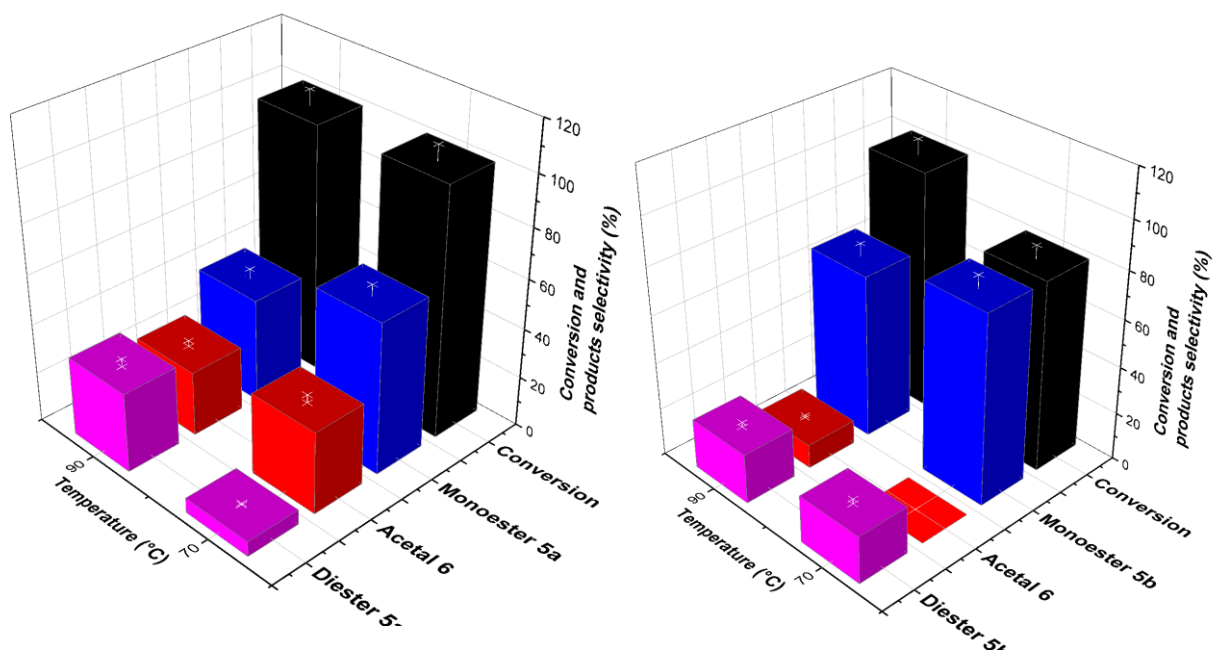
2.2.3 Tandem reactions of ethylene glycol (5)

Ethylene glycol (EG, **5**) was chosen as another 1,2-diol to explore the reaction with isopropenyl-acetate (**2a**), phenylbutyrate (**2b**), and octanoate (**2c**). Batch experiments were carried out under the conditions previously described for PG in Figure 2.23 and Figure 2.30, by varying the temperature in the range 50-90 °C. GC/MS analyses proved the formation of mono- (**5a-5c**) and *di*-transesterification (**5a'-5c'**) products and of dimethyl acetal **6** derived from EG (Scheme 2.27).

a: X=H, n=0; **b**: X=Ph, n=3; **c**: X=Me n=6
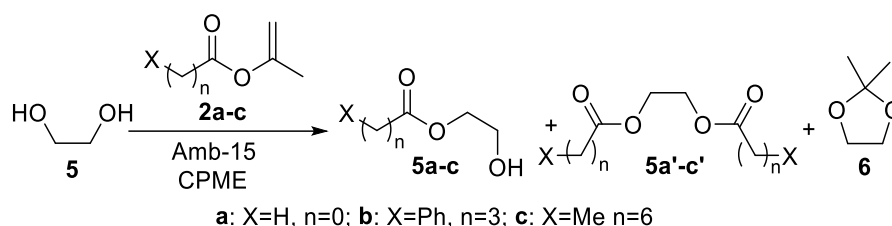
Scheme 2.27. *Tandem transesterification/acetalization reactivity between EG (**5**) and enol esters **2a-c***

Figure 2.34 detail the profiles of conversion and selectivity for the reaction of each single enol ester, at 70 and 90 °C, respectively. The previously observed reactivity scale, acetate > phenylbutyrate > octanoate, was confirmed also with EG. For example, at 70 °C after 4 h, conversion of **5** was 30%, 80%, and 100% in the reactions with **2c**, **2b**, and **2a**, respectively. In the case of **2a**, conversion was >99% even at 50 °C. The tandem selectivity, however, could not be controlled efficiently. At 50 °C, derivatives **5a**, **5a'**, and **6** were obtained in 60%, 2%, and 38% amounts, respectively. Increasing T to 70 and 90 °C further favored the transesterification reaction: the total selectivity toward mono- and diester products (**5a**-**5c** and **5a'**-**5c'**) was in the range 74−100% regardless of the enol ester used (Figure 2.34, **blue** and **magenta** bars).
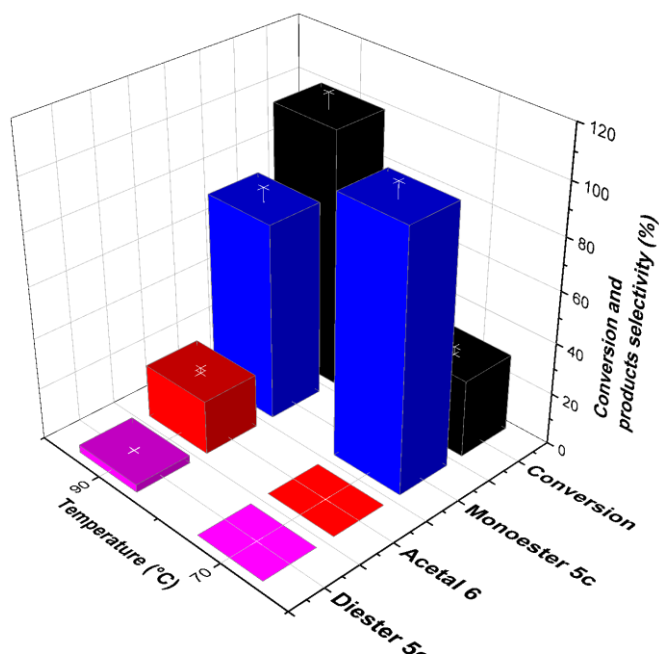
Figure 2.34. *The reaction of an equimolar solution of ethylene glycol (**5**, 1.39 mmol) with: **a)** i-propenyl acetate (**2a**); **b)** i-propenyl phenylbutyrate (**2b**); **c)** i-propenyl octanoate (**2c**). Other conditions: CPME solvent (1 mL) and Amberlyst-15 (15 wt%). (-■-) conversion of **5**; (-■-) acetal (**5**) selectivity; (-■-) mono-ester product (**5a** or **5b** or **5c**) selectivity; (-■-) di-ester product (**5a'** or **5b'** or **5c'**) selectivity*

The reaction of ethylene glycol (**5**) and iPAc (**2a**) was then investigated in the CF mode under a variety of conditions by changing T (30-70 °C), flow rate (0.1–0.9 mL min^{-1}), reactant concentration (1.2-4.8 M), and relative molar ratio (**2a:5** = 1-0.5 mol mol^{-1}). Details are in Table 2.10.

Table 2.10. *Continuous-flow reaction of ethylene glycol (**5**) with iPAc (**2a**)*

Entry	Flow rate (mL/min)	T (°C)	2a:5 (mol:mol)	Conc. (M)[a]	Conv (%)[b]	Product selectivity (%)[b]		
						5a	5a'	6
1	0.1	30	1:1	1.2	73	69		31
2	0.1	50	1:1	1.2	98	69	4	27
3	0.1	70	1:1	1.2	99	69	9	22
4	0.3	50	1:1	1.2	94	67	2	31
5	0.6	50	1:1	1.2	75	67	1	32
6	0.9	50	1:1	1.2	65	69	1	30
7	0.1	50	1:1	2.4	97	69	4	27
8	0.1	50	1:1	4.8	99	79	3	18
9	0.1	50	0.5:1	1.2	68	71		29

[a] Molar concentration of **5** in THF. [b] Conversion of ethylene glycol, and products distribution determined by an external standard.

As for batch reactions, conversions of **5** as high as 98% were reached at T ≥ 50 °C, though the best selectivity toward the acetal product **6** did not exceed 31%. The most plausible reason for this behavior was ascribed to the presence of two equivalent primary hydroxyl groups in EG. Both these functions underwent a rapid transesterification reaction with enol esters, reducing the availability of EG for the subsequent step of acetalization. When the enol ester (iPAc) was more reactive, the transesterification was easier, and the amount of corresponding *mono-* and *di*-ester derivatives (**5a** and **5a'**) was higher.

2.2.4 Conclusions

A never previously reported tandem sequence has been accomplished by the reaction of propylene glycol with isopropenyl esters, during which the transesterification of the diol occured first, generating acetone that triggered a subsequent acetalization step. Reaction products, the monoester and the acetal derivatives of the diol, were obtained with equal selectivity and 100% carbon efficiency. The temperature, the acid catalyst (Amberlyst-15), and the solvent (THF or CPME) played multiple roles in steering the tandem selectivity, by controlling the kinetics of the two steps, activating electrophilic partners of the reaction, and accelerating the keto−enol equilibrium which yielded acetone. The tandem sequence has proven feasible for three different enol esters, showing a reactivity order, i.e., isopropenyl-acetate > phenylbutyrate > octanoate, consistent with the effect of the alkyl chain length in the α position at the ester function. In all cases, the reaction was efficiently scaled up by a factor of 10, providing products in isolated yields of 81−92%, and it was transferred to continuous-flow mode with improved productivity, milder operating conditions (30 °C, 1 atm), and steady catalytic performance for at least 160 h of time-on-stream. When propylene glycol was replaced by ethylene glycol, a fast transesterification reaction occurred with enol esters, hindering the formation of the acetal product.

2.2.5 Experimental

Procedures for tandem reactions of transesterification and acetalization. Batch mode: at atmospheric pressure, a glass reactor shaped as a test tube (5 mL) was charged with an equimolar mixture of chosen enol esters (**2a-2c**, 1.45-1.67 mmol) and diol (propylene or ethylene glycol), Amberlyst-15 (14.7−15.8 mg, 15 wt%) as a catalyst, and cyclopentyl methyl ether (CPME) or tetrahydrofuran (THF) (0−2.5 mL) as a solvent. After three evacuation/backfill cycles with N_2, the mixture was set to react in the range 50-110 °C under stirring. Samples were withdrawn at time intervals for GC/MS analyses. A similar procedure was used to carry out reactions under pressure, by placing the glass reactor charged with the solution of reactants and the catalyst in a stainless-steel autoclave. After evacuation/backfill cycles with N_2, the autoclave was pressurized with N_2 at 8 bar and heated 90-110 °C under stirring. Conversion of diols and selectivity toward tandem products (esters and acetals) were determined by GC/MS, while the structures of products were assigned by GC/MS and ^1H and ^{13}C NMR (see the Appendix A.2). All reactions were performed twice: conversion and selectivity values differed by less than 5% in duplicated experiments, thereby confirming the reproducibility of the procedure. Continuous-flow mode: experiments were performed using the continuous-flow (CF) apparatus described in Figure 2.29. In a typical procedure, the CF apparatus was first conditioned with the solvent of choice (30 mL at 5 mL min^{-1}), and then, a homogeneous 1.2-4.8 M solution of the reactants (isopropenyl ester and propanediol or ethylene glycol) in THF or CPME solvent was delivered to the catalytic bed (Amberlyst-15: 0.8 g) at the desired T and flow rates (30-70 °C, 0.1-0.9 mL min^{-1}). Aliquots (0.3 mL) of the reaction mixture were sampled at the outlet of the reactor every 30 min and analyzed by GC-MS. Reactions were usually allowed to proceed for 3 h, though some prolonged tests were carried out for up to 12 h.

General procedure for the synthesis and the isolation of isopropenyl esters (iPEs). The preparation of iPEs was carried out by adapting already reported protocols based on both the esterification of carboxylic acids and the nucleophilic substitution of acyl chlorides. In a typical

example, a mixture of octanoic acid (0.51 g, 3.55 mmol) or octanoyl chloride (0.52 g, 3.20 mmol), isopropenyl acetate (**2a**, 3.47 g, 34.70 mmol), and H_2SO_4 (17.4 mg, 0.17 mmol) as a catalyst, was subjected to four evacuation/back-fill cycles with N_2 and set to react at 95 °C under stirring for 4h. Once the reaction was complete, the product (isopropenyl octanoate, **2c**) was purified by FCC (see below), and isolated as a colorless liquid. Yields were 31 and 90 % starting from the acid and the chloride as reactants, respectively. Isopropenyl phenylbutyrate (**2b**) was prepared by the same methods: yields of **2b** were 42 and 85% starting from phenylbutyric acid and phenylbutyric chloride, respectively. The synthesis of compound **2c** was also carried out starting from the reaction of isopropenyl acetate with either octanoic acid or octanoyl chloride in the presence of BSMIMHSO$_4$ (55.0 mg, 0.17 mmol) as a catalyst, in place of H_2SO_4. Product **2c** was obtained in 45 and 56% GC/MS-yields, form acid and chloride, respectively. Isopropenyl esters (**2b**, **2c**) were isolated by flash column chromatography (stationary phase: neutral Al_2O_3, eluent: petroleum ether/ethyl acetate 9:1 v/v). Products **2b** and **2c** were characterized by both ^1H and ^{13}C NMR, and GC/MS analyses. Spectra are reported in the Appendix A.2.

The results of this work have been the object of the paper:

Davide Rigo, Giulia Fiorani, Alvise Perosa, Maurizio Selva "Acid-Catalyzed Reactions of Isopropenyl Esters and Renewable Diols. A 100% Carbon Efficient Transesterification/Acetalization Tandem Sequence, from Batch to Continuous Flow", *ACS Sustainable Chem. Eng,* **2019***, 7*, 18810-18818; doi: 10.1021/acssuschemeng.9b03359

2.3 iPEs and glycerol: the pivotal role of isopropenyl acetate (iPAc)

2.3.1 Introduction

As discussed in the Chapter 1 of this Thesis work, glycerol (Glyc) plays a preeminent role in the family of biobased platform chemicals.[34] Several reasons concur to its chemical appeal, among which the most relevant are its versatility as a solvent and/or a reagent, the impressive number of applications of its derivatives, and its market availability as a co-product of biodiesel manufacture.[35,36] These aspects have been highlighted by many recent extensive reviews on its reactivity, *e.g.* on its catalytic oxidation, hydrogenolysis, aqueous phase and steam reforming, dehydration, O-alkylation, oligomerization, and transcarbonation[37,38,39,40] and the extension of such protocols to continuous-flow operation.[41] Of particular significance in this context is also the conversion of glycerol into esters and acetals: both families of products have been and are largely investigated and used as renewable-based solvents, plasticizers, fuel additives, surfactants, flavorings, etc.[42,43,44] Two representative cases are triacetin (1,2,3-triacetoxypropane, TA) and solketal (2,2-dimethyl-1,3-dioxolane-4-methanol) derived from the triacetylation of glycerol and its condensation with acetone, respectively (Figure 2.35).

Triacetin   **Solketal**
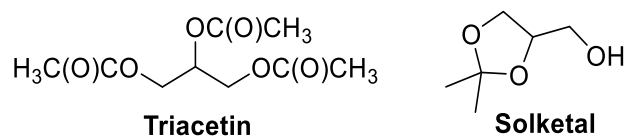
Figure 2.35. Most common derivatives of esterification and acetalization of glycerol

With a global demand of 110000 tonnes per year and an estimated CAGR (Compound Annual Growth Rate) of 4.4% for the next 8 years, TA alone accounts for ca. 10% of the worldwide glycerol market, while the current production of solketal amounts to 22 million USD.[45,46] Although both the esterification and acetalization of glycerol are apparently simple reactions, the implementation of such processes is not without issues. For example, the acetylation of glycerol with acetic anhydride (Ac$_2$O) is an excellent low energy-demanding transformation,[47] but the high potential of explosion for acetic anhydride makes its application not suitable for large-scale manufacturing (vapour/air mixtures are explosive above 49 °C),[47] not to mention the corrosivity of Ac$_2$O and the legislative restrictions to its use in many countries.[48] The same reaction in the presence of acetic acid as an acetylating agent suffers from a poor selectivity since mixtures of mono-, di-, and tri-esters are often obtained, whose isolation and purification are complicated.[49] Acetic acid may also induce undesired etherification and hydrolysis reactions, as observed during the acetylation of some glycerol derivatives.[50] On the other hand, a major difficulty with the acetalization of glycerol is the formation of water as an equilibrium coproduct, which not only weakens the acid strength of the catalyst involved in the process, decreasing the reaction conversion, but also entails corrosion and work-up problems.[51,52] As a part of a research program aimed at integrating eco-friendly synthetic protocols with the upgrading of glycerol and its derivatives,[53,26] the group with which this Thesis work was developed, recently discovered that the thermal (catalyst-free) transesterification of glycerol with isopropenyl esters was an effective option to prepare glyceryl esters: this reaction was already discussed in the paragraph 3.1.[20] Isopropenyl acetate (iPAc) emerged as a privileged reagent in this context: iPAc is a non-toxic, commercially available and cheap compound, and its reaction with glycerol resulted in the rapid irreversible formation of the corresponding methyl

esters accompanied by acetone (resulting from tautomerization of 2-propenol). It was demonstrated that when the process was carried out at T = 180-300 °C and p = 8-50 bar, glycerol underwent an exhaustive acetylation producing triacetin (>99%) in the presence of excess iPAc (20 molar equiv.; Scheme 2.28, top), while mixtures of mono-, di-, and triacetins were obtained under stoichiometric conditions (Glyc : iPAc = 1 : 1 molar ratio; Scheme 2.28, bottom: path a). For further details of this study, the discussion of Scheme 2.23 in paragraph 3.1 should be considered.
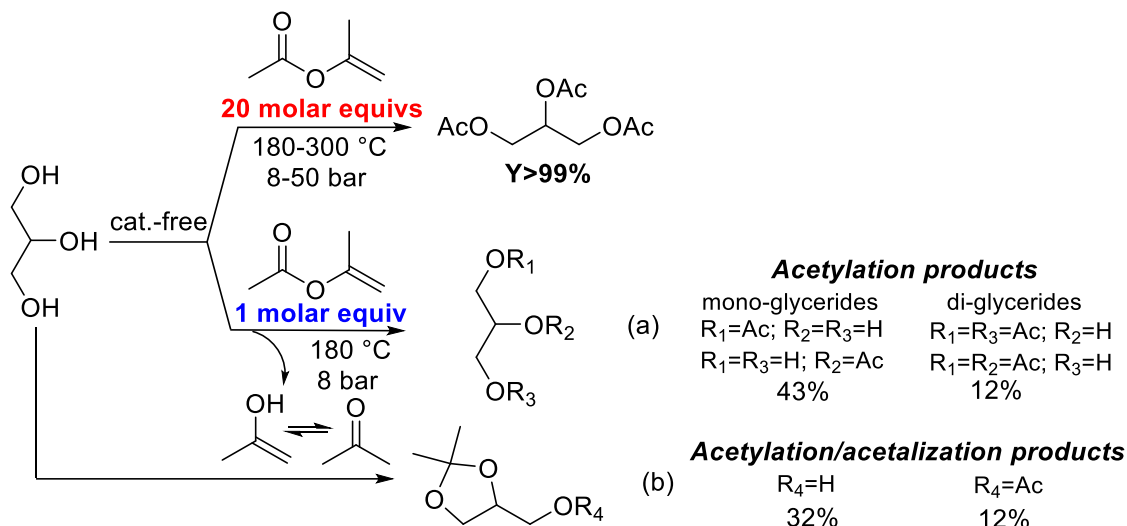
Scheme 2.28. *The reaction of glycerol promoted by isopropenylacetate (iPAc)*

Thermal conditions, however, proved not suitable to control the relative kinetics of the transesterification reaction with respect to the acetalization of glycerol, being the former largely dominant on the latter [paths (a) and (b) of Scheme 2.28].

These results prompted the research program of this Thesis work at exploring new conditions to tune the distribution of cascade products. Based on the analysis of the literature and the inspection of the reactivity of 1,2-diols with iPAc examined in the paragraph 3.2,[54,55,56] the reaction of Scheme 2.28 was studied by using Amberlyst-15 as a heterogenous acid catalyst and acetic acid (AcOH) and acetone (Ace) as co-acetylation and co-acetalization reagents, respectively. Albeit less effective than acetic anhydride, AcOH was preferred thanks to its greener features and the solvency properties. This work demonstrated that not only that the reaction of glycerol with iPAc/AcOH in the presence of Amberlyst-15 proceeded with quantitative glycerol conversion at 30-70 °C and ambient pressure, but also that its selectivity was tuned by optimizing T and the Glyc : iPAc : AcOH : Ace molar ratio. The overall process could be steered either towards the formation of solketal acetate (up to 91%) or to a 1 : 1 mixture of solketal acetate–triacetin. Such a degree of control of the product distribution, triggered by the cooperative effect of the catalyst and the combination of an enol ester, acetic acid and acetone, proved for the first time the potential of the strategy of Scheme 2.28 for preparative purposes via tandem (trans)esterification and acetalization of glycerol. Besides, this exemplified an archetypal green protocol whereby innocuous reagents and solvents allowed the selective upgrading of glycerol under mild catalytic conditions. Experiments with isotopically labelled reagents, specifically CD₃COOD and CD₃C(O)CD₃, have shed light on the mechanism and the role of each reaction partner, confirming the multiple roles of iPAc for the success of the protocol. Notably, this analysis has also proved the intermediacy of acetic

anhydride in the formation of glyceryl acetates and the unusual reactivity of iPAc which assisted the acetalization process even in the presence of excess acetone as the reagent.

2.3.2   Results and discussion

2.3.2.1 The tandem synthesis of solketal acetate and triacetin

The identification of the solvent and the catalyst was the first step in the design of experimental conditions for the reaction of glycerol (**1**) with isopropenyl acetate (**2**). Previous study of our group on such transformation proved that a polar solvent was necessary due to the very poor mutual solubility of the reagents.[20] After screening several solvents, acetic acid was chosen for its non-toxicity and its acetylating reactivity that could be complementary to that of isopropenyl acetate. A commercial Amberlyst-15 catalyst was selected based on the literature and for its comparatively better performance in terms of activity and stability for both acetylation and acetalization of glycerol compared to other heterogenous acids such as K-10, montmorillonite, niobic acid, and zeolites (H-beta, HZSM-5 and HUSY).[40]

Effect of temperature, time and reactant molar ratio. Reactions were carried out using a solution of glycerol (1; 1 mmol) in acetic acid (10 mL; 0.1 M), a variable amount of isopropenyl acetate (**2**; the molar ratio (Q) **2** : **1** = 1-10), and Amberlyst-15 (Amb15: 15 mg; 15 wt%) as the catalyst. Control experiments were performed over a range of temperatures 30-70 °C, and times varying between 4-24 h. In all cases, the observed products were: (i) solketal (**3**) and solketal acetate (**4**), along with trace amounts of the corresponding 6-membered ring isomers (**3'**: 2,2-dimethyl-dioxane-5-ol, and **4'**: 2,2- dimethyl-1,3-dioxan-5-yl acetate); (ii) two regio-isomers of both glycerol monoacetate (monoacetins: **5/5'**) and glycerol diacetate (diacetins, **6/6'**); and (iii) glycerol triacetate (triacetin, **7**) (Scheme 2.29).
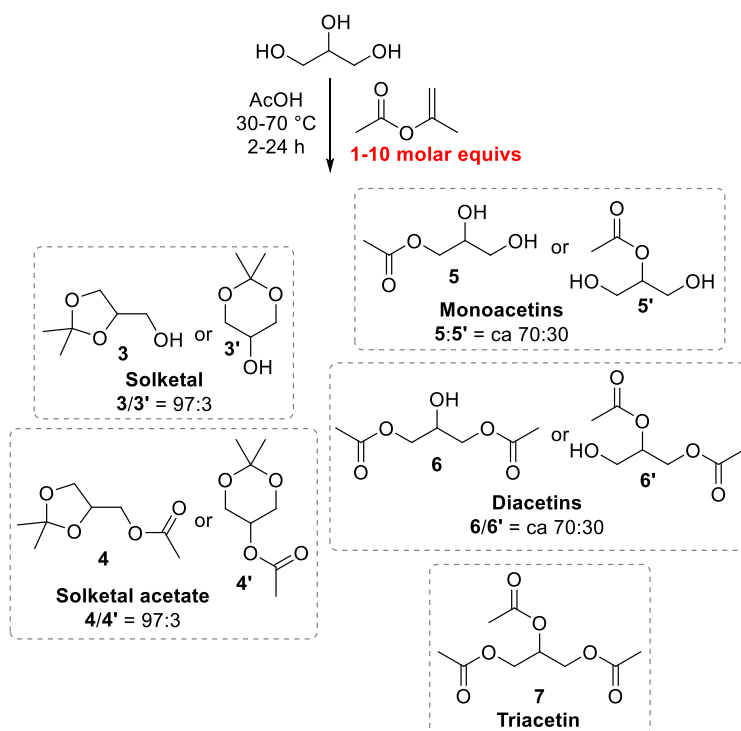
Scheme 2.29. *Products of the reaction between glycerol and iPAc. The relative ratio **3:3'**, **4:4'**, **5:5'**, and **6:6'** was determined by GC analyses and was constant regardless of reaction conditions*

The structures of derivatives **3**-**7** were assigned by GC/MS and NMR analyses and by comparison, when possible, with authentic commercial samples. Under the above-described conditions, blank tests were also carried out either without a catalyst or without iPAc. The results of this screening are summarized in Table 2.11.

Table 2.11. *The reaction of glycerol (**1**) and isopropenyl acetate (**2**) catalyzed by Amberlyst-15 in the presence of AcOH as a solvent*

Entry	iPAc:Glyc, Q (mol:mol)	Cat	T/t (°C, h)	Conv. (%)[a]	Products distribution (%)[b]				
					Acetals		Esters		
					3+3'[c]	4+4'[c]	5+5'[c]	6+6'[c]	7
1		Amb 15	30, 4	≥99	20	51	25	1	3
2	1		50, 4	≥99	12	35	41	7	6
3			70, 4	≥99	2	21	56	8	13
4			30,24	≥99	6	14		77	3
5	0 (iPAc absent)	Amb 15	30,4	31			81	19	
6			50,4	71			68	30	2
7	1	none	30, 24	1	99				
8	3	Amb 15	30, 24	≥99	7	28		60	5
9	5		30, 24	>99	9	31		42	18
10	10		30, 24	>99	4	41		11	44
11	10		30, 32	>99		51			49

All reactions were carried out using a solution of glycerol (**1**: 1.1 mmol) in AcOH (10 mL; 0.1 M) in the presence of Amberlyst-15 (Amb15: 15.2 mg; 15 wt %) as the catalyst, except for entry 6 where the catalyst was absent. Entries 1 -3: an equimolar mixture of glycerol and isopropenyl acetate was used (Q=1). Entries 5-6: isopropenyl acetate was absent. Entries 7-11: an increasing amount of isopropenyl acetate (**2**) was used with **2**:1 (Q) molar ratio in the range of 1÷10. [a] Conversion of glycerol. [b] Selectivity towards products **3/3'**, **4/4'**, **5/5'**, **6/6'** and **7**. [c] Total amount of isomers.

The conversion of glycerol and the product distribution, both measured by calibration with standard solutions (details are in the Experimental section) are shown for the most representative experiments performed at 30, 50 and 70 °C for 4 h and at 30 °C for 24 h, respectively. In this work, given the interest in the tandem sequence, the selectivity (product distribution) for each of the binary mixtures **3 + 3'**, **4 + 4'**, **5 + 5'**, and **6 + 6'** and compound **7** was defined according to the following expression:

$$S_i = [\text{mol } i/\text{conv. glyc.}] \times 100$$

where S_i is the selectivity (%) for compound i (i = **3 + 3'**, **4 + 4'**, **5 + 5'**, **6 + 6'** and **7**), mol i stands for the total moles of compound i (by GC calibration) and conv. glyc. is the total conversion of glycerol for the combined transesterification and acetalization processes. The reaction of an equimolar mixture of glycerol (**1**) and isopropenyl acetate (**2**) (Q = 1) showed that a quantitative conversion could be reached after 4 h even at the lowest investigated temperature (30 °C, entry 1). The increase of the temperature modified the product distribution: (i) at 30 °C the total of glyceryl acetals (**3 + 4**) was 71% compared to glyceryl esters (28%) that were mainly constituted by mono-acetins (**5 + 5'** = 25%) (entry 1); (ii) At 50 and 70 °C, the amounts of glyceryl acetals decreased in favor of glyceryl esters: *mono*-acetins became the major products (**5 + 5'** = 41-56%) along with *di*-acetins (**6 + 6'** = 7-8%) and triacetin (**7**: 6-13%) (entries 2 and 3). The results were consistent with our previous studies on the competitive reactions of 1,2-diols with iPAc and acetone that had demonstrated that acetalization was faster than acetylation,

though the latter became predominant by increasing the temperature (Paragraph 3.2 in this chapter). The tandem acetylation-acetalization selectivity could however not be controlled, as confirmed by prolonging the reaction for 24 h at 30 °C: under such conditions, both the transesterification and acetalization reached equilibrium with an amount of glyceryl esters (**6/6'** + **7**: 80%) significantly exceeding that of acetal products (**3/3'** + **4/4'**: 20%) (entry 4). The product distribution was not altered by doubling the reaction time to 48 h. Blank experiments carried out in the absence of iPAc (entries 5 and 6) proved that AcOH acted not only as a solvent but also contributed to the formation of glyceryl esters. However, notwithstanding the large (175) molar excess of AcOH with respect to glycerol, only mixtures of mono- and diacetins were obtained with moderate conversions of 31% and 71% at 30 °C and 50 °C, respectively (cfr. entries 1 and 5, and 2 and 6). Longer 24 h tests at 30-70 °C further proved that the reaction of glycerol with AcOH was in no way a selective process (Figure 2.36). Moreover, acetic acid was a far less active acetylating agent than iPAc. This behavior matched the results previously reported by Mota and coworkers for the same process run under similar conditions.[49]
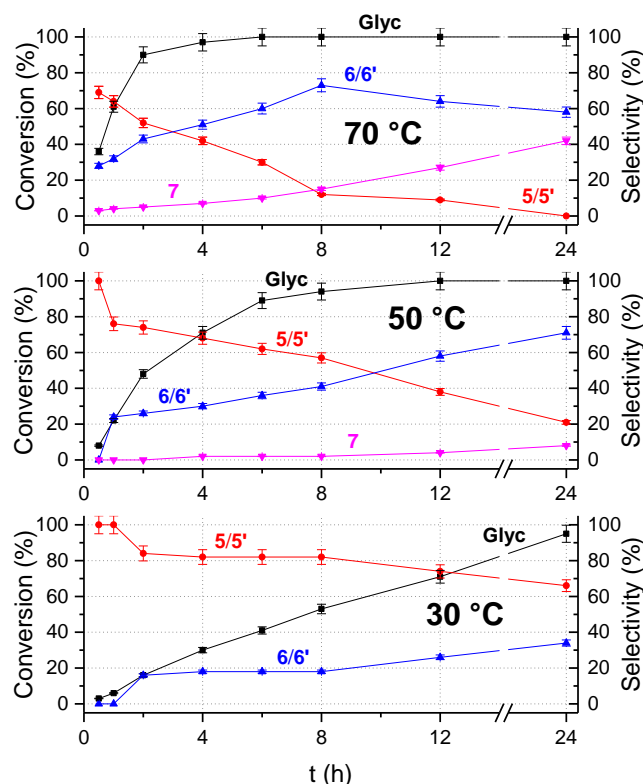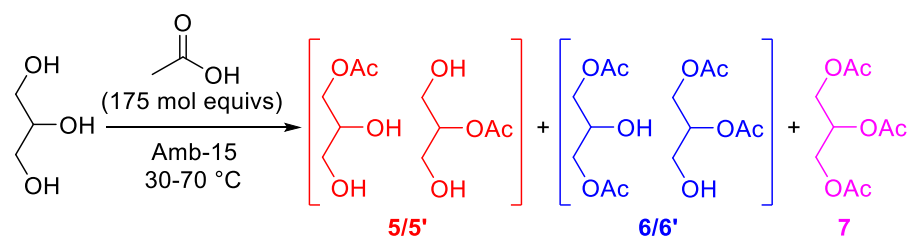
Figure 2.36. *The reaction between glycerol and acetic acid at different temperatures of 30, 50 and 70 °C (bottom, mid, and top, respectively). Conditions: solution of glycerol (1.0 mmol) in acetic acid (10 mL, 0.1 M), Amberlyst-15 (15.0 mg; 15 wt%) as a catalyst. (-■-) Glycerol conversion; (-●-) selectivity towards monoacetin (**5/5'**); (-▲-) selectivity towards diacetin (**6/6'**); (-▼-) selectivity towards triacetin (**7**)*

76

The blank experiment in the absence of Amberlyst-15 demonstrated the need for an acidic catalyst since negligible conversion (1%) was observed after 24 h at 30 °C (entry 7). Significantly better selectivity of the tandem sequence was finally achieved at 30 °C, by simultaneously increasing both the iPAc : glycerol molar ratio (Q) from 3 to 5 to 10, and the reaction time from 4 to 24 h. Indeed, this increase brought about a progressive and concurrent increase of acetal acetates (**4/4'**) from 28 to 41% and triacetin (**7**) from 5 to 44%, at the expense of diacetins (**6/6'**) whose amount dropped from 60 to 11% (entries 8-10). Thereafter, at Q = 10, a further control test prolonged for 32 h showed that compounds **4/4'** and **7** could be obtained as sole products with a comparable selectivity of 51 and 49% *i.e.* in a 1 : 1 ratio (entry 11). These results proved our concept demonstrating for the first time that through a cooperative effect between the electro-philic reactivity of isopropenyl acetate, the solvent/acetylating properties of AcOH, and the use of an acid catalyst, conditions could be tuned to control the product distribution of the tandem sequence: glycerol was successfully upgraded into two derivatives by transesterification and acetalization reactions. An additional optimization study proved that the same (1 : 1) selectivity profile for compounds **4/4'** and **7** was obtained at 30 °C by reducing the iPAc excess from 10 to 7.5 equivalents with respect to glycerol, and the AcOH volume of up to 20 times, from 10 to 0.5 mL. The latter was the minimum volume to obtain a homogenous solution of reactants 1 and 2. This process intensification was not only beneficial to improve the carbon footprint and the safety of the procedure, but also to increase its overall efficiency since the higher reactant concentrations enhanced the rates of all the involved reactions. To gain a detailed insight into this aspect, the reaction mixture was monitored at intervals and the conversion of glycerol and the corresponding product distribution were measured against time for 24 h. Figure 2.37 summarizes the results.
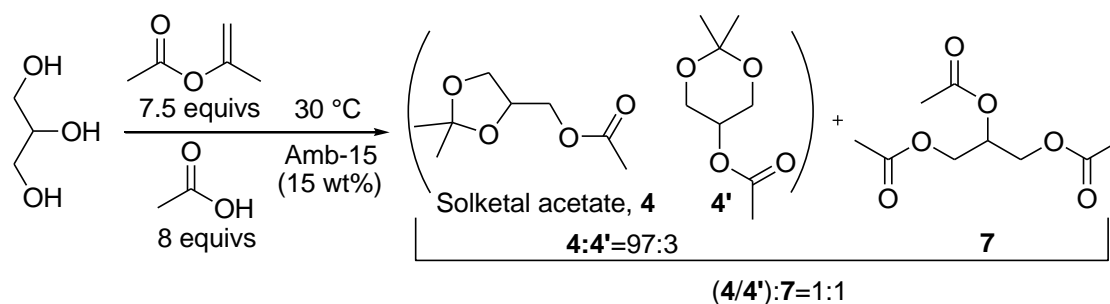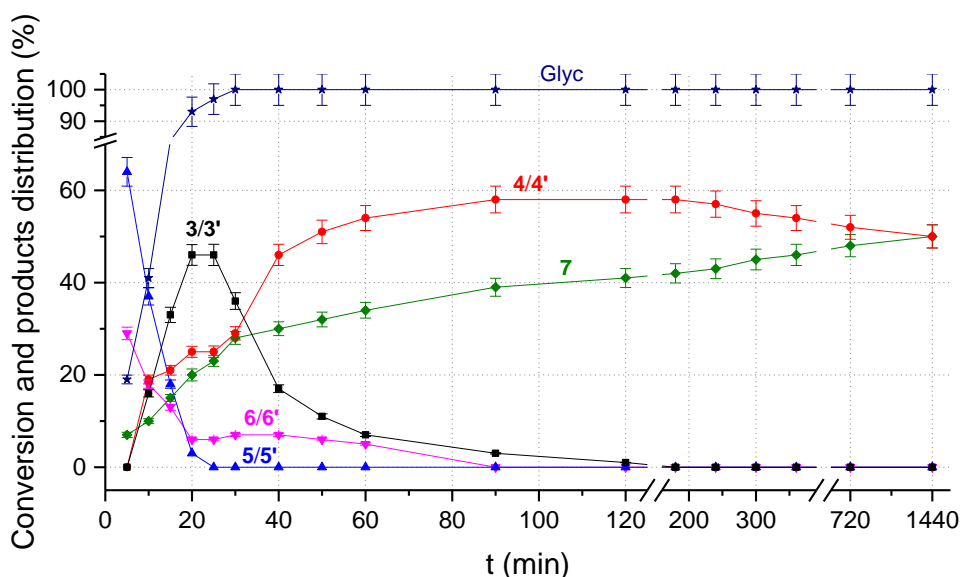
Figure 2.37. *The products distribution of the reaction of a mixture of glycerol (1.1 mmol), iPAc (7.52 mmol) acetic acid (0.5 mL; 8.75 mmol), and Amberlyst-15 (15.0 mg; 15 wt%), T = 30°C. (-★-) Glycerol (1) conversion; (-■-) solketal (3/3') selectivity; (-●-) solketal acetate (4/4') selectivity; (-▲-) monoacetin (5/5') selectivity; (-▼-) diacetin (6/6') selectivity; (-◆-) triacetin (7) selectivity*

With respect to Table 2.11, the reduction of the reaction volume highly impacted the kinetics. The conversion of glycerol was quantitative within the first 30 minutes and in the same time interval, the multiple transesterification of glycerol favored the formation of triacetin (**7**: 28%; green profile). Almost simultaneously, the onset of the acetalization reaction gave rise to a steep increase of acetals (**3/3'**: black profile), mostly solketal that reached a maximum (45%) after 25 min and then dropped with the parallel increase of acetal acetates (**4/4'**) up to ca. 30% (red curve). These derivatives (**4/4'**) were plausibly obtained by the direct esterification of acetals (**3/3'**) and the acetalization of monoacetins (**5/5'**), thereby explaining the decline of the blue profile from 62% to zero in less than 20 min. Indeed, once formed, monoacetins (**5/5'**) were consumed to feed both the transesterification process and the parallel acetalization reaction. In the next 90 min, competitive reactions proceeded with the gradual decrease of acetals (**3/3'**) and diacetins (**6/6'**, magenta curve) until their disappearance in favor of the acetal acetates (**4/4'**) and triacetin that increased to 58 and 41%, respectively (after 120 min from the start). The final part of the sequence was a slow interconversion of (**4/4'**) into triacetin (**7**) until the mixture reached the thermodynamic equilibrium distribution after 24 h with the final products present in equal quantities. From that moment on, the relative proportions of (**4/4'**) and (**7**) did not change anymore. Two further tests on the effect of the catalyst amount have been performed. Experiments were carried out under the same conditions of Figure 2.37 (glycerol: 1.00 mmol; iPAc: 7.50 mmol; AcOH: 8.00 mmol, 0.5 mL; 30 °C), except for the glycerol : catalyst weight ratio that was changed: the amount of Amberlyst-15 was reduced to 10 and 5 wt% with respect to glycerol. Results are reported in after 24 h. For comparison, data of Figure 2.37 (Amberlyst-15: 15 wt%) are also included.

Table 2.12. *Effect of the catalyst amount on the reaction of glycerol with a mixture of iPAc/AcOH*

Entry	Amb-15 (wt%)	Conv. (%)[a]	Products distribution (%)[b]	
			4/4'[c]	7

1	15	≥99	50	50
2	10	≥99	61	39
3	5	≥99	67	33

Conditions: mixture of glycerol (1.00 mmol), iPAc (7.50 mmol), and AcOH (8.00 mmol, 0.5 mL) in the presence of variable amounts of Amberlyst-15 (5.00, 10.00, and 15.00 mg; 5, 10, and 15 wt%), t = 24h. [a] Conversion of glycerol. [b] Selectivity towards compounds **4/4'** and **7** was defined as reported in the main text. [c] Total amount of isomer products

Under the conditions of Figure 2.37, changing the glycerol : catalyst weight ratio altered the kinetics of the different reactions, without however affecting the selectivity of the formation of acetal acetates and triacetin. Decreasing the catalyst amount brought about a drop of the rate of all the reactions involved: after 24 h, albeit acetal acetates **4/4'** and triacetin **7** were the only observed products in all cases, the corresponding amounts increased and decreased, respectively, from 50 to 61 and 67% for **4/4'**, and from 50 to 39 and 33% for **7** (entries 1-3). Results were consistent with profiles of Figure 2.37 where at the highest investigated catalyst amount (15 wt%), the (**4/4'**):**7** ratio reached a maximum of ca 60:40 after 120 min, comparable to that achieved after 24 h with Amberlyst-15 at 10 wt%. No further investigations were carried out on this aspect.

The overall picture was consistent with the reactions in Scheme 2.30.
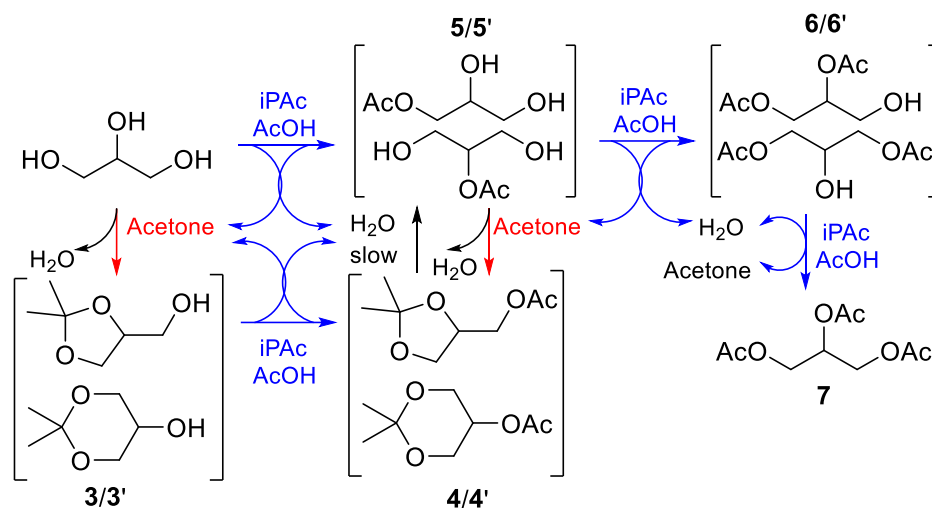
Scheme 2.30. *Reactions involved in the selective formation of (4/4') and (7)*

The transesterification pathways (**blue**) mediated by iPAc/AcOH release acetone which is consumed in the acetalization pathways (**red**). Both processes form water as a co-product. Glycerol yields first mono-acetins (**5/5'**) and as soon as acetone is made available, acetals (**3/3'**). Mono-acetins (**5/5'**) undergo either transesterification to di-acetins (**6/6'**) or acetalization to acetal acetates (**4/4'**). Di-acetins (**6/6'**) react further to form triacetin (**7**). In the last part of the sequence, acetal acetates (**4/4'**) undergo slow hydrolysis to mono-acetins (**5/5'**) and slowly equilibrate to a 1 : 1 thermodynamic mixture of (**4/4'**) and (**7**). The reaction of Figure 2.37 involved a simple and safe experimental setup as well as an equally convenient procedure for the work-up and purification of the products. Once the reaction was complete (24 h), the catalyst was filtered off and the mixture of **4/4'** and **7** could be isolated by vacuum distillation (5 mBar, 50-80 °C) of the oily residue in nearly quantitative yields of 47% and 48%, respectively (based on glycerol as the limiting reagent). Moreover, the procedure could be scaled up by a factor of 10 without any appreciable variation in terms of product distribution, yields, and time.

79

The role of iPAc and acetic anhydride. Curiously, from Figure 2.37, although the acetylating mixture of iPAc/AcOH was in a very large excess compared to acetone, the amount of acetal acetates was higher than that of triacetin in the initial stages of the reaction (red and green profiles). Since the direct acetalization of glycerol by iPAc was not plausible, the results led us to hypothesize that (excess) iPAc acted not only as a transesterification agent, but also as a source of acetone for acetalization through some kind of parallel reaction. The inspection of the literature indicated that at 100 °C, in the presence of H_2SO_4 as a catalyst, an equimolar mixture of AcOH and iPAc underwent an acyl nucleophilic substitution (acidolysis of iPAc) to provide acetone and acetic anhydride in almost quantitative yields (Scheme 2.31).[57]
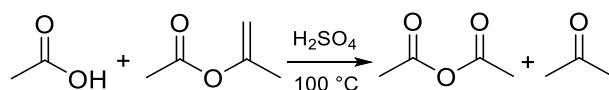
Scheme 2.31. *The reaction of acetic acid with iPAc*

Presuming that the same reaction took place under the conditions of Table 2.11 and Figure 2.37, the desired tandem sequence could be assisted by both acetone and acetic anhydride (Ac_2O) for the acetalization and acetylation reactions, respectively. Additional experiments were therefore carried out aiming at investigating the acidolysis of iPAc at 30 °C with Amberlyst-15 as a catalyst. The first test was performed by replicating the conditions of Figure 2.37. The complexity of the product mixture did not allow satisfactory GC/MS or NMR analyses to resolve signals of acetone and iPAc, but the presence of acetic anhydride was nonetheless verified and quantified. Since Ac_2O was obtained from iPAc as an excess reactant, the anhydride amount was conveniently calculated as a percentage with respect to the total number of products obtained from glycerol (**3/3'**, **4/4'**, **5/5'**, **6/6'** and **7**; Figure 2.38).
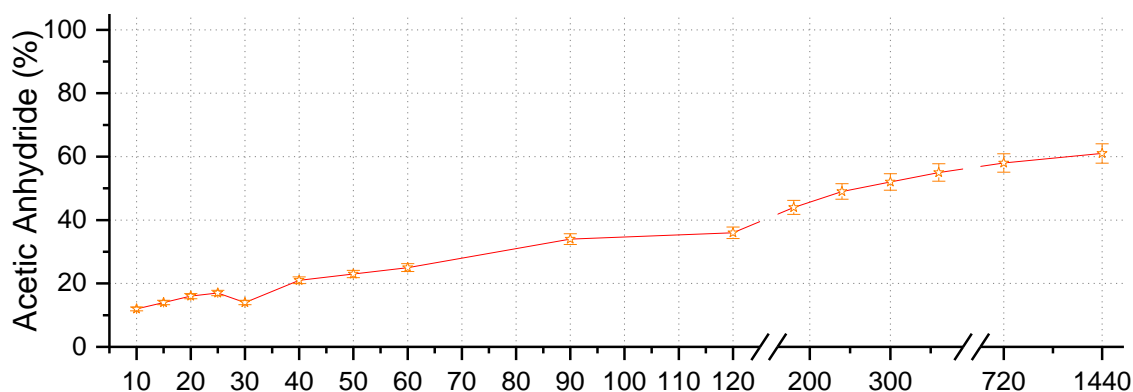
Figure 2.38. *The formation of Ac_2O during the reaction of a mixture of glycerol (1.1 mmol), iPAc (7.52 mmol), acetic acid (0.5 mL; 8.75 mmol), and Amberlyst-15 (15.0 mg; 15 w%), at = 30°C. (-☆-) Amount calculated as the % of acetic anhydride with respect to other products (3/3', 4/4', 5/5', 6/6' and 7) observed during the reaction*

The gradual increase of Ac_2O throughout the process offered convincing, albeit indirect, proof for the corresponding formation of an increasing amount of acetone which could in turn feed the acetalization of glycerol and monoacetins (Scheme 2.31). Additional evidence for this mechanism of acetone formation was then gathered by the reaction of an equimolar mixture of isopropenyl acetate (5.00 mmol) and acetic acid in the presence of Amb-15 as a catalyst (14.8 mg; 15 wt%). At 30 °C, after 24 h, acetic anhydride was observed in 80% yield (by GC). It was excluded that Ac_2O was obtained from the catalytic dehydration of AcOH since this reaction

was reported only at temperatures above 500 °C.[58] The process also allowed to identify minor amounts of by-products (≤10% with respect to Ac_2O), the mass spectra of which was consistent with the formation of acetylacetone plausibly derived from an acid-promoted rearrangement of iPAc,[59] and the aldol conden-sation of acetone (see Appendix A.2 for MS spectra). A not optimal resolution of acetone and iPAc prevented their quantification also in this case. The *in-situ* formation of Ac_2O during the reactions of both Table 2.11 and Figure 2.37 allowed us also to envisage another consequence: the involvement of the anhydride as an acetylating reagent in parallel with iPAc and AcOH. In this respect, a detailed study was carried out on the acetylation of glycerol with acetic anhydride under conditions as close as possible to those of Table 2.11, in which iPAc was replaced by Ac_2O. Experiments were performed at 30 °C, using a solution of glycerol (1 mmol) in acetic acid (0.1 M, 10 mL: conditions of Table 2.11) and a glycerol : Ac_2O molar ratio variable in the range from 5 to 0.2. Amberlyst-15 (15 mg, 15 wt% with respect to glycerol) was the catalyst. To do that, a solution of glycerol (1.00 mmol) in acetic acid (0.1 M, 10 mL) was set to react at 30 °C, in the presence of different amounts of acetic anhydride and Amberlyst-15 (15.0 mg, 15 wt% with respect to glycerol) as the catalyst. The most representative results, reported in Figure 2.39 in which the glycerol:Ac_2O (W) molar ratio was 5, 2, 1 and 0.2, respectively, and briefly summarized in Scheme 2.32, suggested that the esterification of glycerol occurred much faster with Ac_2O than with AcOH alone, and the higher the anhydride amount, the higher the formation of products of multiple (double and triple) acetylation. Hence, this was manifest even when sub-stoichiometric amounts of the anhydride were used: in the first 60-120 min of reaction, as long as Ac_2O was present in the reaction mixture, both the conversion of glycerol and the proportion of bis- versus mono- acetylated products [diacetins **6/6'** vs mono-acetins **5/5'**] were higher than that achieved with AcOH (cfr Figure 2.36 and Figure 2.39). No to mention that in the same time interval, triacetin **7** was obtained as a single product when 5 molar equivs of Ac_2O were used (bottom right, Figure 2.39). Notably, after the consumption of Ac_2O, all reactions slowed down significantly: the further conversion of glycerol and the formation of its multiple transesterification derivatives was ascribable to the acetylating activity of AcOH.
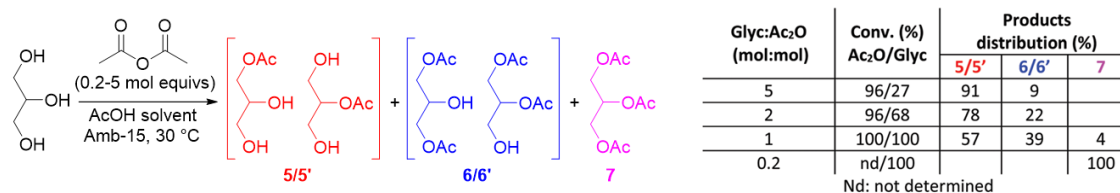
Scheme 2.32. *The acetylation of glycerol with acetic anhydride at 30 °C, over Amberlyst-15*

Glyc:Ac_2O (mol:mol)	Conv. (%) Ac_2O/Glyc	Products distribution (%)		
		5/5'	6/6'	7
5	96/27	91	9	
2	96/68	78	22	
1	100/100	57	39	4
0.2	nd/100			100

Nd: not determined
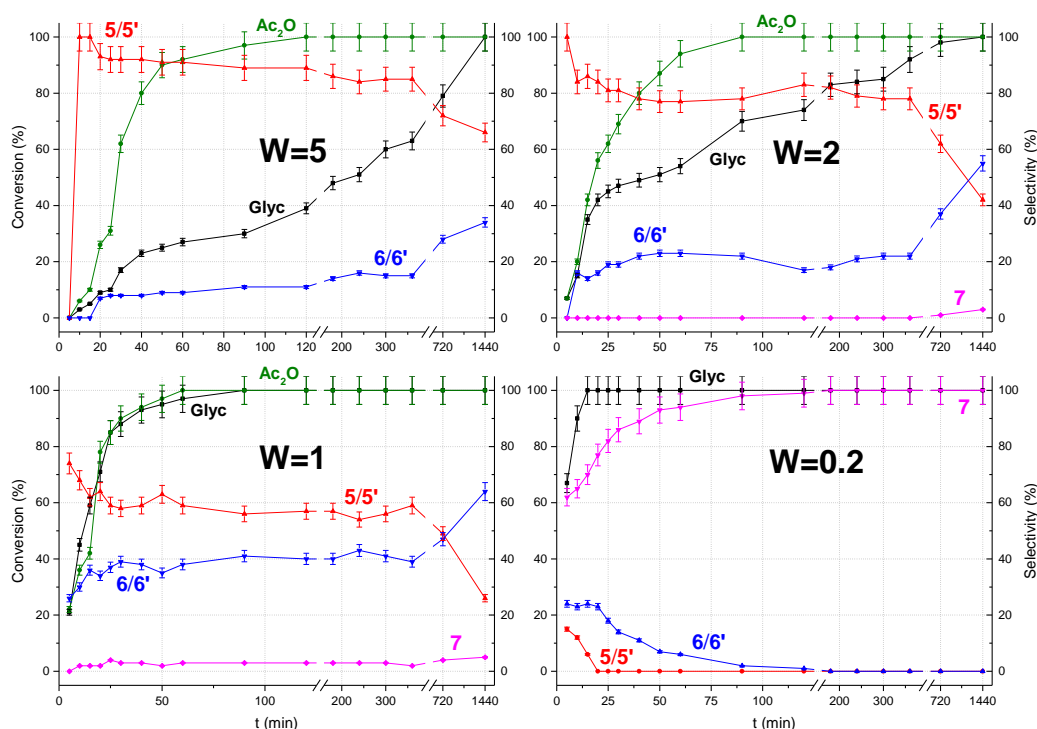
Figure 2.39. The reaction of a solution of glycerol (1.00 mmol) in acetic acid (10 mL; 0.1 M) carried out at 30 °C, in the presence of variable amounts of and acetic anhydride and Amberlyst-15 catalysis (15.0 mg; 15 wt%) as the catalyst. The glycerol:Ac₂O molar ratio (W) was 5, 2, 1 and 0.2: the corresponding four reaction profiles are shown in top left, top right, bottom left, and bottom right figures, respectively. (-■-) conversion of glycerol; (-●-) conversion of acetic anhydride; (-▲-) selectivity towards mono-acetins (5/5'); (-▼-) selectivity towards diacetin (6/6'); (-♦-) selectivity towards triacetin (7)

The emerging picture confirmed the multiple roles of iPAc and indicated that the investigated sequence was even more complicated than that shown in Scheme 2.30. In addition to the competitive (parallel or consecutive) processes there described, the occurrence of the acidolysis of iPAc provided an extra supply of acetone and acetic anhydride, the latter serving as a co-acetylating agent. A limited hydrolysis of iPAc and glyceryl esters could also not be ruled out.[60,50] Nonetheless, the combined relative kinetics and equilibria of such a network of transformations led towards the selective formation of a 1 : 1 mixture of **4/4'** and **7**. It should be noted that our attempts to achieve the same result by replacing iPAc with a mixture of Ac₂O and acetone (in variable proportions) were unsuccessful. Not to mention dangers and possible regulatory constraints associated with the direct use of Ac₂O.

Insights into the tandem mechanism. The complexity of a system in which different components (the enol ester, the acid and the anhydride) could simultaneously express the same reactivity as acetylating agents made it rather challenging to discriminate the contribution of each single partner. To shed light on this aspect, additional experiments were devised using D-isotope labelled acetic acid. A control experiment was carried out under the conditions of Figure 2.37 by replacing AcOH with its perdeuterated analogue, CD_3COOD (glycerol: 1 mmol, iPAc: 7.5 mmol; CD_3COOD: 0.5 mL, 8.75 mmol); Amberlyst-15: 15 mg, 15 wt%; 30 °C; 24 (h). The GC/MS analysis of the reaction mixture allowed the identification of the expected products. Acetal acetates were detected as two species per isomer: the non- and the tri-deuterated compounds, **4/4'** and **4*/4'*** respectively. Triacetin was detected in the form of

four species, the non-, the tri-, the hexa-, and the nona-deuterated products, respectively (Scheme 2.33).
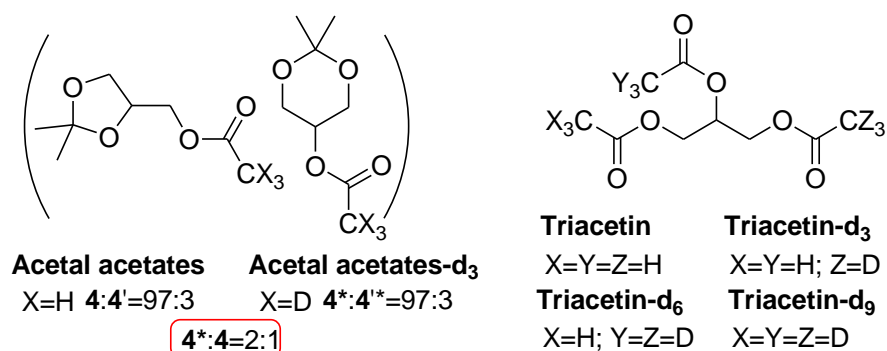
Scheme 2.33. *D-isotope labelled products observed in the reaction of glycerol with iPAc/CD$_3$COOD*

A satisfactory GC resolution was achieved only for the acetal acetates, particularly solketal acetate (**4** and **4***), while signals of the different triacetins were substantially superimposed. Figure 2.40 reports the result by showing enlarged regions of GC/MS analyses corresponding to the two signals of solketal acetate, the most abundant 5-membered ring acetal ester (top), and the four signals of triacetin (bottom). In the figure, red profiles were the authentic GC/MS analyses, while green profiles were obtained by the deconvolution of the red ones, carried out by the "Gaussian polynomial fitting" available in the OriginPro Software (ver. 9.1, Origin Lab. Corp.). Thanks to a more satisfactory resolution, signals of solketal acetate (compounds **4** and **4***, top) allowed not only a more reliable integration of the area under the corresponding peaks, but also a better reading/interpretation of GC/MS spectra, than those of different triacetins. The investigation was then continued considering only products **4** and **4***. From deconvolution, the relative amounts of **4*** and **4** were 67% and 33%, meaning that the quantity of the tri-deuterated solketal acetate was twice as much the non-deuterated derivative.
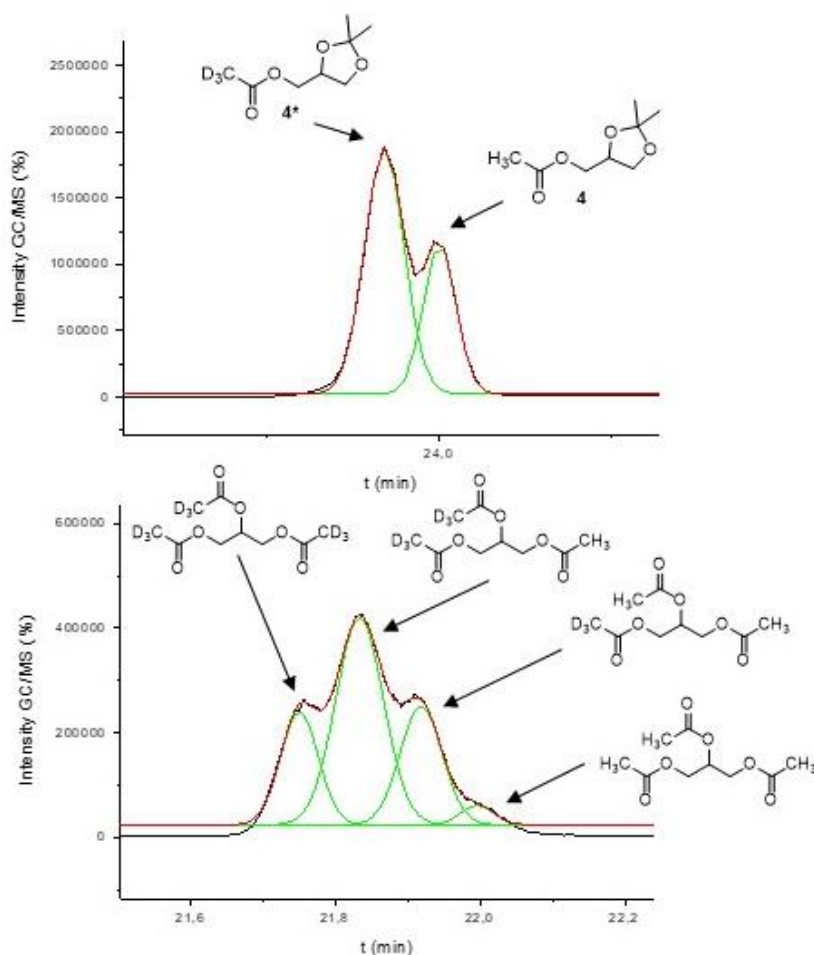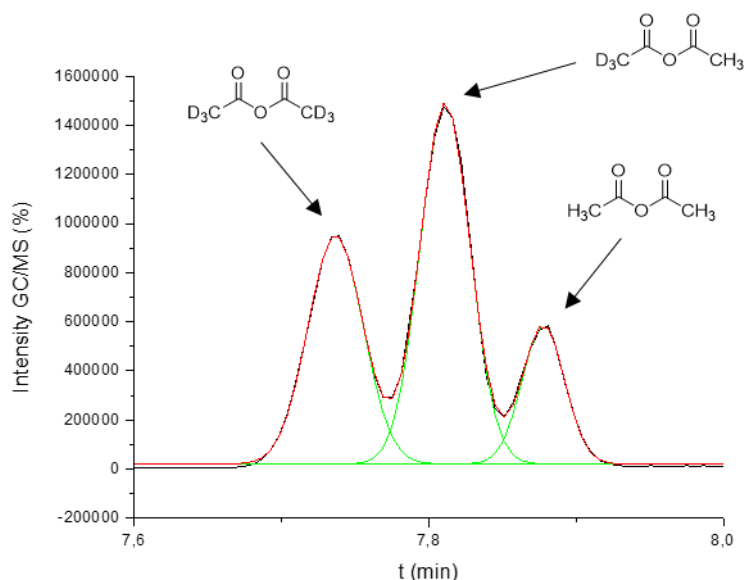
Figure 2.40. *Top: the red profile shows the GC/MS signals for solketal acetate; the corresponding d₃- and non-deuterated derivatives are indicated from left to right, respectively. Bottom: the red profile shows the GC/MS signals for triacetin; the corresponding d₉-, d₆-, d₃- and non-deuterated derivatives are indicated from left to right, respectively. Green profiles for both top and bottom represent the deconvolution of the red profiles carried out by the "Gaussian polynomial fitting" available in the OriginPro Software (ver. 9.1)*

From the mass spectra recorded in the full scan (TIC, 70 eV), fragment ions at m/z = 159 and 162 were recognized as the most abundant and easily distinguishable ions for **4** and **4***, respectively (Figure 2.41). The characteristic absence of the molecular ion peak (M$^+$=174 and 177 for **4** and **4***, respectively) was already noticed in a previous paper reported by us.[20] The fragment ions 159 and 162 were consistent with the loss of a methyl radical from the acetal ring (Scheme 2.34).
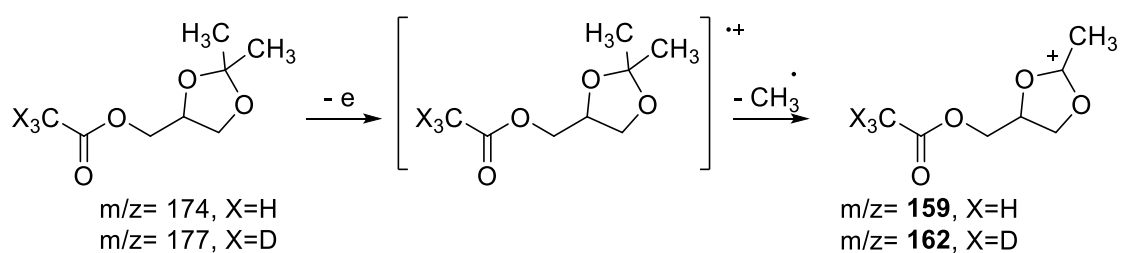
Scheme 2.34. *Plausible fragmentation pathway for the formation of ions 159 and 162 from compounds **4** and **4****

84
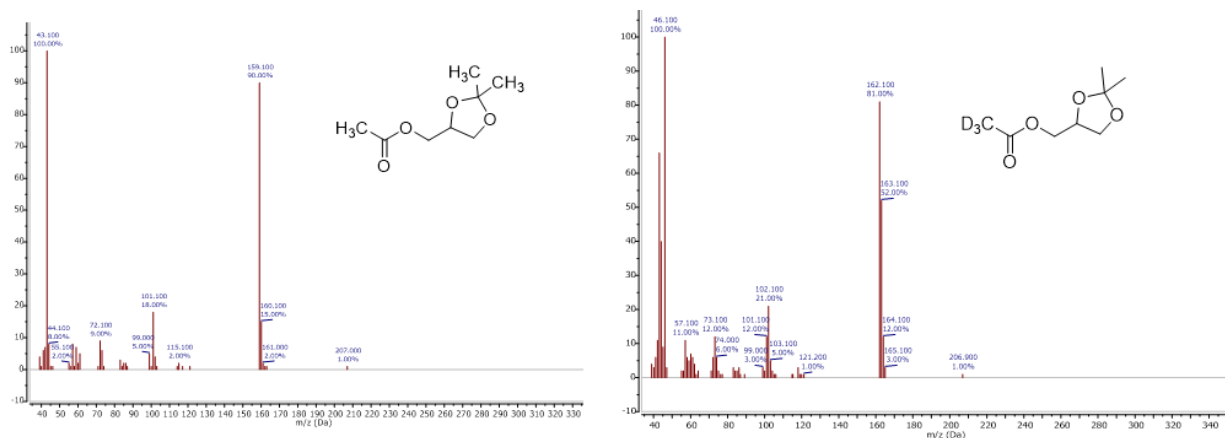
Figure 2.41. *Mass spectra (TIC) of product **4** (top) and **4*** (bottom)*

To improve sensitivity, mass spectra were then acquired in the SIM mode on the characteristic fragment ions m/z = 159 and 162 (70 eV) (Figure 2.42). Comparison of the analytical data recorded in the full scan (TIC) and the SIM mode (set at the most abundant fragment ions, m/z = 159 and 162 for 4 and 4*, respectively) indicated that the relative amounts of **4*** and **4** were 65% and 35%, meaning that the quantity of the tri-deuterated product was approximately twice that of the non-deuterated derivative.
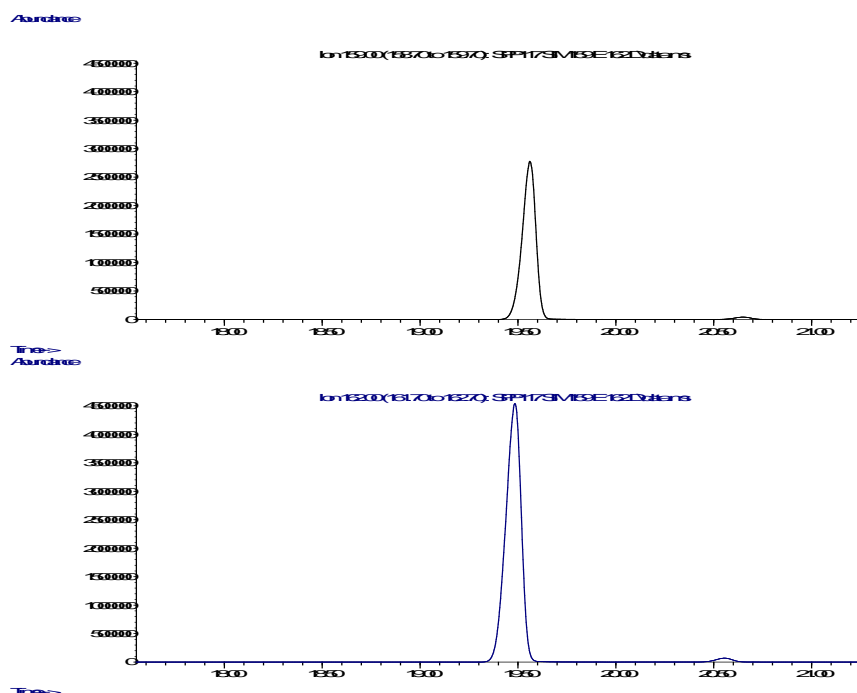
Figure 2.42. *SIM chromatograms of selected fragment ions m/z = 159 and 162 for products **4** (top) and **4*** (bottom), respectively*

Relevant to this study was also the evidence of the formation of three differently deuterated acetic anhydrides, i.e. the non-, the tri-, and hexa-deuterated products which were present in a 1 : 3 : 2 ratio (by GC/MS) in the reaction mixture (Figure 2.43). From deconvolution (green profile), the integration of the area under the corresponding peaks allowed to estimate that non-deuterated, d_3- and d_6- species of acetic anhydride were present in a 1:3:2 ratio, respectively.

85

Figure 2.43. *The red profile shows the GC/MS signals for acetic anhydride: the corresponding d_6-, d_3-, and non-deuterated derivatives are indicated from left to right, respectively. The green profile represents the deconvolution of the red profiles carried out by the "Gaussian polynomial fitting" available in the OriginPro Software (ver. 9.1)*

These results were consistent with Scheme 2.35 in which CD_3COOD mediated the acidolysis not only of iPAc, but also of the produced (deuterated) anhydride.[61]
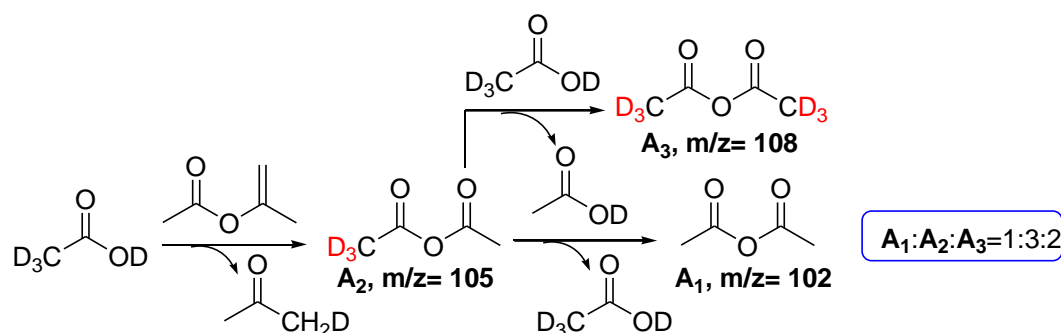
Scheme 2.35. *Plausible pathways for the formation of the three observed species of acetic anhydride*

As a first approximation, excluding kinetic and equilibrium isotope effects,[62] the relative contributions of CD_3COOD and iPAc as acetylating agents could be inferred from the observed 2 : 1 ratio for products **4*** and **4**, respectively (Scheme 2.33). The deuterated acid acted directly or indirectly (via the formation of A_2 and A_3) to produce twice the amount of **4*** with respect to **4**. The latter instead was obtained from iPAc as such or its derivative A_1. From the stoichiometry of acidolysis and the 1 : 3 : 2 ratio of A_1 : A_2 : A_3 in Scheme 2.35, one could also estimate that about 54% of the total mixture of anhydrides was sourced from the deuterated acid.

An additional experiment was then carried out by doubling the amount of CD_3COOD, keeping all the other conditions unaltered (glycerol: 1 mmol, iPAc: 7.5 mmol; CD_3COOD: 1 mL, 17.5 mmol; Amberlyst-15: 15 mg, 15 wt%, 30 °C, 24 h). GC/MS analyses carried out using the above-described procedure in full scan and sim mode indicated that the relative quantities of products **4*** and **4** were 73 and 27%, respectively. Albeit with a modest increase, the higher the amount

86

of CD₃COOD, the higher the formation of the labelled acetal ester with respect to the corresponding non-labelled derivative.

3.3.2.2 The tandem synthesis of acetal acetates

The reaction of glycerol with the mixture iPAc/AcOH was further investigated with the aim to steer the overall process towards the selective formation of the products deriving from a single acetylation and acetalization step, *i.e.* the solketal acetate (**4**) and its 6-membered ring isomer (**4'**) couple. To this end, several new experiments were carried out by modifying the conditions of Figure 2.37, particularly by changing the reactant molar ratio and by adding a large excess of acetone (20 molar equiv. with respect to glycerol) as a co-acetalizing agent. Although acetone (alike iPAc) was scantly soluble with glycerol,[63] in the presence of AcOH a homogeneous solution of reactants was achieved. The salient aspects of this study are summarized in Figure 2.44, which shows the product distribution obtained during the reaction of a mixture of glycerol (1.0 mmol), acetic acid (0.5 mL, 8.75 mmol), and acetone (0.9 mL, 20.0 mmol), in the presence of Amberlyst-15 (15.0 mg; 15 wt% with respect to glycerol) as a catalyst and variable amounts of isopropenyl acetate (1–4 mmol), at 30 °C, after 24 h.
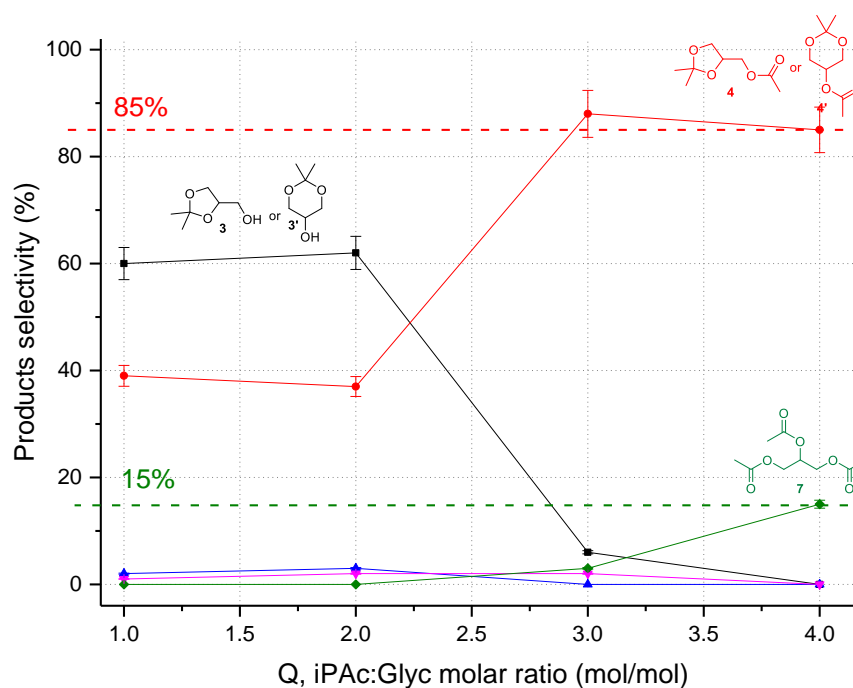
Figure 2.44. *The reaction of glycerol with a mixture of iPAc/AcOH and acetone: effect of increasing amounts of iPAc. Conditions: glycerol (1.00 mmol), isopropenyl acetate (1.00-4.00 mmol), acetic acid (8.75 mmol), acetone (20.00 mmol), Amberlyst-15 (15.0 mg; 15 wt%), 30 °C, 24 h. Selectivity towards: (-■-) acetals (**3/3'**); (-●-) acetal acetates (**4/4'**); (-▲-) mono-acetins (**5/5'**); (-▼-) di-acetins (**6/6'**); (-◆-) triacetin (**7**). Glycerol conversion was ≥99% in each test*

Conversion of glycerol is not reported since it was quantitative in all tests. The product distribution mirrored the intrinsic reactivity of acetone and iPAc. In the presence of equimolar amounts of glycerol and iPAc (Q = 1, left), acetals (**3/3'**) were the predominant products (60%, **black** profile) followed by acetal acetates (**4/4'**: 37%, **red** profile) and traces of glyceryl esters implying that excess acetone favored acetalization versus acetylation. The result was comparable when the amount of IPA was doubled (Q = 2). Instead, for Q = 3 the formation of acetals dropped strikingly from 60% to 6% and the acetal acetates **4/4'** increased from 37% to

88%. The greater availability of iPAc and acetic anhydride (from the acidolysis of the enol ester) brought about a significant improvement of the transesterification reaction which, however, involved mainly the OH function of the acetals and not of glycerol. Indeed, the total amount of glyceryl esters remained low at ca. 6%. The results were consistent with the higher electrophilicity of acetone compared to esters and anhydrides that favored acetalization of glycerol to yield acetals (**3/3'**), which in turn underwent transesterification with iPAc/Ac$_2$O to the corresponding acetal acetates (**4/4'**). A further increase of the iPAc : glycerol molar ratio (Q = 4) caused complete disappearance of the acetals (**3/3'**), albeit with slightly lower selectivity towards acetal acetates (**4/4'**: 85%) due to the formation of triacetin (15%) by exhaustive acetylation of glycerol. In all cases the binary mixtures of compounds **3/3'** and **4/4'** maintained a 97 : 3 ratio between 5- and 6-membered ring products. Additional tests demonstrated that the selectivity of the tandem sequence towards **4/4'** could be further optimized by reducing the quantities of acetone and AcOH to 5 and 1.5 equivalents with respect to glycerol, respectively. After 16 h under these conditions the acetal acetates (**4/4'**) were obtained in up to 91% yield (Scheme 9). Co-products were acetals (**3/3'**: 3%) and di- and triacetins (**5/5'**: 2% and 7: 4%). With respect to Figure 2.38, decreasing the reaction volume allowed to reduce the reaction time to 16 hours and at the same time, to slightly increase the yield of (**4/4'**). Under such conditions, the reaction was scaled up by a factor of 10. Once the experiment was complete (16 h), the catalyst was filtered and vacuum distillation (5 *m*Bar, 50-80 °C) of the oily residue allowed us to isolate **4/4'** in an 87% yield (1.51 g, 8.7 mmol; based on glycerol as the limiting reagent), thereby further vali-dating the mass balance and the synthetic efficiency of the process. The results of Figure 2.38 and Scheme 9 proved the second major novelty of this paper and the originality of the approach used.
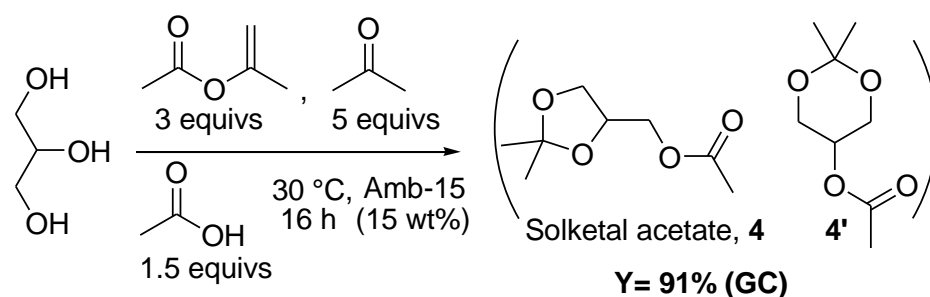
Scheme 2.36. *The tandem synthesis of acetal acetates. The amounts of iPAc, AcOH, Ace and the catalysts are referred to glycerol. Other conditions were those of Figure 2.44 (glycerol: 1.00 mmol, iPAc: 3.00 mmol, Amberlyst-15: 15.0 mg)*

The strategy based on the cooperative reactivity of multiple compounds, pivoted on isopropenyl acetate, could be finetuned to yield a one-pot tandem acetalization and acetylation sequence of glycerol that produced the binary mixture of isomers **4/4'** with high selectivity. To the best of our knowledge, the direct synthesis of acetal acetates **4/4'** from glycerol has no precedent in the literature. Although in the presence of Amberlyst-15 the acetylation of solketal with acetic anhydride was reported with >90% conversion and >80% selectivity towards solketal acetate,[50] earlier studies on the reaction of glycerol with mixtures of acetone and Ac$_2$O under reflux conditions yielded at best solketal (**3**) and its acylated derivative (**4**) in a 9 : 1 ratio (with no mention of isomers **3'** and **4'**).[64] This reaction system was further examined by us under the conditions of Figure 2.44. Experiments showed that reactants (glycerol, Ac$_2$O and acetone) were not mutually miscible. AcOH was used as a solvent. At complete conversion,

acetal acetates (**4/4'**) were obtained in a maximum 82% selectivity along with triacetin (18%). Compared to iPAc, not only the selectivity was lower, but acetone and Ac$_2$O had to be used in a significantly large excess of 20 and 5 equiv., respectively, with respect to glycerol (details are shown in Table 2.13).

Table 2.13. *The reaction of glycerol with acetone and acetic anhydride*

Entry	Solvent	Glyc:Ace:Ac$_2$O[a] (mol:mol:mol)	Conversion[b] (%)	Selectivity[c] (%)				
				3/3'	4/4'	5/5'	6/6'	7
1	AcOH (1.5 equivs.)	1:1:1	≥99	10	30	34	23	1
2		1:1:10	≥99		30		1	69
3		1:3:10	≥99		58		1	41
4		1:5:10	≥99		68		1	31
5		1:20:5	≥99		82			18
6		1:20:2.5	≥99	15	78		3	5
7[d]		1:5:3	≥99		61		1	38

Conditions: T=30 °C, Amberlyst-15 (15 mg; 15 wt%, with respect to glycerol), t=24 h. [a] Molar ratio of the reactants. [b] Conversion of glycerol, by GC. [c] Products selectivity (by GC) calculated as described in the main text. [d] iPAc was replaced with Ac$_2$O under the conditions of Scheme 2.36.

Additional experiments to confirm the role of iPAc further demonstrated that the tandem selectivity was elusive also by reacting glycerol with different mixtures of AcOH and acetone, in the presence of Amberlyst-15 as a catalyst: the amount of **4/4'** did not exceed 32% (further details are shown in Table 2.14). In no way could the use of iPAc be replaced.

Table 2.14. *The reaction of glycerol with acetone and acetic acid*

Entry	Glyc:Ace:AcOH[a] (mol:mol:mol)	Conversion[b] (%)	Selectivity[c] (%)				
			3/3'	4/4'	5/5'	6/6'	7
1	1:1:1	70	56	12	30	2	-
2	1:1:10	95	8	15	51	25	1
3	1:3:10	96	33	26	33	7	-
4	1:5:10	≥99	48	32	15	5	-
5	1:20:5	≥99	95	5	-	-	-
6	1:20:2.5	≥99	97	3	-	-	-

Conditions: T=30 °C, Amberlyst-15 (15.00 mg; 15 wt%, with respect to glycerol), t=24 h. [a] Molar ratio of the reactants. [b] Conversion of glycerol, by GC. [c] Products selectivity (by GC) calculated as described in the main text

Additional experiments to confirm the role of iPAc further demonstrated that the tandem selectivity was elusive also by reacting glycerol with different mixtures of AcOH and acetone, in the presence of Amberlyst-15 as a catalyst: the amount of **4/4'** did not exceed 32% (further details are shown in Table 2.14). In no way could the use of iPAc be replaced.

Acetal acetates with d$_6$-acetone. With the aim to investigate the relative role of iPAc and acetone as acetalization agents, the tandem formation of acetal acetates (**4/4'**) was explored by replacing acetone with its d$_6$-isotope labelled analogue, CD$_3$COCD$_3$. An experiment was carried out under the same conditions of Scheme 2.36 (glycerol: 1 mmol; isopropenyl acetate: 3 mmol; acetic acid: 1.5 mmol; Amberlyst-15: 15 mg; t = 16 h; d$_6$-acetone: 5 mmol). The GC/MS analysis of the reaction mixture allowed us to identify the expected acetal acetates as two species (per isomer), the non and the hexa-deuterated compounds, respectively (**4/4'** and **4$_{d6}$=4'$_{d6}$**). Scheme 2.37 offers a pathway for the formation of the d$_6$- and the non-deuterated solketal acetate.

Scheme 2.37. *Pathways for the formation the non-deuterated and the d₆- solketal acetate (4 and 4_d6, respectively)*

Data analysis was focused on the most abundant isomer solketal acetate (**4**) and its d₆-labelled derivative (**4_d6**). The comparison of the analytical data recorded in the full scan (TIC) and the SIM mode (set at the most abundant fragment ions, m/z = 159 and 162 for **4** and **4_d6**, respectively) indicated that their relative amounts were 35% and 65%, *i.e.* the hexa-deuterated species was approximately twice as much the non-deuterated one (Figure 2.45).

Figure 2.45. Top: Plausible fragmentation pathway for the formation of ions 159 and 162 from compounds **4** and **4**$_{d6}$. Bottom: SIM chromatograms of fragment ions m/z = 159 and 162 from products **4** and **4**$_{d6}$, respectively

Noteworthy is the correspondence between the ions analyzed in SIM mode both for the tests with labelled acetic acid and acetone. Although ions with m/z = 159 and 162 were selected for both the investigations, the comparison of mass spectra proved that different fragmentation pathways occurred: (i) using d$_4$-acetic acid the isotopic marking of the considered ion regarded the acetyl group; (ii) when d$_6$-acetone was used, the marking was set on the acetalized portion of acetal acetates (compare Figure 2.41 and Figure 2.46).
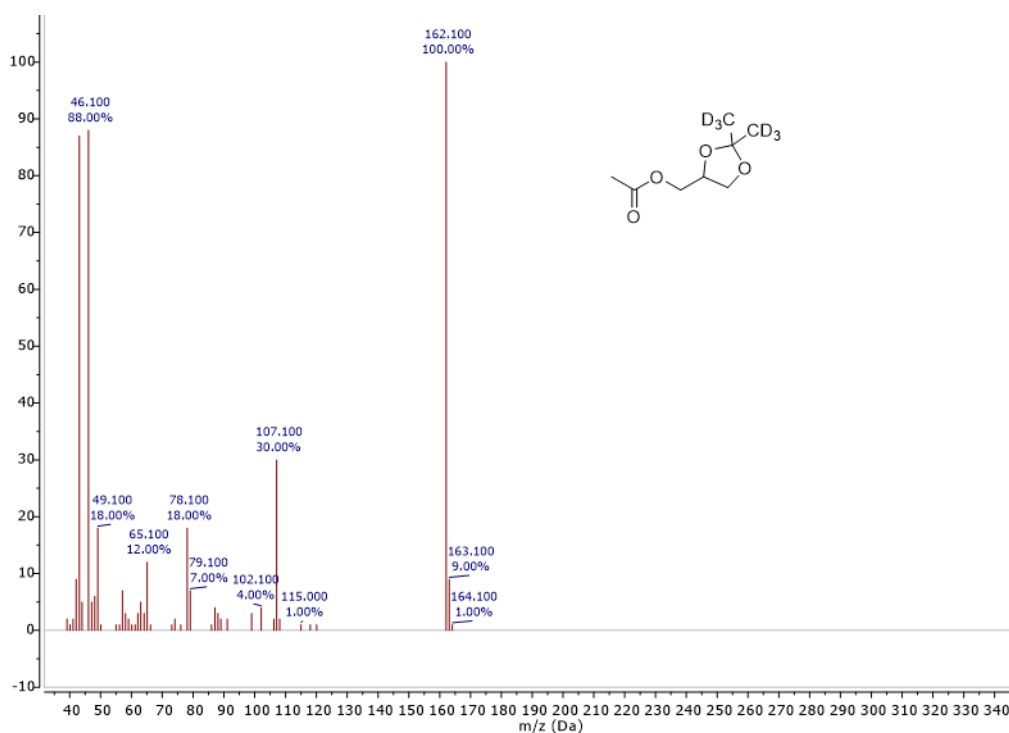
Figure 2.46. *Mass spectrum of product 4$_{d6}$*

Although the apparent contribution of CD$_3$COCD$_3$ to the acetalization reaction was almost double that of acetone released by iPAc, the acetalizing capability of the enol ester was still remarkable considering the excess d$_6$-acetone used. Even more so considering the inverse secondary deuterium isotope effect described for the formation of ketals from the reaction of methanol and acetone/d$_6$-acetone, the measured KH/KD (equilibrium constants for non-deuterated and deuterated ketals) ratio was ~0.7.[65]

2.3.3 Conclusions

This study reported for the first time a one-pot tandem catalytic acetalization-acetylation sequence of glycerol where the presence of multiple reagents allowed one to control the product distribution. Crucial to this result was the cooperative reactivity of isopropenyl acetate, acetic acid, and acetone in the presence of Amberlyst-15. The major role was played by the enol ester that acted as the acetylating agent of glycerol and at the same time, it underwent acidolysis with AcOH. Both these processes released acetone which in turn triggered the acetalization of glycerol. Moreover, acetic anhydride co-generated during the acidolysis of iPAc further contributed to the acetylation of glycerol. Notwithstanding the complex network of reactions, this investigation demonstrated that the experimental conditions could be tuned to obtain the selective conversion of glycerol to either a 1 : 1 mixture of acetal acetates (**4/4'**: 97% of which is solketal acetate) and triacetin, or solely acetal acetates **4/4'** in up to 91% yield. The latter result was achieved simply by supplying extra acetone to the iPAc/AcOH mixture. Experiments using d$_4$-acetic acid and d$_6$-acetone suggested that acetic acid, mostly through the formation of acetic anhydride, was the major contributor (for about 65%) to the final products, while curiously acetone released by iPAc provided ca. 35% of acetal acetates (**4/4'**) even when excess acetone was sourced externally. Acetic acid, along with acidolysis, also served as a solvent to overcome the issue of poor mutual solubility of iPAc and acetone with glycerol. The approach used was original and genuinely green. The synthetic potential of the tandem sequence for the upgrading of glycerol took advantage from the use of a pool of innocuous reactants (glycerol, iPAc, acetic acid and acetone) and mild/simple reaction conditions (30 °C

and atmospheric pressure) which made the scale-up of the protocol safe and easy. This study also proved that intensification of the process was achieved by controlling (reducing) the reactant molar ratio. In this respect, studies are currently in progress to transfer the procedure from batch to continuous flow to further enhance its productivity.

2.3.4 Experimental

General. Reagents and solvents were commercially available compounds and were used as received unless otherwise stated. Glycerol, acetic acid, acetic anhydride, acetone, isopropenyl acetate, Amberlyst-15, d_4-acetic acid, and d_6-acetone, were sourced from Sigma Aldrich (now Merck). GC/MS (EI, 70 eV) analyses were performed on a HP5-MS capillary column (L = 30 m, Ø = 0.32 mm, film = 0.25 mm), and GC analyses (CG/FID) were performed on an Elite-624 capillary column (L = 30 m, Ø = 0.32 mm, film = 1.8 mm). ^{1}H and ^{13}C NMR spectra were recorded at 400 and 100 MHz, respectively. The chemical shifts were reported downfield from tetramethylsilane (TMS), and CDCl$_3$ was used as the solvent.

General procedure for the tandem synthesis of solketal acetate and triacetin. Experiments were carried out under different conditions (Table 2.11 and Figure 2.37) which can be summarized as follows: in a 25- or 50-mL round-bottomed flask equipped with a condenser and a magnetic stir bar, a mixture of glycerol (1 mmol), isopropenyl acetate (1-10 mmol), acetic acid (0.5-10 mL) and Amberlyst-15 (5-15 mg) as a catalyst (5-15 wt%) was set to react at the temperature of choice (30-70 °C) and atmospheric pressure, for 24-32 h. Conversion of glycerol and product selectivity were determined by GC/FID analysis upon calibration. Compounds **4/4'** ((2,2-dimethyl-1,3-dioxolan-4-yl)methyl acetate and 2,2-dimethyl-1,3-dioxan-5-yl acetate, respectively) and **7** (propane-1,2,3-triyl triacetate) were isolated from a reaction scaled up by a factor of 10, using 10 mmol of glycerol (other conditions: T = 30 °C; *p* = 1 atm; molar ratio Glyc : iPAc : AcOH = 1 : 7.5 : 8.75; Amberlyst 15 = 15 wt%; t = 24 h). Once the experiment was complete, the solid catalyst was filtered off, and the liquid solution was distilled under vacuum (5 mBar, 50-80 °C). Isolated yields were 47% and 48% for **4/4'** and **7**, respectively. Products were characterized by both ^{1}H and ^{13}C NMR and GC/MS analyses. Data were in agreement with those reported in the literature.[20,66]

General procedure for the selective tandem synthesis of acetal acetates. Experiments were carried out under different conditions (Figure 2.44 and Scheme 2.36) which can be summarized as follows: in a 25- or 50-mL round-bottomed flask equipped with a condenser and a magnetic stir bar, a mixture of glycerol (1 mmol), isopropenyl acetate (1–4 mmol), acetic acid (0.5 mL), acetone (1–20 mmol) and Amberlyst-15 as a catalyst (15 wt%) was set to react at the temperature of choice (30–70 °C) and atmospheric pressure, for 16–24 h. Conversion of glycerol and product selectivity were determined by GC/FID analysis, upon calibration. Acetal acetates **4/4'** ((2,2-dimethyl-1,3-dioxolan-4-yl)methyl acetate and 2,2-dimethyl-1,3-dioxan-5-yl acetate, respectively) were isolated from a reaction scaled up by a factor of 10, using 10 mmol of glycerol (other conditions: T = 30 °C; *p* = 1 atm; molar ratio Glyc : iPAc : AcOH : Ace = 1 : 3 : 1.5 : 5; Amberlyst 15 = 15 wt%; t = 16 h). Once the experiment was complete, the solid catalyst was filtered off, and the liquid solution was distilled under vacuum (5 mBar, 50-80 °C). The isolated yield of **4/4'** was 87%. Products were characterized by both ^{1}H and ^{13}C NMR and GC/MS analyses; data were in agreement with those reported in the literature.[20,66]

The reactions with D-labelled compounds. Experiments with labelled reagents were carried out by replacing AcOH or acetone with the same quantity of the perdeuterated analogues, CD$_3$COOD or CD$_3$COCD$_3$. In the case of d_4-acetic acid, a mixture of glycerol (1 mmol), iPAc (7.5 mmol), CD$_3$COOD (0.5 mL, 8.75 mmol), and Amberlyst-15 (15 mg, 15 wt%) was set to react in a

25 mL round-bottomed flask at T = 30 °C and atmospheric pressure, under stirring for 24 h. In the case of d_6-acetone, a mixture of glycerol (1 mmol), isopropenyl acetate (4 mmol), d_6-acetone (5 mmol), acetic acid (1.5 mmol), and Amberlyst-15 (15 mg; 15 wt%) was set to react in a 25 mL round bottomed flask, at T = 30 °C and atmospheric pressure, under stirring for 16 h. The mixtures of labelled products were analyzed by GC/MS both in the full scan mode (TIC, 70 eV) and in the SIM mode on the characteristic fragment ions m/z = 159 and 162.

The results of this work have been the object of the paper:

2.4 iPEs and glycerol-derived aminodiols: concatenated procedures

2.4.1 Introduction

3-Amino-1,2-propanediol (3-APD) and 2-amino-1,3-propanediol (2-APD, serinol) are formally classified as glycerol derivatives obtained by the replacement of a primary or a secondary hydroxyl group of glycerol with a primary amine function. Notwithstanding this categorization, no examples have been reported so far for the straightforward preparation of 3-APD and 2-APD regioisomers from glycerol. Major synthetic routes of both substrates are summarized in Scheme 2.38.
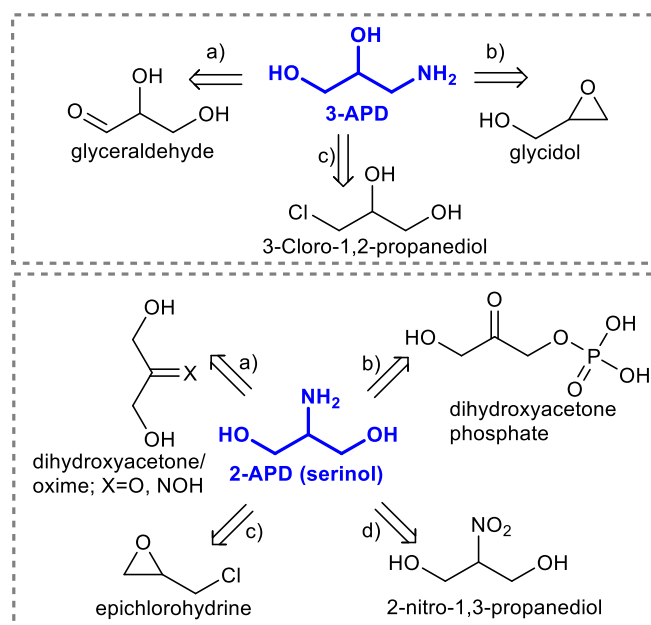
Scheme 2.38. *Top and bottom: major routes for 3-APD and 2-APD (serinol) synthesis, respectively*

3-APD is more often obtained from the reductive amination of biomass-derived glyceraldehyde or the nucleophilic attack of ammonia on glycidol that, in turn, is achieved by the catalytic decarboxylation of glycerol carbonate [Scheme 2.38, top: (a)–(b)].[67,68,69,70] Other, less attractive procedures have proposed the use of a carcinogenic starting reagent as 3-chloro-1,2-propanediol (Scheme 2.38, top: (c)).[71,72] 2-APD (serinol), besides being a naturally occurring substrate, is preferably synthesized from dihydroxyacetone (DHA) which is a popular innocuous product of the partial oxidation of glycerol.[73] DHA can be used as such or in the form of oxime or phosphate derivatives (Scheme 2.38, bottom: (a)–(b)).[73,74,75] Other approaches start from epichlorohydrine or 2-nitro-1,3-propanediol (Scheme 2.38, bottom: (c)–(d)): the epicerol®technology of Solvay produces the first reactant (epichlorohydrine) straight from the catalytic chlorination of glycerol, while protocol (d) is fully based on non-renewable compounds as nitromethane and paraformaldehyde.[76,77,26]

The compresence of three nucleophilic functions (OH and NH_2) makes both 2- and 3-APD appealing intermediates for a variety of transformations. Yet, the upgrading of these regioisomers still represents a largely unexplored area. As a part of a research program on the design of eco-friendly protocols for the valorization of bio-based products, particularly glycerol and its derivatives,[78] the program of this Thesis work was focused also on the investigation of new reactions for the chemoselective conversion of either the amino or the hydroxyl group of

APD compounds. N-acetylation and acetalization processes mediated by isopropenyl acetate (iPAc) and acetone were selected to this purpose, based on a literature survey and results recently published by our group.[56,79,80,81] Nontoxic, commercially available, and cheap iPAc has emerged as a privileged compound since its reactions with a variety of N- and O-nucleophiles result in the formation of acetylated derivatives and prop-1-en-2-ol that, as an enol, quickly converts into acetone, thereby making the overall transformations irreversible. Scheme 2.39 describes some representative examples, some of them described in detail throughout paragraphs 3.2 and 3.3.
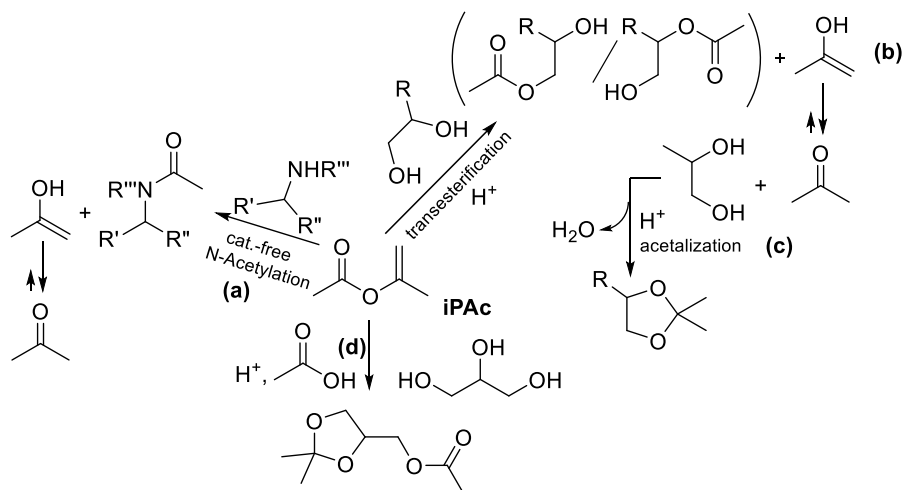
Scheme 2.39. *Examples of N-acetylation, transesterification and acetalization reactions mediated by iPAc (R, R', R''= alkyl, aryl; R, R'''= H, alkyl)*

The N-acetylation of primary and secondary amines has been achieved with iPAc under solventless and catalyst-free conditions (path a). Of note, polyfunctional amines, such as aminoalcohols and aminophenols, have been selectively amidated while primary and secondary hydroxyls or aromatic OH groups were fully preserved.[57] On the other hand, the acid-catalyzed reaction of (renewable) 1,2-diols and iPAc proceeded through a tandem sequence: an initial irreversible transesterification process took place (path b), releasing acetone which then promoted acetalization on a second molecule of glycol (path c). A follow-up of this study highlighted the even more attractive case of glycerol that in the presence of a mixture of iPAc and acetone, underwent simultaneous acetylation and acetalization to provide solketal acetate in almost quantitative yields (91%, path d). In light of these results, this work developed in this Thesis reports an original two-steps approach for the conversion of APD isomers, comprised of an initial N-acetylation reaction promoted by iPAc under batch conditions, followed by a continuous flow (CF) acetalization of the amide derivatives with acetone over a solid acid catalyst. The two processes have been first investigated separately by exploring the effect of major parameters (T, p, t, flow rate, and solvent) and then concatenated as shown in Scheme 2.40.
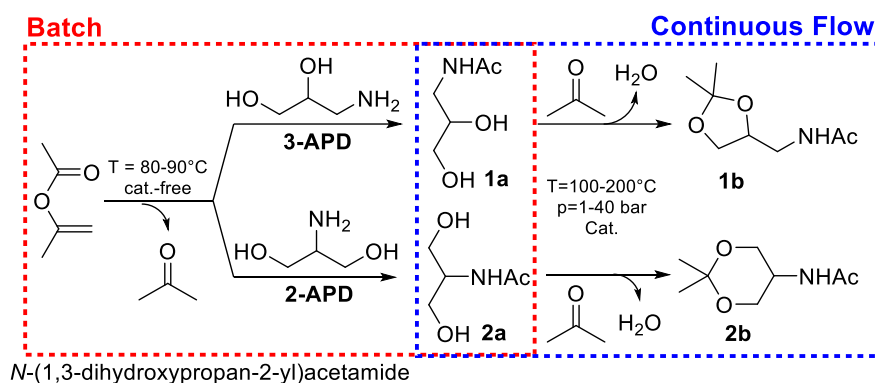
Scheme 2.40. *Concatenated batch and CF reactions used in this work*

In the overall sequence, solutions of crude products **1a** and **2a** as obtained from the batch N-acetylation were used without any treatment, to feed a CF-reactor for the second acetalization step. Highly (chemo)selective and quantitative reactions were achieved with selectivity towards N-acetylated diols (**1a**-**2a**) and N-acetylacetals (**1b**-**2b**) up to 99% and 92%, respectively.

2.4.2 Results and discussion

2.4.2.1 Batch catalyst-Free N-acetylation of 2- and 3-APD with iPAc

The N-acetylation of 2- and 3-APD with iPAc could not be carried out under the conditions previously described for primary and secondary amines (path a, Scheme 2.39), because the highly polar nature of both regioisomers made them fully immiscible with iPAC and with most of conventional organic liquids. After a screening of several candidates, two solvents were identified, *i.e.*, 1,4-dioxane and dimethyl sulfoxide (DMSO) in which the solubilities of APDs were ca 0.2 and 1 mmol/mL, respectively. The lower-boiling 1,4-dioxane (b.p. = 101 °C) was selected to start the investigation since its removal (distillation) was simpler during work-up procedures.

Temperature and reaction time. Initial experiments were performed to explore the effects of the temperature and the reaction time. A mixture of the selected APD (1 mmol), iPAc (1.1 equivs.), and 1,4-dioxane (5 mL, C = 0.2M) was set to react at T = 80–100 °C for up to 62 h, in the absence of any catalyst. Results are described in Figure 2.47 for the acetylation of 3-APD and 2-APD on top and bottom, respectively. The three profiles shown in each plot report the GC-yields of the N-acetylation products **1a** and **2a** (N-(2,3-dihydroxypropyl) acetamide and N-(1,3-dihydroxypropan-2-yl) acetamide, respectively; Scheme 2.40) at 80, 90, and 100 °C (**black**, **red**, and **blue** curves) as a function of time. Both compounds **1a** and **2a** were fully characterized by GC/MS, ^{1}H and ^{13}C NMR (see Appendix A.2). All reactions were run in duplicate for reproducibility ensuring <5% difference in yields between repeated tests.
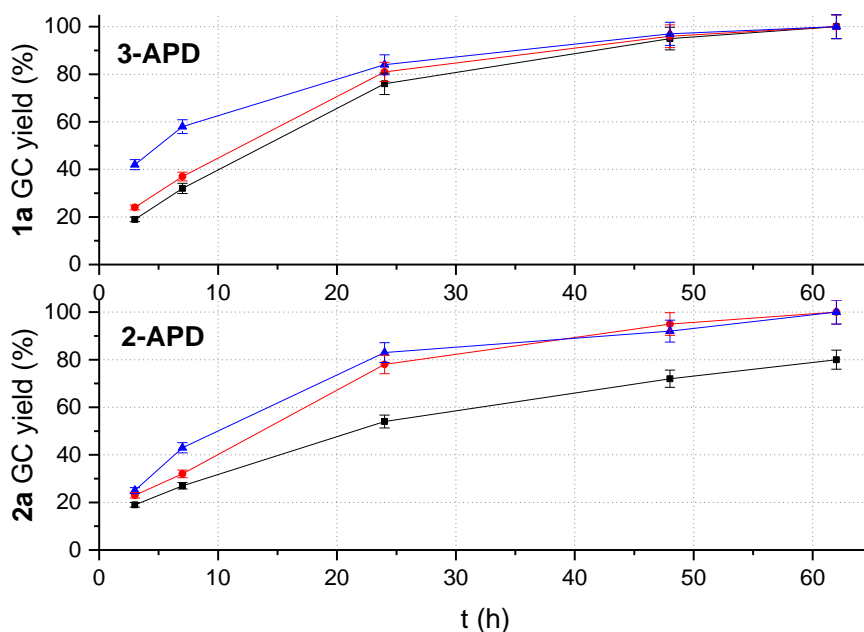
Figure 2.47. *Batch reactions of APD isomers with iPAc. Top and bottom: GC yields of amide products **1a** and **2a** from 3-APD and 2-APD, respectively, at T = 80 °C (-■-), 90 °C (-●-), and 100 °C (-▲-). Other conditions: mixture of APD (1 mmol), iPAc (1.1 equivs.), and 1,4-dioxane as a solvent (5 mL)*

Experiments demonstrated that not only the N-acetylation reactions was effective under the chosen conditions, but it proceeded with an excellent chemoselectivity (>99%). Regardless of the reaction time and the temperature, amides **1a** and **2a** were the only observed products. This was confirmed by the match of the yields of **1a** and **2a** and the conversion of reagents 3- and 2-APD, both determined by GC response calibration with an internal standard. internal standard**.** The exclusive N-acetylation was consistent with the better nucleophilicity of the amino group of both APDs compared to the primary and secondary hydroxyls which were preserved from any reaction. Indeed, no other products were detected.

On the other hand, both the temperature and the nature of the APD isomer affected the N-acetylation kinetics. Increasing T from 80 to 100 °C resulted in a general increase of yields of amides **1a** and **2a** from ca. 25–30% to 45–60% in the first 6 h. After 24 h, however, the acetylation of 3-APD appeared slightly influenced by the temperature and it proceeded to completion in all experiments (Figure 1, top), while a slower conversion of 2-APD was noticed at 80 °C, not exceeding 80% even after 62 h of reaction (Figure 2.47, bottom; **black** profile). The amide **2a** was obtained in quantitative yield only at T = 90 °C. The higher steric hindrance of the secondary amino group of serinol with respect to primary one of 3-APD was plausibly responsible for this behavior. Overall, the optimized temperatures to continue the study of the N-acetylation reaction were set to 80 and 90 °C for 3- and 2-APD, respectively.

The APD:iPAc molar ratio and the solvent. The effect of the iPAc:APD molar ratio (Q) was investigated by doubling and quadrupling the molar amount of iPAc with respect to conditions of Figure 2.47. The increased quantity of iPAc had no adverse consequences on APDs solubilities. Additional experiments were carried out also by replacing 1,4-dioxane (5 mL) with DMSO (0.5–5 mL) as the solvent. Table 2.15 summarizes the results. For a convenient comparison, some results of Figure 2.47 are also indicated (entries 1 and 5).

Table 2.15. *The iPAc-mediated selective N-amidation of 3- and 2-APD regioisomers*

Entry	Substrate	T (°C)	Qa (mol/mol)	Solvent (mL)	t (h)	Amide Yieldb (%)
1	3-APD	80	1.1	1,4-dioxane (5)	48	**1a**: 94%c
2			2.2	1,4-dioxane (5)	24	**1a**: ≥99%
3c			4.4	1,4-dioxane (5)	16	**1a**: ≥99% Isolated: ≥99%
4			4.4	DMSO (5)	3	**1a**: ≥99%
5			4.4	DMSO (1)	1	**1a**: ≥99%
6			4.4	DMSO (0.5)	0.75	**1a**: ≥99%
7c	2-APD	90	1.1	1,4-dioxane (5)	62	**2a**: ≥99%c
8			2.2	1,4-dioxane (5)	48	**2a**: ≥99%
9			4.4	1,4-dioxane (5)	24	**2a**: ≥99% Isolated: ≥99%
10			4.4	DMSO (5)	8	**2a**: ≥99%
11			4.4	DMSO (1)	2.5	**2a**: ≥99%
12			4.4	DMSO (0.5)	2	**2a**: ≥99%

Conditions: mixture of APD (1 mmol), iPAc (1.1-4.4 equivs.), and the solvent of choice (0.5-5 mL): T = 80 and 90 °C for 3-APD and 2-APD, respectively. [a] iPAc:APD molar ratio (Q). [b] Yields of amide derivatives determined by GC or after isolation of the products (entries 3 and 9). [c] Results from Figure 2.47.

Both changes of the Q ratio and the solvent did not affect the chemoselectivity which remained >99% towards the formation of amide derivatives. However, for the reaction of 3-APD in dioxane, increasing Q from 1.1 to 2.2 and 4.4 induced an almost linear drop of the time for complete conversion from 48 to 24 and 16 h, respectively (entries 1-3); while, for 2-APD, the reaction rate increased to a lesser extent consistent with the lower reactivity of this isomer (entries 7-9: time for complete reactions of 62, 48, and 24 h). Under the conditions of entries 3 and 9, two further experiments were carried out upscaling the reactants/solvent amounts by a factor of 10 (APD: 10 mmol; iPAc: 44 mmol; dioxane: 50 mL). The total conversion of 3- and 2-APD required 24 and 32 h, respectively, meaning that reactions were slower than those in Table 2.15; nonetheless, products **1a** and **2a** were easily isolated in >99% yields and 99% purity after rotary-evaporation of the unreacted iPAc and the solvent. The latter (iPAc and dioxane) were then recovered quantitatively by fractionated distillation. Overall, the protocol proved suitable for preparative purposes on the gram scale. The batch N-acetylation of 3- and 2-APD was then investigated using DMSO as a solvent. Compared to 1,4-dioxane (ε = 2.3, LD50 = 4200 mg/kg), the remarkably higher polarity, the excellent H-bonding accepting ability, and the non-toxicity of DMSO (ε = 46.7, LD50 = 14,500 mg/kg) made it not only more efficient at solubilizing both

APDs but also a greener alternative solvent.[82] A recent interesting study close to this subject inspected effects due to H-bonding in glycerol/DMSO binary mixtures.[80] Homogeneous solutions of reactants (APD: 1 mmol; iPAC: 4.4 mmol) were obtained by replacing dioxane either with the same volume of DMSO (5 mL) or by reducing the volume to 1 and 0.5 mL, respectively. Very fast N-acetylations were observed yielding to a quantitative formation of products **1a** and **2a** in all experiments. At the same concentration (0.1 M, 5 mL), the reactions of 3-APD and 2-APD in DMSO were 16- and eight-times faster than the corresponding processes in dioxane, thereby suggesting remarkable solvation effects on the kinetics (entries 4 and 10). On the other hand, the reduction of the solvent volume brought about a further acceleration of the reactions which, again, was more pronounced for the more active 3-APD (entries 5-6 and 11-12). Similar rapid reactions were achieved even by increasing the reactants/solvent amounts up to 10 times. Albeit attempts to isolate the products by distillation or extraction with several water/organic solvent systems failed, DMSO proved obviously advantageous from both the reaction rate and the process intensification standpoints. Results of Table 2.15 prompted us to conceive a concatenated sequence by which amides **1a** and **2a**, once prepared in either dioxane or DMSO, could be further converted into higher acetal homologues. The new products were expected to be quite less polar than amides and APDs, and so they could be more easily separated and handled. Flow chemistry appeared the best option to implement the second functionalization step.

2.4.2.2 The continuous flow (CF) acetalization of APD-amides under acid catalysis

CF-synthesis of N-((2,2-dimethyl-1,3-dioxolan-4-yl) methyl) acetamide (1b). Experiments were designed based on our previous results on the upgrading of glycerol via either sequential transesterification and acetalization processes (tandem) (Scheme 2.39) and CF-acetalization.[80] Among available catalysts for such reactions, solid acids were the most suited systems to cope with issues of deterioration and deactivation of flow reactors and catalytic beds, co-formation of water and not least in the case of glycerol and its derivatives, clogging due to the viscosity of the solutions of reactants and products. Accordingly, three heterogenous catalysts including an organic resin as Amberlyst-15 (Amb-15), and two inorganic solids as aluminum fluoride trihydrate (AlF3·3H2O: AF) and an acid exchanged Y-zeolite (HY) were chosen and compared in this study. Both Amb-15 and AF were commercially available compounds, while HY was obtained by calcination of a NH_4Y faujasite through a procedure reported elsewhere.[83]

Acetone as a reagent and a solvent/carrier. Initial tests were carried out using a 0.1 M solution of amide **1a** (prepared as described in Table 2.15) in acetone that acted as a reagent and a solvent/carrier. This mixture was continuously conveyed to a cylindrical steel reactor (L · D = 12mm · 6 mm, internal volume = 1.4 mL) filled with the catalyst (Amberlyst-15 or AlF3·3H2O or HY: 0.8 g in each case. The employed apparatus was in-house assembled (Figure 2.48). The features were substantially the same of the apparatus described in Figure 2.29, Chapter 2.2.
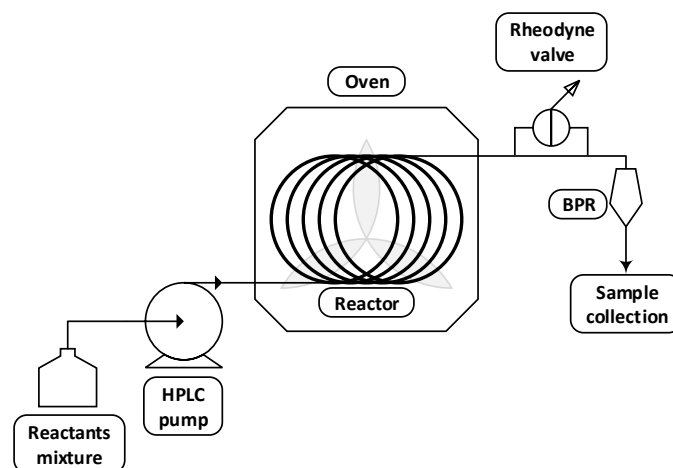
Figure 2.48. Experimental setup used for continuous-flow reactions of APD derivatives

The temperature, the pressure, and the flow rate (F) were varied in the range of 30–150 °C, 1–20 bar, and 0.1-0.2 mL·min^{-1}, respectively. Most representative results are reported in Table 2.16 and refer to reactions run for 5 h.

*Table 2.16. The CF-acetalization of amide **1a** over different catalysts*

Entry	Catalyst[a]	T/p (°C/bar)	Flow (mL/min)	Conv. (%)[b]	Sel. (%)[b]	Mass balance (%)[c]
1	Amb-15	30/1	0.1	>99	>99	>99
2			0.2	>99	>99	>99
3	AF	100/20	0.2	40	96	nd
4		150/20	0.2	79	99	
5	HY	100/20	0.2	27	92	
6		150/20	0.2	76	91	

All reactions were carried using a 0.1 M solution of amide **1a** in acetone. [a] A15: Amberlyst-15; AF: AlF$_3$·3H$_2$O; HY. In each case, the same amount of catalyst was used (0.8 g). [b] Conversion of amide **1a** and selectivity towards N-(1,3-dihydroxypropan-2-yl) acetamide **1b**, both determined by GC/MS. [c] Mass balance evaluated from the recovery of the mixture of the reactor outlet and the isolation of the product. nd: not determined

CF-tests proved the feasibility of the CF-acetalization of amide **1a**, though significantly different outcomes were observed by changing the catalyst. With respect to AF and HY, Amb-15 was a far more active system allowing the acetalization reaction to proceed at 30 °C and atmospheric pressure with excellent conversion and selectivity towards acetal **1b**, both higher than 99% (entries 1-2). Other solid catalysts instead, were effective only at temperatures of 100–150 _C that required to operate under pressure (20 bar) to keep acetone in a condensed phase. Notwithstanding these harsher conditions, the conversion of amide **1a** did not exceed 79 and 76% at 150 °C using AF and HY, respectively (entries 4 and 6). This trend was in line with the results of our previous study on the acetalization of glycerol glycerol that demonstrated a comparatively better performance of Amberlyst 36 with respect to AlF$_3$·3H$_2$O.[84]

In the case of the reaction catalyzed by Amb-15, after 5 h at F = 0.1 mL·min^{-1}, the volume of the solution collected at the reactor outlet was 30 mL (>99% of the expected value) and the yield of crude acetal **1b** isolated after rotary evaporation of acetone was 99% (518 mg) (entry 1). ^{1}H NMR confirmed that the purity of the product (**1b**) was >95% (Appendix A.2). The same volume/yield correspondence was achieved when F was doubled at 0.2 mL·min^{-1} (entry 2).

These results validated the mass balance of the CF-process and ruled out the occurrence of side-reactions.

Under the conditions of entries 1-2 (30 °C, 1 atm) further experiments were then performed to investigate the effect of the flow rate by changing it in a relatively wide range from 0.1 to 1.5 mL min^{-1}. Results are shown in Figure 2.49.
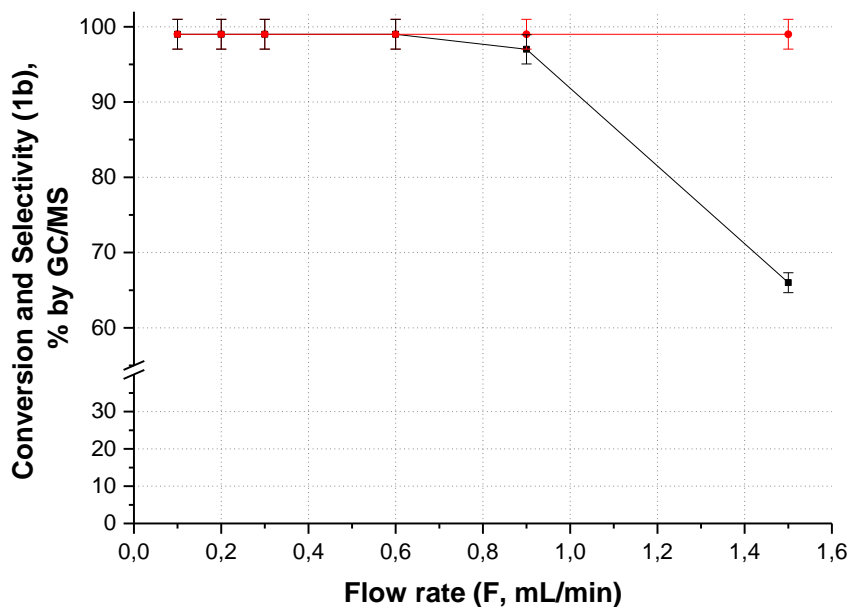
Figure 2.49. *The effect of the flow rate (F) on the CF-acetalization of amide **1a**. Other conditions were those of entries 1-2 in Table 1: 30 °C, 1 atm, Amb-15 catalyst (0.8 g), 0.1 M solution of **1a** in acetone. (-■-) **1a** conversion; (-●-) **1b** selectivity*

The formation of acetal **1b** took place with selectivity >99% regardless of the set flow rate (**red** profile). The conversion of amide **1a** was steady at a quantitative value until F was ≤0.6 mL·min^{-1}; then, it (conversion) showed a slight decrease to 95% and a more pronounced drop to 66% at F = 0.9 and 1.5 mL·min^{-1}, respectively (**black** profile). Results demonstrated that the acetalization protocol was highly efficient throughout the investigated range of F: by reducing the contact time (τ) from 14 min (F = 0.1 mL·min^{-1}) to 0.9 min (F = 1.5 mL·min^{-1}), the specific productivity (WHSV) was enhanced by a factor of 10, from 0.13 up to 1.3 g/(g$_{cat}$ h). An additional prolonged test run for 10 h at F = 0.1 mL·min^{-1}, proved the (long-term) stability of the catalyst: both conversion (>99%) and selectivity (>99%) did not show any appreciable change with respect to results of Figure 2.49.

Dioxane and DMSO as solvents/carriers. A concatenated sequence was then investigated with the aim to convert directly the crude amide **1a** as achieved from the batch N-acetylation, into the corresponding acetal **1b** in the flow mode. Once the reaction of 3-APD with iPAc (in a 1:4 molar ratio) was carried out under the conditions of entries 3 and 4 in Table 1, the resulting solution of amide **1a** (0.2 M) plus unconverted iPAc in dioxane or DMSO solvent, was added with different amounts of acetone (Q$_1$ = Ace:**1a** = 5-40 mol:mol). Without any further treatment, the mixture was used to feed the CF-reactor, by continuously conveying it to a catalytic bed of Amberlyst-15 (0.8 g). All CF-experiments were run for 5 h at atmospheric pressure through the same procedure and apparatus described in Table 2.16 and Figure 2.49. The temperature and the flow rate were changed in the range of 30-50 °C, and 0.1-0.6 mL·min^{-1}, respectively. Results are reported in Table 2.17.

Table 2.17. *The CF-acetalization of crude amide **1a** in the presence of dioxane and DMSO as solvents*[a]
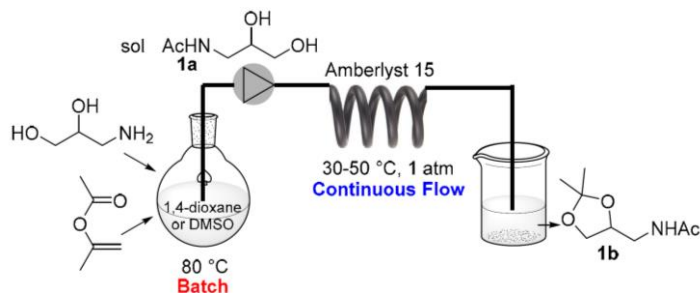
Entry	Substrate	Solvent	Ace:1a, Q_1 (mol:mol)[b]	T/p (°C/bar)	Flow (mL/min)	Conv. (%)[c]	Sel. (%)[c]
1			5	30/1	0.1	33	94
2				50/1		73	91
3		dioxane	20	30/1	0.1	83	>99
4	**1a**				0.3	61	>99
5					0.6	53	>99
6			40	30/1	0.1	95	>99
7					0.3	86	>99
8		DMSO	40	30/1	0.3	11	88
9				50/1		32	92
10		acetone[d]	135	30/1	0.3	24	94
				50/1		37	95
11	**2a**	dioxane	40	30/1	0.3	15	96
				50/1		24	97
12		DMSO	40	30/1	0.3	11	17
13				50/1		18	45

All reactions were carried using a 0.2 M solution of amide **1a** in dioxane or DMSO in the presence of added acetone. [a] The catalytic bed was made up of Amberlyst-15 (0.8 g). [b] Molar ratio of acetone and **1a** (Q_1). [c] Conversion of amide **1a** and selectivity towards N-(1,3-dihydroxypropan-2-yl) acetamide **1b**, both determined by GC/MS. [d] a 0.1M solution of amide **2a** in acetone (conditions of figure 2) was delivered to the Amb-15 catalytic bed

Tests demonstrated that the concatenated protocol was successfully implemented in dioxane as a solvent. Notwithstanding the presence of residual iPAc in the reacting mixture, the competitive acid-catalyzed transesterification of hydroxyl groups of amide **1a** took place to a very minor extent or was not observed at all, it even at a high/quantitative conversion: the acetal was obtained on an exclusive basis (>99%) in the presence of ≥20 molar equivs of acetone (entries 3-7); while, if the Q_1 ratio was reduced to 5, the selectivity towards compound **1b** decreased to 91-94% due to the concurrent formation of O-acetyl derivatives of **1a** (6-9%) (Figure 2.50).
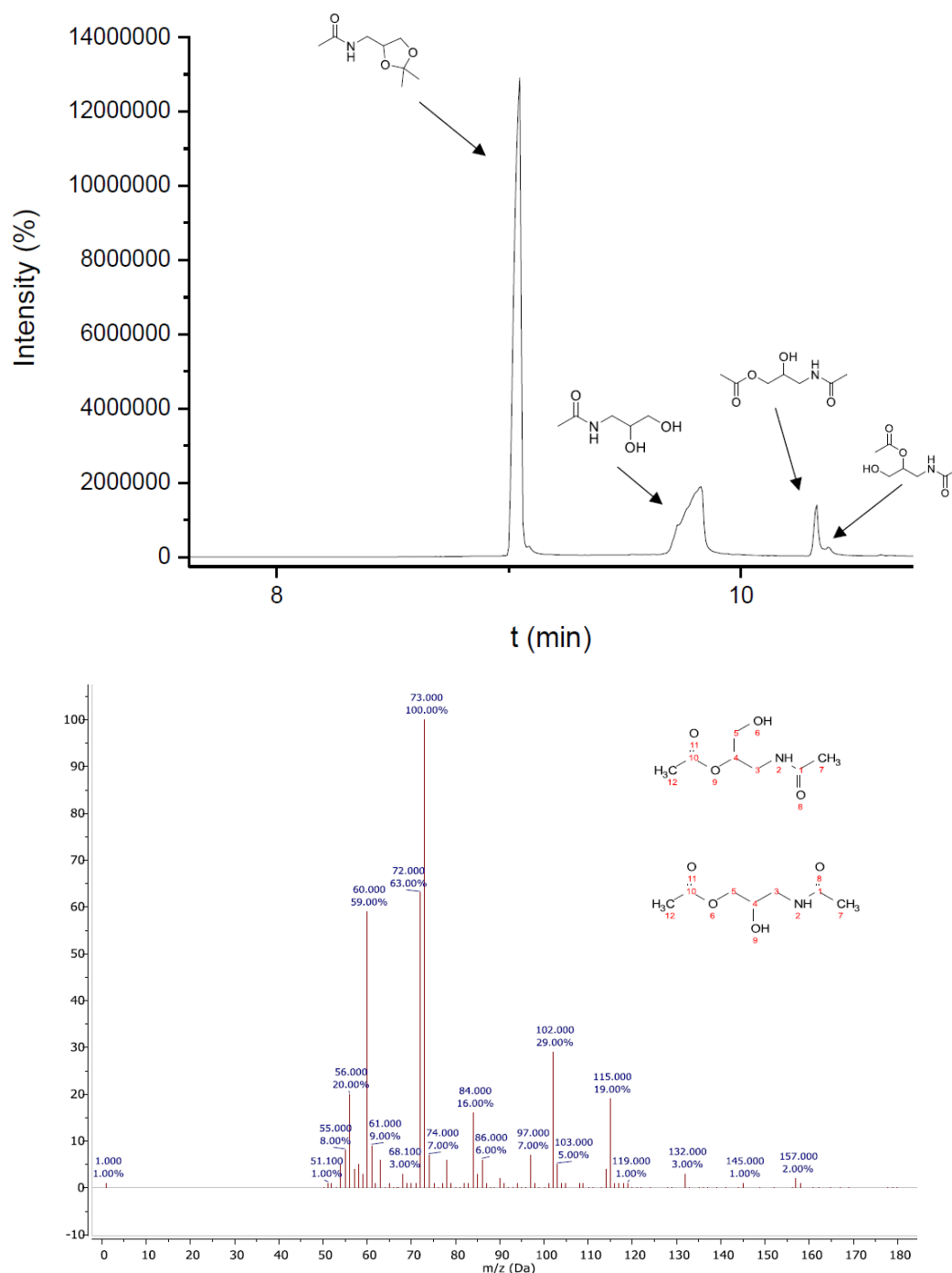
Figure 2.50. *Top: GC/MS chromatogram of the mixture from the concatenated reaction of compound **1a** in 1,4-dioxane (conditions: 0.2 M mixture of **1a** in 1,4-dioxane, 40 equivs. of acetone, T = 50 °C, p = 1 bar, F = 0.1 mL/min). Bottom: MS spectrum (70 eV) of monoacetate esters of amide **1a***

The GC/MS analysis could not resolve the two regioisomers products deriving from the transesterification of the primary and the secondary OH group of amide **1a**. The GC-peaks of these compounds appeared largely overlapped (Figure 2.50, top). The reported MS-spectrum was acquired in a median position of the total GC-signal (Figure 2.50, bottom). The heaviest ion fragment was observed at m/z = 157 corresponding to the loss of water from the molecular ion ($[M^{+\cdot}]$-H_2O = 175-18 = 157). Other relevant fragments were 132, 115 and 102, consistent with the loss of CH_3CO (43), CH_3COO + H (59-1=60), and CH_3COOCH_2 (73) from the molecular ion.

The most abundant fragment (100%) was detected at m/z=73 consistent with $[CH_3COOCH_2]^+$ ion.

A similar remarkable preference for the acetalization with respect to the transesterification process was noticed by us also during previous studies on the tandem reactions of diols mediated by iPAc.[84] This behavior was consistent with the higher reactivity of carbonyl compounds compared to esters toward nucleophilic additions/substitutions. Albeit the Q_1 molar ratio (acetone:**1a**) had no or little effect on selectivity, it significantly altered the kinetics. At T = 30 °C, p = 1 atm, and F = 0.1 mL·min^{-1}, a progressive improvement of the reaction conversion from 33% up to a nearly quantitative value (95%) was observed when the excess acetone was increased from 5 to 40 equivs. (entries 1, 3, and 6). These experiments also confirmed the results of Figure 2.49, further demonstrating that changing the flow rate greatly enhanced the reaction productivity. For example, at Q_1 = 20 and 40, by triplicating F from 0.1 to 0.3 mL·min^{-1}, WHSV was improved from 0.21 to 0.45 and 0.18 to 0.48 g/(g_{cat} h, respectively (entries 3-4 and 6-7).

A strikingly poor result was instead obtained using the crude amide **1a** in DMSO solvent. After addition of acetone (40 equivs with respect to **1a**), when the mixture was set to react in the flow mode at T = 30 °C and F = 0.3 mL·min^{-1}, the conversion was as low as 11% (entry 8). This (conversion) only slightly improved to 32% at 50 °C. The acetalization selectivity did not exceed 92% due to competitive formation of acetate derivatives of amide **1a**. Further investigations of this behavior were beyond the scope of the present paper; though, among plausible reasons for the adverse influence of DMSO on the acetalization kinetics, it was postulated that the occurrence of a strong (mostly H-bonding) interaction between DMSO and OH groups of the amide **1a** played a role in disfavoring/inhibiting the reaction.[80] Solvent effects on the catalyst (Amb-15) seemed less plausible since, for example, it was demonstrated that 1,4-dioxane and DMSO induced a comparable swelling on different Amberlyst solids.[88]

CF-synthesis of N-(2,2-dimethyl-1,3-dioxan-5-yl)acetamide (**2b**). Experiments were carried out either using a 0.1 M solution of (purified) amide **2a** in acetone as a reagent/solvent, or a 0.2 M solution of crude amide **2a** as obtained from the N-acetylation reaction with iPAc in the presence of dioxane solvent (entry 7, Table 2.15). In the latter case, acetone was added in 40 molar equivs with respect to **2a**. Other conditions were set according to the results optimized for amide **1a** (Table 2.16, Figure 2.49 and **Table 2.17.** The CF-acetalization of crude amide **1a** in the presence of dioxane and DMSO as solventsaTable 2.17): T = 30-50 °C, p = 1 atm, F = 0.3 mL·min^{-1}, Amb-15 = 0.8 g. Further experiments were run also at 100 °C and 10 bar. Table 4 reports the reaction conversion and the selectivity towards acetals **2b** after 5 h.

Table 2.18. *The CF-acetalization of amide 2a[a]*

Entry	Solvent	T/p (°C/bar)	Conv. (%)[b]	Sel. (%)[b]
1	acetone	30/1	24	94
2		50/1	37	95
3		100/10	62	92
4	1,4-dioxane	30/1	15	96
5		50/1	24	97
6		100/10	87	43

| 7 | DMSO | 30/1 | 11 | 17 |
| 8 | | 50/1 | 18 | 45 |

CF-reactions were carried using a 0.1 M solution of amide **2a** in acetone (entries 1–1) or a 0.2 M solution of **2a** in 1,4-dioxane (entries 3–4) or DMSO (entries 5–6) in the presence of added acetone (40 molar equivs with respect to **2a**). [a]The catalytic bed was made up of Amberlyst-15 (0.8 g). [b]Conversion of amide **2a** and selectivity towards N-(2,2-dimethyl-1,3-dioxan-5-yl) acetamide **2b**, both determined by GC/MS.

The acetalization of amide **2a** was far more difficult than amide **1a**, in line with the higher stability expected for the five- versus the six-membered ring cyclic acetal.[85] At atmospheric pressure, even increasing the temperature from 30 to 50 °C, the conversion did not exceed 37% and 24% in the presence of acetone alone (entries 1-2) and in dioxane solvent (entries 4-5), respectively. The formation of acetal **2b** (≥94%) was almost exclusive. Increasing the temperature to 100 °C greatly improved the reaction outcome in acetone, with conversion and selectivity of 62 and 92%, respectively (entry 3). A significant change was, however, noticed for the concatenated sequence: in the presence of iPAc, competitive acetalization and transesterification of **2a** took place yielding product **2b** (43%) along with mono- and di-acetate esters of the reactant amide in 16 and 41% selectivity, respectively (entry 6). Under such conditions, the pressure was set to 10 bar to allow acetone reacting in a condensed phase.[86] The acetal **2b** was fully characterized by ^{1}H- and ^{13}C-NMR, and GC/MS (Appendix A.2), while the structure of acetate side-products was assigned by GC/MS (Appendix A.2).

2.4.3   Conclusions

This work described an original protocol demonstrating how a catalyst-free N-acetylation reaction carried out under batch conditions, could be efficiently concatenated to a continuous-flow acid-catalyzed acetalization process for the upgrading of aminodiol regioisomers (APDs) of glycerol. A double functionalization of APDs was achieved through the proposed strategy: reagents were first converted into the corresponding N-acetyl derivatives which without isolation, were further transformed to cyclic C5 and C6 acetal homologues, though, only through a careful choice of reaction conditions, both steps (N-acetylation and acetalization) were successful. In addition to the optimization of the temperature, aspects highlighted by this study especially included the role/effect of: (i) the solvent for the batch N-acetylation which was critical to obtain homogenous solutions of hardly soluble substrates as APDs; (ii) the nature of the solvent/catalyst and the reagent (amide):acetone molar ratio which affected the conversion and steered the selectivity of the CF-acetalization. Of the two identified solvents, DMSO and 1,4-dioxane, the former was far more efficient at solubilizing APDs, but it failed as an acetalization solvent probably because of strong (H-bonding) solvation effects of amide reactants. The less polar and lower boiling dioxane, albeit implying longer reaction times and the use of diluted solutions, proved to be suitable for the concatenated procedure, allowing also a facile separation of both amides and acetals derivatives. In line with previous studies on the acetalization of glycerol, this study confirmed that acid organic resins, specifically Amberlyst 15 (Amb-15) showed a far better performance than other solid catalysts (faujasite (HY) and $AlF_3 \cdot 3H_2O$) for the CF conversion of APD-derived amides into the corresponding acetals. Beyond advantages of Amb-15 in terms of reduced equipment corrosion and environmental acceptability, the flow protocol could be easily tuned to improve the reaction productivity which for the case of acetal **1b**, was enhanced to 1.3 and 0.48 g/(g$_{cat}$ h) in acetone and in dioxane solvent, respectively. A conclusive note was the remarkably different behavior of

amide **1a** and **2a** towards acetalization, being the former much more active than the latter, with consequences not only on the reaction rate but also on the products distribution. The five-membered ring product **1b** was achieved with >99% selectivity, while the formation of the less stable six-membered cyclic acetal **2b** was always accompanied by a competitive transesterification process.

2.4.4 Experimental

General. Reagents and solvents were commercially available compounds and were used as received unless otherwise stated. 3-amino-1,2-propanediol, 2-amino-1,3-propanediol, isopropenyl acetate, 1,4-dioxane, dimethyl sulfoxide, ethanol, acetone, Amberlyst-15, AlF3·3H2O were sourced from Sigma Aldrich (now Merck Life Science S.r.l., Milano, IT). Zeolite HY HY was obtained by calcination of a commercial NH$_4$Y solid.[80] GC/MS and GC/FID (EI, 70 eV) analyses were performed on HP-35 and ELITE-624, respectively, capillary columns (L = 30 m, Æ = 0.32 mm, film = 0.25 mm). ^{1}H and ^{13}C NMR spectra were recorded at 400 and 100 MHz, respectively. The chemical shifts were reported downfield from tetramethylsilane (TMS), and CDCl$_3$, CD$_3$OD or d$_6$-DMSO were used as the solvent, depending on the compounds solubility.

General procedure for the batch N-acetylation of 3-APD and 2-APD (serinol). Experiments were carried out under the conditions described in Table 2.15 and Figure 2.47. In a typical procedure, a 10-mL round-bottomed flask, equipped with a condenser and a magnetic stir bar, a mixture of 3-amino-1,2-propanediol (APD) or 2-amino-1,3-propanediol (serinol) (1 mmol), iPAc (1.1–4.4 equivs.), and 1,4-dioxane (5 mL) or DMSO (0.5–5 mL) as a solvent was set to react at T = 80-90 °C and atmospheric pressure, for 1-62 h. Conversion of APDs and products selectivity were determined by GC-FID analysis upon calibration. The same procedure was also scaled up by a factor of 10, using a mixture of the selected APD (10 mmol), isopropenyl acetate (4.4 equivs.), and 1,4-dioxane as a solvent (50 mL). Once the experiment was complete, the excess of solvent and iPAc was distilled off by vacuum evaporation, affording the N-(2,3-dihydroxypropyl) acetamide (**1a**) or N-(1,3- dihydroxypropan-2-yl) acetamide (**2a**) in quantitative yields. In addition, the recovery of the iPAc was performed by vacuum fractionated distillation. Products **1a** and **1b** were isolated and fully characterized by MS (70 eV), ^{1}H NMR, and ^{13}C NMR. Spectra are reported in Appendix A.2.

*General procedure for the CF acetalization of amides **1a, 2a**.* Experiments were performed using an in-house assembled continuous-flow (CF) apparatus (Figure 2.48), under the conditions described in Table 2.16Table 2.17Table 2.18, and Figure 2.49. In a typical procedure, the CF apparatus was conditioned with acetone (30mL at 5 mL·min^{-1}). Then, a homogeneous 0.1 M solution of the reactants (amides **1a, 2a**) in acetone, acetone/dioxane, acetone/DMSO was delivered to the catalytic bed of choice (Amberlyst 15, AlF$_3$·3H$_2$O, or HY: 0.8 g in each case) at the desired T, *p*, and flow rates (30-100 °C, 1-10 bar, and 0.1-1.5 mL·min^{-1}). Aliquots (0.3 mL) of the reaction mixture were sampled at the outlet of the reactor every 30 min and analyzed by GC/MS. Reactions were allowed to proceed for 5 h, though some prolonged tests were carried out for up to 12 h. Acetal products **1b** and **2b** were isolated according to the following procedure. Compound **1b** was directly isolated in >99% yield and very high purity (>96%, GC) after simple rotary-evaporation of excess acetone and the solvent (dioxane, if present). Compound **2b** instead, after rotary-evaporation of the final reaction mixture, was isolated by

FCC (stationary phase: SiO_2; eluent: Et_2O) in 49% yield. Products were characterized both by MS (70 eV), ^{1}H NMR, and ^{13}C NMR. Spectra are reported in Appendix A.2.

The results of this work have been the object of the paper:

Davide Rigo, Nadia Alessandra Carmo Dos Santos, Alvise Perosa, Maurizio Selva "Concatenated batch and continuous flow procedures for the upgrading of glycerol-derived aminodiols via N-acetylation and acetalization reactions", *Catalysts* **2021**, *11*, 21; doi: 10.3390/catal11010021

References

[1] J. Otera, Transesterification, *Chem. Rev.*, **1993**, *93*, 1449. https://doi.org/10.1021/cr00020a004

[2] G. A. Grasa, R. Singh, and S. P. Nolan, Transesterification/Acylation Reactions Catalyzed by Molecular Catalysts, *Synthesis* **2004**, *2004*, 971. https://doi.org/10.1055/s-2004-822323

[3] M. Selva, A. Perosa, S. Guidi, and L. Cattelan, Ionic liquids as transesterification catalysts: applications for the synthesis of linear and cyclic organic carbonates, *Beilstein J. Org. Chem.*, **2016**, *12*, 1911. https://doi.org/10.3762/bjoc.12.181

[4] A. Drazic, L. M. Myklebust, R. Ree, T. Arnesen, The world of protein acetylation, *Biochim. Biophys. Acta, Proteins Proteomics*, **2016**, *1864*, 1372. https://doi.org/10.1016/j.bbapap.2016.06.007

[5] P. F. Corregidor, Isoamyl acetate preparation from reaction of vinyl acetate and Isoamyl alcohol catalyzed by H-ZSM-5 zeolite: a kinetic study, *Mol. Catal.*, **2018**, 100611. https://doi.org/10.1016/j.mcat.2018.06.009

[6] E. S. Rothman, S. Serota, T. Perlstein, and D. Swern, Acid- Catalyzed Interchange Reactions of Carboxylic Acids with Enol Esters, *J. Org. Chem.*, **1962**, *27*, 3123. https://doi.org/10.1021/jo01056a033

[7] J. Bassut, A. M. R. Rocha, A. França, R. A. C. Leão, C. M. F. T. Monteiro, C. A. M. Afonso, and R. O. M. A. de Souza, PEG600-carboxylates as acylating agents for the continuous enzymatic kinetic resolution of alcohols and amines, *Mol. Catal.* **2018**, *459*, 89. https://doi.org/10.1016/j.mcat.2018.08.019

[8] E. S. Rothman, S. S. Hecht, P. E. Pfeffer, and L. S. Silbert, Enol esters. XV. Synthesis of highly hindered esters via isopropenyl ester intermediates, *J. Org. Chem.*, **1972**, *37*, 3551. https://doi.org/10.1021/jo00795a041

[9] Y. F. Wang, J. J. Lalonde, M. Momongan, D. E. Bergbreiter, and C. H. Wong, Lipase-Catalyzed Irreversible Transesterifications Using Enol Esters as Acylating Reagents: Preparative Enantio and Regioselective Syntheses of Alcohols, Glycerol Derivatives, Sugars, and Organometallics, *J. Am. Chem. Soc.*, **1988**, *110*, 7200. https://doi.org/10.1021/ja00229a041

[10] K. Naemura, M. Murata, R. Tanaka, M. Yano, K. Hirose, and Y. Tobe, Enantioselective acylation of alcohols catalyzed by lipase QL from Alcaligenes sp.: A predictive active site model for lipase QL to identify the faster reacting enantiomer of an alcohol in this acylation, *Tetrahedron: Asymmetry,* **1996**, *7*, 1581. https://doi.org/10.1016/0957-4166(96)00186-3

[11] J. W. J. Bosco, and A. K. Saikia, Palladium(ii) chloride catalyzed selective acetylation of alcohols with vinyl acetate. *Chem. Commun.*, **2004**, 1116. https://doi.org/10.1039/B401218F

[12] S. Magens, M. Ertelt, A. Jatsch, and B. Plietker, A Nucleophilic Fe Catalyst for Transesterifications under Neutral Conditions, *Org. Lett.*, **2008**, *10*, 53. https://doi.org/10.1021/ol702580a

[13] I. Chiarotto, Tetraethylammonium hydrogen carbonate: A cheap, efficient, and recyclable catalyst for transesterification reactions under solvent-free conditions. *Synth. Commun.*, **2016**, *46*, 1840. https://doi.org/10.1080/00397911.2016.1233343

[14] G. Assaf, G. Checksfield, D. Critcher, P. J. Dunn, S. Field, L. J. Harris, R. M. Howard, G. Scotney, A. Scott, S. Mathew, G. M. Walker, and A. Wilder, The use of environmental metrics to evaluate green chemistry improvements to the synthesis of (S,S)-reboxetine succinate, *Green Chem.*, **2012**, *14*, 123. https://doi.org/10.1039/C1GC15921F

[15] A. Orita, A. Mitsutome, and J. Otera, Distannoxane-Catalyzed Highly Selective Acylation of Alcohols, *J. Org. Chem.* **1998**, *63*, 2420. https://doi.org/10.1021/jo9800412

[16] W. J. Croxall, F. J. Glavis and H. T. Neher, Preparation of Acetals or Ketals from Vinyl-type Esters, *J. Am. Chem. Soc.*, **1948**, *70*, 2805. https://doi.org/10.1021/ja01188a049

[17] D. Hirsh, R. Hoaglin and D. Kubler, Preparation of Acetals and Ketals from Enol Esters, *J. Org. Chem.*, **1958**, *23*, 1083. https://doi.org/10.1021/jo01101a628

[18] C. J. Chapman, C. G. Frost, J. P. Hartley and A. J. Whittle, Efficient aromatic and heteroatom acylations using catalytic indium complexes with lithium perchlorate, *Tetrahedron Lett.*, **2001**, *42*, 773. https://doi.org/10.1016/S0040-4039(00)02122-5

[19] D. Mukherjee, B. A. Shah, P. Gupta and S. C. Taneja, Tandem acetalation–acetylation of sugars and related derivatives with enolacetates under solvent-free conditions, *J. Org. Chem.*, **2007**, *72*, 8965. https://doi.org/10.1021/jo070363i

[20] R. Calmanti, M. Galvan, E. Amadio, A. Perosa, and M. Selva, M. High-Temperature Batch and Continuous-Flow Transesterification of Alkyl and Enol Esters with Glycerol and Its Acetal Derivatives, *ACS Sustainable Chem. Eng.*, **2018**, *6*, 3964. https://doi.org/10.1021/acssuschemeng.7b04297

[21] R. A. Sheldon, Fundamentals of green chemistry: efficiency in reaction design, *Chem. Soc. Rev.*, **2012**, *41*, 1437. https://doi.org/10.1039/C1CS15219J

[22] H. Yue, Y. Zhao, X. Ma, and J. Gong, Ethylene glycol: properties, synthesis, and applications, *Chem. Soc. Rev.*, **2012**, *41*, 4218. https://doi.org/10.1039/C2CS15359A

[23] A. Gonzalez-Garay, M. Gonzalez-Miquel, and G. Guillen-Gosalbez, High-Value Propylene Glycol from Low-Value Biodiesel Glycerol: A Techno-Economic and Environmental Assessment under Uncertainty, *ACS Sustainable Chem. Eng.*, **2017**, *5*, 5723. https://doi.org/10.1021/acssuschemeng.7b00286

[24] J. L. Dong, L. S. Yu, and J. W. Xie, A Simple and Versatile Method for the Formation of Acetals/Ketals Using Trace Conventional Acids, *ACS Omega*, **2018**, *3*, 4974. https://doi.org/10.1021/acsomega.8b00159

[25] B. Mukhopadhyay, Sulfuric acid immobilized on silica: an efficient promoter for one-pot acetalation–acetylation of sugar derivatives, *Tetrahedron Lett.*, **2006**, *47*, 4337. https://doi.org/10.1016/j.tetlet.2006.04.118

[26] S. Guidi, R. Calmanti, M. Noè, A. Perosa, and M. Selva, Thermal (catalyst-free) transesterification of diols and glycerol with dimethyl carbonate: A flexible reaction for batch and continuous-flow applications, *ACS Sustainable Chem. Eng.*, **2016**, *4*, 6144. https://doi.org/10.1021/acssuschemeng.6b01633

[27] L. Chen, B. Nohair, and S. Kaliaguine, Glycerol acetalization with formaldehyde using water-tolerant solid acids, *Appl. Catal., A*, **2016**, *509*, 143. https://doi.org/10.1016/j.apcata.2015.08.014

[28] N. Boz, N. Degirmenbasi, and D. M. Kalyon, Esterification and transesterification of waste cooking oil over Amberlyst 15 and modified Amberlyst 15 catalysts, *Appl. Catal., B*, **2015**, *165*, 723. https://doi.org/10.1016/j.apcatb.2014.10.079

[29] A. D. Curzons, D. J. C. Constable, D. N. Mortimer, and V. L. Cunningham, So you think your process is green, how do you know? Using principles of sustainability to determine what is green a corporate perspective, *Green Chem.*, **2001**, *3*, 1. https://doi.org/10.1039/B007871I

[30] M. B. Smith, and J. March, Eds. March's Advanced Organic Chemistry, Reactions, Mechanisms, and Structure, 6th ed.; Wiley: Hoboken, NJ, 2007.

[31] Y. Liu, E. Lotero, J. G. Goodwin, Effect of carbon chain length on esterification of carboxylic acids with methanol using acid catalysis, *J. Catal.*, **2006**, *243*, 221. https://doi.org/10.1016/j.jcat.2006.07.013

[32] D. Datta, and D. Majumdar, Steric effects of alkyl groups: A 'cone angle' approach, *J. Phys. Org. Chem.*, **1991**, *4*, 611. https://doi.org/10.1002/poc.610041005

[33] A. Randová, O. Vopička, L. Bartovská, and K. Friess, Cyclopentyl methyl ether, *tert*-amyl methyl ether and *tert*-butyl methyl ether: density, dynamic viscosity, surface tension and refractive index, *Chem. Pap.,* **2018**, *72*, 947. https://doi.org/10.1007/s11696-017-0338-x

[34] C. L. Gargalo, A. Carvalho, K. V. Gernaey and G. Sin, Optimal Design and Planning of Glycerol-Based Biorefinery Supply Chains under Uncertainty, *Ind. Eng. Chem. Res.*, **2017**, *56*, 11870. https://doi.org/10.1021/acs.iecr.7b02882

[35] M. Pagliaro, Glycerol: The Renewable Platform Chemical, Elsevier, 2017.

[36] M. R. Monteiro, C. L. Kugelmeier, R. S. Pinheiro, M. O. Batalha and A. da Silva César, Glycerol from biodiesel production: Technological paths for sustainability, *Renew. Sust. Energ. Rev.*, **2018**, *88*, 109. https://doi.org/10.1016/j.rser.2018.02.019

[37] A. Villa, N. Dimitratos, C. E. Chan-Thaw, C. Hammond, L. Prati and G. J. Hutchings, Glycerol oxidation using gold-containing catalysts, *Chem. Res.*, **2015**, *48*, 1403. https://doi.org/10.1021/ar500426g

[38] Y. Wang, J. Zhou and X. Guo, Catalytic hydrogenolysis of glycerol to propanediols: a review, *RSC Adv.*, **2015**, *5*, 74611. https://doi.org/10.1039/C5RA11957J

[39] A. Fasolini, D. Cespi, T. Tabanelli, R. Cucciniello and F. Cavani, Hydrogen from renewables: a case study of glycerol reforming, *Catalysts*, **2019**, *9*, 722. https://doi.org/10.3390/catal9090722

[40] P. S. Kong, M. K. Aroua and W. M. A. W. Daud, Conversion of crude and pure glycerol into derivatives: A feasibility evaluation, *Renew. Sust. Energ. Rev.*, **2016**, *63*, 533. https://doi.org/10.1016/j.rser.2016.05.054

[41] R. S. Varma and C. Len, Glycerol valorization under continuous flow conditions-recent advances, *Curr. Opin. Green Sustain. Chem.*, **2019**, *15*, 83. https://doi.org/10.1016/j.cogsc.2018.11.003

[42] P. S. Kong, M. K. Aroua, W. M. A. W. Daud, H. V. Lee, P. Cognet and Y. Pérès, Catalytic role of solid acid catalysts in glycerol acetylation for the production of bio-additives: a review, *RSC Adv.*, **2016**, *6*, 68885. https://doi.org/10.1039/C6RA10686B

[43] P. U. Okoye and B. H. Hameed, Review on recent progress in catalytic carboxylation and acetylation of glycerol as a byproduct of biodiesel production, *Renew. Sust. Energ. Rev.*, **2016**, *53*, 558. https://doi.org/10.1016/j.rser.2015.08.064

[44] A. R. Trifoi, P. Ş. Agachi and T. Pap, Glycerol acetals and ketals as possible diesel additives. A review of their synthesis protocols, *Renew. Sust. Energ. Rev.*, **2016**, *62*, 804. https://doi.org/10.1016/j.rser.2016.05.013

[45] https://www.globenewswire.com/news-release/2019/07/15/ 1882588/0/en/Triacetin-Glyceral-Triacetate-Market-To-Reach- USD-255-6-Million-By-2026-Reports-And-Data.html (accessed 17/11/2021).

[46] https://www.globalinforesearch.com/global-solketal-cas-100-79-8-market_p106784.html (accessed 17/11/2021).

[47] L. J. Konwar, P. Mäki-Arvela, P. Begum, N. Kumar, A. J. Thakur, J. P. Mikkola, R. C. Deka and D. Deka, Shape selectivity and acidity effects in glycerol acetylation with acetic anhydride: Selective synthesis of triacetin over Y-zeolite and sulfonated mesoporous carbons, *J. Catal.*, **2015**, *329*, 237. https://doi.org/10.1016/j.jcat.2015.05.021

[48] L. R. Odell, J. Skopec and A. McCluskey, A 'cold synthesis' of heroin and implications in heroin signature analysis: Utility of trifluoroacetic/acetic anhydride in the acetylation of morphine, *Forensic Sci. Int.*, **2006**, *164*, 221. https://doi.org/10.1016/j.forsciint.2006.02.009

[49] V. L. C. Goncalves, B. P. Pinto, J. C. Silva and C. J. A. Mota, Acetylation of glycerol catalyzed by different solid acids, *Catal. Today*, **2008**, *133–135*, 673. https://doi.org/10.1016/j.cattod.2007.12.037

[50] J. R. Dodson, T. d. C. M. Leite, N. S. Pontes, B. Peres Pinto and C. J. A. Mota, Green acetylation of solketal and glycerol formal by heterogeneous acid catalysts to form a biodiesel fuel additive, *ChemSusChem*, **2014**, *7*, 2728. https://doi.org/10.1002/cssc.201402070

[51] J. Deutsch, A. Martin and H. Lieske, Investigations on heterogeneously catalysed condensations of glycerol to cyclic acetals, *J. Catal.*, **2007**, *245*, 428. https://doi.org/10.1016/j.jcat.2006.11.006

[52] C. X. A. da Silva, V. L. C. Goncalves and C. J. A. Mota, Water-tolerant zeolite catalyst for the acetalisation of glycerol, *Green Chem.*, **2009**, *11*, 38. https://doi.org/10.1039/B813564A

[53] M. Selva, S. Guidi and M. Noè, Upgrading of glycerol acetals by thermal catalyst-free transesterification of dialkyl carbonates under continuous-flow conditions, *Green Chem.*, **2015**, *17*, 1008. https://doi.org/10.1039/C4GC01750A

[54] U. I. Nda-Umar, I. Ramli, Y. H. Taufiq-Yap and E. N. Muhamad, An overview of recent research in the conversion of glycerol into biofuels, fuel additives and other bio-based chemicals, *Catalysts*, **2019**, *9*, 15. https://doi.org/10.3390/catal9010015

[55] L. Zhou, T. H. Nguyen and A. A. Adesina, The acetylation of glycerol over amberlyst-15: Kinetic and product distribution, *Fuel Process. Technol.*, **2012**, *104*, 310. https://doi.org/10.1016/j.fuproc.2012.06.001

[56] D. Rigo, G. Fiorani, A. Perosa and M. Selva, Acid-Catalyzed Reactions of Isopropenyl Esters and Renewable Diols: A 100% Carbon Efficient Transesterification/Acetalization Tandem Sequence, from Batch to Continuous Flow, *ACS Sustainable Chem. Eng.*, **2019**, *7*, 18810. https://doi.org/10.1021/acssuschemeng.9b03359

[57] H. J. Hagemeyer Jr. and D. C. Hull, Reactions of isopropenyl acetate, *Ind. Eng. Chem.*, **1949**, *41*, 2920. https://doi.org/10.1021/ie50480a063

[58] N. Y. He, C. S. Woo, H. G. Kim and H. I. Lee, Catalytic formation of acetic anhydride over tungstophosphoric acid modified SBA-15 mesoporous materials, *Appl. Catal., A*, **2005**, *281*, 167. https://doi.org/10.1016/j.apcata.2004.11.026

[59] E. S. Rothman, Formation of Heneicosane-2, 4-dione by Acid-Catalyzed Rearrangement of Isopropenyl Stearate, J. *Org. Chem.*, **1966**, *31*, 628. https://doi.org/10.1021/jo01340a528

[60] J. A. Landgrebe, Kinetics and Mechanism of Acid-Catalyzed Enol Ester Hydrolysis, *J. Org. Chem.*, **1965**, *30*, 2997. https://doi.org/10.1021/jo01020a024

[61] J. Huanc, J.-P. Leblanc and H. K. Hall, Model studies on the kinetics and mechanism of polyarylate synthesis by acidolysis, *J. Polym. Sci., Part A: Polym. Chem.*, **1992**, *30*, 345. https://doi.org/10.1002/pola.1992.080300301

[62] J. F. Marlier, Multiple isotope effects on the acyl group transfer reactions of amides and esters, *Acc. Chem. Res.*, **2001**, *34*, 283. https://doi.org/10.1021/ar000054d

[63] S. Guidi, M. Noè, P. Riello, A. Perosa and M. Selva, Towards a Rational Design of a Continuous-Flow Method for the Acetalization of Crude Glycerol: Scope and Limitations of Commercial Amberlyst 36 and AlF3·3H2O as Model Catalysts, *Molecules*, **2016**, *21*, 657. https://doi.org/10.3390/molecules21050657

[64] V. B. Vol'eva, I. S. Belostotskaya, A. V. Malkova, N. L. Komissarova, L. N. Kurkovskaya, S. V. Usachev and G. G. Makarov, New approach to the synthesis of 1,3-dioxolanes, *Russ. J. Org. Chem.*, **2012**, *48*, 638. https://doi.org/10.1134%2FS1070428012050028

[65] V. A. Stoute and M. Winnik, Secondary β-Hydrogen Isotope Effects in Ketal Formation Equilibria, *Can. J. Chem.*, **1975**, *53*, 3503. https://doi.org/10.1139/v75-505

[66] (a) M. Hatano, Y. Tabata, Y. Yoshida, K. Toh, K. Yamashita, Y. Ogura and K. Ishihara, Metal-free transesterification catalyzed by tetramethylammonium methyl carbonate, *Green Chem.*, **2018**, *20*, 1193. https://doi.org/10.1039/C7GC03858E; (b) K. Sugahara, N. Satake, K. Kamata, T. Nakajima and N. Mizuno, A basic germanodecatungstate with a− 7 charge: Efficient chemoselective acylation of primary alcohols, *Angew. Chem., Int. Ed.*, **2014**, *53*, 13248. https://doi.org/10.1002/ange.201405212

[67] G. Liang, A. Wang, L. Li, G. Xu, N. Yan, and T. Zhang, Production of Primary Amines by Reductive Amination of Biomass-Derived Aldehydes/Ketones. *Angew. Chem.-Int. Ed.* **2017**, *56*, 3050. https://doi.org/10.1002/ange.201610964

[68] A. Horiguchi, A. Takabe, and E. Takemoto, A Process for the Preparation of a Dihydroxyamino Compound. EP1201644 (A2), 2 May 2002.

[69] E. Felder, M. Roemer, H. Bardonner, H. Haertner, and W. Fruhstorfer, Process for the Preparation of Hydroxyamines. US5023379 (A), 11 June 1991.

[70] A. Borregaard, and F. Tjosaas, Process for the Production of Amino Alcohols. WO2012108777 (A1), 16 August 2012.

[71] K. Baum, W. T. Maurice, The Mannich Condensation of 3-amino-1,2-propanediol with 2,2-dinitropropanol and the nitration of the product, *J. Org. Chem.* **1962**, *27*, 2231. https://doi.org/10.1021/jo01053a518

[72] B. Andreeßen, and A. Steinbüchel, Serinol: Small molecule-big impact. *AMB Express* **2011**, *1*, 1. https://doi.org/10.1186/2191-0855-1-12

[73] L. Cerioli, M. Planchestainer, J. Cassidy, D. Tessaro, and F. Paradisi, Characterization of a novel amine transaminase from Halomonas elongata. *J. Mol. Catal. B Enzym.* **2015**, *120*, 141. https://doi.org/10.1016/j.molcatb.2015.07.009

[74] D. Cespi, R. Cucciniello, M. Ricciardi, C. Capacchione, I. Vassura, F. Passarini, and A. Proto, A simplified early stage assessment of process intensification: Glycidol as a value-added product from epichlorohydrin industry wastes. *Green Chem.*, **2016**, *18*, 4559. https://doi.org/10.1039/C6GC00882H

[75] A. L. Fedorov, T. I. Davidenko, I. I. Kotlyar, and V. V. Kuznetsov, Reduction of nitro groups in aliphatic compounds. *Russ. J. Org. Chem.* **1982**, *18*, 1161.

[76] E. Felder, S. Bianchi, and H. Bollinger, Process for the Preparation of Serinol and of Serinol Derivatives, and Products Obtained Therefrom. US Patent 4503252 (A), 5 March 1985.

[77] A. Nardi, and M. Villa, M. Process for the Preparation of 2 amino-1,3-propanediol. US Patent 5922917 (A), 13 July 1999.

[78] G. Fiorani, A. Perosa, and M. Selva, Dimethyl carbonate: A versatile reagent for a sustainable valorization of renewables. *Green Chem.* **2018**, *20*, 288. https://doi.org/10.1039/C7GC02118F

[79] R. Pelagalli, I. Chiarotto, M. Feroci, and S. Vecchio, Isopropenyl acetate, a remarkable, cheap and acylating agent of amines under solvent- and catalyst-free conditions: A systematic investigation. *Green Chem.* **2012**, *14*, 2251. https://doi.org/10.1039/C2GC35485C

[80] D. Rigo, R. Calmanti, A. Perosa, and M. Selva, A transesterification–acetalization catalytic tandem process for the functionalization of glycerol: The pivotal role of isopropenyl acetate. *Green Chem.* **2020**, *22*, 5487. https://doi.org/10.1039/D0GC01775B

[81] P. V. Rui Faria, C. S. M. Pereira, V. M. T. M. Silva, J. M. Loureiro, and E. A. Rodrigues, Glycerol valorisation as biofuels: Selection of a suitable solvent for an innovative process for the synthesis of GEA. *Chem. Eng. J.*, **2013**, *233*, 159. https://doi.org/10.1016/j.cej.2013.08.035

[82] G. Angulo, M. Brucka, M. Gerecke, G. Grampp, D. Jeannerat, J. Milkiewicz, Y. Mitrev, C. Radzewicz, A. Rosspeintner, E. Vautheyf, et al. Characterization of dimethylsulfoxide/glycerol mixtures: A binary solvent system for the study of "friction-dependent" chemical reactivity, *Phys. Chem. Chem. Phys.*, **2016**, *18*, 18460. https://doi.org/10.1039/C6CP02997C

[83] K. Zhang, C. Huang, H. Zhang, S. Xiang, S. Liu, D. Xu, and H. Li, Alkylation of phenol with tert-butyl alcohol catalysed by zeolite HY. *Appl. Catal.* **1998**, *166*, 89. https://doi.org/10.1016/S0926-860X(97)00244-5

[84] D. Mun, N. T. T. Huynh, S. Shin, Y. J. Kim, S. Kim, Y.-J. Shul, and J. K. Cho, Facile isomerization of glucose into fructose using anion-exchange resins in organic solvents and application to direct conversion of glucose into furan compounds. *Res. Chem. Intermed.* **2017**, *43*, 5495. https://doi.org/10.1007/s11164-017-2942-3

[85] A. R. Trifoia, P. S. Agachi, and T. Pap, Glycerol acetals and ketals as possible diesel additives. A review of their synthesis protocols. *Renew. Sustain. Energy Rev.* **2016**, *62*, 804. https://doi.org/10.1016/j.rser.2016.05.013

[86] Available online: https://webbook.nist.gov/ (accessed on 07/10/2021).

3 Isopropenyl esters (iPEs) in green organic synthesis

Foreword. The research project of this PhD Thesis was originally intended within a cotutelle program which included a one-year mobility of the candidate at the University of Sydney under the supervision of prof. Thomas Maschmeyer. However, due the pandemic which hindered any travel to Australia, the planned experimental research was converted into the writing of a review article on a topic of common interest for both the Italian and Australian groups. The content of the article was designed, organized, and revised through video-meetings of the PhD candidate and his Australian and Italian supervisor. This chapter reports the result.

3.1 Introduction

Isopropenyl esters (iPEs) are a class of enol esters (EEs), characterized by the presence of a methyl substituted vinyl group adjacent to an ester functionality (Scheme 3.)
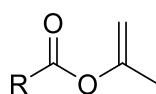
Scheme 3.1. *General iPEs structure (R= alkyl, aryl)*

These polyfunctional compounds can address a range of applications in organic synthesis and material science, with a major focus on intermediates in organic and pharmaceutical chemistry for the preparation of antibiotics and steroids (*vide infra*),[1,2,3] for the synthesis of drugs and drugs intermediates,[4,5,6] building blocks for polymer synthesis in emulsion phase coatings,[7] and acylating agents in presence of alcohols and amines.[8,9,10]

This review showcases the uses of isopropenyl esters (iPEs) with particular emphasis on sustainability-related aspects. After an initial section dedicated to the synthesis of iPEs, an in-depth literature analysis of their reactivity is described, including irreversible O-/N-/C-acylation processes, Friedel-Kraft and thiol-ene reactions, polymerizations, epoxidations, cross couplings, and others. Then, a conclusive part is devoted to the most promising future applications of iPEs in green organic synthesis.

3.2 Synthesis

3.2.1 General

Isopropenyl acetate (iPAc) is the simplest and most readily available iPE. It is currently produced on an industrial scale via the thermal cracking of acetic acid. This process generates ketene that, in the presence of sulfuric acid, in turn reacts with acetone. The overall pathway is illustrated in Scheme 3.2.[11,12]
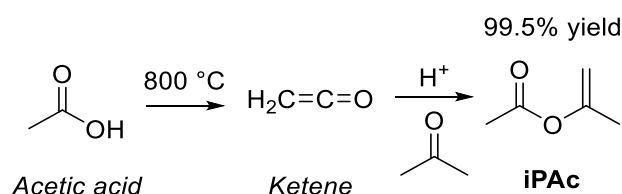
Scheme 3.2. *Industrial synthesis of iPAc*

iPAc is a non-toxic, inexpensive, colorless liquid, provided by major chemicals suppliers. Due to its versatility and anticipated future growth for various applications, the development of renewables-based protocols for iPAc production is an attractive step towards promoting more sustainable synthetic strategies. Relevant in this respect are renewable reagents such as acetic acid obtained by the catalytic reforming of biomass waste streams or acetone prepared by the ABE fermentation of sugars.[13]

Different approaches have been designed for the preparation of higher iPEs homologues. From the first pioneering work dating back to 1894 where Krüss and co-workers reported the preparation of ethyl prop-1-en-2-yl carbonate (ethyl isopropenyl carbonate) starting from ethyl carbonchloridate and sodium prop-1-en-2-olate,[14] far more productive alternative routes have been proposed being the main ones described in
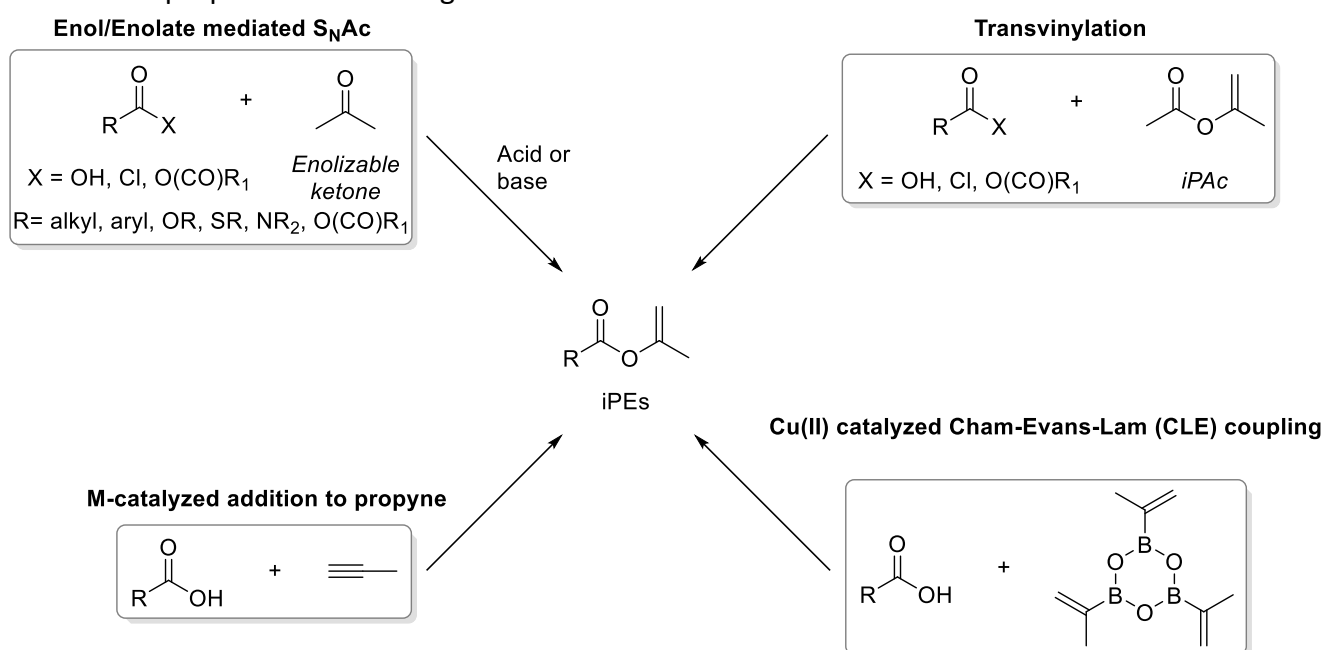
Scheme 3.**3**.
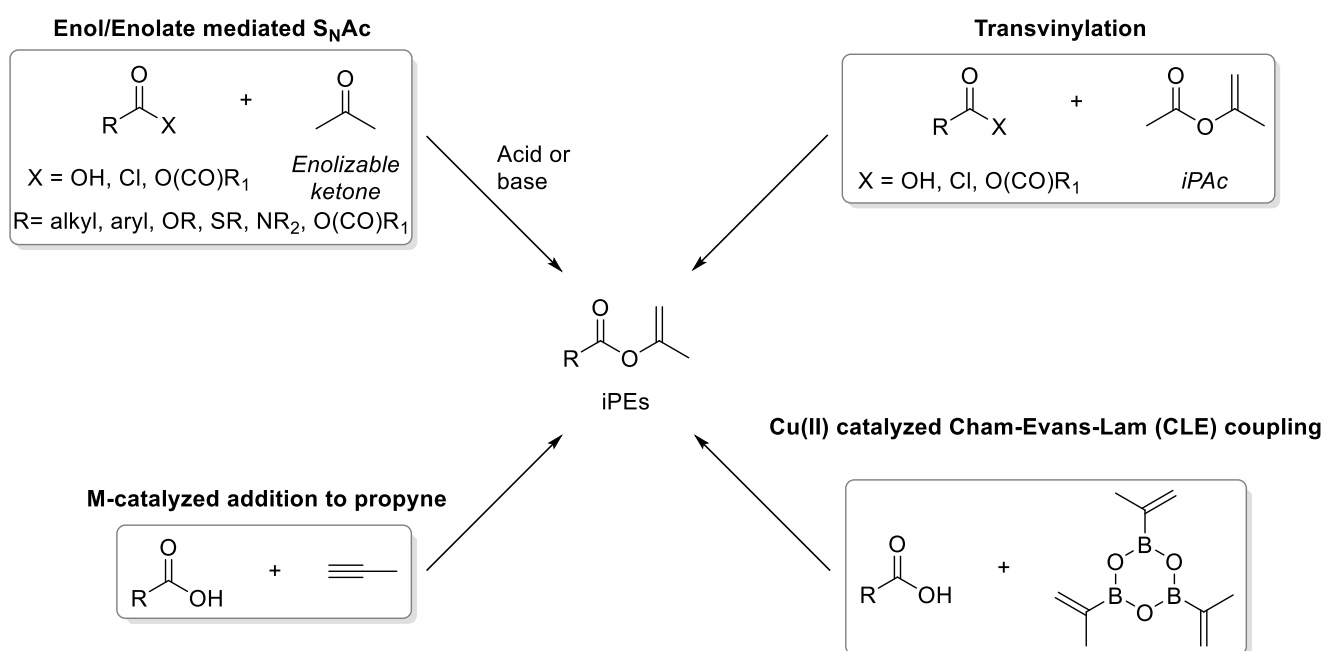
Scheme 3.3. *Main synthetic methodologies for the preparation of iPEs upon nucleophilic substitution on carboxylic acids and/or carboxylic acids derivatives*

114

3.2.1.1 Enol/Enolate-mediated S_NAc

The most straightforward synthesis of iPEs involves a nucleophilic acyl substitution (S_NAc) on activated acyl derivatives (*e.g.* acyl chlorides, anhydrides and ketenes) in presence of enolizable ketones as nucleophiles. Scheme 3.3 (top left) exemplifies the case of acetone that can be protonated/deprotonated by strong acids/bases with formation of the corresponding enol or enolate, respectively. The latter two species then act as nucleophiles.

Ketene was the first acyl derivative used for the reaction with enolizable ketones to yield the corresponding enol acetates.[15] The study demonstrated that the S_NAc pathway was affected by both the nature of the ketone co-reagent and the extent of enolization, and was promoted in presence of H_2SO_4 as the acid catalyst. The protocol was optimized for acetone with which the formation of iPAc was achieved with 45% conversion of ketene (yield of iPAc not reported) at T = 55 °C. Under similar conditions, the scope of the reaction was extended to other ketones as 2-butanone, acetophenone, 2,4-dimethyl-3-pentanone and pinacolone. At lower temperatures (below 55 °C) extensive ketene polymerizations occurred. Further studies proved that the latter processes were due to the reaction of ketene with both the oxygen or carbon nucleophilic centers of enolates, particularly polyacetals and polyketones were obtained by *O*-acylations in dipolar aprotic solvents and by *C*-acylations in non-polar solvents, respectively. [16, 17, 18]

A small library of iPEs (6 examples, yields of 34-44%) was obtained by the *O*-acylation of acetone enolates with different acyl chlorides. Enolates were generated from acetone and KH in 1,2-DME (dimethoxyethane) and the overall reaction proceeded at T = 0 °C.[19]

Chloroformates were investigated as electrophiles for the synthesis of iPEs, but any attempts to generate formate-based products by *O*-acylation of enolates were not successful.[20]

Structurally similar to enol esters, enol carbonates also gained attention as building blocks, especially for the design of polymer precursors.[21] The most straightforward pathway for the preparation of enol carbonate esters involves the *O*-acylation of enolates with chloroformate esters. This transformation is generally characterized by a low chemoselectivity because of the concurrent formation of *C*-acylation by-products.[22] Though, an effective strategy was reported through the reaction of fluoroformate esters with aldehydes [23] and ketones[24] carried out at 35-70 °C for 1-36 h, in the presence of excess KF and 18-crown-6 as a co-catalyst (27 examples; yields in the range 35-93%). The same Authors reported that unsaturated carbonyl compounds (such as substituted crotonaldehydes) were selectively acylated using potassium *tert*-butoxide (KO*t*Bu) at -78 °C (13 examples; yields in the range 32-87%).[25] More recently, Seeman and co-workers prepared a library of enol carbonates (7 examples) by chloroformates mediated *O*-acylation of sodium enolates generated from various ketones in the presence of tetramethylethylenediamine (TMEDA). Interestingly, sodium enolates were quantitatively generated by TMEDA in ethereal solvents and then quenched by the rapid addition at T = 0 °C of chloroformate esters.[26] Tamura *et al.* reported that isopropenyl carbonates were obtained also by the treatment of chloromercuriacetone ($ClHgCH_2COCH_3$) as the acetone-enolate equivalent with alkyl and aryl chloroformates in hexamethylphosphoric triamide.[27] Comparably high yields (48-78 %, 5 examples) were achieved.

3.2.1.2 Transvinylation reactions

The first reported transvinylation process was the reaction of butyric acid and iPAc carried out at 25 °C for 24h in the presence of mercuric acetate and boron trifluoride etherate (Scheme 3.3; top, right). The corresponding isopropenyl butyrate was isolated in 33 % yield with acetic acid as co-product.[9] In the same paper, using sulfuric acid as the catalyst, the reaction of iPAc with several carboxylic acids including acetic and butyric acids was also explored. However, the corresponding mixed anhydrides were the major products. This behavior was clarified by a subsequent study where the H_2SO_4-catalysed reaction of stearic acid with iPAc was investigated with excess iPAc (5 equiv.). The formation of equimolar amounts of isopropenyl stearate (iPSt) and stearic anhydride was observed, while if stearic anhydride (1 equiv.) was added in the reaction mixture, the yield of iPSt was almost doubled, from 53 to 93 %. [28] This led to the conclusion that the transvinylation process was promoted by the presence of activated carboxylic acids derivatives as anhydrides. This result and its interpretation were consistent with the content of a patent on the synthesis of iPEs from the reaction of 2-ethylhexoic, butyric, propionic, benzoic and sorbic anhydrides catalyzed by sulfuric acid.[29]

The product distribution (iPEs/anhydrides ratio) is also influenced by the nature of the carboxylic acid. For example, in the reaction of valeric acid with freshly distilled iPAc and two drops of H_2SO_4, the addition of valeric anhydride enabled the formation of isopropenyl valerate in a 60% yield at T= 97 °C in 10 h.[30]

Just as iPAc, vinyl acetate was effective in the reaction with benzoic and crotonic acids in the presence of mercuric acetate as a catalyst.[31] The protocol was extended to the synthesis of other mono enol esters (4 examples),[32] diisopropenyl esters (2 examples), [33] and isopropenyl propionate.[34] A mechanistic study hypothesized that the formation of enol esters was mediated by an organo-mercurial intermediate (Scheme 3.4).[35]
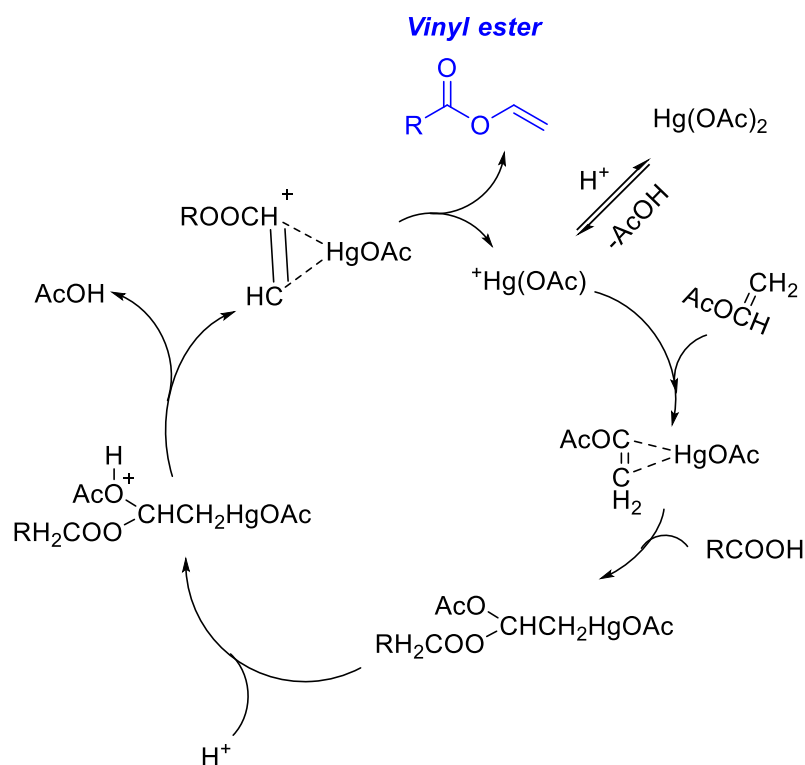
Scheme 3.4. *Mechanism for the formation of enol esters in the presence of Hg-based catalysts*

More recently, Park and co-workers synthesized isopropenyl benzoate starting from iPAc and benzoic acid with H_2SO_4 as a catalyst. Isopropenyl benzoate was then employed together with iPAc for isopropenyl/vinyl transfer upon metallacycle fragmentation (Scheme 3.5).[36] The same procedure was developed also for vinyl esters.

R = Me, Ph
X = Me, H
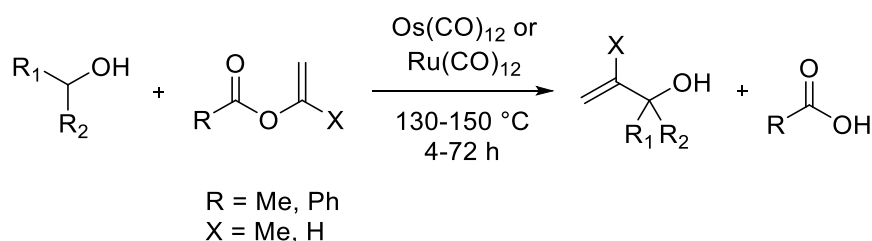
Scheme 3.5. The synthesis of iPEs with isopropenyl/vinyl transfer

This transvinylation has been extensively described with Ru-based catalysts.[37] Interestingly, a first paper was reported in 2013 by Ziriakus *et al.,*[38] who examined the regioselectivity of the reaction of iPAc and propionic acid to obtain isopropenyl propionate with RuCl$_3$ as the catalyst precursor.

Transvinylations were also carried out using acyl chlorides in place of carboxylic acids: for example, isopropenyl benzoate was synthesized with variable yields (21-58%) starting from benzoyl chloride and iPAc.[39]

3.2.1.3 Chan-Evans-Lam Coupling (CLE coupling)

An alternative protocol for the synthesis of iPEs has been recently proposed by Steemers and van Maarseveen who demonstrated that the Chan-Evans-Lam (CLE) coupling between N-protected amino acids and a tri(isopropenyl)boroxine pyridine complex was effective to achieve a variety of dipeptide derived isopropenyl esters (6 examples, 80-97% yields) (Scheme 3.3: right, bottom).[40] The reaction was catalyzed by a catalytic system composed of Cu(Otf)$_2$, Et3N and 1,3-diethyl urea. In all cases, the methodology proved scalable up to 2 mmol and it allowed the selective transformation of the *C*-terminus portion of dipeptides into the corresponding iPEs with complete stereoretention. A mechanism was not proposed in the paper in analogy with the investigation of Watson and co-workers who reported that the analysis of the reaction mechanism was complicated by the instability of the copper complexes used and the multicomponent nature of the reaction.[41]

3.2.1.4 Addition of carboxylic acids to propyne

The pioneering work of Nieuwland and co-workers dating back to the thirties of the last century, described the reactivity of alkyl acetylenes with a variety of oxy compounds, among which carboxylic acids were used to obtain the corresponding alkenyl esters (iPEs) (

Enol/Enolate mediated S$_N$Ac

$X = OH, Cl, O(CO)R_1$

$R=$ alkyl, aryl, OR, SR, NR$_2$, O(CO)R$_1$

Enolizable ketone

Transvinylation

$X = OH, Cl, O(CO)R_1$

iPAc

Acid or base

iPEs

M-catalyzed addition to propyne

Cu(II) catalyzed Cham-Evans-Lam (CLE) coupling
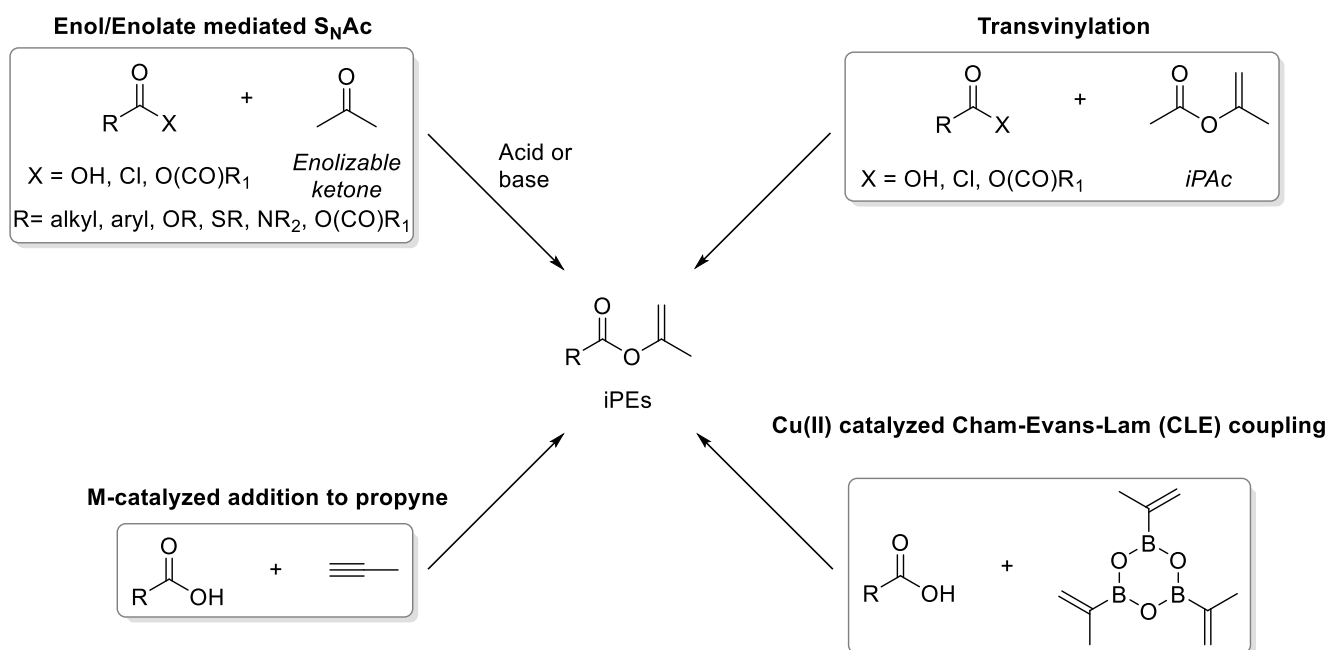
Scheme 3.**3**, bottom left).[42,43] The latter compounds were prepared at T= 30-40 °C starting from methyl, butyl and amyl acetylenes and acetic, chloroacetic, benzoic acids using (C$_2$H$_5$)$_2$O·BF$_3$ and mercuric oxide as the catalytic system at room temperature. Typical yields were in the range 30-68% and were limited by the formation of anhydrides and ketones as by-products, as depicted in Scheme 3.6.

a)

b)
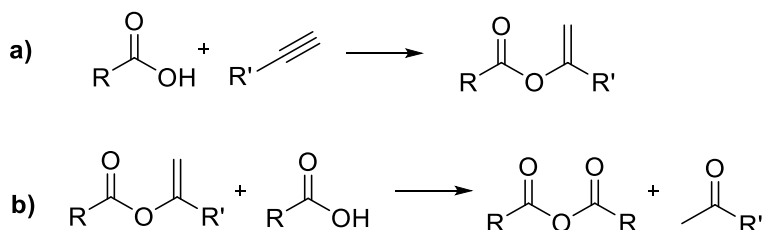
Scheme 3.6. Formation of alkenyl esters and their further reaction with carboxylic acids

The protocol was improved years later using propyne and long chain carboxylic acids (> C$_{18}$) in the form of zinc salts:[44] at high temperatures and pressures (T = 150 °C, p = 35 bar) the desired enol esters were isolated in >90% yields (10 examples). The reaction was further implemented in a continuous mode procedure, where stearic acid and propyne were set to react in a continuous stirred tank reactor (CSTR: p = 38 bar and T = 205 °C) with zinc stearate. The production of isopropenyl stearate was performed in a short tubular reactor connected to the outflow of the CSTR:[45] the overall reaction time was 10 min at a flow rate of 5-18 Kg/h.

Additional recent studies proved that the addition of carboxylic acids to alkynes was effectively catalyzed by homogeneous Ru complexes as for example, [Ru$_3$(CO)$_{12}$][46], [(cyclooctadienyl)$_2$Ru][47] or [(arene)RuCl$_2$(PR$_3$)][48] and other Ru-based systems.[49] Under such (catalytic) conditions, iPEs were obtained at 60-80 °C and atmospheric pressure with 80-99% yields. Ru complexes also promoted the addition of Z-*N* or Boc-*N* protected amino-acids to propyne, providing the corresponding enol esters without racemization of the amino acid moiety.[50] Interestingly, in the presence of a base [e.g., PPh$_3$, P(p-ClC$_6$H$_4$)$_3$, and P(Fur)$_3$], simple commercially available Ru-based catalysts as RuCl$_3$ and dichloro(p-cymene)Ru(II) dimer [((p-cymene)RuCl$_2$)$_2$] proved efficient for the regioselective synthesis of vinyl esters from terminal alkynes (R-C≡CH, R= n-

C₄H₉, Phenyl, Me, *t*-Butyl) and aromatic acids, favoring the formation of the Markovnikov product with up to 97% selectivity and quantitative yields (15 examples).[51] Similarly, XPhos-modified ruthenium(0) or osmium(0) complexes [M₃(CO)₁₂; M=Ru, Os] have been proposed by Krische *et al.*[36] to design a strategy for catalytic vinyl transfer from enol carboxylates to activated secondary alcohol C−H bonds. The same and other commercial Ru-precursors [Ru₃(CO)₁₂ and Ru(methylallyl)₂(COD)] were used for the synthesis of catalytic systems as [Ru(O₂CH)(CO)₂(PPh₃)]₂ and [Ru(CH₂CMeCH₂)₂(dppb)] that promoted the formation of 1-(*trans*-2-Ethoxycyclopropyl)ethenyl esters from (*trans*-2-ethoxycyclopropyl)ethyne and various carboxylic acids (Scheme 3.7).[52]
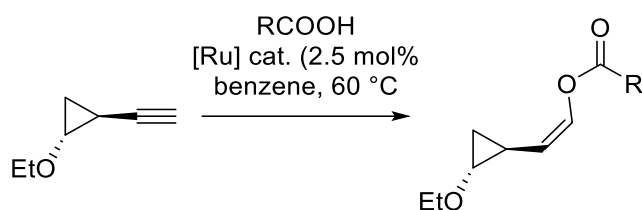
Scheme 3.7. *Anti-Markovnikov Addition of Carboxylic Acids to (trans-2-ethoxycyclopropyl) ethyne (R = Bu, Ph, CH2=CH; Y = 69-92%)*

3.2.1.5 Isopropenyl chloroformate (iPCF)

Isopropenyl chloroformate (iPCF), prepared from acetone and phosgene,[53] was reported to act as an active electrophile for a variety of substrates such as isopropenyl carbonates and carbamates. Although this chemistry is no longer recommended today for safety reasons, its development is interesting for the Reader from both historical and mechanistic standpoints. A two-step strategy was designed to prepare amino acid derivatives: a iPCF-mediated nucleophilic substitution was initially carried out to obtain mixed isopropenyl-based carbonates; then, an irreversible decarboxylation/transesterification reaction followed by which the corresponding Boc-protected amino acid ester derivatives were achieved (Scheme 3.8).[54]
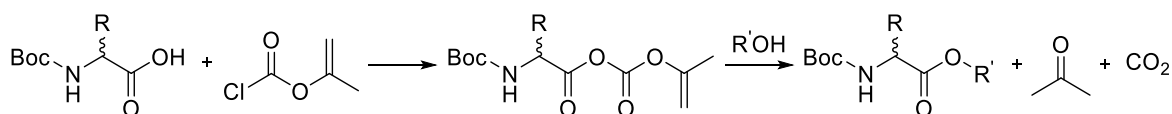
Scheme 3.8. *Two-step esterification of amino acids with configurational retention*

Mild operating conditions (0 °C, and atmospheric pressure) were used to isolate the final products with configurational retention in yields of 60-96 % (33 examples for esters and 10 examples for depsipeptides).

Takeda and co-workers followed a similar approach to prepare a series of mixed isopropenyl-based carbonates (iPCs) from iPCF and N-hydroxy compounds at 0°C in the presence of triethylamine as the catalyst (5 examples, 70-98% yields). The products were further reacted with protected amino acids at room temperature.[55]

iPCF was also effective in the synthesis of other carbonates. For instance, allyl isopropenyl dicarbonate (49 % yield) was prepared in THF at room temperature from the reaction of

isopropenyl chloroformate and sodium allyl carbonate in the presence of 15-crown-5 as a catalyst.[56] The product, allyl isopropenyl decarbonate, was used for the synthesis of allyl esters using a two-step methodology (yields of 81-99%, 9 examples; Scheme 3.9).
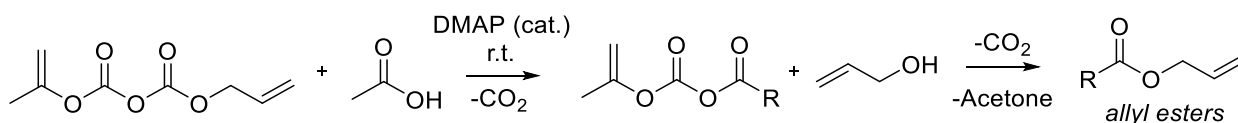
Scheme 3.9. *Two-step synthesis of allyl esters promoted by allyl isopropenyl carbonates*

Isopropenyl glycosyl carbonates were prepared from the reaction of iPCF with glycosides (4 examples in nearly quantitative yields). Products in the form of glucosyl and galactosyl carbonates were derived from the corresponding monosaccharide hemiacetal donors and displayed glycosylating properties towards other sugars.[57] iPCF was also used in the reaction with amines (L-leucine and 1-naphthylamin) to achieve isopropenyl carbamates (iPCMs) that, in turn, [58,59] were converted into unsymmetrical ureas.

3.2.1.6 Isopropylidene deprotonation

Cope and Hancock designed an inventive procedure to achieve enol esters, via the quantitative deprotonation of isopropylidene malonic esters with sodamide (NaNH$_2$).[60] The resulting enolates were excellent nucleophiles able to react with ordinary alkylating agents (e.g. alkyl halides or dialkyl sulfates) to produce alkyl isopropenyl malonic esters (Scheme 3.10).

R$_1$/R$_2$ = Me; Et; Allyl; Propyl;
iso-propyl; Butyl; *iso*-butyl;
Amyl; *iso*-amyl
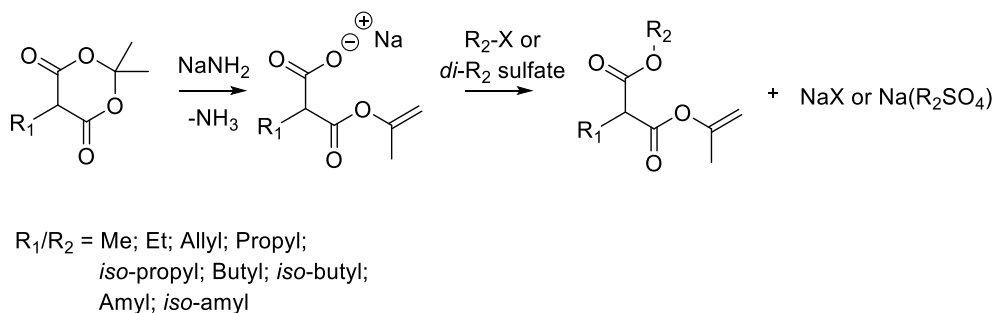
Scheme 3.10. *The synthesis of iPEs via isopropylidene deprotonation*

The alkylation step sequence was performed at 135 °C and atmospheric pressure with the isopropenyl esters being isolated in up to 90% yields (9 examples). The Authors extended the reaction scope by preparing isopropenyl alkyl barbituric and thiobarbituric acids.[61]

3.2.1.7 Claisen reactions of iPAc

Claisen-like reactions of iPAc with suitable acceptors (RX; X= leaving group) were proposed as an efficient route to the synthesis of iPEs (Scheme 3.11).

X = leaving group
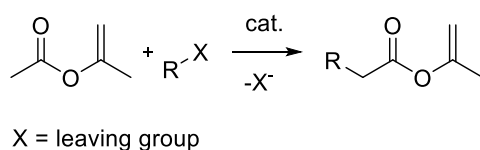
Scheme 3.11. *Claisen-like synthesis of iPAc derivatives*

The first example was reported by Larson and co-workers, who investigated the methyldiphenylsilylation of esters and lactone enolates in the presence of a strong non-

nucleophilic base catalyst as lithium diisopropylamide (LDA).[62] The Authors observed that when iPAc was the reactant, the corresponding enolate originated prop-1-en-2-yl 2-(methyldiphenylsilyl)acetate as the final product (Scheme 3.12, top). A similar strategy was proposed some years later by Trost *et al.* who prepared a novel hydroxy isopropenyl compound from the reaction of iPAc and a tert-butyldimethylsilyl-protected acceptor (Scheme 3.12, mid).[63] The protocol was extended to the asymmetric synthesis of (*S*)-Prop-1-en-2-yl-4,4,4-trifluoro-3-[(*S*)-2-methylpropan-2-ylsulfinamido]butanoate (Scheme 3.12, bottom).[64]
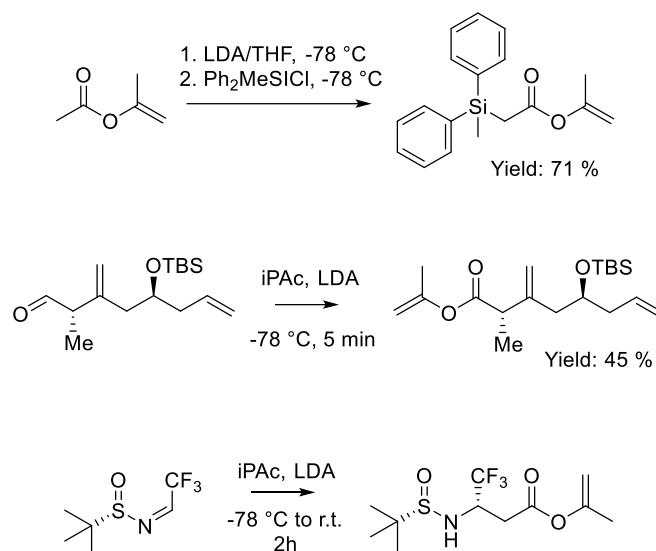
Scheme 3.12. *Claisen-like reactions of iPAc for the preparation of various iPEs*

3.2.1.8 Future directions

Apart from iPAc whose synthesis is well established, the synthesis of higher iPE homologues is still an open challenge.

According to the concepts of green chemistry and green engineering, the most promising routes seem the transvinylations and the additions of carboxylic acids to propyne. Key factors are the cost of the starting materials (iPAc ≈ 1$/Kg; carboxylic acids 1-100 $/Kg,[65,66]) and the design of novel catalysts based on Lewis acids able to replace the old-fashioned systems as H_2SO_4 or *p*-TSA, facilitate the work-up procedures, the catalyst recycle, and minimize the waste disposal.

3.3 Reactivity

3.3.1 Reactions of the acyl group

3.3.1.1 Esterification

The preparation of esters is one of the major transformations in organic synthesis. The most straightforward protocol for the preparation of esters involves the direct coupling of carboxylic acids and/or their derivatives (anhydrides or acyl halides) with over stoichiometric quantities of alcohols (*e. g.* Fisher esterification). Several reagents, promoters and acidic or basic catalysts have been employed to the scope.[67] Compared to these processes, transesterification reactions

stand out as more sustainable routes for the esters preparation since volatile by-products (alcohols) are usually formed and these can be easily removed from the reaction mixture by distillation. The transesterification reactions have been extensively used also for large-scale sequences of biomass valorization, one for all the catalytic conversion of natural triglycerides into biodiesel. The transesterification, however, is a reversible process requiring over-stoichiometric quantities of reactants (alcohol or ester) and active catalytic systems to ensure quantitative product formation. Enol esters (EEs) offer a privileged transesterification pathway because of the formation of an enol as a reaction co-product that quickly converts into the corresponding ketone. This feature makes the overall transformation irreversible. Isopropenyl esters (iPEs) are excellent substrates to this scope, particularly the lightest term of the series, the non-toxic isopropenyl acetate (iPAc), which generates an enol able to tautomerize to acetone (Scheme 3.13).[68]
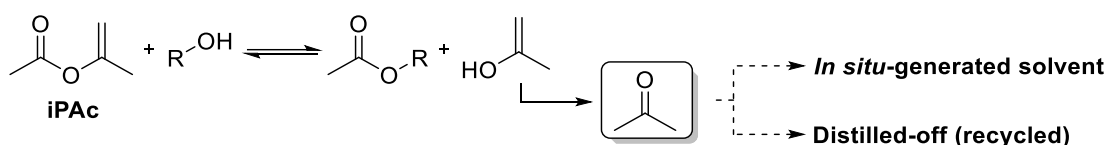
Scheme 3.13. *General reactivity of iPAc in transesterification reactions. The process is made irreversible due to the rapid tautomerization of the enol-leaving group*
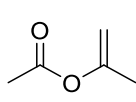
Acetone continuously released during the transesterification reaction can be either used as a solvent/co-solvent or it is easily distilled off and recycled during work-up. This behavior is not general for EEs. For comparison, transesterification reactions starting from vinyl esters produce acetaldehyde as co-product, which is far more reactive than acetone and can acetalize the alcohol co-reagent or undergo self-polymerization processes.[69,70]
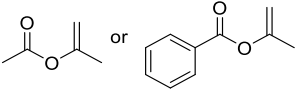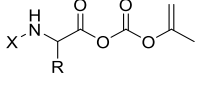
Table 3.19 sums up various routes and conditions for the iPEs-mediated esterifications.

The first example of iPEs transesterification was reported by Hagemeyer in 1949 for the reactivity of iPAc: in presence of catalytic amounts of an acid (sulfuric or *p*-toluensulfonic acid) iPAc reacted with primary, secondary, tertiary alcohols, phenols, polyhydroxy compounds and hydroxy esters to form the corresponding acetylated products (entry 2).[9] The general applicability of iPAc as an acetylating agent was thus demonstrated. The protocol was further improved in a subsequent study by Rothman and co-workers, who performed a systematic study of transesterification reactions between a model iPE, namely 2-butyl-2-heptyldecanoic isopropenyl ester, and alcohols with a variable steric hindrance, like *n*-octanol, 2-methyl-2-propanol and 2-butyl-2-heptyldecanol, under acid catalysis (entry 1).[71]

Table 3.19. *The employment of iPEs in esterification reactions promoted by various alcohols under different conditions*

Entry	iPE	Alcohol	Catalyst	T (°C)	Other conditions	Yield (%)[a]	Ref.
1	*n*-C₇H₁₅ *n*-C₈H₁₇ *n*-C₄H₉	- *n*-octanol - 2-methyl-2-propanol - 2-butyl-2-heptyldecanol	H⁺	175	neat	75-95	71

		Primary, Secondary, Tertiary, Phenols, Polyols					
2		Primary, Secondary, Tertiary, Phenols, Polyols	p-TSA or H$_2$SO$_4$	n.r.	n.r.	n.r.	9
3		Tertiary	Oxime/Cp*Sm(thf)$_2$	r.t.	15h, toluene	90-99	72
4		Primary Secondary Phenols	I$_2$	85-90	5-30 min, neat	70-99	10
5		Primary Secondary Polyols Phenols Thiols	Al(OTf)$_3$	r.t.	5-7 min	90-95	74
6		Primary Secondary Polyols Benzylic Phenols	distannoxanes	30-50	5-24h, neat or toluene	36-99	75
7		Benzylic Primary	Electrogenerated NHC	60	2h, neat	52-98	77
8		Benzylic Furanic Aliphatic	TEAHC	60	2h, neat	10-99	78
9		Primary	IMes (NHC)	r.t	3h, neat	95	79
10		Phenol n-octanol	K$_2$CO$_3$/Aliquat	70	0.5-24h, neat	65-99	80
11		Glycerol	Cat.-free	300	CF	99	81
12		N-acetyl-D-mannosamine	protease N	r.t.	n.r.	6-O-acetylated product: 70	83
13		Various sugars	p-TSA	80	Neat, 2h	per-acetylated product: 85	84
14		Poly-O-benzylated sugars	I$_2$/tetraethylsilane	0	DCM,	6-O-acetylated products: 60-78	85

123

15	![structure] or ![structure]	Primary, secondary	$Y_5(OiPr)_{13}O$	r.t.	5 min-1.5h	95-99	76
16	![structure]	Primary Secondary tertiary	DMAP	0-35	n.r.	60-96	54

[a]Yield of the corresponding acylated product. n.r. = nor reported.

In search for alternative routes of iPEs mediated esterifications, a wide range of catalysts have been developed. For example, Tashiro and co-workers reported the catalytic activity of an oxime/Cp*$_2$Sm(thf)$_2$ towards acylation of tertiary alcohols with iPAc (entry 3).[72] This method allowed the acylation of tertiary alcohols under acid-free conditions and was particularly suitable for acid-sensitive terpene-based alcohols, like linalool. Interestingly, molecular iodine was described as a highly efficient catalyst for the acetylation of a variety of alcohols and phenols under solvent free conditions (entry 4).[73] It was suggested that iodine acted as Lewis acid, stabilizing iPAc polarization (Scheme 3.14).
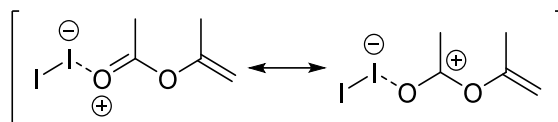
Scheme 3.14. *Iodine-mediated activation mechanism of iPAc*

Al(OTf)$_3$ was reported as another Lewis acid catalyst for the transesterification of iPAc with substituted and unsubstituted alcohols, phenols, and thiols:[76] the reaction took place at room temperature and the corresponding acetates were prepared in good yields (90-95 %) in t = 5-7 min with only 0.5 mol % of Al(OTf)$_3$ (entry 5).[74] Distannoxane and Y$_5$(OiPr)$_{13}$O systems catalyzed the reaction of EEs, including iPAc, with primary and secondary alcohols or phenols (entries 6 and 15). Primary alcohols, in particular, were acylated preferentially compared to secondary alcohols and phenols.[75,76] The yttrium based-catalyst displayed a variety of other features: i) it promoted the *O*-acylation of amino alcohols; ii) it favored the acylation selectivity of unsymmetrical diols: for example, the transesterification of 1-phenyl-1,2- ethanediol proceeded with up to 90% selectivity towards the monoacetate product; iii) compared to vinyl acetate, the transesterification of cyclohexanol with isopropenyl acetate proceeded with considerably higher yields.[78] Ionic liquids (ILs) were described as both solvents and catalysts for iPEs transesterifications: i*n situ* electrogenerated *N*-heterocyclic carbenes (NHC), obtained upon electrochemical reduction of the 1,3-dialkylimidazolium based ILs used as reaction media, promoted the proton transfer from the alcohol to iPAc, yielding the corresponding acetate product (entry 7).[77] A similar mechanism was proposed for the iPAc transesterification with benzylic, furanic and aliphatic alcohols catalyzed by tetraethylammonium hydrogen carbonate (TEAHC). The corresponding acetates were observed in moderate up to very good yields (10 examples, 10-90 % yield, entry 8) under solventless conditions.[78] Similarly, another family of NHC, imidazol-2-ylidenes, catalyzed the transesterification of several esters including iPAc with alcohols (entry 9).[79] Simple alkaline carbonates as K$_2$CO$_3$ were active for the transesterification of iPAc with primary alcohols or phenols both in the presence or in the absence of the phase transfer catalysts (entry 10).[80] More recently, a catalyst-free protocol was described by some of

us for the selective, high yielding synthesis of triacetin starting from glycerol and iPAc: iPAc displayed a superior performance compared to other esters, like ethyl acetate. At high temperature (T = 300°C) the upgrading of glycerol was achieved yielding triacetin (glycerol triacetate) in 99% isolated yield, both under batch and continuous flow (entry 11).[81]

Rothman *et al.* studied the reactivity of fatty acids-derived iPEs, such as isopropenyl stearate, for the acylation of isethionic acid and N-methyl taurine to achieve surface-active agents.[82] For instance, the reaction of isopropenyl stearate at 200 °C for 30 min gives 95% yield of sodium 2-sulfoethyl stearate (Scheme 3.15), acetone being the only byproduct.
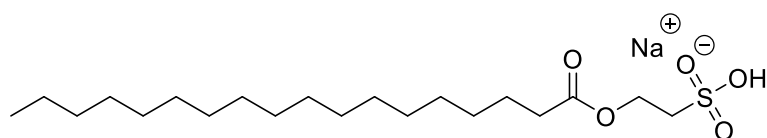
Scheme 3.15. *Structure of sodium 2-sulfoethyl stearate*

The iPEs-mediated transesterification of sugars was also extensively investigated. The acetylation of *N*-acetyl-D-mannosamine (mannose-NAc) with iPAc occurred regioselectively, forming exclusively the 6-*O*-acetylated product in 70 % yield in the presence of protease-N as the catalyst (entry 12; Scheme 3.16; top).[83] In addition, iPAc was employed for the selective acetylation of sugar tertiary alcohols (entry 13; Scheme 3.16: bottom, left).[84] The acetolytic de-O-benzylation of poly-O-benzylated sugars took place regioselectively via the reaction of iPAc triggered by an iodine/silane combined reagent or iodine alone (entry 14; Scheme 3.16; bottom, right).[85]
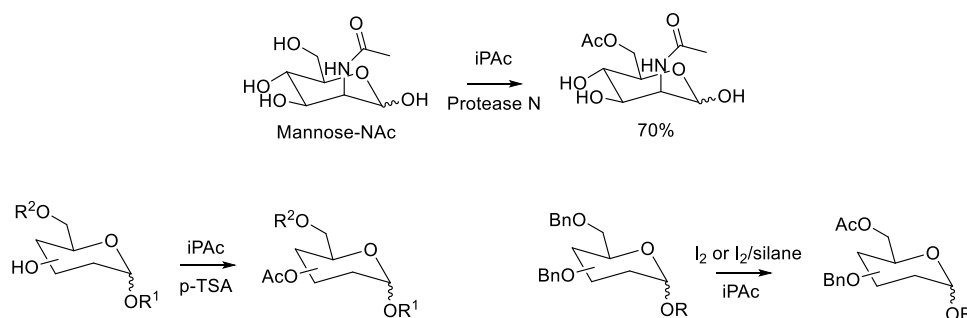
Scheme 3.16. *Various routes for the acetylation of sugars promoted by iPAc*

Enzymes were employed as catalysts for the regio- and/or stereoselective acylation of alcohols with iPAc. These investigations were mainly focused to the dynamic kinetic resolution (DKR) of racemic mixtures of alcohols. A widespread range of iPAc-mediated DKR protocols was developed over the years: for a discussion of this topic, the Reader is referred to an exhaustive review of R. Ward.[86]

A convenient one-pot esterification of N-protected aminoacids was reported by Jouin and co-workers (entry 16),[87,88] who developed a two-step route for depsipeptide bond formation through: a) an isopropenyl chloroformate activation of the N-protected aminoacid of choice; b) a DMAP catalyzed esterification/decarboxylation to obtain the final esterified peptide (Scheme 3.17).[89,90] Similarly, by exploiting the reactivity of iPCF, Franck and Li developed a methodology for the selective preparation of γ- of δ-amino-β-ketoesters starting from C-protected amino acids (10 examples, 77-92 % yield).[89]
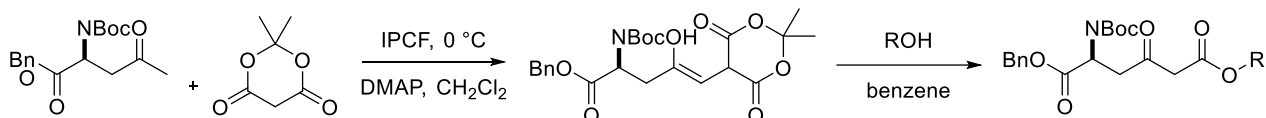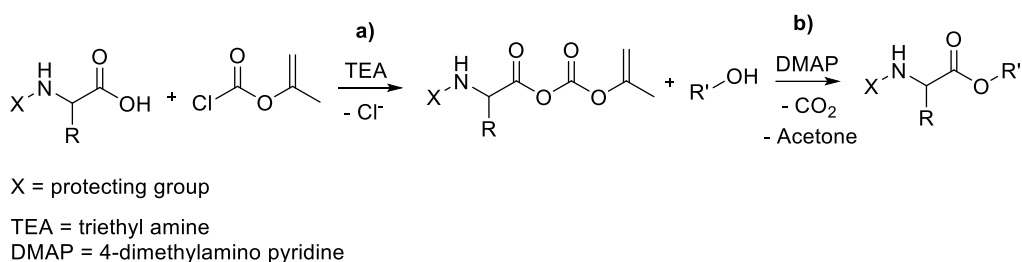
Scheme 3.17. *Top: Jouin's strategy for the synthesis of depsipeptides. Bottom: preparation of γ- of δ-amino-β-ketoesters using iPCF*

3.3.1.2 O-acetylation of aldehydes and ketones

The reaction of carbonyl compounds with iPAc allow the formation of the corresponding O-acetylated derivatives under several conditions (Scheme 3.18).
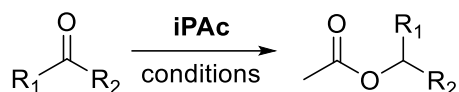
Scheme 3.18. *General example for the iPAc-mediated O-acetylation of carbonyl groups*

Trost et al. found that the reaction of an unsymmetrical ketone with isopropenyl acetate in the presence of a catalytic amount of *p*-toluenesulfonic acid yields a mixture of enol acetates in which the less highly substituted isomer was the more abundant component (2 examples; yields 82-85%).[90] Using the same catalyst (*p*-TSA), a convenient synthesis of aryl acetates was achieved from the reaction of α-tetralones with iPAc, followed by dehydrogenation with air or 2,3-dichloro-5,6- dicyanoquinone (DDQ) in a one-pot procedure (7 examples; yields 68-84%).[91] Similarly, iPAc and *p*-TSA were used for i) the preparation of enol acetates derived from their corresponding aryl alkyl ketones (6 examples; yields 80-90%; Scheme 3.19, top),[92,93] and ii) to convert steroid ketones to enol acetates (11 examples; yields 31-76 %; Scheme 3.19, bottom). In the latter case, starting from 20-keto steroids, the formed enol acetates displayed the double bond between the 20- and 21-carbon atoms.[94]
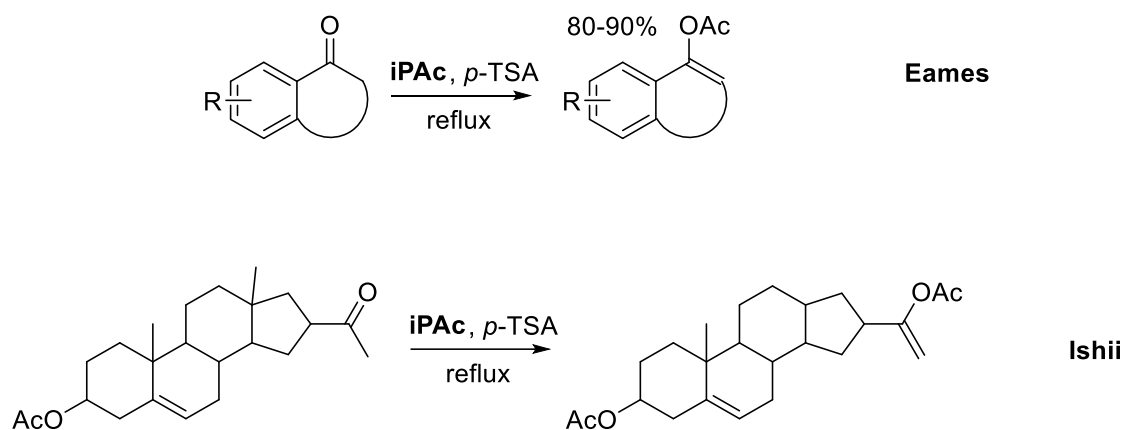
Scheme 3.19. Top: O-acetylation of aryl alkyl ketones promoted by iPAc. Bottom: prototype reaction for the O-acetylation of steroids with iPAc

The acetyl-cyanation of aldehydes with acetone cyanohydrin and iPAc by $Cp*_2Sm(THF)_2$ occurred at ambient conditions (6 examples; yields 49-87%; Scheme 3.20, top).[95] Meerwein–Ponndorf–Verley-type reductive acetylation of carbonyl compounds to acetates was successfully carried out in the presence of iPAc in the presence of $Ln(OiPr)_3$ as a catalytic amount at room temperature. Several carbonyl compounds were converted into the corresponding acetates in fair to good yields (17 examples; yields 10-95%; Scheme 3.20, bottom).[96]

Ln = Sm, Gd, Yb, La
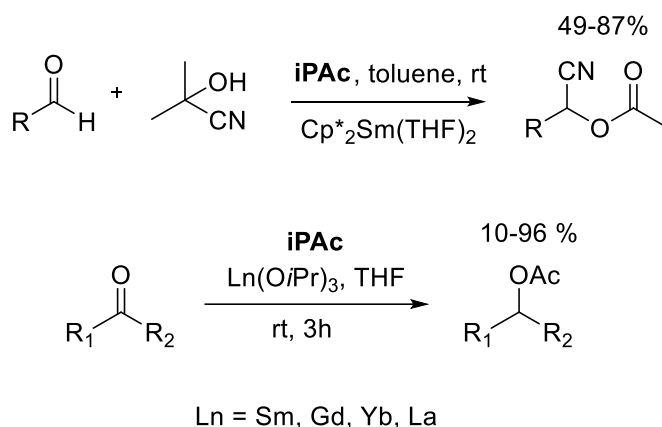
Scheme 3.20. Top: acetyl-cyanation of aldehydes with iPAc. Bottom: Meerwein–Ponndorf–Verley-type reductive acetylation of carbonyl compounds to acetates with iPAc

An appealing sequence was developed by Shono et al. for the regioselective synthesis of α-methylene ketones in satisfactory overall yields (10 examples; yields 79-89%). The procedure involved a first reaction of enol acetates (synthesized by means of iPAc) with α-chloromethyl methyl ether in the presence of active Zn/Cu compounds, followed by an acid-catalyzed elimination of methanol from the resulting α-methoxymethyl ketones (Scheme 3.21).[97]
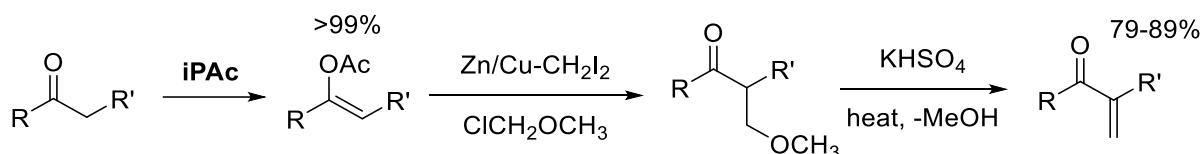
Scheme 3.21. Enol acetates conversion into α-methylene ketones

Man et al. found that under H_2SO_4 catalysis at T = 100 °C the iPAc-mediated *O*-acetylation of methyl-methylene ketones gave different results depending on the starting compound: i) methyl n-hexyl ketone gave the corresponding methylene derivative, whereas methyl neopentyl ketone formed the methyl derivative. Other methyl-methylene ketones produced mixtures of the two isomers (Scheme 3.22).[98]

R = *n*-hexyl (**A**:**B** = 0:100)
  3,3-dimethylbutyl (**A**:**B** = 18:82)
  isobutyl (**A**:**B** = 72:28)
  neopentyl (**A**:**B** = 100:0)
  dibenzyl ketone (not given)
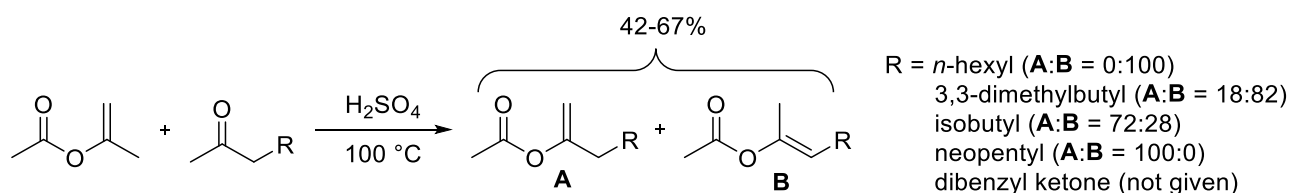
Scheme 3.22. *Regioselectivity of the O-acetylation of methyl-methylene ketones under H_2SO_4 catalysis*

Jacobi and co-workers found that the conversions of acetylenic enones into their corresponding intramolecularly annulated products took place at a markedly enhanced rate in the presence of iPAc, yielding the corresponding phenol acetates in 30-89 % yield (3 examples; Scheme 3.23; top, left).[99] Similarly, iPAc played a key role during the enol acetylation step in an efficient and metal-free multicomponent synthesis of biaryls and heterobiaryls (13 examples; yields 20-60%; Scheme 3.23; top, right).[100] In addition, a variety of iPEs reacted with amidoximes in a straightforward manner forming the corresponding 1,2,4-oxadiazoles (9 examples; yields 21-69%; Scheme 3.23, bottom). This reaction involved an initial amidoxime *O*-acylation followed by an irreversible cyclization/dehydration step yielding to the final oxadiazole product. Interestingly, when the transesterification reaction was performed in the presence of aliphatic esters such as ethyl acetate, oxadiazoles were not detected.[101]
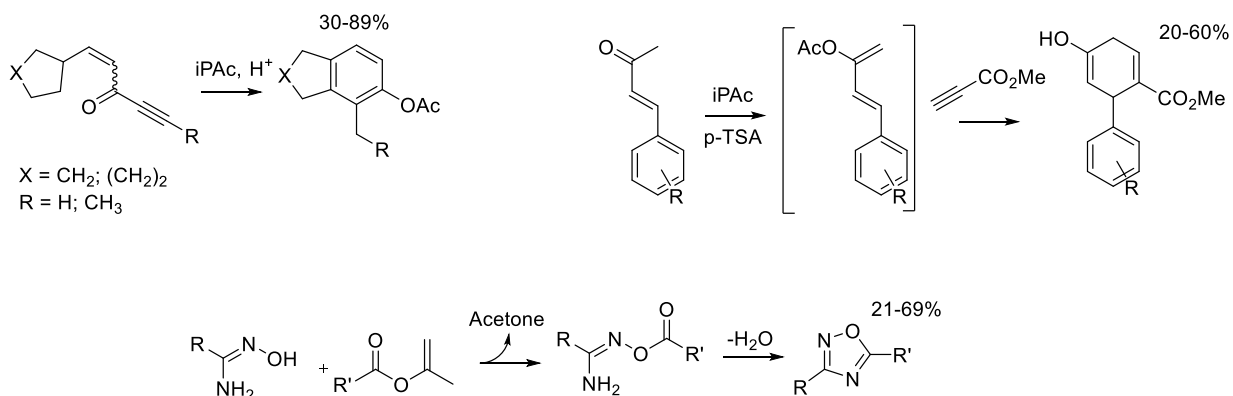
Scheme 3.23. *top, left: iPAc improves the yields of the phenol acetates in the cyclization of acetylenic enones; top, right: iPAc-mediarted enol acetylation in the multicomponent synthesis of biaryls; bottom: iPEs-mediated synthesis of 1,2,4-oxadiazoles*

Acylase catalyzed Markovnikov addition of iPAc could be performed starting from 4-nitroimidazole via a three-step mechanism consisting of acylation, hemiaminal intermediate formation and transesterification. This reactivity was observed employing several different aliphatic and aromatic aldehydes and imidazole-based nucleophiles.[102]

3.3.1.3 C-acylation

Corey and Ghosh found that Mn^{III} promoted the addition of various 1,3-dicarbonyl compounds to enol ethers or terminal enol esters, including iPAc. After a subsequent hydrolysis of the resulting adducts and a base catalyzed aldol cyclization, a range of 2-cyclopentenones were synthesized (7 examples, yields 71-96%).[103] The reaction between 2-carbethoxy cyclopentanone and iPAc was reported to explain the mechanism (Scheme 3.24, a). Rothman et al. reported that isopropenyl stearate was used to acylate diethyl malonate under basic conditions (Scheme 3.24, b).[82]
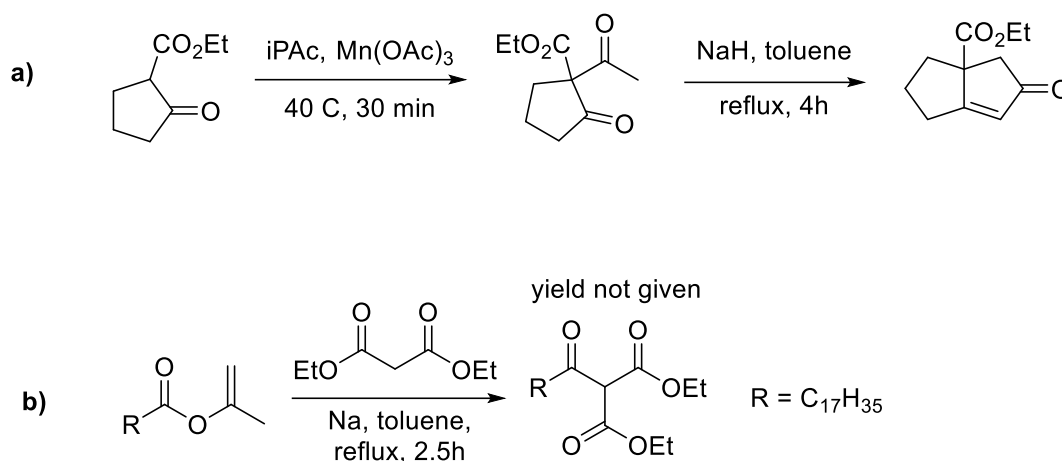
Scheme 3.24. C-acylations with iPEs

3.3.1.4 Amidation

The acylation of amines is a commonly employed organic transformation, occurring in the presence of a variety of Lewis bases and acids catalysts.[104] As for the above-mentioned acylation of alcohols, iPEs represents a greener acylating agent also for amines. An irreversible reaction takes place thanks to the tautomerization of the leaving group, an enol, to the corresponding ketone (Scheme 3.19)

Table 3.20 summarizes the main protocols reported for the iPEs-mediated acylation of amines and amides. The first procedure was described by Hagemeyer in 1949 who observed that primary and secondary aliphatic amines reacted vigorously with iPAc in the absence of catalysts, forming the corresponding N-alkylacetamides. Aromatic amines were less reactive, requiring a strong acid catalyst (entry 2).[9] Subsequently, Rothman and co-workers developed a methodology for the selective N-acylation of amides and imides:[105] starting from a mixture of isopropenyl stearate or laurate and cyclic imides (such as succinimide, maleimide, phthalimide, barbituric acids), cyclic imide-amides (spirohydantoins), N-alkyl amides, or N-aryl amides, were converted into the corresponding N-acylated products in the presence of an acid catalyst. Moderate to good yields (35-87%) were achieved at T = 150-175 °C (entry 1). Authors proposed two different iPEs activation mechanisms (Scheme 3.25). The first one (left) consisted in an initial enol ester protonation (on the C=C bond), which brought to the resonance-stabilized carbonium ion A formation. In turn, intermediate A reacted with the amide to produce the adduct B with the regeneration of the proton catalyst. Finally, adduct B underwent a thermally induced collapse to the observed products, acetone and acylamide. In the second mechanism instead (right), a direct carbonyl protonation activated the iPE. Then, in a concerted step, the

amide nucleophilic attack towards the activated ester followed by an intermolecular rearrangement produced the amidated product and acetone.
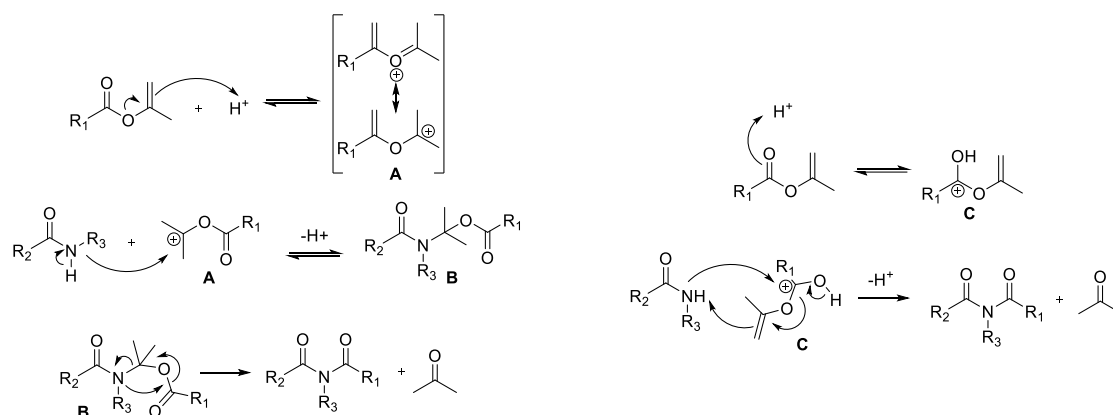
Scheme 3.25. E. S. Rothman's iPEs activation mechanisms
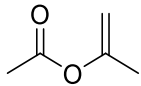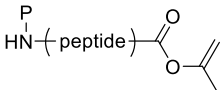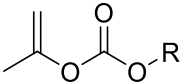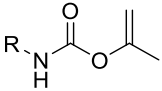
iPEs are also active acylating agents towards aminoacids. [74,106] For example, Jones and co-workers reported the facile, chemoselective acetylation of cysteine, occurring at pH = 7 in presence of iPAc, forming exclusively *N*-acetylcysteine in 60 % yield (entry 3).[109] RajanBabu *et al.* found that phenylglycine and phenylalanine esters readily reacted with neat iPAc (9 equivs.) at room temperature, giving a quantitative yield of the expected amides (entry 4).[78] Further studies on the iPEs reactivity with aminoacids were performed by Dixneuf *et al.*[48b] Their investigation was focused on the iPEs-mediated amidation of peptides: *N*-protected amino iPEs (structure A, Scheme 3.26) were easily transformed into the corresponding amino amides (70-90 % yields) using ammonia, primary amines and amino acids as the N-nucleophiles (entry 11).[48b] When amino-acids were used as the nucleophiles a facile method for the synthesis of dipeptides came out (Scheme 3.26).
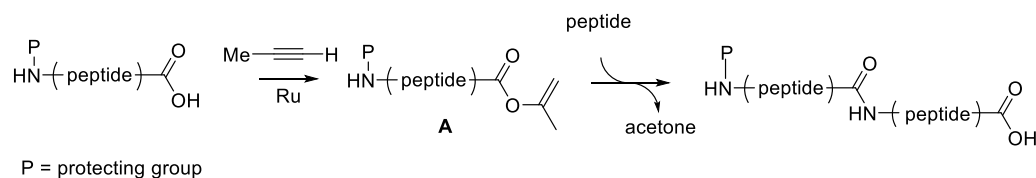
Scheme 3.26. iPEs-mediated strategy for the synthesis of dipeptides

Table 3.20. The employment of iPEs in amidation reactions under different conditions

Entry	iPE	Amine/amide	Catalyst	T (°C)	Other conditions	Yield (%)[a]	Ref.
1	$R = C_{11}H_{23}: C_{17}H_{35}$	succinimide, maleimide, phthalimide, 5,5-Diethylbarbituric acids, spirohydantoins, N-alkyl amides,	H^{+}	150-175	neat	35-87	105

		N-aryl amides					
2		Primary, Secondary	Cat-free	n.r.	neat	81-94	9
3		Cysteine	Cat-free	20	In H_2O, pH = 7, 1h	60	106
4		Phenylglycine Phenylalanine esters	Cat-free	r.t.	neat	99	76
5		Azide-amine	Cat-free	r.t.	EtOAc, 30 min	99	110
6		Amido-sugar	p-TSA	85	neat	99	113
7		Octyl amine Aniline 2-amino Acetophenone	I_2	85-90	Neat, 5-20 min	86-98	10
8		Primary Secondary Enantiopure	1,2,4-Triazole anion/DBU	r.t.	MeCN, 10 h	89-98	68f
9		Primary Secondary Aromatic	Cat-free	60	Neat, 3-24h	99	77
10		Primary Aromatic	Cat-free	r.t.	Neat, 24h	70-92	107
11	P = protecting group	NH_3 Primary Amino-acids	Cat-free	r.t.	EtOAc	70-90	48b
12		Primary Secondary Aromatic	Cat-free	50-70	neat	80-95	114
14		Boc-Cicloesyl Diamines	Cat-free	n.r.	n.r.	57-60	115

Lier *et al.* found that iodine was a highly efficient catalyst for the acetylation of amines (and alcohols, too: see Scheme 3.14) with iPAc (they found also that it was active for the acetylation. They reported that octyl amine, 2-amino acetophenone and aniline were easily acetylated in good to excellent yield at 85-90 °C (entry 7).[10] Another example of an active catalyst was 1,2,4-

triazole anion by which acyl transfer took place during the aminolysis of iPAc (8 examples, 89-98% yields; entry 8).[68f]

The development of catalyst-free and/or solvent free protocols is a highly desirable from the sustainability standpoint. In this respect, iPEs-mediated solvent- and catalyst-free amidations represent an alternative, eco-compatible pathway for the valorization of amines that has been systematically investigated.[107] Catalyst-free conditions (but not solvent-free) were adopted by Takaoka and co-workers: they reported that iPAc fully acetylated an azide-functionalized amine at room temperature in 30 min in EtOAc (Scheme 3.27).[108]
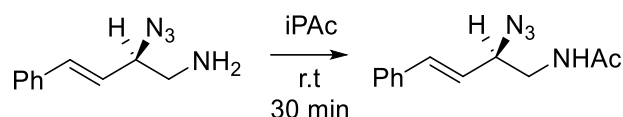
Scheme 3.27. *iPAc-mediated amidation of an azide-functionalized amine*

Pelagalli and co-workers reported the acylating activity of iPAc towards amines in the absence of additional solvent and/or catalyst, obtaining the corresponding amides in very high yields (34 examples with quantitative yield in most cases; entry 9).[77] This solvent- and catalyst-free protocol was suitable for the selective acetylation of primary, secondary and tertiary aliphatic amines, aromatic, chiral amines (with different steric hindrance), diamines (aliphatic and aromatic), hydroxyamines (aliphatic and aromatic), chiral hydroxyamines and thioamines. In almost all cases, quantitative conversion of the amine reagent was observed at T = 60 °C for t = 3 h. While the degree of substitution on the *N-* heteroatom did not influence the reaction outcome, an increased steric hindrance paired with an electron effect of the alkyl substituents in the amines slowed down the reaction. For instance, with aromatic amines the yields were low (even as low as 20 %) or the reaction did not take place at all (for example with aniline). Interestingly, when starting from bifunctional amines bearing both aromatic and aliphatic *N-* functionalities or hydroxyamines, the acetylation occurred chemoselectively on the *N*-aliphatic group for bifunctional amines, while hydroxyamines underwent an exclusive amidation (Scheme 3.28).[77]
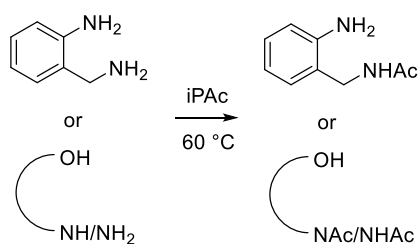
Scheme 3.28. *Chemoselective reactions of iPAc with amines*

Alalla and co-workers described another clean and sustainable protocol for iPAc-mediated amidation, again under solvent/catalyst-free conditions at room temperature (19 examples with variable yields; entry 10):[107] The reaction was successful with various primary amines, aromatic, benzylic, cyclic, heterocyclic amines and aminoalcohols. Similarly to the results described by Pelagali *et al.* it was confirmed that aromatic amines were less active than aliphatic ones. In addition, EWG groups on the phenyl ring led to a decrease in the products yield, while the presence of *meta*-acetyl substituents afforded the corresponding acetamide in good yield. For bifunctional compounds such as amino alcohols, the primary amine

functionality was selectively *N*-acetylated albeit the isolated yields were affected by steric effects.[107]

iPAc acted as an acyl donor for the biocatalytic kinetic resolution (KR) of amines.[109] For example, Gill and co-workers reported the improved performance of iPAc compared to vinyl acetate towards biocatalyzed *N*-acetylations: while vinyl acetate was too reactive and resulted in high levels (12-34 %) of unselective non-enzymatic acetylation with the formation of several side products, iPAc formed exclusively the corresponding *N*-acylated products.[109a] Several lipases were active towards enantioselective *N*-acylation with iPAc: the best results were obtained with Chirazyme-L2 and Novozym-435, which provided full conversion of (*R*)-1-(30-bromophenyl)ethylamine with very high enantioselectivity (>99.8% *ee*; Scheme 3.29).
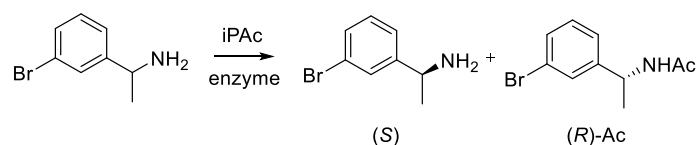
Scheme 3.29. *Enzymatic KR of (R/S)-1-(30-bromophenyl)ethylamine, promoted by iPAc*

Notwithstanding these good results, further experiments demonstrated the poor reproducibility of the kinetic resolution mediated by the iPAc.[109a,c] Other investigations on the enzymatic acetylation of amines with iPAc in water, catalyzed by acyltransferase enzymes, showed that no stereoselectivity could be achieved.[110]

iPAc was used as the acyl donor for quantitative and selective acetylation of sugar derivatives in the presence of *p*-toluensulfonic acid as a catalyst. Examples are shown in Scheme 3.30.[111,112]

CAc = chloroacetyl
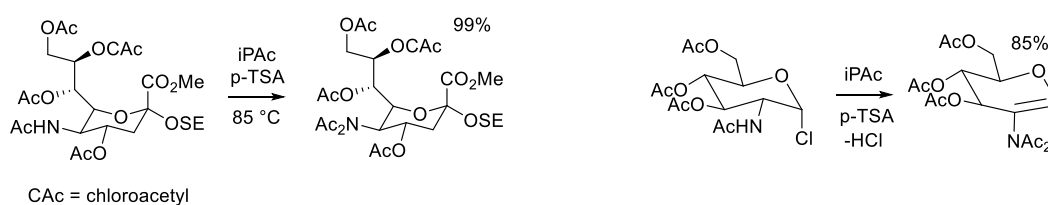
Scheme 3.30. *iPAc-promoted amidation of N-functionalized sugar derivatives*

Selective alkoxy- and/or amidoxy-carbonylation reactions have been reported using isopropenyl carbonates (iPCs) and carbamates (iPCMs).[113,114] iPCs were obtained by the treatment of chloromercuriacetone (ClHgCH$_2$COCH$_3$) with alkyl or aryl chloroformates (Scheme 3.31: top, path a).
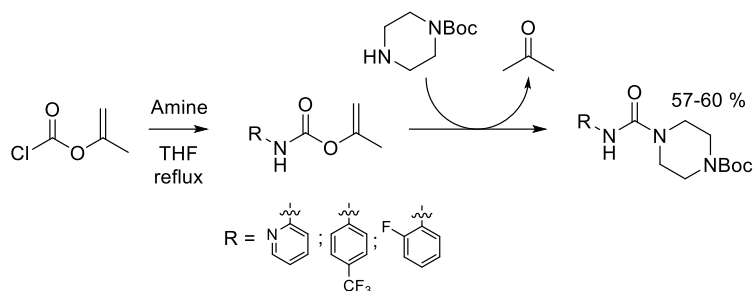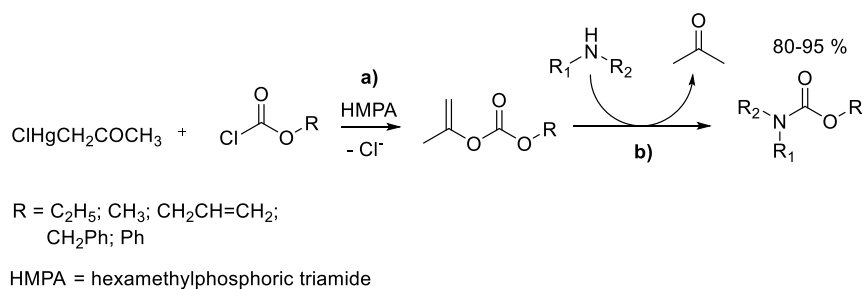
Scheme 3.31 *Synthesis and reactivity of isopropenyl carbonates (iPCs) and carbamates (iPCMs) with amines*

iPCs reacted with various amines at 50-70 °C to form the corresponding *N*-carboalkoxylated and *N*-carboaryloxylated products (12 examples: yields 80-95 %; Scheme 3.31: top, route b). The reactions took place in the absence or in the presence of catalytic amounts of p-TSA, depending on the amine.

iPCMs were prepared starting from iPCF. Isopropenyl carbamates were then set to react with N-Boc cyclohexyl amine to synthesize the corresponding ureas (3 examples: 57-60 % yield; Scheme 3.31, bottom).[59]

To conclude, the sole example of acylation of thiols is aggregated to this section. Kucinski et al. reported an efficient, mild, and chemoselective synthesis of various thioesters via a HOTf-catalyzed S-acetylation of aromatic and aliphatic thiols using iPAc as a cheap and convenient acetylating agent (17 examples; yields 80-93%; Scheme 3.32).[115]
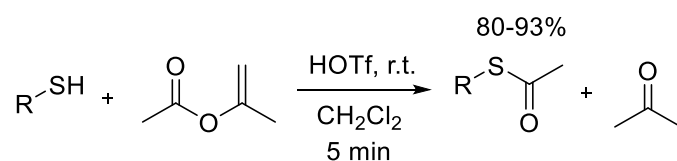
Scheme 3.32 *Acetylation of thiols with iPAc*

3.3.1.5 Friedel-Crafts

To the best of our knowledge, only a few papers have been reported on iPEs-mediated Friedel-Crafts (FC) reactions. Rothman and co-workers initially described the activity of isopropenyl stearate as an acylating agent in AlCl$_3$ catalyzed Friedel-Crafts reaction of benzene.[116] Stearophenone was achieved in a 60% yield (Scheme 3.33, route a). In addition, the paper highlighted the versatility of isopropenyl stearate in comparison with saturated esters which showed poor, if any, reactivity with aromatic systems.

iPAc was also employed for Friedel-Crafts acetylation reactions in the presence of a series of Lewis acid heterogeneous catalysts including zeolites HBEA, HMFI, and HFAU, in place of the conventional $AlCl_3$ system. Under batch conditions, a model substrate as anisole afforded *p*-methoxyacetophenone in around 40% yield at 80 °C (Scheme 3.33, route b).[117] The competitive absorption rates/constants of reactants and solvents in the zeolite framework was thoroughly investigated, and iPAc displayed the highest absorption equilibrium constant. Furthermore, it was found that absorption of the co-product acetone was neglectable, thereby concluding that it (acetone) did not contribute to catalyst deactivation.

Schmidt *et al.* described the use of an acyltransferase bacterium by which the Friedel-Crafts C-acylation of various resorcinol derivatives with iPAc could be successfully carried out. Variable yields (up to 95 %) of the products were achieved (Scheme 3.33, route c).[118] This was the first example of bio-catalyzed F.-C. acetylation of aromatic compounds highlighting the role of iPAc as a bio-compatible acetyl donor.

Another peculiar catalyst was diphenylboryl hexachloroantimonate (Ph_2BSbCl_6) which was reported for the activation of acyl enolates in the Friedel-Crafts reaction of iPAc with alkyl aromatics. The corresponding aromatic ketones were obtained in moderate to fairly good yields (46-71%) under almost neutral conditions and at room temperature (Scheme 3.33, route d).[119]
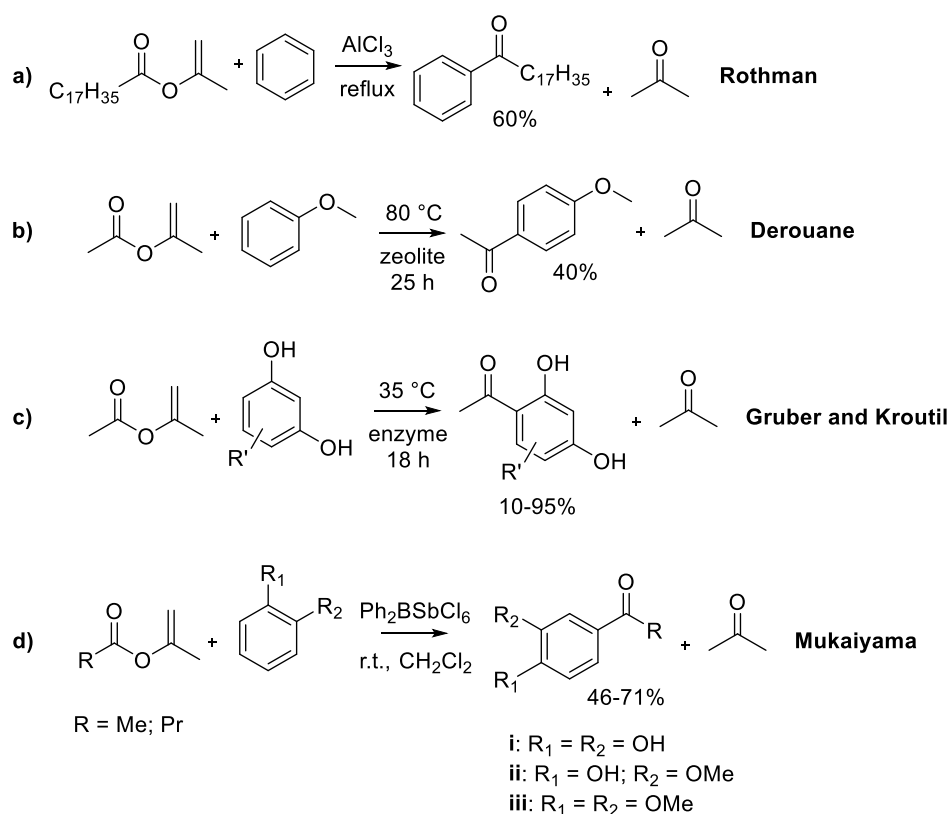
Scheme 3.33. *All the reported procedures for the iPEs-mediated FC reaction*

Overall, the study of iPEs-mediated Friedel-Crafts reactions remains a largely underexplored field. The substitution of toxic conventional acyl halides with more eco-friendly ones, like iPEs, in combination to the design of halide-free catalysts may therefore represent a promising sustainable alternative for FC strategies.

3.3.2 Reactions of the C=C double bond

3.3.2.1 Polymerization

iPAc has been the most employed isopropenyl ester for polymer synthesis. In the perspective of synthesizing iPAc from bio-based acetic acid and acetone (see paragraph 3.2.1), iPAc-derived polymers could be, in principle, viewed as renewable plastics. The first papers on the homopolymerization of iPAc reported the use of peroxide based-initiators as for example, benzoyl peroxide, to obtain viscous liquids with low molecular weight.[9,120] Authors recognized that iPAc showed a reactivity almost identical to that of allyl acetate. Later on, Nishino and co-workers employed α,α'-azobisisobutylonitrile (AIBN) to induce the radical polymerization of iPAc: at room temperature a very low-molecular weight homopolymer was obtained, while poly (isopropenyl acetate) (PiPAc) with a weight average molecular weight over 10^4 was synthesized at high-pressure (1 GPa, T = 70 °C).[121] Poly-isopropanol (PiPOH) was then achieved by hydrolysis of the acetyl moieties (Scheme 3.34, a).

Helium ions irradiation effects towards liquid iPAc and isopropyl acetate have been studied at room temperature and at 80 °C by Newton et al.[122] It was found a factor of thirty higher "polymer" yield when iPAc was used in place of isopropyl acetate, indicating that the polymerization occurs through the double bond.[125] iPAc was also investigated for various copolymerization processes. Vinyl chloride and iPAc were emulsion copolymerized in sealed tubes at 45° C.[7] Colorless, clear resins ternary copolymers were prepared by the reaction of iPAc with esters of maleic and fumaric acid in different molar ratios and combinations[7] McNeill et al. reported thermal degradation studies of alternating copolymers in which the copolymerization of iPAc with maleic anhydride was involved.[123] The isothermal studies proved that isopropenyl acetate units in the alternating copolymer chain had lower stability than other acetate monomer units, such as those from allyl acetate. Other copolymers of iPAc with vinyl chloride were synthesized by Unruh et al. and Basche et al.[124] A copolymer of isopropenyl acetate with indene monomer was described by De et al. who carried out a radical polymerization at a high pressure.[125] Wu et al. reported a random poly (styrene-co-isopropenyl acetate) (SIPA) copolymer achieved by free radical polymerization at 70 °C using AIBN as initiator. SIPA was used as macroinitiator for the cationic polymerization (TiCl$_4$ catalysis) of isobutylene (IB) at -40 °C in CH$_2$Cl$_2$, to produce graft copolymers of SIPA-g-PIB (Scheme 3.34, b).[126] Sabnis et al. examined one of few preparations of acrylic polymers via an emulsion technique in the presence of iPAc.[127] Authors claimed for iPAc as a low-cost monomer for radical polymerization, which could be a partial replacement for various acrylic monomers. Though, polymerization techniques needed improvement (Scheme 3.34, c).
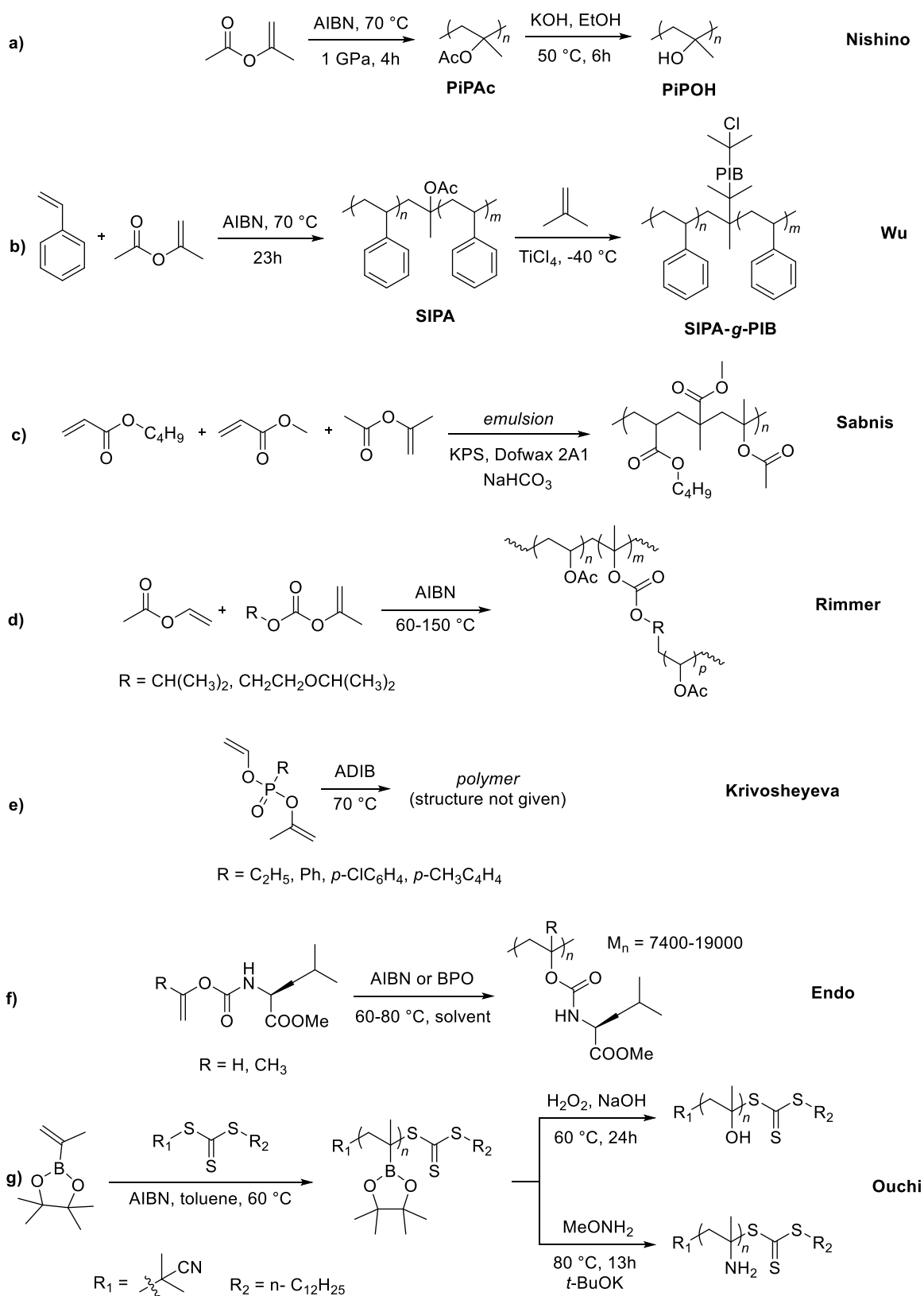
Scheme 3.34. *Polymerizations of iPEs*

Kuwae et al. reported that a kinetic study using electron spin resonance. They found that although iPAc and its radical were reactive enough for chain propagation, high-molecular weight homopolymers were not easily formed because of the rate of chain transfer to monomers.[128] The theoretical determination of infrared spectra of poly-isopropenyl acetate were investigated by Borowsky et al.[129] Simple procedures for the calculation were adopted

and the results reflected well the experimental results. Tong and co-workers investigated the (co)polymerization of iPAc with maleic anhydride, using benzoyl peroxide as a catalyst, and observed that the final materials contained substantially alternating units of the two monomeric species.[130]

Some works have been reported on the iPEs polymerization using higher homologues of iPAc. Rimmer et al. employed two isopropenyl carbonates (isopropyl prop-1-en-2-yl carbonate and carbonic acid isopropenyl ester 2-isopropoxy-ethyl ester) in the radical copolymerization with vinyl acetate to synthesize highly branched (poly)vinyl acetate (Scheme 3.34, d).[131] They found that the isopropenyl functionality showed lower reactivity during the propagation step when compared to the allyl carbonate homologue of choice. Nevertheless, the work demonstrated the applicability of isopropenyl carbonates to control the characteristics of the polymer and to tune its properties.

Krivosheyeva and co-workers performed the polymerization of allyl-isopropenyl esters of ethyl/aryl-phosphinic acids by electrical conductivity measurements, dilatometry, and infrared spectroscopy (Scheme 3.34, e).[132] On the basis of the physical properties and the infrared spectra of the polymers, it was concluded that polymerization occurred through the allyl group and not the isopropenyl one. It was also hypothesized that isopropenyl groups took part in a secondary process of crosslinking of the polymer along with allyl groups. The radical polymerization of an isopropenyl carbamate having L-leucine methyl ester structures, N-isopropenyloxycarbonyl-L-leucine methyl ester, chosen as model compound, was carried out (Scheme 3.34, f).[133] Using benzoyl peroxide (BPO; 1 mol%) as initiator, a low molecular weight polymer was achieved at 80 °C, meanwhile using AIBN no polymer was afforded. The glass transition temperature of poly-N-isopropenyloxycarbonyl-L-leucine methyl ester was 65 °C. The ability of isopropenyl boronate pinacol ester to serve as a monomer in radical polymerizations was established and exploited for the synthesis of polymers that are difficult to access using other polymerization techniques (Scheme 3.34, g).[134] The boronyl pendants, which were directly attached to the polymer backbone, can be replaced with -OH or -NH_2 to yield poly(a-methyl vinyl amine) or poly(a-methyl vinyl alcohol), which has been inaccessible by conventional synthetic methods.

3.3.2.2 Thiol-Ene reactions

The formation of a carbon-sulfur bond (C-S) is relevant in the synthesis of organosulfur moieties within natural products, pharmaceuticals and modern materials.[135] Various strategies for the construction of C-S bonds have been developed. Among others, the thiol-ene Michael type addition provides efficient access to sulfur containing products, fulfilling the "click" chemistry concept and exemplifying a sustainable atom economical process.[136] These Micheal type additions occur through a nucleophilic attack of a thiol to an α,β-unsaturated carbonylic compound. A similar, though conceptually different, pathway has been described in few papers reporting the reactivity of iPEs with thiols.
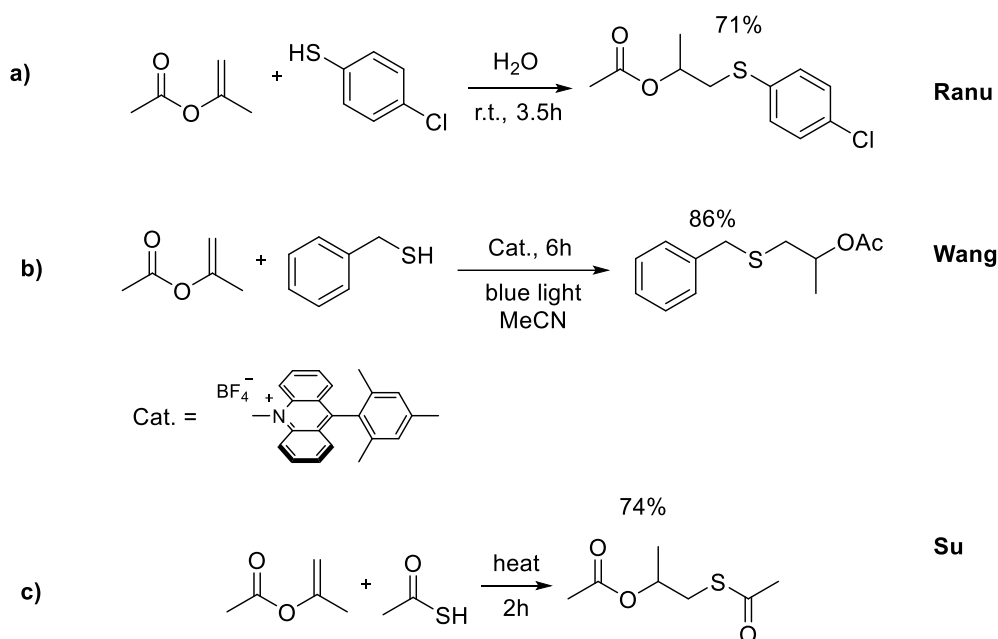
Scheme 3.35. *Thiol-ene reactions, promoted by iPAc*

Ranu et al. claimed a highly selective anti-Markovnikov addition of aromatic thiols to iPAc in water at room temperature without any additive (Scheme 3.35, a). [137] Winking the eye towards green chemistry, this process represented a very simple and efficient method for the synthesis of linear thioethers: mild conditions (room temperature), high regioselectivity, water as a solvent, high yields of products, and absence of catalyst were major advantages. Wang et al. reported the combined work of 9-mesityl-10-methylacridinum tetrafluoroborate and visible light as a green photocatalyst for the reaction between benzyl mercaptane and iPAc (Scheme 3.35, b).[138] The supposed mechanism involves the formation of thiyl radicals, generated upon quenching of the photoexcited catalyst, as active species for the addition to the olefin. Su et al. prepared 1 -Acetylthio-isopropy 1 acetate from isopropenyl acetate and thiolacetic acid (Scheme 3.35, c).[139]

3.3.2.3 Epoxidation

The epoxidation of olefins is a well-known transformation for the synthesis of a plethora of intermediates.[140] iPEs have been also investigated to this purpose.

a)

m-CPBA = m-chloroperbenzoic acid

b)
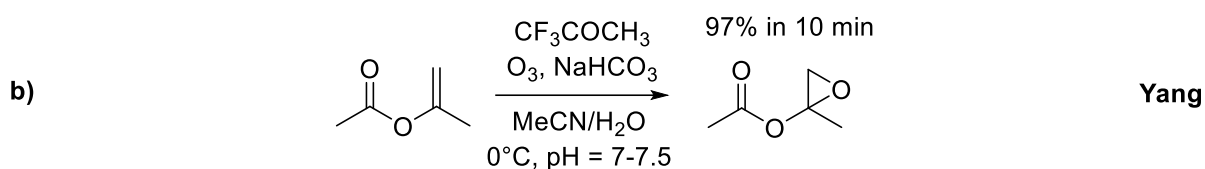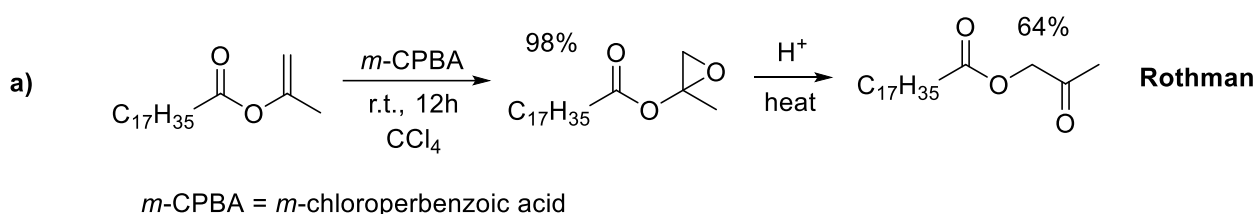
Scheme 3.36. *iPEs epoxidations*

The first example of iPEs epoxidation is dated back to 1968, in a study that described the use of iPEs-derived from mono- and di-basic fatty acids with m-chloroperbenzoic acid in carbon tetrachloride (Scheme 3.36, a).[141] Authors highlighted the difficult isolation of the oxirane products due to its spontaneous rearrangement to a hydroxyacetone ester. Rapid gel filtration was the only method that consistently afforded good yields of the epoxide.

Lately, Yang et al. demonstrated that a high yield (97%) of 2-acetoxy-1,2-epoxipropan in 97% was achieved by the reaction of iPAc with ozone under neutral reaction conditions: the process took place through an *in situ* generated methyl(trifluoromethyl)dioxirane (Scheme 3.36, b)[142]

3.3.2.4 Reactions with H_2 and CO

The cyclocarbonylation of iPAc was investigated in the presence of $PdCl_2(PPh_3)_2$ and methanol as a catalyst and a solvent, respectively. At 100 °C, the reaction produced 2-methoxy-2,5,5-trimethyl-1,3-dioxolan-4-one with a 67% selectivity at ≥98% conversion of iPAc.[143] The relevance of methanol for the reaction was described according to the catalytic cycle of Scheme 3.37. Interestingly, no reaction took place without methanol. The cycle involves a first iPAc coordination, followed by a CO insertion; the final addition of the alcohol brings to the corresponding product. The same Authors also reported a similar method for the carbonylation of different enol esters (8 examples; yields 46-64%).[144]
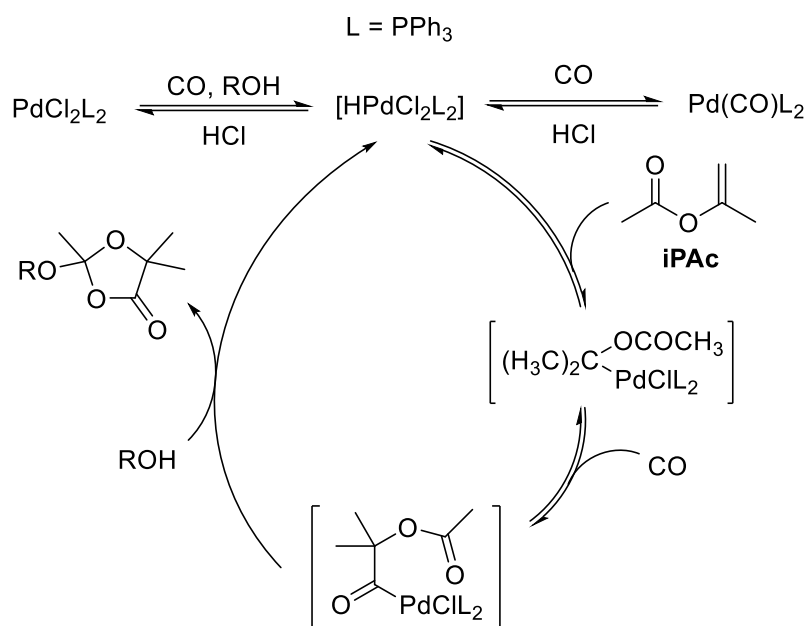
Scheme 3.37. *Catalytic cycle of iPAc carbonylation in the presence of methanol, catalyzed by PdCl$_2$(PPh$_3$)$_2$*

The stereoselective hydroformylation of tri-fluorinated iPAc, namely 3,3,3-trifluoroprop-1-en-2-yl acetate, was studied using Rh-based catalysts (Scheme 3.38). The reaction product was subsequently oxidized to yield enantiomerically pure 2-trifluoromethyllactic acid with >99 ee (S).[145]
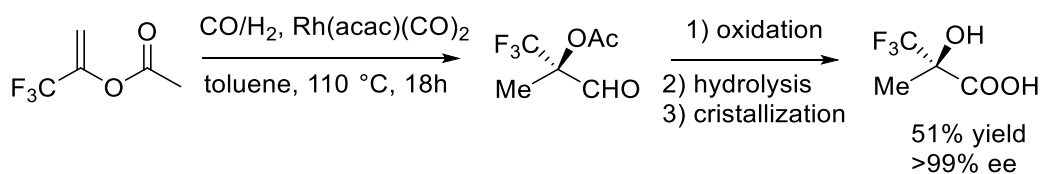
Scheme 3.38. *Stereoselective hydroformylation of 3,3,3-trifluoroprop-1-en-2-yl acetate*

Based on this result, a hydroformylation protocol was developed using both iPAc and two of its derivatives, as 1-(trifluoromethyl)vinyl acetate and 1-cyanovinyl acetate (3 examples; yields 29-97%).[146]

3.3.2.5 Etherification

Only few papers report on the conversion of iPEs into isopropenyl ethers. Interestingly, one of the first syntheses of isopropenyl ethers started from the reaction of propyne and alcohols.[147] Albeit this protocol did not involve the use of iPEs, the study was important to highlight the behavior of isopropenyl ethers bearing alkyl chains of different length. The systematic analysis of these compounds showed that isopropenyl ethers were more sensitive to hydrolysis than the corresponding enol esters, thereby paving the way for converting ethers into value added chemicals and polymers (when, for instance, diisopropenyl ethers were involved).
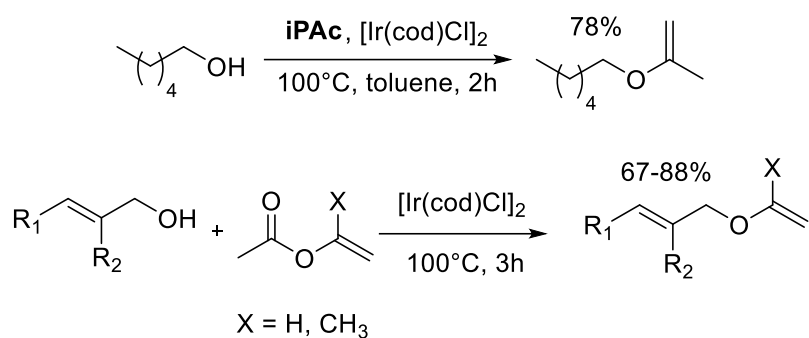
Scheme 3.39. *Synthesis of isopropenyl ethers*

iPAc was successfully used in the reaction with *n*-octyl alcohol catalysed by [Ir(cod)Cl]$_2$ to prepare the corresponding isopropenyl ether (78% yield) (Scheme 3.39).[148] They also proposed a mechanism for the reaction (Scheme 3.40). In another investigation of the same Authors, a one-pot synthesis of α,β-unsaturated carbonyl compounds from allyl alcohols and iPAc or vinyl acetate was achieved through the in situ generation of allyl isopropenyl/vinyl ethers as key intermediates. Ir-complexes, such as [IrCl(cod)]$_2$, catalyzed both the isopropenyl ether synthesis and the further rearrangement of ethers to the Claisen products (8 examples; yields 67-88%) (Scheme 3.39).[149]
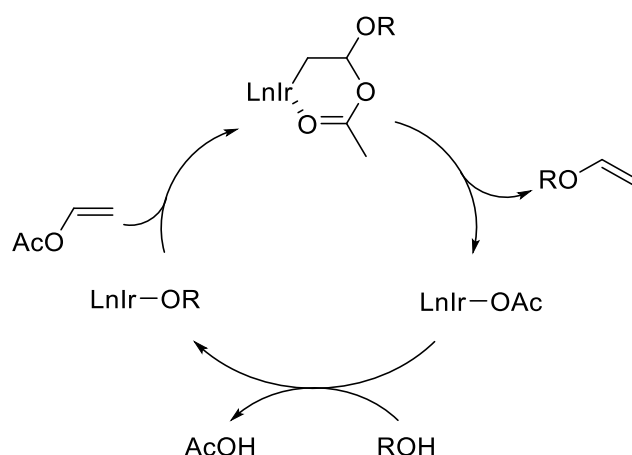
Scheme 3.40. *Ishii's mechanism for the synthesis of isopropenyl ethers*

3.3.2.6 Mannich reaction

The Mannich reaction allows the design of complex structures through a straightforward multicomponent process where a Schiff base formed in-situ generates a β-aminocarbonyl compound (a Mannich base).[150]

An iPEs-mediated Mannich reaction has been reported using diversely substituted anilines and ethyl glyoxalate, in the presence of Sc(OTf)$_3$ as a Lewis acid catalyst. Under such conditions, vinyl acetate yielded quinoline derivatives selectively, whereas iPAc led to the corresponding Mannich adducts in moderate to good yields (20-76 %) (Scheme 3.41, top).[151] Authors, however, did not propose any mechanism for the reaction. The hypothesis illustrated by Scheme 3.41 (bottom) was formulated by us. Four major steps were considered: i) a Sc(OTf)$_3$ activation of the C=O group of the aldehyde followed by a nucleophilic attack of the amine; ii) a concerted intramolecular N to O proton transfer (t-H), which brought to the formation of the corresponding imine intermediate after the elimination of H$_2$O; iii) a iPAc-promoted Michael-

142

type attack towards the imine; iv) an internal cascade rearrangement to form the final acetylated Mannich product.
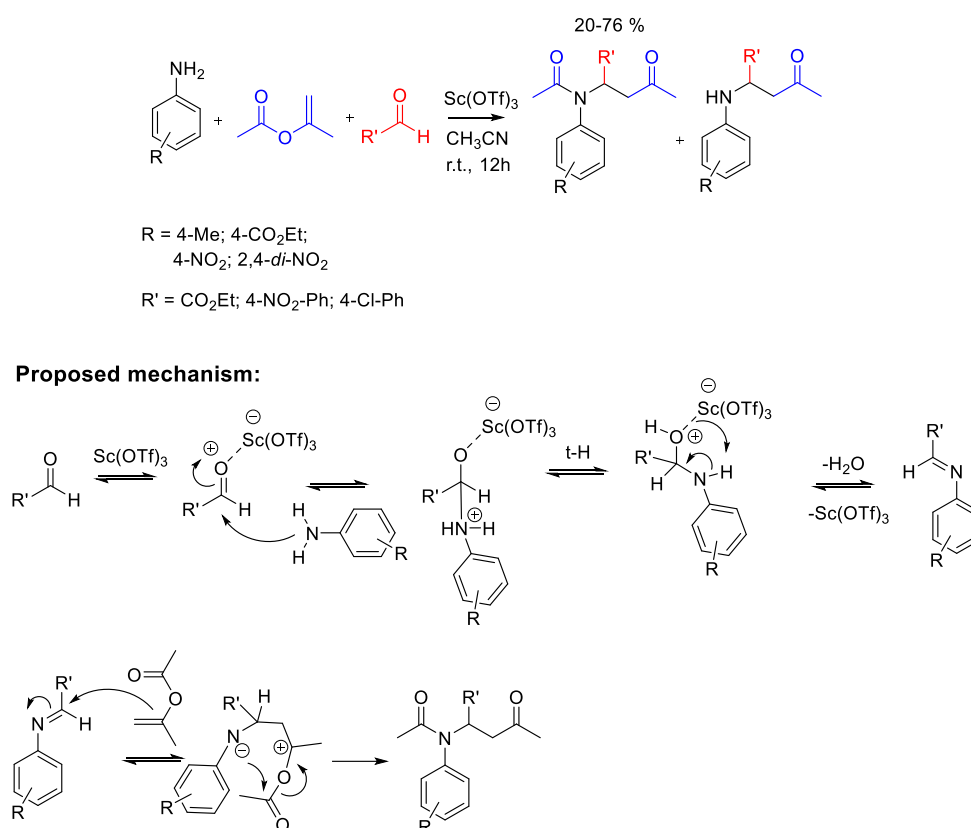
Scheme 3.41. *Sc(OTf)₃ catalyzed Mannich reaction promoted by iPAc and its proposed mechanism*

Stainforth *et al.* employed a combination of $Mg(ClO_4)_2$, 2,2'-bipyridine, and N-methylmorpholine as the catalyst for the direct addition of isopropenyl carbonate ketones to aryl N-Ts imines, providing cyclic carbamate adducts (4 examples; 61-72% yields). The *anti*-configured Mannich products dominated.[152]
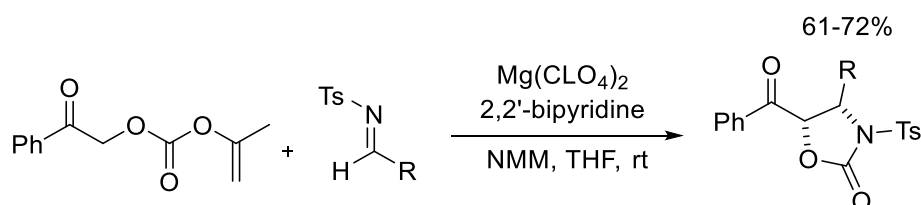
Scheme 3.42. *Mannich reaction of isopropenyl carbonates*

3.3.2.7 Radical reactions

iPEs have been involved for several types of radical reactions. iPAc in particular, has been used as an electron-rich terminal alkene to carry out a reductive alkylation processes promoted by organic halides.[153] Reactions were performed at 60-80 °C in benzene or dioxane solvent, using di-tert-butyl hyponitrite (TBHN) or dilauroyl peroxide as initiators. The overall transformation proceeded via electrophilic carbon-centred radicals and produced esters in good yields (7 examples: 72-88%; Scheme 3.43, top).

Similarly, thiols catalyzed the radical-chain addition of primary aldehydes to enol esters and to silyl enol ethers to give aldol derivatives in good yields under mild conditions.[154] For example,

the addition of butanal (2 equiv.) to iPAc in the presence of TBHN (2 × 2.5 mol%) and methyl thioglycolate (2 × 5 mol%) afforded the corresponding adduct in 80% yield. It was found that also the TBHN-promoted radical-chain addition of dimethylphenylsilane to iPAc proceeded smoothly in hexane or dioxane solvent in 2.5 h at 60 °C, in the presence of tert-dodecanethiol as catalyst.[155] Leonel *et al.* found that the activation of CBr$_4$ and CCl$_4$ by a bimetallic iron/copper couple in acetonitrile was efficient for gem-dibromo- and gem-dichloromethylenation of nucleophilic alkenes including iPAc. This route involved dihalocarbene species to produce gem-dihalocyclopropanes (Scheme 3.43, bottom).[156]
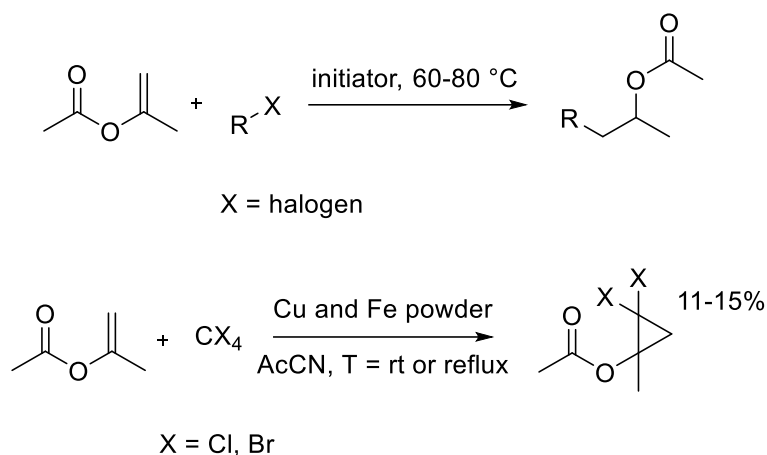
Scheme 3.43. Top: radical addition to iPAc. Bottom: synthesis of dihalo cyclopropanes

Crabtree and co-workers developed a novel photochemical methodology for the Hg^{II}-photosynthesized alkene hydrodimerization in presence of H$_2$ as radical source. In particular, when performing the hydrodimerization reaction starting from iPAc, the product, 2,3-dimethylbutane-1,4-diyl diacetate, was obtained in 50 % yield.[157] The same reaction was successfully carried out to produce 2,3-dimethylbutane-2,3-diyl diacetate in 92 % yield from iPAc and H$^•$ generated via Hg photosensitization.[158]

A Fe^0 (iron filings) catalyzed radical addition of CCl$_4$ (1.5 equiv.) to iPAc provided the formation of 4,4-dichloro-but-3-en-2-one in a 36 % yield. Notwithstanding the quantitative conversion of iPAc, the low product yield was ascribed to the dehydrohalogenation of a transient intermediate (Kharasch adduct).[159] The study of the reaction between perfluorinated electrochemically generated radicals, obtained by the reductive electrolysis of perfluorocarboxylic acids R$_f$CF$_2$COOH, and iPAc proved that perfluoroalkylacetones were achived in 30-37 % yield. The overall sequence involved a radical addition process followed by deacetylation.[160]

3.3.2.8 Cross Coupling

The use of iPEs and other enol esters in cross coupling reactions has been proposed as an alternative halogen-free methodology for the construction of C-C bonds. The main reported routes are discussed below.

Stille

A series of α-heteroarylacetone derivatives have been synthesized upon Pd-catalyzed coupling of heteroaromatic bromides, chlorides, and triflates, tributyltinmethoxide and iPAc (8

examples, 10-90 % yield).[161] From a mechanistic point of view, the observed reactivity was in agreement with the observations of Buchwald and Palucki,[162] who postulated an initial *in-situ* formation of tin enolate from tributyltin methoxide and iPAc, followed by transmetallation and coupling to the aryl partner to deliver the α-aryl acetone (Scheme 3.44).
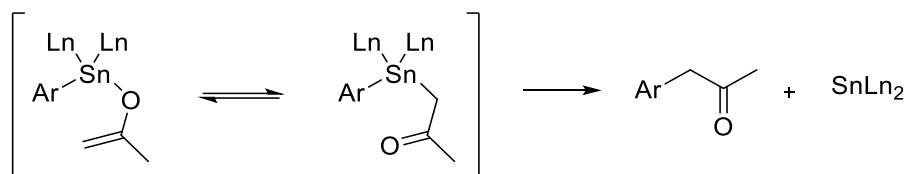
Scheme 3.44. Proposed pathway for the Stille coupling of iPAc with tributyltinmethoxide

Bailey and co-workers reported a methodology for the synthesis of 8-substituted-6-phenyl-6,7,8,9-tetrahydro-3H-pyrazolo[4,3-f]-isoquinolines, which included the preparation of a chiral amino substituted indazone derivative obtained by a Stille coupling of 4-bromoidazone and iPAc in the presence of (Bu)$_3$SnOMe.[163] The reaction of tributyltin enolates, prepared from tributyltin methoxide and enol acetates in situ, with 1-bromo-l-alkenes in the presence of a catalytic amount of PdC$_{12}$(o-tolyl$_3$P)$_2$ was described for the preparation of allyl ketones (12 examples; yields 32-86%)[164] and α-phenyl ketones with complete retention of the acetate regiochemistry (8 examples; yields 33-90 %).[165] The case of iPac is represented in Scheme 3.45.
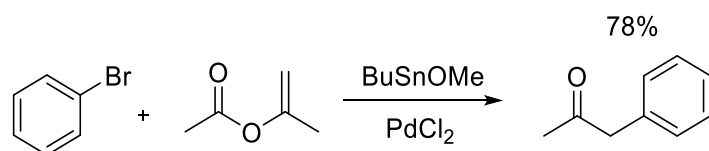
Scheme 3.45. Pd-catalysed α-phenylation of henylbromide with iPac

Similarly, the reaction of acetonyltributyltin obtained *in-situ* from tributyltin methoxide and iPAc, and aryl bromide was successfully performed in toluene at 100 °C under Ar atmosphere to provide arylacetones in good yields (8 examples; yields 51-91%).[166] To conclude, an iPEs-mediated Stille coupling was used for the total synthesis of tricyclic pyrazoles as potentphosphodiesterase 10A inhibitors.[167]

Olefin metathesis

Xu and Nicolaou proposed a cross-coupling strategy for the total syntheses of the cytotoxin marine natural product floresolide B and its $\Delta^{6,7}$-Z isomer through an olefin metathesis-based strategy: benzyl methyl ketones were intermediates synthesized starting from substituted benzyl bromides, iPAc and (Bu)$_3$SnOMe in the presence of catalytic amounts of Pd$_2$(dba)$_3$ and Buchwald ligand A5.[168]

Miscellaneous Cross Coupling

A 1,4-diketone was selectively prepared from a β-ketoester and iPAc. As depicted in Scheme 3.46, the reaction occurred under mild and sustainable conditions, using atmospheric oxygen as the oxidant, non-toxic and inexpensive CeCl$_3$·7 H$_2$O as a catalyst precursor and 2,2,2-trifluoroethanol (TFE) as the solvent. The sequence involved an initial oxidative coupling of iPAc with formation of a diacetal dioxolane intermediate which in turn, was hydrolyzed in acidic media to the final product.[169,170]
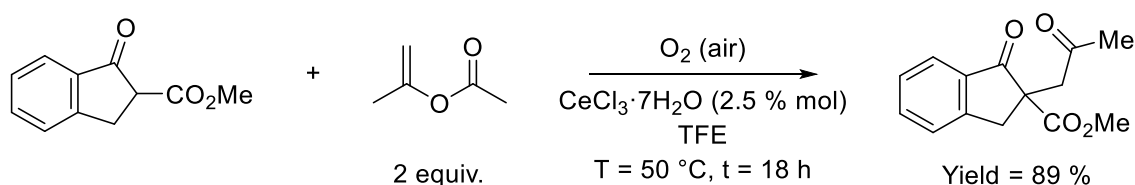
Scheme 3.46. *Synthesis of methyl 2-(2-oxopropyl)-1-indanone-2-carboxylate via Ce-catalyzed oxidative coupling between methyl 1-indanone-2-carboxylate and iPAc*

Wang and co-workers reported a Fe^{III}-based protocol for the selective synthesis of symmetrical diethynyldiethiane derivatives from 2-alkylthiophenes and substituted vinyl acetates. For example, 5,5'-(propane-2,2-diyl)bis(2-ethylthiophene) was obtained from 2-ethylthiophene and iPAc in 23 % yield, in the presence of FeCl$_3$ (20 mol %) and TsOH (20 mol %) as catalysts.[171] 2-Substituted allylic arenes were achieved by a Ni^{II}-catalyzed reaction of aryl ammonium salts and vinyl/aryl C–O electrophiles: as an example, 1-methoxy-4-(2-methylallyl) naphthalene was synthesized in a 73 % yield from 1-(4-methoxynaphthalen-1-yl)-*N,N,N*-trimethylmethanaminium trifluoromethane sulfonate and iPAc (Scheme 3.47).[172]
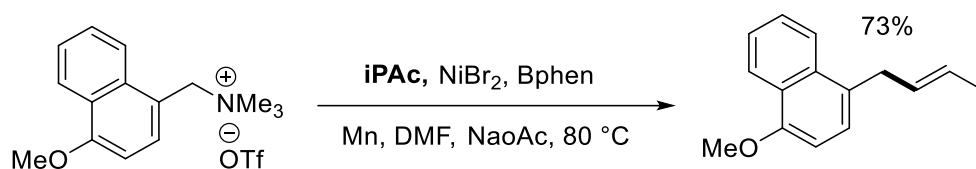
Scheme 3.47. *The reaction between 1-(4-methoxynaphthalen-1-yl)-N,N,N-trimethylmethanaminium trifluoromethane sulfonate and iPAc*

Tanaka and co-workers prepared a series of tri- and tetra-substituted benzenes using a cationic Rh^I/*rac*-BINAP complex to catalyze chemo- and regioselective cross-cyclotrimerizations between alkynes and enol ethers or acetates, including iPAc. Interestingly, three component cyclotrimerizations of a mixture of terminal alkynes afforded the corresponding 1,2,3,4-tetrasubstituted benzenes in good yields (41-73 %) and excellent regioselectivity (> 99:1).[173] The same group employed iPAc as a cycloaddition partner for intermolecular cross-[2+2+2] cycloadditions with substituted alkynes in the presence of the above-quoted cationic Rh^I/BINAP catalyst: when the cyclotrimerization reaction occurred with terminal monoynes, a mixture of trisubstituted benzenes regioisomers was formed, while 1,2,3,4-substituted benzenes as a single regioisomer (11 examples, 35-72 % yield) were achieved starting from a mixture of terminal and internal alkynes.[174] Another cycloaddition was reported by Cheng *et al.*, who developed an iron-catalyzed intermolecular [4 + 2] cyclization of arylnitrones with geminal-substituted vinyl acetates. 2,4-disubstituted quinolines with good functional group compatibility was prepared in moderate to good yields (14 examples; yields 33-83%). Preliminary mechanistic studies suggested an iron-catalyzed C–H activation process under external-oxidant-free conditions.[175] The same group also proposed the synthesis of 3-substituted or non-C3-substituted isoquinolines through Rh-catalyzed sequential oxidative C–H activation/annulation with geminal-substituted vinyl acetates (16 examples; yields 33-82%; Scheme 3.48).[176]

33-82%
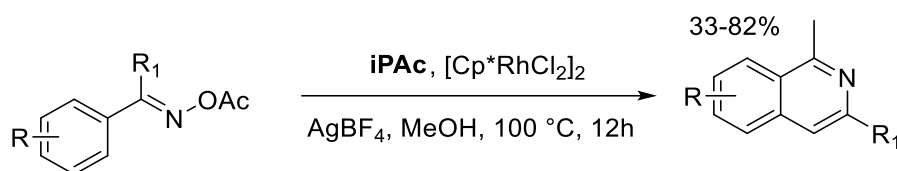
Scheme 3.48. *Synthesis of isoquinolines mediated by iPAc*

A Co^{II}-catalyzed electrophilic alkenylation protocol was developed using functionalized aryl and/or alkenyl zinc pivalates and various alkenyl acetates: for example, 1,2,3-trimethoxy-5-(prop-1-en-2-yl)benzene was synthesized in 92 % yield starting from oxo(pivaloyl)(3,4,5-trimethoxyphenyl)zinc (1.5 equiv.) and iPAc under mild reaction conditions (5 % mol CoBr$_2$, 5 % mol 2,2'-bipyridyl, rt, t = 23 h).[177] A gold-catalyzed olefin cyclopropanation reaction of propargyl esters with vinyl ester or vinyl sulfonamide derivatives was investigated for the synthesis of highly substituted cyclo-propane derivatives. Products were achieved with good moderate to good *cis-/trans*-diastereoselectivity (*cis:trans*=99-21:1-79; 4 examples; yields 58-75%; Scheme 3.49).[178]

58-75%

R$_1$ = Ac, Piv
R$_2$, R$_3$ = Ph, Me
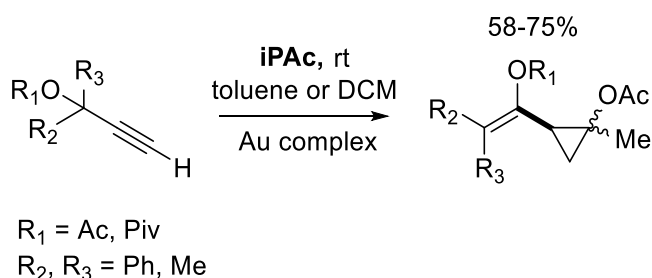
Scheme 3.49. *Cyclopropanation of propargyl esters*

Substituted aza-fused 7-azaindoles (16 examples, 30-94 % yield) were synthesized through a Rh^{III}-catalyzed *N*-directed *ortho* C–H activation followed by a roll-over C–H activation between 1-aryl-7-azaindole and iPAc.[179] Ishii and co-workers prepared a diester product, 1-acetoxy-2-methylpentan-3-yl propionate, using the cross coupling of propanal and iPAc in the presence of Sm^{II}-catalyst: the reaction took place under mild conditions (T = 0° C, t = 0.5 h followed by T = 25 °C and t = 2.5 h).[180] The same group reported the first example of a Pd-catalysed oxidative cross-coupling between acrylates and vinyl carboxylates: Scheme 3.50 shows the reaction of 2-ethylhexylacrylate and iPAc in excess. The coupling reaction was performed in acetic acid at T = 90 °C for t = 5 h under O$_2$ and in the presence of catalytic amounts of Pd(OAc)$_2$ and H$_4$PMo$_{11}$VO$_{40}$·nH$_2$O. The product was obtained in 71 % yield.[181]

Pd(OAc)$_2$ (10 % mol)
H$_4$PMo$_{11}$VO$_{40}$ (2 % mol)

NaOAc (10 % mol)
O$_2$ (1 atm)
AcOH (5 ml)
T = 90 °C, t = 5 h

5 equiv.

2-ethyloctyl (2*E*)-5-acetoxyhexa-2,4-dienoate
Yield = 71 %
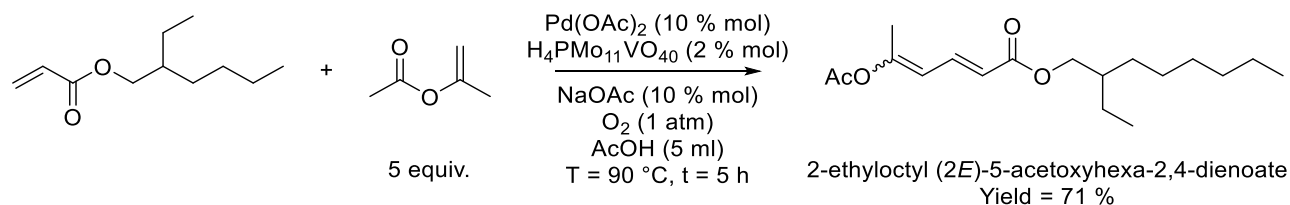
Scheme 3.50. *Synthesis of 2-ethyloctyl (2E)-5-acetoxyhexa-2,4-dienoate upon Pd-catalysed oxidative cross coupling between 2-ethylhexylacrylate and iPAc*

A combined Lewis acid system comprised of InI$_3$ and Me$_3$SiI was described to catalyze the direct coupling of enol acetates with alkyl acetates or alkyl ethers without generating metal waste.[182]

147

In a similar fashion, the coupling of iPAc and monosubstituted silyl ethers generated α-alkylated carbonyl products (14 examples, 23-99 % yield).[183] A strategy for the catalytic vinyl transfer from enol carboxylates (including iPAc) to activated C–H bonds of secondary alcohols was described using XPhos-modified Ru⁰ or Os⁰ complexes as the catalysts.[184] An example is given in Scheme 3.51.

PhMe, 130 °C

iPAc, $Ru_3(CO)_{12}$
XPhos

85%
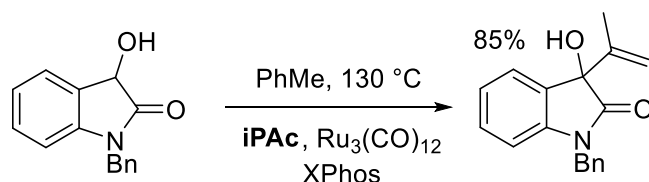
Scheme 3.51. An example of vinyl transfer from iPAc to an activated secondary alcohol

To conclude, Abdelwahaba and co-workers recently reported that in the presence of iron powder, aryl diazonium salts reacted with methyl vinyl ketone, acrylates, and iPAc to produce the corresponding arylated products (11 examples; yields 27-69%).[185]

iPAc derived α-substituted styrenes

α-Substituted styrene derivatives (23 examples, 15-92 % yield) were prepared via the coupling of vinyl acetates, including iPAc, and aryl halides (ArX; X = Cl, Br).[186] The case of iPAc is illustrated in Scheme 3.52.

ArX + (iPAc) → Ar

MeCN, pyridine   CoBr₂

bpy, Iron anode
stainles steel grid cathode
Bu4NBF4, rt, I=0.2A
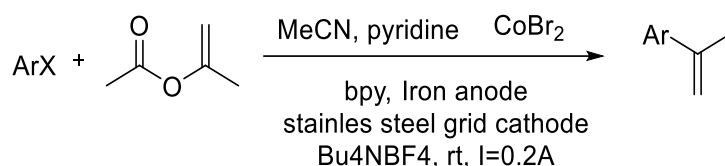
Scheme 3.52. Coupling reaction between aryl chlorides and iPAc

Likewise, an approach for the synthesis of α-substituted styrene derivatives was described starting from aryl and heteroaryl halides and iPAc, in the presence of a catalytic system comprised of equimolar amounts of CoBr₂ and 2,2'-bipyridine. Under mild conditions a T = 50 °C, products were isolated in moderate to very good yields (16-86 %: 13 examples).[187] Zhang and co-workers prepared aryl substituted styrenes and *N*-acetylanilides through a dehydrogenative arylation of electron rich alkenes catalyzed by Rhᴵᴵᴵ-based systems. Scheme 3.53 illustrates the use of iPAc. The most effective catalysts were electron-deficient Rhᴵᴵᴵ complexes, [CpRh] and [CpCF3Rh].[188]

Rhᴵᴵᴵ cat. (5 % mol)
AgSbF₆ (10 % mol)
Cu(OAc)₂·H₂O (1.1 equiv.)
THF
T = 80 °C, t = 12 h

X = (CO)N^{i}Pr₂   10 equiv.
X = NHAc

X = (CO)N^{i}Pr₂, Yield = 98 % [CpRh], 85 % [Cp^{CF3}Rh]
X = NHAc, Yield = 79 % [CpRh], 66 % [Cp^{CF3}Rh]
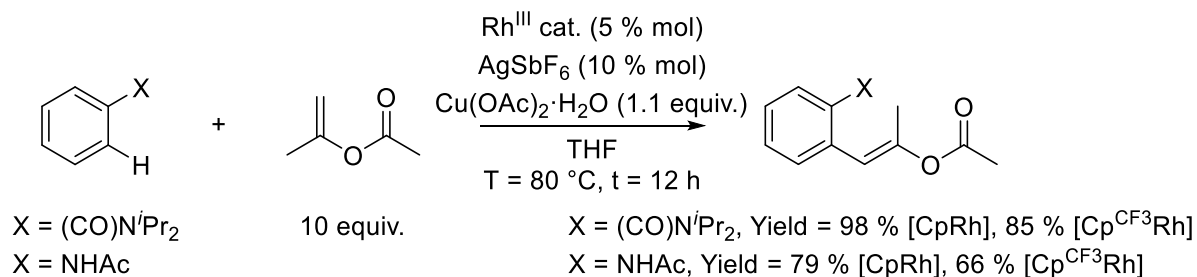
Scheme 3.53. RhIII catalyzed dehydrogenative arylation of iPAc

Heck olefination

Goossen *et al.* reported the decarbonylative Heck olefination of iPEs (8 examples; 67-98% yield; Scheme 3.54).[189] In contrast to traditional Heck reactions, the reaction was environmentally benign: the addition of base was avoided, and the use of iPEs implied the generation of volatile by-products instead than waste salts.

TBHAB = tri-n-butyl(2-hydroxyethyl)ammonium bromide
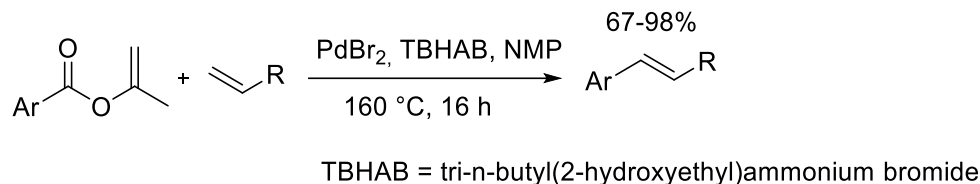
Scheme 3.54. Decarbonylative Heck olefinatin of iPEs

Another Heck-type reaction was described through a Pd-catalyzed oxidative β-arylation of electron-rich olefins as vinyl acetate and iPAc (Scheme 3.55). The coupling reaction was performed using both EWG- and EDG-substituted arylboronic acids under mild and additive-free conditions.[190]
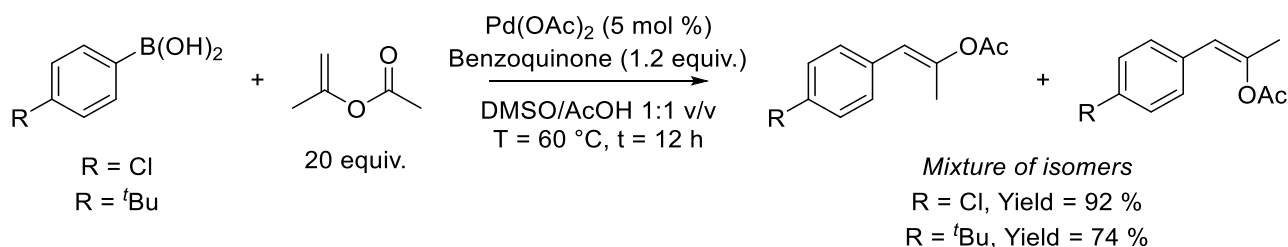
Scheme 3.55. Pd-catalyzed β-selective Heck oxidation between 4-substituted arylboronic acids and iPAc (ref. 138)

Paetzold and Gooßen reported the first optimized protocol for base- and solvent-free Pd-catalyzed Heck olefination between isopropenyl carboxylates and substituted styrenes (16 examples: 63-98 % yield). Interestingly, the *E* isomer of the stilbene products was synthesized preferentially.[191] The vinylation of substituted arylboronic acids with iPAc was catalysed also by Rh-based systems: for example, starting from [1,1'-biphenyl]-4-ylboronic acid, the corresponding vinylation product was obtained in 35 % yield.[192]

3.3.2.9 Photo-induced reactions

A photoredox alkylation of halopyridines with functionalized alkenes (including iPAc) and alkynes was reported at room temperature in the presence of [Ir(ppy)$_2$dtbbpy]PF$_6$ (24 examples: yields of 38-76%).[193] He and co-workers prepared and characterized a PANI (polyaniline)-*g*-C$_3$N$_4$-TiO$_2$ composite, active towards radical C–H arylation reactions. The process involved an initial photocatalyzed *in situ* generation of aryldiazonium salts (starting from substituted anilines in presence of ^{t}BuONO and MeSO$_3$H). Aryl radicals then formed and reacted with heteroarenes, benzoquinones or enol acetates under visible light (Scheme 3.56). The coupling products were isolated in good to excellent yields in water-based solvents, and the heterogeneous photocatalyst was recycled up to ten times without any loss of activity.[194]

^{t}BuONO (1.5 equiv.)

MeSO$_3$H (1.0 equiv.)

PANI (40 %)-g-C$_3$N$_4$-TiO$_2$

Acetone/H$_2$O 2:1 v/v

14 W CFL, t = 6 h

10 equiv.

12 examples
Yields = 72-85 %
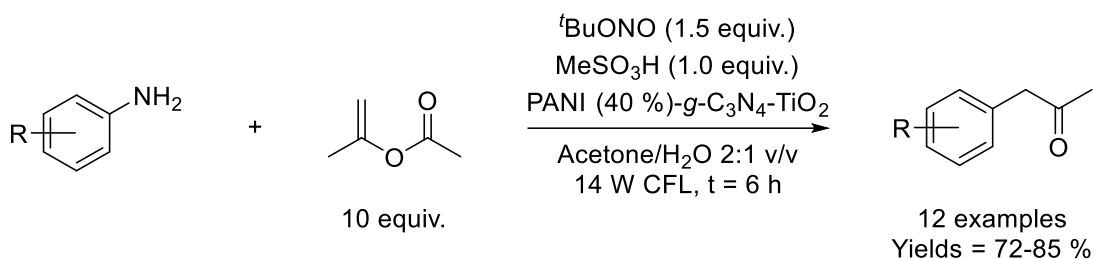
Scheme 3.56. *Photocatalyzed synthesis of α-aryl methyl ketones from substituted anilines and iPAc*

The first example of visible light photoinduced electron transfer (PET) reactions for the α-arylation of enol acetates with aryl diazonium salts was described using [Ru(bpy)$_3$]Cl$_2$ as a photosensitizer. This protocol allowed the preparation of 2-substituted indoles via a two-step process which included an initial photochemical ketone arylation with *o*-nitroaryldiazolium salts, followed by the reductive cyclization to the indole.[195] An aqueous photocatalytic system was designed by combining a visible-light photoredox catalysis with micellar catalysis. Notably, the arylation of iPAc with *p*-nitro aniline was performed in good yield (89%) (Scheme 3.57).[196]

89%

Eosin B, t-BuONO

TX100/H$_2$O
20 W CFL, rt

TX100 = Triton X-100 (surfactant)
CFL = compact fluorescent light
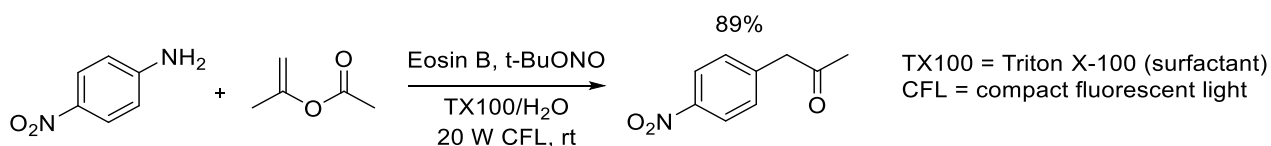
Scheme 3.57. *Photocatalytic α-arylation of iPAc in water*

Cyclobutanones were synthesized in moderate-to-good yields and with a high degree of stereo- and regioselectivity by the photolytic reaction between a variety of chromium alkoxycarbene complexes and olefins. The use of iPAc as an olefin afforded the corresponding product in only 16 % yield (Scheme 3.58, top).[197] Better results were achieved using iPAc for the radical cyclization of 4-hydroxycoumarin and for the synthesis of tricyclic ring systems: products were isolated in 54 and 87% yields, respectively (Scheme 3.58, centre and bottom).[198,199]

(CO)$_5$Cr

OMe

hv
Et$_2$O, CO

16%

OH

iPAc, Mn(OAc)$_3$
100 °C

54%

CO$_2$CH$_3$

n-BuSSBu
benzene, hv

87%

CO$_2$CH$_3$

OCOCH$_3$
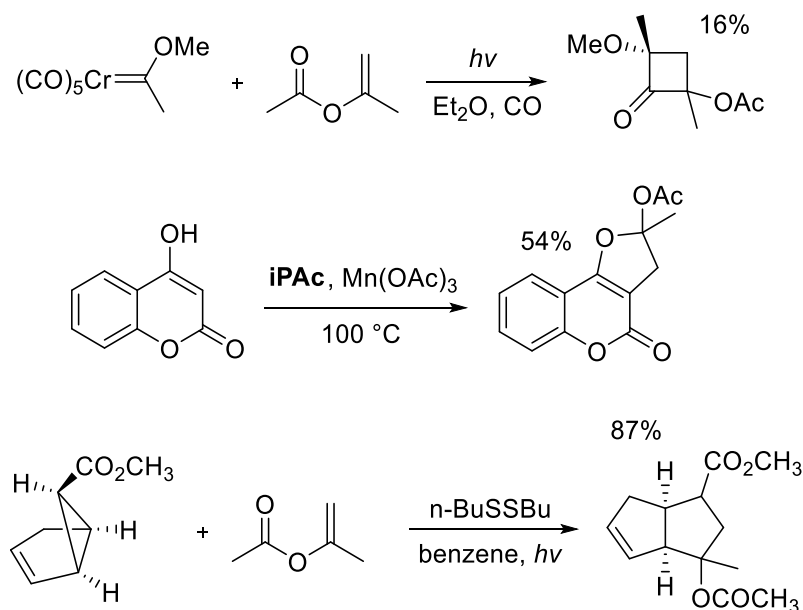
Scheme 3.58. *Photo-induced reactions of iPAc*

3.3.2.10 Metal-free approaches for C-C bond formation

In recent years important efforts have been devoted to implement transition-metal-free arylation protocols.[200] As an effort to exclude the use of transitional metals, metal-free Meerwein arylation was performed under basic catalysis conditions: Molinaro and his coworker described the reaction of diazonium tetrafluoroborate salts and iPAc to synthesize α-aryl methyl ketones (12 examples; yields 13-76%).[201] The C–H arylation of both enol acetates and heteroarenes was also carried out in aqueous medium in the presence of UiO-66 microcrystals as a catalyst without any metal assistance (11 examples; yields 45-67%).[202]

3.3.2.11 Aldol-type reactions

Teruaki *et al.* found that Lewis acids as $TiCl_4$, $AlCl_3$, $SnCl_4$, $ZnCl_2$, and $BF_3 \cdot O(C_2H_5)_2$, effectively catalysed the reaction of enol acetates, including iPAc, with acetals to afford aldol-type addition products in good yields at T = 0-78 °C (6 examples; yields 1-65%; Scheme 3.59, top).[203] The same group reported the crossed aldol reaction of enol esters, as stable carbon nucleophiles, with carbonyl compounds, catalyzed by diethylaluminum ethoxide at 0 °C (10 examples; 56-82% yields; Scheme 3.59, bottom).[204]

MeO R OMe + (enol acetate) →[TiCl₄] 41-81% + 1-65%

(enol acetate) + R X O →[Cat. / 0 °C, THF] R X O / HO   Cat. = Et₂AlOEt

X = H, CH₃
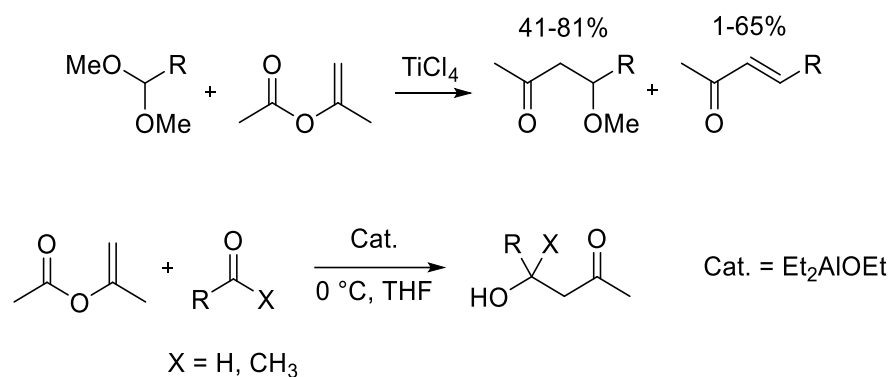
Scheme 3.59. Aldol-type reactions of iPAc

The crossed aldol condensation of enol ester (including iPAc) with aldehydes was effectively promoted by different systems as tetrakys(pentafluorophenyl)borate, a binary mixture of N-chlorosuccinimide (NCS)/$SnCl_2$, and $PdCl_2(PhCN)_2$-$SnCl_2$.[205,206,207] 4-substituted 4-benzyloxybutan-2-ones were achieved as products (11 examples, yields 19-91 %). A Lewis acid reagent derived from NCS/$SnCl_2$ proved active for the synthesis of 2-acetonyl cyclic ethers from lactols and enol acetates.[208]

3.3.2.12 Michael-type additions

Baba et al. reported that the direct Michael addition of enol acetates to α,β-unsaturated ketones was achieved at room temperature using a combination of Lewis acid catalysts, $InCl_3$ and Me_3SiCl, which provided stable enol-form products (Scheme 3.60, a; 12 examples; yields: 15-99%).[209]
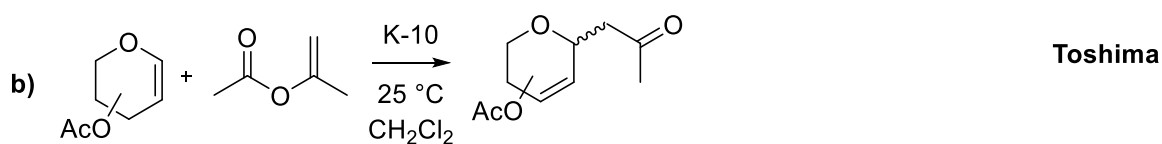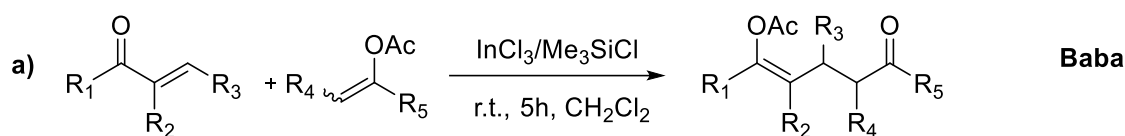
Scheme 3.60. *Michael-type reactivity of iPAc*

Similar to the Michael addition, the C-glycosidations of some glycal acetates with iPAc was carried out over montmorillonite K-10 as a green, inexpensive catalyst under mild conditions (T = 25 °C). 2,3-Unsaturated C-glycosides were obtained in high yields (4 examples; yields 85-97%; Scheme 3.60, b).[210]

3.3.2.13 Claisen-type condensations

1,3-Dioxin-4-ones were prepared from β-ketoacids and iPAc (9 examples; yields 50-82%; Scheme 3.61, top).[211] In accordance with this finding, it was proposed that the acid-catalyzed reaction of diketene with acetone to form 2,2,6-trimethyl-4H-1,3-dioxin-4-one took place *via* a isopropenyl acetoacetate intermediate (Scheme 3.61, bottom).[212] A similar annulation reaction was described by Trost and co-workers, who employed iPAc for the preparation of protected dioxanone derivatives as part of the total synthesis of Amphidinolide P.[213]
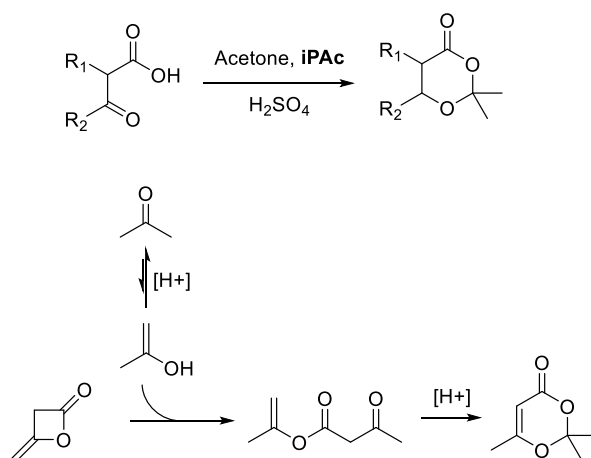
Scheme 3.61. *The synthesis of 1,3-dioxin-4-ones, using iPAc*

The α-alkylation of aldehydes and ketones through the direct use of alcohols and enol acetates was accomplished in the presence of either InI_3, $GaBr_3$, or $FeBr_3$ catalysts (15 examples; yields in the range 40-95%).[214] The same reaction was implemented by Umeda et al., who discovered that when benzylic and allylic alcohols were treated with enol acetate in the presence of a catalytic amount of a rhenium complex, $ReBr(CO)_5$, a C-C bond forming reaction occurred affording ketones and aldehydes in moderate to good yields (14 examples; yields 0-84%).[215]

An efficient procedure was developed for the synthesis of 1-(2-oxopropyl) adamantane by the reaction of 1-bromo(chloro)adamantanes with isopropenyl acetate in the presence of manganese and iron acetoacetates (2 examples; yields 45-90%; Scheme 3.62).[216]
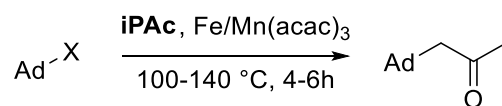
Ad = adamantane
X = halogen

Scheme 3.62. *The Claisen-type reaction of halo-adamantanes with iPAc*

3.3.2.14 Miscellaneous

The last part of this section is devoted to the description of some unusual reactions occurring with iPEs.

A non-classical Grignard reactivity was found using substituted aryl Grignard reagents and iPAc: in a one-step reaction, symmetrical aromatic 1,3-diols were efficiently synthesized forming anti products as the major species (17 examples; yields 20-85%; Scheme 3.63).[217]
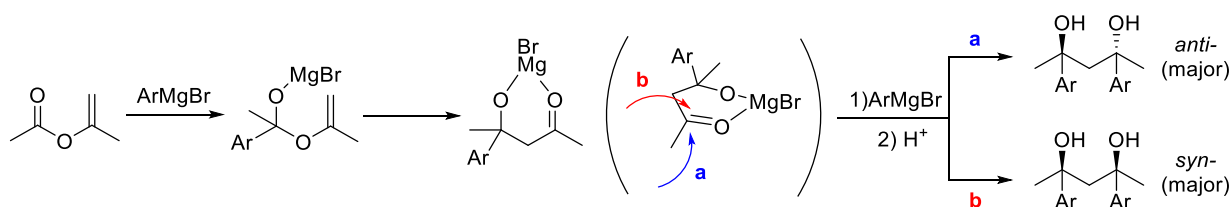
Scheme 3.63. *Non-classical Grignard reaction with iPAc*

The reaction of amidoximes with iPAc in the presence of KSF and under microwave irradiation, gave 1,2,4-oxadiazoles (2 examples; yields 50-67%; Scheme 3.64).[218]
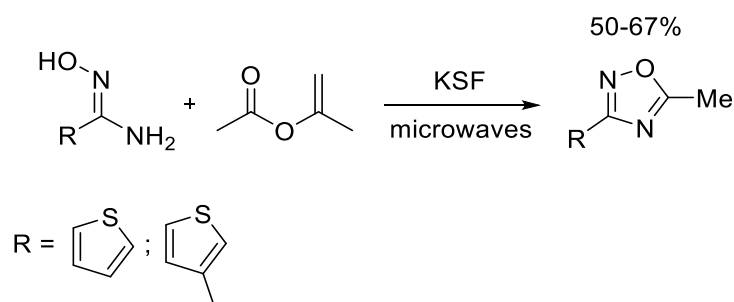
Scheme 3.64. *Synthesis of oxadiazoles with iPAc*

The electrochemical oxidation of triphenylphosphine in the presence of enol esters (including iPAc) yielded 2-oxocycloalkyltriphenylphosphonium salts, which were suitable reagents for the Wittig reaction with aldehydes (Scheme 3.65, top).[219] Similarly, the electrochemical oxidation of 1,3-diketones in the presence of iPAc originated a [3+2] cycloadduct (Scheme 3.65, bottom).[220]

153
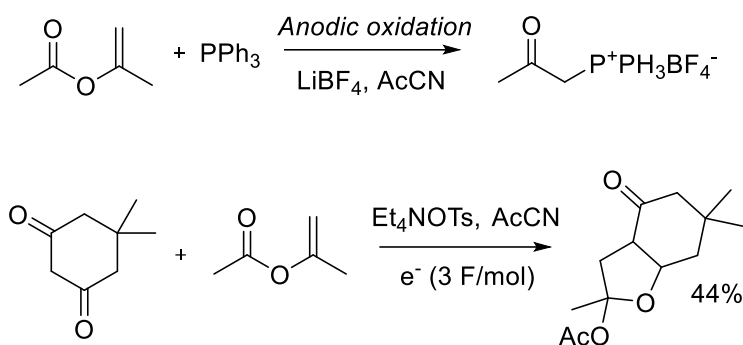
Scheme 3.65. Top: anodic oxidation of triphenylphosphine in the presence of iPAc. Bottom: electrochemical oxidation of 1,3-diketones and 2-substituted 1,3-diketones in the presence of iPAc

Toshimitsu *et al.* investigated the reaction of phenylselenenyl chloride with iPAc in aqueous acetonitrile. A phenyl selenyl derivative was isolated in a 91% yield (Scheme 3.66).[221] With a similar procedure, the reaction of iPAc with Bu$_3$SnOMe afforded a Sn-functionalized product in 89% yield (Scheme 3.66, bottom). [222]
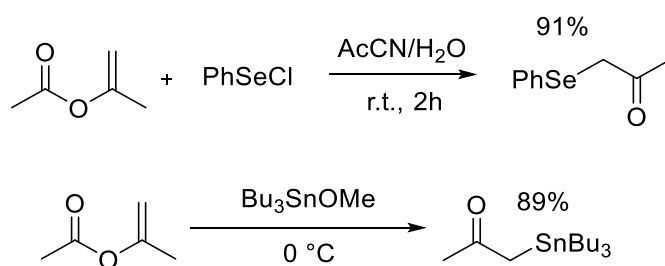
Scheme 3.66. Selenation (top) and stannation (bottom) of iPAc

A peculiar tandem scission-allylation,-alkylation, or -arylation reactions mediated by iPEs was developed for the synthesis of non-natural amino acids as synthetic blocks in peptidomimetics. In the case of iPAc, the corresponding product was obtained in a 75% yield (Scheme 3.67).[223]
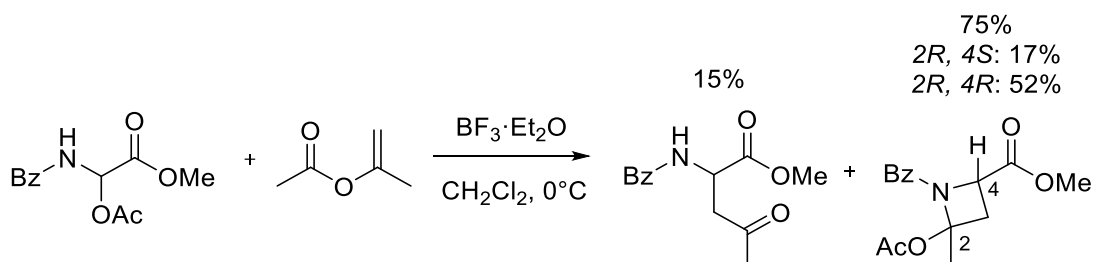
Scheme 3.67. Synthesis of unnatural aminoacids using iPAc

Oshima and co-workers synthesized a cyclopentanes from vinylciclopropanes in 54-77% yields (Scheme 3.68). iPAc was present within the scope of olefins.[224]

R = COOEt, COPh, SO$_2$Ph
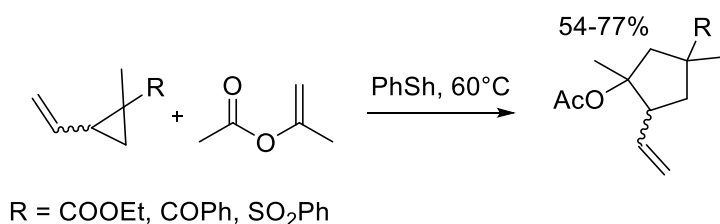
Scheme 3.68. Synthesis of cyclopentanes using iPAc

3.3.2.15 Self-reactions of iPEs catalyzed by AlCl₃

AlCl₃ catalysed the self-reaction of iPEs: i) at 50-100 °C they produced β-diketones with yields of 50-70% (Scheme 3.69, top);[119] the self-reaction of iPAc in refluxing 1,2-dichloroethane formed 3,5-diacetyl-2,6-dimethyl-4*H*-pyran-4-one in 17 % yield (Scheme 3.69, bottom).[225]

Scheme 3.69. *iPEs reactions under AlCl₃ catalysis*
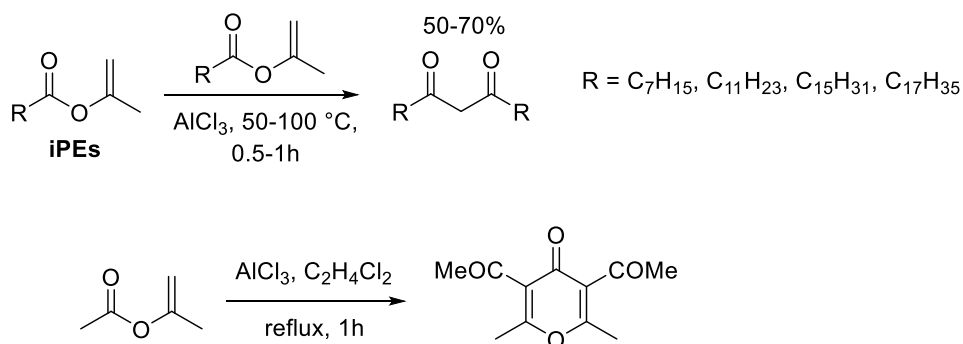
3.3.2.16 Biomass modification

iPEs were employed for the chemical modification of wood, fabrics, cellulose, and lignin. For example, an iPEs-based transesterification protocol was adopted for the preparation of cellulose-based water-repellent fabrics: the free -OH functionalities of cellulose were esterified with isopropenyl stearate.[226] The resulting material was characterized by minor changes in tensile strength with respect to the starting polymer. The transformation was quite challenging using classical esterification reactants/conditions especially because the polymeric structure of cellulose may be severely degraded in the presence of acidic catalysts.[231] iPAc was used for a chemical modification of rubberwood in the presence of anhydrous aluminum chloride as a catalyst.[227] The results of the treatment with respect to UV-light resistance are shown in Figure 3.51. A similar procedure has been reported also using I₂ as the catalyst.[228]
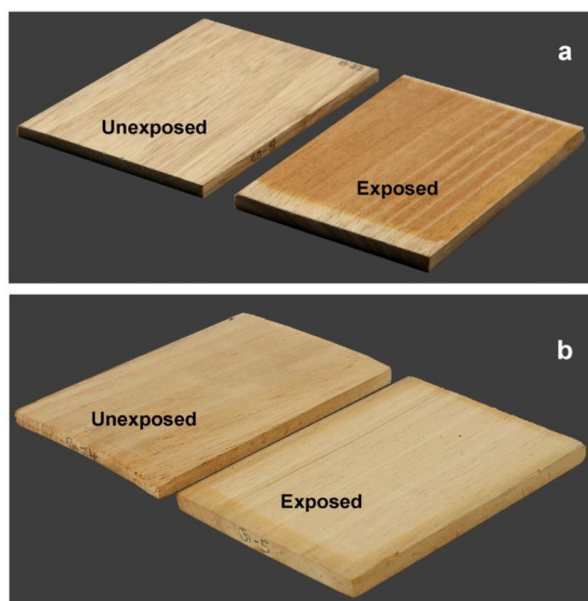
Figure 3.51. *Changes in color of (a) unmodified (upper panel) and (b) IPA modified rubber wood surfaces (lower panel) after 250 h UV light exposure. Left side samples are unexposed and right-side samples are exposed samples. Taken from ref 232.*

More recently Takahashi and co-workers reported a novel protocol for the facile transesterification reaction between cellulose and iPAc without any additional catalysts and corrosive chemicals, using ionic liquids, in particular ethylmethylimidazolium acetate [Emim][OAc] as both a solvent and a catalyst.[229] [Emim][OAc] was active also in the catalysis of the acetylation of lignin with iPAc.[230]

In this case, a one-pot, two-step process was observed during which iPAc first rapidly reacted with aromatic -OH groups (Ar–OH) but slowly with aliphatic ones (R–OH); then, the generated Ar–OAc species were subjected to a gradual deacetylation by heating in the presence of EmimOAc, while the aliphatic acetyl esters (R–OAc) were thermodinamically more stable and persisted as such.[231] In another paper, Takahashi's group proposed a holistic approach for the treatment of sugarcane bagasse. A homogeneous transesterification of the bagasse was carried out at 50 °C using iPAc as the acetyl donor and [Emim][OAc] as a catalyst/solvent. Parallelly, the production of hemicellulose acetate and lignin acetate were achieved by a multi-step precipitation procedure (Figure 3.52).[232]
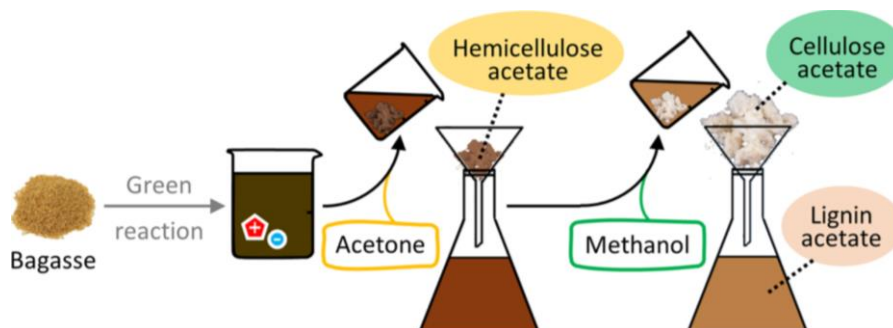
Figure 3.52. *Holistic approach to the acetylation of bagasse derived feedstocks, mediated by iPAc. Taken from Ref 238*

An even more recent work described a controlled acetylation of lignin using iPAc in a DMSO/EmimOAc mixture. A step-by-step increase of the degree of substitution of lignin and a fine-tuning of its thermal characteristics were achieved. This modification of lignin improved its the miscibility of its blends with acrylonitrile.[233] The resulting material was subjected to fabricate electrospun carbonfiber mats whose morphological and mechanical properties changed and could be improved by the tunable functionalization with iPAc.

A bio-catalytic acetylation of various lignin model compounds with iPAc was successfully carried out using carried a CALB catalyst. The reaction was performed in a ball mill and produced fully compounds (8 examples, yields 45-89%; Scheme 3.70).[234]
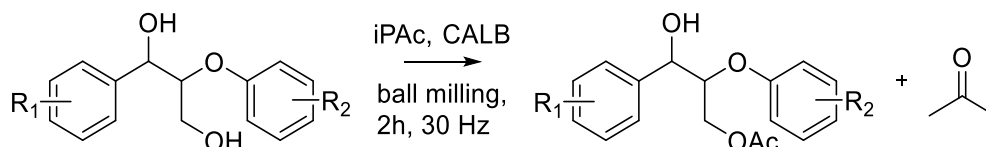
Scheme 3.70. *iPAc-mediated acetylation of lignin model compounds in the ball mill*

References

[1] K. Matsumoto, C. Feng, S. Handa, T. Oguma and T. Katsuki, Asymmetric epoxidation of (Z)-enol esters catalyzed by titanium (salalen) complex with aqueous hydrogen peroxide, *Tetrahedron*, **2011**, *67*, 6474. https://doi.org/10.1016/j.tet.2011.06.022

[2] Y. Kita, H. Maeda, F. Takahashi, and S. Fukui, A convenient synthesis of dicarboxylic monoesters using isopropenyl esters: synthesis of oxaunomycin derivatives, *J. Chem. Soc., Chem. Commun.*, **1993**, 410. https://doi.org/10.1039/C39930000410

[3] F. S. Crossley, E. Miller, W. H. Hartung, and M. L. Moore, Thiobarbitures III. Some N-Substituted Derivatives, *J. Org. Chem.* **1940**, *5*, 238. https://doi.org/10.1021/jo01209a004

[4] T. Gizur and K. Harsanyi, Some Applications of Isopropenyl Acetate To O-, N-and C-Acetylation, *Synthetic Commun.*, **1990**, *20*, 2365. https://doi.org/10.1080/00397919008053182

[5] W. Collins, N. Lowen and D. J. Blake, Caffeic acid esters are effective bactericidal compounds against Paenibacillus larvae by altering intracellular oxidant and antioxidant levels, *Biomolecules*, **2019**, *9*, 312. https://doi.org/10.3390/biom9080312

[6] V. R. Shanbhag, A. M. Crider, R. Gokhale, A. Harpalani and R. M.Dick, Ester and amide prodrugs of ibuprofen and naproxen: synthesis, anti-inflammatory activity, and gastrointestinal toxicity, *J. Pharm. Science*, **1992**, *81*, 149. https://doi.org/10.1002/jps.2600810210

[7] R. E. Murray and D. M. Lincoln, New catalytic route to vinyl esters, *Catal. Today*, **1992**, *13*, 93. https://doi.org/10.1016/0920-5861(92)80189-T

[8] R. Pelagalli, I. Chiarotto, M. Feroci and S. Vecchio, Isopropenyl acetate, a remarkable, cheap and acylating agent of amines under solvent-and catalyst-free conditions: a systematic investigation, *Green Chem.*, **2012**, *14*, 2251. https://doi.org/10.1039/C2GC35485C

[9] HJ Hagemeyer, DC Hull, Reactions of isopropenyl acetate, Ind. Eng. Chem., **1949**, *41*, 2920. https://doi.org/10.1021/ie50480a063

[10] N. Ahmed, J. E. van Lier, Molecular iodine in isopropenyl acetate (IPA): a highly efficient catalyst for the acetylation of alcohols, amines and phenols under solvent free conditions, *Tetrahedron Lett.*, **2006**, *47*, 5345. https://doi.org/10.1016/j.tetlet.2006.05.122

[11] R. Miller, C. Abaecherli, A. Sais and B. Jackson, Ketenes in *Ullmann's Encyclopedia of Industrial Chemistry*, Wiley, New York, 2012; Vol. 20; p. 171-185.

[12] Quzhou Xinbu Chemical Technology Co Ltd; Yan, zhaochun CN105777540, 2016, Location in patent: Paragraph 0050-0055

[13] M. Sauer, Industrial production of acetone and butanol by fermentation—100 years later, *FEMS Microbiol. Lett.*, **2016**, *363*, 134. https://doi.org/10.1093/femsle/fnw134

[14] G. Krüss, Liebigs Annalen der Chemie, **1894**, *283*, 381.

[15] B. H. Gwynn and E. F. Degering, Condensation Products of Ketene with Ketones, *J. Am. Chem. Soc.*, **1942**, *64*, 2217. https://doi.org/10.1021/ja01261a051

[16] Y. Yamashita, S. Miura and M. Nakamura, Ambident nature of the polydimethylketene anion, *Macromol. Chem.*, **1963**, *68*, 31. https://doi.org/10.1002/macp.1963.020680104

[17] L. M. Bairgrie, R. Leung-Toung and T. T. Tidwell, Oxygen and carbon-acylation of enolates by ketenes, *Tetrahedron Lett.*, **1988**, *29*, 1673. https://doi.org/10.1016/S0040-4039(00)82014-6

[18] R. J. Clemens and J. Stewart Witzeman, Kinetic and spectroscopic studies on the thermal decomposition of 2, 2, 6-trimethyl-4H-1, 3-dioxin-4-one. Generation of acetylketene, *J. Am. Chem. Soc.*, **1989**, *111*, 2186. https://doi.org/10.1021/ja00188a037

[19] Y. Kita, H. Maeda, F. Takahashi and S. Fukui, Convenient synthesis of alcohol O-hemiesters using isopropenyl esters as acylating reagents: synthesis of hydrophilic oxaunomycin 10-O-hemiester derivatives, *J. Chem. Soc. Perk. T. 1*, **1993**, *21*, 2639. https://doi.org/10.1039/P19930002639

[21] a) G. Meunier, P. Hemery, J-P. Senet and S. Boileau, Polymerization and copolymerization of vinyl carbamates and vinyl carbonates, *Polymer Bull.*, **1981**, *4*, 705. https://doi.org/10.1007/BF00285137; b) S. Boivin, A. Chettouf, P. Hemery and S. Boileau, Polymérisation du chloroformiate de vinyle et de ses dérivés, *Polym. Bull.*, **1983**, *9*, 114. https://doi.org/10.1139/v85-227; c) G. Meunier, P. Hemery, S. Bofleau, J-P. Senet and H. Cheyaclan, Poly (vinyl chloroformate) and derivatives: 1. Polymerization of vinyl chloroformate, vinyl carbamates and vinyl carbonates, *Polymer*, **1982**, *23*, 849. https://doi.org/10.1016/0032-3861(82)90145-8; d) G. Meunier, S. Boivin, P. Hemery, S. Boileau and J-P. Senet, Poly (vinyl chloroformate) and derivatives: 3. Chemical modification of poly (vinyl chloroformate), *Polymer*, **1982**, *23*, 861. https://doi.org/10.1016/0032-3861(82)90147-1; e) S. Boileau, F. Kassir, S. Boivin, H. Cheradame, G. P. Wooden and R. A. Olofson, Poly (vinyl chloroformate) and its derivatives: 5. New poly

(vinyl carbamates) and poly (vinyl thiocarbonates), *Polymer*, **1985**, *26*, 443. https://doi.org/10.1016/0032-3861(85)90209-5

[22] a) H. O. House, Modern Synthetic Reactions. 2nd ed., 1972, 492-570; b) W.A. Benjamin Inc. and T. H. Black, *Org. Prep. Proc. Int.*, **1989**, *21*, 179.

[23] R. A. Olofson, V. A. Dang, D. S. Morrison and P. F. de Cusati, Simple one-step preparations of vinylic carbonates from aldehydes, *J. Org. Chem.*, **1990**, *55*, 1. https://doi.org/10.1021/jo00288a001

[24] R. A. Olofson and J. Cuomo, A regiospecific and stereospecific route to enol carbonates and carbamates: closer look at a "naked anion, *Tetrahedron Lett.*, **1980**, *21*, 819. https://doi.org/10.1016/S0040-4039(00)71514-0

[25] P. F. de Cusati and R. A. Olofson, A simple synthesis of 1-(1, 3-butadienyl) carbonates and carbamates, *Tetrahedron Lett.*, **1990**, *31*, 1405. https://doi.org/10.1016/S0040-4039(00)88817-6

[26] L. M. Harwood, Y. Houminer, A. Manage and J. I. Seeman, Efficient preparation of enol carbonates by selective O-acylation of ketone sodium enolates generated in the presence of TMEDA, *Tetrahedron Lett.*, **1994**, *35*, 8027. https://doi.org/10.1016/0040-4039(94)80040-5

[27] Y. Tamura, J. Haruta, S. Okuyama and Y. Kita, Preparation and reactions of alkyl and aryl isopropenyl carbonatesnovel alkoxy-and aryloxycarbonylations of amines, *Tetrahedron Lett.*, **1978**, *39*, 3737. https://doi.org/10.1016/S0040-4039(01)95045-2

[28] E. S. Rothman, S. Serota, T. Perlstein and D. Swern, Acid-Catalyzed Interchange Reactions of Carboxylic Acids with Enol Esters, *J. Org. Chem.*, **1962**, *27*, 3123. https://doi.org/10.1021/jo01056a033

[29] B. Phillips, Jr., U. S. Patent 2.466.738, April 12, 1949.

[30] Y. F. Wang, J. J. Lalonde, M. Momongan, D. E. Bergbreiter and C. H. Wong, sters as Acylating Reagents: Preparative Enantio- and Regioselective Syntheses of Alcohols, Glycerol Derivatives, Sugars, and Organometallics, *J. Am. Chem. Soc.*, **1988**, *110*, 7200. https://doi.org/10.1021/ja00229a041

[31] W. O. Herrmann and W. Haehnel, U. S. Patent, 2, 245, 131.

[32] R. L. Adelman, The interchange reaction of vinyl acetate with organic acids, *J. Org. Chem.*, **1949**, *14*, 1057. https://doi.org/10.1021/jo01158a015

[33] E. S. Rothman, S. Serota and D. Swern, Enol Esters. III.1 Preparation of Diisopropenyl Esters of Dicarboxylic Acids, *J. Org. Chem.*, **1966**, *31*, 629. https://doi.org/10.1021/jo01340a529

[34] P. M. Henry, Palladium (II)-Catalyzed Exchange and Isomerization Reactions. VII. Isomerization and Exchange of Enol Propionates in Acetic Acid Catalyzed by Palladium (II) Chloride, *J. Am. Chem. Soc.*, **1972**, *94*, 7316. https://doi.org/10.1021/ja00776a602

[35] H. Hopff and M. A. Osman, The vinyl interchange reaction: I—Vinyl acetate with carboxylic acids stronger than acetic acid, *Tetrahedron*, **1968**, *24*, 2205. https://doi.org/10.1016/0040-4020(68)88123-2

[36] B. Y. Park, T. L. Hiroki, S. Michael and J. Krische, A Metallacycle Fragmentation Strategy for Vinyl Transfer from Enol Carboxylates to Secondary Alcohol C–H Bonds via Osmium- or Ruthenium-Catalyzed Transfer Hydrogenation, *J. Am. Chem. Soc.*, **2015**, *137*, 7652. https://doi.org/10.1021/jacs.5b04688

[37] a) R. E. Murray, U.S. Patent 005155253A, 1991; b) R. E. Murray, European Patent EP O0506070A2, 1992; c) R. E. Murray, European Patent EPO0351603A2, 1989.

[38] J. Ziriakus T. K. Zimmermann, A. Pöthig, M. Drees, S. Haslinger, D. Jantke and F. E. Kühn, Ruthenium-Catalyzed Transvinylation–New Insights, *Adv. Synth. Catal.*, **2013**, *355*, 2845. https://doi.org/10.1002/adsc.201300447

[39] a) A. L. Henne, J. W. Shepard and E. J. Young, Conversion of Ketone Enol Esters to β-Diketones by Intramolecular Thermal Rearrangement and by Intermolecular Acylations using Boron Fluoride, *J. Am. Chem. Soc.*, **1950**, *72*, 3635. https://doi.org/10.1021/ja01164a088; b) W. M. Muir, P. D. Ritchie and D. J. Lyman, Acylation. I. The Mechanisms of Enol Ester and 1, 3-Diketone Formation in the Reaction of Ketone—Enol Systems with Acyl Halides, *J. Org. Chem.*, **1966**, *31*, 3790. https://doi.org/10.1021/jo01349a070

[40] L. Steemers and J. H. van Maarseveen, Stereoselective C-terminal peptide elongation from Chan–Lam–Evans reaction generated isopropenyl esters, *Org. Biomol. Chem.*, **2019**, 17, 2103. https://doi.org/10.1039/C8OB02102C

[41] J. C. Vantourout, H. N. Miras, A. Isidro-Llobet, S. Sproules, and A. J. B. Watson, A.J.B., Spectroscopic studies of the Chan–Lam amination: a mechanism-inspired solution to boronic ester reactivity, *J. Am. Chem. Soc.*, **2017**, *139*, 4769. https://doi.org/10.1021/jacs.6b12800

[42] G. F. Hennion, D. B. Killian, T. H. Vaughn and J. A. Nieuwland, Condensation of alkyl acetylenes with oxy compounds, *J. Am. Chem. Soc.,* **1934**, *56*, 1130. https://doi.org/10.1021/ja01320a039

[43] G. F. Hennion and J. A. Nieuwland, The Addition of Some Organic Acids to Alkyl Acetylenes, *J. Am. Chem. Soc.*, **1934**, *56*, 1802. https://doi.org/10.1021/ja01323a047

[44] E. S. Rothman and S. Serota, Enol esters XIII: Synthesis of isopropenyl esters by addition of carboxylic acids to propyne, *J. Am. Oil Chem. Soc.*, **1971**, *48*, 373. https://doi.org/10.1007/BF02637352

[45] J. C. Craig, M. F. Kozempel, H. I. Sinnamon, M. J. Calhoun, and W. K. Heiland, Development of a continuous process for enol esters of fatty acids, *J Am Oil Chem Soc,* 1977, *54*, 24. https://doi.org/10.1007/BF02671368

[46] M. Rotem and Y. Shvo, Addition of carboxylic acids to alkynes catalyzed by ruthenium complexes. Vinyl ester formation, *Organometallics*, **1983**, *2*, 1689. https://doi.org/10.1021/om50005a037

[47] T. Mitsudo, Y. Hori, Y. Yamakawa and Y. Watanabe, Ruthenium-catalyzed selective addition of carboxylic acids to alkynes. A novel synthesis of enol esters, *J. Org. Chem.*, **1987**, *52*, 2230. https://doi.org/10.1021/jo00387a024

[48] a) C. Ruppin and P. H. Dixneuf, Synthesis of enol esters from terminal alkynes catalyzed by ruthenium complexes, *Tetrahedron Lett.*, **1986**, *27*, 6323. https://doi.org/10.1016/S0040-4039(00)87798-9 b) C. Bruneau, M. Neveux, Z. Kabouche, C. Ruppin and P. H. Dixneuf, Ruthenium-catalysed additions to alkynes: synthesis of activated esters and their use in acylation reactions, *Synlett.*, **1991**, *11*, 755. https://doi.org/10.1055/s-1991-20866

[49] M. Neveux, B. Seiller, F. Hagedorn, C. Bruneau and P. H. Dimeuf, Novel ruthenium-catalyzed synthesis of 1, 3-dioxolan-4-ones from α-hydroxy acids and terminal alkynes via enol esters, *J. Organometallic Chem.*, **1993**, *451*, 133. https://doi.org/10.1016/0022-328X(93)83017-P

[50] C. Ruppin, P. H. Dixneuf and S. Lecolier, Regioselective synthesis of isopropenyl esters by ruthenium catalysed addition of N-protected amino-acids to propyne, *Tetrahedron Lett.*, **1988**, *29*, 5365. https://doi.org/10.1016/S0040-4039(00)82869-5

[51] L. J. Goossen, J. Paetzolda and D. Koleya, Regiocontrolled Ru-catalyzed addition of carboxylic acids to alkynes: practical protocols for the synthesis of vinyl esters, *Chem. Commun.*, **2003**, *6*, 706. https://doi.org/10.1039/B211277A

[52] I. Emmea, C. Bruneaub, P. H. Dixneuf, H-C. Militzera and A. de Meijere, Ruthenium-catalyzed transformations of cyclopropylethynes, *Synthesis*, **2007**, *22*, 3574. https://doi.org/10.1055/s-2007-990874

[53] M. P. Matuszak. The Action of Phosgene on Acetone, *J. Am. Chem. Soc.*, **1934**, *56*, 1934. https://doi.org/10.1021/ja01324a504

[54] a) M. Jaouadi, C. Selve, J. R. Dormoy, B. Castro and J. Martinez, Le chloroformiate d'isopropenyle (ipcf) en chimie des amino-acides et des peptides-iii synthese d'esters actifs d'amino acides n-proteges, *Tetrahedron Lett.*, **1985**, *26*, 1721. https://doi.org/10.1016/S0040-4039(00)98321-7 b) C. Zeggaf, J. Poncet, P. Jouin, M-N. Dufour and B. Castro, Isopropenyl chlorocarbonate (IPCC)1 in amino acid and peptide chemistry: Esterification of N-protected amino acids; Application to the synthesis of the depsipeptide valinomycin, *Tetrahedron*, **1989**, *45*, 5039. https://doi.org/10.1016/S0040-4020(01)81083-8

[55] K. Takeda, A. Ayabe, M. Suzuki, Y. Konda and Y. Harigaya, An improved method for the synthesis of active esters of N-protected amino acids and subsequent synthesis of dipeptides, *Synthesis*, **1991**, *9*, 689. https://doi.org/10.1055/s-1991-26545

[56] K. Takeda, A. Akiyama, Y. Konda, H. Takayanagi and Y. Harigaya, Allyl Isopropenyl Dicarbonate; a convenient reagent for the preparation of allyl esters of carboxylic acids, *Tetrahedron Lett.*, **1995**, *36*, 113. https://doi.org/10.1016/0040-4039(94)02179-F

[57] A. Marra, J. Esnault, A. Veyrieres and P. Sinay, Isopropenyl glycosides and congeners as novel classes of glycosyl donors: theme and variations, *J. Am. Chem. Soc.*, **1992**, *114*, 6354. https://doi.org/10.1021/ja00042a010

[58] F. Sanda, T. Abe, and T. Endo, Syntheses and radical polymerizations of novel optically active vinyl and isopropenyl carbamates having L-leucine structures, *Polymer Chem.*, **1996**, *34*, 1969. https://doi.org/10.1002/(SICI)1099-0518(19960730)34:10<1969::AID-POLA15>3.0.CO;2-G

[59] I. Gallou, M. Eriksson, X. Zeng, C. Senanayake and V. Farina, Practical synthesis of unsymmetrical ureas from isopropenyl carbamates, *J. Org. Chem.*, **2005**, *70*, 6960. https://doi.org/10.1021/jo0507643

[60] A. C. Cope and E. M. Hancock, The introduction of substituted vinyl groups I Isopropenyl alkyl malonic esters, *J. Am. Chem. Soc.*, **1938**, *60*, 2644. https://doi.org/10.1021/ja01278a028

[61] A. C. Cope and E. M. Hancock, Substituted vinyl barbituric acids. I. Isopropenyl derivatives, *J. Am. Chem. Soc.*, **1939**, *61*, 96. https://doi.org/10.1021/ja01870a031

[62] G. L. Larson, V. C. Maldonado, L. M. Fuentes, L. E. Torres, The chemistry of. alpha.-silyl carbonyl compounds. 17. Methyldiphenylsilylation of ester and lactone enolates, *J. Org. Chem.*, **1988**, *53*, 633. https://doi.org/10.1021/jo00238a029

[63] B. M. Trost, J. P. N. Papillon and T. Nussbaumer, Ru-catalyzed alkene– alkyne coupling. Total synthesis of amphidinolide P, *J. Am. Chem. Soc.*, **2005**, *127*, 17921. https://doi.org/10.1021/ja055967n

[64] Y. Dai, C. Xie, H. Mei, J. Han, V. A. Soloshonok and Y. Pan, Asymmetric synthesis of β-trifluoromethyl-β-amino acids, including highly sterically constrained α, α-dialkyl derivatives, *Tetrahedron*, **2015**, *71*, 9550. https://doi.org/10.1016/j.tet.2015.10.071

[65] https://dir.indiamart.com/impcat/carboxylic-acid.html (accessed 12/11/2021)

[66] https://www.chemicalbook.com/ProductList_En.aspx?kwd=Isopropenyl%20acetate&gclid=CjwKCAiAvriMBhAuEiwA8Cs5lUzp-u-pmS3Cn2Uh8pEgrzM7QM8qK9YYA6fhu-5fc9yGHS6a48c9rBoCA0cQAvD_BwE (accessed 12/11/2021)

[67] (a) Green, T. W.; Wuts, P. G. M. Protective Groups in Organic Synthesis, 3rd ed.; Wiley: New York, 1999; (b) Larock, R. C. In Comprehensive Organic Transformations; VCH: New York, 1989; p 980; (c) P. N. Rao, J. W. Cessac, T. L. Tinley, S. L. Mooberry, Synthesis and antimitotic activity of novel 2-methoxyestradiol analogs, *Steroids*, **2002**, *67*, 1079. https://doi.org/10.1016/S0039-128X(02)00066-1

[68] a) Y. Ishii, M. Takeno, Y. Kawasaki, A, Muromachi, Y. Nishiyama and S. Sakaguchi, Acylation of Alcohols and Amines with Vinyl Acetates Catalyzed by Cp*2Sm(thf)2, *J. Org. Chem.*, **1996**, *61*, 3088. https://doi.org/10.1021/jo952168m; b) X. Zhu, B. Qian, R. Wei, J-D. Huang and H. Bao, Protection of COOH and OH groups in acid, base and salt free reactions, *Green Chem.*, **2018**, *20*, 1444. https://doi.org/10.1039/C8GC00037A;; d) A. Temperini, L. Minuti, T. Morini, O. Rosati and F. Piazzolla, Isopropenyl acetate: A cheap and general acylating agent of alcohols under metal-free conditions, *Tetrahedron Lett.*, **2017**, *58*, 4051. https://doi.org/10.1016/j.tetlet.2017.09.007; e) T. Zeng, G. Song and C-J. Li, Separation, recovery and reuse of N-heterocyclic carbene catalysts in transesterification reactions, *Chem. Commun.*, **2009**, 6249. https://doi.org/10.1039/B910162D; f) X. Yang and V. B. Birman, Acyl transfer catalysis with 1, 2, 4-triazole anion, *Org. Lett.*, **2009**, *11*, 1499. https://doi.org/10.1021/ol900098q.

[69] S. Kamal, S. Mahajani, Kinetic study for oligomerization of acetaldehyde over cation exchange resin, *Applied Cat. A: general*, **2020**, *608*, 117841. https://doi.org/10.1016/j.apcata.2020.117841

[70] R. P. V. Faria, C. S. M. Pereira, V. M. T. M. Silva, J. M. Loureiro, and A. E. Rodrigues, Glycerol valorization as biofuel: thermodynamic and kinetic study of the acetalization of glycerol with acetaldehyde *Ind. Eng. Chem. Res.* **2013**, *52*, 1538. https://doi.org/10.1021/ie302935w

[71] E. S. Rothman, S. S. Hecht, P. E. Pfeffer and L. S. Silbert, Enol esters. XV. Synthesis of highly hindered esters via isopropenyl ester intermediates, *J. Org. Chem.*, **1972**, *37*, 3551. https://doi.org/10.1021/jo00795a041

[72] D. Tashiro, Y. Kawasaki, S. Sakaguchi and Y. Ishii, An Efficient Acylation of Tertiary Alcohols with Isopropenyl Acetate Mediated by an Oxime Ester and Cp*2Sm(thf)2, *J. Org. Chem.*, **1997**, *62*, 8141. https://doi.org/10.1021/jo971204+

[73] N. Ahmed and J. E. van Lier, Molecular iodine in isopropenyl acetate (IPA): a highly efficient catalyst for the acetylation of alcohols, amines and phenols under solvent free conditions, *Tetrahedron Lett.*, **2006**, *47*, 5345. https://doi.org/10.1016/j.tetlet.2006.05.122

[74] A. Kamal, M. Naseer, A. Khan, K. Srinivasa Reddy, Y. V. V. Srikanth and T. Krishnaji, Al (OTf) 3 as a highly efficient catalyst for the rapid acetylation of alcohols, phenols and thiophenols under solvent-free conditions, *Tetrahedron Lett.*, **2007**, *48*, 3813. https://doi.org/10.1016/j.tetlet.2007.03.162

[75] A. Orita, K. Sakamoto, Y. Hamada, A. Mltsutome and J. Otera, Mild and practical acylation of alcohols with esters or acetic anhydride under distannoxane catalysis, *Tetrahedron*, **1999**, *55*, 2899. https://doi.org/10.1016/S0040-4020(99)00072-1

[76] M-H. Lin and T. V. RajanBabu, Metal-Catalyzed Acyl Transfer Reactions of Enol Esters: Role of Y5(OiPr)13O and (thd)2Y(OiPr) as Transesterification Catalysts, *Org. Lett.*, **2000**, *2*, 997. https://doi.org/10.1021/ol0057131

[77] I. Chiarotto, M. Feroci, G. Sotgiu and A. Inesi, Electrogenerated N-Heterocyclic Carbenes in the Room Temperature Parent Ionic Liquid as an Efficient Medium for Transesterification/Acylation Reactions, *Eur. J. Org. Chem.*, **2013**, 326. https://doi.org/10.1002/ejoc.201201023

[78] I. Chiarotto, Tetraethylammonium hydrogen carbonate: A cheap, efficient, and recyclable catalyst for transesterification reactions under solvent-free conditions, *Synth. Commun.*, **2016**, *46*, 1840. https://doi.org/10.1080/00397911.2016.1233343

[79] G. A. Grasa, T. Guveli, R. Singh and S. P. Nolan, Efficient Transesterification/Acylation Reactions Mediated by N-Heterocyclic Carbene Catalysts, *J. Org. Chem.*, **2003**, *68*, 2812. https://doi.org/10.1021/jo0267551

[80] J. Barry, G. Bram and A. Petit, Organic syntheses without solvent: Base-catalysed ester interchange, *Tetrahedron Lett.*, **1988**, *29*, 4567. https://doi.org/10.1016/S0040-4039(00)80548-1

[81] R. Calmanti, M. Galvan, E. Amadio, A. Perosa, and M. Selva, High-temperature batch and continuous-flow transesterification of alkyl and enol esters with glycerol and its acetal derivatives, *ACS Sustainable Chem. Eng.,* **2018**, *6*, 3964. https://doi.org/10.1021/acssuschemeng.7b04297

[82] R. G. Bistline Jr., E. S. Rothman, S. Serota, A. J. Stirton, A. N. Wrigley, Surface active agents from isopropenyl esters: acylation of isethionic acid and n-methyltaurine, *J. Am. Oil Chem. Soc*., **1971**, *48*, 657. https://doi.org/10.1007/BF02638512

[83] M-J. Kim, W. J. Hennen, H. M. Sweers and C-H. Wong, Enzymes in carbohydrate synthesis: N-acetylneuraminic acid aldolase catalyzed reactions and preparation of N-acetyl-2-deoxy-D-neuraminic acid derivatives, *J. Am. Chem. Soc.*, **1988**, *110*, 6481. https://doi.org/10.1021/ja00227a031

[84] a) M. M. Green, C. Andreola, B. Muñoz, M. P. Reidy, and K. Zero, Macromolecular stereochemistry: a cooperative deuterium isotope effect leading to a large optical rotation, *J. Am. Chem. Soc.,* **1988**, *110*, 4063. https://doi.org/10.1021/ja00220a070; b) C. Collet, F. Chrétien, Y. Chapleur and S. Lamandé-Langle,

Diasteroselective synthesis of new O-alkylated and C-branched inositols and their corresponding fluoro analogues, *Beilstein J. Org. Chem.*, **2016**, *12*, 353. https://doi.org/10.3762/bjoc.12.39

[85] M. Giordano, A. Iadonisi and A. Pastore, Solvent-free synthesis of glycosyl chlorides based on the triphenyl phosphine/hexachloroacetone system, *Eur. J. Org. Chem.*, **2013**, 3137. https://doi.org/10.1016/j.tetlet.2017.03.068

[86] R. S. Ward, Dynamic kinetic resolution, *Tetrahedron-Asymm.,* **1995**, *6*, 1475. https://doi.org/10.1016/0957-4166(95)00179-S

[87] P. Jouin, B. Castro, C. Zeggaf, A. Pantaloni, J. P. Senet, S. Lecolier, and G. Sennyey, Convenient one-pot esterification of N-protected aminoacids via isopropenyl chloroformate activation, *Tetrahedron Lett.,* **1987**, *28*, 1661. https://doi.org/10.1016/S0040-4039(00)95387-5

[88] P. Jouin, J. Poncet, M-N. Dufour, A. Pantaloni and B. Castro, Synthesis of the cyclodepsipeptide nordidemnin B, a cytotoxic minor product isolated from the sea tunicate Trididemnum cyanophorum, *J. Org. Chem.*, **1989**, *54*, 617. https://doi.org/10.1021/jo00264a022

[89] B. Li and R. W. Franck, Facile synthesis of N-protected γ and δ-Amino-β-Keto-esters, *Bioorg. Med. Chem. Lett.*, **1999**, *9*, 2629. https://doi.org/10.1016/S0960-894X(99)00449-7

[90] H. O. House and B. M. Trost, The Chemistry of Carbanions. X. The Selective Alkylation of Unsymmetrical Ketones, *J. Org. Chem.,* **1965**, *30*, 2502. https://doi.org/10.1021/jo01019a003

[91] G. Wang and M. Cushman, A Convenient Method for the Conversion of α-Tetralones to Aryl Acetates, *Synthetic Commun.*, **1991**, *21*, 989. https://doi.org/10.1080/00397919108019787

[92] S. Buksha, G. S. Coumbarides, M. Dingjan, J. Eames, M. J. Suggate and N. Weerasooriya, Investigations into the C-deuteriation of enol acetates derived from aryl alkyl ketones, *J. Label Compd. Radiopharm.*, **2005**, *48*, 337. https://doi.org/10.1002/jlcr.928

[93] J. Eames, G. S. Coumbarides, M. J. Suggate, and N. Weerasooriya, Investigations into the regioselective C-deuteration of acyclic and exocyclic enolates, *European J. Org. Chem.*, **2003**, *4*, 634. https://doi.org/10.1002/ejoc.200390103

[94] R. B. Moffett and D. I. Weisblat, Δ20(21)-Steroid Enol Acetates1, *J. Am. Chem. Soc.*, **1952**, *74*, 2183. https://doi.org/10.1021/ja01129a010

[95] Y. Kawasaki, A. Fujii, Y. Nakano, S. Sakaguchi, and Y. Ishii, Acetylcyanation of aldehydes with acetone cyanohydrin and isopropenyl acetate by Cp*2Sm(thf)2, *J. Org. Chem.*, **1999**, *64*, no. 11, 4214. https://doi.org/10.1021/jo990030o

[96] Y. Nakano, S. Sakaguchi, and Y. Ishii, Meerwein-Ponndorf-Verley-type reductive acetylation of carbonyl compounds to acetates by lanthanide complexes in the presence of isopropenyl acetate, *Tetrahedron Lett.*, **2000**, *41*, 1565. https://doi.org/10.1016/S0040-4039(00)00012-5

[97] T. Shono, I. Nishiguchi, T. Komamura, and M. Sasaki, Novel Synthesis of α-Methylene Carbonyl Compounds, *J. Am. Chem. Soc.*, **1979**, *101*, 984. https://doi.org/10.1021/ja00498a031

[98] E. H. Man, F. C. Frostick, and C. R. Hauser, Proportions of Isomeric Ketone Enol Acetates from O-Acetylations of Methyl-methylene Ketones with Isopropenyl Acetate, *J. Am. Chem. Soc.*, **1952**, *74*, 3228. https://doi.org/10.1021/ja01133a007

[99] P. A. Jacobi and J. I. Kravitz, Enynones in organic synthesis. III. A novel synthesis of phenols, *Tetrahedron Lett.*, **1988**, *29*, 6873. https://doi.org/10.1016/S0040-4039(00)88463-4

[100] L. Minuti, F. Piazzolla, and A. Temperini, High-Pressure-Promoted Multicomponent and Metal-Free Synthesis of Polyfunctionalized Biaryls, *European J. Org. Chem.*, **2017**, *2017*, 5370. https://doi.org/10.1002/ejoc.201700898

[101] J. A. Durden Jr. and D. L. Heywood, Reaction of" activated" esters with amidoximes. Convenient synthesis of 1, 2, 4-oxadiazoles, *J. Org. Chem.*, **1971**, *36*, 1306. https://doi.org/10.1021/jo00808a034

[102] B. K. Liu, Q. Wu, D. S. Lv, X. Z. Chen, and X. F. Lin, New view of acylase promiscuity: An extended study on the acylase-catalyzed Markovnikov addition, *J. Mol. Catal. B Enzym.*, **2011**, *73*, 85. https://doi.org/10.1016/j.molcatb.2011.08.002

[103] E. J. Corey and A. K. Ghosh, Mn(III)-promoted annulation of enol ethers and esters to fused or spiro 2-cyclopentenones, *Tetrahedron Lett.*, **1987**, *28*, 175. https://doi.org/10.1016/S0040-4039(00)95679-X

[104] a) W. B. Jensen, The Lewis acid-base definitions: a status report, *Chem. Rev.*, **1978**, *78*, 1. https://doi.org/10.1021/cr60311a002; b) S. E. Denmark and G. L. Beutner, Lewis base catalysis in organic synthesis, *Angew. Chem., Int. Ed.*, **2008**, *47*, 1560. https://doi.org/10.1002/anie.200604943

[105] E. S. Rothman, S. Serota and D. Swern, Enol Esters. II. N-Acylation of Amides and Imides, *J. Org. Chem.*, **1964**, *29*, 646. https://doi.org/10.1021/jo01026a031

[106] J. B. Jones and J. M. Young, Carcinogenicity of lactones. The reactions of unsaturated. Gamma-lactones with l-cysteine, *J. Med. Chem.*, **1968**, *11*, 1176. https://doi.org/10.1021/jm00312a017

[107] A. Alalla, M. Merabet-Khelassi, L. Aribi-Zouioueche, and O. Riant, Green synthesis of benzamides in solvent- and activation-free conditions, *Synth. Commun.*, **2014**, *44*, 2364. https//doi.org/10.1080/00397911.2014.898072

[108] Y. Takaoka, T. Kajimoto and C-H. Wong, Inhibition of N-acetylglucosaminyl transfer enzymes: chemical-enzymic synthesis of new five-membered acetamido azasugars, *J. Org. Chem.*, **1993**, *58*, 4809. https://doi.org/10.1021/jo00070a013

[109] a) I. I. Gill, J. Das and R. N. Patel, Enantioselective enzymatic acylation of 1-(3'-bromophenyl)ethylamine, *Tetrahedron Asymm.*, **2007**, *18*, 1330. https://doi.org/10.1016/j.tetasy.2007.05.039; b) B. G. Vaz, C. D. F. Milagre, M. N. Eberlin, and H. M. S. Milagre, Shvo's catalyst in chemoenzymatic dynamic kinetic resolution of amines-inner or outer sphere mechanism?, *Org. Biomol. Chem.*, **2013**, *11*, 6695. https://doi.org/10.1039/c3ob41318g; c) Y. Zhang, F. Cheng, H. Yan, J. Zheng, and Z. Wang, The enzymatic resolution of 1-(4-chlorophenyl)ethylamine by Novozym 435 to prepare a novel triazolopyrimidine herbicide, *Chirality*, **2018**, *30*, 1225. https://doi.org/10.1002/chir.23016; d) M. Pérez-Venegas, M. M. Tellez-Cruz, O. Solorza-Feria, A. López-Munguía, E. Castillo, and E. Juaristi, Thermal and Mechanical Stability of Immobilized Candida antarctica Lipase B: an Approximation to Mechanochemical Energetics in Enzyme Catalysis., *ChemCatChem*, **2020**, *12*, 803. https://doi.org/10.1002/cctc.201901714

[110] A. Zadło-Dobrowolska, N. G. Schmidt, and W. Kroutil, Promiscuous activity of C-acyltransferase from: Pseudomonas protegens: Synthesis of acetanilides in aqueous buffer, *Chem. Commun.*, **2018**, *54*, 3387. https://doi.org/10.1039/c8cc00290h; b) M. L. Contente, A. Pinto, F. Molinari, and F. Paradisi, Biocatalytic N-Acylation of Amines in Water Using an Acyltransferase from Mycobacterium smegmatis, *Adv. Synth. Catal.*, **2018**, *360*, 4814. https://doi.org/10.1002/adsc.201801061

[111] M. Yamagishi *et al.*, Structure-activity relationship study of the neuritogenic potential of the glycan of starfish ganglioside LLG-3, *Mar. Drugs*, **2015**, *13*, 7250. https://doi.org/10.3390/md13127062

[112] a) L. Zhang, M. M. Muthana, H. Yu, J. B. McArthur, J. Qu, and X. Chen, Characterizing non-hydrolyzing Neisseria meningitidis serogroup A UDP-N-acetylglucosamine (UDP-GlcNAc) 2-epimerase using UDP-N-acetylmannosamine (UDP-ManNAc) and derivatives, *Carbohydr. Res.*, **2016**, *419*, 18. https://doi.org/10.1016/j.carres.2015.10.016; b) N. Pravdić, I. Franjić-Mihalić, and B. Danilov, An improved synthesis of the 2-acetamido-d-glucal derivative 3,4,6-tri-O-acetyl-2-(N-acetylacetamido)-1,5-anhydro-2-deoxy-d-arabino-hex-1-enitol, *Carbohydr. Res.*, **1975**, *45*, 302. https://doi.org/10.1016/S0008-6215(00)85889-9

[113] Y. Tamura, J. Haruta, S. Okuyama and Y. Kita, Preparation and reactions of alkyl and aryl isopropenyl carbonatesnovel alkoxy- and aryloxycarbonylations of amines, *Tetrahedron Lett.*, **1978**, *39*, 3737. https://doi.org/10.1016/S0040-4039(01)95045-2

[114] Otrubova, V. Srinivasan and D. L. Boger, Discovery libraries targeting the major enzyme classes: the serine hydrolases, *Bioorg. Med. Chem. Lett.*, **2014**, *24*, 3807. https://doi.org/10.1016/j.bmcl.2014.06.063

[115] K. Kuciński and G. Hreczycho, S-Acetylation of Thiols Mediated by Triflic Acid: A Novel Route to Thioesters, *Org. Process Res. Dev.*, **2018**, *22*, 489. https://doi.org/10.1021/acs.oprd.7b00378

[116] E. S. Rothman and G. C. Moore, Enol esters. XII. C-acylations with enol esters, *J. Org. Chem.*, **1970**, *35*, 2351. https://doi.org/10.1021/jo00832a054

[117] E. G. Derouane, G. Crehan, C. J. Dillon, D. Bethell, H. He, and S. B. Derouane-Abd Hamid, Zeolite catalysts as solid solvents in fine chemicals synthesis: 2. Competitive adsorption of the reactants and products in the Friedel-Crafts acetylations of anisole and toluene, *J. Catal.*, **2000**, *194*, 410. https://doi.org/10.1006/jcat.2000.2933

[118] N. G. Schmidt, T. Pavkov-Keller, N. Richter, B. Wiltschi, K. Gruber, and W. Kroutil, Biocatalytic Friedel–Crafts Acylation and Fries Reaction, *Angew. Chemie - Int. Ed.*, **2017**, *56*, 7615. https://doi.org/10.1002/anie.201703270

[119] T. Mukaiyama, H. Nagaoka, M. Oshima and M. Murakami, The Diphenylboryl Hexachloroantimonate Promoted Friedel-Crafts Acylation Reaction, *Chem. Lett.*, **1986**, 165. https://doi.org/10.1246/cl.1986.165

[120] N. G. Gaylord, F. R. Eirich, Peroxide-catalyzed polymerization of isopropenyl acetate. *J Polymer Sci A: Polymer Chem*, **1950**, *5*, 743. https://doi.org/10.1002/pol.1950.120050615

[121] T. Nishino, N. Kitamura, and K. Murotani, High-pressure-synthesis of poly(isopropenyl alcohol) and its biocompatibilities, *J. Polym. Sci. Part A Polym. Chem.*, **2009**, *47*, 754. https://doi.org/10.1002/pola.23191

[122] A. S. Newton and P. O. Strom, The radiation chemistry of isopropyl acetate and isopropenyl acetate, *Preprints*, **1957**, *2*, 24. https://doi.org/10.1021/j150559a007

[123] I. C. McNeill, S. Ahmed, and J. G. Gorman, Thermal degradation studies of alternating copolymers VII. Degradation of the alternating copolymer of allyl acetate and maleic anhydride: Structural changes and degradation mechanism, *Polym. Degrad. Stab.*, **1999**, *64*, 21. https://doi.org/10.1016/S0141-3910(98)00166-9

[124] a) Unruh CC, Kenyon WO (1948) Heteropolymer of isopropenyl acetate and maleic anhydride. US Patent 2,452,165, 10 Oct 1948; b) Hasche RL, McMahon EM (1947) Copolymer of isopropenyl acetate and vinyl chloride. US Patent 2,453,317, 3 Sept 1947.

[125] P. De and D. N. Sathyanarayana, Free radical oxidative copolymerization of indene with vinyl acetate and isopropenyl acetate: Synthesis and characterization, *J. Appl. Polym. Sci.*, **2002**, *86*, 639. https://doi.org/10.1002/app.10918

[126] W. Y. Ma, Y. X. Wu, L. Feng, and R. W. Xu, Synthesis of poly(styrene-co-isopropenyl acetate) -g-polyisobutylene graft copolymers via combination of radical polymerization with cationic polymerization, *Polymer (Guildf).*, **2012**, *53*, 3185. https://doi.org/10.1016/j.polymer.2012.05.028

[127] N. Shinde, M. Kathalewar, and A. Sabnis, Synthesis and characterization of emulsion polymers using isopropenyl acetate, *Int. J. Ind. Chem.*, **2012**, *3*, 1. https://doi.org/10.1186/2228-5547-3-28

[128] Y. Kuwae, M. Kamachi, and S. Nozakura, Kinetic and electron spin resonance studies on radical polymerization of isopropenyl acetate, *Macromolecules*, **1986**, *19*, 2912. https://doi.org/10.1021/ma00166a006

[129] P. Borowski, S. Pasieczna-Patkowska, M. Barczak, and K. Pilorz, Theoretical determination of the infrared spectra of amorphous polymers, *J. Phys. Chem. A*, **2012**, *116*, 7424. https://doi.org/10.1021/jp303209v

[130] L. K. J. Tong and W. O. Kenyon, Heats of Polymerization. IV. Copolymerization, *J. Am. Chem. Soc.*, **1949**, *71*, 1925. https://doi.org/10.1021/ja01174a008

[131] S. Rimmer, S. Collins, and P. Sarker, Preparation of highly branched poly(vinyl acetate) by transfer to allylic carbonate comonomers, *Chem. Commun.*, **2005**, *48*, 6029. https://doi.org/10.1039/b511870k

[132] I. A. Krivosheyeva, T. B. Borisova, and A. I. Razumov, Study of the initiated polymerization of mixed allyl-isopropenyl esters of ethylphosphinic and arylphosphinic acids by electrical conductivity measurements, dilatometry and infrared spectroscopy, *Polym. Sci. U.S.S.R.*, **1969**, *11*, 287. https://doi.org/10.1016/0032-3950(69)90170-1

[133] F. Sanda, T. Abe, and T. Endo, Syntheses and radical polymerizations of novel optically active vinyl and isopropenyl carbamates having L-leucine structures, *J. Polym. Sci. Part A Polym. Chem.*, **1996**, *34*, 1969. https://doi.org/10.1002/(SICI)1099-0518(19960730)34:10<1969::AID-POLA15>3.0.CO;2-G.

[134] T. Kanazawa, T. Nishikawa, and M. Ouchi, RAFT polymerization of isopropenyl boronate pinacol ester and subsequent terminal olefination: precise synthesis of poly(alkenyl boronate)s and evaluation of their thermal properties, *Polym. J.*, **2021**, *53*, 1167. https://doi.org/10.1038/s41428-021-00498-8

[135] a) P. Chauhan, S. Mahajan and D. Enders, Organocatalytic carbon–sulfur bond-forming reactions, *Chem. Rev.*, **2014**, *114*, 8807. https://doi.org/10.1021/cr500235v; b) J. Clayden and P. MacLellan, Beilstein J. Org. Chem., 2011, 7, 582. J. Clayden and P. MacLellan, Asymmetric synthesis of tertiary thiols and thioethers, *Beilstein J. Org. Chem.*, **2011**, *7*, 582. https://doi.org/10.3762/bjoc.7.68

[136] a) H. C. Kolb, M. G. Finn and K. B. Sharpless, The growing impact of click chemistry on drug discovery, *Angew. Chem., Int. Ed.*, **2001**, *40*, 2004. https://doi.org/10.1016/S1359-6446(03)02933-7; b) M. G. Finn and V. V. Fokin, Click chemistry: Function follows form, *Chem. Soc. Rev.*, **2010**, *39*, 1231. https://doi.org/10.1039/c003740k

[137] B. C. Ranu and T. Mandal, Water-promoted highly selective anti-Markovnikov addition of thiols to unactivated alkenes, *Synlett*, **2007**, *6*, 925. https://doi.org/10.1055/s-2007-973877

[138] a) G. Zhao, S. Kaur, and T. Wang, Visible-Light-Mediated Thiol-Ene Reactions through Organic Photoredox Catalysis, *Org. Lett.*, **2017**, *19*, 3291. https://doi.org/10.1021/acs.orglett.7b01441; b) S. Kaur, G. Zhao, E. Busch, and T. Wang, Metal-free photocatalytic thiol-ene/thiol-yne reactions, *Org. Biomol. Chem.*, **2019**, *17*, 1955. https://doi.org/10.1039/c8ob02313a

[139] K. Kuciński, and G. Hreczycho, S-acetylation of thiols mediated by triflic acid: a novel route to thioesters, *Org. Proc. Res. Dev.*, **2018**, *22*, 489. https://doi.org/10.1021/acs.oprd.7b00378

[140] G. Sienel, R. Rieth and K. T. Rowbottom, Epoxides. In Ullmann's Encyclopedia of Industrial Chemistry; Wiley–VCH, 2000.

[141] S. Serota and E. S. Rothman, Enol esters. VII. Isolation and rearrangement of terminal fatty oxirane esters, *J. Am. Oil Chem. Soc.*, **1968**, *45*, 525. https://doi.org/10.1007/BF02541341

[142] D. Yang, M-K. Wong and Y-C. Yip, Epoxidation of olefins using methyl (trifluoromethyl) dioxirane generated in situ, *J. Org. Chem.*, **1995**, *60*, 3887. https://doi.org/10.1021/jo00117a046

[143] K. Kudo, K. Mitsuhashi, S. Mori, K. Komatsu and N. Sugita, Palladium (II)-catalyzed cyclocarbonylation of enol ester of acetone. A novel synthesis of 1, 3-dioxolan-4-one, *Chem. Lett.*, **1993**, 1615. https://doi.org/10.1246/cl.1993.1615

[144] K. Kudo, Y. Oida, K. Mitsuhashi, S. Mori, K. Komatsu, and N. Sugita, Hydrocarbonylation of Enol Esters Catalyzed by a Palladium(II) Complex, *Bulletin of the Chemical Society of Japan*, **1996**, *69*, 1337. https://doi.org/10.1246/bcsj.69.1337

[145] X. Wang and S. L. Buchwald, Synthesis of optically pure 2-trifluoromethyl lactic acid by asymmetric hydroformylation, *J. Org. Chem.*, **2013**, *78*, 3429. https://doi.org/10.1021/jo400115r

[146] J. Eshon, F. Foarta, C. R. Landis and J. M. Schomaker, α-Tetrasubstituted aldehydes through electronic and strain-controlled branch-selective stereoselective hydroformylation, *J. Org. Chem.*, **2018**, *83*, 10207. https://doi.org/10.1021/acs.joc.8b01431

[147] a) M. F. Shostakovskii, A. V Bogdanova, and G. I. Plotnikova, Addition of Alcohols and Mercaptans To Compounds With Triple Bonds, *Russ. Chem. Rev.*, **1964**, *33*, 66. https://doi.org/10.1070/rc1964v033n02abeh001378; b) E. S. Rothman, G. G. Moore, J. M. Chirinko, and S. Serota, Enol esters XVI: Enol ethers in synthesis, *J. Am. Oil Chem. Soc.*, **1972**, *49*, 376. https://doi.org/10.1007/BF02633393

[148] Y. Okimoto, S. Sakaguchi and Y. Ishii, Development of a highly efficient catalytic method for synthesis of vinyl ethers, *J. Am. Chem. Soc.*, **2002**, *124*, 1590. https://doi.org/10.1021/ja0173932

[149] M. Morita, S. Sakaguchi, and Y. Ishii, One-pot synthesis of γ,δ-unsaturated carbonyl compounds from allyl alcohols and vinyl or isopropenyl acetates catalyzed by [IrCl(cod)] 2, *J. Org. Chem.*, **2006**, *71*, 6285. https://doi.org/10.1021/jo060860j

[150] For an overview, see: Multicomponent reactions; Zhu, J., Bienayme´, H., Eds.; Wiley-VCH: Weinheim, 2005.

[151] N. Isambert, M. Cruz, M. J. Arévalo, E. Gómez, and R. Lavilla, Enol esters: Versatile substrates for mannich-type multicomponent reactions, *Org. Lett.*, **2007**, *9*, 4199. https://doi.org/10.1021/ol701717z

[152] N. E. Stainforth, G. A. Cutting, M. P. John, and M. C. Willis, Direct catalytic diastereoselective Mannich reactions: the synthesis of protected α-hydroxy-β-aminoketones, *Tetrahedron Asymmetry*, **2009**, *20*, 741. https://doi.org/10.1016/j.tetasy.2009.03.026

[153] H. S. Dang, K. M. Kim, and B. P. Roberts, Radical-chain reductive carboxyalkylation of electron-rich alkenes: Carbon-carbon bond formation mediated by silanes in the presence of thiols as polarity-reversal catalysts, *Chem. Commun.*, 1998, 13, 1413. https://doi.org/10.1039/a802826e

[154] H. S. Dang and B. P. Roberts, Radical-chain addition of aldehydes to alkenes catalysed by thiols, *J. Chem. Soc. - Perkin Trans. 1*, **1998**, *1*, 67. https://doi.org/10.1039/a704878e

[155] M. B. Haque and B. P. Roberts, Enantioselective radical-chain hydrosilylation of prochiral alkenes using optically active thiol catalysts, *Tetrahedron Lett.*, vol. 37, no. 50, pp. 9123–9126, 1996, https://doi.org/10.1016/S0040-4039(96)90165-3

[156] E. Leonel, M. Lejaye, S. Oudeyer, J. P. Paugam and J-Y. Nedelec, gem-Dihalocyclopropane formation by iron/copper activation of tetrahalomethanes in the presence of nucleophilic olefins. Evidence for a carbene pathway, *Tetrahedron Lett.*, **2004**, *45*, 2635. https://doi.org/10.1016/j.tetlet.2004.01.124

[157] C. A. Muedas, R. R. Ferguson and R. H. Crabtree, Hydrodimerization of unsaturated alcohols, esters, nitriles, ketones, amines, silanes, epoxides and fluorocarbons by mercury-photosensitization, *Tetrahedron Lett.*, **1989**, *30*, 3389. https://doi.org/10.1016/S0040-4039(00)99252-9

[158] C. A. Muedas, R. R. Ferguson, S. H. Brown and R. H. Crabtree, Hydrogen atoms as convenient synthetic reagents: mercury-photosensitized dimerization of functionalized organic compounds in the presence of molecular hydrogen, *J. Am. Chem. Soc.*, **1991**, *113*, 2233. https://doi.org/10.1021/ja00006a048

[159] F. Bellesia, L. Forti, F. Ghelfi and U. M. Pagnoni, The Fe0 Promoted Addition of CCl4, and CCl3Br to Olefins, *Synth. Commun.*, **1997**, *27*, 961. https://doi.org/10.1080/00397919708003040

[160] I. M. Vol'pin, M. A. Kurykin, V. A. Grinberg, Y. B. Vasilev and L. S. German, Electrochemical synthesis of perfluoroalkylacetones, *Bull. Acad. Sci. USSR, Div. Chem. Sci.*, **1991**, *40*, 1395. https://doi.org/10.1007/BF00961239

[161] P. Liu, T. J. Lanza, J. P. Jewell, C. P. Jones, W. K. Hagmann and L. S. Lin, A highly active catalyst system for the heteroarylation of acetone, *Tetrahedron Lett.*, **2003**, *44*, 8869. https://doi.org/10.1016/j.tetlet.2003.09.176

[162] M. Palucki and S. L. Buchwald, Palladium-catalyzed α-arylation of ketones, *J. Am. Chem. Soc.*, **1997**, *119*, 11108. https://doi.org/10.1021/ja972593s

[163] R. D.M. Davies, J. H. Pink, J. S. Scott, A. Bailey, Synthesis of 8-substituted-6-phenyl-6, 7, 8, 9-tetrahydro-3H-pyrazolo [4, 3-f] isoquinolines using Pictet-Spengler and Bischler-Napieralski cyclisation methods, *Tetrahedron Lett.*, **2018**, *59*, 2917. https://doi.org/10.1016/j.tetlet.2018.06.041

[164] M. Kosugi, I. Hagiwara and T. Migita, 1-Alkenylation on α-position of ketone: palladium-catalyzed reaction of tin enolates and 1-bromo-1-alkenes, *Chem. Lett.*, **1983**, 839. https://doi.org/10.1246/cl.1983.839

[165] M. Kosugi, I. Hagiwara, T. Sumiya and T. Migita, α-Phenylation of ketones via tin enolates catalysed by a palladium complex, *J. Chem. Soc., Chem. Commun.*, **1983**, 344. https://doi.org/10.1039/C39830000344

[166] M. Kosugi, M. Suzuki, I. Hagiwara, K. Goto, K. Saitoh and T. Migita, A new palladium catalyzed aromatic acetonylation by acetonyltributyltin, *Chem. Lett.*, **1982**, *11*, 939. https://doi.org/10.1246/cl.1982.939

[167] A. Dore, B. Asproni, A. Scampuddu, G. Aime Pinna, C. T. Christoffersen, M. Langgård and J. Kehler, Synthesis and SAR study of novel tricyclic pyrazoles as potent phosphodiesterase 10A inhibitors, *Eur. J. Med. Chem.*, **2014**, *84*, 181. https://doi.org/10.1016/j.ejmech.2014.07.020

[168] K. C. Nicolaou and H. Xu, Total synthesis of floresolide B and Δ 6, 7-Z-floresolide B, *Chem. Commun.*, **2006**, 600. https://doi.org/10.1039/B517385J

169 A) I. Geibel, C. Kahrs, and J. Christoffers, Formation of Bicyclic Cyclopentenone Derivatives by Robinson-Type Annulation of Cyclic β-Oxoesters Containing a 1,4-Diketone Moiety, *Synth.*, **2017**, *49*, 3874. https://doi.org/10.1055/s-0036-1590812

170 I. Geibel and J. Christoffers, Synthesis of 1,4-Diketones from β-Oxo Esters and Enol Acetates by Cerium-Catalyzed Oxidative Umpolung Reaction, *European J. Org. Chem.*, **2016**, *2016*, 918. https://doi.org/10.1002/ejoc.201600057

171 T. Zhang, N-X. Wang, Y-H. Wu, Z. Yan, Y. Xing, J-L. Wen and X-W. Gao, Synthesis of 1, 4-Diketones from β-Oxo Esters and Enol Acetates by Cerium-Catalyzed Oxidative Umpolung Reaction, *Tetrahedron Lett.*, **2018**, *59*, 4525. https://doi.org/10.1002/ejoc.201600057

172 R-D. He, C.-L. Li, Q.-Q. Pan, P. Guo, X.-Y. Liu and X-Z. Shu, Reductive coupling between C–N and C–O electrophiles, *J. Am. Chem. Soc.*, **2019**, *141*, 12481. https://doi.org/10.1021/jacs.9b05224

173 H. Hara, M. Hirano, and K. Tanaka, Liquid enol ethers and acetates as gaseous alkyne equivalents in Rh-catalyzed chemo- and regioselective formal cross-alkyne cyclotrimerization, *Org. Lett.*, **2008**, *10*, 2537. https://doi.org/10.1021/ol800813g

174 H. Hara, M. Hirano, and K. Tanaka, Commercially available liquid enol ethers and acetates as gaseous alkyne equivalents in cationic Rh(I)/BINAP-catalyzed chemo- and regioselective formal cross-alkyne cyclotrimerizations, *Tetrahedron*, **2009**, *65*, 5093. https://doi.org/10.1016/j.tet.2009.02.047

175 M. Zhong, S. Sun, J. Cheng and Y. Shao, Iron-catalyzed cyclization of nitrones with geminal-substituted vinyl acetates: A direct [4+ 2] assembly strategy leading to 2, 4-disubstituted quinolines, *J. Org. Chem.*, **2016**, *81*, 10825. https://doi.org/10.1021/acs.joc.6b01910

176 H. Chu, S. Sun, J-T. Yu and J. Cheng, Rh-catalyzed sequential oxidative C–H activation/annulation with geminal-substituted vinyl acetates to access isoquinolines, *Chem. Commun.*, **2015**, *51*, 13327. https://doi.org/10.1039/C5CC04708K

177 J. Li and P. Knochel, Cobalt-Catalyzed Cross-Couplings between Alkenyl Acetates and Aryl or Alkenyl Zinc Pivalates, *Angew. Chem. Int. Ed.*, **2018**, *57*, 11436. https://doi.org/10.1002/anie.201805486

178 C. A. Sperger, J. E. Tungen and A. Fiksdahl, Gold (I)-Catalyzed Reactions of Propargyl Esters with Vinyl Derivatives, *Eur. J. Org. Chem.*, **2011**, 3719. https://doi.org/10.1002/ejoc.201100291

179 S.-S. Li, C-F. Liu, Y-Q. Xia, W-H. Li, G-T. Zhang, X-M. Zhang and L. Dong, A unique annulation of 7-azaindoles with alkenyl esters to produce π-conjugated 7-azaindole derivatives, *Org. Biomol. Chem.*, **2016**, *14*, 5214. https://doi.org/10.1039/C6OB00730A

180 M. Takeno, S. Kikuchi, K-I. Morita, Y. Nishiyama and Y. Ishii, A new coupling reaction of vinyl esters with aldehydes catalyzed by organosamarium compounds, *J. Org. Chem.*, **1995**, *60*, 4974. https://doi.org/10.1021/jo00121a008

181 Y. Hatamoto, S. Sakaguchi and Y. Ishii, Oxidative Cross-Coupling of Acrylates with Vinyl Carboxylates Catalyzed by a Pd(OAc)2/HPMoV/O2 System, *Org. Lett.*, **2004**, *6*, 4623. https://doi.org/10.1021/ol047971u

182 Y. Onishi, Y. Nishimoto, M. Yasuda and A. Baba, InI3/Me3SiI-catalyzed Direct Alkylation of Enol Acetates Using Alkyl Acetates or Alkyl Ethers, *Chem. Lett.*, **2011**, *40*, 1223. https://doi.org/10.1246/cl.2011.1223

183 Y. Onishi, Y. Nishimoto, M. Yasuda, and A. Baba, InCl3/Me3SiBr-catalyzed direct coupling between silyl ethers and enol acetates, *Org. Lett.*, **2011**, *13*, 2762. https://doi.org/10.1021/ol200875m

184 B. Y. Park, T. Luong, H. Sato and M. J. Krische, A Metallacycle Fragmentation Strategy for Vinyl Transfer from Enol Carboxylates to Secondary Alcohol C–H Bonds via Osmium- or Ruthenium-Catalyzed Transfer Hydrogenation, *J. Am. Chem. Soc.*, **2015**, *137*, 7652. https://doi.org/10.1021/jacs.5b04688

185 A. B. Abdelwahaba, E. R. El-Sawya and G. Kirscha, Iron powder and tin/tin chloride as new reducing agents of Meerwein arylation reaction with unexpected recycling to anilines, *Synth. Comm.*, **2020**, *50*, 526. https://doi.org/10.1080/00397911.2019.1704786

186 P. Gomes, C. Gosmini and J. Perichon, Cobalt-catalyzed electrochemical vinylation of aryl halides using vinylic acetates, *Tetrahedron*, **2003**, *59*, 2999. https://doi.org/10.1016/S0040-4020(03)00404-6

187 M. Amatore, C. Gosmini and J. Périchon, Cobalt-Catalyzed Vinylation of Functionalized Aryl Halides with Vinyl Acetates, *Eur. J. Org. Chem.*, **2005**, 989. https://doi.org/10.1002/ejoc.200400897

188 W. Lin, W. Li, D. Lu, F. Su, T-B. Wen and H-J. Zhang, Dual effects of cyclopentadienyl ligands on Rh (III)-catalyzed dehydrogenative arylation of electron-rich alkenes, *ACS Catal.*, **2018**, *8*, 8070. https://doi.org/10.1021/acscatal.8b01753

189 L. J. Gooßen and J. Paetzold, Decarbonylative Heck Olefination of Enol Esters: Salt-Free and Environmentally Friendly Access to Vinyl Arenes, *Angew. Chem. Int. Ed.*, **2004**, *43*, 1095. https://doi.org/10.1002/anie.200352357

190 L. Meng, C. Liu, W. Zhang, C. Zhoua and A. Lei, Palladium catalysed β-selective oxidative Heck reaction of an electron-rich olefin, *Chem. Commun.*, **2014**, *50*, 1110. https://doi.org/10.1039/C3CC47045H

[191] L. J. Gooßen and J. Paetzold, Decarbonylative Heck Olefination of Enol Esters: Salt-Free and Environmentally Friendly Access to Vinyl Arenes, *Angew. Chem. Int. Ed.*, **2004**, *43*, 1095. https://doi.org/10.1002/anie.200352357

[192] H. W. Lee and F. Y. Kwong, Rhodium-catalyzed cross-coupling of arylboronic acids using vinyl acetate as the electrophilic partner, *Synlett*, **2009**, *19*, 3151. https://doi.org/10.1055/s-0029-1218283

[193] C. P. Seath, D. B. Vogt, Z. Xu, A. J. Boyington and N. T. Jui, Radical hydroarylation of functionalized olefins and mechanistic investigation of photocatalytic pyridyl radical reactions, *J. Am. Chem. Soc.*, **2018**, *140*, 15525. https://doi.org/10.1021/jacs.8b10238

[194] L. Wang, J. Shen, S. Yang, W. Liu, Q. Chen and M. He, C–H arylation reactions through aniline activation catalysed by a PANI-gC 3 N 4-TiO 2 composite under visible light in aqueous medium, *Green Chem.*, **2018**, *20*, 1290. https://doi.org/10.1039/C8GC00012C

[195] T. Hering, D. Prasad Hari and B. König, Visible-light-mediated α-arylation of enol acetates using aryl diazonium salts, *J. Org. Chem.*, **2012**, *77*, 10347. https://doi.org/10.1021/jo301984p

[196] M. Bu, G. Lu, J. Jiang and C. Cai, Merging visible-light photoredox and micellar catalysis: arylation reactions with anilines nitrosated in situ, *Catal. Sci. Technol.*, **2018**, *8*, 3728. https://doi.org/10.1039/C8CY01221K

[197] B. C. Soderberg, L. S. Hegedus and M. A. Sierra, Synthesis of cyclobutanones by the photolytic reaction of chromium carbene complexes with olefins: inter-and intramolecular reactions, *J. Am. Chem. Soc.*, **1990**, *112*, 4364. https://doi.org/10.1021/ja00167a038

[198] M. Yilmaz, M. Yakut and A. T. Pekel, Synthesis of 2,3-Dihydro-4H-furo[3,2-c] chromen-4-ones and 2,3-Dihydronaphtho[2,3-b]furan-4,9-diones by the Radical Cyclizations of Hydroxyenones with Electron-Rich Alkenes using Manganese(III) Acetate, *Synthetic Commun.*, **2008**, *38*, 914. https://doi.org/10.1080/00397910701845456

[199] M. E. Jung and H. L. Rayle, Generation of [5.5.n] Tricyclic Ring Systems by Radical-Promoted Inter- and Intramolecular [3 + 2] Cycloadditions, *J. Org. Chem.*, **1997**, *62*, 4601. https://doi.org/10.1021/jo9706133

[200] D. Felipe-Blanco and J. C. Gonzalez-Gomeza, Salicylic acid-catalyzed arylation of enol acetates with anilines, *Adv. Synth. Catal.*, **2018**, *360*, 2773. https://doi.org/10.1002/adsc.201800427

[201] C. Molinaro, J. Mowat, F. Gosselin, P. D. O'Shea, J.-F. Marcoux, R. Angelaud, and I. W. Davies, A Practical Synthesis of α-Aryl Methyl Ketones via a Transition-Metal-Free Meerwein Arylation, *J. Org. Chem.*, **2007**, *72*, 1856. https://doi.org/10.1021/jo062483g

[202] Z.-H. Sun, W. Chen, B-B. Qian, L. Wang, B. Yu, Q. Chen, M-Y. He, Z-H. Zhang, UiO-66 microcrystals catalyzed direct arylation of enol acetates and heteroarenes with aryl diazonium salts in water, *Appl Organometal Chem.*, **2020**, *34*, 5482. https://doi.org/10.1002/aoc.5482

[203] M. Teruaki, S. Jun, S. Tadashi and S. Isamu, The insulated gate field effect transistor (IGFET) as a microluminometer, *Chem. Lett.*, **1973**, *3*, 323.

[204] M. Teruaki, S. Jun, S. Tadashi and S. Isamu, Diethylaluminum ethoxide mediated crossed aldol reaction of enol esters with carbonyl compounds, *Chem. Lett.*, **1999**, *28*, 951. https://doi.org/10.1246/cl.1999.951

[205] M. Yanagisawa, T. Shimamura, D. Iida, J. Matsuo and T. Mukaiyama, Aldol reaction of enol esters catalyzed by cationic species paired with tetrakis (pentafluorophenyl) borate, *Chem. Pharm. Bull.*, **2000**, *48*, 1838. https://doi.org/10.1248/cpb.48.1838

[206] Y. Masuyama, Y. Kobayashi, R. Yanagi and Y. Kurusu, Aldol-Type Reaction by Propen-2-yl Acetate with NCS/SnCl2/ROH, *Chem Lett*, **1992**, *21*, 2039. https://doi.org/10.1246/cl.1992.2039

[207] Y. Masuyama, T. Sakai and Y. Kurusu, Palladium-catalyzed aldol-type condensation by enol esters with SnCl2, *Tetrahedron Lett.*, **1993**, *34*, 653. https://doi.org/10.1016/S0040-4039(00)61644-1

[208] Y. Masuyama, Y. Kobayashi and Y. Kurusu, Aldol reaction of enol acetates and lactols with N-chlorosuccinimide and tin (II) chloride. Diastereoselective synthesis of disubstituted cyclic ethers, *J. Chem. Soc., Chem. Commun.*, **1994**, 1123. https://doi.org/10.1039/C39940001123

[209] Y. Onishi, Y. Yoneda, Y. Nishimoto, M. Yasuda and A. Baba, InCl3/Me3SiCl-Catalyzed Direct Michael Addition of Enol Acetates to α,β-Unsaturated Ketones, *Org. Lett.*, **2012**, *14*, 5788. https://doi.org/10.1021/ol302888k

[210] K. Toshima, N. Miyamoto, G. Matsuo, M. Nakata and S. Matsumura, Environmentally compatible C-glycosidation of glycals using montmorillonite K-10, *Chem. Commun.*, **1996**, 1379. https://doi.org/10.1039/CC9960001379

[211] M. Sato, H. Ogasawara, K. Oi and T. Kato, Synthesis of 1, 3-dioxin-4-one derivatives, *Chem. Pharm. Bull.*, **1983**, *31*, 1896. https://doi.org/10.1248/cpb.31.1896

[212] J. A. Hyatt, Isopropenyl acetoacetate and the reaction of diketene with acetone, *J. Org. Chem.*, **1984**, *49*, 5102. https://doi.org/10.1021/jo00200a017

[213] B. M. Trost, J. P. N. Papillon, and T. Nussbaumer, Ru-catalyzed alkene-alkyne coupling. Total synthesis of amphidinolide P, *J. Am. Chem. Soc.*, **2005**, *127*, 17921. https://doi.org/10.1021/ja055967n

[214] Y. Nishimoto, Y. Onishi, M. Yasuda and A. Baba, α-Alkylation of Carbonyl Compounds by Direct Addition of Alcohols to Enol Acetates, *Angew. Chem. Int. Ed.*, **2009**, *48*, 9131. https://doi.org/10.1002/ange.200904069

[215] R. Umeda, Y. Takahashi, T. Yamamoto, H. Iseki, I. Osaka and Y. Nishiyama, Rhenium-catalyzed α-alkylation of enol acetates with alcohols or ethers, *J. Organomet. Chem.*, **2018**, *877*, 92. https://doi.org/10.1016/j.jorganchem.2018.09.010

[216] R. I. Khusnutdinov, N. A. Shchadneva, K. S. Kislitsina, V. A. Veklov and B. I. Kutepov, Synthesis of 1-(2-oxopropyl) adamantane from 1-bromo (chloro) adamantanes and isopropenyl acetate in the presence of iron and manganese compounds, *Russ. J. Org. Chem.*, **2014**, *50*, 1272. https://doi.org/10.1134/S1070428014090061

[217] Y. Jiao, C. Cao and Z. Zhou, Direct Synthesis of anti-1,3-Diols through Nonclassical Reaction of Aryl Grignard Reagents with Isopropenyl Acetate, *Org. Lett.*, **2011**, *13*, 180. https://doi.org/10.1021/ol102520y

[218] B. Oussaid, L. Moeini, B. Martin, D. Villemin and B. Garrigues, Improved synthesis of oxadiazoles under microwave irradiation, *Synthetic Commun.*, **1995**, *25*, 1451. https://doi.org/10.1080/00397919508011757

[219] T. Takanami, A. Abe, K. Suda and H. Ohmori, Anodic oxidation of triphenylphosphine in the presence of enol silyl ethers or enol esters. Electrochemical one-step preparation of 2-oxocycloalkyltriphenylphosphonium tetrafluoroborates, *J. Chem. Soc., Chem. Commun.*, **1990**, *19*, 1310. https://doi.org/10.1039/C39900001310

[220] J. Yoshida, K. Sakaguchi and S. Isoe, Oxidative [3+ 2] cycloaddition of 1, 3-diketone and olefin using electroorganic chemistry, *J. Org. Chem.*, **1988**, *53*, 2525. https://doi.org/10.1021/jo00246a022

[221] A. Toshimitsu, T. Aoai, H. Owada, S. Uemura and M. Okano, Phenylselenenyl chloride in acetonitrile-water: a highly convenient reagent for hydroxyselenation of olefins and preparation of cyclic ethers from dienes, *Tetrahedron*, **1985**, *41*, 5301. https://doi.org/10.1016/S0040-4020(01)96781-X

[222] S. E. Denmark, R. A. Stavenger, S. B. D. Winter, K-T. Wong and P. A. Barsanti, Preparation of chlorosilyl enolates, *J. Org. Chem.*, **1998**, *63*, 9517. https://doi.org/10.1021/jo981740h

[223] A. Boto, J. A. Gallardo, D. Hernandez and R.Hernandez, Synthesis of unnatural amino acids from serine derivatives by β-fragmentation of primary alkoxyl radicals, *J. Org. Chem.*, **2007**, *72*, 7260. https://doi.org/10.1021/jo071155t

[224] K. Miura, K. Fugami, K. Oshima, and K. Utimoto, Synthesis of vinylcyclopentanes from vinylcyclopropanes and alkenes promoted by benzenethiyl radical, *Tetrahedron Lett.*, **1988**, *29*, 5135. https://doi.org/10.1016/S0040-4039(00)80701-7

[225] V. L. Novikov, O. P. Shestak, and V. A. Denisenko, Unusual aluminum chloride-assisted conversion of isopropenyl acetate into 3-acetyl-and 3, 5-diacetyl-2, 6-dimethyl-4 H-pyran-4-ones, *Russ. Chem. Bull.*, **2010**, *59*, 1600. https://doi.org/10.1007/s11172-010-0283-0

[226] L. S. Silbert, S. Serota, G. Maerker, W. E. Palm, J. G. Phillips, Acylation of Cotton Fabric with Isopropenyl Stearatel, *Textile Research Journal*, **1978**, 48, 422, 426. https://doi.org/10.1177/004051757804800710

[227] G.B. Nagarajappa and K.K. Pandey, UV resistance and dimensional stability of wood modified with isopropenyl acetate, *J. Photochem. Photobio., B: Bio.*, **2016**, *155*, 20. https://doi.org/10.1016/j.jphotobiol.2015.12.012

[228] B. N. Giridhar, K. K. Pandey, B. E. Prasad, S. S. Bisht, and H. M. Vagdevi, Dimensional stabilization of wood by chemical modification using isopropenyl acetate, *Maderas Cienc. y Tecnol.*, **2017**, *19*, 15. https://doi.org/10.4067/S0718-221X2017005000002

[229] R. Kakuchi, M. Yamaguchi, T. Endo, Y. Shibata, K. Ninomiya, T. Ikai, K. Maedac and K. Takahashi, Efficient and rapid direct transesterification reactions of cellulose with isopropenyl acetate in ionic liquids, *RSC Adv.*, **2015**, *5*, 72071. https://doi.org/10.1039/C5RA14408F

[230] S. Suzuki, A. Ishikuro, D. Hirose, K. Ninomiya, and K. Takahashi, Dual catalytic activity of an ionic liquid in lignin acetylation and deacetylation, *Chem. Lett.*, **2018**, *47*, 860. https://doi.org/10.1246/cl.180350

[231] S. Suzuki, S. Kurachi, N. Wada and K. Takahashi, Selective Modification of Aliphatic Hydroxy Groups in Lignin Using Ionic Liquid, *Catalysts*, **2021**, *11*, 120. https://doi.org/10.3390/catal11010120

[232] S. Suzuki, R. Yada, Y. Hamano, N. Wada, and K. Takahashi, Green Synthesis and Fractionation of Cellulose Acetate by Controlling the Reactivity of Polysaccharides in Sugarcane Bagasse, *ACS Sustainable Chem. Eng.*, **2020**, *8*, 9002. https://doi.org/10.1021/acssuschemeng.0c01639

[233] L. Szabó, R. Milotskyi, H. Ueda, T. Tsukegi, N. Wada, K. Takahashi, Controlled acetylation of kraft lignin for tailoring polyacrylonitrile-kraft lignin interactions towards the production of quality carbon nanofibers, *Chem. Eng. J.*, **2021**, *405*, 126640. https://doi.org/10.1016/j.cej.2020.126640

[234] U. Weißbach, S. Dabral, L. Konnert, C. Bolm and J. G. Hernández, Selective enzymatic esterification of lignin model compounds in the ball mill, *Beilstein J. Org. Chem.*, **2017**, *13*, 1788. https://doi.org/10.3762/bjoc.13.173

4 CO_2 insertion into terminal epoxides

4.1 Introduction

In recent years, the range of synthetically relevant applications of carbon dioxide (CO_2) has extended tremendously, shifting from a niche research area to an established stimulating, interdisciplinary research topic.[1,2] The most notable examples of non-reductive transformations employing CO_2 as C^1 electrophilic synthon include carboxylation and CO_2 insertion reactions,[3] which are highly desirable from the green chemistry perspective as they valorise a renewable resource through atom economical chemical processes. Among them, a cornerstone is represented by the synthesis of cyclic organic carbonates (COCs) *via* CO_2 insertion in epoxide rings (Scheme 4.1).
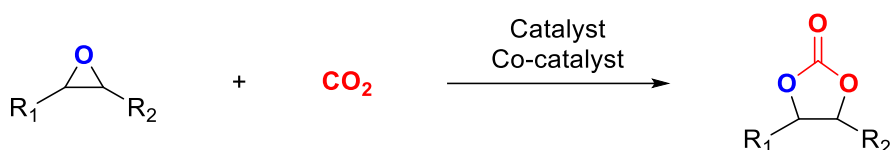
Scheme 4.1. *Formation of 5-membered COCs via CO_2 insertion in epoxide rings in presence of a suitable catalytic system*

Although the reaction often proceeds with good to excellent yields, it exemplifies some of the typical issues/challenges associated to the use of CO_2 in synthesis. Indeed, due to the high thermodynamic stability and low kinetic reactivity of CO_2, the process requires: i) high-energy co-reactants (epoxides) and active (and often tailor-made) catalytic systems embedding Lewis/Brønsted acid and nucleophilic moieties; ii) relatively high temperatures and/or CO_2 pressures which imply the design of engineering solutions through (pressurized) reaction vessels. Figure 4.1 depicts the mechanism proposed for COCs synthesis from epoxides and CO_2 in the presence of a bi-functional catalytic system (M-Nu).[4,5]
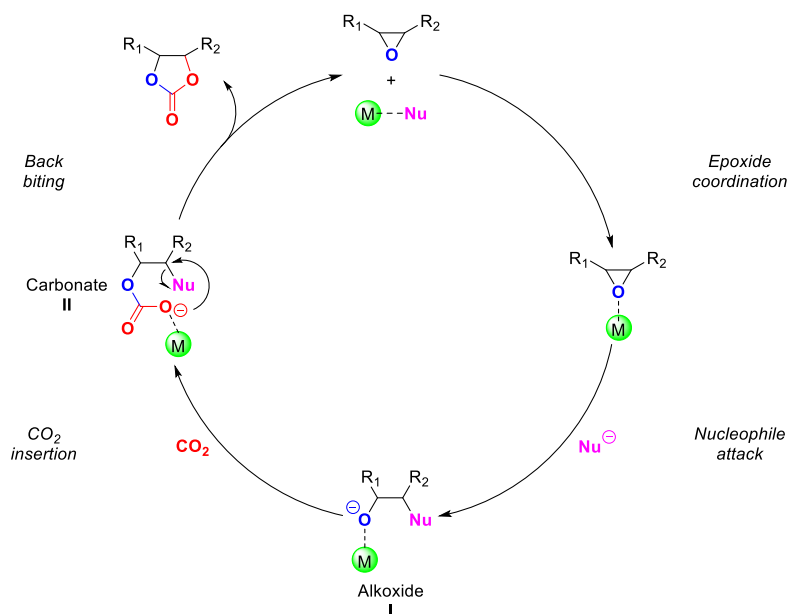
Figure 4.1. *Proposed mechanism for the synthesis of 5-membered COC by reacting CO_2 with epoxides in the presence of a bifunctional catalytic system*

The acidic moiety (M) of the catalyst coordinates the epoxide activation; the resulting activated substrate undergoes attack by the nucleophilic component (Nu) of the catalyst, generally a halide, resulting in the formation of an alkoxide intermediate (I). Thereafter, the reaction of I and CO_2 forms a carbonate intermediate (II) which undergoes ring closure via a back-biting reaction. This final step releases the COC product, and concurrently restores the catalytic system. A plethora of such systems active for terminal, internal and trisubstituted epoxides have been reported so far.[6] In view of more sustainable protocols, special emphasis has been devoted to non-endangered metal catalysts[7] such as salts and complexes of Fe, Al, Co and Zn,[8,9,10,11] and, even more interesting, some of these systems have proved efficient in continuous-flow (CF) mode, *i.e.* under highly reliable conditions for process optimization, intensification and upscaling.[12] One of the first CF-examples described a Co(II)-salen complex immobilized on MCM-41 silica gel: at T = 110 °C, $p(CO_2)$ = 125 bar and F = 10-20 mL·h^{-1}, in the presence of tetrabutylammonium bromide (TBAB) as a co-catalyst, ethylene oxide (EO) was converted up to 86% into ethylene carbonate (EC) with > 99 % selectivity.[13] Another approach proposed a Zn-based imidazolium ionic liquid ([AeMIM][Zn_2Br_5]) supported on MCM-22 molecular sieves, to obtain propylene carbonate (PC) from propylene oxide (PO). A steady PC yield of 62% was reported after > 50 h of time-on-stream, at T = 130 °C, $p(CO_2)$ = 20 bar, LHSV = 0.75 h^{-1} employing a molar ratio CO_2/PO = 3.[14] An Al(III)-salen complex modified with (diethylbenzyl)ammonium bromide tethers and immobilized on amorphous silica proved effective for the first continuous-flow synthesis of EC designed for using waste CO_2 originated for example, in the exhaust stream of a fossil fuel power station. At T = 150 °C, when a binary mixture of N_2 and CO_2 at a total flow rate of 4.7 mL·min^{-1}, was allowed to pass through (pressurized) liquid EO, 57 % of the carbon dioxide was converted into ethylene carbonate, with a TOF of 7.6 h^{-1}.[15] More recently, the CF insertion of CO_2 was performed in a tube-in-tube gas-liquid reactor comprised of a CO_2 permeable inner coil continuously fed by styrene oxide (SO) and a mixture of tetrabutylammonium bromide and zinc bromide (TBAB/$ZnBr_2$ as a homogeneous catalyst), surrounded by an external jacket pressurized with CO_2: this configuration allowed a quantitative SO conversion under relatively mild conditions (T = 120 °C, $p(CO_2)$ = 6 bar).[16] Heterogeneous catalytic systems based on d-block metal catalysts were also employed for CO_2 insertion in CF conditions. For instance, $NbCl_5$ and the ionic liquid 1-hydroxypropyl-3-n-butylimidazolium chloride, supported on protonated carboxymethylcellulose (HBimCl-$NbCl_5$/HCMC), were tested as catalysts for CO_2 insertion in a library of epoxides at T = 130 °C and $p(CO_2)$ = 15 bar (6 examples, yields = 68 - 99%).[17] More recently, a metal-organic framework modified with Sc [MOF MIL-101(Sc)] was active for the conversion of PO to PC in up to 57 % yield, using chlorobenzene as a solvent at T = 100 °C and $p(CO_2)$ = 5 bar.[18] On the other hand,, catalytic systems based on salts/complexes of alkali and alkaline earth metals have been less investigated for the preparation of COCs. One of the few available studies reported a Cs-P-Si fixed bed reactor which, albeit active for the transformation of propylene oxide (PO) to propylene carbonate (T = 200 °C, $p(CO_2)$ = 140 bar, PO/CO_2 at F = 0.2 mL·min^{-1}, conversions up to 81%), showed extensive catalyst leaching in the reaction mixture with complete deactivation in t = 5 h.[19] Other strategies to carry out the insertion of CO_2 into terminal epoxides over alkali/alkaline earth metal-based catalysts were limited only to batch conditions. Typically, reactions were performed in homogenous conditions in the presence of cocatalysts acting as both hydrogen bond donor and cation coordinating agents,[20] *e. g.* glycols, crown ethers and polyethers,[21,22,23] which were also necessary to overcome the well-known

solubility issues of metal salts in epoxides/organic solvents. For example, a system comprised of KBr embedded in polyethylene glycol 400 (PEG400) was reported for the conversion of a library of epoxides (13 examples) into the corresponding carbonates with yields > 90 % in all cases.[24] More recently, in a similar fashion, CaI_2 in combination with poly(ethyleneglycol) dimethyl ether (PEG DME 500) proved effective towards CO_2 insertion into both terminal and internal epoxides: at T = 25-90 °C and $p(CO_2)$ of 10-50 bar, the corresponding COCs (27 examples) were obtained in variable yields from 51 to 99%. The catalytic system was then further optimized using PEG400 dimethyl ether as a complexing agent, allowing a scaling up of the CO_2 insertion reaction starting from 10 g of reacting epoxides.[25,26,27,28,29] In the light of these results, the long-standing interest in sustainable CF reactions by the group with which this Thesis work has been carried out [30,31,32,33] prompted part of the research program of this PhD thesis to investigate whether mixtures of organic ligands based on oligo- and poly-glycols and alkali/alkaline earth metal halides, could be used for the preparation of COCs in CF mode. This was a substantially unexplored area with major challenges associated to the control of the viscosity of the complexing agent and the design of a liquid/gas biphasic system able to ensure reactants/catalyst miscibility and suitable contact time for the process. This chapter reports that the CO_2 insertion in model epoxides succeeded by using a diethylene glycol (DEG)/NaBr catalytic system. DEG was chosen as a model hydrogen bond donor moiety due to its ability to coordinate Na^+ cations. After an initial screening on the effects of reaction parameters in batch conditions (in an autoclave), the reaction was implemented in the continuous mode by making a homogenous mixture of DEG, NaBr and the selected epoxide flow through a capillary steel column (the CF-reactor), under controlled flow/pressure of CO_2. At T = 140 - 220 °C and $p(CO_2)$ = 120 bar, conversions of the tested epoxides (styrene oxide, SO; butyl glycidyl ether, BGE and 1,2-epoxyhexane, EO) ranged from 75 to > 99 %, and the corresponding COCs were achieved with selectivity up to 93 %. The CF-setup proved robust and flexible since the products were separated by continuous extraction at the reactor outlet, while the (homogenous) catalyst as a DEG/NaBr mixture was recovered and reused**.**
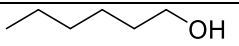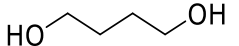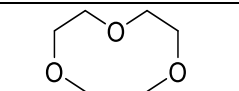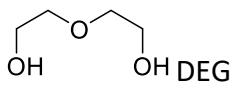
4.2   Results and discussion

4.2.1   Batch conditions

Choice of complexing agent (co-catalyst). The insertion of CO_2 into styrene oxide (**1a**: SO) was chosen as a model reaction to investigate in the presence of NaBr as the catalyst and different glycols and alcohols as co-catalysts/complexing agents. Diethylene glycol (DEG), diethylene glycol dimethyl ether (DEGDME), 1-hexanol, and 1,6-hexanediol were tested. With the aim to preliminarily explore the effects of reaction parameters, initial experiments were carried out in the batch mode. A steel pressure vessel (autoclave, 200 mL) was charged with a homogenous solution of SO (0.4 g, 3.33 mmol), NaBr and the selected glycol in SO/NaBr/glycol 1:0.1:0.3 molar ratio. The mixture was then heated at 50-100 °C under 40 bar of CO_2, under magnetic stirring. Results are summarized in Table 4.1 which reports the conversion of SO and the yield of styrene carbonate (SC: 4-phenyl-1,3-dioxolan-2-one) determined after 5 h.

Table 4.1. *The insertion of CO_2 in styrene oxide catalyzed by NaBr: effects of the co-catalyst and the temperature under batch conditions*

Entry	Co-catalyst	T (°C)	Yield (%)[a,b]

1	1-hexanol	100	12
2	1,6-hexanediol	100	14
3	DEGDME	100	3
4	DEG	50	20
5		75	60
6		100	99

All reactions were carried out in an autoclave charged with a mixture of SO, NaBr and the co-catalyst in a 1:0.1:0.3 molar ratio, respectively. [a] Yield were determined by ^{1}H NMR using mesitylene as an internal standard. [b] Selectivity were always >99% according to ^{1}H NMR and GC/MS analysis

Hexanol, 1,6-hexanediol and the methyl capped-glycol (DEGDME) offered poor reaction conversions not exceeding 12, 14 and 3 % at T = 100 °C, respectively (Entries 1-3, Table 4.1). By contrast, quantitative and exclusive formation of SC was achieved when DEG was used as a co-catalyst (entry 6). Diethylene glycol proved active even at temperatures between 50 and 70 °C, albeit with lower conversions (21 and 62%, respectively: entries 4-5). These comparative experiments demonstrated the superior performance of DEG suggesting that its structure was particularly suited for the complexation and activation of NaBr and the reactant epoxide. To the best of our knowledge, the use of DEG/NaBr was an unprecedented combination to promote CO_2 insertion reactions. The study of this mixture was continued at 100 °C.

Effects of reaction time, reactant:catalyst molar ratio, and CO_2 pressure. A series of experiments was carried out at 100 °C by changing one at a time, the reaction parameters of Table 4.1, specifically by decreasing: i) the reaction time (t) from 5 to 3 and 2 h, respectively; ii) the SO:NaBr:DEG molar ratio (W) from 1:0.1:0.3 to 1:0.05-0.025:0.3 and then 1:0.1:0.2 and finally, in the absence of either DEG or NaBr; iii) the CO_2 pressure from 40 to 10, 2 and 1 bar. In the latter case (1 bar = atmospheric pressure), the CO_2 insertion process was carried out in a conventional glass flask (50 mL) equipped with a 2 L CO_2 reservoir. The experimental set-up for batch reactions run using conventional lab glassware is illustrated in Figure 4.2. The CO_2 pressure, *p* = 1.06 bar, was measured by a portable digital manometer. At *p* = 1.06 bar, the 2 L reservoir used in the experiments, supplied an amount of CO_2 which exceeded by several orders of magnitude that required for the quantitative conversion of the reactant epoxide (3.3 mmol). Therefore, no measurable pressure drop was appreciated during the reaction.
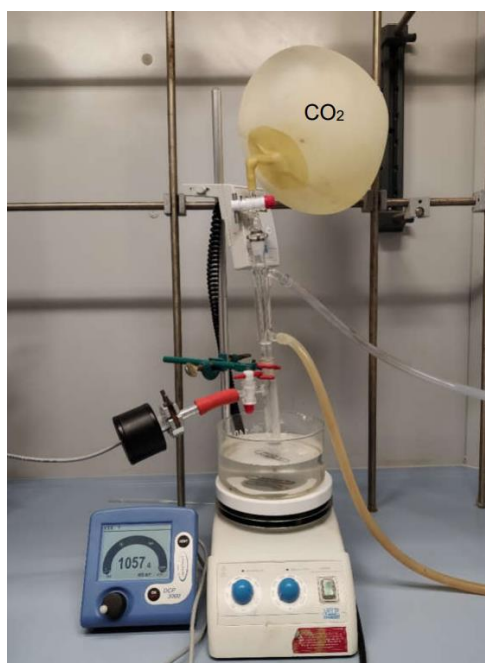
Figure 4.2. *CO$_2$ insertion into styrene oxide carried out at atmospheric pressure*

All reactions were run in duplicate for reproducibility ensuring <5% difference in conversion and selectivity between repeated tests. The results are reported in Table 4.2.

Table 4.2. *The insertion of CO$_2$ in styrene oxide catalyzed by NaBr/DEG: effects of relevant reaction parameters under batch conditions*

Entry	p0(CO$_2$) (bar)	t (h)	SO:NaBr:DEG (molar ratio)	Yield (%)[a,b]
1	40	5	1:0.1:0.3	> 99
2	40	3	1:0.1:0.3	> 99
3	40	2	1:0.1:0.3	96
4	40	3	1:0.05:0.3	62
5	40	3	1:0.025:0.3	20
6	40	3	1:0.1:0.2	85
7	40	3	1:0:0.3	0
8	40	3	1:0.1:0	0
9	10	3	1:0.1:0.3	> 99
10	2	3	1:0.1:0.3	> 99
11	1	3	1:0.1:0.3	> 99

All reactions were carried out at 100 °C, in an autoclave charged with a mixture of SO (3.33 mmol), NaBr and DEG in the reported molar ratio. [a] Yield were determined by ^{1}H NMR using mesitylene as an internal standard. [b] Selectivity were always >99% according to ^{1}H NMR and GC/MS analysis

Compared to the 5 h tests of Table 4.1, 3 h were sufficient for quantitative reactions, while a slight decrease of the conversion (from 99 to 96%) was noticed after 2 h (Entries 1-3, Table 4.2). Further experiments were conducted on this basis (3 h). A pronounced effect, particularly on the extent of the SO conversion, was observed by varying the reactant/catalyst/DEG molar ratio. Indeed, when the catalyst (NaBr) was reduced from 10 to 5 mol % and then to 2.5 mol%, the conversion of the epoxide dropped from 99 to 62 and 20%, respectively (Entries 2, 4 and 5). This clearly indicated the role of the halide salt concentration in the process kinetics, pointing out how the bromide-mediated ring opening of the epoxide was the rate-determining step of the overall CO$_2$ insertion process. In line with this observation, decreasing the loading of the co-

catalyst (DEG) from 30 to 20 mol % caused a reduction of the SO conversion, from 99 to 85%, (Entries 2 and 6) consistent with a lower bromide activation. In addition, DEG could assist the reaction through its hydrogen bond donor activity, making the epoxide ring cleavage easier (see later, Scheme 4.2). The synergic action of the catalyst and the co-catalyst was unambiguously proved by the tests in the absence of either NaBr or DEG where no reaction took place (Entries 7 and 8). Conditions investigated so far suggested that the best results were achieved using the mixture of SO, NaBr, and DEG in the W= 1:0.1:0.3 molar ratio, respectively. This (W) ratio was set to study the pressure effect. Experiments demonstrated that the reaction outcome was not affected by the pressure over the range 1-40 bar, wherein SO was quantitatively converted into styrene carbonate (Entries 9-11, Table 4.2). In agreement with Figure 4.1, CO_2 insertion was apparently much faster compared to the RDS (rate determining step), *i.e.* epoxide ring opening. A plausible mechanistic hypothesis for catalyst activation by DEG is shown in Scheme 4.2.
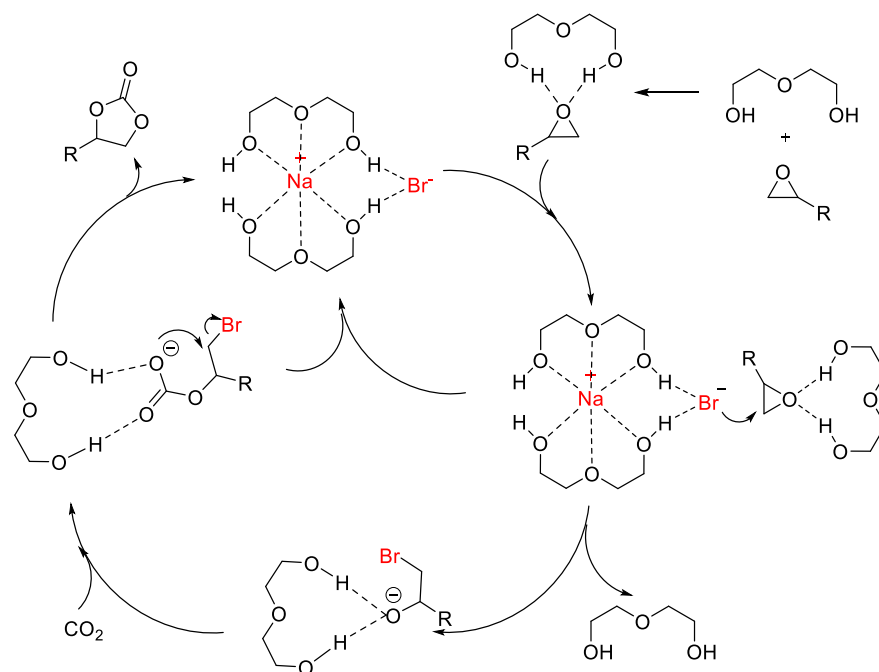
Scheme 4.2. *Proposed mechanism for the co-catalytic effect of DEG. Top, mid: the activation of NaBr; top-to-bottom, right: hydrogen bond donor assistance to the epoxide ring cleavage*

Diethylene glycol plausibly played a double role acting as a chelating agent for Na$^+$ but also as a hydrogen bond donor (HBD) that assisted the ring-opening of the reactant epoxide. Both the complexing and HBD activity of polyethylene glycols are indeed widely reported.[23-28,34] Overall, TablesTable 4.1Table 4.2 show that an effective and robust batch synthesis of styrene carbonate was achieved. These results were further examined by assessing the performance of NaBr/DEG with respect to that of 7 other recently reported halide-based catalysts, with characteristics in terms of commercial availability and ease of handling comparable to our system. These included combination of iodide salts (KI and CaI$_2$) with polyethylene glycols, crown ethers, β-cyclodextrin, polyvinyl alcohol, etc. Albeit the range of operating conditions was widely variable (T, *p*, and t from 25 to 140 °C, 1 to 60 bar, and 3 to 48 h, respectively), on balance, the DEG/NaBr mixture was equally, if not more, active and economic than other systems. (Table 4.3).

Table 4.3. *The performance of the DEG/NaBr mixture compared to other catalyst for the CO_2 insertion into styrene oxide*

Entry	Catalyst	Co-catalyst	T (°C)	t (h)	p (bar)	SC, Yield (%)	Ref.
1	NaBr	DEG	100	3	1	99	This work
2	CaI_2	PEGDME 500[a]	25	24	10	91-93	25,26
3	CaI_2	CE 18C6[b]	23	24	1	82	27
4	KI	TEG[c]	40	48	1	99	23
5	KI	β-Cyclodextrin	120	24	60	94	35
6	KI	PVA[d]	120	17	15	99	36
7	KI	Lignin	140	12	20	87	37
8	KI	Pentaerythrol	130	4	25	95	38

[a] Poliethylen glycol dimethyl ether [b] Crown Ether 18C6 [c] Tetraethylene glycol [d] polyvinyl alcohol

Substrate scope. Under the best conditions for the conversion of SO (Entries 2 and 11, Table 4.2), the activity of the binary mixture of NaBr/DEG was tested for 6 other terminal epoxides including 1,2-epoxybutane (**1b**), 1,2-epoxyhexane (**1c**), 1,2-epoxydecane (**1d**), butyl glycidyl ether (**1e**), phenyl glycidyl ether (**1f**), and 1,4-butanediol diglycidyl ether (**1g**). Reactions were carried out at T = 100 °C for t = 3 h, using a solution of the epoxide, NaBr, and DEG in a 1:0.1:0.3 molar ratio, respectively. Experiments were performed at both $p^0(CO_2)$ = 40 bar and atmospheric pressure. All the tested epoxides were quantitively and selectively converted into the corresponding COCs (**2b-g**), (Scheme 4.3), thereby confirming that: i) the batch protocol could be extended to a range of different epoxides; ii) CO_2 insertion reactions were not substantially affected by the CO_2 pressure. In the case of the diepoxide **1g**, the bis-cyclic carbonate **2g** was obtained.

1b:R= Et; **1c**: R=n-Bu; **1d**: R= *n*-Oct
1e: $CH_3(CH_2)_3OCH_2$; **1f**: $C_6H_5OCH_2$

1g:
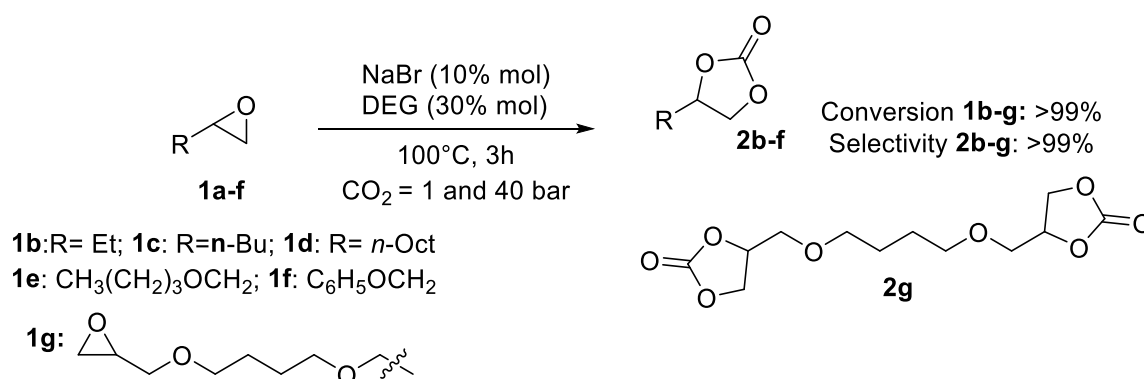
Scheme 4.3. *NaBr/DEG catalyzed CO_2 insertion in terminal epoxides: substrate scope. Conversion and selectivity were determined by GC in the presence of mesitylene as internal standard*

The batch protocol was also examined using the internal epoxide of methyl oleate, *i.e.* methyl 8-(3-octyloxiran-2-yl) octanoate (**1h**) in its pure diastereomeric *cis-* form. Under the conditions of Scheme 4.3, the reaction conversion was 66% and the selectivity to the carbonate derivative, methyl 8-(5-octyl-2-oxo-1,3-dioxolan-4-yl) octanoate (**2h**), was 50% (60:40 *cis-/trans-*). The only observed by-product (16%) was methyl 9-oxooctadecanoate coming from a known isomerization process of the starting epoxide,[39] (Scheme 4.4).
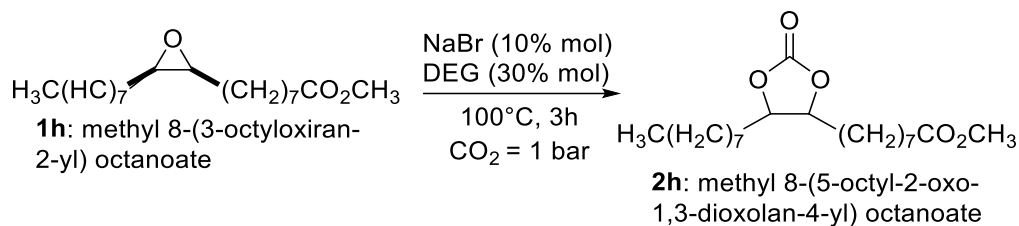
Scheme 4.4. *NaBr/DEG catalyzed CO_2 insertion in the internal epoxide **1h**. Conversion and selectivity were determined by GC in the presence of mesitylene as internal standard*

Under the reaction conditions, the *cis*-epoxide plausibly underwent the formation of trans-epoxidized methyl oleate which accounted for the presence of the carbonate **2h** product in a 60:40 *cis-/trans-* mixture. Carbonate products were characterised by ^{1}H- and ^{13}C-NMR and GC/MS (details are reported in Appendix A.2).
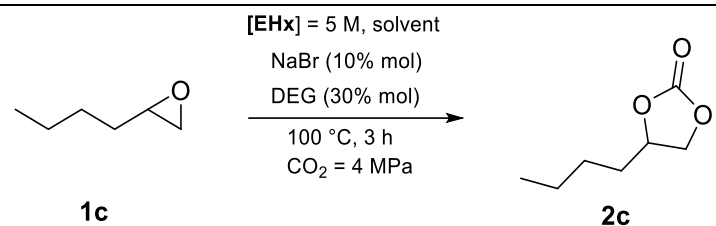
4.2.2 Continuous Flow (CF)

CF-setup. The encouraging results obtained investigating the CO_2 insertion in batch mode prompted us to extend the protocol under continuous-flow conditions. Flow chemistry is one of the top ten emerging technologies with high potential for sustainable syntheses,[40,41] yet, from a chemical engineering standpoint, the transfer from a batch to a continuous process poses some issues especially when a setup comprised of a polar liquid mixture and nonpolar (gaseous or liquid/supercritical) CO_2 are present as in the case of this work. We focused on two main aspects: i) identification of a liquid carrier (solvent) to achieve a homogeneous solution of epoxide, NaBr and DEG and with low enough viscosity for continuous pumping for extended time; ii) design of an experimental setup with full control of liquid and CO_2 flows (*i.e.* pressure/contact time) able to ensure miscibility of all the components (reactants/catalyst/co-catalyst/CO_2).

In search for a solvent for the insertion of CO_2 into epoxides catalyzed by NaBr/DEG, five conventional liquid solvents ordered by increasing polarity as toluene, chloroform, THF, 2-butanone, and acetonitrile were initially chosen. To a mixture of 1,2-epoxyhexane (**1c**: 3.33 mmol), NaBr, and DEG in a 1:0.1:0.3 molar ratio, respectively, the chosen solvent (667 µL) was added to obtain a 5 M solution of the epoxide. Thereafter, the solution was used to carry out the cycloaddition of CO_2 to compound **1c** in the batch mode, under the conditions of Scheme 4.3 (T = 100 °C, $p^0(CO_2)$ = 40 bar, t = 3 h). Results are reported in

Table **4.4**. The reaction conversion showed a decreasing trend with the solvent polarity, from 40-50 % in toluene and chloroform (Entries 1-2), to 18% in 2-butanone and acetonitrile (Entries 4-5). However, the higher the conversion the lower the selectivity, due to the formation of by-products. In all cases, these by-products could not be identified unambiguously by ^{1}H NMR and GC-MS. Whichever the reasons for this behavior, the overall results were unsatisfactory with respect to those in the absence of solvents where 100 % selectivity was achieved at complete conversion (compare Table 4.1Table 4.2).

Table 4.4. *Insertion of CO_2 in 1,2-epoxyhexane (EHx) catalyzed by NaBr/DEG, in the presence of a solvent*

Entry	Solvent	ε^a	1c, Conv. (%)	2c, Sel. (%)	By-products (%)
1	Toluene	2.38	41	54	19
2	Chloroform	4.81	49	70	15
3	THF	7.58	28	39	17
4	2-butanone	18.6	18	67	6
5	Acetonitrile	37.5	18	>99	-

All reactions were run in batch conditions (autoclave). Conversion of **1c** and selectivity towards **2c** were determined by ^{1}H NMR in presence of an internal standard (mesitylene). ^{a}The polarity of the investigated solvents was compare through the corresponding dielectric constant.

This study proved that DEG was not only an excellent complexing agent, but it could also act as the best reaction medium. Hence, when reacting a mixture of 1,2-epoxyhexane (**1c**: 3.33 mmol) and NaBr in a 1:0.1 molar ratio, respectively, DEG (500 µL) was added to achieve a 5 M solution of the epoxide. Thereafter, the solution was used to carry out the CO_2 insertion into compound **1c** in batch mode, under the conditions of Scheme 2 (T = 100 °C, $p^0(CO_2)$ = 40 bar, t = 3 h). The reaction occurred smoothly, retaining the high conversion/selectivity (both > 99%) reported in Scheme 4.3. Similar outcomes were observed with other terminal epoxides, such as styrene oxide (**1a**) and butyl glycidyl ether (**1e**) as reactants (Scheme 4.5).
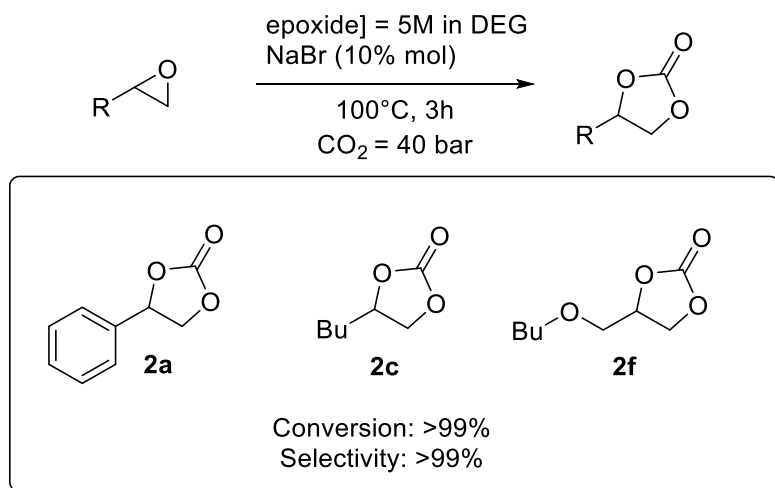
Scheme 4.5. *Insertion of CO_2 into terminal epoxides catalyzed by NaBr using DEG as co-catalysts and solvent. Conversion and selectivity determined by ^{1}H NMR*

Based on the expertise in flow chemistry of our group,[32-33,42] the CF-apparatus was designed and in-house assembled, using a microfluidic reactor in the shape of 1/16'' stainless-steel coil (Figure 4.3).

176
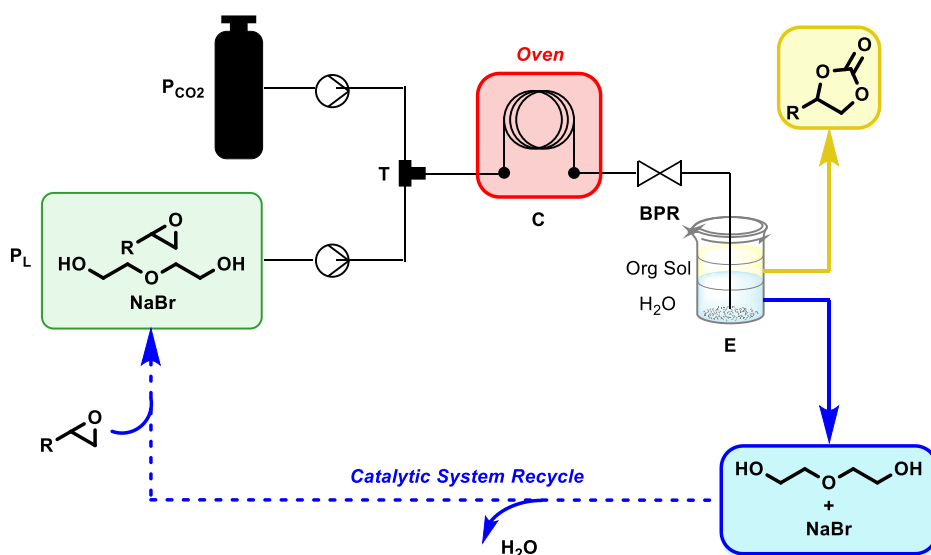
Figure 4.3. *CF apparatus used for CF CO_2 insertion into epoxides*

CO_2 was supplied as a liquid from a commercial CO_2 cylinder equipped with a dip tube and then compressed at the desired pressure and flow by a refrigerated dual head pump (**PCO₂**). The solution of epoxide, NaBr and DEG was delivered by an HPLC pump (**PL**). The CO_2 and liquid streams were mixed in T junction (**T**) and conveyed to the CF-reactor (**coil C**) placed inside an oven for the temperature control. A backpressure regulator (**BPR**) maintained a constant operating pressure throughout the system and allowed the depressurization and recovery of the reaction mixture in the extractor (**E**) where the COC product was separated from the NaBr catalyst and DEG cocatalysts which were recycled (*vide infra*).

The CF insertion of CO_2 into 1,2-epoxyhexane (1c). Compound **1c** was chosen as a model terminal epoxide to begin the study of CF CO_2 insertions, due to its relatively low toxicity and reduced the risks associated to its use in CF systems under pressure. Experiments were carried out using a 1 M solution of **1c** in DEG in the presence of NaBr (0.1-1 molar equiv. with respect to **1c**). This mixture was fed along with CO_2 to the CF-reactor of Figure 4.3: for screening tests, the dimensions of the steel coil were 2500 x 0.2 mm (length x internal diameter; $7.85 \cdot 10^{-2}$ cm^3 internal volume). Check valves were placed to avoid cross-contamination. All tests were run for t = 2 h by changing different pressure, temperature, and flow rates of the liquid solution (FL) and CO_2 (FCO₂) stream in the range of 60-150 bar, 150-220 °C, 0.1-1.0 mL min^{-1}, and 1.0-4.0 mL min^{-1}, respectively. GC and GC-MS analyses of reaction mixtures samples confirmed the formation of 3 different products: hexene carbonate (**2c**), 1-bromohexan-2-ol (**3c**: BHO), and hexane-1,2-diol (**4c**) (Scheme 4.6).
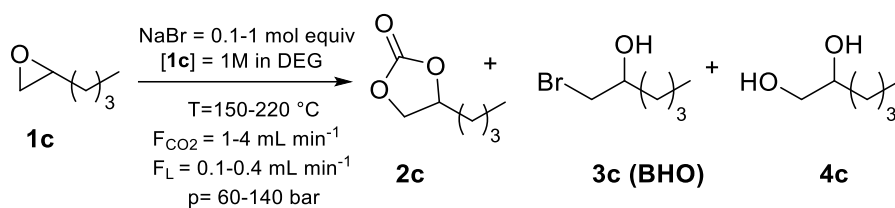
Scheme 4.6. *The CO_2 insertion in EHx in the presence of NaBr/DEG under CF conditions*

According to the mechanism of Scheme 4.2, the bromohydrin (**3c**: BHO) was the reaction intermediate formed by the nucleophilic attack of the bromide anion to the primary carbon

atom of the epoxide ring, as confirmed by GC-MS and NMR (see Appendix A.2 for further details) Formation of the diol **4c** (MS spectrum in Appendix A.2) was due to hydrolysis of the starting epoxide plausibly promoted by traces of water in the highly hygroscopic DEG.[43]

Initial CF experiments proved that the recovery of the reaction products and the unreacted starting material was problematic because volatile species, particularly the starting epoxide, were stripped from the flow of CO_2. This was an issue for the quantitative evaluation of conversion and products' distribution (and therefore, for the reproducibility and the mass balance of the protocol). For the recovery of the products of Scheme 4.6, the simplest method was to convey the reaction mixture to a separatory flask containing a biphasic system of water and an organic solvent (30 mL of each phase). Different organic solvents including diethyl ether, diethyl carbonate (DEC), cyclopentyl methyl either (CPME), *n*-hexane and ethyl acetate were compared to this purpose. Hexene oxide (**1c**) was chosen as model for this investigation. The CF insertion of CO_2 into **1c** was carried out under the following conditions: [**1c**] = 1M in DEG, NaBr 1 equiv., T = 220°C, *p* = 120 bar, F_{CO2}= 1 mL·min^{-1}, and F_L=0.1 mL·min^{-1}. From GC and GC-MS analyses, the products detected in the organic phase were hexylene carbonate (**2c**), 1-bromohexan-2-ol (**3c**: BHO), and hexane-1,2-diol (**4c**) (Scheme S2). Results are summarized in Table 4.5.

Table 4.5. *Comparative experiments for the recovery/analysis of CF-reactions*

Entry	Solvent[a]	Conv.[b] (%)	Products selectivity (%)[c]			Mass recovery (%)[d]
			2c	3c	4c	
1	diethyl ether	88	81	15	4	98
2	DEC	86	82	13	5	98
3	CPME	85	80	16	4	97
4	*n*-hexane	89	78	17	5	97
5	ethyl acetate	87	81	15	4	n.d.

[a] A liquid biphasic system comprising of water (10 mL) and an immiscible organic solvent (10 mL) was used to recover the reaction mixture out of the CF-reactor. [b] Conversion of EHx. [c] Selectivity (%) towards hexene carbonate, bromohexan-2-ol, and hexane-1,2-diol. [d] Mass recovery of reactant and products in the organic phase. n.d. = not determined.

The extraction efficiency in each solvent was defined by the % mass recovery, defined as:

Mass Recovery (%) = [total molar amount of unconverted epoxide and reaction products extracted in the organic phase (mmol) / molar amount of the starting epoxide (mmol)] x 100. The molar amount of unconverted epoxide and reaction products in the organic phase were evaluated after collecting the reaction mixture for 2 hours. Once the experiment was complete, the two phases were separated. The aqueous phase was dried under vacuum, and the DEG + NaBr mixture was quantitively recovered. The organic phase was dried with Na_2SO_4, filtered, and then the excess of solvent (Et_2O, *n*-hexane, Et_2OAc) was removed and recovered in vacuo. Quantitative isolation of the resulting carbonate **2c**, **3c**, and **4c** mixture was easily achieved.

Similar high efficiencies (> 97%) were obtained in diethyl ether, DEC, CPME and *n*-hexane (Entries 1-2). In these extraction solvents, it was noticed that the hydrophilic reaction solvent/carrier, diethylene glycol, was absent. Indeed, DEG was completely dissolved in the aqueous phase. This result was beneficial not only for the isolation of the reaction products, but also for the catalyst and co-catalyst (NaBr and DEG) recycling. Ethyl acetate proved instead, unsuitable for the recovery of the reaction mixture due to the partition of DEG between the

organic and the aqueous phases, and the corresponding mass recovery (%) was not determined. The choice of the extraction solvent finally fell on diethyl carbonate (DEC) which was not only safer and greener than other tested solvents, but also the most suited to dissolve carbonate products. Figure 4.4 reports a gas-chromatogram of the reaction mixture extracted in DEC.
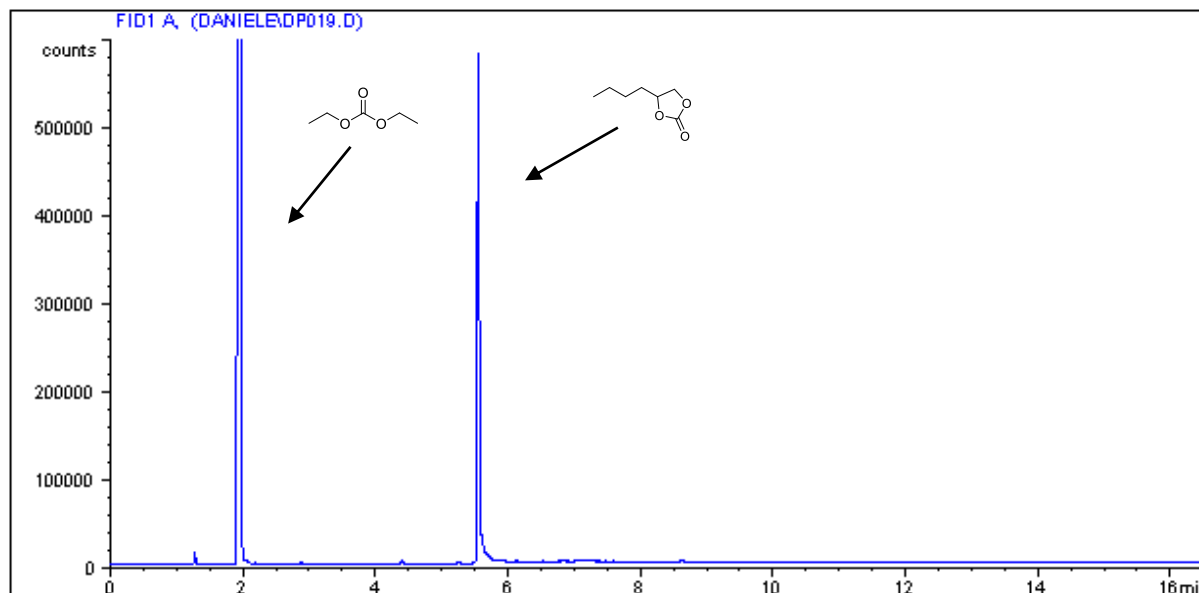
Figure 4.4. *GC-chromatogram of carbonate **2c** in DEC solvent*

Then, all tests were run in duplicate for reproducibility: in repeated reactions, conversion and selectivity differed <5% from one experiment to another. Results are reported in Table 4.6. The reaction outcome depended on multiple parameters such as temperature, reactant/NaBr (Q) molar ratio, flow rate, and CO_2 pressure. At the lowest investigated pressure, Q ratio and flow rates (60 bar, FL = 0.1 and mL·min^{-1}, FCO_2 = 1 mL min^{-1} and Q = 0.2), the epoxide conversion was very low at T = 150 °C (8 %) and it was limited even at T = 200 °C, not exceeding 15 % (Entries 1 and 2). Formation of the desired COC product, 4-butyl- 1,3-dioxolan-2-one (**2c**), was also unsatisfactory (up to 13 %), because of the predominant presence of the bromohydrin intermediate (BHO, 80 %). Doubling the system pressure up to p = 120 bar had a modest influence: the corresponding epoxide conversion and selectivity to **2c** were 18 and 19 %, respectively (Entry 3). Further testing showed that significant improvements of the reaction outcome could be reached through the cooperative effects of T and the Q ratio variation. This was exemplified by the results of Entries 4 and 5: at p = 120 bar, when the temperature and the catalyst loading were progressively raised from 200 to 220 °C and from 0.1 to 0.3 and 1 molar equiv., respectively, the epoxide conversion also increased from 18 to 25 and 88% and the carbonate selectivity was enhanced to 81% (Entry 5). Under such conditions, an effect of the pressure was also noticed: albeit an increase to p = 140 bar did not produce appreciable changes, a decrease to p = 100 bar brought about a 9 % reduction of the conversion (from 90 to 82%, compare Entries 6 and 7). Minor variations of products distribution were observed. The CF system pressure, therefore, must be set at a sufficiently high threshold value ($p \geq$ 120 bar) to ensure a constant CO_2 concentration in the reaction environment. In light of these results, the study was continued at T, p, and Q (NaBr:**1c** molar ratio) of 220 °C, 120 bar, and 1, respectively. This choice was corroborated by the following considerations taken from the literature:

179

a) The MSDS reported for diethylene glycol by the supplier (Aldrich-Merck) indicated that the compound distills at 245 °C and atmospheric pressure, without any detectable decomposition. In addition, NMR spectra of DEG recorded before and after its use for CF-reactions run in this work, were perfectly superimposable and did not indicate the presence of degradation by-products, not even at traces level (Figure 4.5).

b) The MSDS reported for propylene carbonate by the supplier (Aldrich-Merck) indicated that the decomposition temperature of the compound is 350 °C;

c) a recent study based on TG–FTIR investigated the thermal pyrolysis of carbonate derivatives of glycerol carbonate.[44] As a measure of the thermal behavior, Authors determined the 5% weight loss temperature ($T_{5\%}$) as the temperature at which each single compound lost 5% of its initial weight. In all cases, $T_{5\%}$ was above 250 °C.
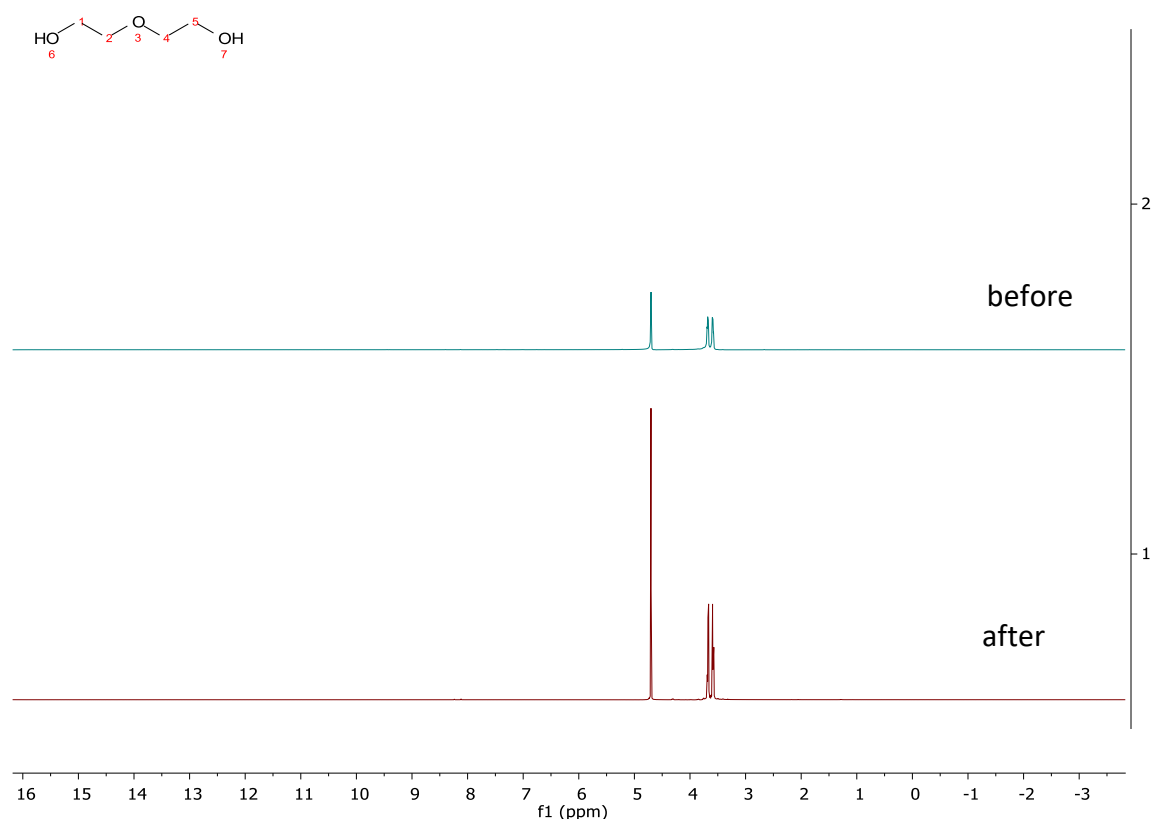
Figure 4.5. *Comparison of ^1H NMR spectra in D_2O of DEG before and after its use in the CF-synthesis of hexylene carbonate **2c** (220 °C, 120 bar)*

Albeit data (a-c) offer only a partial picture of the thermal behavior of DEG and cyclic carbonates, they suggest that these products were generally stable at temperatures above that used for CF-processes studied in this work (220 °C). This observation was further corroborated by the evaluation of the mass balance of CF-experiments (see the paragraph "Catalytic system recycling and mass balance") which proved how the yields of isolated products were consistent with the conversion and selectivity, thereby indicating that side-reactions of (thermal) degradation did not occur appreciably under the explored conditions.

Overall, temperatures > 220 °C were not explored in this work: indeed, a partial thermal degradation of DEG was noticed above 220 °C resulting in clogging of the CF-reactor.

The influence of changing the flow rate of both the reactant solution (FL) and CO_2 (FCO_2) stream was then investigated. Experiments were first carried out by increasing FL from 0.1 to 0.2 and 0.4 mL·min^{-1}, at a constant FCO_2 (1 mL min^{-1}). No apparent effects on the reaction outcome were noticed (Entries 5 and 8-9). The reaction productivity [defined as moles of carbonate product · (h · cat. equivs)$^{-1}$], however, was substantially enhanced: by quadrupling FL, the rate of EHxC formation went up from 4.3 mmol h^{-1} equiv^{-1} to 15.9 mmol h^{-1} equiv^{-1} with an increase by a factor of 3.7. When FL was further raised to 1 mL min^{-1}, a drop of both the conversion (73 %) and the carbonate selectivity (63 %) was observed (Entry 10); yet, the productivity continued to increase up to 27.6 mmol h^{-1} equiv^{-1}. No further investigations were carried out in this respect, but it should be noted here that under batch conditions, the maximum productivity for carbonate **2c** was 11.1 mmol h^{-1} equiv^{-1} (Scheme 4.3), about 2.5-fold lower than that in the CF-mode.

Table 4.6. *Synthesis of carbonate **2c** (hexylene carbonate) from 1,2-epoxyhexane (**1c**) and CO_2 in the continuous mode. Effects of key reaction parameters*

Entry	1c:NaBr (Q, mol:mol)	F_L/F_{CO2} (mL/min)	p (bar)	T (°C)	Conv. (%) [a]	Sel. (%) [a]		
						2c	3c	4c
1	0.1	0.1/1	60	150	8	-	>99	-
2	0.1	0.1/1	60	200	15	13	80	7
3	0.1	0.1/1	120	200	18	19	74	7
4	0.3	0.1/1	120	200	25	26	67	7
5	1	0.1/1	120	220	88	81	15	4
6	1	0.1/1	140	220	90	82	15	3
7	1	0.1/1	100	220	82	79	18	4
8	1	0.2/1	120	220	88	78	17	5
9	1	0.4/1	120	220	84	79	16	4
10	1	1/1	120	220	73	63	30	7
11	1	0.1/4	120	220	69	77	19	4

All reactions were run for t = 2 h. [a] Conversion and selectivity were determined by GC-MS analysis

Increasing FCO_2 from 1 to 4 mL min^{-1} (at constant FL = 0.1 mL min^{-1}) was also detrimental for the epoxide conversion, which was reduced from 88 to 69 % (compare Entries 5 and 11). These findings highlighted how the feeding rates of the liquid solution (FL) and of supercritical CO_2 (FCO_2) affected the CF reaction: higher flow rates resulted in lower contact times, lower epoxides conversion and lower COC selectivity. Overall, the concept was proved: the CO_2 insertion into **1c** could be engineered to proceed in CF mode in the presence of a homogenous catalyst/co-catalyst system (NaBr/DEG).

Two major challenges remained open: i) devising a purification protocol to allow an efficient separation of products, while effectively recycling the NaBr/DEG "catalytic" mixture; ii) improving the formation of the carbonate product (**2c**). None of the changes of reaction parameters in Table 4.6 was effective in this respect: the selectivity to compound **2c** apparently levelled off, never exceeding 82 %, mainly because of the formation of the BHO intermediate which persisted in the final reaction mixtures. The selectivity to the diol (**4c**) showed instead, a general decreasing trend from 7% to 3-4% as the epoxide conversion increased from ca 20 to >80%, respectively.

Catalytic system recycling and mass balance. Experiments on the recycling of the NaBr/DEG system were carried out under the experimental conditions of Entry 5, Table 4.6 ([**1c**] = 1 M in DEG; NaBr (1.0 equiv.); FL = 0.1 mL·min⁻¹, FCO₂ = 1 mL·min⁻¹, *p* = 120 bar, T = 220 °C), as summarized in Scheme 4.7.
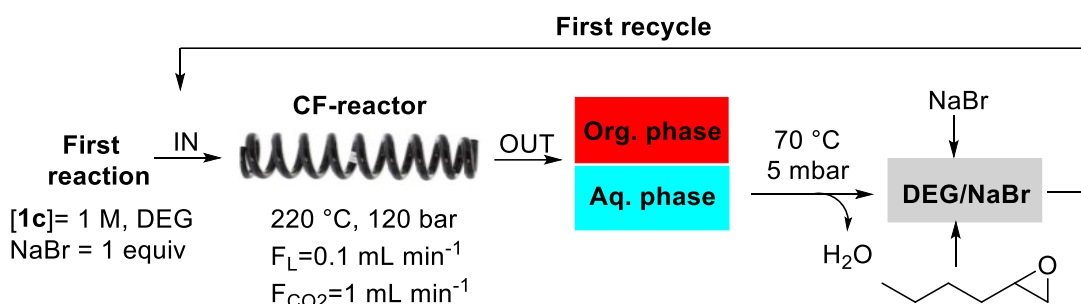
Scheme 4.7. *Catalytic system recycling in CF-mode*

In a typical setup, a CF-reaction was allowed to proceed for t = 2 h and continuously collected at the reactor outlet by venting it in a biphasic mixture consisting of diethyl carbonate and water (Figure 4.3). The catalytic system (DEG and NaBr) present exclusively in the aqueous layer, was collected and evaporated under reduced pressure (T = 70 °C, *p* = 5 mbar) until complete removal of water. To the resulting liquid was added fresh epoxide (**1c**: 12 mmol to obtain a 1 M solution in DEG) and an additional aliquot of NaBr (163 mg, 1.6 mmol). The latter was necessary to integrate the amount of catalyst consumed by the formation of the bromohydrin intermediate (**3c**: BHO), and it was calculated to restore the initial quantity of NaBr (*i.e.* to achieve an epoxide:catalyst molar ratio of 1, based on 88% conversion and 15% selectivity towards BHO, see Entry 5, Table 4.6). A similar topping-up procedure was reported for CO_2 insertion in epoxides also in the presence of dual component organocatalysts based on pyrogallol and onium iodides.[45] The solution was then delivered to the CF-reactor for the first recycle run. The steps of Scheme 4.7 were repeated for 4 subsequent recycles. The amount of fresh NaBr was adjusted after each experiment according to the conversion and the selectivity achieved case-by-case. Results are reported in Figure 4.6.
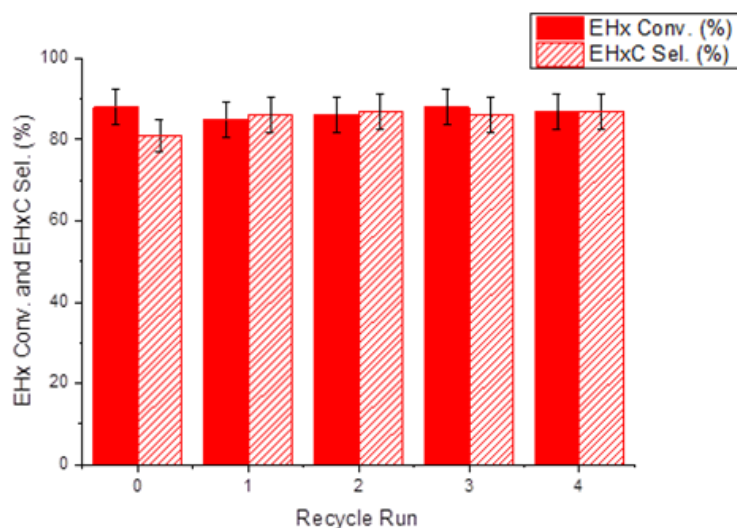
Figure 4.6. *DEG/NaBr system recycling upon CF synthesis of hexylene carbonate (**2c**). Conditions: [**1c**] = 1 M in DEG, NaBr:**1c** = 1.0 mol/mol; F_L = 0.1 mL·min^{-1}, F_{CO2} = 1 mL·min^{-1}, p = 120 bar, T = 220 °C. Run 0 (first reaction) refers to the result of Entry 5, Table 4.6*

After each recycle, both the conversion and EHxC selectivity were substantially steady at ca 85-90% and 80-85%, respectively, thereby proving that the NaBr/DEG catalytic mixture was reusable without loss of performance. It should be noted however, that undesired hydrolysis of the alcoholate precursor of the bromohydrin intermediate (Scheme 4.8), produced NaOH as byproduct which accumulated in the DEG solution, making it denser and (slightly) more viscous after each cycle.
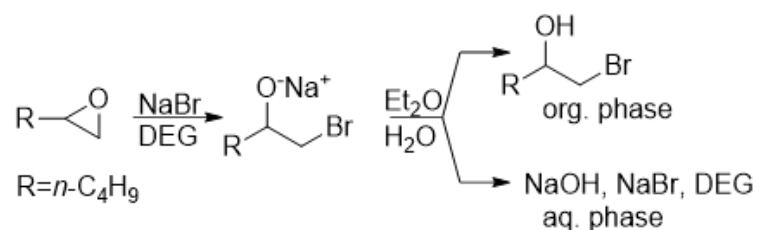
Scheme 4.8. *Hydrolysis of the alcoholate precursor of bromohydrin*

Although this feature was not investigated in detail, nor its consequences were apparent from Figure 4.3, nevertheless it could plausibly bring about a limitation in view of an indefinite recycle of the DEG solution: the higher its viscosity/density, the more difficult the mass transport, especially in microfluidic reactors.[46] Moreover, part of NaBr was irreversibly consumed in each reaction run. Recycle experiments allowed to confirm the reaction mass balance. To this aim, the organic phase (containing exclusively the products) was collected and concentrated *in vacuo* (T = 30 °C, p = 50 mbar) and dried. The desired product, EHxC was then isolated by FCC, with isolated yields ranging between 66 and 71 %, consistent with the conversion and selectivity reported in Table 4.6.

Further experiments have been performed for the validation of the mass balance during recycle experiments. The mass balance (mass recovery) was validated during recycle experiments with respect to the catalyst/co-catalyst system (DEG/NaBr) and the reaction products (for hexene oxide: compounds **2c**, **3c**, and **4c**). Under the conditions of Scheme 4.6 and Figure 4.3, the mixture at the reactor outlet was recovered into a H_2O/DEC biphase, during four subsequent

recycle tests. The separation of DEG/NaBr and reaction products occurred in the aqueous and organic phases, respectively, in each case. The water solution was dried *in vacuo*, while the organic phase was dried over Na_2SO_4, filtered, and rotary-evaporated (T = 30°C, *p* = 50 mbar) for the removal of the solvent. Both mixtures of DEG/NaBr and products **2c**, **3c**, and **4c** were recovered in >97% and >96% yield, respectively, after all recycles. Results are reported in Table 4.7.

Table 4.7. *Mass recovery of the DEG/NaBr and mixtures of products* **2c**, **3c**, *and* **4c** *during the recycles*

Entry	Mixture	First reaction (g)[a]	Recycle (g)[b]				Mass recovery (%)[c]
			1	**2**	**3**	**4**	
1	DEG/NaBr	14.32	14.24	14.20	14.09	13.92	97
2	products 2c, 3c, and 4c	1.20	1.19	1.18	1.17	1.15	96

[a] Amounts (g) of DEG/NaBr and products **2c**, **3c**, and **4c** recovered after the first reaction. [b] Amounts (g) of DEG/NaBr and products **2c**, **3c**, and **4c** recovered after each recycle. [c] Mass Recovery (%) = [total molar amount of unconverted epoxide and reaction products extracted in the organic phase (mmol) / molar amount of the starting epoxide (mmol)] x 100.

The mass recovery of the DEG/NaBr was reported considering the loss of Br$^-$ ions due to the formation of bromohydrin **3c**. In addition, the carbonate **2c** was isolated by FCC (stationary phase: Silica gel, eluent: hexane/ethyl acetate 3:1 v/v) after each of the four recycle test. The corresponding (isolated) yields were 66%, 71%, 65 %, and 68%. These values were consistent with the results of GC-MS analyses of Figure 4.3.

Improving the selectivity: effect of reactor length (contact time) and substrate scope. Previous experiments highlighted that the selectivity towards the EHxC product was mostly limited by formation of BHO. Increasing the contact (residence) time could plausibly favour the conversion of BHO into hexylene carbonate **2c**. However, the technical specs of the pumps of our CF system did not allow flow rates lower than the values specified in Table 4.6 (FL = 0.1 mL·min^{-1} and FCO$_2$ = 1 mL·min^{-1}). A redesign of the CF reactor was therefore required. The same 1/16" steel coil (internal diameter = 0.2 mm) of Figure 4.3 was used, but the reactor length and internal volume were doubled from 250 to 500 cm, and from 7.85·10^{-2} to 0.157 cm^3, respectively. Experiments were performed under the conditions of Entry 5, Table 4.6 ([**1c**] = 1 M in DEG; NaBr (1.0 equiv.); FL = 0.1 mL·min^{-1}, FCO$_2$ = 1 mL·min^{-1}, *p* = 120 bar, T = 220 °C). Epoxides **1c** and **1e** (butyl glycidyl ether) were set to react in both the available reactors of 250 and 500 cm; while, two additional tests were run with epoxides **1f** and **1g** using only the longer coil (500 cm). Results are reported in Table 4.8, which compares the conversion and the selectivity towards the desired COC products (**2**) and the corresponding bromohydrins (**3**).

Table 4.8. *CO$_2$ insertion reactions in terminal epoxides: influence of CF reactor length*

Epoxide in DEG = 1 M
NaBr = 1 equiv.
F_L = 0.1 mL min^{-1}
F_{CO_2} = 1 mL min^{-1}

R = $CH_3(CH_2)_3$; $CH_3(CH_2)_3OCH_2$; $C_6H_5OCH_2$;
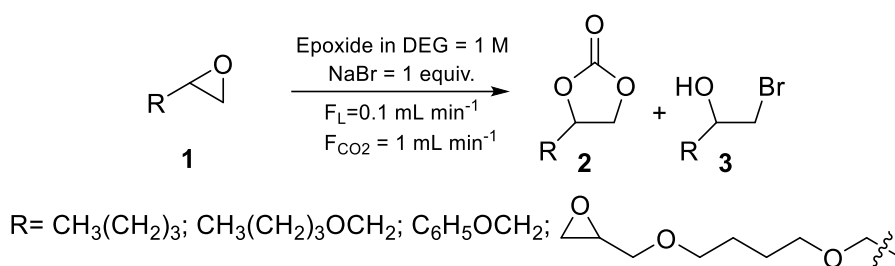
Entry	Epoxide	CF-reactor length (mm)	T (°C)	Conv (%)	Product Sel. (%)	
					2	3
1	1c	250[a]	220	88	81	15
2		500		92	91	9
3	1e	250	220	95	85	15
4		500		99	93	7
5	1f	500	220	>99	>99	
6	1g	500	220	>99	>99[b]	

t = 2 h for all reactions. Conversion and selectivity were determined by GC-MS analysis. [a] Result of entry 5 in Table 1: hexane-1,2-diol (4c: 4%) was also detected among reaction products. [b] The bis-cyclic carbonate 2g was the final product.

When choosing 1c as a model substrate, increasing the reactor length improved the conversion from 88 to 92%, but had an even more pronounced effect on the selectivity towards the desired hexylene carbonate (2c) which increased from 81 to 91% (Entries 1 and 2, Table 4.8). The diol (4c: hexane-1,2-diol in Scheme 4.6) was not detected, not even in trace levels (compare Entries 1 and 2): this result was consistent with the correlation previously noticed in Table 4.6, between the diol selectivity and the epoxide conversion. Apparently, the initially formed 4c gradually disappeared if the CF-reaction was allowed to proceed at high conversion (>90%), thereby suggesting that even the diol could transform into carbonate 2c *via* direct addition of CO_2 and dehydration. Albeit thermodynamically disfavored, this last sequence (addition/dehydration) has been described under a range of different conditions.[29] A similar outcome was observed when performing CF CO_2 insertion reactions on epoxide 1e: increasing coil length resulted in a quantitative conversion with an excellent selectivity to the corresponding COC 2e (93%, entry 4). These results supported the mechanism of Scheme 4.2 since the increase of the carbonate product at the expenses of the bromohydrin clarified the role of the bromohydrin itself as a reaction intermediate. Finally, using phenyl glycidyl ether and 1,4-butanediol diglycidyl ether (1e and 1f) as reactants, conversions were quantitative with excellent carbonate selectivity in both cases (>99%: entries 5 and 6). This general improvement of the reaction outcome positively impacted also on the DEG/NaBr recycling, reducing if not avoiding topping-up of the catalyst. Indeed, once the reaction run under conditions of entry 4 was complete, a successful recycle test was carried out by integrating NaBr of an amount (85 mg) equal to only 7% of its initial loading: the observed conversion of 1e and selectivity to the carbonate 2e were 99% and 92%, respectively. A similar effective recycle was achieved even after the reaction of epoxide 1f in entry 5, though, in this case, no addition (integration) of fresh catalyst was necessary since the process was quantitative and the corresponding bromohydrin intermediate was not observed at all. Overall, the CF system could be flexibly engineered by adjusting the length of the CF reactor to overcome issues associated to the kinetics of the consecutive reactions involved (bromohydrin and CO_2 insertion). A more quantitative explanation of these results should have considered the estimation and

comparison of the contact time under the investigated conditions. This was beyond the scope of the present paper: a flowing system comprising a polar liquid (epoxide in DEG/NaBr) and a non-polar supercritical gas-like phase (CO_2 with a density as low as 0.14 g·mL^{-1} at 220 °C and 120 bar) made this study challenging, if at all possible.[47,48]

Additional experiments were performed using also styrene oxide (**1a**: SO). In this case, however, the onset of a competitive isomerization side-reaction due to Meinwald rearrangement of SO did not allow to increase the selectivity towards styrene carbonate above 73 % even when with longer coils. Experiments were run under the conditions of Table 4.8 ([SO] = 1 M in DEG; NaBr (1.0 equiv.); F_L = 0.1 mL·min^{-1}, F_{CO2} = 1 mL·min^{-1}, p = 120 bar) except for the temperature which was varied in the range of 140-220 °C. Results are reported in Table 4.9. For a clearer view, the reaction outcomes were compared with both the available reactors of 250 and 500 cm.

Table 4.9. Effect of CF reactor length on CO_2 insertion into styrene oxide
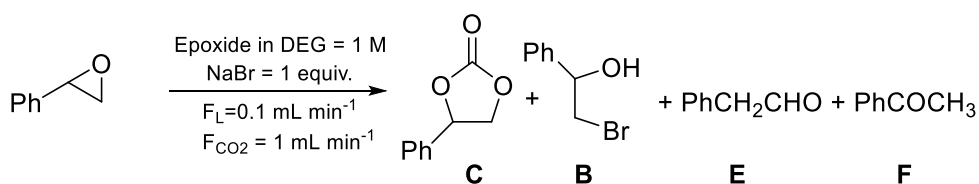
Entry	CF reactor (cm)	T (°C)	Conv. (%)	Product Sel. (%)			
				C	B	E	F
1	250	220	99	52	7	36	5
2	250	140	64	70	26	3	1
3	500		75	73	23	3	1

All reactions were run for 2 h. Conversion and selectivity were determined by GC-MS analysis.

The presence of an electron withdrawing substituent as the aryl ring,[49] altered the reactivity of SO with respect to both hexene oxide (**1c**) and butyl glycidyl ether (**1e**) (cfr. Table 4.8). At T = 220 °C, when the shorter reactor (250 cm) was used, the conversion of SO was 99% but a significant formation of products deriving for the epoxide isomerization, phenylacetaldehyde (**E**, 36%) and to a lesser extent acetophenone (**F**, 5%), was noticed (entry 1, Table 4.9).[50] The isomerization side-reaction was almost suppressed by lowering the temperature at 140 °C. Under such conditions, however, the conversion was reduced to 64% and a significant amount of unreacted bromohydrin intermediate (**B**, 2-bromo-1-phenylethan-1-ol: 26%) was detected in the final mixture (entry 2). Increasing the reactor length to 500 cm, improved the conversion to 75% with no appreciable effects on the products distribution. The selectivity towards styrene carbonate (**C**) and the bromohydrin intermediate (**B**) were 73% and 23%, respectively (entry 3).

Comparison with other protocols for CO_2 insertion into epoxides. A comparative assessment of the present procedure with other methods was carried out by selecting two recent representative papers that report effective catalytic systems and even more importantly, that describe in detail applications on CO_2 insertion into terminal epoxides under batch conditions and in continuous flow.[51,52] Table 4.10 shows the data examined in this comparison. The discussion is divided in three sections [(i)-iii)] for convenience.

Table 4.10. Comparison of different catalytic system in the CO2 insertion to epoxide under batch and continuous flow

Entry	Catalyst (synthesis)	Substrate:R	BATCH Epx:Cat (wt%)[b]	BATCH T/p/t (°C/bar/h)	CONTINUOUS FLOW FL/FCO2 (mL/min)[c]	CONTINUOUS FLOW T/p (°C/bar)	CONTINUOUS FLOW CO2/Epx (v/v)[d]	Solv.	Conv./Sel./Yield (%)[e]	TP (g/h)[f]	SP (g/gcath)[g]
1	NaBr/DEG	Ph	7-9	100/1/3					>99/>99/>99	0.18	5.29
2		CH3(CH2)3OCH2							>99/>99/>99	0.19	5.59
3		n-C4H9							>99/>99/>99	0.16	4.71
4		CH3CH2							>99/>99/>99	0.17	4.95
5	(none: commercial products)	n-C4H9							92/91/84	0.73	1.18
6		CH3(CH2)3OCH2							99/93/92	0.96	1.56
7		C6H5OCH2			0.1/1	220/120	71-83	none	>99/>99/>99	1.12	1.97
8[54]	Melamine formald. resins (solgel/ hydrotherm polym.)	CH3CH2	2-3.5	140/20/24					90/88/na	0.08	1.6
9		Ph							88/99/na	0.12	2.4
10		ClCH2		140/20/2					>99/>99/na	1.21	24.2
11		CH3CH2			0.01/15	120/13	150	none	86[h]/>99/na	0.69	0.35
12		ClCH2							>99/>99/na	0.93	0.47
13[55]	Ionic liquids, SILC, SILP (surface modified silica with ILs)	CH3	16-18	70/50/18					na/na/99	0.11	0.37
14		CH3			0.02/1.98	120/100	198	Hexane	na/na/65	0.50	0.37
15		CH3				120/160			na/na/89	0.68	0.51

[a] No solvent used; [b] Epoxide:catalyst weight ratio. [c] F_L: flow rate of liquid solution (epoxide+solvent); F_{CO_2}: flow rate of CO_2. [d] Epoxide:CO_2 volumetric ratio. [e] Conv.: conversion of the epoxide; Sel. and Yield: selectivity and yield on the corresponding carbonate product. [f] TP: total productivity of the protocol defined as grams of carbonate product obtained per hour (g/h). [g] SP: specific productivity defined as grams of carbonate product obtained per g of catalyst in an hour (g/g_{cat}h). [h] Long-term performance due to catalyst deactivation. na= not

i) Catalysts. Ref.[51] proposed catalysts based on melamine formaldehyde resins (MFRs) prepared by sol-gel hydrothermal polymerizations, while ref.[52] described silica supported ionic liquids (both chemo- and physi-sorbed as SILC and SILP, respectively). Albeit different, both these approaches implied preparation/characterization steps and reproducibility control, increasingly

challenging for large scale syntheses. No to mention the use of harmful chemicals as paraformaldehyde and ionic liquids, and the catalysts deactivation by build-up of products especially during long-term (on-stream) operations in flow mode. Such drawbacks could be by-passed by using the system investigated in the present work which was effectively a homogenous catalytic one based on inexpensive, sustainable, and commercially available NaBr and glycol. Catalyst deactivation was also not an issue since the NaBr/DEG mixture was continuously recovered by a simple green extraction with diethylcarbonate and re-used. Refs[51,52] did not consider recycling probably due to an energy and resource intensive recovery processes.

ii) Productivity and substrate scope. From the sustainability standpoint, the comparison of the productivity of different protocols is a complex issue since it should include aspects dealing with life cycle, from the synthetic step to the preparation of catalyst and its recycle, the disposal and associated costs. In the absence of these details, simpler and more direct indicators were taken into account: both the total productivity (TP) defined as the grams of carbonate produced per hour ($g \cdot h^{-1}$) and the specific productivity (SP) referred to the mass unit (g) of catalyst were examined. Except for the reaction of epichlorohydrin (an extremely reactive substrate not investigated in the present work), the analysis indicated that for alkyl or aryl substituted terminal epoxides (R=CH_3, CH_3CH_2, $CH_3(CH_2)_3OCH_2$, $C_6H_5OCH_2$, *n*-C_4H_9, and C_6H_5) our protocol allowed comparably better results than the others. Under batch conditions, the average TP and SP of the NaBr/DEG system were 0.13-0.19 $g \cdot h^{-1}$ and 3.82-5.29 $g \cdot (g_{cat}h)^{-1}$ (Entries 1-4, **Error! Reference source not found.**), well over those calculated for MFRs and ILs based catalysts (0.08-0.12 $g \cdot h^{-1}$ and 0.37-2.4 $g \cdot (g_{cat}h)^{-1}$, cfr. Entries 8-10 and 13); in the flow mode, albeit TP was of the same order of magnitude for the different procedures, SP was more 3-times higher for NaBr/DEG with respect to other catalysts (Entries 5-7: TP=0.73-1.17 $g \cdot h^{-1}$, SP = 1.18-1.89 $g \cdot (g_{cat}h)^{-1}$; Entries 11-12 and 14-15: TP = 0.69-0.93 and 0.50-0.68 $g \cdot h^{-1}$, SP = 0.35-0.47 and 0.37-0.51 $g \cdot (g_{cat}h)^{-1}$). The intrinsic reactivity of different epoxides could be co-responsible for some differences of productivity; however, the consistent comparison of the reaction of styrene oxide confirmed that NaBr/DEG was more efficient for the formation of styrene carbonate (cfr. Entries 1 and 9).

iii) Reaction conditions. For batch processes, MFRs and ILs systems required considerably higher pressure and longer reaction times of 20-50 bar and 18-24 hours compared to our catalyst that promoted quantitative reactions at atmospheric pressure in 3 hours. With respect to NaBr/DEG, SILP/SILC operated at a lower temperature (70 °C vs 100 °C), while MFRs were active at 140 °C; the corresponding catalyst loading (Epox:Cat weight ratio) were however twice and half, respectively, the amount of NaBr/DEG. The latter therefore proved most effective. This advantage was less evident in the flow reactions: albeit our CF system was more productive and operated with a far lower CO_2 flow (2-15 times smaller), the use of NaBr/DEG necessitated a higher temperature (220 °C, entries 5-7) compared to other systems (120 °C, entries 11-12 and 14-15). As a general observation, this apparent discrepancy could be hardly ascribed to chemical restraints or limitations due to the nature of the DEG/NaBr mixture. Since our batch protocol was active under similar, if not milder conditions (T, *p*, t) than those used for other catalysts (Table 4.3 and **Error! Reference source not found.**), the higher energy demand of CF reactions was likely due to a still-unoptimized engineering of our CF-apparatus, particularly by a finer tuning of flow rates which were crucial to improve the contact of reactants and the

kinetics. CO_2 consumption, which is often underestimated, should also be considered: for example, CF-procedures of entries 11-12 and 14- 15 in **Error! Reference source not found.** involve a large excess CO_2, most of it being wasted implying environmental and economic burden. On a final note, energetic issues associated to elevated reaction temperatures can be efficiently mitigated especially as the preparation scale is increased. Modern chemical plants always integrate heat recovery or exchange necessary for reactions within heat sinks and the usage of excess heat as part of the cogeneration plants.[53] Pertinent to this context is the commercial Shell Omega process for the CF-production of ethylene glycol via CO_2 insertion in ethylene oxide followed by hydrolysis, which exemplifies the relevance of both heat recovery and CO_2 recycle.[54]

4.3 Conclusion

The current literature describes a limited number of examples reporting alkali metal halides as catalysts for CO_2 insertion into epoxides. This paper reports the first application of a simple nonpolymeric glycol such as diethylene glycol (DEG) for the catalytic activation of NaBr in the insertion of CO_2 to terminal epoxides. The binary system made of NaBr/DEG has proven efficient for the batch conversion of different substrates including 7 terminal and one internal epoxides, but even more importantly, the characteristics of DEG (viscosity, density, diffusivity) made it suitable to act concurrently as a co-catalyst (cation coordinating agent and hydrogen bon donor) and a solvent/carrier for the implementation of the reaction in continuous-flow. However, translating the reaction conditions from batch to continuous flow is challenging. The results gathered so far highlight that the batch reaction can be run under conditions far milder (T = 100 °C, $p^0(CO_2)$ = 1 bar) than those required in CF-mode (T = 220 °C, $p(CO_2)$ = 120 bar); nevertheless, the potential of CF in terms of process intensification can be appreciated. Notably, in the explored range of flow rates, a microfluidic reactor with a capacity of just $7.85 \cdot 10^{-2}$ cm^3 allows a productivity 2.5 higher compared to the corresponding batch process carried out on a gram scale. Recycle experiments have also confirmed that the NaBr/DEG catalytic mixture is reusable without loss of performance, for at least four subsequent CF-runs. Moreover, a comparative analysis has proven that the NaBr/DEG system is competitive with other systems based on organic resins and ionic liquids, particularly regarding productivity, greenness, and possibly (economic) sustainability. A significant advance with respect to previous data is the continuous recyclability of the homogeneous mixture that bypasses typical drawbacks associated to heterogeneous catalyst deactivation. Although further optimization is required in terms of process engineering to improve the CF system design and maximize delivery/contact between the polar liquid solution of reactant/catalyst/co-catalyst and gas-like apolar supercritical CO_2, the study provides a proof of concept which paves the way for future advances in the field.

4.4   Experimental Section

General. Commercially available reagents and solvents were used as received unless otherwise stated. 1,2-epoxyhexane (hexene oxide, EHx), 2-phenyloxirane (styrene oxide, SO), 2-(propoxymethyl)oxirane (butyl glycidyl ether; BGE), diethylene glycol (DEG), ethanol, NaBr, diethylene glycol (DEG), diethylene glycol dimethyl ether (DEGME) 1-hexanol and 1,6-hexanediol were sourced from Sigma-Aldrich (now Merck). GC-MS (EI, 70 eV) analyses were performed with an Agilent 6890N GC, equipped with a HP5-MS capillary column (l = 30 m, Ø = 0.32 mm, film thickness = 0.25 mm), coupled with an Agilent 5975 EI detector. GC-FID analyses were performed with a HP 6890 GC mounting an Elite-624 capillary column (l = 30 m, Ø = 0.32 mm, film thickness = 1.8 mm). ^{1}H and ^{13}C NMR spectra were recorded with a Bruker Ascend 400 instrument operating at 400 and 100 MHz, respectively. The chemical shifts were reported downfield from tetramethylsilane (TMS). CDCl$_3$ and DMSO-d$_6$ were chosen as deuterated solvents.

General procedure for CO$_2$ insertion reactions with terminal epoxides in batch conditions, p^0(CO$_2$) = 10-50 bar. The selected epoxide (3.33 mmol, 1 equiv.), NaBr (0.025 – 0.1 eq), the co-catalyst (DEG, DEGME, 1-hexanol or 1,6-hexanediol, 0.2 - 0.3 eq), and mesitylene (0.33 mmol, 0.1 equiv., as the internal standard) were charged in a round-bottomed flask shaped as a test tube and equipped with a pierced glass cap and a stirring bar. The flask was placed inside a 100-mL stainless steel autoclave which was sealed, degassed via three vacuum-CO$_2$ cycles, pressurized with CO$_2$ (10- 50 bar), and finally heated at T of 50-100 °C for 2-5 h. Thereafter, the autoclave was cooled to rt and vented. A sample of the crude mixture was analysed by ^{1}H NMR to determine conversion, yield and selectivity.

General procedure for CO$_2$ insertion reactions in CF conditions. Reactions were performed using the apparatus of Figure 4.3. Experimental conditions were described throughout Table 4.6Table 4.8, and 4 and Figure 4.3. In a typical procedure, the CF apparatus was first conditioned with DEG (FL = 0.5 mL·min^{-1}), and CO$_2$ (FCO$_2$ = 4 mL·min^{-1}) for t = 30 min. Then, a homogeneous 1 M solution of the epoxide of choice (EHx, BGE, SO), and NaBr (0.1-1 equiv. with respect to the epoxide) in DEG was continuously delivered to the CF-reactor at the desired T and flow rates (T = 140-220 °C, FL = 0.1-0.4 mL· min^{-1} and FCO$_2$ = 1-4 mL·min^{-1}). Reactions were allowed to proceed for t = 2 h, though some prolonged tests were carried out for up to t = 6 h. The reaction mixture was collected according to the procedure exemplified by Figure 4.3. After each test, the CF system was washed with distilled water (10 mL) and ethanol (10 mL) and dried with a CO$_2$ flow (FCO$_2$ = 4 mL·min^{-1}) for 10 minutes.

The contribution of DR was in the design and conduction of all CF-experiments and the writing of the draft of the research article.

References

[1] M. Aresta, *Carbon Dioxide as Chemical Feedstock*, Wiley-VCH, Weinheim, 2010.

[2] J. Artz, T. E. Müller, K. Thenert, J. Kleinekorte, R. Meys, A. Sternberg, A. Bardow, W. Leitner, Sustainable conversion of carbon dioxide: an integrated review of catalysis and life cycle assessment, *Chem. Rev.* **2018**, *118*, 434. https://doi.org/10.1021/acs.chemrev.7b00435

[3] Q. Liu, L. Wu, R. Jackstell, M. Beller, Using carbon dioxide as a building block in organic synthesis, *Nat. Commun.* **2015**, *6*, 5933. https://doi.org/10.1038/ncomms6933

[4] C. Martín, G. Fiorani, A. W. Kleij, Recent advances in the catalytic preparation of cyclic organic carbonates, *ACS Catal.* **2015**, *5*, 1353. https://doi.org/10.1021/cs5018997

[5] A. J. Kamphuis, F. Picchioni, P. P. Pescarmona, CO 2-fixation into cyclic and polymeric carbonates: principles and applications, *Green Chem.* **2019**, *21*, 406. https://doi.org/10.1039/C8GC03086C

[6] M. Alves, B. Grignard, R. Mereau, C. Jerome, T. Tassaing, C. Detrembleur, Organocatalyzed coupling of carbon dioxide with epoxides for the synthesis of cyclic carbonates: catalyst design and mechanistic studies, *Catal. Sci. Technol.* **2017**, *7*, 2651. https://doi.org/10.1039/C7CY00438A

[7] J. W. Comerford, I. D. V. Ingram, M. North, X. Wu, Sustainable metal-based catalysts for the synthesis of cyclic carbonates containing five-membered rings, *Green Chem.* **2015**, *17*, 1966. https://doi.org/10.1039/C4GC01719F

[8] C. J. Whiteoak, N. Kielland, V. Laserna, E. C. Escudero-Adán, E. Martin, A. W. Kleij, A powerful aluminum catalyst for the synthesis of highly functional organic carbonates, *J. Am. Chem. Soc.* **2013**, *135*, 1228. https://doi.org/10.1021/ja311053h

[9] V. Laserna, G. Fiorani, C. J. Whiteoak, E. Martin, E. Escudero-Adán, A. W. Kleij, Carbon Dioxide as a Protecting Group: Highly Efficient and Selective Catalytic Access to Cyclic cis-Diol Scaffolds, *Angew. Chem. Int. Ed.* **2014**, *53*, 10416–10419. https://doi.org/10.1002/anie.201406645

[10] G. Fiorani, M. Stuck, C. Martín, M. M. Belmonte, E. Martin, E. C. Escudero-Adán, A. W. Kleij, Catalytic coupling of carbon dioxide with terpene scaffolds: access to challenging bio-based organic carbonates, *ChemSusChem* **2016**, *9*, 1304. https://doi.org/10.1002/cssc.201600238

[11] J. Martínez, F. de la Cruz-Martínez, M. A. Gaona, E. Pinilla-Peñalver, J. Fernández-Baeza, A. M. Rodríguez, J. A. Castro-Osma, A. Otero, A. Lara-Sánchez, Influence of the counterion on the synthesis of cyclic carbonates catalyzed by bifunctional aluminum complexes, *Inorg. Chem.* **2019**, *58*, 3396. https://doi.org/10.1021/acs.inorgchem.8b03475

[12] H. Seo, L. V. Nguyen, T. F. Jamison, Using carbon dioxide as a building block in continuous flow synthesis, *Adv. Synth. Catal.* **2019**, *361*, 247. https://doi.org/10.1002/adsc.201801228

[13] X.-B. Lu, J.-H. Xiu, R. He, K. Jin, L.-M. Luo, X.-J. Feng, Chemical fixation of CO2 to ethylene carbonate under supercritical conditions: continuous and selective, *Appl. Catal. A: Gen.* **2004**, *275*, 73. https://doi.org/10.1016/j.apcata.2004.07.022

[14] L. Guo, L. Deng, X. Jin, Y. Wang, H. Wang, Catalytic conversion of CO2 into propylene carbonate in a continuous fixed bed reactor by immobilized ionic liquids, *RSC Adv.* **2018**, *8*, 26554. https://doi.org/10.1039/C8RA03952F

[15] M. North, P. Villuendas, C. Young, A Gas-Phase Flow Reactor for Ethylene Carbonate Synthesis from Waste Carbon Dioxide, *Chem. Eur. J.* **2009**, *15*, 11454. https://doi.org/10.1002/chem.200902436

[16] A. Rehman, A. M. López Fernández, M. F. M. G. Resul, A. Harvey, Kinetic investigations of styrene carbonate synthesis from styrene oxide and CO2 using a continuous flow tube-in-tube gas-liquid reactor, *J. CO2 Util.* **2018**, *24*, 341. https://doi.org/10.1016/j.jcou.2018.02.001

[17] X. Wu, M. Wang, Y. Xie, C. Chen, K. Li, M. Yuan, X. Zhao, Z. Hou, Carboxymethyl cellulose supported ionic liquid as a heterogeneous catalyst for the cycloaddition of CO2 to cyclic carbonate, *Appl. Catal. A: Gen.* **2016**, *519*, 146. https://doi.org/10.1016/j.apcata.2016.04.002

[18] B. R. James, J. A. Boissonnault, A. G. Wong-Foy, A. J. Matzger, M. S. Sanford, Structure activity relationships in metal–organic framework catalysts for the continuous flow synthesis of propylene carbonate from CO 2 and propylene oxide, *RSC Adv.* **2018**, *8*, 2132. https://doi.org/10.1039/C7RA13245J

[19] H. Yasuda, L. He, T. Takahashi, T. Sakakura, Non-halogen catalysts for propylene carbonate synthesis from CO2 under supercritical conditions, *Appl. Catal. A: Gen.* **2006**, *298*, 177. https://doi.org/10.1016/j.apcata.2005.09.034

[20] V. H. Jadhav, S. H. Jang, H.-J. Jeong, S. T. Lim, M.-H. Sohn, J.-Y. Kim, S. Lee, J. W. Lee, C. E. Song, D. W. Kim, Oligoethylene Glycols as Highly Efficient Mutifunctional Promoters for Nucleophilic-Substitution Reactions, *Chem. Eur. J.* **2012**, *18*, 3918. https://doi.org/10.1002/chem.201102455

[21] G. Rokicki, W. Kuran, B. Pogorzelska-Marciniak, Cyclic carbonates from carbon dioxide and oxiranes, *Monatsh. Chem.* **1984**, *115*, 205. https://doi.org/10.1007/BF00798411

[22] J. Tharun, G. Mathai, A. C. Kathalikkattil, R. Roshan, J.-Y. Kwak, D.-W. Park, Microwave-assisted synthesis of cyclic carbonates by a formic acid/KI catalytic system, *Green Chem.* **2013**, *15*, 1673. https://doi.org/10.1039/C3GC40729B

[23] S. Kaneko, S. Shirakawa, Potassium Iodide–Tetraethylene Glycol Complex as a Practical Catalyst for CO2 Fixation Reactions with Epoxides under Mild Conditions, *ACS Sustainable Chem. Eng.* **2017**, *5*, 2836. https://doi.org/10.1021/acssuschemeng.7b00324

[24] S. Kumar, S. L. Jain, Polyethylene Glycol Wrapped Potassium Bromide Assisted Chemical Fixation of Carbon Dioxide, *Ind. Eng. Chem. Res.* **2014**, *53*, 541. https://doi.org/10.1021/ie4033439

[25] J. Steinbauer, T. Werner, Poly (ethylene glycol) s as Ligands in Calcium-Catalyzed Cyclic Carbonate Synthesis, *ChemSusChem* **2017**, *10*, 3025. https://doi.org/10.1002/cssc.201700788

[26] J. Steinbauer, A. Spannenberg, T. Werner, An in situ formed Ca 2+–crown ether complex and its use in CO 2-fixation reactions with terminal and internal epoxides, *Green Chem.* **2017**, *19*, 3769. https://doi.org/10.1039/C7GC01114H

[27] Y. Hu, J. Steinbauer, V. Stefanow, A. Spannenberg, T. Werner, Polyethers as complexing agents in calcium-catalyzed cyclic carbonate synthesis, *ACS Sustainable Chem. Eng.* **2019**, *7*, 13257. https://doi.org/10.1021/acssuschemeng.9b02502

[28] V. Butera, H. Detz, Cyclic Carbonate Formation from Epoxides and CO2 Catalyzed by Sustainable Alkali Halide–Glycol Complexes: A DFT Study to Elucidate Reaction Mechanism and Catalytic Activity, *ACS Omega* **2020**, *5*, 18064. https://doi.org/10.1021/acsomega.0c01572

[29] C. C. Truong, D. K. Mishra, Recent advances in the catalytic fixation of carbon dioxide to value-added chemicals over alkali metal salts, *J. CO2 Util.* **2020**, *41*, 101252. https://doi.org/10.1016/j.jcou.2020.101252

[30] S. Guidi, M. Noè, P. Riello, A. Perosa, M. Selva, Towards a Rational Design of a Continuous-Flow Method for the Acetalization of Crude Glycerol: Scope and Limitations of Commercial Amberlyst 36 and AlF3·3H2O as Model Catalysts, *Molecules* **2016**, *21*, 657. https://doi.org/10.3390/molecules21050657

[31] L. Cattelan, A. Perosa, P. Riello, T. Maschmeyer, M. Selva, Continuous-Flow O-Alkylation of Biobased Derivatives with Dialkyl Carbonates in the Presence of Magnesium-Aluminium Hydrotalcites as Catalyst Precursors, *ChemSusChem* **2017**, *10*, 1571. http://dx.doi.org/10.1002/cssc.201601765

[32] R. Calmanti, M. Galvan, E. Amadio, A. Perosa, M. Selva, High-temperature batch and continuous-flow transesterification of alkyl and enol esters with glycerol and its acetal derivatives, *ACS Sustainable Chem. Eng.* **2018**, *6*, 3964. https://doi.org/10.1021/acssuschemeng.7b04297

[33] L. Cattelan, G. Fiorani, A. Perosa, T. Maschmeyer, M. Selva, Two-step synthesis of dialkyl carbonates through transcarbonation and disproportionation reactions catalyzed by calcined hydrotalcites, *ACS Sustainable Chem. Eng.* **2018**, *6*, 9488. https://doi.org/10.1021/acssuschemeng.8b02106

[34] M. Liu, X. Wang, Y. Jiang, J. Sun and M. Arai, Hydrogen bond activation strategy for cyclic carbonates synthesis from epoxides and CO2: current state-of-the art of catalyst development and reaction analysis, *Catal. Rev.*, **2018,** *61*, 214. https://doi.org/10.1080/01614940.2018.1550243

[35] J. Peng, S. Wang, H.-J. Yang, B. Ban, Z. Wei, L. Wang and L. Bo, Chemical fixation of CO2 to cyclic carbonate catalyzed by new environmental-friendly bifunctional bis-β-cyclodextrin derivatives, *Catal Today*, **2019**, *330*, 76. https://doi.org/10.1016/j.cattod.2018.06.020

[36] H. Chang, Q. Li, X. Cui, H. Wang, C. Qiao, Z. Bu and T. Lin, Polyvinyl alcohol-potassium iodide: an efficient binary catalyst for cycloaddition of epoxides with CO2, *Mol Catal*, **2018**, *449*, 25. https://doi.org/10.1016/j.mcat.2018.02.007

[37] Z. Wu, H. Xie, X. Yu and E. Liu, Lignin-Based Green Catalyst for the Chemical Fixation of Carbon Dioxide with Epoxides To Form Cyclic Carbonates under Solvent-Free Conditions, *ChemCatChem*, **2013**, *5*, 1328. https://doi.org/10.1002/cctc.201200894

[38] L. Zhou, Y. Liu, Z. He, Y. Luo, F. Zhou, E. Yu, Z. Hou and W. Eli, Pentaerythritol and KI: An Efficient Catalytic System for the Conversion from CO2 and Epoxides to Cyclic Carbonates, *J Chem Res*, **2013**, *37*, 102. https://doi.org/10.3184/174751913X13571500195988

[39] N. Tenhumberg, H. Büttner, B. Schäffner, D. Kruse, M. Blumenstein and T. Werner, Cooperative catalyst system for the synthesis of oleochemical cyclic carbonates from CO 2 and renewables, *Green Chem.*, **2016**, *18*, 3775. https://doi.org/10.1039/C6GC00671J

[40] M. B. Plutschack, B. Pieber, K. Gilmore, P. H. Seeberger, The hitchhiker's guide to flow chemistry, *Chem. Rev.* **2017**, *117*, 11796. https://doi.org/10.1021/acs.chemrev.7b00183

[41] F. Gomollón-Bel, Ten Chemical Innovations That Will Change Our World: IUPAC identifies emerging technologies in Chemistry with potential to make our planet more sustainable, *Chem. Int.* **2019**, *41*, 12. https://doi.org/10.1515/ci-2019-0203

[42] D. Rigo, G. Fiorani, A. Perosa, M. Selva, Acid-Catalyzed Reactions of Isopropenyl Esters and Renewable Diols: A 100% Carbon Efficient Transesterification/Acetalization Tandem Sequence, from Batch to Continuous Flow, *ACS Sustainable Chem. Eng.,* **2019**, *7*, 18810. https://doi.org/10.1021/acssuschemeng.9b03359

[43] https://www.meglobal.biz/products/diethylene-glycol/physicalproperties/ (accessed 08/10/2021).

[44] R. Li, J. Liu, H. Tao, D. Sun, D. Xiao, C. Liu, The investigation of thermal pyrolysis of glycerol carbonate derivatives by TG–FTIR, *Thermochimica Acta* **2016**, *624*, 76. https://doi.org/10.1016/j.tca.2015.12.002

[45] C. J. Whiteoak, A. H. Henseler, C. Ayats, A. W. Kleij, M. Pericas, Conversion of oxiranes and CO 2 to organic cyclic carbonates using a recyclable, bifunctional polystyrene-supported organocatalyst, *Green Chem*., **2014**, *16*, 1552. https://doi.org/10.1039/C3GC41919C

[46] M. Brivio, W. Verboom, D. N. Reinhoudt, Miniaturized continuous flow reaction vessels: influence on chemical reactions, *Lab Chip* **2006**, *6*, 329. https://doi.org/10.1039/B510856J

[47] T. Andersson, P. Pucar, Estimation of residence time in continuous flow systems with dynamics, *J. Process Control* **1995**, *5*, 9. https://doi.org/10.1016/0959-1524(95)95941-6

[48] S. Lohse, B. T. Kohnen, D. Janasek, P. S. Dittrich, J. Franzke, D. W. Agar, A novel method for determining residence time distribution in intricately structured microreactors, *Lab Chip* **2008**, *8*, 431. https://doi.org/10.1039/B714190D

[49] G.-P. Wu, S.-H. Wei, W.-M. Ren, X.-B. Lu, B. Li, Y.-P. Zu, D. J. Darensbourg, Alternating copolymerization of CO2 and styrene oxide with Co(III)-based catalyst systems: differences between styrene oxide and propylene oxide, *Energy Environ. Sci.*, **2011**, *4*, 5084. https://doi.org/10.1039/C1EE02566J

[50] V. V. Costa, K. A. da Silva Rocha, I. V. Kozhevnikov, E. V. Gusevskaya, Isomerization of styrene oxide to phenylacetaldehyde over supported phosphotungstic heteropoly acid, *Appl. Catal. A: Gen.*, **2010**, *383*, 217. https://doi.org/10.1016/j.apcata.2010.06.005

[51] A. Sainz Martinez, C. Hauzenberger, A. R. Sahoo, Z. Csendes, H. Hoffmann, K. Bica, Continuous Conversion of Carbon Dioxide to Propylene Carbonate with Supported Ionic Liquids, *ACS Sustainable Chem. Eng.* **2018**, *6*, 13131. https://doi.org/10.1021/acssuschemeng.8b02627

[52] T. Q. Bui, L. J. Konwar, A. Samikannu, D. Nikjoo, J.-P. Mikkola, Mesoporous Melamine-Formaldehyde Resins as Efficient Heterogeneous Catalysts for Continuous Synthesis of Cyclic Carbonates from Epoxides and Gaseous CO2, *ACS Sustainable Chem. Eng.* **2020**, *8*, 12852. https://doi.org/10.1021/acssuschemeng.0c03123

[53] R. T. L. Ng, D. H. S. Tay, D. K. S. Ng, Simultaneous process synthesis, heat and power integration in a sustainable integrated biorefinery, *Energy Fuels* **2012**, *26*, 7316. https://doi.org/10.1021/ef301283c

[54] K. Kawabe, Development of Highly Selective Process for Mono-Ethylene Glycol Production from Ethylene Oxide via Ethylene Carbonate Using Phosphonium Salt Catalyst, *Catal Surv Asia* **2010**, *14*, 111. https://doi.org/10.1007/s10563010-9094-4

5   Diversified upgrading of 5-hydroxymethylfurfural (HMF)

5.1   Introduction

5-Hydroxymethyl-2-furfural (HMF) is among the most promising platform chemicals derived from the acid-catalyzed hydrolysis of lignocellulose.[1] As illustrated by several comprehensive reviews,[2,3,4] the multiple functionalization of HMF makes it a suitable substrate for a range of reactions, including oxidations, hydrogenations, etherifications, couplings, condensations, and others.[5,6] Carbon-carbon and carbon-heteroatom bond forming processes are an exemplificative large family of transformations where the reactivity of the HMF carbonyl with a variety of nucleophiles has been investigated for the construction of bio-based organic frameworks.[7,8,9,10] A model case is the aldol condensation, particularly with acetone as a donor, which has been explored to produce renewable polymers and pigments.[11,12,13,14] Another relevant route is the reductive amination of HMF for the synthesis of nitrogen functionalized compounds of interest in the pharmaceutical and surfactants sectors.[15,16] Less studied but not less noteworthy is also the conversion of HMF to the corresponding olefins via Wittig-type reactions: an example is the vinylated homologue 5-hydroxymethyl-2-vinylfuran (HMFV) which undergoes free radical polymerization to yield renewable glues.[17] On the other hand, remarkable strategies for the upgrading of HMF have been designed by taking advantage of its benzyl alcohol-like reactivity. Among them, one of most investigated reactions was the transesterification, particularly the acetylation to 5-formylfuran-2-yl)methyl acetate (HMF-acetate or AMF) which thanks to its lower hydrophilicity and improved stability has been proposed as an alternative platform to HMF.[18] Several acetyl donors including acetic anhydride, acetic acid and even simple esters, and catalysts (pyridine, sodium acetate, I_2, etc.)[19,20,21] or biocatalysts (e.g. Lipase Cal-B)[22,23] proved effective for the synthesis of AMF. Intriguingly, albeit similar to the transesterification reaction, the transcarbonation of HMF with organic carbonates is a largely unexplored field. To the best of our knowledge, notwithstanding HMF-derived carbonates are expected to display attractive properties as intermediates and monomers for polycarbonate materials, only one paper has reported a bio-catalyzed carboxymethylation of HMF with dimethyl carbonate for the synthesis of (5-formylfuran-2-yl) methyl carbonate (HMFC) in 91% yield.[22] Reduction of 5-hydroxymethylfurfural is also a key reaction towards a variety of chemicals and biofuels such as, 2,5-bis(hydroxymethyl)furan, 2,5-dimethylfuran, and linear derivatives such as HHD (1-hydroxyhexane-2,5-dione) and polyols, just to name a few.[24] Most if not all of these strategies, however, have issues. These include: i) the limited thermal and chemical stability of HMF which easily undergoes undesired polymerization or degradation to humins and char;[25,26,27] ii) the challenging control of the selectivity between mono- and bis-substituted products in aldol-type reactions;[28] iii) the explosive potential and corrosivity of acetic anhydride, and its legal restrictions for large-scale manufacturing in many countries;[29,30] iv) the use of tailored solvents, e.g. deep-eutectics (DES), to cope with the separation of equilibrium mixtures obtained in transesterification reactions;[22] v) the poor atom economy, the use of harmful solvents and organohalogens, and the formation of stoichiometric salts to dispose of in Wittig-type reactions;[31] vi) severe catalysts poisoning by heavy byproducts during hydrogenation and hydrogenolysis of HMF.[24] Not to mention that even storage of HMF must be controlled (at T below 4 °C) to avoid aging of the substrate and spontaneous formation of dimers and oligomers.[32] This scenario clearly highlights that the design of innovative protocols for the upgrading of HMF still remains a highly desirable target. In light of these considerations,

the interest for the design of green protocols for the conversion of biomass derived platform chemicals prompted part of this Thesis work towards exploring the functionalization of HMF and its derivatives in a logic as much as possible integrated in the green chemistry principles.[33] The five transformations described above, namely acetylation, transcarbonation, aldol condensation, reductive amination, and Wittig vinylation were approached by favoring the use of safe reagents and solvents, and catalytic processes. Scheme 5.1 summarizes the selection of experimental conditions used in this work and the major results achieved.
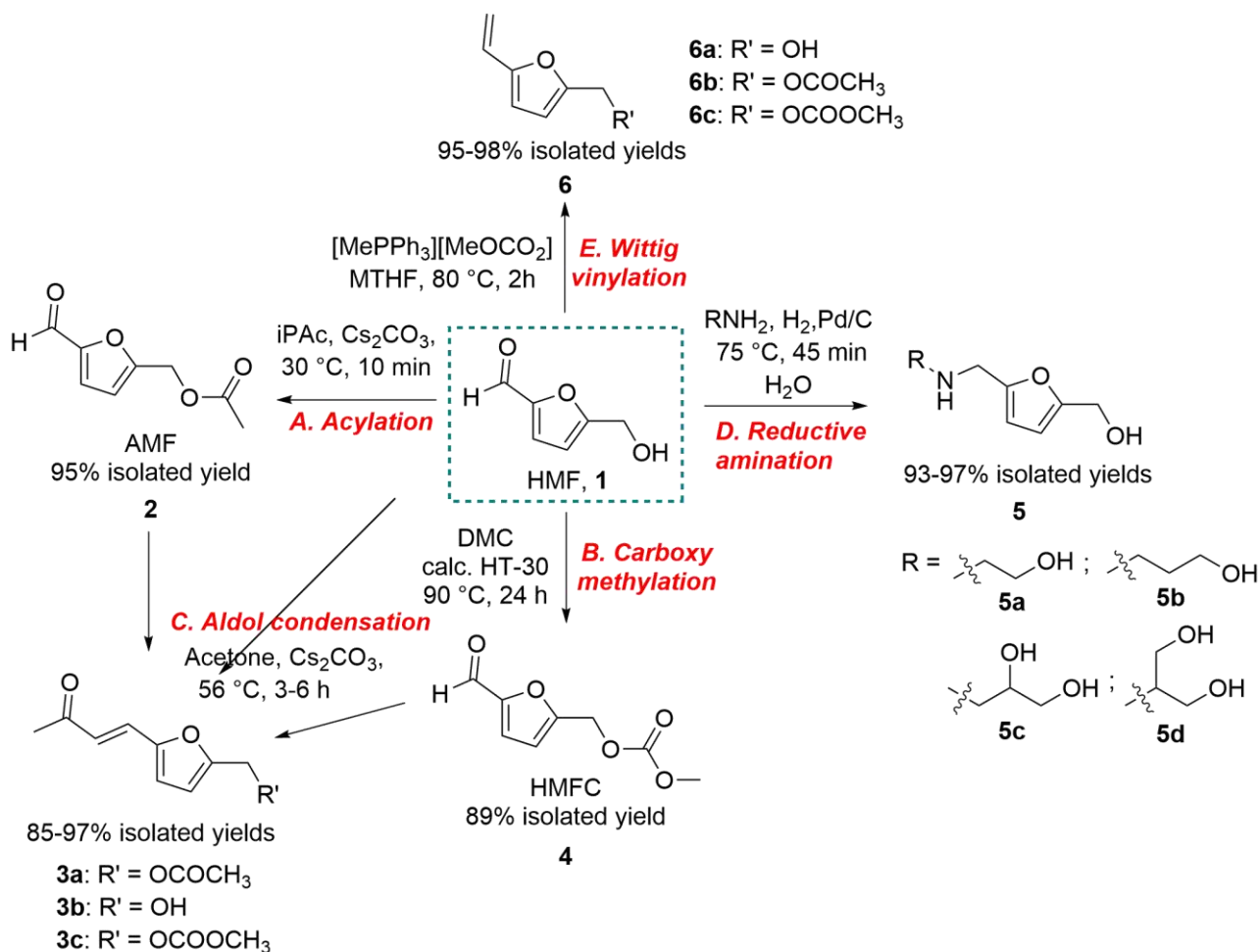
Scheme 5.1. *Pathways for the upgrading of HMF developed in this work*

Nontoxic isopropenyl acetate (iPAc) and dimethyl carbonate (DMC) were selected as acetylating and carboxymethylating agents (reactions A and B) to replace harmful and corrosive compounds (Ac$_2$O, acetyl halides, haloformates), and poorly active reactants (AcOH). Both iPAc and DMC served also as solvents. The use of alkaline heterogenous catalysts such as calcined hydrotalcites and alkali metal carbonates (C-HT-30 and M$_2$CO$_3$; M = K, Cs) was optimized to facilitate work-up, product separation and catalyst recycle. The same catalysts were used in combination with acetone for the aldol condensation (C). Renewable aminated glycerol derivatives 3-amino- (3-APD) and 2-amino-propanediol (2- APD) were investigated for the reductive amination reaction in the presence of water as a solvent (D). Simpler model substrates as ethanolamine (EA) and propanolamine (PA) were also used. Finally, the latent ylide reactivity of the Wittig vinylation reagent developed in our laboratories,[34] methyltriphenylphosphonium methylcarbonate ([MePPh$_3$] [MeOCO$_2$]) was exploited for the vinylation of the carbonyl (E). Contrarily to conventional ylides used for Wittig olefinations, the

vinylation reagent used here was synthesized simply by heating Ph_3P and dimethyl carbonate without added bases or co-product salts to dispose of.[31] All the designed strategies proved not only efficient, but also scalable routes that afford gram-scale quantities of 12 HMF derivatives (85–98% yields), 7 of which novel.

5.2   Results and discussion

5.2.1   General

All reactions were run in duplicate to ensure reproducibility: unless otherwise specified, the conversions, GC and NMR yields and isolated yields differed by less than 5% from one another. Catalysts used in this work were selected from the current literature among most active systems for esterifications, transcarbonations, aldol condensations, and reductive amination reactions.

5.2.2   The acetylation of HMF

As was mentioned in chapter 1, isopropenyl acetate (iPAc) is a privileged reagent for the catalytic transesterification with alcohols not only because it is nontoxic and inexpensive, but also due to the fact that the overall transformation is irreversible thanks to the formation of the enol of acetone as co-product. Based on the previous works described in Chapter 2,[35] the acetylation of HMF with isopropenyl acetate (iPAc) was investigated (Scheme 5.2).
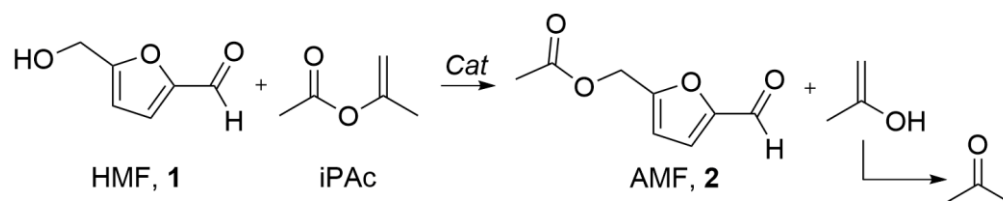
Scheme 5.2. The acetylation of HMF with iPAc

The acetylation protocol required a full design of experimental conditions since the reaction had no precedents in the literature. Both acid and base catalysts were selected for this study: they were either commercially available products or systems *ad-hoc* prepared through procedures described elsewhere by us and by others (Table 5.1). Among heterogeneous catalysts, an organic acid resin as Amberlyst-15, basic alkali metal carbonates (Na_2CO_3, K_2CO_3, and Cs_2CO_3), and two amphoteric solids (C-HT30 and C-HT63) comprised of mixed Mg/Al oxides, were employed. The latter (C-HT30 and C-HT63) were obtained by high-temperature calcination of commercial and cheap hydrotalcites Pural® MG30 and Pural® MG63 (HT30 and HT63) supplied by CONDEA/Sasol GmbH. The full characterization of these solids was reported previously:[36] amphoteric properties were ascribed to the coexistence of basic sites including OH groups, Mg-O or Al-O pairs and low-coordinated O^{2-} anions, and Lewis-acid sites in the form of coordinatively unsaturated Al^{3+} species.[36] Homogenous (organo) catalysts were basic ionic liquids, particularly methyl triphenyl onium methylcarbonates ([MeQPh$_3$] [MeOCO$_2$]; $Q = P$, N) prepared by the methylation of both triphenylphosphine and triphenylamine with dimethyl carbonate (DMC),[36] and conventional liquid acids as H_2SO_4 and AcOH (entries 7-8). The reactants (HMF and iPAc) were mutually miscible in all ratios.

Table 5.1. Catalysts used for the reactions of HMF and iPAc

Entry	Precursor(s)	Catalyst	Preparation	Ref.
1	-	Amberlyst-15 [b]	-	
2	HT30 [a] (MgO/Al$_2$O$_3$=30/70)	c-HT30	Calcination of precursors, 450 °C, dried air, 16 h	37
3	HT63 [a] (MgO/Al$_2$O$_3$=63/37)	c-HT63		
4	-	M$_2$CO$_3$ (M=Na$^+$, K$^+$, Cs$^+$)	-	
5	Ph$_3$P, DMC	[Ph$_3$PCH$_3$][OCO$_2$CH$_3$]	DMC-mediated alkylation, 140 °C, 20 h	38
6	Ph$_3$N, DMC	[Ph$_3$NCH$_3$][OCO$_2$CH$_3$]		
7		H$_2$SO$_4$, ACS reagent, 98%		
8		AcOH glacial, ACS reagent, 99.7%		

[a] MgO/Al$_2$O$_3$ ratio [wt%] specified by the supplier (Sasol); [b] acid capacity: 4.7 meq/g by dry weight.

Experiments were therefore carried out using a solution of HMF (0.5 mmol) and iPAc (1.5 molar equivs.), the latter used also as solvent. The catalyst loading could not be strictly the same for all catalysts because of the different composition/stoichiometry of the solid and liquid systems Table 5.1: with respect to HMF, Amberlyst-15 and calcined hydrotalcites were used in a 15 wt%, while (for most tests) alkali metal carbonates and ionic liquids were employed in 10 mol%. Preliminary tests indicated that the reaction must be run as close as possible to ambient temperature, to minimize HMF degradation and preserve the carbon balance. Experiments were carried out at 30 °C and monitored over a wide time range of 0.1 48 h. The results are summarized in Table 5.2 which also includes a blank test without any catalyst.

Table 5.2. *The reaction of HMF with iPAc at 30 °C, in the presence of different catalysts*

Entry	Catalyst	Cat. Loading[a]	t (h)	Conv. (%)[b]	Products, (%, GC)[b]		Yield (%)[c]	
					2 (AMF)	3a	2+3a	2
1	none		24	-	-	-		
2	Amb-15	15 wt%	24	≥99	93	7	96	
3	c-HT-30		24	-	-	-		
4	c-HT-63		24	4	≥99	-		
5	H$_2$SO$_4$		0.5	≥99	≥99			19
6	AcOH		24	3	≥99			
7	[Ph$_3$PCH$_3$][OCO$_2$CH$_3$]		2	≥99	≥99	-		93
8	[Ph$_3$NCH$_3$][OCO$_2$CH$_3$]	10 mol%	4	≥99	95	5		
9	Na$_2$CO$_3$		48	72	≥99	-		
10	K$_2$CO$_3$		2	≥99	91	9	96	
11	Cs$_2$CO$_3$		1	≥99	91	9	93	89
12	Cs$_2$CO$_3$	70 mol%	0.1	≥99	98	2	95	94

All reactions were carried out using a mixture of HMF (0.5 mmol) and iPAc (1.5 molar equivs.). [a] Catalyst loading was calculated with respect to the weight (entries 2-4) or the molar amount (entries 5-9) of HMF. [b] Conversion of HMF and amounts of products (%) were determined by GC. No other products, but **2** and **3a** were detected. [c] Isolated yields of the mixture of crude products **2+3a** and of product **2** were determined after rotary-evaporation and filtration on celite/silica of the final reaction mixture.

No reaction took place without catalyst (entry 1), while the catalytic experiments proved the feasibility of the desired acetylation of HMF with iPAc. Except for C–HT solids and AcOH which were substantially ineffective (entries 3–4 and 6), both Amberlyst 15 (entry 2), H$_2$SO$_4$ (entry 5),

ionic liquids (entries 7–8) and alkali metal carbonates (entries 9–11) allowed a very high HMF conversion, in most cases quantitative. However, different reaction rates, product distribution, and yields were observed. The acetylated derivative of HMF [**2**, AMF: (5- formylfuran-2-yl)methyl acetate] was always the major product (>90%, by GC), but non-negligible amounts of compound **3a** [Scheme 5.3: (5-(3- oxobut-1-en-1-yl)furan-2-yl)methyl acetate; up to 9%] were detected, thereby indicating that acetone released by the acetylation reaction (Scheme 5.2) underwent aldol condensation with the HMF carbonyl. No products other than **2** and **3a** were detected in all tests. Both **2** and **3a** were isolated by rotary-evaporation and filtration on celite/silica, and their structures were assigned by GC–MS, ^{1}H NMR and ^{13}C NMR analyses (details are in the Appendix A.5). Under acid conditions, the reaction rates apparently followed the order of acid strengths of the catalysts, *i.e.* H_2SO_4 > Amberlyst 15 > AcOH (entries 5, 2 and 6). Very fast conversion (99% in 0.5 h) was achieved with H_2SO_4, but massive HMF degradation took place: the reacting solution turned from pale yellow to black immediately after the catalyst addition and the yield of **2** did not exceed 19%. In the presence of Amberlyst 15, a much slower reaction was observed with a satisfactory isolated yield (**2** + **3a**=96%; **2:3a** = 93:7, after 24 h). Acid catalysis conditions enhanced the electrophilic character of the carboxyl carbon of iPAc (as reported for acid-catalyzed transesterification reactions of conventional esters): however, from Table 5.2 and Scheme 5.2, this (acid) activation step was significantly dependent on the nature of the catalyst and in general, except for Amberlyst 15, it brought about a poor acetylation selectivity. Nucleophilic activation of HMF by both homogeneous and heterogenous basic catalysts proved, instead, more efficient for the transesterification reaction which was complete in only a few hours (1-4 h: entries 7-11). Scheme 5.3 depicts the base-catalyzed reaction pathway.
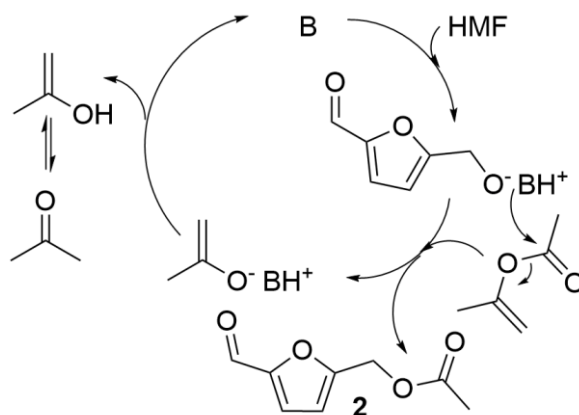
Scheme 5.3. Base (B) catalysed acetylation of HMF with iPAc

With respect to acid conditions, a change of the acetylation mechanism occurred in the presence of a base catalyst (B). The latter activated the OH group of HMF by converting it into a more powerful nucleophile as the corresponding alkoxide anion. Then, an acyl nucleophilic substitution followed providing product **2** and an enolate as a leaving group. An acid-base reaction generated an enol that tautomerized to acetone and restored the B species. The reactivity trend for alkali metal carbonates, particularly the slower conversion with Na_2CO_3 (72% after 48 h: entry 9) compared to the faster reactions observed with K_2CO_3 and even more with Cs_2CO_3 (1–2 h: entries 10–11) was consistent with the effect of ionic radii of alkali metal cations (Cs^+>K^+>Na^+) on solvation and (partial) solubilisation of carbonate salts in the organic mixture.[39,40] For example, in DMC, it was reported that Cs_2CO_3 and K_2CO_3 were almost equally

soluble (~0.6 g/L) and about 3 times more soluble than Na_2CO_3.[41] In general, methyl carbonate ionic liquids gave slightly higher yields of the acetylated derivative **2** (up to 93%, 2 h: entry 7) compared to K_2CO_3 or Cs_2CO_3 (89%, 1 h: entry 11). The latter was preferred because it is readily available commercially and can be more easily separated (by filtration) from the product. Interestingly, an additional test with a larger amount of Cs_2CO_3 (from 10 to 70 mol%) allowed to reduce the reaction time to 0.1 h only, and to further favor AMF (**2**: 98%) over the tandem product (**3a**: 2%). Compound **2** was isolated in 94% yield (entry 12). The synthesis was scaled up by a factor of 10 (HMF: 5 mmol, 630 mg) and AMF was achieved in 92% yield within 15 min. To the best of our knowledge, neither such simple conditions nor the use of iPAc and Cs_2CO_3 as a reagent and a catalyst, respectively, were previously reported for the acetylation of HMF. Scheme 5.4 details for comparison, the results of three effective protocols for the synthesis of AMF using ethyl acetate and acetic anhydride as acetyl donors.[20] These processes gave yields of **2** at best comparable to those of the present work (Table 5.2), but required prolonged reactions or two-steps (protection/deprotection) sequences, harmful solvents, and time-consuming (bio)catalyst/product/ unconverted HMF separations.

R	Cat	T/t (°C/h)	2 (Yield, %)
Et	CAL-B	40/24	90
Ac	BF$_3$-OEt$_2$; BLAP (two steps)	0/0.08 20/0.5	ca 80
Ac	piry	25/18	95

BLAP: bovine liver acetone powder
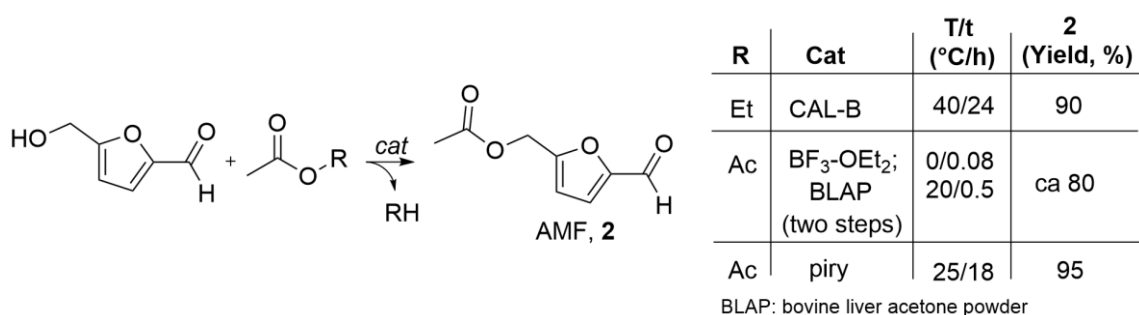
Scheme 5.4. *Biocatalytic methods recently reported for the synthesis of AMF*

5.2.3 The tandem acetylation-aldol condensation of HMF

The formation of compound **3a** during the acetylation of HMF with iPAc (Scheme 5.2) prompted us to investigate whether the tandem acetylation-aldol condensation process could be exploited for synthetic purposes. Similar strategies based on consecutive acetylation and acetalization tandem cascades were successfully reported by us in the reaction of glycerol and diols with iPAc.[35,42] Starting from the conditions of Table 5.2 [entry 11: mixture of HMF (0.5 mmol), iPAc (1.5 molar equivs.), and Cs_2CO_3 (10 mol%)] where the tandem derivative **3a** was achieved in up to a 9% amount, a detailed investigation of the effects of temperature (T, from 30 to 120 °C), time (t, from 1 to 15 h), pressure (*p*, from 1 to 8 bar of N_2), and solvents (polar aprotic such as cyclopentyl methyl ether or diethylene glycol dimethyl ether) were carried out. Results are reported in Table 5.3 and Figure 5.1.

Table 5.3. *The effect of time, pressure and solvent in the reaction between HMF and iPAc at 30 °C*

Entry	Solvent	t (h)	p (bar)	Conv. (%)^a	Products (%, by GC)^a		Yield (%) (2+3a)^b
					2	3a	
1		1		≥99	91	9	93
2		15	1	≥99	86	14	92
3	none	24		≥99	85	15	91
4		1	8^c	≥99	90	10	94
5		24	8^c	≥99	84	16	93

6	CPME	15	1	65	97	3	n.d.
7	DIGLYME			67	97	3	n.d.

All reactions were carried out using a mixture of HMF (0.5 mmol), iPAc (1.5 molar equivs.), and Cs_2CO_3 (10 mol%). [a]Conversion of HMF and amounts of products (%) were determined by GC. No other products, but **2** and **3a** were detected. [b] Isolated yields of the mixture of crude products **2+3a** determined after rotary-evaporation and filtration on celite/silica of the final reaction mixture. [c] Under N_2 pressure.

The effect of pressure, reaction time, and solvents. At atmospheric pressure, full conversion of HMF was reached within 1 h (entry 1). Increasing t from 1 to 15 h slightly improved the amount of **3a** to ca 15% (entry 2). However, the tandem sequence could not be favored any further by prolonging the reaction up to 24 h (entry 3).

Two experiments were carried out under a moderate pressure (8 bar) of N_2 with the aim to ensure that (volatile) acetone released by the acetylation reaction was available in the condensed (liquid) phase for the subsequent aldol process. Results were almost identical to those achieved at 1 bar (compare entries 1 and 3 to 4 and 5), thereby demonstrating the pressure was not beneficial to the tandem product, at least at 30 °C.

Under the conditions of entry 2, other tests were performed in the presence of an added solvent (5 mL in each reaction) as cyclopentyl methyl ether (CPME, $\varepsilon=4.76$ at 25 °C,[43]) and diethylene glycol dimethyl ether (Diglyme; $\varepsilon=7.40$ at 25 °C,[44]). These were selected among polar aprotic solvents with moderate dielectric constants to not deactivate the enolate nucleophile [$MeC(O)CH_2^-$]. Albeit solvents were expected to help the catalyst dissolution, the observed effect was detrimental to the aldol condensation, most plausibly because of the dilution of reactants: after 15 h, the conversion of HMF was similar in both solvents, not exceeding 67%, and the amount of **3a** (3%) was negligible compared to the acetyl derivative (**2**, 97%) (entries 6 and 7). No other solvents were investigated.

The effect of the temperature. Experiments were carried out for 15 h in the range of 30-120 °C. For reactions at T ≥ 60 °C, a pressurized autoclave (8 bar of N_2) was used to make acetone released by the acetylation of HMF available in the condensed (liquid) phase for the aldol condensation. HMF conversion was quantitative in all cases (and not reported in Figure 5.1).

The increase of the temperature from 30 to 90 °C strongly favored the aldol condensation of the acetyl derivative **2** with acetone: since no other products were detected but compounds **2** and **3a**, their relative profiles dropped and increased, respectively, of the same amounts (**2**: blue, from 76 to 14%, and vice versa for **3a**, red). However, it was confirmed that even under an inert atmosphere, the degradation of HMF with the temperature took place to a considerable extent. Indeed, mixtures recovered after experiments above 30 °C, were dark and viscous and their filtration on celite/silica gave isolated yields of **2+3a** (total of the two products) that progressively decreased from 94 at 30 °C, to 52% at 90 °C, respectively (dotted gray profile). The residues were black solids that could not be dissolved in most common solvents and were not further characterized. The sharp discontinuity noticed in both the blue and the red profiles for the experiment at 120 °C was consistent with the presence of part (most) of the acetone in the gaseous phase (not

available

for the aldol condensation with compound **2**), as evinced from the phase diagram of acetone itself.[45] Moreover, the increase of the temperature the increase of the temperature favored the HMF degradation and a further decrease of the isolated yields of **2+3a** to 34% (dotted gray profile).
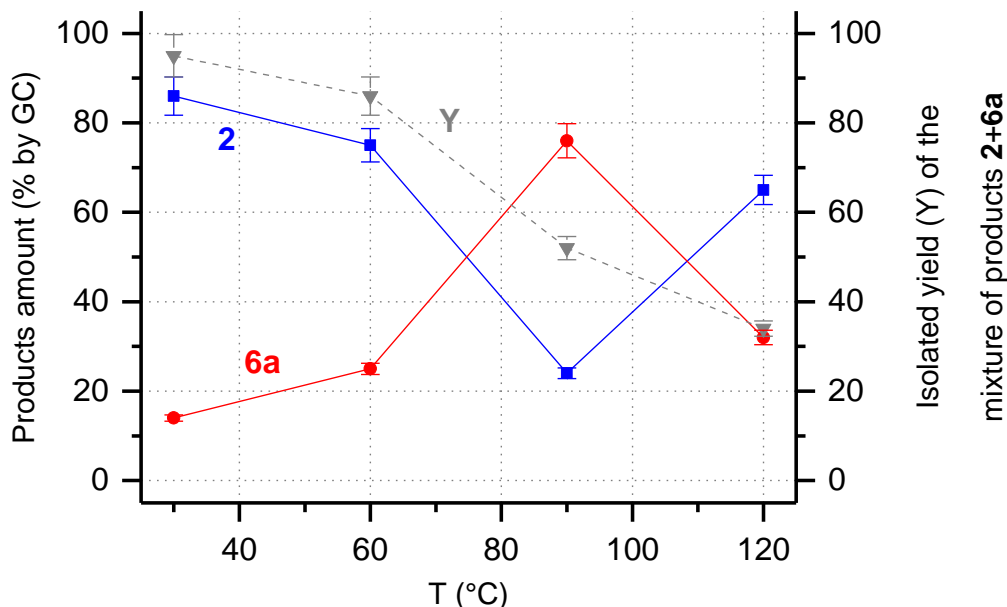
Figure 5.1. *The effect of the temperature in the reaction between HMF and iPAc. Conditions: mixture of HMF (0.5 mmol), iPAc (1.5 equivs.), and Cs$_2$CO$_3$ (10 mol%); t = 15 h. From 60 °C on, reactions were carried out under 8 bar of N$_2$. (-■-) Amount (%, GC) of compound **2**; (-●-) Amount (%, GC) of compound **3a**. (- -★- -) Isolated yield of products **2+3a***

Although none of the above-described experiments was conclusive, these findings led us to conclude that the aldol reaction was limited by the (insufficient) amount of acetone released by the acetylation process. GC and GC/MS analyses of the reaction mixtures showed that regardless of the conditions, the conversion of iPAc did not exceed 75%, which meant that at the best, acetone was available in an equimolar quantity with respect to the acetyl derivative **2**. A further set of reactions was then designed by adding acetone to favor the aldol process. A mixture of HMF (0.5 mmol), iPAc (1.5 molar equivs.), and Cs$_2$CO$_3$ (10 mol%) was set to react at 30 °C for 15 h, and increasing the amount of acetone from 1 to 16 molar equivalents respect to HMF. Results are reported in Figure 5.2 which describes the distribution of products and their isolated yields after purification of the final reaction mixtures by filtration on celite/ silica gel.
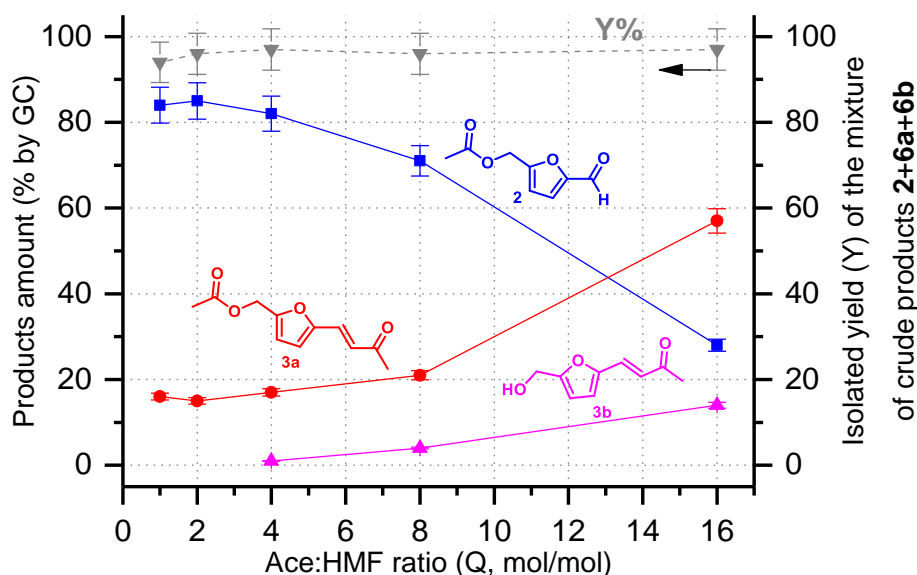
Figure 5.2. *The effect of HMF:acetone molar ratio in the reaction between HMF and iPAc. Conditions: HMF (0.5 mmol), iPAc (1.5 equivs.), Cs₂CO₃ (10 mol%), and acetone (Ace:HMF=1:1-16:1 molar ratio); T= 30 °C; t = 15 h. Left-to-right: (-■-) Amount (%, GC) of compound **2**; (-●-) amount (%, GC) of compound **3a**; ; (-▲-) amount (%, GC) of compound **3b**. Right-to-left: (- -▼- -) Isolated yield of products **2+3a+3b** (total of three products)*

The formation of the tandem product took advantage of the excess acetone, particularly when the Ace:HMF ratio (Q) was increased from 4 to 16, the amount of **3a** increased as well from 18 to 57% (**red** profile). Interestingly, albeit no HMF degradation side-processes were noticed, the onset of a straightforward aldol condensation of HMF with acetone, yielding product **3b**, was observed [**fuchsia** profile; the structure of (E)-4-(5-(hydroxymethyl)furan-2-yl)but-3-en-2-one was confirmed by MS and NMR analyses, (Appendix A.5)]. The combined isolated yields of three observed products (total of **2** + **3a+3b**) were substantially steady at ca 95% in all experiments (**gray** profile). These results finally allowed us to succeed in the desired tandem sequence: under the conditions of Figure 5.2 (Q = 16), but at the reflux temperature (56 °C), compound **3a** was achieved in a 92% yield by GC and 88% isolated yield. (Scheme 5.5).
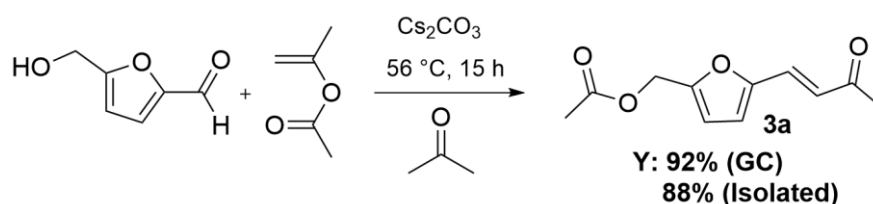
Scheme 5.5. *The one-pot synthesis of the tandem product **3a***

The sole co-product was the acetyl derivative **2** (8% by GC). The excess acetone prevented both the thermal degradation of HMF and the bis-aldol condensation with (two equivs. of) HMF. This latter reaction was instead, noticed when Ace and HMF reactants were combined in the presence of NaOH as a catalyst.[28] Overall, the protocol of Scheme 5.5 was not only highly effective for the one-pot synthesis of the tandem derivative **3a**, but it exemplified an intrinsically green approach in terms of selection of reagents and (mild) conditions. Results proved that the aldol condensation was favored by acetone simultaneously supplied as a reagent and released through the iPAc-promoted acetylation. With the aim to shed light on this aspect and discriminate the contribution of the two sources of acetone, an additional

203

experiment was carried out under the conditions of Scheme 5.5, by replacing acetone with its perdeuterated analogue, CD_3COCD_3. The GC-MS analysis of the reaction mixture allowed us to identify both product **3a** and its d_4-labelled isomer **3a*** (Scheme 5.6, left). The analytical data recorded in the SIM mode for the most abundant fragment ions of compounds **3a** and **3a*** (*m/z* = 135 and 139, respectively; Scheme 5.6, right) indicated that the relative amounts of such products were 8% and 92% (see also Figure 5.3).
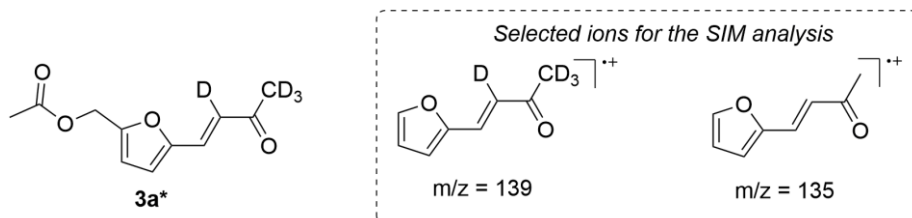
Scheme 5.6. *Left: d_4-labelled product **3a*** observed in the reaction of HMF with d_6-acetone; right: ions selected for SIM GC-MS analysis of products **3a** and **3a***, respectively*
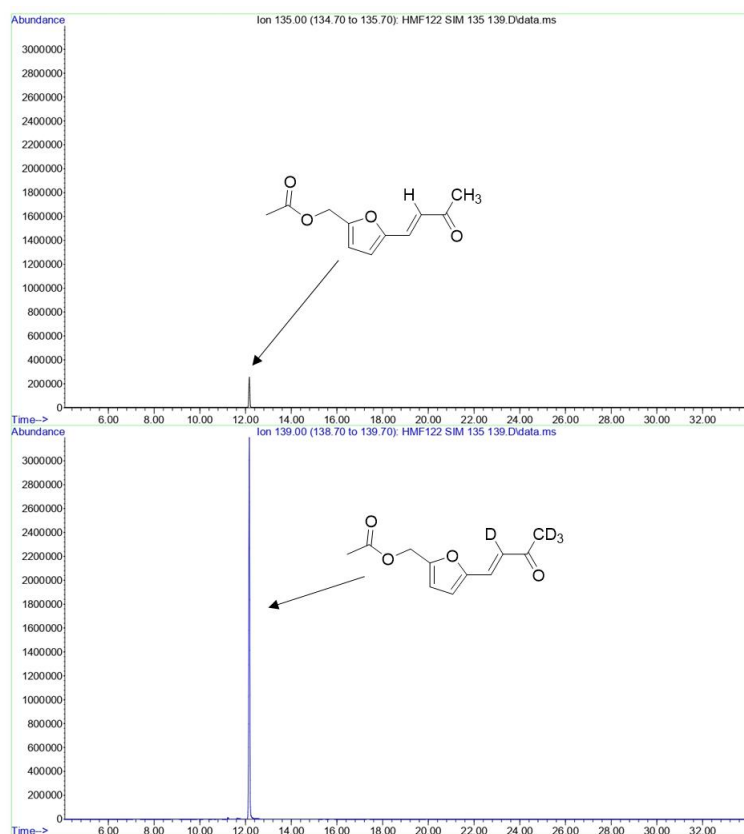
Figure 5.3. *GC-MS signal relative the GC-MS SIM analyses at 135 m/z ion (top) and 139 m/z (bottom)*

As a first approximation, excluding kinetic and equilibrium isotope effects,[46] this meant that the contribution of the iPAc-derived acetone to the aldol condensation, albeit not negligible, was about 10-fold lower than that of CD_3COCD_3. Integration of signals in the SIM chromatogram proved that relative areas under the peaks of target ions 135 and 139 were 8% and 92%, respectively (Figure 5.3), thereby confirming that the parent compounds **3a** and **3a*** were formed in a ratio of about 10:1.

5.2.4 DMC-promoted transcarbonation (carboxymethylation) of HMF combined to aldol condensation

The basic and amphoteric catalysts described in Table 5.1 for the acetylation of HMF, particularly methyl triphenyl phosphonium methylcarbonate ([MePPh$_3$] [MeOCO$_2$]), Cs$_2$CO$_3$, and C–HT30 as a mixed Al/Mg oxides solid, were used to investigate also the transcarbonation of HMF with dimethyl carbonate. Based on previous results of our group on the carboxymethylation of O-nucleophiles,[35] experiments were designed at T in the range of 30-90°C and with a large excess DMC, which served as both a reagent and a solvent. In a typical experiment a mixture of HMF (0.5 mmol), DMC (30 equivs. with respect to HMF) and the catalyst of choice was heated at the desired temperature. The loading of the catalysts was adjusted case-by-case: with respect to HMF, Cs$_2$CO$_3$ and the ionic liquid were employed in 10–70 mol% equivalents, while the calcined hydrotalcite was used in a 15–100 wt% amount (meaning a catalyst mass amount varying from 15% to 100% of the mass amount of HMF). For tests run at reflux conditions (90 °C), the reaction flask was equipped with a condenser thermostated at 70 °C, by which the azeotropic mixture MeOH/DMC (70:30 w/w, bp = 64–67 °C) formed during the process was continuously removed. The main results of this study are summarized in Table 5.4.

Table 5.4. *The reaction of HMF with DMC at 90 °C, in the presence of different catalysts*
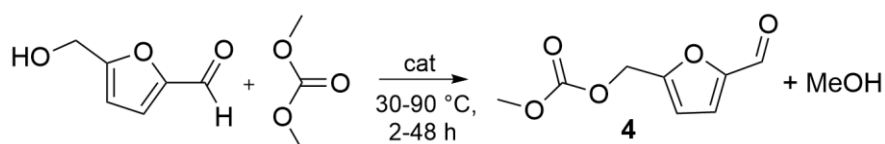
Entry	Catalyst	Cat. Loading[a]	T (°C)	t (h)	Conv. (%)[b]	Product 4, Yield (%)[c]
1	none	-	30	24	-	-
2	[Ph$_3$PCH$_3$][OCO$_2$CH$_3$]	10 mol%	30	24	59	53
3			90	2	≥99	56
4	Cs$_2$CO$_3$	10 mol%	30	24	73	69
5		70 mol%			75	68
6		10 mol%	90	2	≥99	45
7	c-HT-30	15wt%	30	24	-	-
8		50 wt%	90	48	74	70
9		100 wt%		24	95	93

All reactions were carried out using a mixture of HMF (0.5 mmol) and DMC (30 molar equivs.). [a] Catalyst loading was calculated with respect to the molar amount (entries 2-3) or the weight (entries 4-6) of HMF. [b] Conversion of HMF. [c] Yield of product **4** isolated after rotary-evaporation and filtration on celite/silica of the final reaction mixture.

The methyl carbonate derivative of HMF [**4**: 5-formylfuran-2-yl) methyl carbonate] was the only detected product by GC and GC/MS. After each test, compound **4** was isolated by rotary-evaporation the final reaction mixture and filtration/elution of the residue on celite/silica gel (5 g; eluant: Et$_2$O, 30 mL). The structure of the product was confirmed by GC–MS, ^{1}H and ^{13}C NMR (see also the experimental section). Compared to the acetylation with iPAc (Table 5.2), the reversibility of the reaction of HMF with DMC complicates the process as it requires prolonged experiments and/or higher temperature. At 30 °C, in the presence of basic catalysts ([MePPh$_3$]

[MeOCO$_2$]) and Cs$_2$CO$_3$], the HMF conversion was 59–73% after 24 h (entries 2 and 4) and was not improved even by increasing the catalyst loading from 10 to 70 mol% (Cs$_2$CO$_3$: entry 5). The yield of **4** (53–69%) was consistent with the observed conversion. This result was confirmed also by the amount of unconverted HMF (32–40% compared to the starting quantity of 0.5 mmol) that was recovered after purification/filtration on celite/silica gel. Increasing the temperature to 90 ∘C prompted a quantitative process in only 2 h, but about half of HMF underwent decomposition as anticipated by the black color of the reactant solution: the yield of product **4** did not exceed 56% (entries 3 and 6). Under such conditions, the recycle/reuse of catalysts was not even attempted because at the end of the process, both homogeneous and heterogeneous systems [([MePPh$_3$] [MeOCO$_2$]) and Cs$_2$CO$_3$] were contaminated by the presence of high-molecular weight by-products deriving from HMF degradation. The calcined hydrotalcite (C–HT30) was considerably less active than basic catalysts and not effective at 50 wt% and 30 °C (entry 7). However, at higher loading (100 wt%: 1:1 mass ratio with HMF) with respect to HMF, C–HT30 could be used successfully at 90 °C to reach an almost complete conversion (95%) and an isolated yield of **4** of 93% (24 h: entry 9). The milder catalytic performance of this (amphoteric) system apparently prevented the degradation of HMF and the catalyst was perfectly suited for recycle. After filtration, a pale-yellow solution was separated from solid C–HT30. The latter was dried under vacuum (70 °C, 5 mbar, overnight) and reused for another reaction carried out under the conditions of entry 9 in Table 5.4. The overall sequence was repeated for 4 subsequent experiments. Results are reported in Figure 5.4 The catalyst could be recycled without any significant change of its performance: both the conversion (blue bars) and the yield of product **4** (red bars) were steady at 94–95% and 91–93%, respectively.
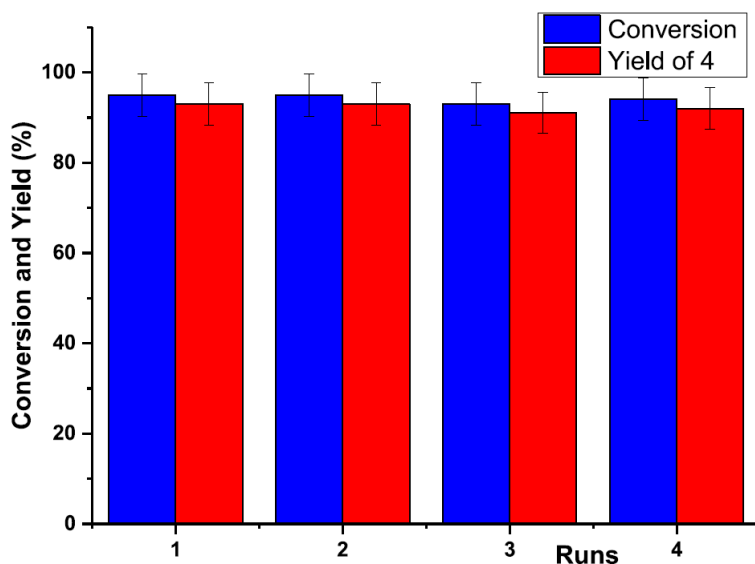
Figure 5.4. *Recycle tests of C−HT30 (100 wt%). Reaction conditions were those of Table 5.4, entry 9: HMF (0.5 mmol), DMC (30 molar equivs.), 90 °C, 24 h. Conversion and yield of **4** isolated were determined as in Table 5.4*

The synthesis was also scaled up by a factor of 10 (HMF: 50 mmol), affording product **4** in an 89% isolated yield after 36 h. Overall, the protocol was robust and reproducible. The excellent HMF/catalyst tolerability along with the simple downstream operations substantially offset the potential issue of the high loading of C–HT30. Compound **4**, once isolated, could be further

functionalized by aldol condensation with acetone. Under the best conditions of Scheme 5.5, additional experiments demonstrated that in the presence of excess acetone, the methyl carbonate of HMF was converted into the corresponding α,β-unsaturated carbonyl product **3c** in a 85% isolated yield after 15 h (Scheme 5.7).
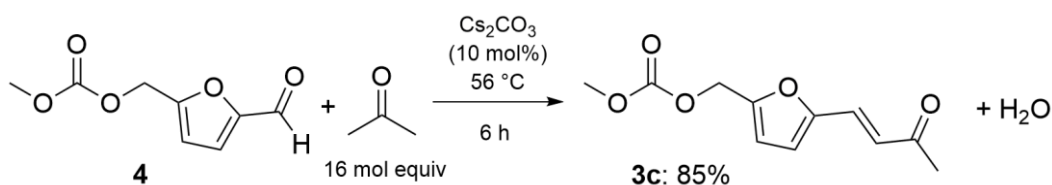
Scheme 5.7. *The acetone promoted aldol condensation of compound **4***

Compound **3c** is a new compound (characterization details including NMR and MS spectra are in the Appendix A.5). The co-presence of a carbonate group and conjugated $C = C$ and $C = O$ bonds make it a promising building block for new HMF-based oligomers and polymers. Interestingly, also the Cs_2CO_3-catalysed aldol condensation of HMF with acetone was very satisfactory: compound **3b** was isolated in a 97% yield in 3 h (conditions of Scheme 5.7).

5.2.5 Pd/C catalyzed reductive amination of HMF and its derivatives in water

Notwithstanding the extensive literature on the reductive amination of carbonyl compounds, there are only few examples of the condensation of HMF with primary amines.[47,48] Reductive amination of HMF has been reported by a two-step method involving formation of an HMF-imine intermediate followed by hydride reduction,[49] or by one-pot metal catalyzed reactions with H_2.[48] Catalytic procedures have been preferred over hydride donors (*e.g.* $NaBH_4$) that generate over-stoichiometric amounts of toxic waste to be disposed of. Although, a key challenge of these transformations remains the development of robust protocols able to operate in aqueous solutions which are more suitable for the upgrading of furanics in biorefineries.[50] With the aim to design an easily accessible method having high synthetic value, we opted to investigate the reductive amination of HMF in the presence of commercial Pd/C as a catalyst, OH-functionalized renewable amines such as 2-aminopropanediol (2-APD) and 3-aminopropanediol (3-APD),[51] and water as the solvent. Ethanolamine (EA) and propanolamine (PA) were used as model substrates in the initial experiments. Accordingly, the effects of temperature, pressure and time were explored using a mixture of HMF (0.5 mmol), EA (1.1 equivs.), water (1 mL), 5% Pd/C (3 mol% of active metal with respect to HMF) that was set to react at T = 50–75 °C, under H_2 pressure (*p* = 1–10 bar) in an autoclave, for 30–60 min. Table 5.5 reports the results.

Table 5.5. *The Pd/C catalyzed reductive amination of HMF with ethanolamine in water*
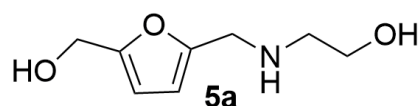
Entry	T (°C)	*p* (bar)	t (min)	5a, Yield (%)[a]
1	50	10	60	19
2	75			≥99
3	75	5		≥99
4		3		≥99

5		1		≥99
6		1	45	≥99
7			30	46

Conversion and product selectivity were determined by ^{1}H NMR upon calibration. Any attempt to characterize the reaction products by GC/MS proved unsuccessful. Experiments proved that none other than the expected derivative of reductive amination of HMF [**5a**: 2-((5-(hydroxymethyl)furan-2-yl) amino)ethan-1-ol] was observed. At 10 bar, increasing the temperature from 50 to 75 °C, a 4-fold increase of the product yield from 19 to ≥99%, was observed after only 1 h (entries 1–2). While the progressive decreasing of p from 10 to 1 bar did not affect the outcome at all: at 75 °C, the reaction was always quantitative with complete selectivity to product **5a** (entries 3–5). It was finally noticed that even the reaction time could be further reduced from 1 to 0.75 min without any appreciable alteration of the **5a** yield (entry 6). Such mild conditions were not previously reported for the reductive amination of HMF with a bidentate nucleophile such as ethanol amine. To the best of our knowledge, this reaction was described only in one recent article where product **5a** was obtained in 86% yield after 6 h at 100 °C (3 bar H_2) in the presence of Ni$_6$AlOx as a catalyst and a water/EtOH (1:2 v/v) mixture as a solvent.[50] The process of Table 5.5 was also fully chemoselective towards amine **5a**; HMF acetalization products deriving from the attack of the OH group to the carbonyl were never detected. The reductive amination of HMF was then explored using propanolamine and the two aminodiol regioisomers derived from glycerol, 3- amino-1,2-propanediol and 2-amino-1,3-propanediol (serinol). Experiments carried out under the conditions of entry 6 of Table 5.5 [T = 75 °C, p (H_2) = 1 bar, t = 45 min] demonstrated the synthetic scope of the protocol. The three tested reactions proved highly efficient yielding the corresponding products **5b, 5c**, and **5d** in 95%, 98% and 97% isolated yields, respectively (Scheme 5.8).
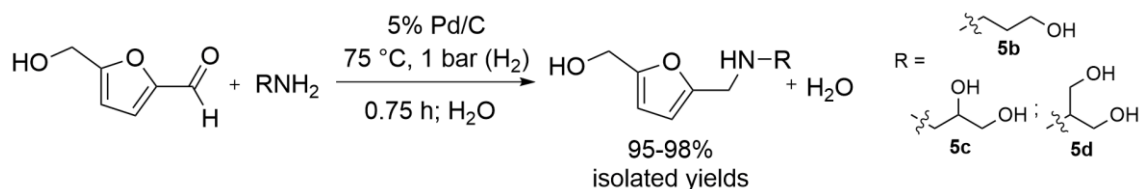
Scheme 5.8. *The reductive amination of HMF with multifunctionalized hydroxyamines*

The operative simplicity and effectiveness of the present procedure proved more efficient for the reductive amination of HMF compared to the above quoted methods,[48-50] especially in aqueous solution. Additionally, compounds **5b, 5c**, and **5d** were fully novel HMF-derivatives (further details on isolation and characterization are in the SD section): the presence of multiple (2–3) OH groups and an amine function made these products appealing for further upgrading, for example, in the synthesis of renewable furanic-based polymeric materials. To confirm the mechanism of formation of **5a-d**, additional experiments were carried out by investigating the reaction of HMF with hydroxyamines of Table 5.5 and Scheme 5.8 at lower temperatures, both with and without Pd/C. Tests confirmed the generally accepted two-step mechanism for reductive amination. i) Initially, quantitative formation of an imine derivative was observed. Notwithstanding this was formally a dehydration of the HMF carbonyl, no adverse effects of water as a solvent were noticed. The reaction proceeded quickly in all cases at 30 °C and in the absence of any catalyst. ii) In the second step, Pd/C-catalyzed hydrogenation of the C = N bond

of the imine at $T \geq 50\ °C$ yielded the desired amine. The results of this study along with the characterization of all imine intermediates are reported in the Appendix A.5. It should be finally noted that any attempt to perform the reductive amination by replacing HMF with derivatives **2** and **4** (the acylated HMF and the methyl carbonate of HMF, respectively) was unsuccessful. A complex mixture of products was obtained in both cases whose characterization/purification failed (Figure 5.5 exemplifies the case of the reaction of **2** with ethanol amine).
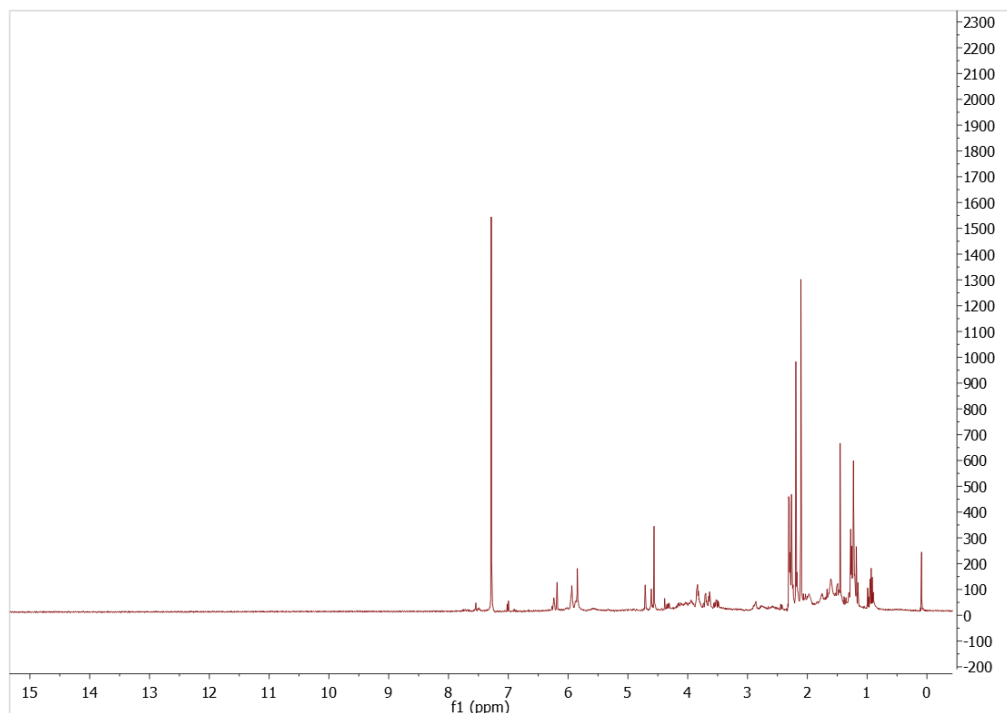
Figure 5.5. ^{1}H *NMR of the crude mixture of the reaction of HMF and ethanolamine (400 MHz, 298 K, CDCl$_3$)*

5.2.6 Wittig vinylation of HMF and its derivatives with triphenyl phosphonium methylcarbonate

As was mentioned in the introduction, some years ago our group discovered that the ylide-like reactivity of a specific ionic liquid as methyl triphenylphosphonium methylcarbonate ([MePPh$_3$] [MeOCO$_2$]), allowed not only the selective Wittig vinylation of a variety of aldehydes and ketones, but also a considerable improvement of the green metrics of the process (atom economy, E-factor, and mass index) with respect to conventional Wittig reactions.[31] We thought that these advantages could be exploited on HMF. Moreover, a further benefit could be the use of a renewable solvent as methyl tetrahydrofuran (Me-THF) that was itself derived from HMF. Experiments were then designed based on the above-mentioned work: a mixture of HMF (0.5 mmol), [MePPh$_3$] [MeOCO$_2$] (1.2 equivs.), and 2Me-THF (1 mL) was set to react at the reflux temperature (80 °C) under a N$_2$ atmosphere, for 2 h. Conditions proved successful in providing both the total conversion of HMF and the full selectivity towards the vinyl derivative **6a** [(5-vinylfuran-2-yl)methanol]. This compound was isolated in an excellent 98% yield. In light of this finding, the reaction scope was extended to HMF derivatives **2** and **4**, with equally good results on the formation of the corresponding terminal olefins **6b** [(5-vinylfuran-2-yl)methyl acetate] and **6c** [methyl ((5-vinylfuran-2-yl) methyl) carbonate], respectively. These were isolated in 96% and 95% yields. (Scheme 5.9).
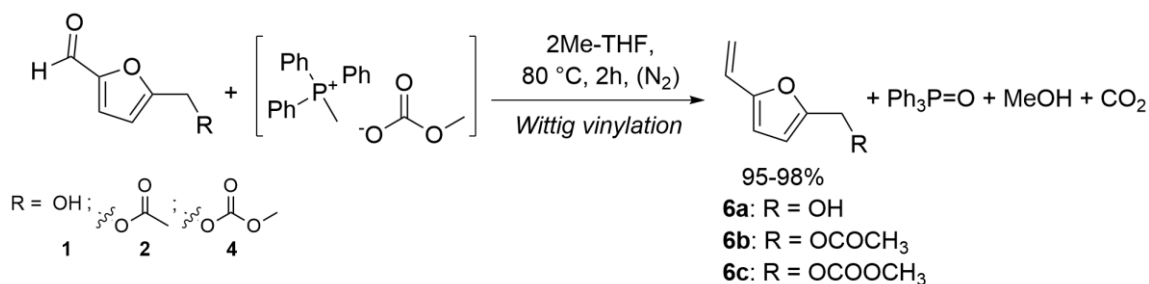
Scheme 5.9. *The Wittig vinylation of HMF and its derivatives **2** and **4** by [MePPh₃][MeOCO₂]*

Products **6a 6c** were purified by FCC on silica gel and fully characterized by NMR and GC/MS analyses (details are in the experimental and SD sections). Only one previous paper described the formation of compound **6a** through a classical Wittig reaction and with a yield of only 69%,[16] while **6b** and **6c** were two new derivatives of HMF. This investigation proved the suitability of the [MePPh₃] [MeOCO₂]-mediated vinylation for multiple-functionalized substrates as HMF and its homologues **2** and **4**, and corroborated the green advantages of the procedure including the total absence of halides throughout the whole process (and the lack of formation of inorganic halide salts to be disposed of) and the isolation of products by filtration over silica to remove the co-product triphenylphosphine oxide (TPPO).

5.3   Conclusions

The present work described diversified, robust, and greener protocols for the chemical upgrading of HMF. A variety of reactions have been described based on new or improved procedures by which a total of 12 different HMF derivatives were synthesized, isolated, and fully characterized, 7 of which new. The design of the transformations has been inspired by the green chemistry principles regarding the choice of catalytic protocols, the safety and/or renewability of reagents and solvents. Reagents include isopropenyl acetate, dimethyl carbonate, acetone, and a halide-free phosphonium vinylation reagent, that were used to carry out reactions of acetylation, carboxymethylation, aldol condensation, and vinylation, respectively, on HMF and on its homologues: acetylated HMF and the methyl carbonate of HMF. In one case, a combination of acetylation and aldol condensation has been successfully accomplished to achieve a double functionalization of HMF through a one-step tandem sequence. Moreover, the reductive amination of HMF has also been performed in the presence of water as a solvent and glycerol-derived aminodiols. In order to make the proposed procedures as accessible as possible and avoid any thermal degradation of HMF, the use of commercial catalysts (e.g. Cs₂CO₃ and Pd/C) has been privileged and experiments have been tuned to operate at 30–90 °C and atmospheric pressure. Notwithstanding the mild conditions adopted, high isolated yields of 85–95% were obtained for all products, often in a few hours or less. These results pave the way for both the study of new applications for such products and the design of new upgrading strategies. Just to name a few promising perspectives, polyhydroxylated or vinylated derivatives of HMF could be used in the materials (polymers) chemistry, while suitable as fuel additives. The work-up and post-reaction treatments of the reported procedures have not been always optimized for what concerns, for instance, the recycle of excess reagents (*e.g.* DMC and acetone which have been concurrently employed as solvents) and/or the recovery/recycle of the catalysts. However, it should be noted here that not only the reaction steps but also the downstream operations become difficult/ delicate in

the presence of sensitive substrates such as HMF and its derivatives. Further improvements of such aspects are currently under study in our laboratories and will be the object of future papers.

5.4   Experimental

5.4.1   General

Reagents and solvents were commercially available compounds and were used as received unless otherwise stated. HMF, isopropenyl acetate, acetone, dimethyl carbonate, ethanolamine, propanolamine, 2- aminopropanediol, 3-aminopropanediol, Na_2CO_3, K_2CO_3, Cs_2CO_3, d_6-acetone, Pd/C (5 wt%), D_2O, $CDCl_3$ were sourced from Sigma Aldrich (now Merck). Hydrotalcites HT-30 and HT-63 were a generous gift of Sasol Italy SpA. Ionic liquids [MePPh$_3$] [MeOCO$_2$] and [MeNPh$_3$] [MeOCO$_2$] were synthesized according to a procedure previously reported.[36] GCMS– (EI, 70 eV) analyses were performed on a HP5-MS capillary column (L = 30 m, Ø = 0.32 mm, film = 0.25 mm). ^1H and ^{13}C NMR spectra were recorded at 400 and 100 MHz, respectively. The chemical shifts were reported downfield from tetramethylsilane (TMS), and $CDCl_3$ or D_2O were used as the solvents.

5.4.2   General procedure for the iPAc-mediated acetylation and tandem acetylation-aldol condensation of HMF

Experiments were performed under different conditions (details are in Table 5.2). In a typical procedure for the acetylation of HMF, a 5-mL round-bottomed flask equipped with a condenser and a magnetic stir bar, was charged with a mixture of HMF (0.5 mmol), isopropenyl acetate (1.5 equivs.), and the catalyst (15 wt% or 10–70 mol%, depending on the chosen catalyst). The flask was then heated at the desired temperature, at atmospheric pressure. Aliquots of the reaction mixture were withdrawn at intervals and analyzed by GC/MS to determine the conversion of HMF and product selectivity. The same procedure was used for the tandem acetylation-aldol condensation process except for the addition of acetone (up to 16 molar equivs with respect HMF). Details are in Figure 5.2 and Scheme 5.5. The same procedure was also used for experiments carried under a N_2 pressure (8 bar, Table 5.3 and Figure 5.1) or above 60 °C. In this case, however, a stainless-steel autoclave (inner volume 10 mL) was the reaction vessel. A typical work-up is reported for the isolation of the acetylated product **2** [(5-formylfuran-2-yl)methyl acetate)] when the acetylation of HMF was scaled up by a factor of 10 (HMF: 5 mmol; HMF:iPAc=1:1.5 mol:mol; T = 30 °C; p = 1 atm; Cs_2CO_3 in 70 mol% (1140 g); t = 15 min). Once the experiment was complete, the solid catalyst and the eventual formed char/humins were filtered off using a short column for chromatography (length = 15 cm; inner diameter = 1 cm) filled with celite and silica (5 g each) and washed with MeOH (20 mL). The excess solvent was rotary evaporated (p = 10 mbar) affording compound **2** in a 92% yield and >98% purity by GC–MS. The product was further characterized by ^1H and ^{13}C NMR and (see Appendix A.5). Data were in agreement with those reported in the literature.[20] The tandem product **3a** ((E)-(5-(3-oxobut-1-en-1-yl)furan-2-yl) methyl acetate) was isolated from the reaction of HMF (0.5 mmol), iPAc (1.5 equivs), acetone (16 equivs.), in the presence of Cs_2CO_3 (10 mol%) as a catalyst. Once the reaction was complete (15 h at T = 56 °C), the solid catalyst and the eventual formed char/humins were filtered off using a short column for chromatography (length = 15 cm; inner diameter = 1 cm) filled with celite and silica (5 g each)

and washed with MeOH (20 mL). Then, the excess solvent was rotary evaporated (p = 10 mbar) affording compound **3a** in 88% yield and > 99% purity by GC–MS. The product was further characterized by ^{1}H and ^{13}C NMR and GC–MS analyses (see Appendix A.5).

5.4.3 General procedure for the DMC-promoted carboxymethylation of HMF and further aldol condensation

Experiments were performed under different conditions (details are in Table 5.4). In a typical procedure for the carboxymethylation of HMF, a 5-mL round-bottomed flask equipped with a condenser and a magnetic stir bar, was charged with a mixture of HMF (0.5 mmol), DMC (1.3 mL, 30 equivs.), and the catalyst (50–100 wt% or 10 mol%, depending on the chosen catalyst). The mixture was set to react at the desired temperature (30–90 °C) and atmospheric pressure. Aliquots of the reaction mixture were withdrawn at intervals and analyzed by GC/MS to determine the conversion of HMF and product selectivity. A typical work-up is reported for the isolation of the carboxymethylated product **4** [(5-formylfuran-2-yl)methyl acetate)] when the reaction of HMF was scaled up by a factor of 10 (HMF: 5 mmol; HMF: DMC=1:30 mol:mol; C– HT30=100 wt%;). Once the experiment was complete (36 h at 90 °C; p = 1 atm, the solid catalyst and the eventual formed char/humins were filtered off using a short column for chromatography (length = 15 cm; inner diameter = 1 cm) filled with celite and silica (5 g each) and washed with MeOH (20 mL). The excess DMC and solvent (MeOH) were rotary evaporated (p = 10 mbar) affording compound **4** in 89% yield. The product was further characterized by ^{1}H and ^{13}C NMR and GC–MS analyses (see Appendix A.5). Data were in agreement with those reported in the literature.[22]

5.4.4 Aldol condensation of compound 4 and acetone

A mixture of compound **4**, acetone (16 equivs.), and Cs$_2$CO$_3$ (10 mol %) was charged in a 10-mL round bottom flask, equipped with a condenser and a magnetic stir bar. The flask was heated at the reflux temperature (56 °C) for 6 h. Once the reactions were complete, the solid catalyst and the eventual formed char/humins were filtered off using a short column for chromatography (length = 15 cm; inner diameter = 1 cm) filled with celite and silica (5 g each) and washed with MeOH (20 mL). The excess acetone was removed by rotary evaporation (p = 10 mbar). Then, compound **3c** was purified by FFC on silica gel (eluant: petroleum ether:ethyl acetate = 1 : 1 v/v) and isolated in a 85% yield. The product was then characterized by ^{1}H and ^{13}C NMR and GC–MS (see Appendix A.5).

5.4.5 Aldol condensation of HMF and acetone

The same procedure described for the aldol condensation of **4** was repeated by using HMF as the substrate. The corresponding product **3b** was isolated in a 97% in 3 h. The product was then characterized by ^{1}H and ^{13}C NMR and GC–MS (see Appendix A.5).

5.4.6 General procedure for the reductive amination of HMF

In a typical experiment, HMF (0.5 mmol), the amino alcohol of choice (1.1 equivs.; RNH$_2$: R=(CH$_2$)nOH, n = 2–3, CH(CH$_2$OH)$_2$, CH$_2$CH (OH)CH$_2$OH]), water (1 mL), 5% Pd/C as a catalyst (3 mol% of Pd with respect to HMF) were mixed in a 5-mL glass tubular reactor, equipped with a pierced glass stopper and a magnetic stir bar. The reactor was placed inside a 10 mL stainless steel autoclave which was purged by three N$_2$-vacuum cycles. The mixture was then pressurized

with H_2 (1–10 bar) and set to react at T = 50–75 °C for t = 30–60 min. Conversion of HMF and product selectivity were determined by ^{1}H NMR analysis. The products **5a**-**5d** (Table 5.5 and Scheme 5.8) were isolated after reactions run under the best conditions found for the reductive amination (p (H_2) = 1 bar, T = 75 °C, t = 45 min). Once reactions were complete, the solid catalyst was filtered, and the crude residue was purified by FFC on silica gel (eluant: MeOH). Then, the excess solvent was rotary evaporated (p = 10 mbar). Compounds **5a, 5b, 5c, 5d** were isolated in 96%, 97%, 93%, 95% yields, respectively. The products were characterized by ^{1}H and ^{13}C NMR (see Appendix A.5).

5.4.7   General procedure for the Wittig vinylation of HMF and its derivatives 2 and 4

In a typical procedure, a 10-mL round bottom flask equipped with a condenser and a magnetic stir bar, was charged with a mixture of HMF or its derivatives **2** or **3** (0.5 mmol), [Ph$_3$PCH$_3$] [CH$_3$OCO$_2$] (1.2 equivs.), and 2Me-THF (5 mL) as a solvent. The mixture was set to react at the reflux temperature (80 °C) for 2 h. Once the reaction was complete, the excess of solvent was removed by rotary evaporation (p = 10 mbar), and the liquid residue purified by FCC on silica gel

The results of this work have been the object of the paper:

The contribution of DR was in the design and conduction of experiments for the acetylation, aldol condensation, carboxymethylation, and vinylation of HMF, and the writing of the draft of the research article. He also collaborated with DP in the conduction of experiments for the reductive amination of HMF.

References

[1] S. Kang, J. Fu, G. Zhang, From lignocellulosic biomass to levulinic acid: a review on acid-catalyzed hydrolysis, *Renew. Sustainable Energy Rev.*, **2018**, *94*, 340. https://doi.org/10.1016/j.rser.2018.06.016

[2] G. De Vries, Hydroxymethylfurfural, a versatile platform chemical made from renewable resources, *Chem. Rev.*, **2013**, *113*, 1499. https://doi.org/ 10.1021/cr300182k

[3] A.A. Rosatella, S.P. Simeonov, R.F.M. Frade, C.A.M. Afonso, 5- Hydroxymethylfurfural (HMF) as a building block platform: biological properties, synthesis and synthetic applications, *Green Chem*, **2021**, *13*, 754. https://doi.org/10.1039/C0GC00401D

[4] F.A. Kucherov, L.V. Romashov, K.I. Galkin, V.P. Ananikov, Chemical transformations of biomass-derived C6-furanic platform chemicals for sustainable energy research, materials science, and synthetic building blocks, *ACS Sustain. Chem. Eng.*, **2018**, *6*, 8064. https://doi.org/10.1021/acssuschemeng.8b00971

[5] X. Zhang, K. Wilson, A.F. Lee, Heterogeneously catalyzed hydrothermal processing of C5–C6 sugars, *Chem. Rev.*, **2016**, *116*, 12328. https://doi.org/10.1021/ acs.chemrev.6b00311

[6] K. Gupta, R.K. Rai, S.K. Singh, Metal catalysts for the efficient transformation of biomass-derived hmf and furfural to value added chemicals, *ChemCatChem*, **2018**, *10*, 2326. https://doi.org/10.1002/cctc.201701754

[7] R.T. Cummings, J.P. DiZio, G.A. Krafft, Photoactivable fluorophores. 2. Synthesis and photoactivation of functionalized 3-aroyl-2-(2-furyl)-chromones, *Tetrahedron Lett*, **1988**, *29*, 69. https://doi.org/10.1016/0040-4039(88)80018-2

[8] J. Van Schijndel, L.A. Canalle, D. Molendijk, J. Meuldijk, Exploration of the role of double schiff bases as catalytic intermediates in the knoevenagel reaction of furanic aldehydes: mechanistic considerations, *Synlett*, **2018**, *29*, 1983. https://doi. org/10.1055/s-0037-1610235

[9] W. Fan, Y. Queneau, F. Popowycz, The synthesis of HMF-based α-amino phosphonates via one-pot kabachnik–fields reaction, *RSC Adv*, **2018**, *8*, 31496. https://doi.org/10.1039/C8RA05983G

[10] K.I. Galkin, V.P. Ananikov, Towards improved biorefinery technologies: 5-methylfurfural as a versatile c6 platform for biofuels development, *ChemSusChem*, **2019**, *12*, 185. https://doi.org/10.1002/cssc.201802126

[11] R.F.A. Gomes, J.A.S. Coelho, C.A.M. Afonso, Direct conversion of activated 5- hydroxymethylfurfural into δ-lactone-fused cyclopentenones, *ChemSusChem*, **2019**, *12*, 420. https://doi.org/10.1002/cssc.201802537

[12] A. Bohre, B. Saha, M.M. Abu-Omar, Catalytic upgrading of 5-hydroxymethylfurfural to drop-in biofuels by solid base and bifunctional metal–acid catalysts, *ChemSusChem*, **2015**, *8*, 4022. https://doi.org/10.1002/cssc.201501136

[13] T. Yutthalekha, D. Suttipat, S. Salakhum, A. Thivasasith, S. Nokbin, J. Limtrakul, C. Wattanakit, Aldol condensation of biomass-derived platform molecules over amine-grafted hierarchical FAU-type zeolite nanosheets (Zeolean) featuring basic sites, *Chem. Commun.*, **2017**, *53*, 12185. https://doi.org/10.1039/ C7CC06375J

[14] R. Lee, J.R. Vanderveen, P. Champagne, P.G. Jessop, CO₂-Catalysed aldol condensation of 5-hydroxymethylfurfural and acetone to a jet fuel precursor, *Green Chem*, **2016**, *18*, 5118. https://doi.org/10.1039/C6GC01697A

[15] J.J. Roylance, K.S. Choi, Electrochemical reductive amination of furfural-based biomass intermediates, *Green Chem*, **2016**, *18*, 5412. https://doi.org/ 10.1039/C6GC01541G

[16] A. Feriani, G. Gaviraghi, G. Toson, M. Mor, A. Barbieri, E. Grana, C. Boselli, M. Guarneri, D. Simoni, S. Manfredini, Cholinergic agents structurally related to furtrethonium. 2. synthesis and antimuscarinic activity of a series of n- [5-[(1'-substituted-acetoxy)methyl]-2-furfuryl]dialkylamines, *J. Med. Chem.*, **1994**, *37*, 4278. https://doi.org/10.1021/jm00051a004

[17] M. Han, X. Liu, X. Zhang, Y. Pang, P. Xu, J. Guo, Y. Liu, S. Zhang, S. Ji, 5- Hydroxymethyl-2-vinylfuran: a biomass-based solvent-free adhesive, *Green Chem*, **2017**, *19*, 722. https://doi.org/10.1039/C6GC02723G

[18] E.S. Kang, Y.W. Hong, D.W. Chae, B. Kim, B. Kim, Y.J. Kim, J.K. Cho, Y.G. Kim, From lignocellulosic biomass to furans via 5-acetoxymethylfurfural as an alternative to 5-hydroxymethylfurfural, *ChemSusChem*, **2015**, *8*, 1179. https://doi.org/10.1002/cssc.201403252

[19] J.A.S. Coelho, A.F. Trindade, V. Andr´e, M.Teresa Duarte, L.F. Veiros, C.A. M. Afonso, Trienamines derived from 5-substituted furfurals: remote ε-functionalization of 2,4-dienals, *Org. Biomol. Chem.*, **2014**, *12*, 9324. https://doi.org/10.1039/C4OB01759E

[20] D. Koszelewski, R. Ostaszewski, The studies on chemoselective promiscuous activity of hydrolases on acylals transformations, *Bioorg. Chem.*, **2019**, *93*, 102825. https://doi.org/10.1016/j.bioorg.2019.02.050

[21] M. Sheykhan, H.F. Moafi, M. Abbasnia, Novel access to carbonyl and acetylated compounds: the role of the tetra-n-butylammonium bromide/sodium nitrite catalyst, *RSC Adv*, **2016**, *6*, 51347. https://doi.org/10.1039/C6RA08672A

[22] M. Krystof, M. P´erez-S´anchez, P. Domínguez De María, Lipase-catalyzed (trans) esterification of 5-hydroxy-methylfurfural and separation from HMF esters using deep-eutectic solvents, *ChemSusChem*, **2013**, *6*, 630. https://doi.org/ 10.1002/cssc.201200931

[23] L. Wiermans, S. Hofzumahaus, C. Schotten, L. Weigand, M. Schallmey, A. Schallmey, P.D. De María, Transesterifications and peracid-assisted oxidations in aqueous media catalyzed by mycobacterium smegmatis acyl transferase, *ChemCatChem*, **2013**, *5*, 3719. https://doi.org/10.1002/cctc.201300683

[24] S. Chen, R. Wojcieszak, F. Dumeignil, E. Marceau, S. Royer, How catalysts and experimental conditions determine the selective hydroconversion of furfural and 5- hydroxymethylfurfural, *Chem. Rev.*, **2018**, *118*, 11023. https://doi.org/10.1021/acs.chemrev.8b00134

[25] G. Tsilomelekis, M.J. Orella, Z. Lin, Z. Cheng, W. Zheng, V. Nikolakis, D.G. Vlachos, Molecular structure, morphology and growth mechanisms and rates of 5-hydroxymethyl furfural (HMF) derived humins, *Green Chem*, **2016**, *18*, 1983. https://doi.org/10.1039/C5GC01938A.

[26] K.I. Galkin, E.A. Krivodaeva, L.V. Romashov, S.S. Zalesskiy, V.V. Kachala, J. V. Burykina, V.P. Ananikov, Critical influence of 5-hydroxymethylfurfural aging and decomposition on the utility of biomass conversion in organic synthesis, *Angew. Chemie*, **2016**, *128*, 8478. https://doi.org/10.1002/ ange.201602883

[27] P.Y. Nikolov, V.A. Yaylayan, Thermal decomposition of 5-(Hydroxymethyl)-2- furaldehyde (HMF) and its further transformations in the presence of glycine, *J. Agric. Food Chem.*, **2011**, *59*, 10104. https://doi.org/10.1021/ jf202470u

[28] W. Fan, C. Verrier, Y. Queneau, F. Popowycz, 5-Hydroxymethylfurfural (HMF) in organic synthesis: a review of its recent applications towards fine chemicals, *Curr. Org. Synth.*, **2019**, *16*, 583. https://doi.org/10.2174/1570179416666190412164738

[29] P. S. Kong, M. K. Aroua, W. M. A. W. Daud, H. V. Lee, P. Cognet, Y. Peres, Catalytic role of solid acid catalysts in glycerol acetylation for the production of bio-additives: a review, *RSC Adv*, **2016**, *6*, 68885. https://doi.org/10.1039/ C6RA10686B

[30] L.R. Odell, J. Skopec, A. McCluskey, A 'cold synthesis' of heroin and implications in heroin signature analysis: utility of trifluoroacetic/acetic anhydride in the acetylation of morphine, *Forensic Sci. Int.*, **2006**, *164*, 221. https://doi.org/10.1016/j.forsciint.2006.02.009

[31] L. Cattelan, M. Noe, M. Selva, N. Demitri, A. Perosa, Methyltriphenylphosphonium methylcarbonate, an all-in-one wittig vinylation reagent, *ChemSusChem*, **2015**, *8*, 3963. https://doi.org/10.1002/cssc.201500935

[32] R.J. Van Putten, J.C. Van Der Waal, E. De Jong, C.B. Rasrendra, H.J. Heeres, J. G. De Vries, Hydroxymethylfurfural, a versatile platform chemical made from renewable resources, *Chem. Rev.*, **2013**, *113*, 1499. https://doi.org/10.1021/cr300182k

[33] P. Anastas, N. Eghbali, Green chemistry: principles and practice, *Chem. Soc. Rev.*, **2010**, *39*, 301. https://doi.org/10.1039/B918763B

[34] https://www.sigmaaldrich.com/catalog/product/aldrich/809551?lang=it&region =IT (Accessed 11/10/2021).

[35] D. Rigo, G. Fiorani, A. Perosa, M. Selva, Acid-catalyzed reactions of isopropenyl esters and renewable diols: a 100% carbon efficient transesterification/ acetalization tandem sequence, from batch to continuous flow, *ACS Sustain. Chem. Eng.*, **2019**, *7*, 18810. https://doi.org/10.1021/acssuschemeng.9b03359

[36] M. Bolognini, F. Cavani, D. Scagliarini, C. Flego, C. Perego, M. Saba, Heterogeneous basic catalysts as alternatives to homogeneous catalysts: reactivity of Mg/Al mixed oxides in the alkylation of m-cresol with methanol, *Catal. Today*, **2002**, *75*, 103. https://doi.org/10.1016/S0920-5861(02)00050-0

[37] L. Cattelan, A. Perosa, P. Riello, T. Maschmeyer, M. Selva, Continuous-flow O-alkylation of biobased derivatives with dialkyl carbonates in the presence of magnesium-aluminium hydrotalcites as catalyst precursors, *ChemSusChem,* **2017**, *10*, 1571. http://dx.doi.org/10.1002/cssc.201601765

[38] M. Fabris, V. Lucchini, M. Noè, A. Perosa, M. Selva, Ionic liquids made with dimethyl carbonate: solvents as well as boosted basic catalysts for the Michael reaction, *Chem. Eur. J.,* **2009**, *15*, 12273. https://doi.org/10.1002/chem.200901891

[39] R. Rabie, M.M. Hammoud, K.M. Elattar, Cesium carbonate as a mediated inorganic base in some organic transformations, *Res. Chem. Intermed.*, **2017**, *43*, 1979. https://doi.org/10.1007/s11164-016-2744-z

[40] V.A. Stenger, Solubilities of various alkali metal and alkaline earth metal compounds in methanol, *J. Chem. Eng. Data*, **1996**, *41*, 1111. https://doi. org/10.1021/je960124k

[41] M. Selva, C.A. Marques, P. Tundo, Selective mono-methylation of arylacetonitriles and methyl arylacetates by dimethyl carbonate, *J. Chem. Soc. Perkin Trans. I*, **1994**, 1323. https://doi.org/10.1039/P19940001323

[42] D. Rigo, R. Calmanti, A. Perosa, M. Selva, A transesterification–acetalization catalytic tandem process for the functionalization of glycerol: the pivotal role of isopropenyl acetate, *Green Chem*., **2020**, *22*, 5487. https://doi.org/10.1039/D0GC01775B

[43] K. Watanabe, N. Yamagiwa, Y. Torisawa, Cyclopentyl Methyl Ether as a New and Alternative Process Solvent, *Org. Proc. Res. Develop*., **2007**, *11*, 251. https://doi.org/10.1021/op0680136

[44] C. F. Riadigos, R. Iglesias, M. A. Rivas, T.P. Iglesias, Permittivity and density of the systems (monoglyme, diglyme, triglyme, or tetraglyme + n-heptane) at several temperatures, *J. Chem. Thermodynamics*, **2011**, *43*, 275. https://doi.org/10.1016/j.jct.2010.09.008

[45] https://www.engineeringtoolbox.com/acetone-2-propanone-dimethyl-ketone-properties-d_2036.html (accessed 10/11/2021)

[46] J.F. Marlier, Multiple isotope effects on the acyl group transfer reactions of amides and esters, Acc. Chem. Res., 2001, 34, 283. https://doi.org/10.1021/ar000054d

[47] J. He, L. Chen, S. Liu, K. Song, S. Yang, A., sustainable access to renewable N-containing chemicals from reductive amination of biomass-derived platform compounds, *Green Chem*., **2020**, *22*, 6714. https://doi.org/10.1039/D0GC01869D

[48] A. García-Ortiz, J.D. Vidal, M.J. Climent, P. Concepcion, A. Corma, S. Iborra, Chemicals from biomass: selective synthesis of N-substituted furfuryl amines by the one-pot direct reductive amination of furanic aldehydes, ACS Sustainable Chem. Eng., 2019, 7, 6243. https://doi.org/10.1021/acssuschemeng.8b06631

[49] A. Cukalovic, C.V. Stevens, Production of biobased HMF derivatives by reductive amination, Green Chem., 2010, 12, 1201. https://doi.org/10.1039/C002340J

[50] H. Yuan, J.-.P. Li, F. Su, Z. Yan, B.T. Kusema, S. Streiff, Y. Huang, M. Pera-Titus, F. Shi, Reductive amination of furanic aldehydes in aqueous solution over versatile niyalox catalysts, *ACS Omega*, **2019**, *4*, 2510. https://doi.org/10.1021/acsomega.8b03516

[51] D. Rigo, N.A. Carmo Dos Santos, A. Perosa, M. Selva, Concatenated batch and continuous flow procedures for the upgrading of glycerol-derived aminodiols via n-acetylation and acetalization reactions, *Catalysts*, **2021**, *11*, 1. https://doi.org/10.3390/catal11010021

6 A new family of renewable thermosets: Kraft lignin polyadipates

6.1 Introduction

Plastics are produced in 368 Mtons per year and are pivotal for our everyday life in vast applications such as sterile hospital instruments, coatings to prolong the lifetime and increase the hydrophobicity of wood products, molecular electronics, materials in electronic devices, *etc*.[1] Even though there is a strive to substitute plastic materials for bio-based ones such as wood, there will still be a demand for plastics in the future. Therefore, there has been an effort to substitute fossil-based plastics for bio-based alternatives. However, to avoid food competition and better exploit the existing resources, waste or side streams should preferably be used. Such waste streams are common in the Kraft pulp and paper industry, which has an estimated annual production of 260 Mtons/y of pulp and where 130 Mtons/y of Kraft lignin (KL), in form of black liquor, is processed.[2] Currently, KL is burnt to a low value for the pulp mill.[3] To make the KL source more valuable, several strategies have been reported to produce lignin-based plastics by either incorporating KL into a thermoplastic polymer and by producing KL-based thermosets.[4,5] However, KL is extracted as an amphiphilic solid with scarce affinity with common plastics, and therefore, to achieve blends or composites with non-polar matrices, further chemical functionalizations are required.[6] These functionalization procedures yield lignin derivatives with increased lipophilicity to allow homogeneous mixing with the polymer. Among the reported methodologies, the esterification of KL is one of the most investigated.[7,8,9] In relation to the production of lignin-based thermosets, the solid nature of lignin hinders the direct generation of a homogeneous prepolymer. A crosslinking mixture (CLM) is generally not able to disperse KL sufficiently where usually one or more pretreatment steps are required, *e.g.* KL fractionation, KL pre-functionalization, use of dispersants such as PEG or solvents. Consequently, a synthetic strategy that allows the direct mixing of KL and a CLM to yield a sufficiently homogeneous liquid prepolymer would be beneficial. The free hydroxyl moieties are the main functional groups on the Kraft lignin chain (approx. 6.5 mmol/g) making the synthesis of esters of lignin with fatty acids a valuable strategy for its functionalization.[10] Polyacids act as crosslinking agents *via* esterification with free hydroxyl groups.[11,12] However, only a few reports based on citric acid showed the reaction between lignin, as a minor component, and polyacids to yield a thermoset.[13,14] Due to the abovementioned compatibility issues, a high concentration of untreated lignin is usually detrimental to the homogeneity of the prepolymer, and the mechanical properties of the resulting resins, reducing their potential application.[15] Aiming to use untreated KL in a two components resin, a new strategy has been designed to use activated dioic acids to generate a homogeneous prepolymer that can be poured and molded as a thermoset material.

6.2 Results and discussion

6.2.1 Synthesis of the crosslinking mixture (CLM)

A diester of AdA has been envisioned to perform the crosslinking of two separate parts of KL. Acid catalysis can promote the AdA esterification.[16,17] However, the direct condensation of KL with carboxylic groups would require high temperatures associated with undesired reactivity.[8] An activated version of AdA was designed by performing the reaction with an excess of

isopropenyl acetate (iPAc) using catalytic amounts of H_2SO_4 (Scheme 6.10). This protocol showed two primary synthetic and safety advantages: i) for one thing, iPAc was a non-toxic acetylating reagent, not strictly regulated as Ac_2O; ii) the low boiling points associated to iPAc and acetone (Ace) and acetic acid as co-products made their removal by distillation easy after the completion of the esterification process.[18,19] Indeed, both the recovered by-products (Ace and AcOH) could in principle be reused to produce iPAc.[20] The effects of experimental conditions were investigated by changing the catalyst amount, the temperature, and the time. The best result was achieved by setting a mixture of AdA (5 g, 34.2 mmol), iPAc (4 equiv) and H_2SO_4 (0.8 mol%) to react for 4 hours at 97 °C. The so-obtained cross-linking mixture (CLM: a total of 6.5 g) was characterized by NMR and high-resolution mass spectrometry (HR-MS) (see Appendix A.6 for spectra) and it was comprised of isopropenyl functional groups (2.4 equiv/g) and anhydrides moieties (8.0 equiv/g). Both acetyl anhydrides (6.2 equiv/g) and adipoyl anhydrides (1.8 equiv/g) were generated. The HR-MS analysis showed up to trimeric poly-adipic anhydride with all the combinations for the terminal groups, either isopropenyl esters or acetyl anhydrides.
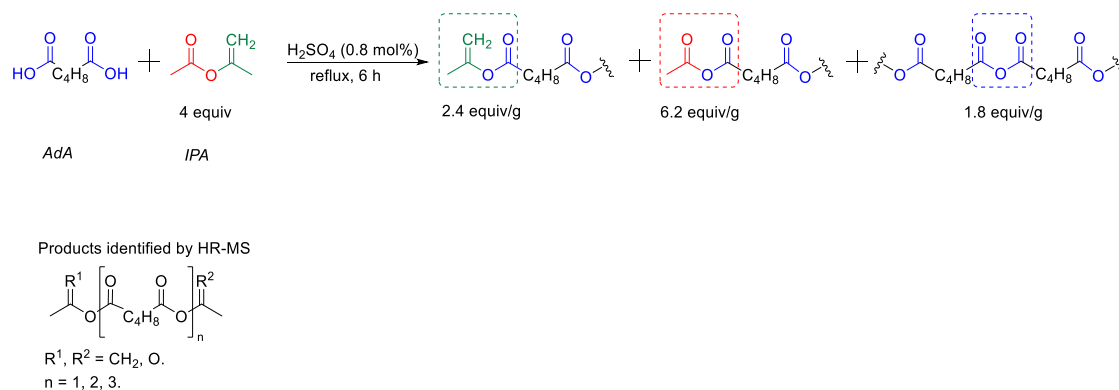
Scheme 6.10. *Optimized synthesis of the crosslinking mixture (CLM)*

The reaction of Scheme 6.1 was easily scaled up to 500 g of AdA giving identical yields and compositions of the resulting CLM.

6.2.2 Synthesis of Lignoboost Kraft lignin polyadipate (KLPA)

The above-described CLM (19.5 g) was set to react with dry Lignoboost KL (30 g). The two components were mixed in an equimolar amount to lignin hydroxyl groups, and the resulting dark brown suspension (primer) was heated swiftly to 100 °C for 10 minutes. When the KL started to react with the CLM, a viscous homogenous liquid, a "masterbatch", was obtained. The masterbatch was poured, while still warm, into a PTFE rectangular mold placed between two flat surfaces and heated at 100 °C for 16 hours (under autogenous pressure) to achieve the crosslinking while maintaining the shape. Thereafter, a Kraft lignin *poly*-adipate in the form of a dark brown rigid solid was obtained. The overall procedure is illustrated in Figure 6.6.
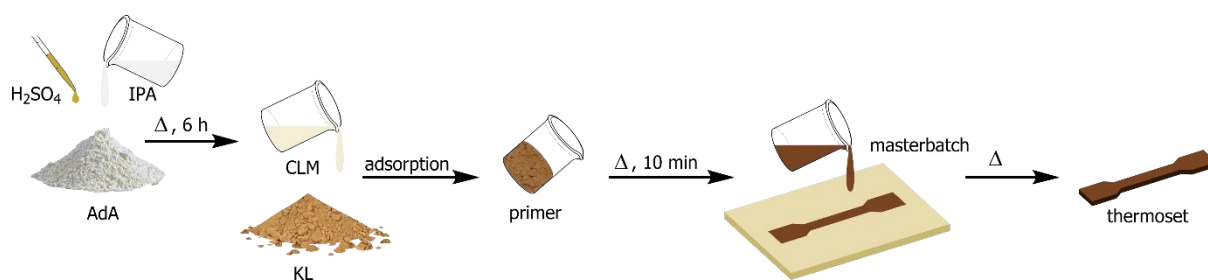
Figure 6.6. *Overall synthetic process of KLPA*

Notably, recent papers have described the preparation of (renewable) AdA directly from lignin instead of fossil feedstocks as is currently the case. According to Scheme 6.1 and Figure 6.1, the use of renewable AdA would potentially allow the fabrication of a thermoset material almost fully based on lignin.[21,22,23,24,25]

6.2.3   KL polyesters tensile properties

The tensile properties of the thermoset materials with different compositions and process parameters were evaluated by performing stress-strain analysis on rectangular samples (70 mm × 15 mm × 1.2 mm, clamp distance 40 mm, and elongation rate 5 mm/min). A negative trend was registered in the elastic behavior of the KLPAs produced with 1, 1.5, and 2 equiv of CLM. A higher CLM:KL ratio led to materials with lower tensile strength and Young's modulus (

Table 6.**6**, entries 1–3), disclosing the plasticizing effect of the extra CLM. The same trend was observed when adding glycerol (10 and 20 wt%) (

Table 6.**6**, entries 4 and 5). In an additional control experiment KL was set to react with a CLM based on hexanoic acid in place of AdA: the presence of a monoacid brought about the formation of a viscous material fully soluble in THF and not suitable for stress/strain analysis, thereby suggesting that crosslinking, if any, was not successful in this case (

Table 6.**6**, entry 6). The corresponding GPC analysis showed a KL with a (increased) molecular weight compatible with a lignin ester (Figure 6.7). This behavior indicated that the mechanical properties of the material could be tuned based on either the ratio of CLM and KL and the addition of glycerol.
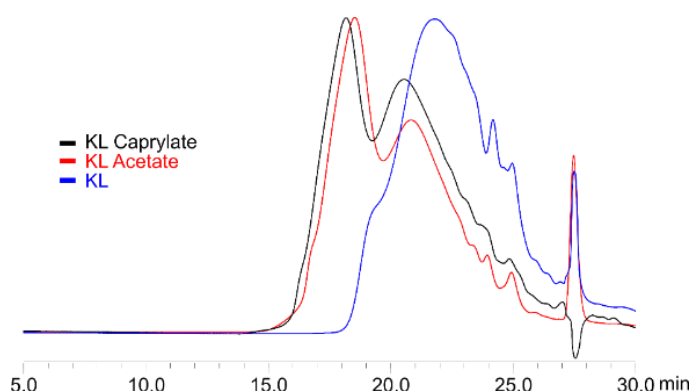
Figure 6.7. *GPC chromatogram KL (blue), KL acetate (red), and KL reacted with Caprylic CLM (black)*

Table 6.6. *KL-based polyester tensile properties*

219

Entry	CLM (equiv)	Tens. Strength (MPa)	Tens. Strain (%)	E (σ/ε MPa)
1	1	15 ± 3	10 ± 3	1400 ± 254
2	1.5	7 ± 1	90 ± 30	300 ± 16
3	2	1.3 ± 0.1	120 ± 14	11 ± 1
4[a]	1	1.9 ± 0.3	6 ± 2	125 ± 7
5[b]	1	0.33 ± 0.01	145 ± 10	14 ± 5
6[c]	1	-	-	-

Reaction conditions: Lignoboost Kraft lignin (30 g), 100 °C, 16 h. [a] Glycerol (10 wt%) added on top. [b] Glycerol (20 wt%) added on top. [c] CLM based on caprylic acid, the resulting material was not analyzable by a tensile stress machine. Mean values of 3 repetitions associated with standard deviation.

6.2.4   KLPA thermal analysis

The materials resulting from the reaction of KL and an equimolar amount of CLM were further tested by differential scanning calorimetry and thermo-gravimetric analysis. The thermograms of the KL-based materials and intermediates are depicted in Figure 6.8, top. The thermogram of CLM alone shows an endo peak at 155 °C, corresponding to the melting point of the residual AdA.[26] Interestingly, both the primer and masterbatch behaved similarly, both showing an exothermic peak at around 150 °C indicating the reaction of the CLM with KL. The thermogram of the corresponding polyester, which only contains fully reacted CLM, showed only an endo peak at 100 °C produced by the evaporation of the residual acetic acid which is a by-product of the reaction of CLM with KL. The TGA analysis showed the thermal stability of the polyester up to 125 °C with a negligible mass loss of 1.0 wt% (Figure 6.8, bottom).
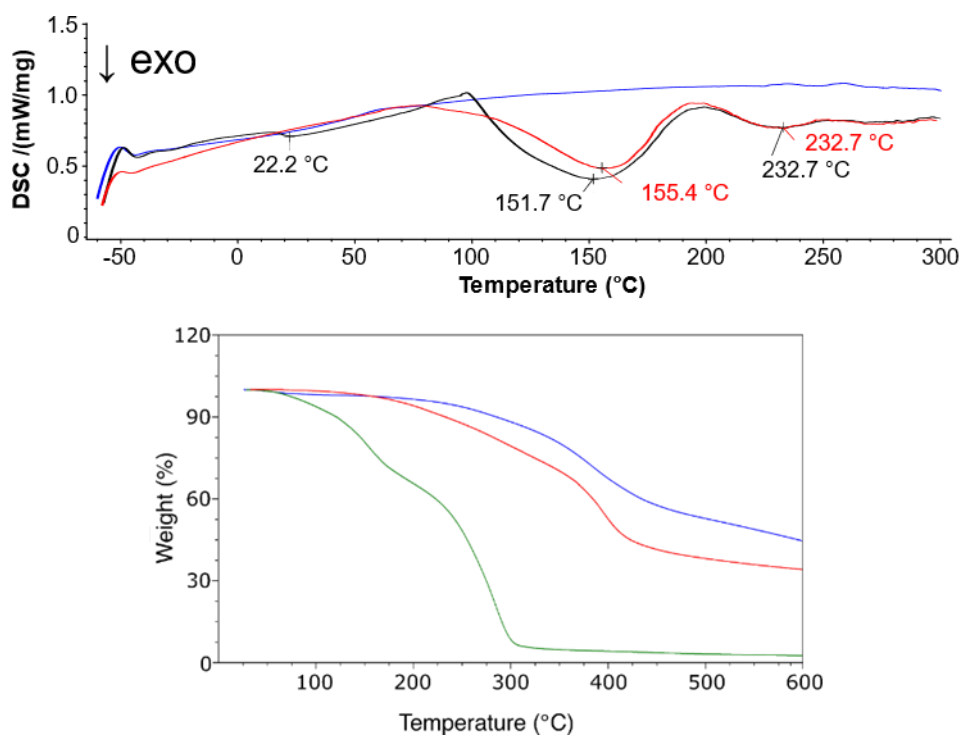
Figure 6.8. *Top: thermograms of KL with equimolar C$_6$-CLM, primer (**black**), masterbatch (**red**), and KLPA (**blue**). Bottom: TGA analysis of KL (**blue**), C$_6$-CLM (**green**), and KLPA (**red**)*

6.2.5 Mechanistic study

Additional characterization tests were carried out to study the chemistry occurring at the masterbatch stage and the crosslinking step to produce the thermoset. IR spectra were therefore recorded at different times during the overall process of formation of the material (Figure 6.9). The band at 3370 cm^{-1}, which corresponds to the free hydroxyl groups of KL, decreased at the masterbatch stage. The same reductions in intensity were observed for the signals at 1744 cm^{-1} and 1816 cm^{-1}, assigned to the C–H stretching of anhydride functions.[27] Notably, as these bands decreased, the intensities of the peaks corresponding to lignin esters at 1708 cm^{-1}, increased: the latter were dominating at the KLPA stage (Figure 6.9, top). In addition, the reaction of KL with 2 equivalents of CLM resulted in full conversion of the free hydroxyl groups (Figure 6.9, bottom).
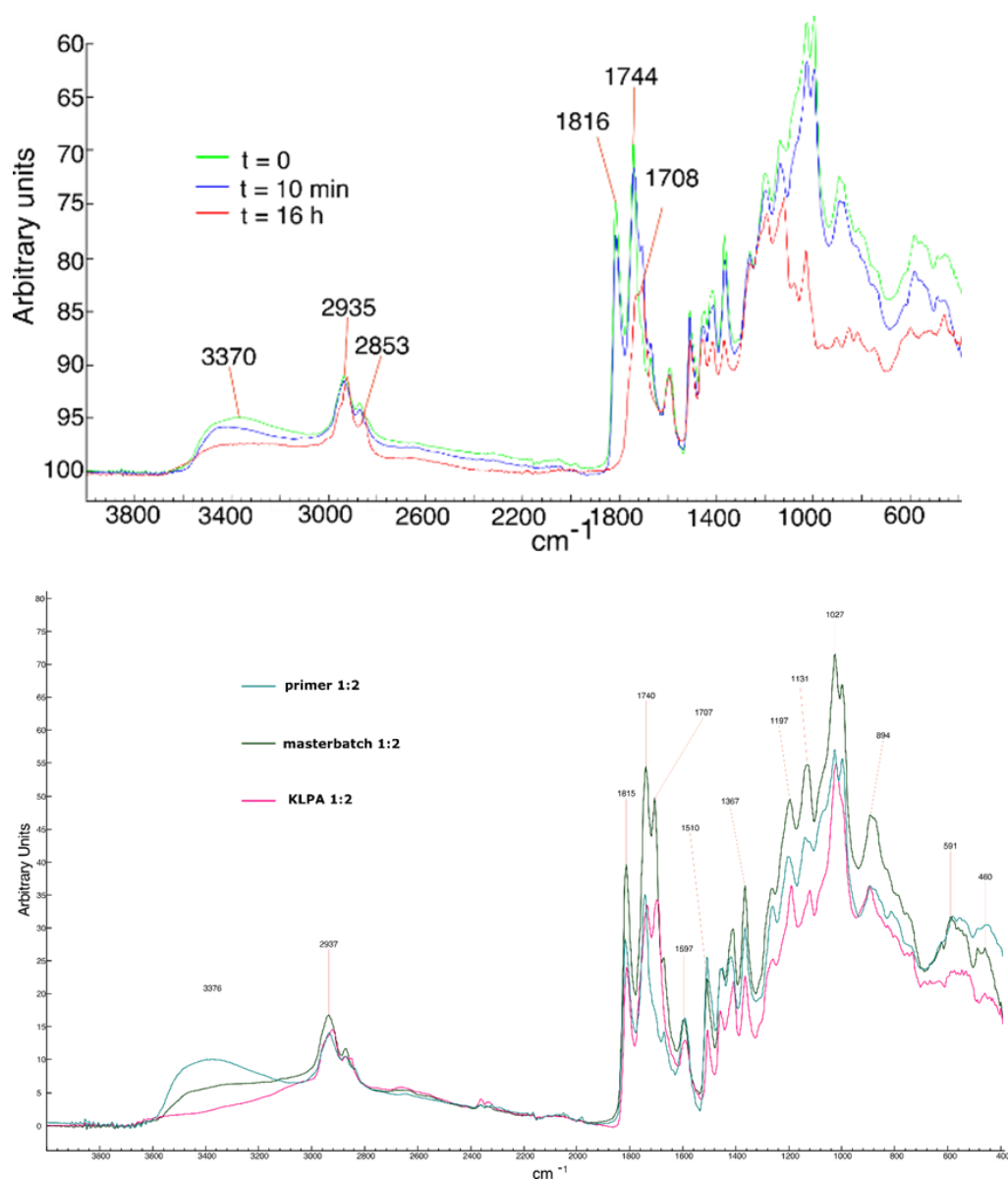
Figure 6.9. *Top: ATR-IR spectra of KL and equimolar amount of CLM at primer (t= 0), masterbatch (t = 10 min) and KLPA (t = 16 h) stages. Bottom: ATR-FTIR spectra of KL and 2 equivalents of CLM at primer, masterbatch, and KLPA stages*

To gain more insight into the crosslinking step that yielded the KLPA, solid-state ^{13}C MAS NMR spectra were recorded. A broad peak at 172 ppm was observed only in the case of KLPA and it

was assigned to the esters formed between KL and AdA (Figure 6.10). Signals corresponding to carboxylic acids were observed in the KLPA. These resonances were assigned to unreacted terminal carboxylic acids of KL adipate: indeed, any residual (unreacted) AdA could not be extracted from the material.
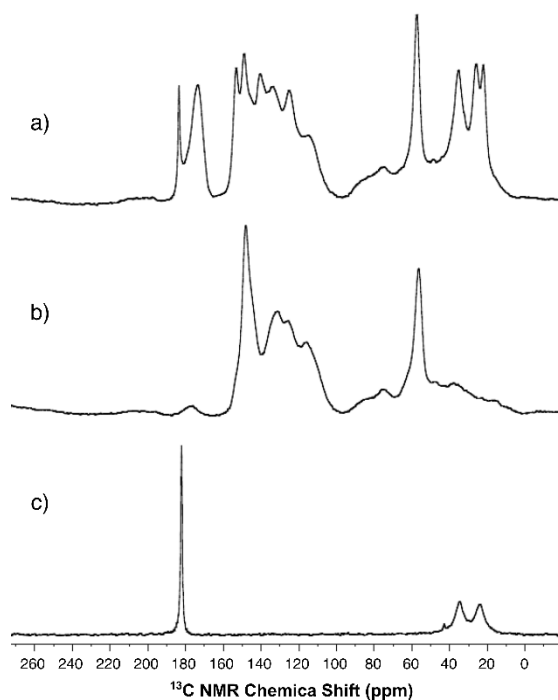
Figure 6.10. ^{13}C MAS NMR spectra of KLPA (a), KL (b), and AdA (c)

To ascertain which of the two species of adipic derivatives, *i.e.* the isopropenyl or the acetate one, reacted faster, the two compounds were synthesized and isolated in a pure form as bis(isopropenyl) adipate (BIPA) and bis(acetyl) adipate (BACA), respectively (Scheme 6.11, top). The corresponding esterification reactions of KL were then independently evaluated. The reactions were performed by mixing KL with an equimolar amount of either BIPA or BACA at 100 °C for 16 hours following the same procedure used for the CLM. As for the CLM, BIPA and BACA were first blended with KL at room temperature to obtain light brown primers. The preheating step (100 °C, 10 min) did not give any effect with BIPA, while BACA produced a homogeneous dark brown mixture soluble in THF. GPC analysis demonstrated that the reaction carried with BACA increased the molecular weight of lignin comparably with the one made with CLM, while no significant modification of KL was achieved with BIPA (Scheme 6.2, bottom). The further reaction of the masterbatches at 100 °C for 16 hours produced an insoluble material in the case of BACA, thereby confirming its role as the crosslinking agent. By contrast, only a slight increase in the molecular weight was obtained for BIPA. This led to conclude that the anhydride portion of the CLM was responsible for esterification reaction during the masterbatch step, and most likely in the crosslinking step too.

bis(isopropenyl) adipate (BIPA)   bis(acetyl) adipate (BACA)
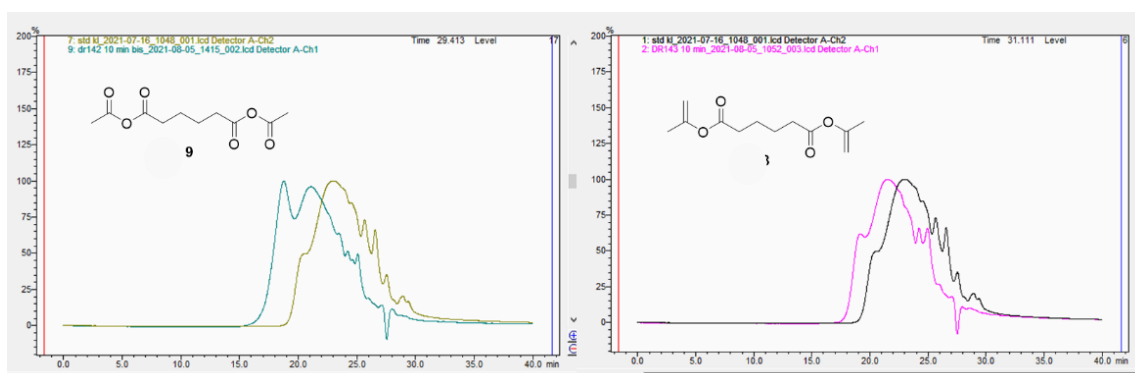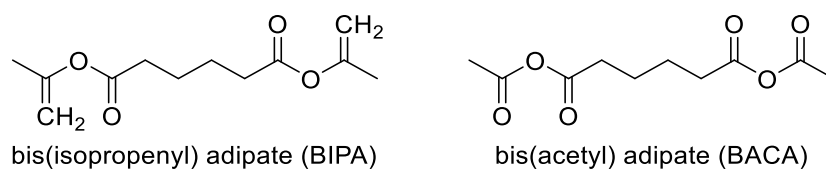
Scheme 6.11. *Top: crosslinking mixture synthesis. Bottom: GPC analyses of KL functionalized with BACA (left) and BIPA (right)*

6.2.6 Lignin model compounds

The reactivity of the above described CLM was further explored by investigating the reaction of AdA-based CLM with lignin model compounds bearing primary and secondary aliphatic, and phenolic hydroxyl moieties which mimicked those present in the KL.[28,29] For each set of reactions, four main products were detected by high-resolution mass spectrometry: acetates, mono adipates, mixed adipates, and symmetrical diesters (Scheme 6.12). The products were quantified by ^{1}H NMR using 1,4-dioxane as an internal standard. Due to overlapped signals, mono- and diesters could not be quantified independently, and the total amount of adipate was reported as yield of esters. The reactions were performed by mixing each lignin model compound (1 mmol) with the CLM (1.1 equiv) at 100 °C for 16 hours. Similar reactivities among the tested compounds were observed. All the substrates bearing hydroxyl moieties were transformed into acetate and adipate in an approximate 1:2 ratio. This was also confirmed by GPC analysis (Table 6.7, entries 1-5, and Figure 6.11). 1-phenyletanol underwent an elimination reaction, probably catalyzed by the residual H_2SO_4 present in the CLM, yielding styrene in 20% amount among the products (Table 6.7, entry 5).

R^1= H, C(=CH$_2$)CH$_3$, **R**.
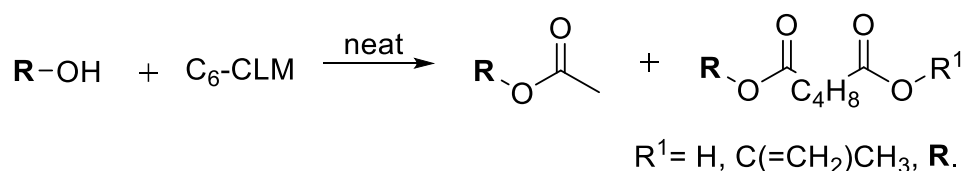
Scheme 6.12. *Lignin model compounds product distribution*

Table 6.7. *Lignin model compound reactivity with CLM*

Entry	Substrate	Conv. (%)	Acetate yield (%)	Esters yield (%)
1		96	28	68
2		97	31	66
3		99	35	64
4		99	38	61
5[a)]		99	24	56

Reaction conditions: substrate (1 mmol), CLM (1.1 equiv), 100 °C, 16 h, neat. Conversions and yield by ^{1}H NMR. a) Styrene was observed among the products.
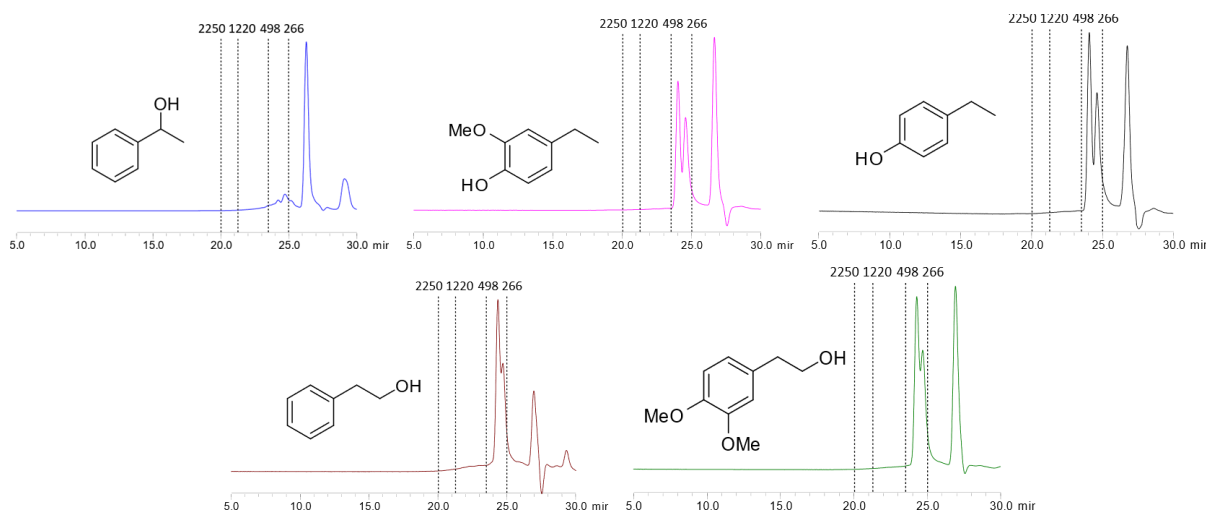
Figure 6.11. *GPC chromatogram of the reaction of 1-phenylethan-1-ol (top, left), 4-ethyl-2-methoxyphenol (top, center), 4-ethylphenol (top, right), 2-phenylethan-1-ol (bottom, left), of 2-(3,4-dimethoxyphenyl)ethan-1-ol (bottom, right) with C$_6$-CLM (100 °C, 16 h)*

Three substrates bearing two hydroxyl groups, *i.e.* 4-(2-hydroxyethyl)phenol, 4-(2-hydroxyethyl)-2-methoxyphenol, and 4-(1-hydroxy-ethyl)-2-methoxyphenol were also set to react with CLM, in order to confirm the crosslinking reactivity. A blank test (conditions in absence of the CLM) was carried out to verify the thermal stability of each compound under the conditions of Scheme 6.3: the results of these reactions were used as references for the GPC analysis (Figure 6.12, **red** profiles).

^{1}H NMR spectroscopy together with high-resolution mass spectrometry proved the formation of acetylated and esterified products. GPC demonstrated the effectiveness of the CLM in the esterification of the diols to give oligomers (Figure 6.12).
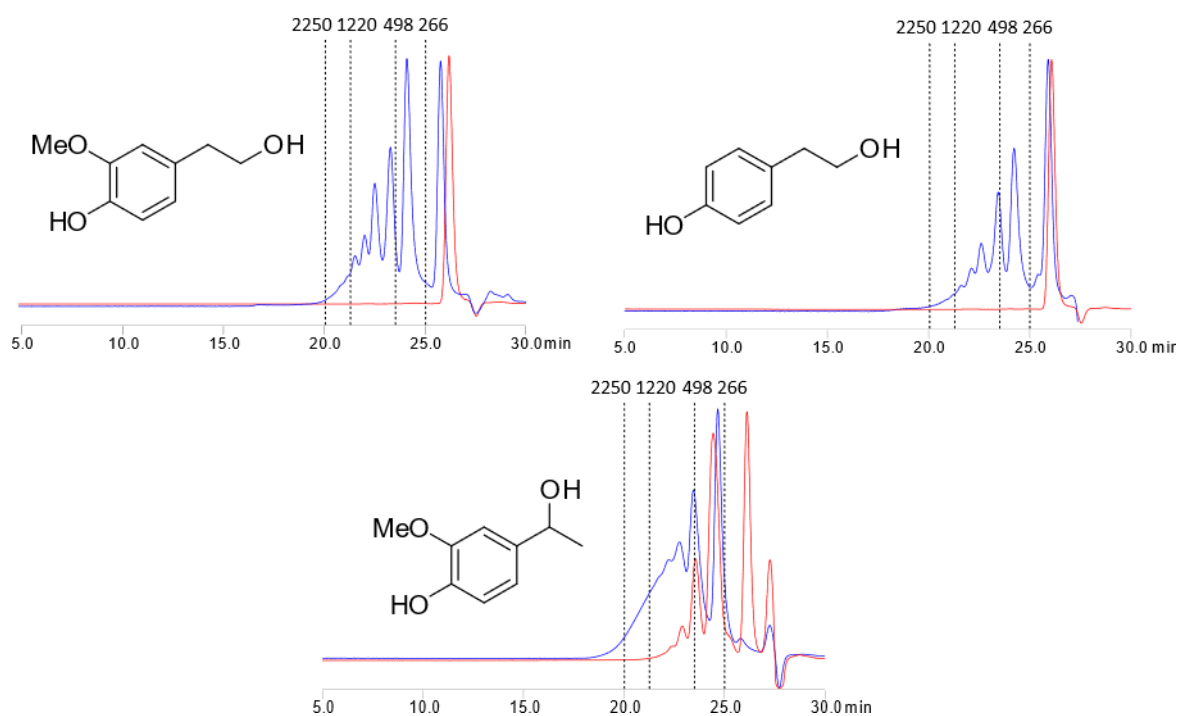
Figure 6.12. *GPC chromatograms of lignin model compounds, as blank (**red**) and reacted with CLM (**blue**). Normalized by height. Dashed lines report apparent molecular weight (Da) based on polystyrene as a reference*

The last part of this investigation was focused on the reaction of simple model substrates as 2-phenylethanol, 4-ethylphenol, and 1-phenylethanol with CLM under neat conditions (Figure 6.13). Experiments were performed at 50 °C and the progress of reactions was followed by ^{1}H NMR. The products were the same observed at 100 °C (Table 6.2), though in the case of 1-phenylethanol, the formation of 1-(phenyl)ethyl ether was also detected (Figure 6.13, a). A substantially quantitative conversion (>95%) was reached in 16 hours for each reactant, thereby corroborating the reactivity of CLM. The efficiency of acetylation and esterification were almost independent of the type of hydroxyl functionality in the substrate.
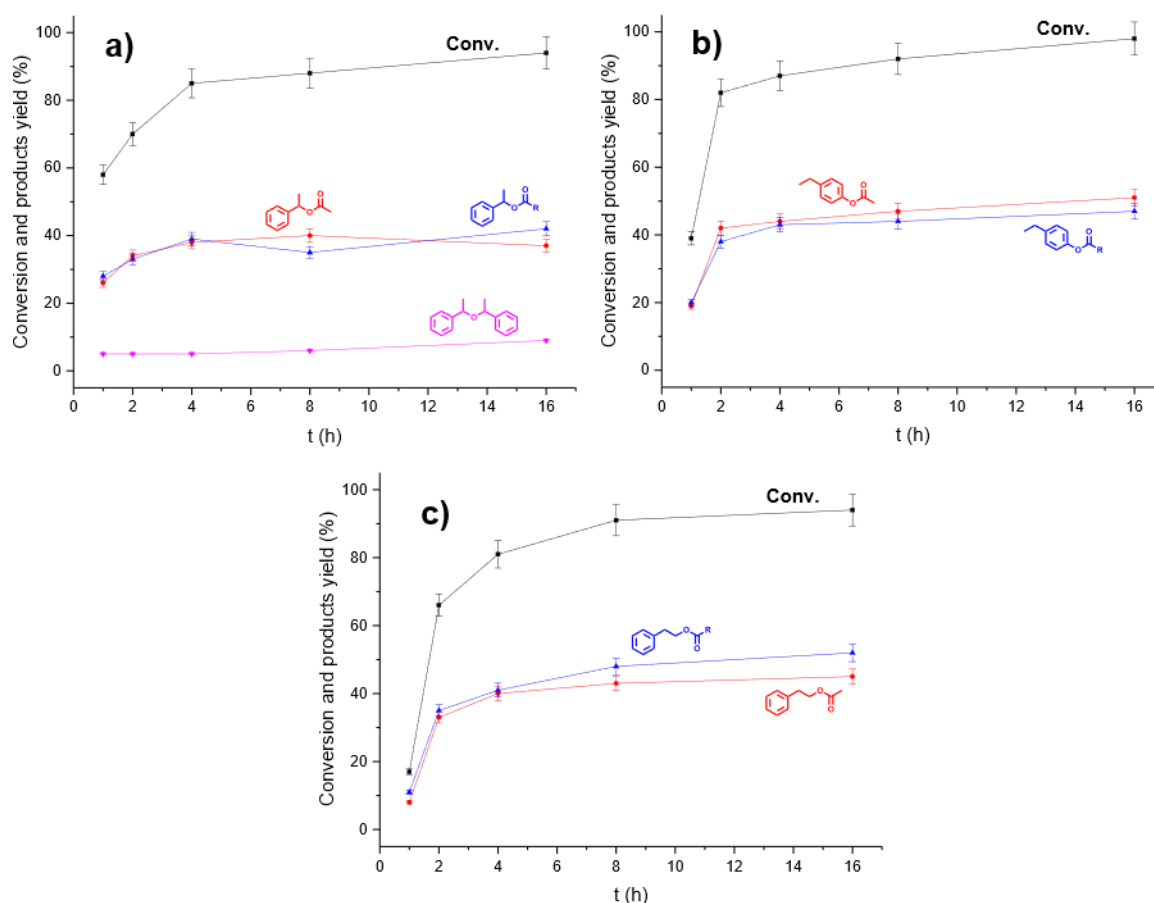
Figure 6.13. *Real-time analysis of the reactions of Ada-based CLM with 1-phenylethanol (a), 4-ethylphenol (b), and 2-phenylethanol (c). Reaction conditions: substrate (1 mmol), CLM (1.1 equiv), 50 °C, neat*

6.3 Conclusions

This study discloses a novel procedure to obtain thermoset plastic materials from KL, by the reaction of dry KL powder with a crosslinking liquid mixture based on an activated dicarboxylic acid. All components, KL, AdA, iPAc, and H_2SO_4 are relatively inexpensive, and widely available. In the synthesis of the material, the diester of AdA undergoes a condensation reaction with the KL which proceeds through the initial formation of a homogeneous prepolymer by the partial esterification of lignin. This step requires only heating at 100 °C. The resulting viscous liquid becomes easily pourable and moldable under pressure to yield a plastic solid whose mechanical properties can be modulated over time by changing the KL:CLM ratio or by adding glycerol. The proposed strategy for KL valorization overcomes issues usually associated to lignin-based materials, such as the need for pre-functionalization or fractionation.[9] In addition, if bio-based AdA (from lignin) could be used, up to 90 wt% of the material would be, directly and indirectly, derived from a side-stream of an existing biorefinery industry not competing with food cultivation.[35]

The results of this work have been the object of a paper which has been submitted for publication:

The contribution of DR was in the design and conduction of the experiments together with DDF. DR also collaborated with DDF and KRB in the characterization of the materials and in writing of the draft of the paper.

References

[1] Global plastic production 1950-2020, https://www.statista.com/statistics/282732/global-production-of-plastics-since-1950/, (accessed 18/11/2021).

[2] Forest products statistics, http://www.fao.org/forestry/statistics/81757/en/, (accessed 18/11/2021).

[3] I. F. Demuner, J. L. Colodette, A. J. Demuner and C. M. Jardim, Biorefinery review: Wide-reaching products through kraft lignin, *BioResources*, **2019**, *14*, 7543.

[4] M. Jawerth, M. Lawoko, S. Lundmark, C. Perez-Berumen and M. Johansson, Allylation of a lignin model phenol: a highly selective reaction under benign conditions towards a new thermoset resin platform, *RSC Adv.*, **2016**, *6*, 96281. https://doi.org/10.1039/C6RA21447A

[5] Y. Li and S. Sarkanen, Alkylated kraft lignin-based thermoplastic blends with aliphatic polyesters, *Macromolecules*, **2002**, *35*, 9707. https://doi.org/10.1021/ma021124u

[6] D. Kun and B. Pukánszky, Polymer/lignin blends: Interactions, properties, applications, *Eur. Polym. J.*, **2017**, *93*, 618. https://doi.org/10.1016/j.eurpolymj.2017.04.035

[7] K. A. Y. Koivu, H. Sadeghifar, P. A. Nousiainen, D. S. Argyropoulos and J. Sipilä, Effect of Fatty Acid Esterification on the Thermal Properties of Softwood Kraft Lignin, *ACS Sustain. Chem. Eng.*, **2016**, *4*, 5238. https://doi.org/10.1021/acssuschemeng.6b01048

[8] D. Di Francesco, C. Dahlstrand, J. Löfstedt, A. Orebom, J. Verendel, C. Carrick, Å. Håkansson, S. Eriksson, H. Rådberg, H. Wallmo, M. Wimby, F. Huber, C. Federsel, M. Backmark and J. S. M. Samec, Debottlenecking a Pulp Mill by Producing Biofuels from Black Liquor in Three Steps, *ChemSusChem*, **2021**, *14*, 2414. https://doi.org/10.1002/cssc.202100496

[9] A. Orebom, D. Di Francesco, P. Shakari, J. S. M. Samec and C. Pierrou, Thermal and Mechanical Properties of Esterified Lignin in Various Polymer Blends, *Molecules*, **2021**, *26*, 3219. https://doi.org/10.3390/molecules26113219

[10] W. Thielemans and R. P. Wool, Lignin Esters for Use in Unsaturated Thermosets: Lignin Modification and Solubility Modeling, *Biomacromolecules*, **2005**, *6*, 1895. https://doi.org/10.1021/bm0500345

[11] B. Martel, M. Weltrowski, D. Ruffin and M. Morcellet, Polycarboxylic acids as crosslinking agents for grafting cyclodextrins onto cotton and wool fabrics: Study of the process parameters, *J. Appl. Polym. Sci.*, **2002**, *83*, 1449. https://doi.org/10.1002/app.2306

[12] L. Shen, H. Xu, L. Kong and Y. Yang, Non-Toxic Crosslinking of Starch Using Polycarboxylic Acids: Kinetic Study and Quantitative Correlation of Mechanical Properties and Crosslinking Degrees, *J. Polym. Environ.*, **2015**, *23*, 588. https://doi.org/10.1007/s10924-015-0738-3

[13] Y. Xu, K. Odelius and M. Hakkarainen, Levulinic Acid as a Versatile Building Block for Plasticizer Design, *ACS Sustain. Chem. Eng.*, **2019**, *7*, 13456. https://doi.org/10.1021/acssuschemeng.9b02439

[14] X. He, F. Luzi, W. Yang, Z. Xiao, L. Torre, Y. Xie and D. Puglia, Citric Acid as Green Modifier for Tuned Hydrophilicity of Surface Modified Cellulose and Lignin Nanoparticles, *ACS Sustain. Chem. Eng.*, **2018**, *6*, 9966. https://doi.org/10.1021/acssuschemeng.8b01202

[15] M. Mariana, T. Alfatah, A. K. H.p.s., E. B. Yahya, N. G. Olaiya, A. Nuryawan, E. M. Mistar, C. K. Abdullah, S. N. Abdulmadjid and H. Ismail, An Investigation of the Moderating Effect of IT Personnel Capability on the Relationship between Intangible IT Resources and IT Infrastructure Flexibility on the Sustainable Competitive Advantages, *J. Mater. Res. Technol.*, **2021**, *15*, 2287. https://doi.org/10.18488/journal.2.2018.89.277.286

[16] V. Santacroce, F. Bigi, A. Casnati, R. Maggi, L. Storaro, E. Moretti, L. Vaccaro and G. Maestri, Selective monomethyl esterification of linear dicarboxylic acids with bifunctional alumina catalysts, *Green Chem.*, **2016**, *18*, 5764. https://doi.org/10.1039/C6GC01900E

[17] G. T. Morgan and E. Walton, New derivatives of p-arsanilic acid. Part V. p-Arsonomethyl-malonanilic acid and related compounds, *J. Chem. Soc. Resumed*, **1933**, 91. https://doi.org/10.1039/JR9330001064

[18] D. Rigo, G. Fiorani, A. Perosa and M. Selva, Acid-Catalyzed Reactions of Isopropenyl Esters and Renewable Diols: A 100% Carbon Efficient Transesterification/Acetalization Tandem Sequence, from Batch to Continuous Flow, *ACS Sustain. Chem. Eng.*, **2019**, *7*, 18810. https://doi.org/10.1021/acssuschemeng.9b03359

[19] D. Rigo, R. Calmanti, A. Perosa and M. Selva, A transesterification–acetalization catalytic tandem process for the functionalization of glycerol: the pivotal role of isopropenyl acetate, *Green Chem.*, **2020**, *22*, 5487. https://doi.org/10.1039/D0GC01775B

[20] H. J. Hagemeyer and D. C. Hull, Reactions of isopropenyl acetate, *Ind. Eng. Chem.*, **1949**, *41*, 2920. https://doi.org/10.1021/ie50480a063

[21] W. Yan, G. Zhang, J. Wang, M. Liu, Y. Sun, Z. Zhou, W. Zhang, S. Zhang, X. Xu, J. Shen and X. Jin, Recent Progress in Adipic Acid Synthesis Over Heterogeneous Catalysts, *Front. Chem.*, **2020**, *8*, 185. https://doi.org/10.3389/fchem.2020.00185

[22] J. Rios, J. Lebeau, T. Yang, S. Li and M. D. Lynch, A critical review on the progress and challenges to a more sustainable, cost competitive synthesis of adipic acid, *Green Chem.*, **2021**, *23*, 3172. https://doi.org/10.1039/D1GC00638J

[23] A. Corona, M. J. Biddy, D. R. Vardon, M. Birkved, M. Z. Hauschild and G. T. Beckham, Life cycle assessment of adipic acid production from lignin, *Green Chem.*, **2018**, *20*, 3857. https://doi.org/10.1039/C8GC00868J

[24] D. R. Vardon, M. A. Franden, C. W. Johnson, E. M. Karp, M. T. Guarnieri, J. G. Linger, M. J. Salm, T. J. Strathmann and G. T. Beckham, Adipic acid production from lignin, *Energy Environ. Sci.*, **2015**, *8*, 617. https://doi.org/10.1039/C4EE03230F

[25] W. K. Ng, J. W. Kwek, A. Yuen, C. L. Tan and R. Tan, Effect of milling on DSC thermogram of excipient adipic acid, *AAPS PharmSciTech*, **2010**, *11*, 159. https://doi.org/10.1208/s12249-009-9372-5

[26] J. P. McEvoy, Characterizing Carbonyls with Infrared Spectroscopy: An Introductory Chemistry Experiment in a Molecular Bioscience Program, *J. Chem. Educ.*, **2014**, *91*, 726. https://doi.org/10.1021/ed4001427

[27] C. Crestini, H. Lange, M. Sette and D. S. Argyropoulos, On the structure of softwood kraft lignin, *Green Chem.*, **2017**, *19*, 4104. https://doi.org/10.1039/C7GC01812F

[28] C. S. Lancefield, S. Constant, P. de Peinder and P. C. A. Bruijnincx, Linkage Abundance and Molecular Weight Characteristics of Technical Lignins by Attenuated Total Reflection-FTIR Spectroscopy Combined with Multivariate Analysis, *ChemSusChem*, **2019**, *12*, 1139. https://doi.org/10.1002/cssc.201802809

[29] Y. Wang, H. Meng, D. Cai, B. Wang, P. Qin, Z. Wang and T. Tan, Improvement of l-lactic acid productivity from sweet sorghum juice by repeated batch fermentation coupled with membrane separation, *Bioresour. Technol.*, **2016**, *211*, 291. https://doi.org/10.1016/j.biortech.2016.03.095

7. Concluding remarks and future perspectives

This PhD project was developed as part of a cotutelle agreement among Università Ca' Foscari di Venezia, Università degli Studi di Trieste, and the University of Sydney. As it was presented in the introduction, this PhD work was focused on the development of eco-friendly procedures for the upgrading of biobased chemical platforms. The starting compounds were chosen among those considered to be the most promising for the development of a modern biorefinery. The experimental work was divided into four main areas, which were all commonly aimed at combining green technologies and biobased compounds for the development of sustainable protocols.

1. *Isopropenyl esters (iPEs) in tandem reactions*

In Chapter 2, the implementation of unique tandem reactions of esterification/amidation and acetalization mediated by isopropenyl esters (iPEs) is described. In particular, biobased 1,2-diols (ethylene glycol and 1,2-propanediol), glycerol, and glycerol-derived aminodiols, have been used as substrates for this purpose. The procedures involve a first esterification/amidation, which generates acetone as co-product. In turn, acetone triggers a subsequent acetalization step.

i) Starting from 1,2-diols and using Amberlyst-15 as an heterogenous acid catalyst, the fine tuning of reactions parameters allowed for the development of a 100% carbon efficiency (CE) process mediated by iPEs. The tandem sequence has proven feasible for three enol esters, showing a different reactivity: isopropenyl-acetate > phenylbutyrate > octanoate. In all cases, the reaction was efficiently scaled up by a factor of 10, providing products in isolated yields of 81−92%, and it was transferred to continuous-flow mode with improved productivity, milder operating conditions (30 °C, 1 atm), and steady catalytic performance for at least 160 h of time-on-stream.

ii) The cooperative reactivity of isopropenyl acetate, acetic acid, and acetone in the presence of Amberlyst-15 promoted a tandem sequence for the upgrading of glycerol. The major role was played by the enol ester that acted as the acetylating agent of glycerol and at the same time, it underwent acidolysis with AcOH. Notwithstanding the complex network of reactions, this investigation demonstrated that the experimental conditions could be tuned to obtain the selective conversion of glycerol to either a 1 : 1 mixture of acetal acetates (97% of which is solketal acetate) and triacetin, or solely acetal acetates in up to 91% yield. Insights into the reaction mechanism have been also investigated using D-labelled compounds.

iii) A catalyst-free N-acetylation reaction carried out under batch conditions has been successfully concatenated to a continuous-flow acid-catalyzed acetalization process for the upgrading of aminodiol regioisomers (APDs) of glycerol. A double functionalization of APDs was achieved through the proposed strategy: reagents were first converted into the corresponding N-acetyl derivatives which without isolation, were further transformed to cyclic C5 and C6 acetal homologues, though, only through a careful choice of reaction conditions. In addition, this investigation highlighted the role/effect of: (i) the solvent for the batch N-acetylation; (ii) the nature of the solvent (1,4-dioxane vs. DMSO), and catalyst (Amberlyst 15 vs.

faujasite (HY) vs. AlF$_3$·3H$_2$O) (iii) the reagent (amide regioisomers), affording the five-membered ring acetal in >99% selectivity, while the formation of the less stable six-membered cyclic product was always accompanied by a competitive transesterification process.

Future trends may be directed towards the application of tandem sequences for the direct upgrading of more complex -OH rich systems, such as sugars and their derivatives. In addition, valuable routes can be developed starting from -OH and -NH$_2$ bearing biomasses and/or biomass-derived crude feedstocks (*i.e.* lignin, cellulose, hemicellulose, chitin, etc.). Hence, the functionalization of biobased raw feedstocks is a timely field of investigation which produces several scientific reports per year. Notwithstanding the importance of the nature of the starting material, the possibility of developing one-pot (maybe 100% carbon efficient) procedures can make biorefinery not only more efficient, but also more cost-effective. For instance, important effort is currently put into the compatibilization of lignins of various nature/type into thermoplastic matrices, like polylactic acid and others. To date, the field is still an open challenge since most of the times the addition of lignin over a certain amount (roughly around 30%) is detrimental for the mechanical properties of the final plastic. Isopropenyl esters might play a preeminent role in that regard, as green and efficient compounds for lignin functionalization throughout tandem esterification and acetalization.

2. CO$_2$ insertion into epoxides

In Chapter 4, the first application of a catalytic system composed by diethylene glycol (DEG) and NaBr has been reported in the insertion of CO$_2$ to terminal epoxides. The binary system made of NaBr/DEG has proven efficient for the batch conversion of different substrates including 7 terminal and one internal epoxides, but even more importantly, the characteristics of DEG (viscosity, density, diffusivity) made it suitable to act concurrently as a co-catalyst (cation coordinating agent and hydrogen bon donor) and a solvent/carrier for the implementation of the reaction in continuous-flow. However, translating the reaction conditions from batch to continuous flow is challenging. The results gathered so far highlight that the batch reaction can be run under conditions far milder (T = 100 °C, p^0(CO$_2$) = 1 bar) than those required in CF-mode (T = 220 °C, p(CO$_2$) = 120 bar). Nevertheless, the potential of CF in terms of process intensification can be appreciated. Recycle experiments have also confirmed that the NaBr/DEG catalytic mixture is reusable without loss of performance, for at least four subsequent CF-runs.

Though CO$_2$ insertion into epoxides is a widely investigated field, two major challenges are still open: i) the implementation of batch protocols under CF and ii) the direct tandem one step epoxidation of olefins and subsequent CO$_2$ insertion. In this context, the above-described work finds a way to solve objective i). Nevertheless, the procedure lacks mainly from a chemical engineering standpoint: the improvement of the CF apparatus (*i.e.* an improvement of the heat transfer, the use of more precise pumps especially for CO$_2$, etc.) may bring to a decrease of the harsh requested conditions (T = 220 °C) to carry the CF synthesis of cyclic organic carbonates. On the other hand, the replacement of epoxides with their corresponding olefins is a challenging but innovative issue. The addition of an oxidant and/or a catalyst able to activate the oxidation of alkenes into the reaction mixture may be the solution for the implementation of such tandem one-pot sequence first in batch and then under CF. Our group recently developed W-based catalysts (*i.e.* ionic liquids) which have been found active for both oxidation of olefins and CO$_2$ insertion. The immobilization of such type of ionic liquids on an

heterogenous support may be a solution for the implementation of tandem procedures of that type under CF.

3. Diversified upgrading of HMF

Chapter 5 describes diversified, robust, and greener protocols for the chemical upgrading of HMF. A variety of reactions have been described based on new or improved procedures by which a total of 12 different HMF derivatives were synthesized, isolated, and fully characterized, 7 of which new. Reagents include isopropenyl acetate, dimethyl carbonate, acetone, and a halide-free phosphonium vinylation reagent, that were used to carry out reactions of acetylation, carboxymethylation, aldol condensation, and vinylation, respectively, on HMF and on its homologues: acetylated HMF and the methyl carbonate of HMF. The most active catalytic systems were composed by commercially available reagents, as Cs_2CO_3 and Pd/C. High isolated yields of 85–95% were obtained for all products, often in a few hours or less.

Considering the high yields of all these products, these results pave the way for both the study of new applications for such products and the design of new upgrading strategies. Just to name a few promising perspectives, polyhydroxylated or vinylated derivatives of HMF could be used in the materials (polymers) chemistry. In particular, the use of DMC-derived ionic liquids and/or inorganic carbonates as the catalysts in step growth polymerization could make polycarbonates production circular and sustainable. Other compounds, such as the acetylated and alkylated homologues of HMF, are suitable as such to improve fuels specifications.

4. The synthesis of Kraft-lignin polyadipates

Chapter 6 illustrates how Kraft lignin-derived thermoset polyesters can be prepared by the reaction of dry KL powder with a crosslinking liquid mixture based on an activated dicarboxylic acid. All components, KL, AdA, iPAc, and H_2SO_4 are relatively inexpensive, and widely available. The procedure involves a two-step sequence: i) a partial esterification reaction of Kraft lignin allows for the formation of a homogeneous pourable prepolymer; ii) the facile molding of the first step liquid yields a thermoset whose mechanical properties can be modulated over time. The proposed strategy for KL valorization overcomes issues usually associated to lignin-based materials, such as the need for pre-functionalization or fractionation. In addition, if bio-based AdA (from lignin) could be used, up to 90 wt% of the material would be, directly and indirectly, derived from a side-stream of an existing biorefinery industry not competing with food cultivation.

On the other hand, this investigation opens three major challenges which can be summarized as follows: i) the improvement of the mechanical properties of Kraft ligin polyadipates; ii) the use of the activated carboxylic acids mixture (CLM) for the crosslinking of other lignin containing feedstocks and others (*i.e.* cellulose); iii) improvements on the CLM synthesis (i.e. using different carboxylic acids, replacing H_2SO_4 as the catalyst with greener ones, etc.). Depending on the reaction conditions/procedure the work on the synthesis of Kraft lignin polyadipates opens a plethora of possibility for further upgrading (*i.e.* by blending this lignin-based matrix with other polymers) or for direct applications, such as coatings, foams, and insulators. The latter work is a starting point for further investigations on the synthesis of biobased materials and polymers.

Overall, this PhD Thesis represents a step forward in upgrading of biomass derived chemical platforms throughout diversified green and sustainable methodologies and procedures. It is hoped that efforts made during this PhD journey may be beneficial to inspire future scientists sharing interests on the investigated chemistry, procedures, and technologies.

8. List of publications

- Davide Rigo, Giulia Fiorani, Alvise Perosa, Maurizio Selva "Acid-Catalyzed Reactions of Isopropenyl Esters and Renewable Diols. A 100% Carbon Efficient Transesterification/Acetalization Tandem Sequence, from Batch to Continuous Flow", *ACS Sustainable Chem. Eng.,* **2019**, *7*, 18810-18818; doi: 10.1021/acssuschemeng.9b03359

- Davide Rigo, Roberto Calmanti, Alvise Perosa, Maurizio Selva "A transesterification-acetalization catalytic tandem process for the functionalization of glycerol: the pivotal role of isopropenyl acetate", *Green Chem.,* **2020**, *22*, 5487–5496*;* DOI: 10.1039/D0GC01775B

- Davide Rigo, Nadia Alessandra Carmo Dos Santos, Alvise Perosa, Maurizio Selva "Concatenated batch and continuous flow procedures for the upgrading of glycerol-derived aminodiols via N-acetylation and acetalization reactions", *Catalysts,* **2021**, *11*, 21; doi: 10.3390/catal11010021

- Davide Rigo, Roberto Calmanti, Alvise Perosa, Maurizio Selva and Giulia Fiorani, "Diethylene Glycol/NaBr catalyzed CO_2 insertion into terminal epoxides: from batch to continuous flow", *ChemCatChem,* **2021**, 13, 2005-2016; DOI: 10.1002/cctc.202002010.

- Davide Rigo, Daniele Polidoro, Alvise Perosa, Maurizio Selva, "Diversified upgrading of HMF *via* green acetylation, aldol condensation, carboxymethylation, vinylation and reductive amination reactions", *Mol. Catal.,* **2021**, *514*, 111838. DOI: 10.1016/j.mcat.2021.111838.

Acknowledgements

I would like to express my special appreciation and thanks to my supervisors and advisors Professor Maurizio Selva and Professor Thomas Maschmeyer, for encouraging my research and for allowing me to mature as a research scientist. All my gratitude to Professor Joseph Samec who initiate me into the world of lignin chemistry. I would like to give a big thank also to Professor Alvise Perosa, Professor Giulia Fiorani and Professor Anthony Masters, for their useful advice, contributions, and guidance. This project would not have been as successful without the assistance of professors and staff from both Università Ca' Foscari di Venezia, the University of Sydney, and Stockholm University. I would also like to thank Dr. Francesca Guidi, who allowed me to master all the bureaucracy during my PhD.

Then, I really want to thank all my colleagues (and friends) from GOST team: Carlotta Campalani, aka my secretary, for her overwhelming hilarity, Daniele Polidoro for all the nice discussions on HMF and multiphasic systems, Filippo Rizzo for all his super funny impersonations, Roberto Calmanti for his brother's olive oil, Simone Cailotto for being always helpful and kind, Alessandro Bellè for being one of the craziest person I ever met, Andrea Morandini for running GPCs for me, Nicola Bragato for his lessons on fishing, Matteo Bertoldini for keeping the lab tidy, and Daily Rodriguez for the short time spent together. Again other friends from Ca' Foscari, thanks to Robi Sole and Seba Tieuli for being the toughest soccer opponents, Giulia, Somi, and Luca for being 34th cycle PhD students like me, and again all others in Ca' Foscari, Sandro and Matteo from Luleå, the "beghette", the "signorette" and all the other "stanzino" guys. Of course, I also have to thank all my friends from Stockholm University: Davide di Francesco for teaching me the word "inchiommo" (and nothing else), Luca Massaro for his carbonara at 11 pm, Federico Riu for his mother's pappassini (or how they should be written), Matteo Costantini for pyramid training, Alessandro Ruda for climbing with me and buying small size shoes, Ester di Tommaso for listening to my boring argumentations, Emanuele Silvi for introducing me to "il Marchese del Grillo", Stefano Parisotto for his lasagna, Axel Furevi for being the only Swedish person in the department, and again, Domenica, Marie, Alba, Thanya for being the best lab manager ever, Kiran Reddy for helping me with DSC and other stuff, Igor for pull ups, Dasha for midnight swimming, Gonzalo for being always happy and for his happy songs, Kuntawit "Kun" for his noodles, Suthawan "Dear" for the help with calibration curves. You all made my three and a half years of PhD unforgettable: I had a really great time with you guys, thank you!

A thank is given to all my family (Rigo's and Lupo's), especially to Alvise who I consider more a brother than a cousin. A lovely thanks is devoted to Tere, who has really been the best girlfriend I could find during that period of my life. A big thank is given to all my friends outside the university, thank you for helping me strike a balance between my PhD studies and my social life, especially during the toughest moments.

Finally, I would like to dedicate this thesis to my parents. To them my deepest gratitude for their support, patience, and encouragements. Without them I could never reach this goal.

Appendix A.2 – Chapter 2

A.2.1 The tandem reaction of iPEs and renewable 1,2-diols: from batch to continuous flow: characterization data and other supporting information

General isolation procedure of isopropenyl esters. Isopropenyl esters (**2b**, **2c**) were isolated by flash column chromatography (stationary phase: neutral Al$_2$O$_3$, eluent: petroleum ether/ethyl acetate 9:1 v/v).

Prop-1-en-2-yl 4-phenylbutanoate (isopropenyl phenylbutyrate, 2b)

The product was isolated in a 85% yield from the reaction of the phenylbutyryl chloride (0.510 g, 2.49 mmol) and isopropenyl acetate (2.503 g, 24.9 mmol) in the presence of H$_2$SO$_4$ (25.5 mg, 0.26 mmol) as a catalyst.
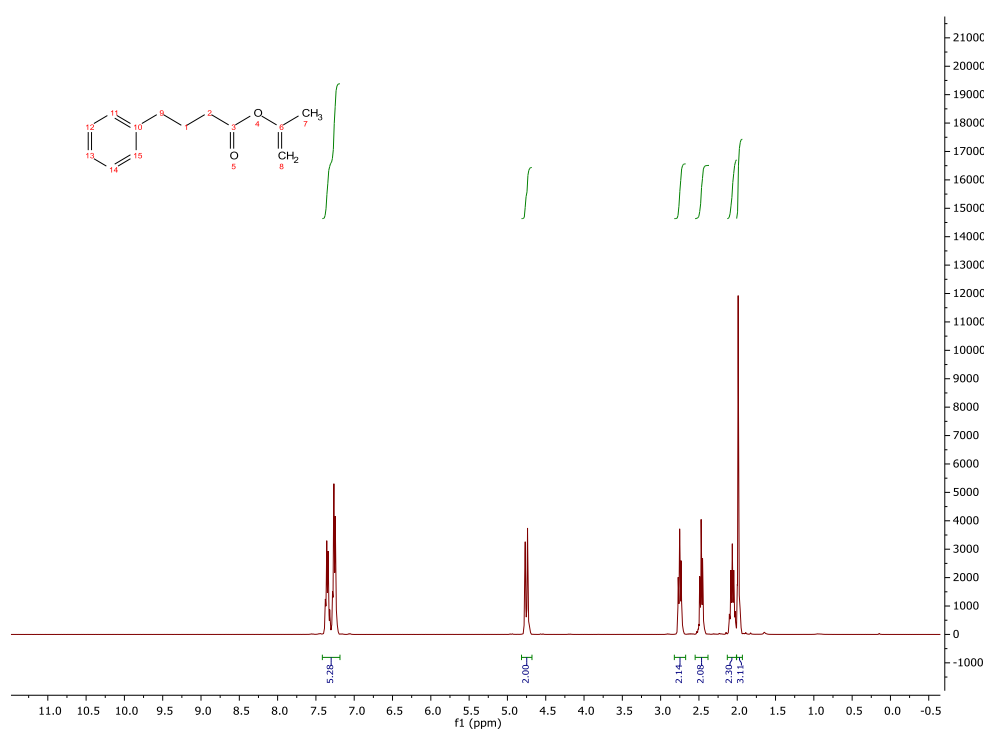
Figure A.2.1.1. *^{1}H NMR spectrum of compound **2b***

^{1}H NMR (400 MHz, 298 K, CDCl$_3$) δ: 7.32-7.23 (m, 5H), 4.70 (m, 2H), 2.71 (m, 2H), 2.43 (t, 2H), 2.10 (m, 2H), 1.95 (d, 3H).
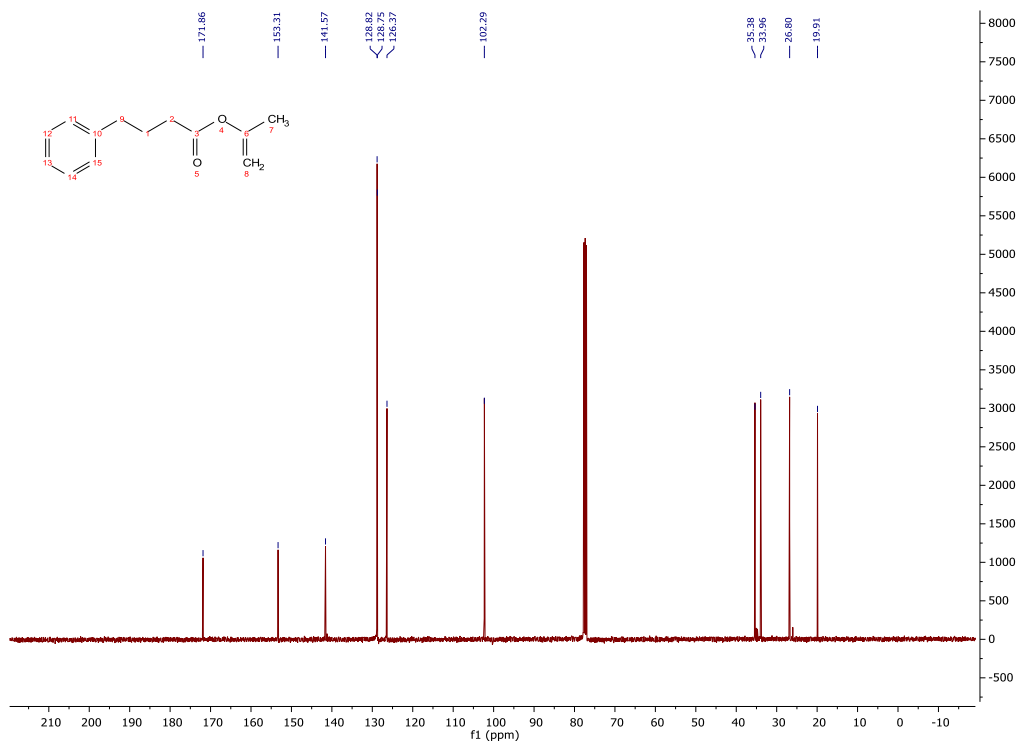
Figure A.2.1.2. *^{13}C NMR spectrum of compound **2b***

^{13}C{H} NMR (101 MHz, 298 K, CDCl$_3$) δ: 171.86, 153.31, 141.57, 128.82, 128.75, 126.37, 102.29, 36.38, 33.96, 26.80, 19.91.
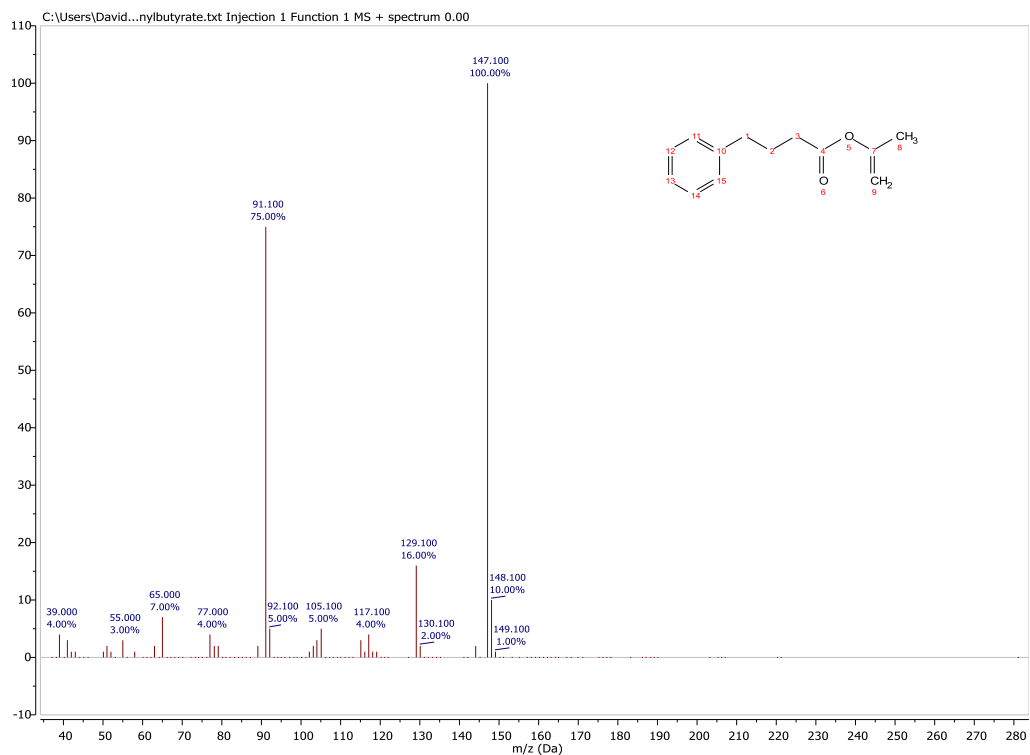
Figure A.2.1.3. *MS spectrum of compound **2b***

GC/MS (relative intensity, 70 eV) *m/z*: 148 (10), 147 (100), 129 (16), 117 (4), 105 (5), 92 (5), 91 (75), 65 (7), 39 (4).

Prop-1-en-2-yl octanoate (isopropenyl octanoate, 2c)

The product was isolated in a 90% yield from the reaction of the octanoyl chloride (0.502 g, 3.09 mmol) and isopropenyl acetate (3.101 g, 30.9 mmol) in the presence of H_2SO_4 (25.1 mg, 0.25 mmol) as a catalyst.
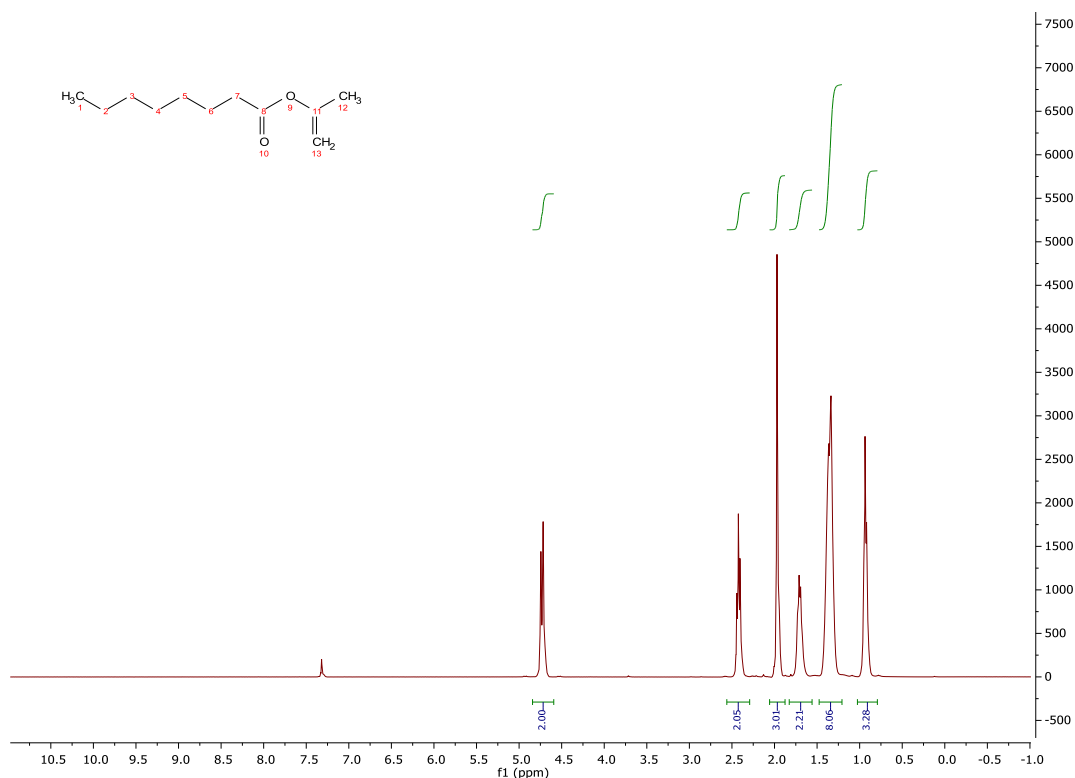
Figure A.2.1.4. ^1H NMR spectrum of compound 2c

^1H NMR (400 MHz, 298 K, CDCl$_3$) δ: 4.69 (m, 1H), 4.67 (dd, 1H), 2.38 (t, 2H), 1.92 (d, 3H), 1.58-1.72 (m, 2H), 1.20-1.40 (m, 8H), 0.89 (m, 3H).
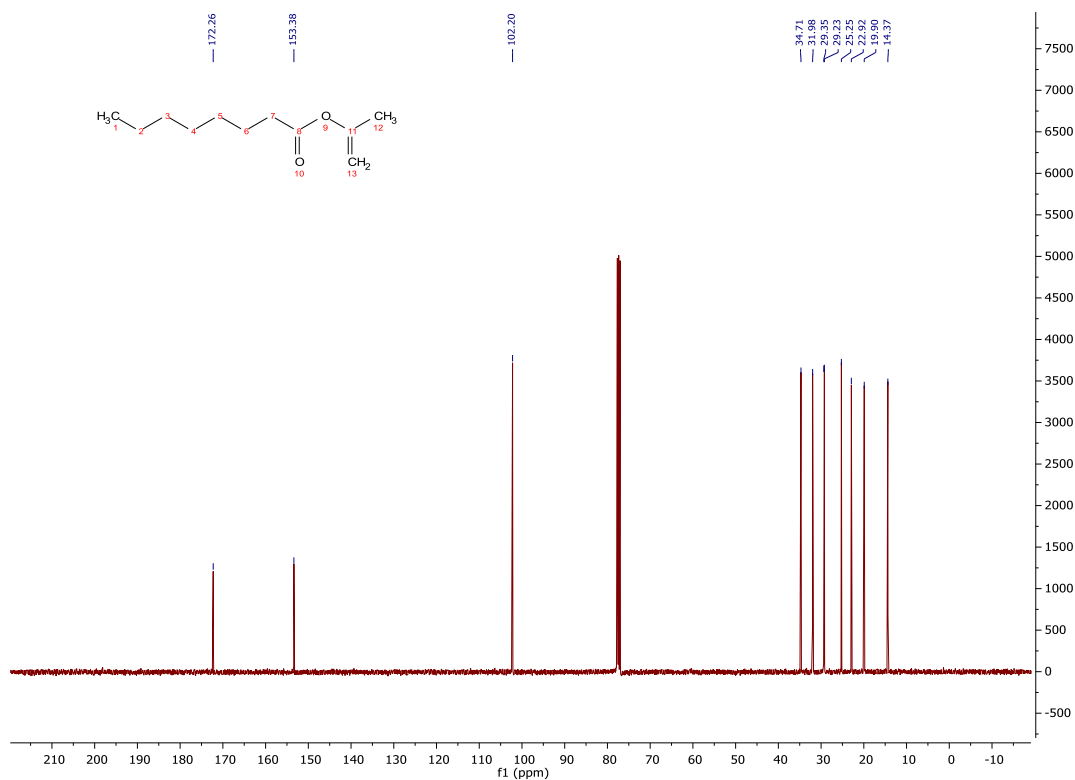
Figure A.2.1.5. ^{13}C NMR spectrum of compound *2c*

^{13}C{H} NMR (101 MHz, 298 K, CDCl$_3$) δ: 172.26, 153.38, 102.20, 34.71, 31.98, 29.35, 29.23, 25.25, 22.92, 19.90, 14.37.
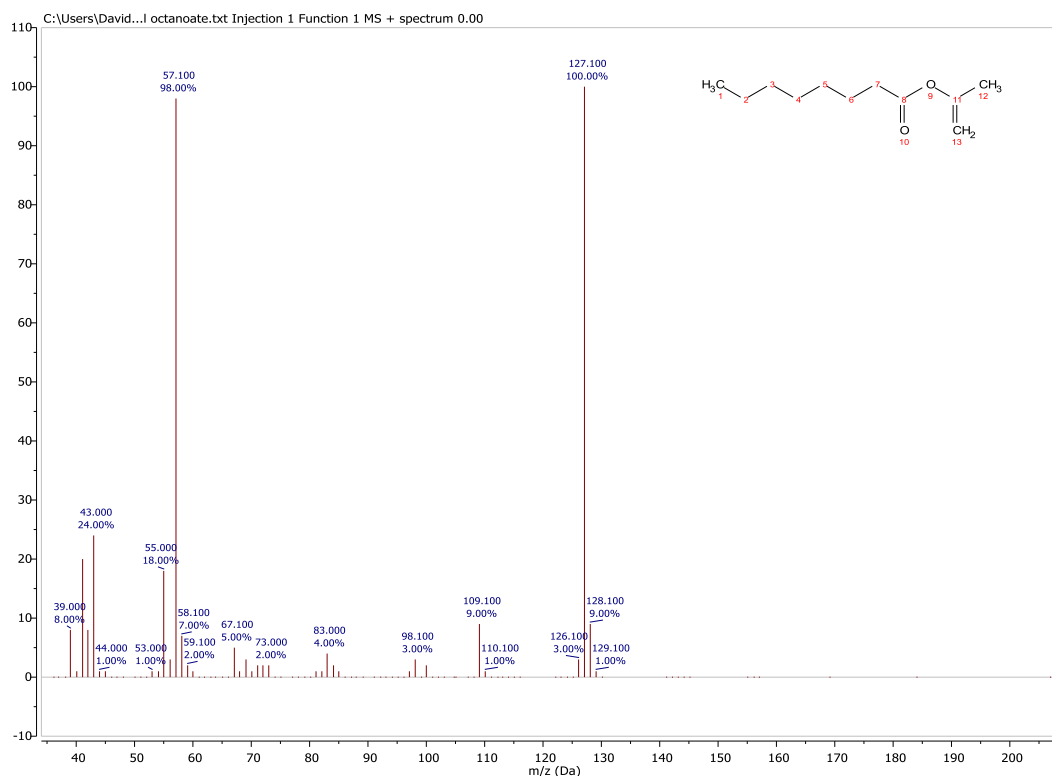
Figure A.2.1.6. MS spectrum of compound *2c*

GC/MS (relative intensity, 70 eV) *m/z*: 128 (9), 127 (100), 109 (9), 67 (5), 57 (98), 55 (18), 43 (24), 42 (8), 41 (20), 39 (8).

General isolation procedure for propanediol monoesters. Propanediol monoesters (**3a/3a***, **3b/3b***, **3c/3c***) were isolated by flash column chromatography (stationary phase: SiO$_2$, eluent: petroleum ether/ethyl acetate 9:1 v/v).

General isolation procedure for propanediol diesters. Propanediol diesters (**3a'**, **3b'**, **3c'**) were isolated upon washing the reaction mixture with a saturated solution of NaHCO$_3$ (3x10 mL).

General isolation procedure for ethylene glycol diesters. Ethylene glycol diesters (**5a'**, **5b'**, **5c'**) were isolated upon washing the reaction mixture with a saturated solution of NaHCO$_3$ (3x10 mL).

2-Hydroxypropyl acetate, 1-hydroxypropan-2-yl acetate (propanediol monoacetates, 3a,3a*)

The products were isolated both in batch and continuous flow conditions, in: i) a 89% yield from the batchwise reaction of isopropenyl acetate (1.315 g, 13.14 mmol) and 1,2-propanediol (1.004 g, 13.19 mmol) in the presence of Amberlyst-15 (150.5 mg) as a catalyst; ii) a 94% yield from the CF-reaction of isopropenyl acetate and 1,2-propanediol in THF as a solvent (molar ratio 1:1:10) for 8h (conditions: Flow = 0.3 mL/min, T = 30°C, C = 1.2 M).
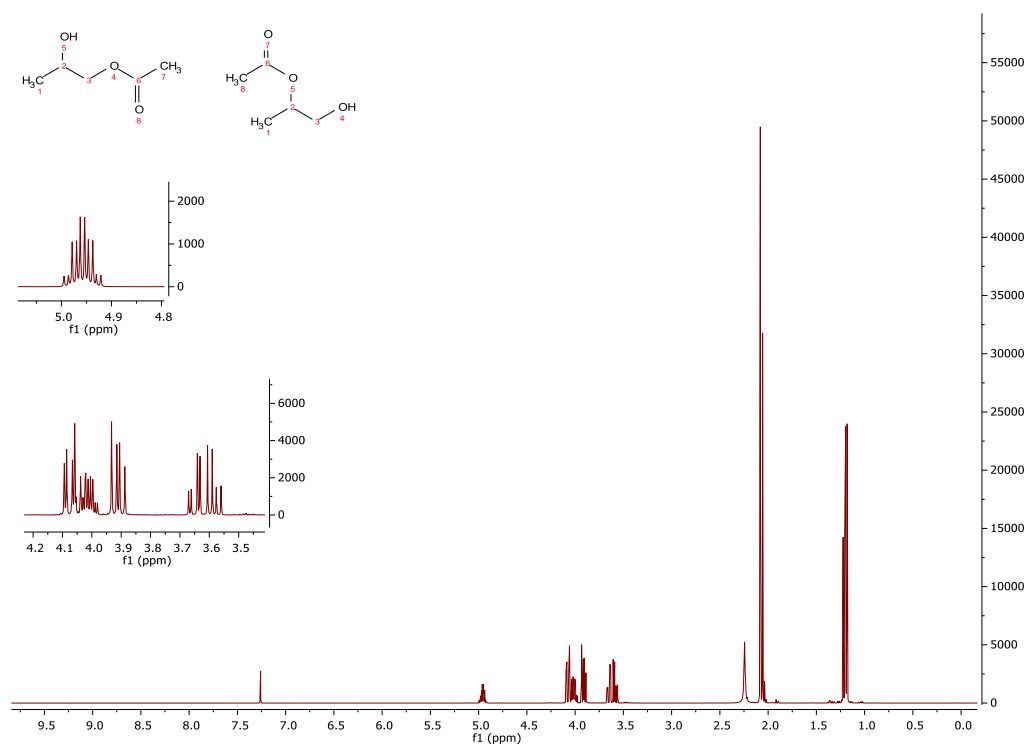
Figure A.2.1.7. *^{1}H NMR spectrum of compounds **3a**, **3a***

3a: ^{1}H NMR (400 MHz, 298 K, CDCl$_3$) δ: 4.09-3.90 (m, 2H), 4.02 (m, 1H), 2.08 (s, 3H), 1.19 (d, 3H).

3a*: ^{1}H NMR (400 MHz, 298 K, CDCl$_3$) δ: 4.95 (m, 1H), 3.60 (m, 2H), 2.09 (s, 3H), 1.21 (d, 3H).
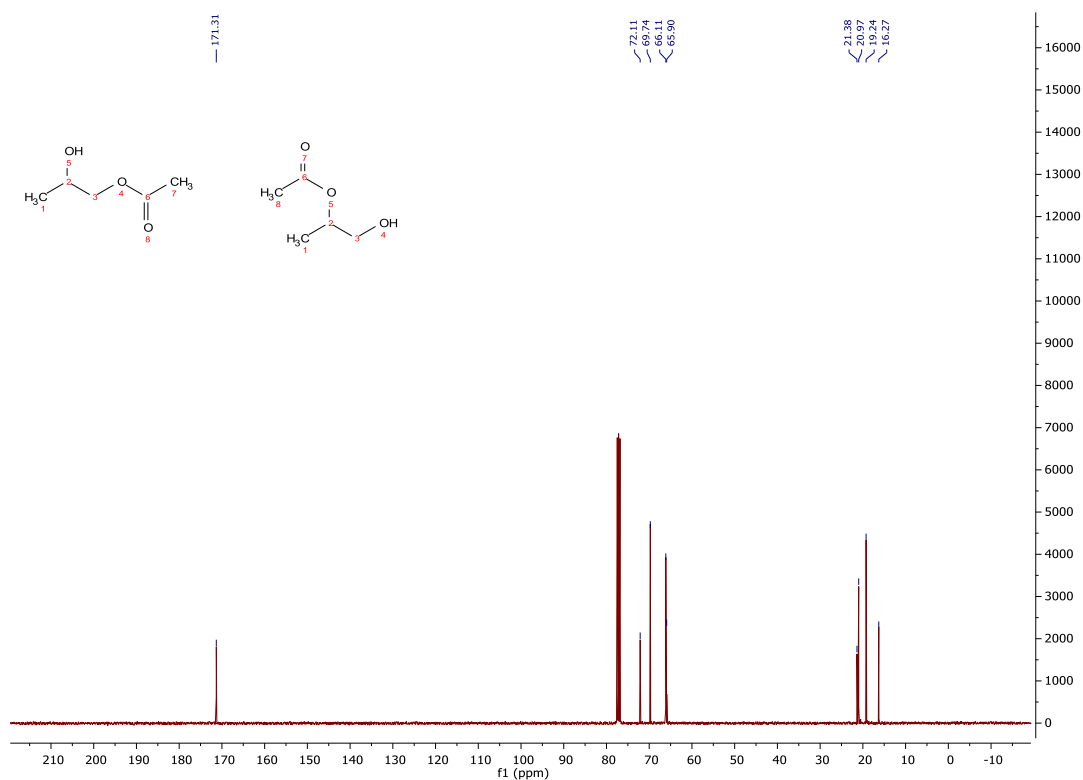
Figure A.2.1.8. *^{13}C NMR spectrum of compounds **3a**, **3a***

3a: ^{13}C{H} NMR (101 MHz, 298 K, CDCl$_3$) δ: 171.31, 69.74, 66.11, 20.97, 19.24.

240

3a*: $^{13}C\{H\}$ NMR (101 MHz, 298 K, CDCl$_3$) δ: 171.31, 72.11, 65.90, 21.38, 16.27.
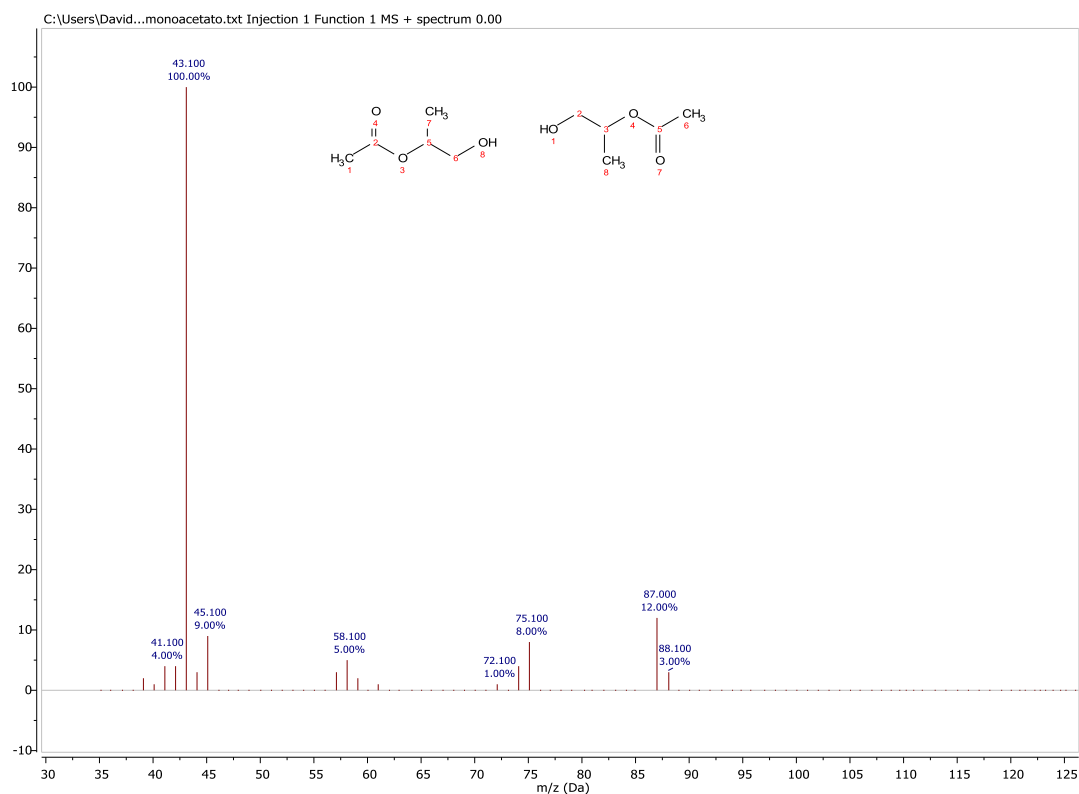
Figure A.2.1.9. MS spectrum of compounds **3a, 3a***

GC/MS (relative intensity, 70 eV) *m/z*: 87 (12), 75 (8), 58 (5), 45 (9), 43 (100).

2-Hydroxypropyl 4-phenylbutanoate, 1-hydroxypropan-2-yl 4-phenylbutanoate (propanediol monophenylbutyrates, 3b,3b*)

The products were isolated both in batch and continuous flow conditions in: i) a 92% yield from the batchwise reaction of isopropenyl phenylbutyrate (2.715 g, 13.29 mmol) and 1,2-propanediol (1.012 g, 13.29 mmol) in the presence of Amberlyst-15 (150.4 mg) as a catalyst; ii) a 87% from the CF-reaction of isopropenyl phenylbutyrate and 1,2-propanediol in THF as a solvent (molar ratio 1:1:10) for 8h (conditions: Flow = 0.3 mL/min, T = 50°C, C = 1.2 M).
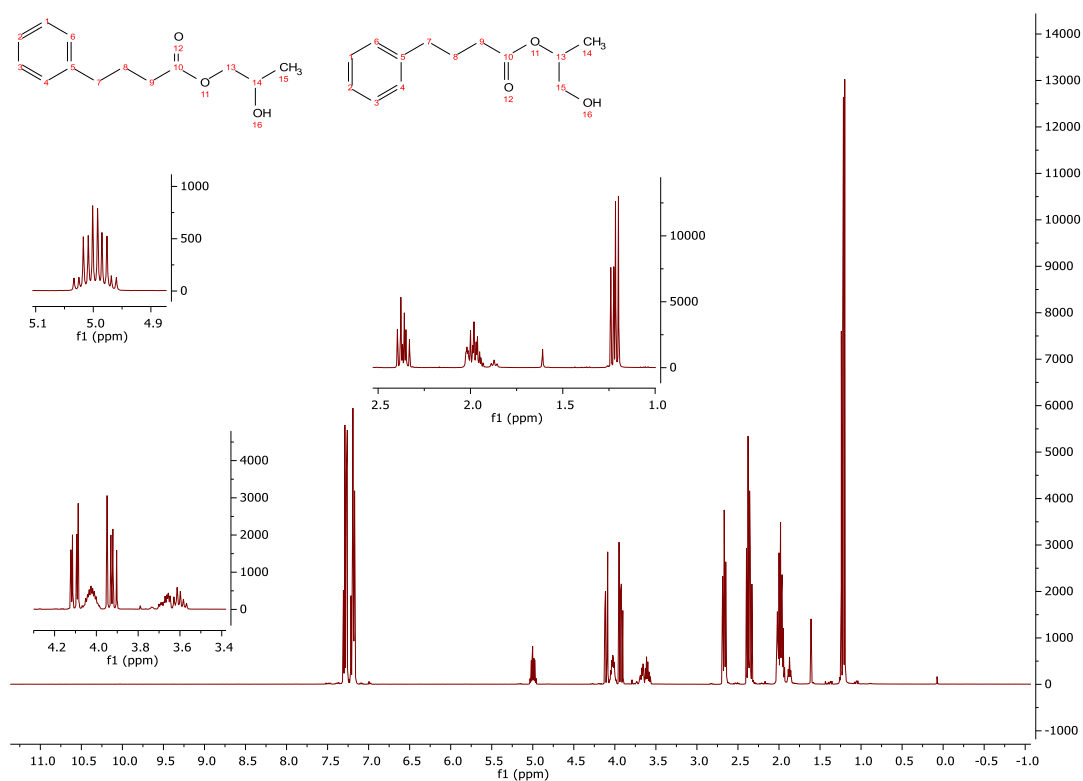
Figure A.2.1.10. *¹H NMR spectrum of compounds **3b, 3b***

3b: ¹H NMR (400 MHz, 298 K, CDCl₃) δ: 7.32-7.16 (m, 5H), 4.15-3.90 (m, 2H), 4.03 (m, 1H), 2.65 (m, 2H), 2.35 (m, 2H), 1.95 (m, 2H), 1.20 (d, 3H).

3b*: ¹H NMR (400 MHz, 298 K, CDCl₃) δ: 7.32-7.16 (m, 5H), 5.00 (m, 1H), 4.15-3.90 (m, 2H), 2.65 (m, 2H), 2.35 (m, 2H), 1.95 (m, 2H), 1.22 (d, 3H).
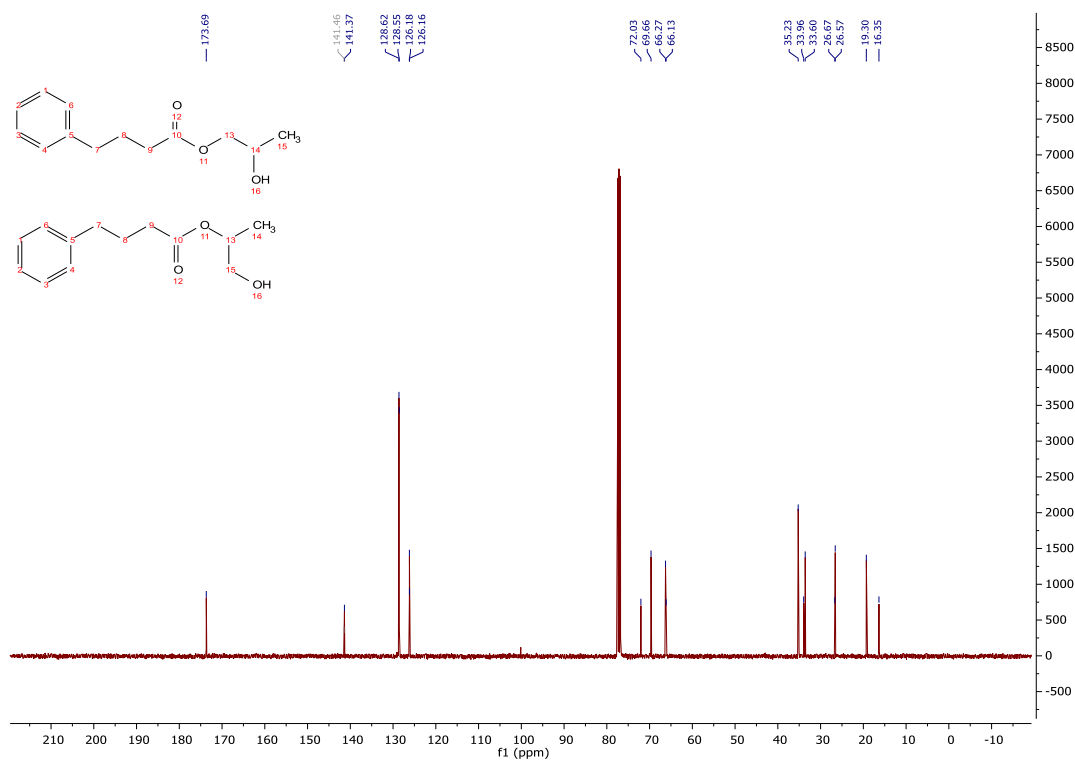
Figure A.2.1.11. *¹³C NMR spectrum of compounds **3b, 3b***

3b: ^{13}C{H} NMR (101 MHz, 298 K, CDCl$_3$) δ: 173.69, 141.37, 128.62, 128.55, 126.18, 69.66, 66.27, 35.23, 33.60, 26.57, 19.30.

3b*: ^{13}C{H} NMR (101 MHz, 298 K, CDCl$_3$) δ: 173.69, 141.46, 128.62, 128.55, 126.16, 72.03, 66.13, 35.23, 33.96, 26.67, 16.35.
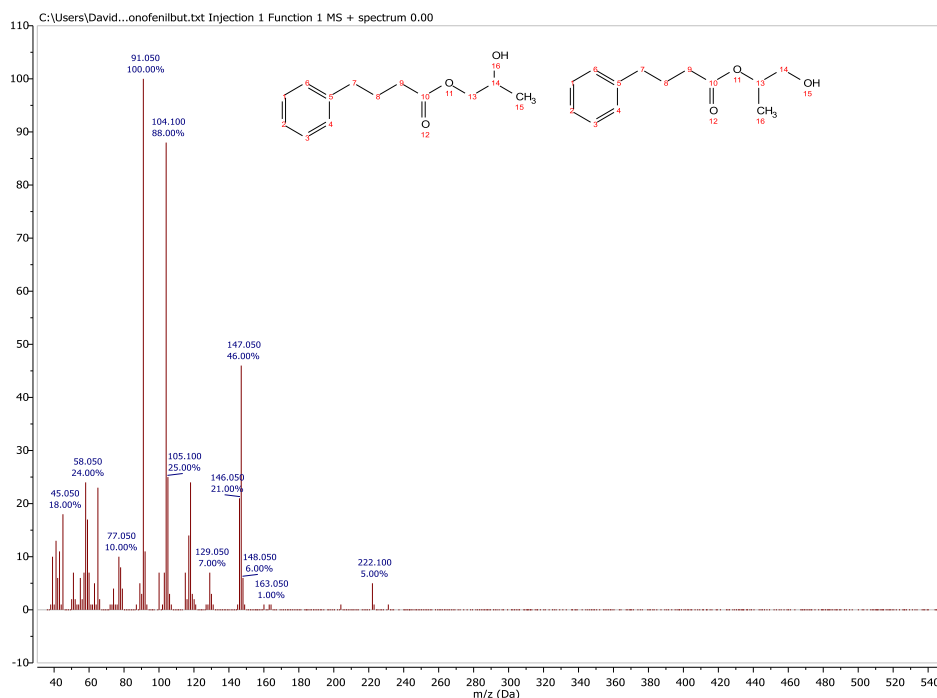
*Figure A.2.1.12. MS spectrum of compounds **3b, 3b***

GC/MS (relative intensity, 70 eV) *m/z*: 222 (M$^+$, 5), 147 (46), 118 (24), 105 (25), 104 (88), 91 (100), 65 (23), 58 (24), 45 (18).

2-Hydroxypropyl octanoate, 1-hydroxypropan-2-yl octanoate (propanediol monooctanoates, 3c,3c*)

The products were isolated both in batch and continuous flow conditions in i) a 92% yield from the batchwise reaction of isopropenyl octanoate (2.445 g, 13.26 mmol) and 1,2-propanediol (1.009 g, 13.26 mmol) in the presence of Amberlyst-15 (150.7 mg) as a catalyst; ii) a 81% yield from the CF-reaction of isopropenyl octanoate and 1,2-propanediol in THF as a solvent (molar ratio 1:1:10) for 8h (conditions: Flow = 0.3 mL/min, T = 70°C, C = 1.2 M).
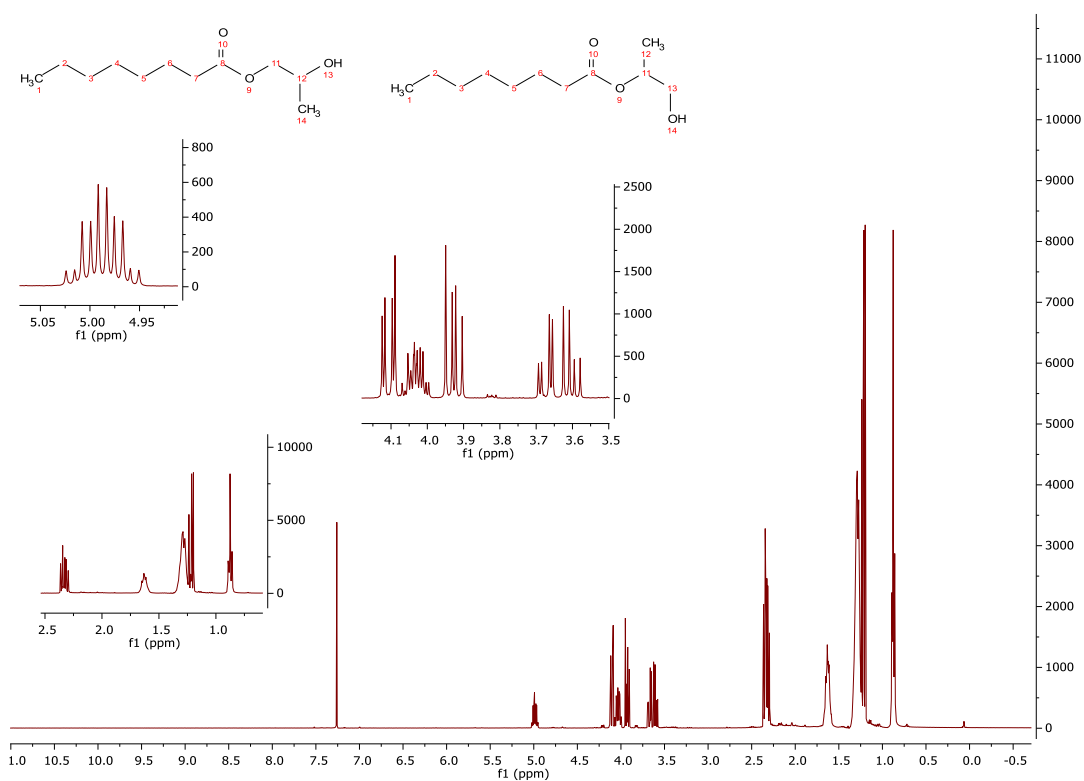
Figure A.2.1.13. ^{1}H NMR spectrum of compounds 3c, 3c*

3c: ^{1}H NMR (400 MHz, 298 K, CDCl$_3$) δ: 4.15-3.90 (m, 2H), 4.04 (m, 1H), 2.35 (m, 2H), 1.65 (m, 2H), 1.30 (m, 8H), 1.20 (d, 3H), 0.9 (t, 3H).

3c*: ^{1}H NMR (400 MHz, 298 K, CDCl$_3$) δ: 5.00 (m, 1H), 3.70-3.55 (m, 2H), 2.35 (m, 2H), 1.65 (m, 2H), 1.30 (m, 8H), 1.24 (d, 3H), 0.9 (t, 3H).
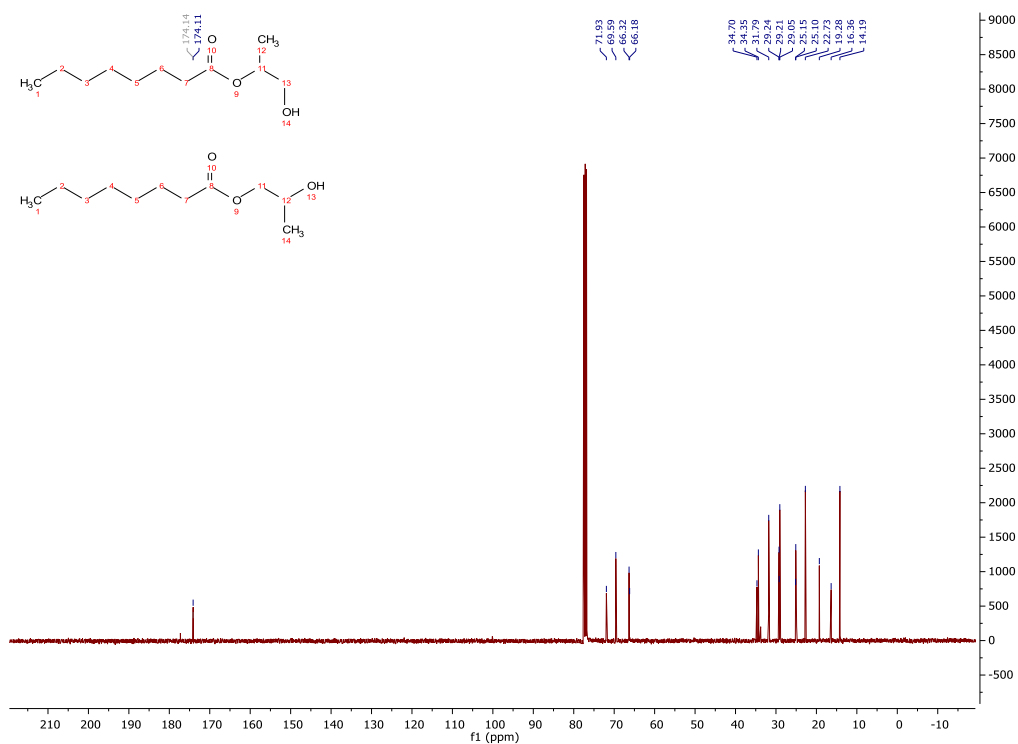
Figure A.2.1.14. ^{13}C NMR spectrum of compounds 3c, 3c*

244

3c: $^{13}C\{H\}$ NMR (101 MHz, 298 K, CDCl$_3$) δ: 174.11, 69.59, 66.32, 34.35, 31.79, 29.05, 25.10, 22.73, 19.28, 16.36, 14.19.

3c*: $^{13}C\{H\}$ NMR (101 MHz, 298 K, CDCl$_3$) δ: 174.14, 71.93, 66.18, 34.70, 29.24, 29.21, 25.15, 22.73, 19.28, 16.36, 14.19.
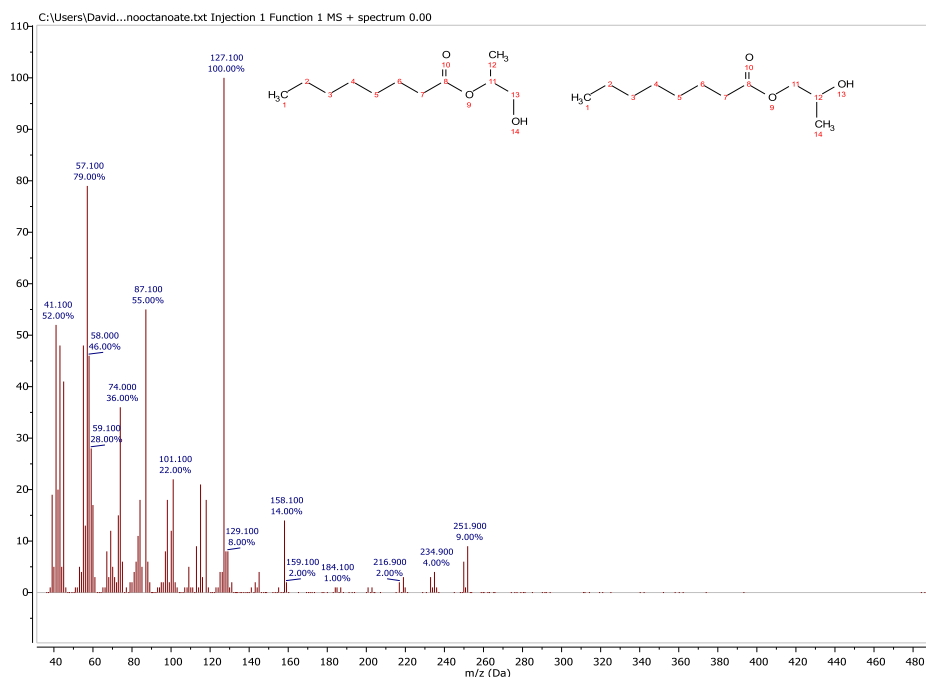
Figure A.2.1.15. MS spectrum of compounds *3c, 3c**

GC/MS (relative intensity, 70 eV) *m/z*: 158 (14), 128 (8), 127 (100), 118 (18), 115 (21), 101 (22), 100 (12), 98 (18), 87 (55), 84 (18), 74 (36), 59 (28), 58 (46), 57 (79), 55 (48), 45 (41), 43 (48), 41 (52).

Propane-1,2-diyl diacetate (propanediol diacetate, 3a')

The product was isolated in a 72% yield from the reaction of isopropenyl acetate (6.69 g, 66.75 mmol) and 1,2-propanediol (1.016 g, 13.35 mmol) in the presence of H$_2$SO$_4$ (50.8 mg, 0.51 mmol) as a catalyst.
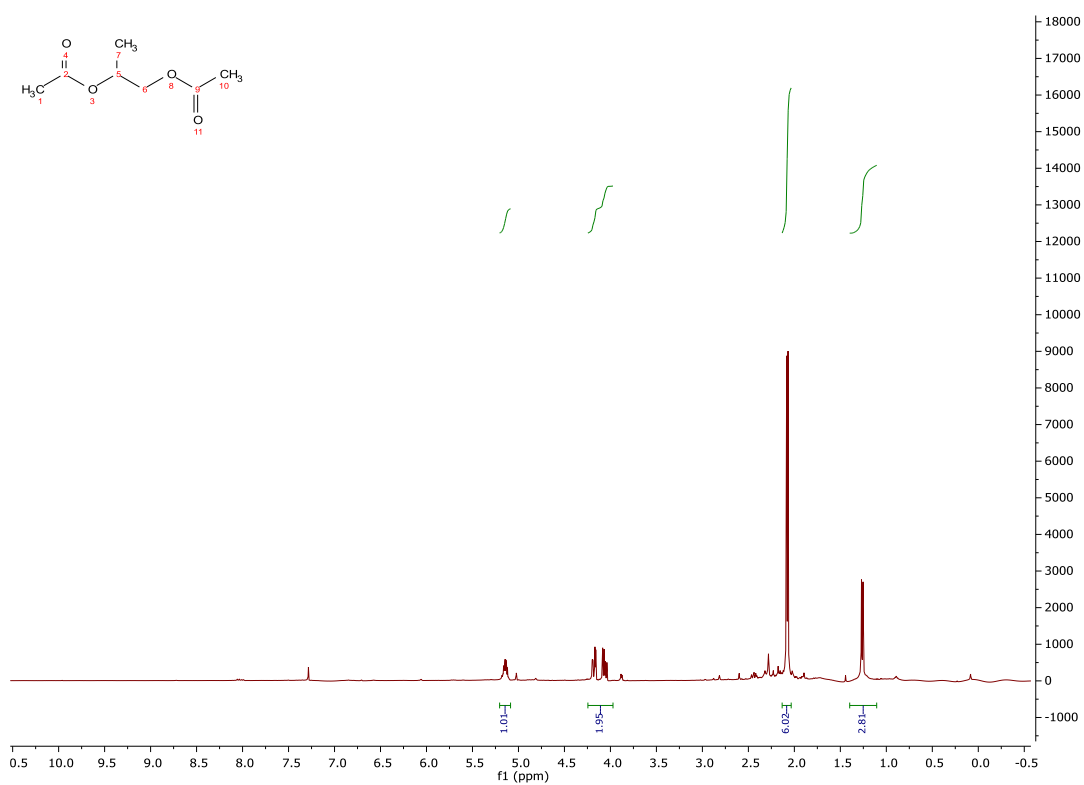
Figure A.2.1.16. *^{1}H NMR spectrum of compound **3a'***

^{1}H NMR (400 MHz, 298 K, CDCl$_3$) δ: 5.15 (m, 1H), 4.20-4.00 (m, 2H), 2.08 (d, 6H), 1.25 (d, 3H).
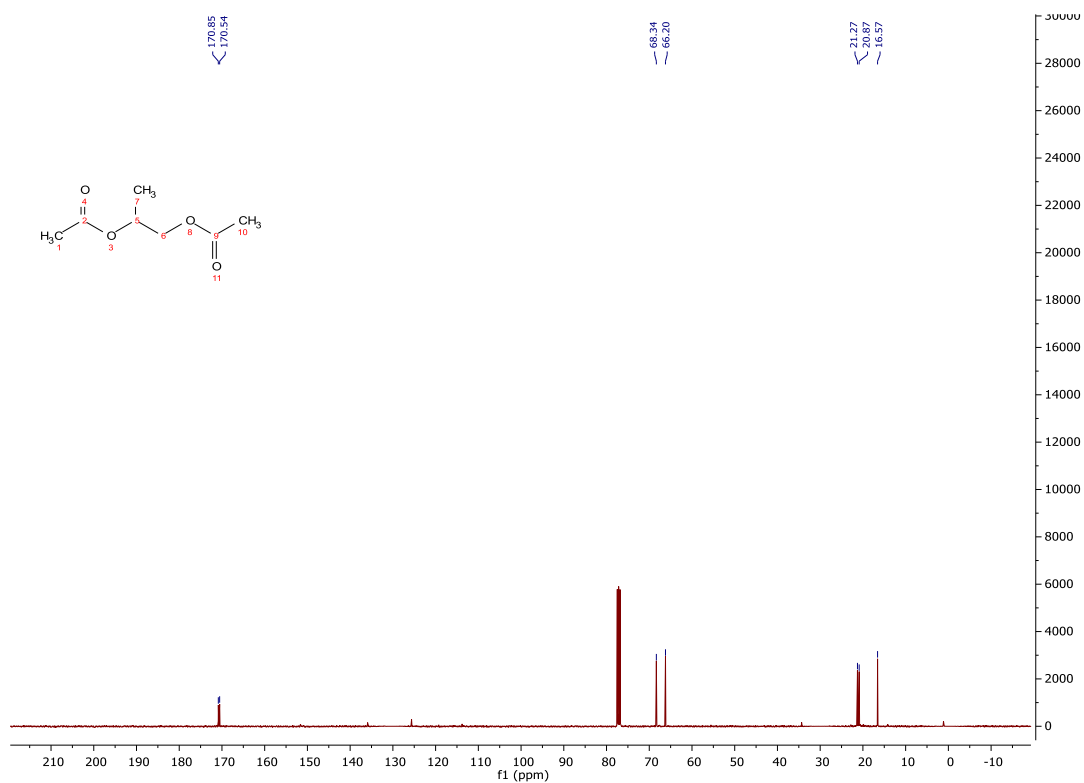
Figure A.2.1.17. *^{13}C NMR spectrum of compounds **3a'***

^{13}C{H} NMR (101 MHz, 298 K, CDCl$_3$) δ: 170.85, 170.54, 68.34, 66.20, 21.27, 20.87, 16.57.

246
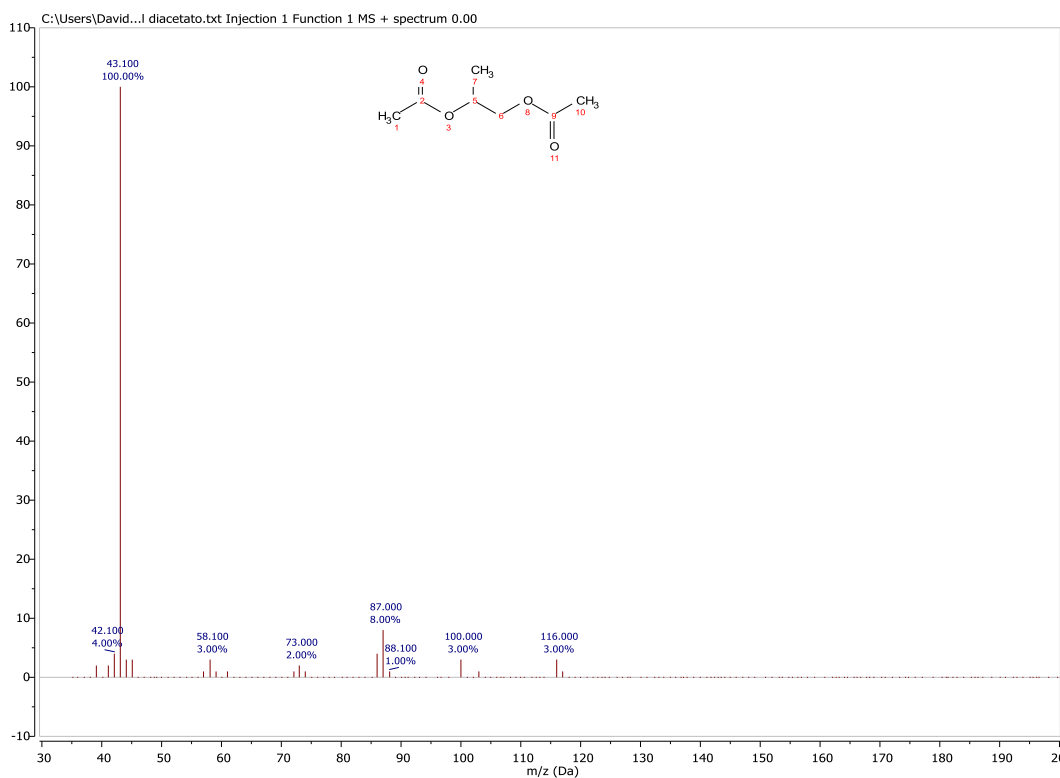
Figure A.2.1.18. MS spectrum of compound **3a'**

GC/MS (relative intensity, 70 eV) *m/z*: 116 (3), 100 (3), 87 (8), 58 (3), 43 (100).

1-(3-Phenylpropoxy)propan-2-yl 4-phenylbutanoate (propanediol diphenylbutyrate, 3b')

The product was isolated in a 95% yield from the reaction of phenylbutyric acid (10.798 g, 65.77 mmol) and 1,2-propanediol (1.001 g, 13.15 mmol) in the presence of H_2SO_4 (50.0 mg) as a catalyst.
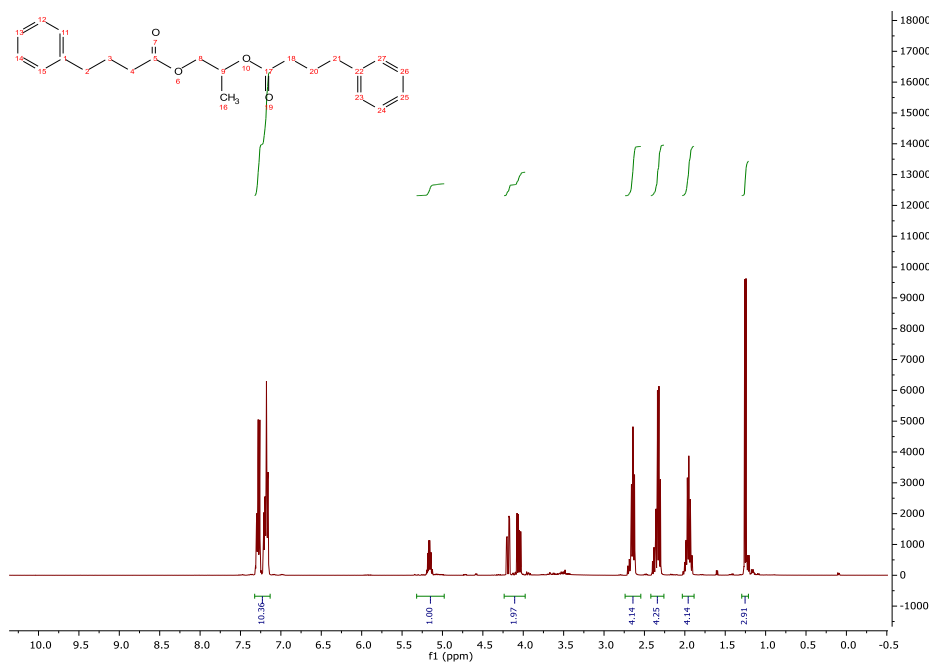
Figure A.2.1.19. ^1H NMR spectrum of compounds **3b'**

247

^{1}H NMR (400 MHz, 298 K, CDCl$_3$) δ: 7.32-7.16 (m, 10H), 5.15 (m, 1H), 4.20-4.00 (m, 2H), 2.65 (m, 4H), 2.35 (m, 4H), 1.95 (m, 4H), 1.25 (d, 3H).
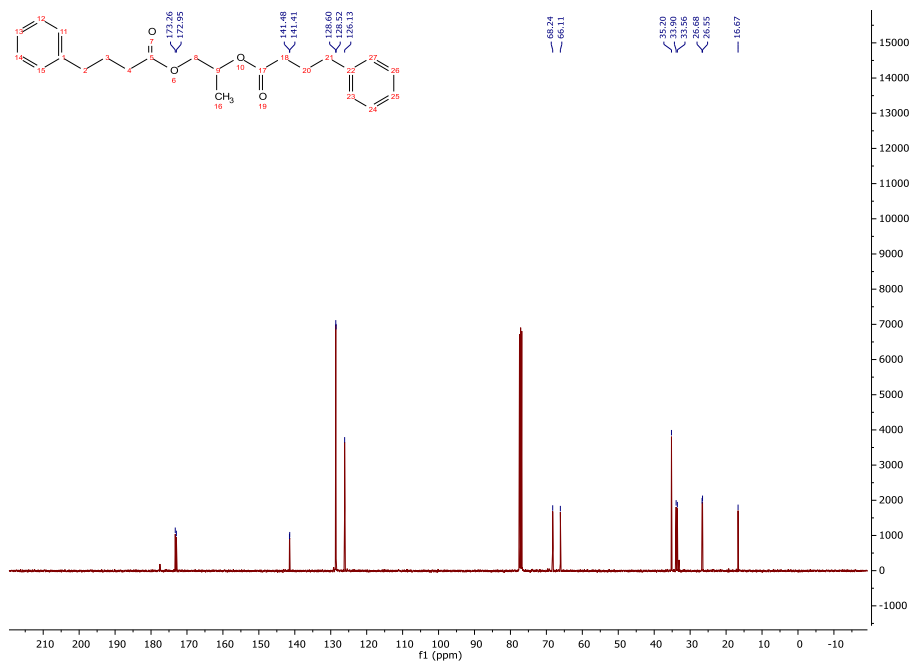
Figure A.2.1.20. ^{13}C NMR spectrum of compounds **3b'**

^{13}C{H} NMR (101 MHz, 298 K, CDCl$_3$) δ: 173.26, 172.95, 141.48, 141.41, 128.60, 128.52, 126.13, 68.24, 66.11, 35.20, 33.90, 33.56, 26.68, 26.55, 16.67.
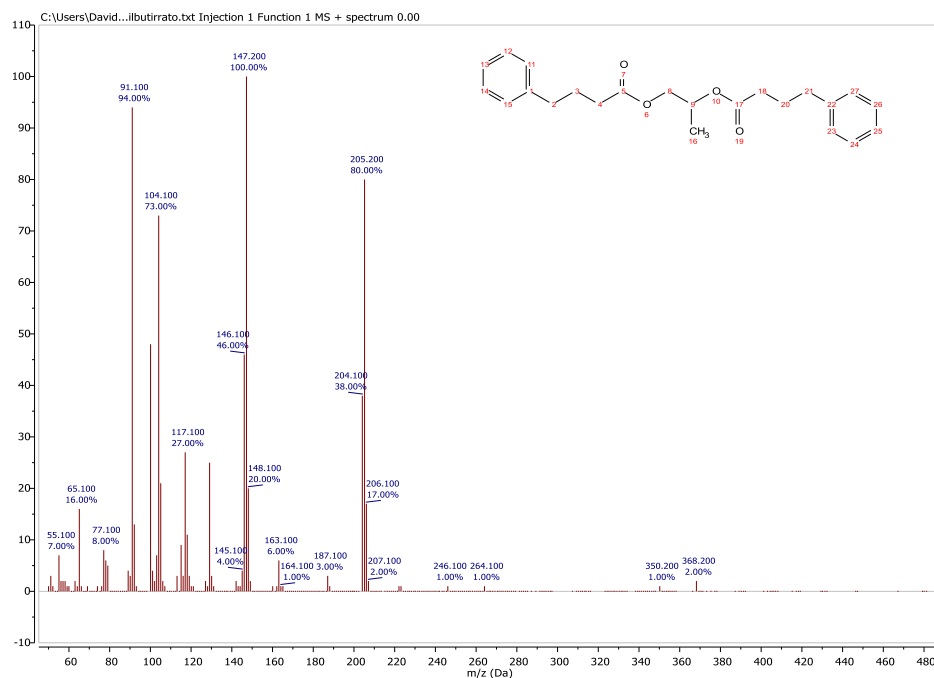
Figure A.2.1.21. MS spectrum of compound **3b'**

GC/MS (relative intensity, 70 eV) *m/z*: 368 (M$^+$, 2), 206 (80), 147 (100), 117 (27), 104 (73), 91 (94), 65 (16).

248

Propane-1,2-diyl dioctanoate (propanediol dioctanoate, 3c')

The product was isolated in a 87% yield from the reaction of octanoic acid (9.985 g, 69.25 mmol) and 1,2-propanediol (1.054 g, 13.85 mmol) in the presence of Amberlyst-15 (49.9 mg) as a catalyst.
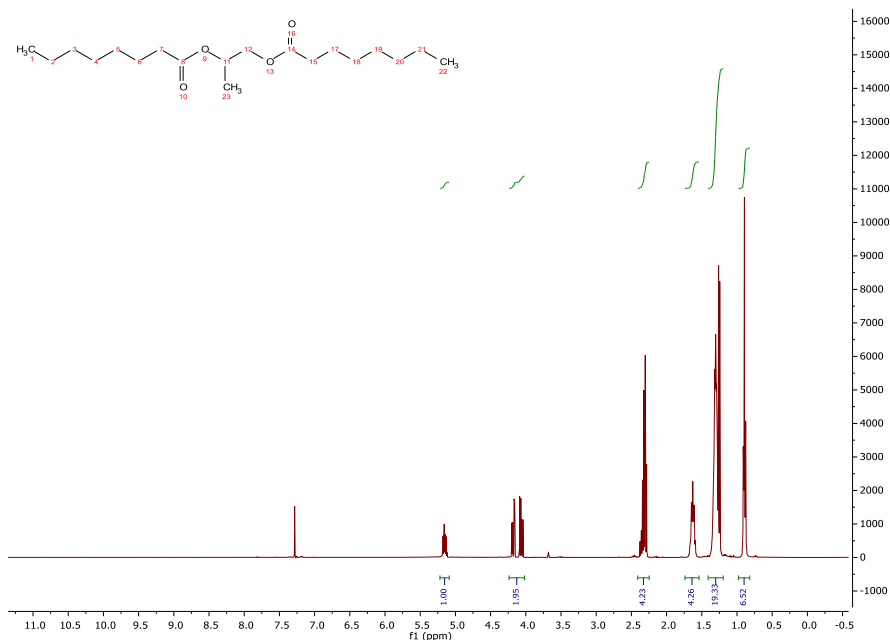
Figure A.2.1.22*. ^{1}H NMR spectrum of compounds **3c'***

^{1}H NMR (400 MHz, 298 K, CDCl$_3$) δ: 5.15 (m, 1H), 4.20-4.00 (m, 2H), 2.30 (m, 4H), 1.63 (m, 4H), 1.30 (m, 19H), 0.90 (t, 6H).
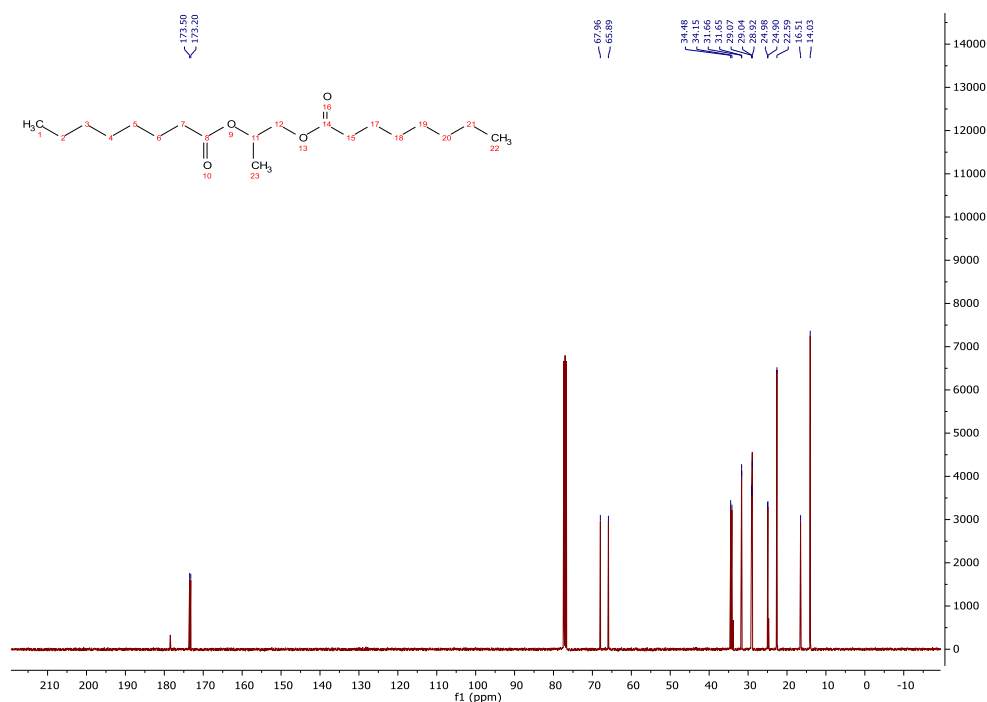
Figure A.2.1.23*. ^{13}C NMR spectrum of compounds **3c'***

^{13}C{H} NMR (101 MHz, 298 K, CDCl$_3$) δ: 173.50, 173.20, 67.96, 65.89, 34.48, 34.15, 31.66, 31.65, 29.07, 29.04, 28.92, 24.98, 24.90, 22.59, 16.51, 14.03.
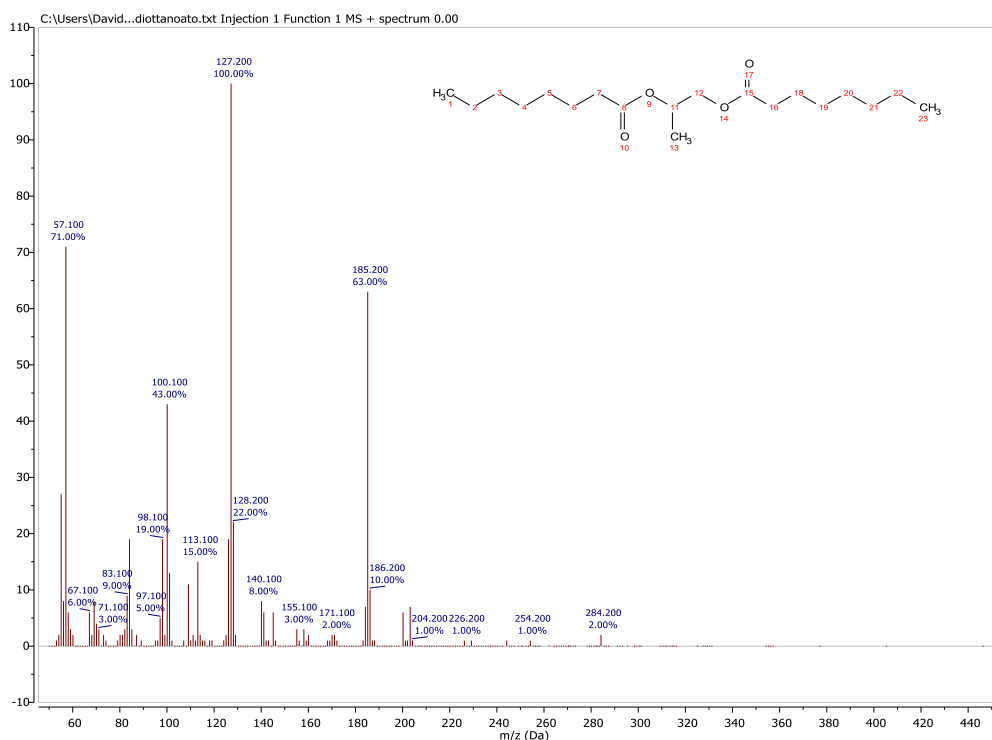
Figure A.2.1.23. MS spectrum of compound **3c'**

GC/MS (relative intensity, 70 eV) *m/z*: 281 (2), 185 (63), 127 (100), 100 (43), 57 (71).

2,2,4-Trimethyl-1,3-dioxolane (propanediol acetal) (4)
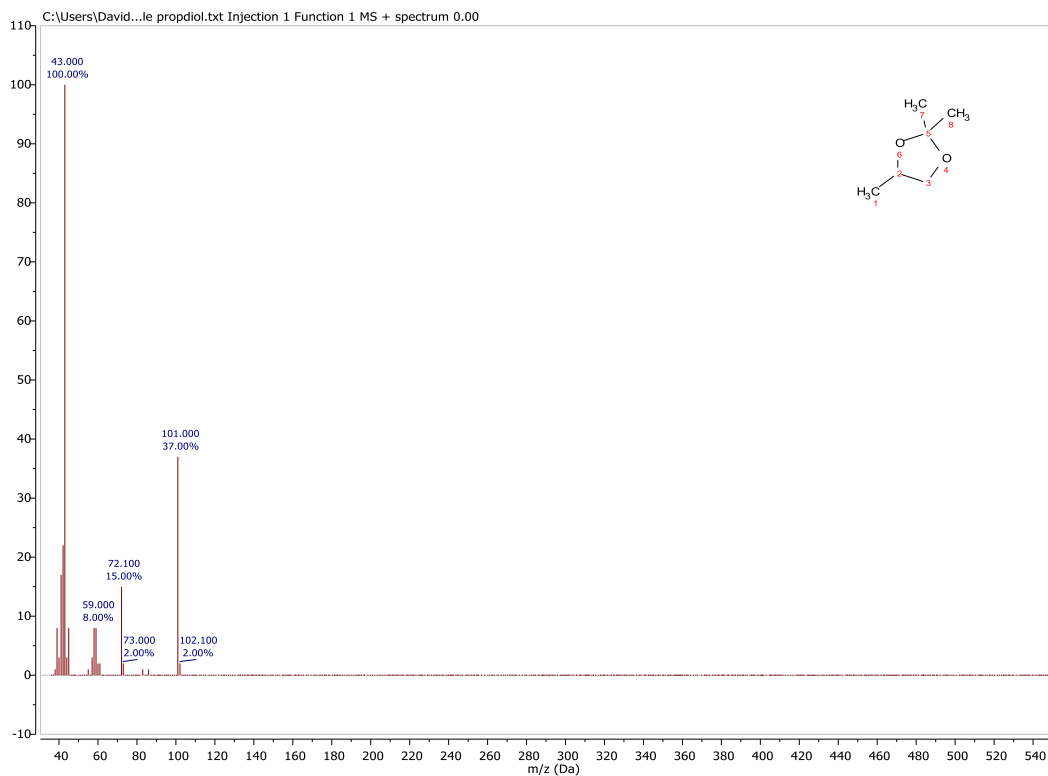
Figure A.2.1.24. MS spectrum of compound **4**

GC/MS (relative intensity, 70 eV) *m/z*: 101 (37), 72 (15), 59 (8), 58 (8), 43 (100), 42 (22), 41 (17).

2-Hydroxyethyl acetate (ethylene glycol monoacetate) (5a)
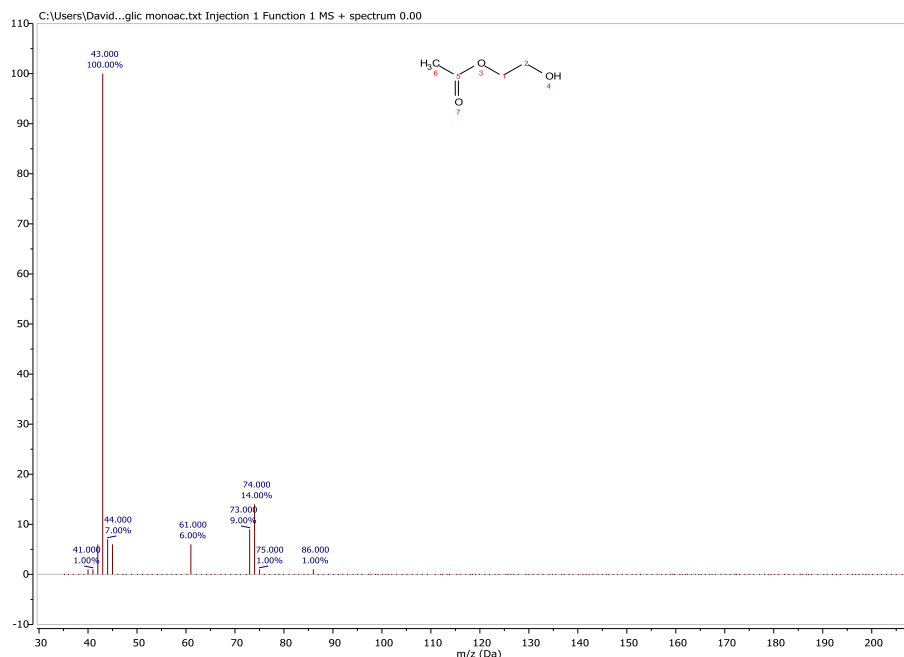
Figure A.2.1.25. *MS spectrum of compound **5a***

GC/MS (relative intensity, 70 eV) *m/z*: 74 (14), 61 (6), 44 (7), 43 (100).

2-Hydroxyethyl 4-phenylbutanoate (ethylene glycol monophenylbutyrate) (5b)
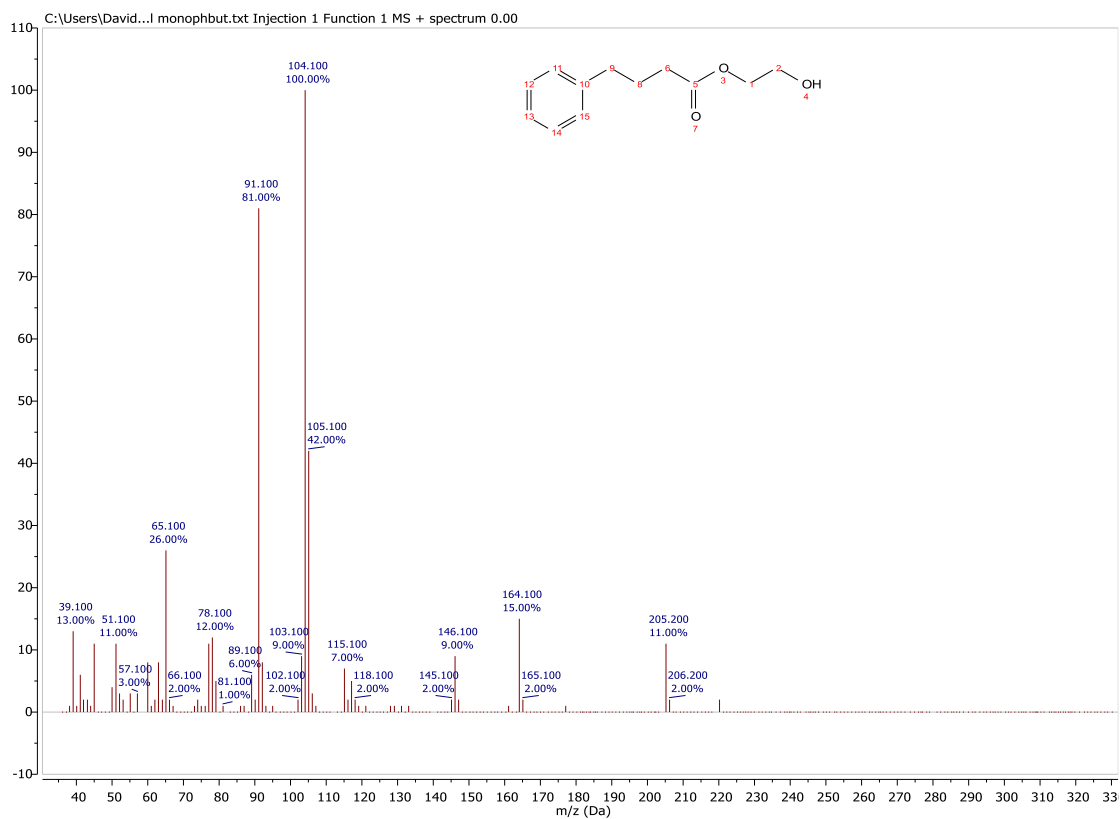
Figure A.2.1.26. *MS spectrum of compound **5b***

GC/MS (relative intensity, 70 eV) *m/z*: 205 (11), 164 (15), 146 (9), 105 (42), 104 (100), 91 (81), 78 (12), 65 (26), 45 (11).

2-Hydroxyethyl octanoate (ethylene glycol monooctanoate) (5c)
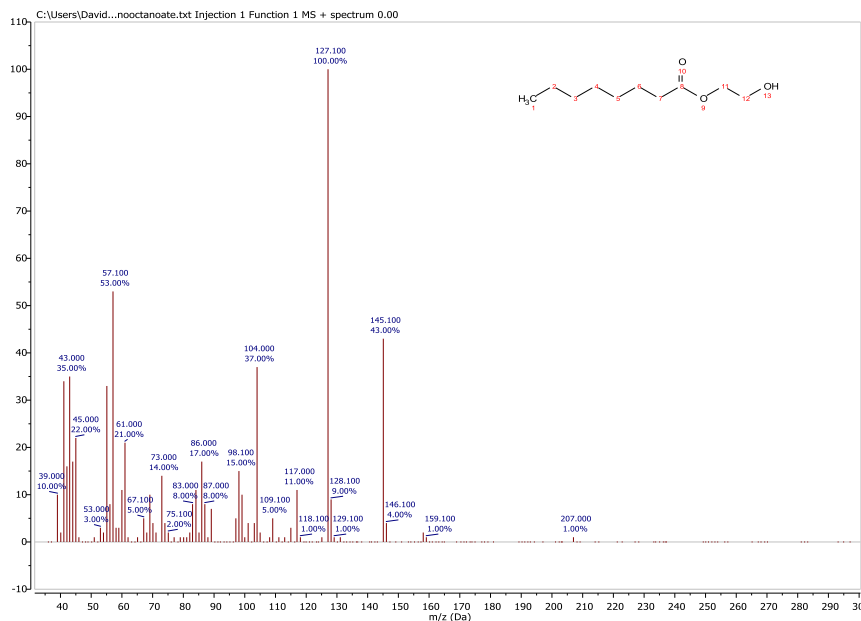
Figure A.2.1.27. MS spectrum of compound **5c**

GC/MS (relative intensity, 70 eV) *m/z*: 159 (1), 145 (43), 127 (100), 117 (11), 104 (37), 98 (15), 86 (17), 61 (21), 57 (53), 43 (35).

Ethane-1,2-diyl diacetate (ethylene glycol diacetate, 5a')

The product was isolated in a 75% yield from the reaction of isopropenyl acetate (8.258 g, 82.5 mmol) and ethylene glycol (1.023 g, 16.5 mmol) in the presence of H_2SO_4 (49.7 mg) as a catalyst.
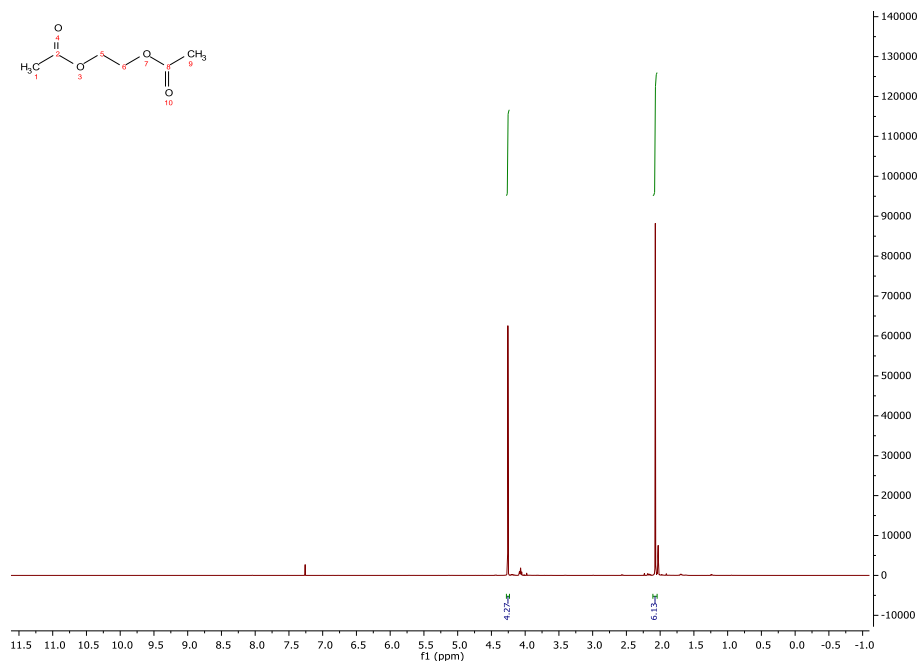
Figure A.2.1.28. ¹H NMR spectrum of compound **5a'**

^{1}H NMR (400 MHz, 298 K, CDCl$_3$) δ: 4.26 (s, 4H), 2.75 (s, 6H).
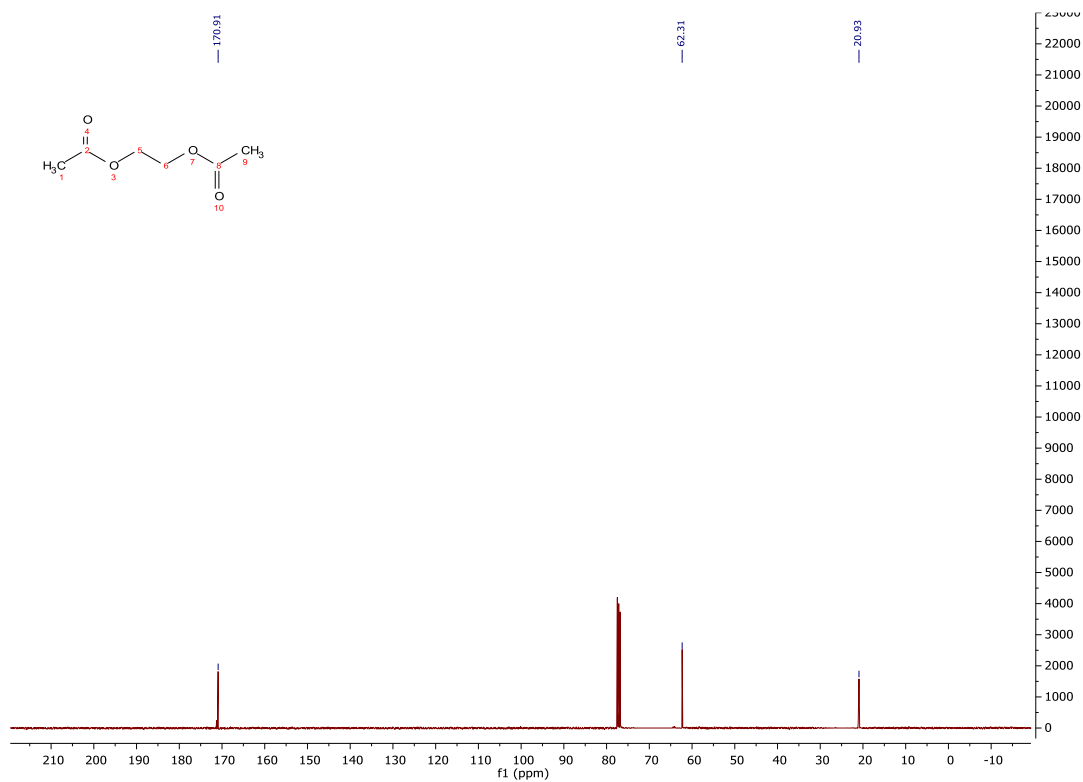
Figure A.2.1.29. ^{13}C NMR spectrum of compound **5a'**

^{13}C{H} NMR (101 MHz, 298 K, CDCl$_3$) δ: 170.91, 62.31, 20.93.
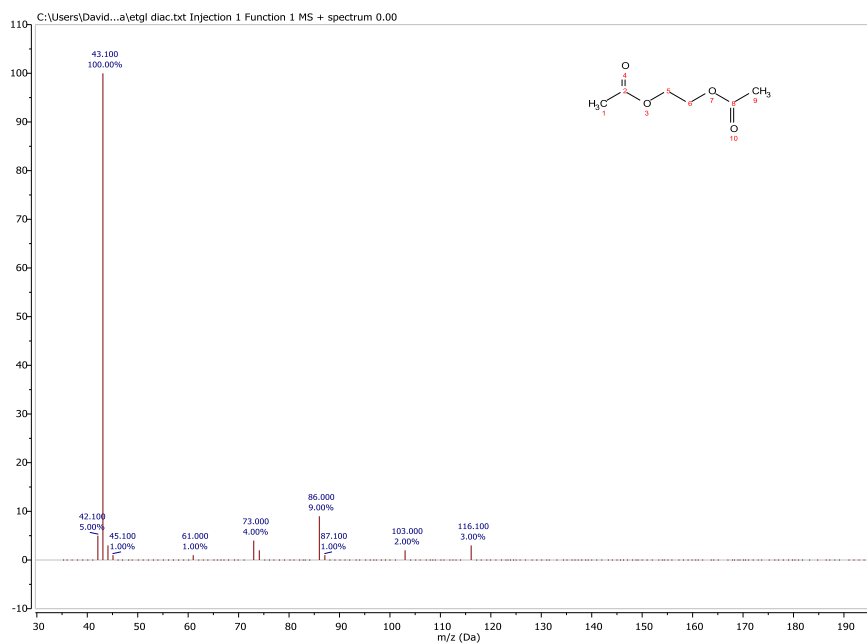
Figure A.2.1.30. MS spectrum of compound **5a'**

GC/MS (relative intensity, 70 eV) *m/z*: 116 (3), 103 (2), 86 (9), 73 (4), 44 (3), 43 (100).

Ethane-1,2-diyl bis(4-phenylbutanoate) (ethylene glycol diphenylbutyrate, 5b')

The product was isolated in a 81% yield from the reaction of phenylbutyric acid (13.4 g, 81.8 mmol) and ethylene glycol (1.013 g, 16.3 mmol) in the presence of H_2SO_4 (51.1 mg) as a catalyst.
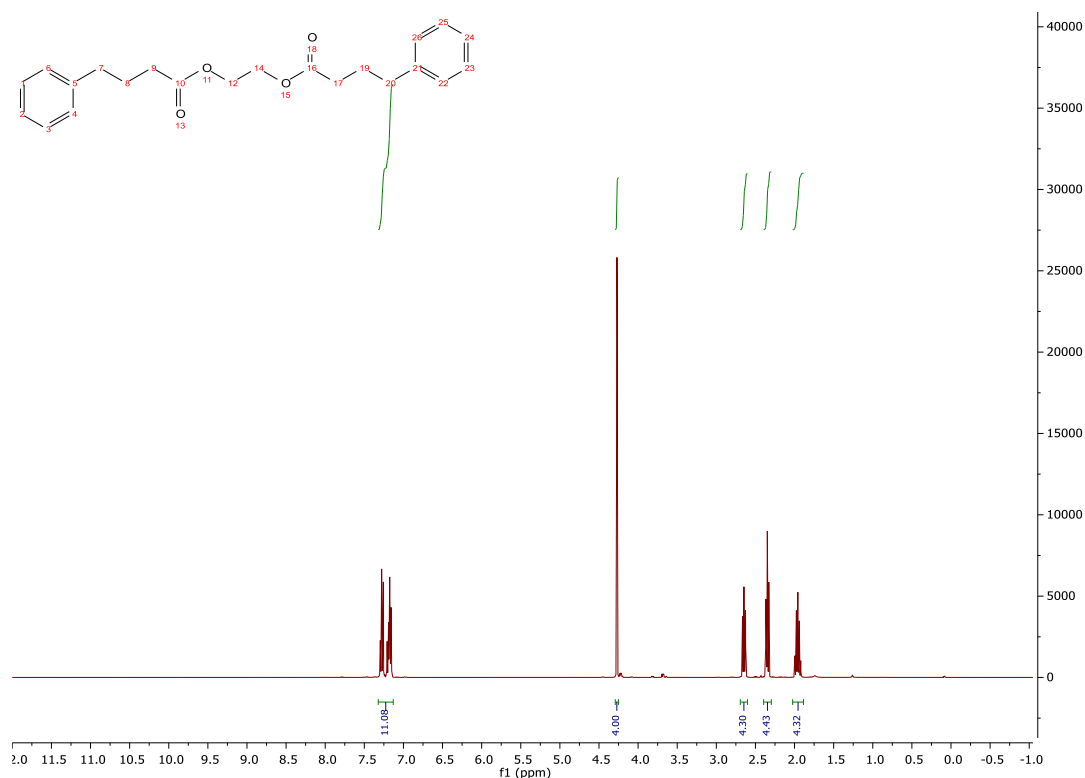
Figure A.2.1.31. ^1H NMR spectrum of compound **5b'**

^1H NMR (400 MHz, 298 K, CDCl$_3$) δ: 7.30-7.15 (m, 10H), 4.27 (s, 4H), 2.65 (t, 4H), 2.35 (t, 4H), 1.95 (m, 4H).

254
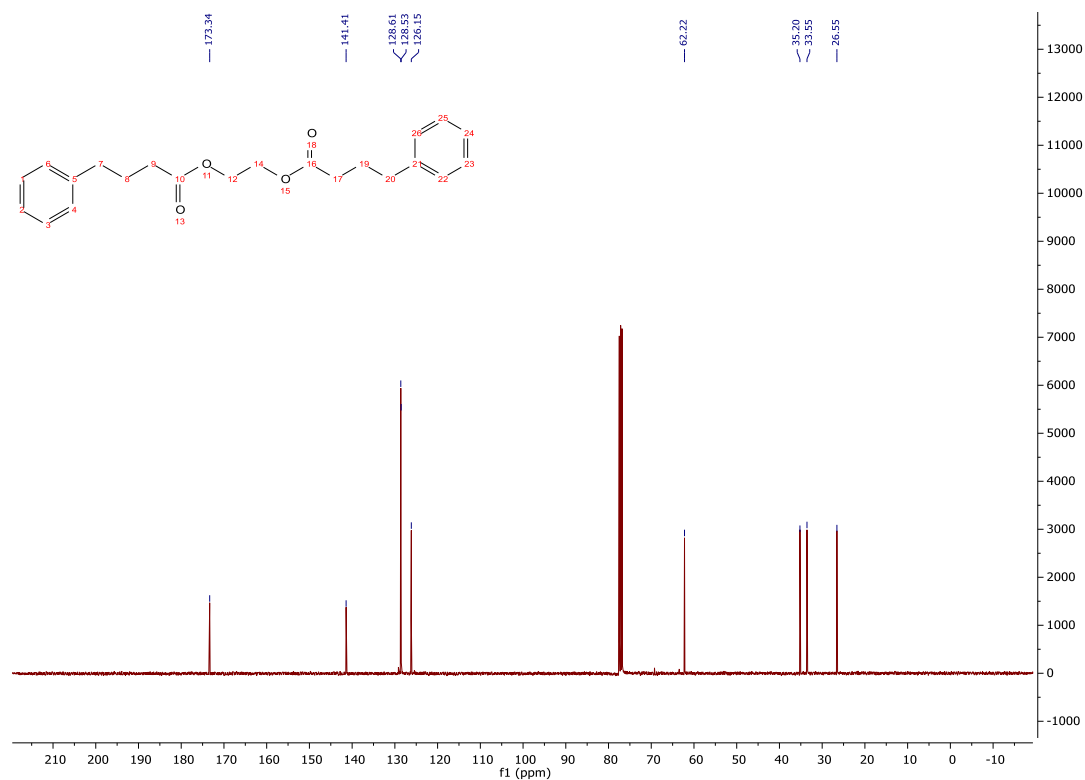
¹³C{H} NMR (101 MHz, 298 K, CDCl₃) δ: 173.34, 141.41, 128.61, 128.53, 126.15, 62.22, 35.20, 33.55, 26.55.
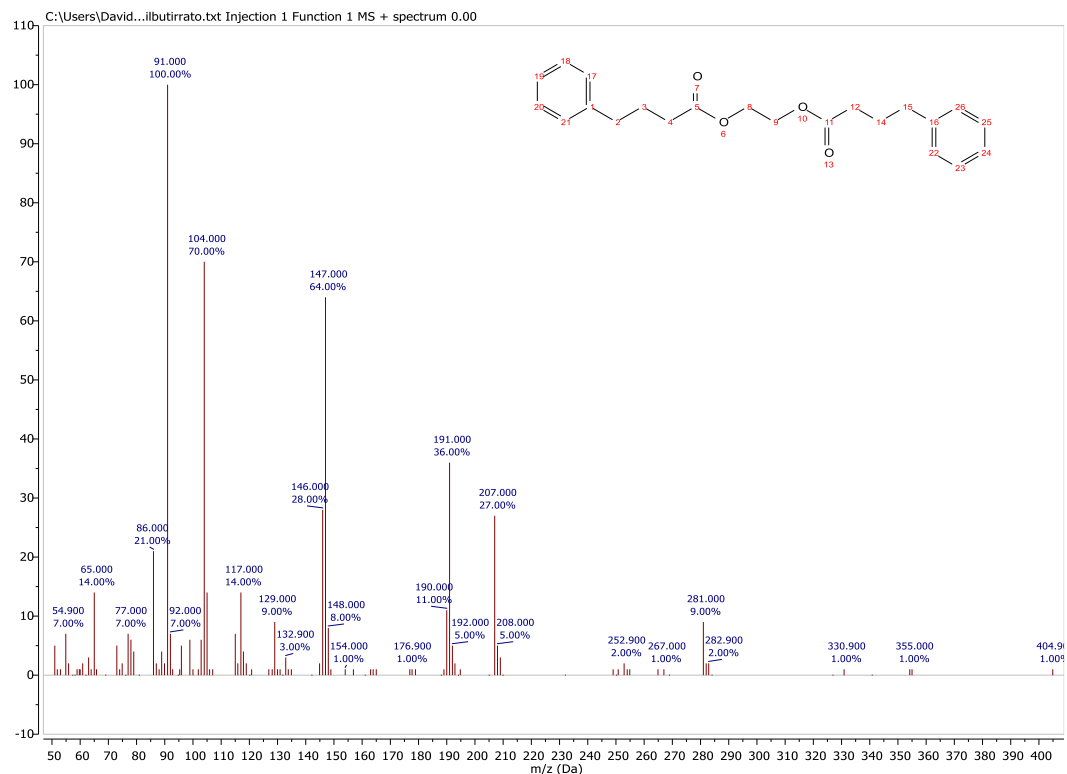
Figure A.2.1.33. *MS spectrum of compound 5b'*

GC/MS (relative intensity, 70 eV) *m/z*: 355 ([M+1]⁺, 1), 281 (9), 207 (27), 191 (36), 147 (61), 101 (70), 91 (100), 86 (21), 65 (14).

Ethane-1,2-diyl dioctanoate (ethylene glycol dioctanoate, 5c')

The product was isolated in a 88% yield from the reaction of octanoic acid (11.6 g, 80.8 mmol) and ethylene glycol (1.002 g, 16.2 mmol) in the presence of H₂SO₄ (50.1 mg) as a catalyst.
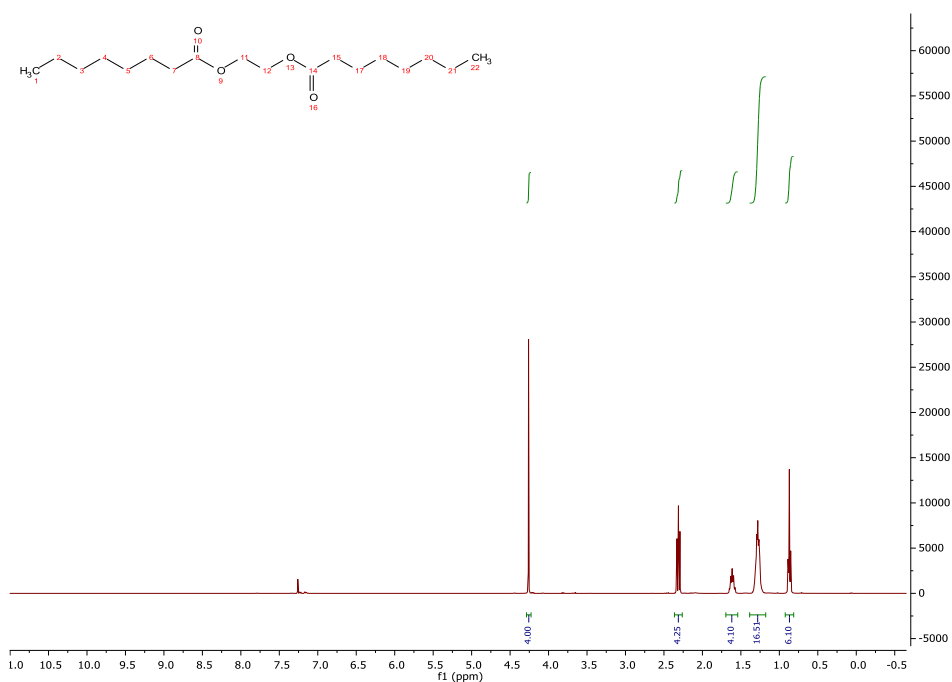
Figure A.2.1.34. *¹H NMR spectrum of compound **5c'***

¹H NMR (400 MHz, 298 K, CDCl₃) δ: 4.26 (s, 4H), 2.31 (t, 4H), 1.61 (m, 4H), 1.28 (m, 16H), 0.87 (t, 6H).
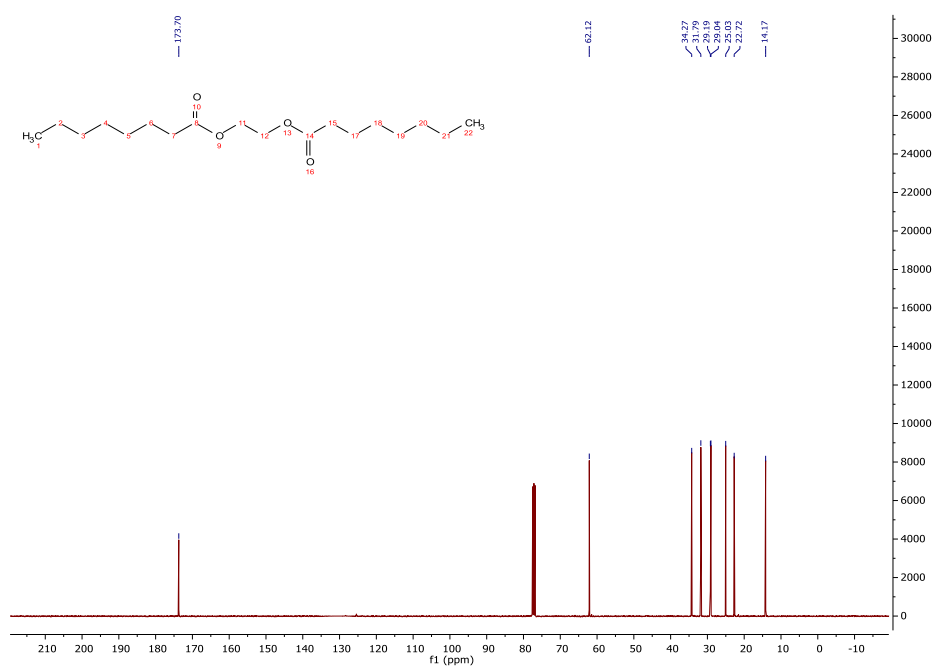
Figure A.2.1.35. *¹³C NMR spectrum of compound **5c'***

¹³C{H} NMR (101 MHz, 298 K, CDCl₃) δ: 173.70, 62.12, 34.27, 31.79, 29.19, 29.04, 25.03, 22.72, 14.17.

256
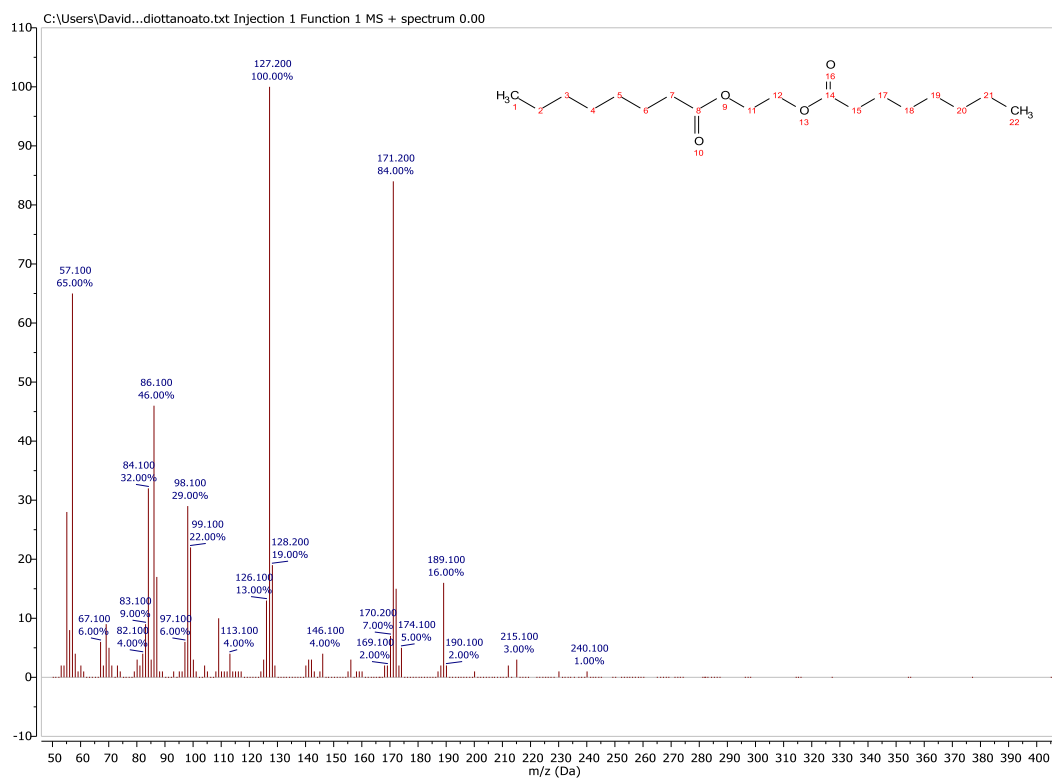
Figure A.2.1.36. MS spectrum of compound 5c'

GC/MS (relative intensity, 70 eV) *m/z*: 240 (1), 189 (16), 171 (84), 127 (100), 98 (29), 86 (46), 57 (65).

2,2-Dimethyl-1,3-dioxolane (ethylene glycol acetal) (6)
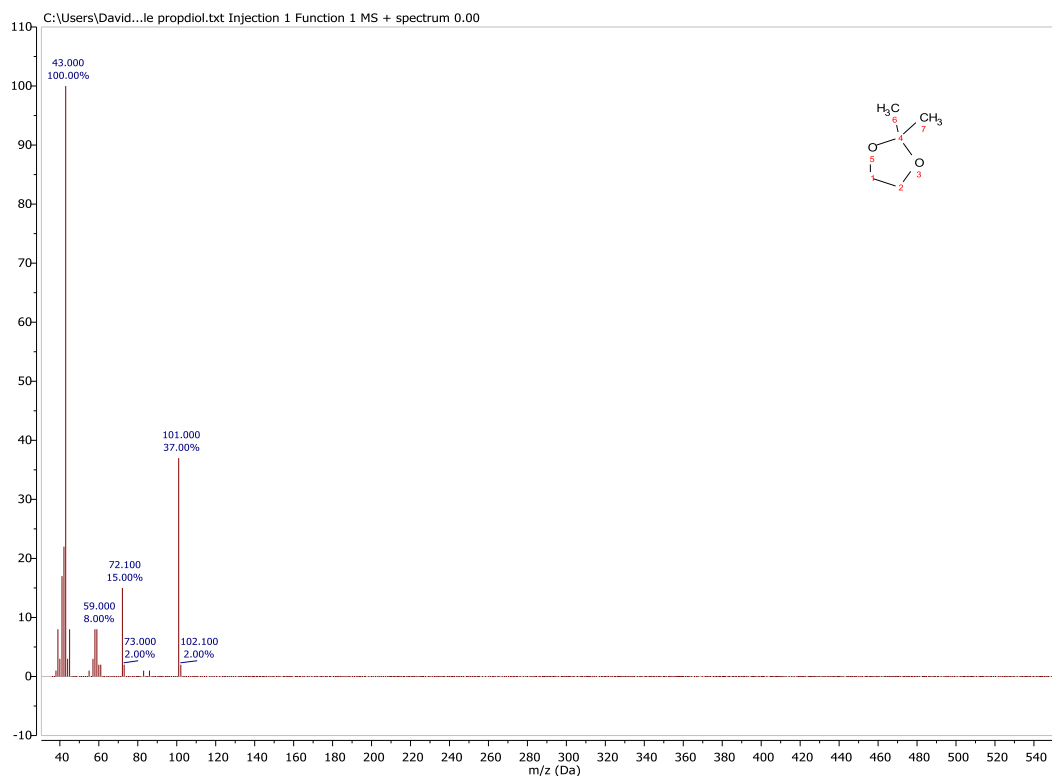
Figure A.2.1.36. MS spectrum of compound 6

GC/MS (relative intensity, 70 eV) *m/z*: 101 (37), 72 (15), 59 (5), 57 (10), 443 (100).

257

A.2.2 iPEs and glycerol: the pivotal role of isopropenyl acetate (iPAc)

The reaction of iPAc and acetic acid

At 30 °C, after 24 h, the reaction of an equimolar mixture of isopropenyl acetate (5.0 mmol) and acetic acid in the presence of Amberlyst-15 as a catalyst (45.0 mg; 15 wt% with respect to AcOH) mainly afforded acetic anhydride (80% yield, by GC), though minor amounts by-products (≤10% with respect to Ac_2O) were detected. The mass spectra of these compounds are reported in Figure S2, and were consistent with the formation of acetylacetone, and of products of the aldol condensation of acetone, both the aldol, 4-hydroxy-4-methylpentan-2-one, and the two α,β-unsaturated isomers carbonyl derivative, 4-methylpent-3-en-2-one and 4-methylpent-4-en-2-one. In addition, the formation of 4-oxopentan-2-yl acetate was observed. Comparison with spectra of authentic compounds available from the NIST library of the GC/MS ChemStation afforded a match quality >60% in all cases.

260
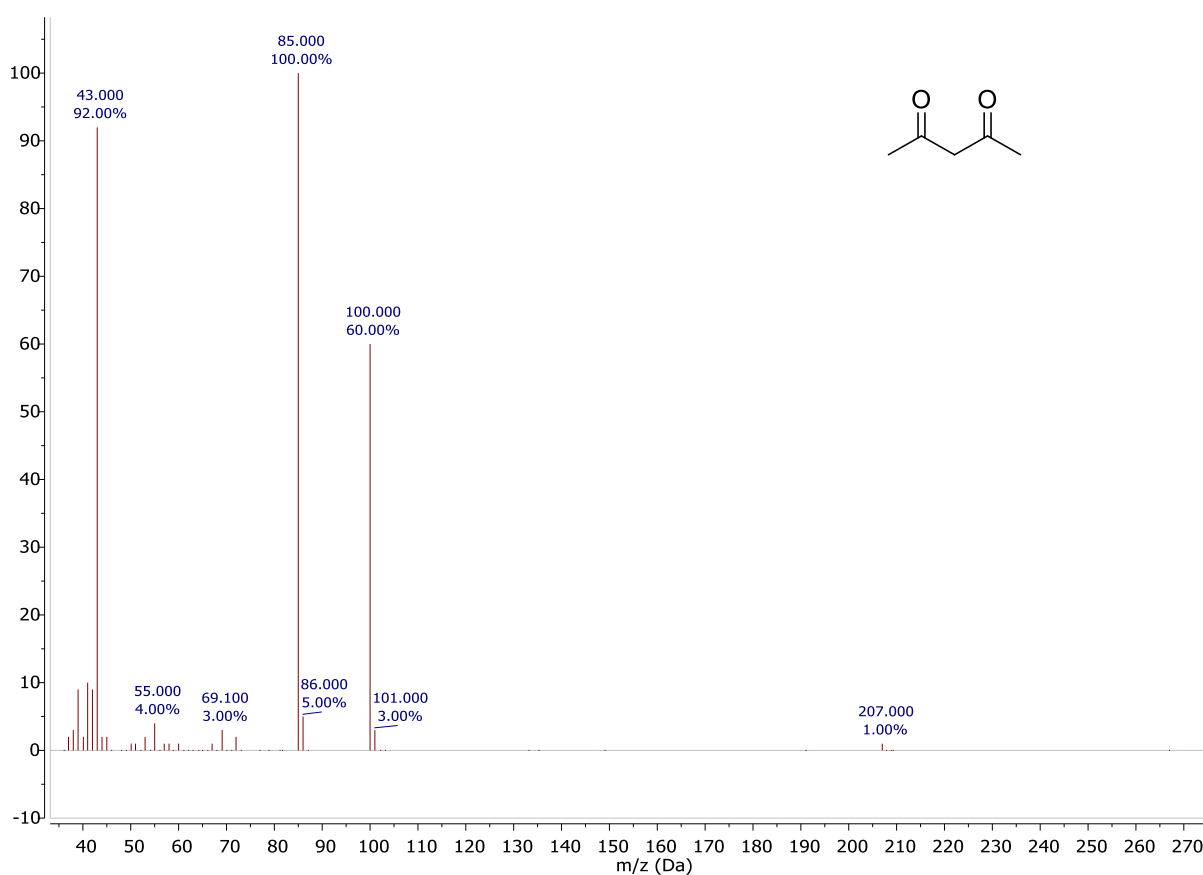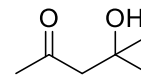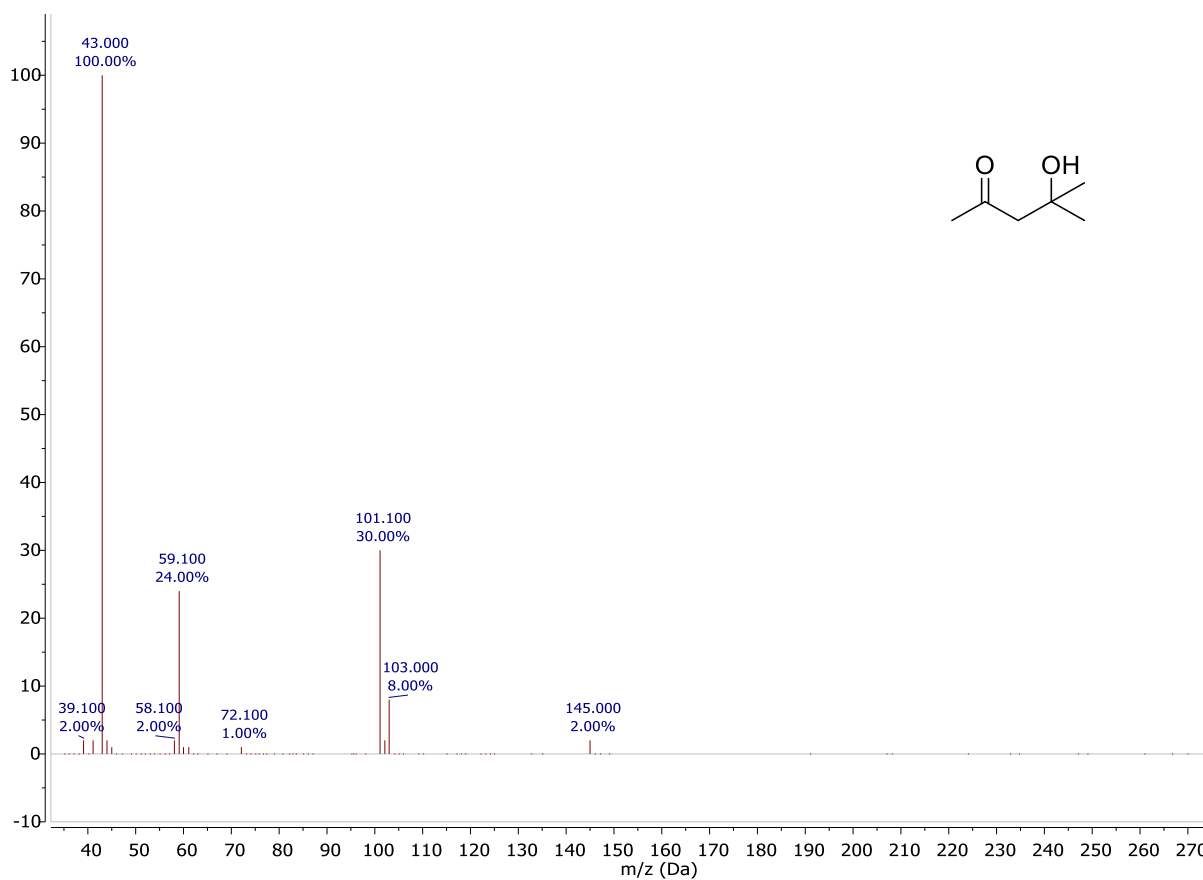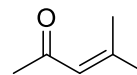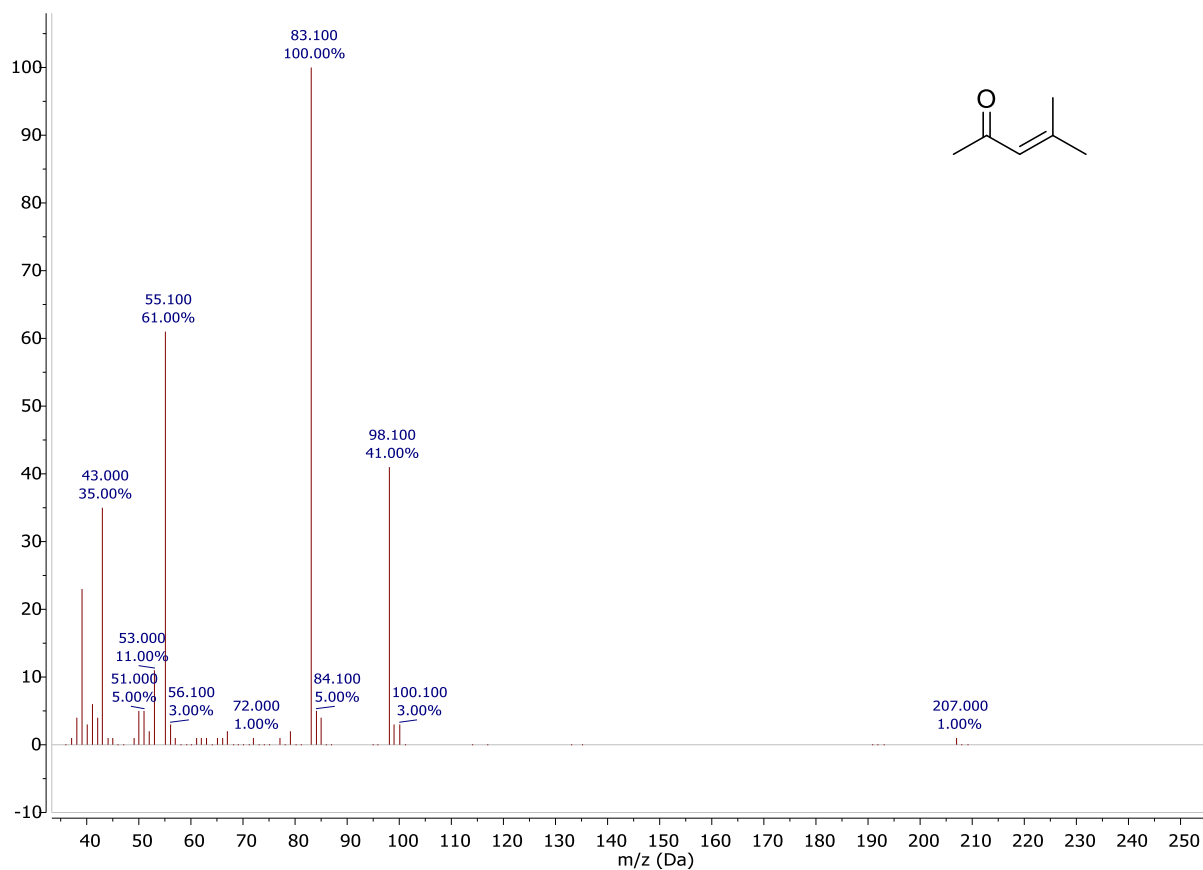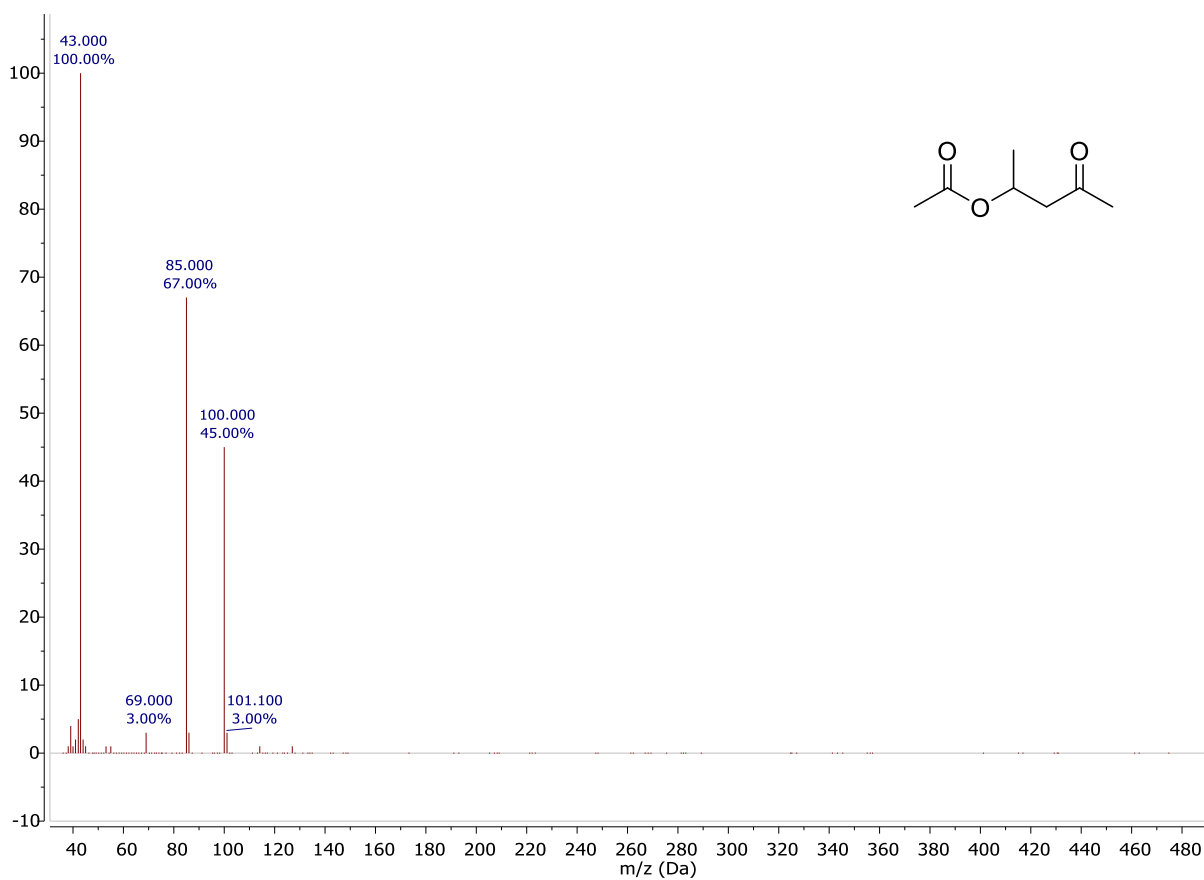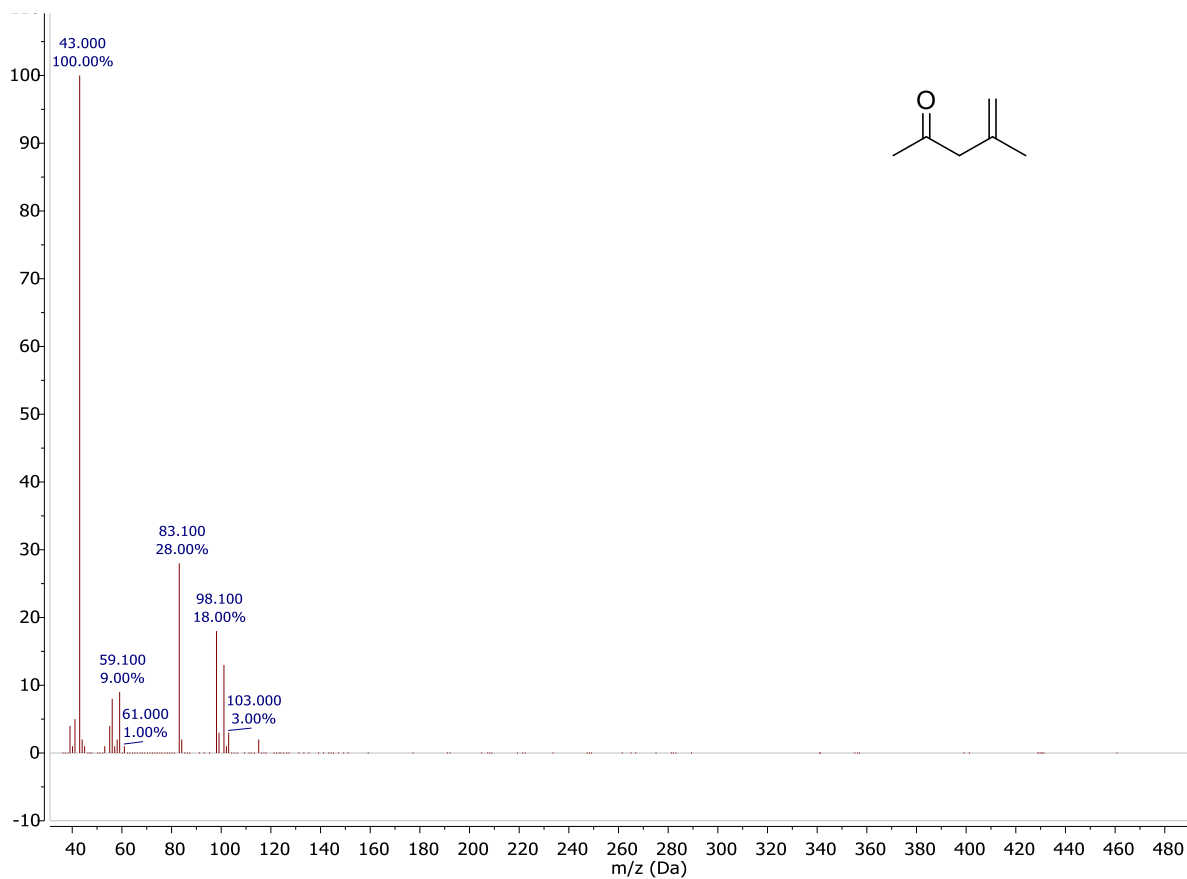
Figure A.2.2.1. *Mass spectra of by-products of the reaction of iPAc and acetic acid*

261

A.2.3 iPEs and glycerol-derived aminodiols: concatenated procedures

N-(2,3-dihydroxypropyl)acetamide, 1a

Figure A.2.3.1. *^{1}H NMR of compound **1a** in CD$_3$OD*
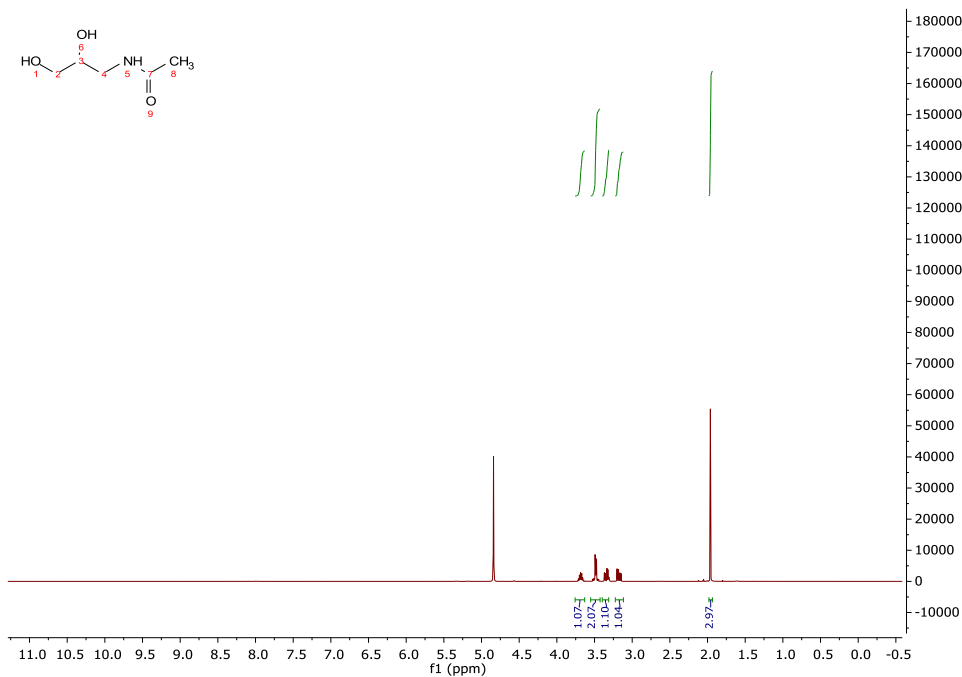
^{1}H NMR (400 MHz, 298 K, CD$_3$OD) δ: 3.75 (m, 1H), 3.5 (m, 2H), 3.33 (m, 1H), 3.27 (m, 1H), 1.97 (s, 3H).

Figure A.2.3.2. *^{13}C NMR of compound **1a** in CD$_3$OD*
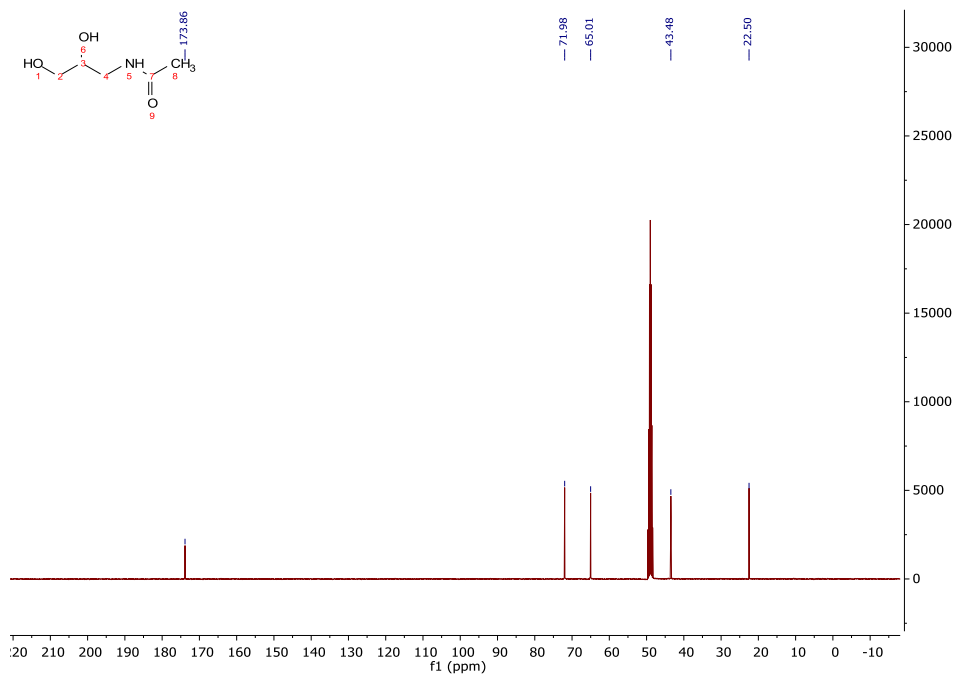
^{13}C{H} NMR (101 MHz, 298 K, CD$_3$OD) δ: 71.98, 65.01, 43.48, 22.50.
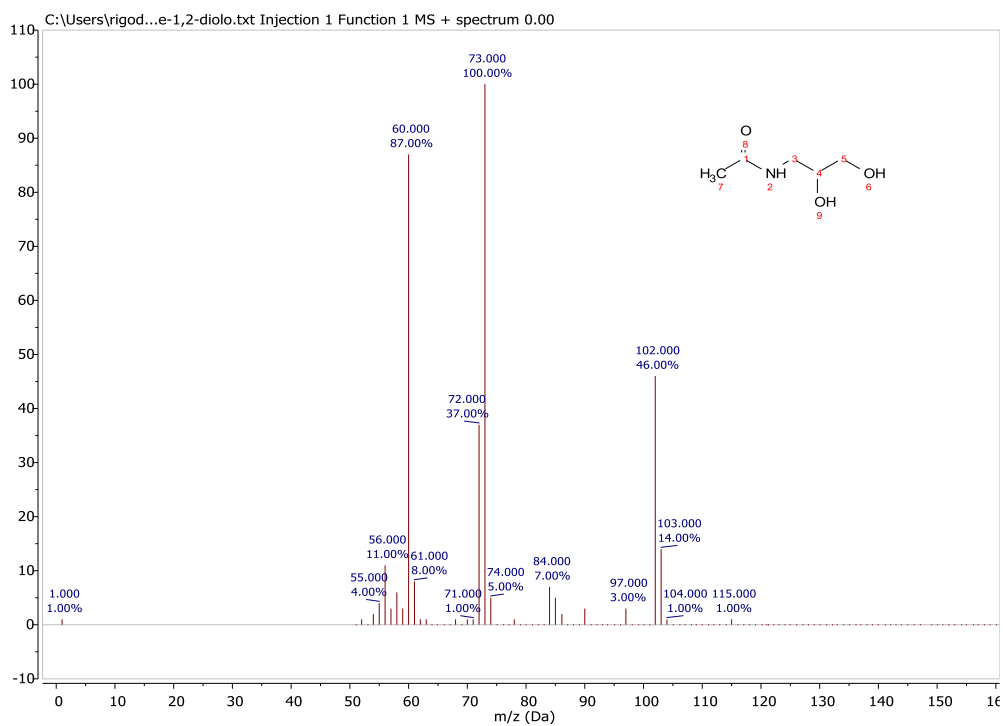
Figure A.2.3.3. *MS spectrum (70eV) of compound* **1a**

GC/MS (relative intensity, 70 eV) *m/z*: 102 (46), 73 (100), 60 (87), 56 (11).

N-(1,3-dihydroxypropan-2-yl)acetamide, 2a
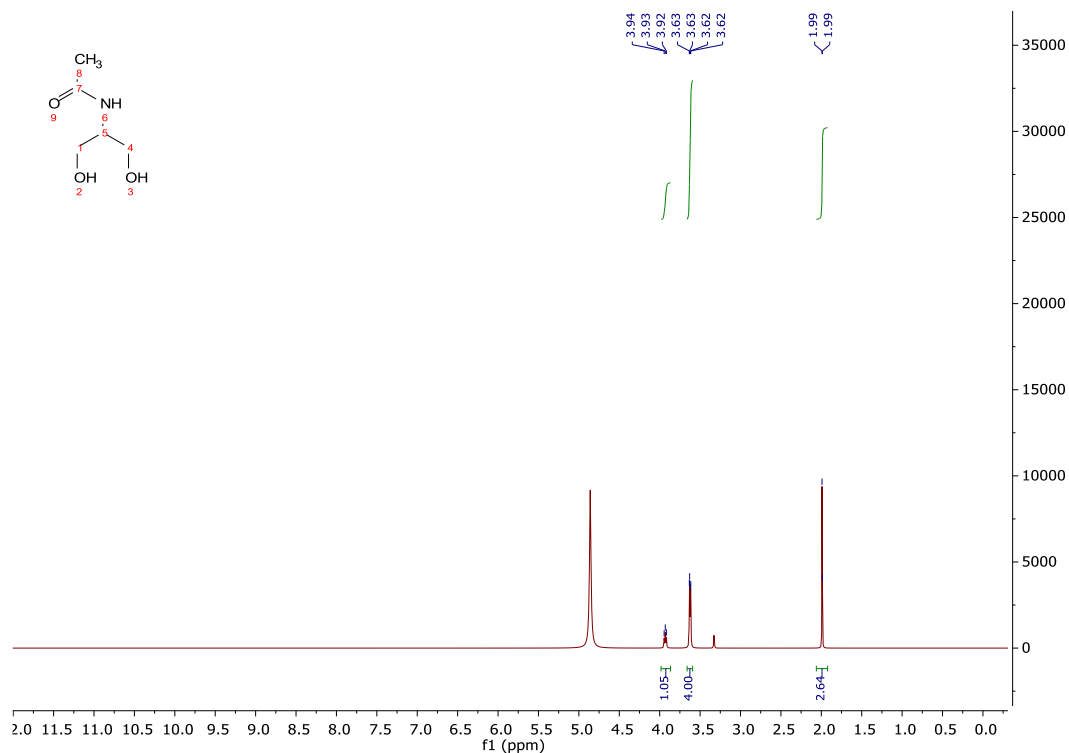
Figure A.2.3.4. *¹H NMR of compound* **2a** *in CD₃OD*

¹H NMR (400 MHz, 298 K, CD₃OD) δ: 3.95 (m, 1H), 3.37 (m, 4H), 1.97 (s, 3H).
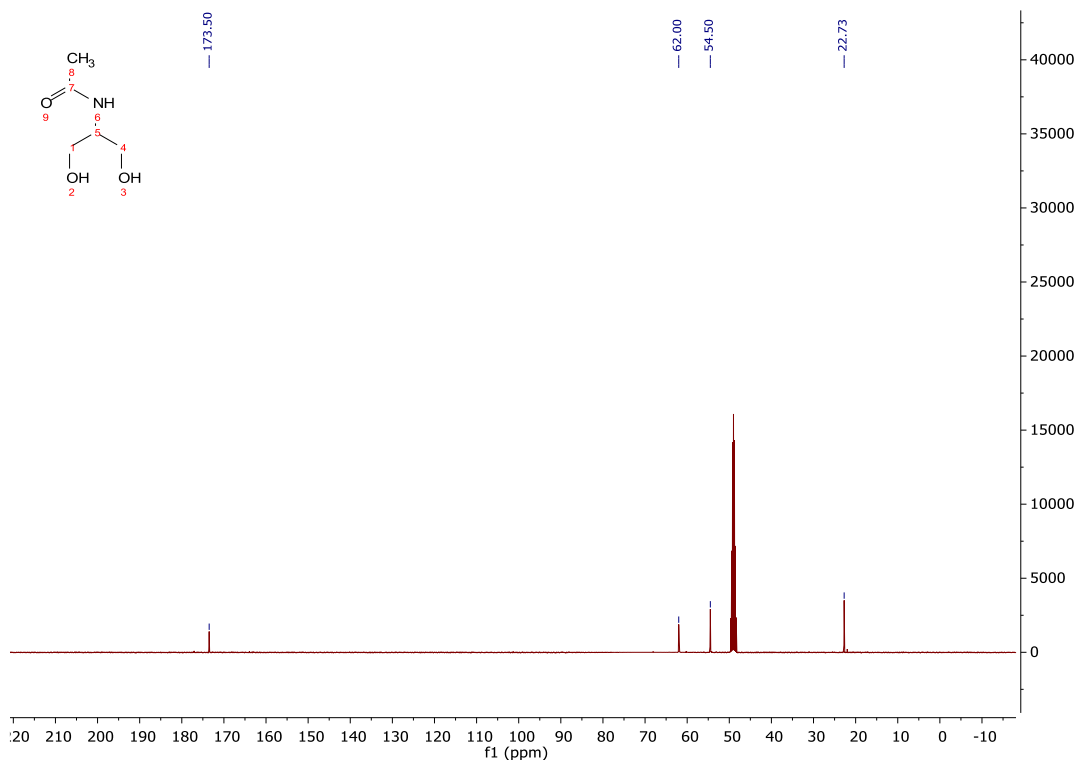
Figure A.2.3.5. *¹³C NMR of compound **2a** in CD₃OD*

¹³C{H} NMR (101 MHz, 298 K, CD₃OD) δ: 173.50, 62.00, 54.50, 22.73.
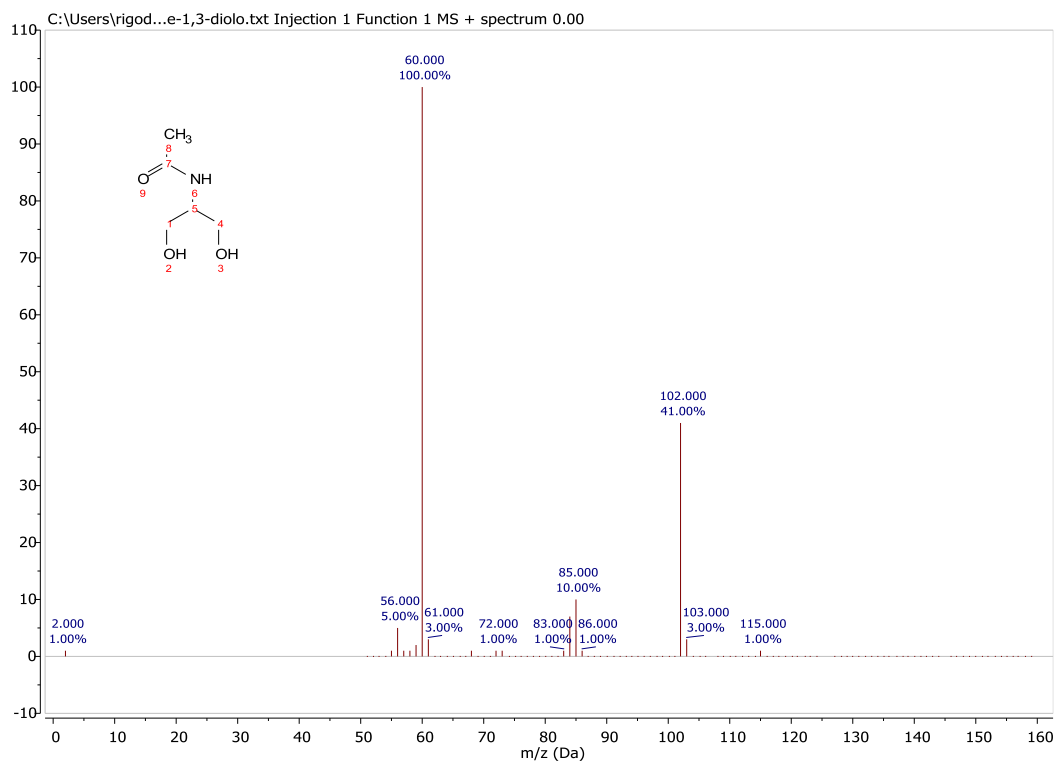
Figure A.2.3.6. *MS spectrum (70eV) of compound **2a***

GC/MS (relative intensity, 70 eV) *m/z*: 102 (41), 85 (10), 60 (100).

264

N-((2,2-dimethyl-1,3-dioxolan-4-yl)methyl)acetamide, 1b
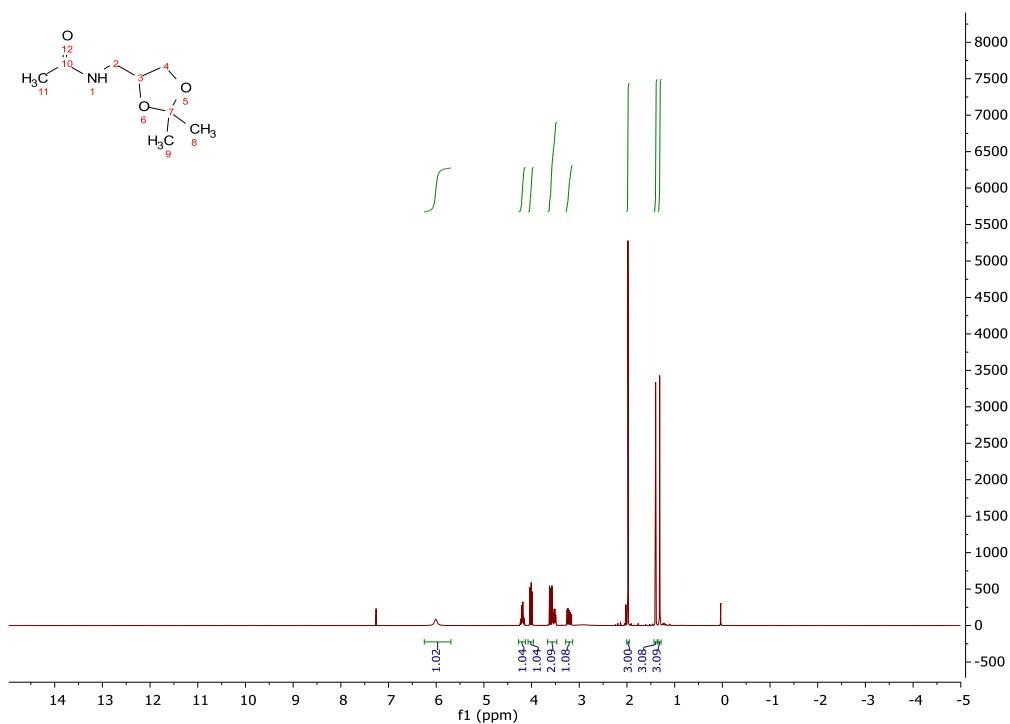
Figure A.2.3.7. *^{1}H NMR of compound **1b** in CDCl$_3$*

^{1}H NMR (400 MHz, 298 K, CDCl$_3$) δ: 4.11 (m, 1H), 4.01 (m, 1H), 3.57 (m, 2H), 3.25 (m, 1H), 1.98 (s, 3H), 1.46 (s, 3H), 1.43 (s, 3H).
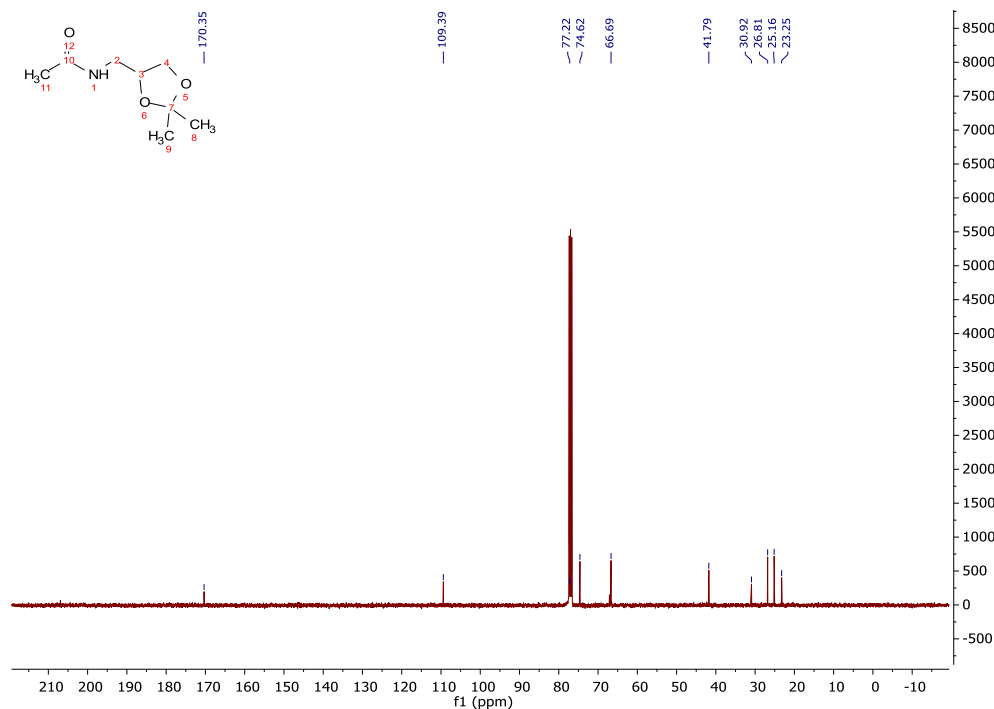
Figure A.2.3.8. *^{13}C NMR of compound **1b** in CDCl$_3$*

^{13}C{H} NMR (101 MHz, 298 K, CDCl$_3$) δ: 170.35, 109.39, 77.22, 74.62, 66.69, 41.79, 30.92, 26.81, 25.16, 23.25.
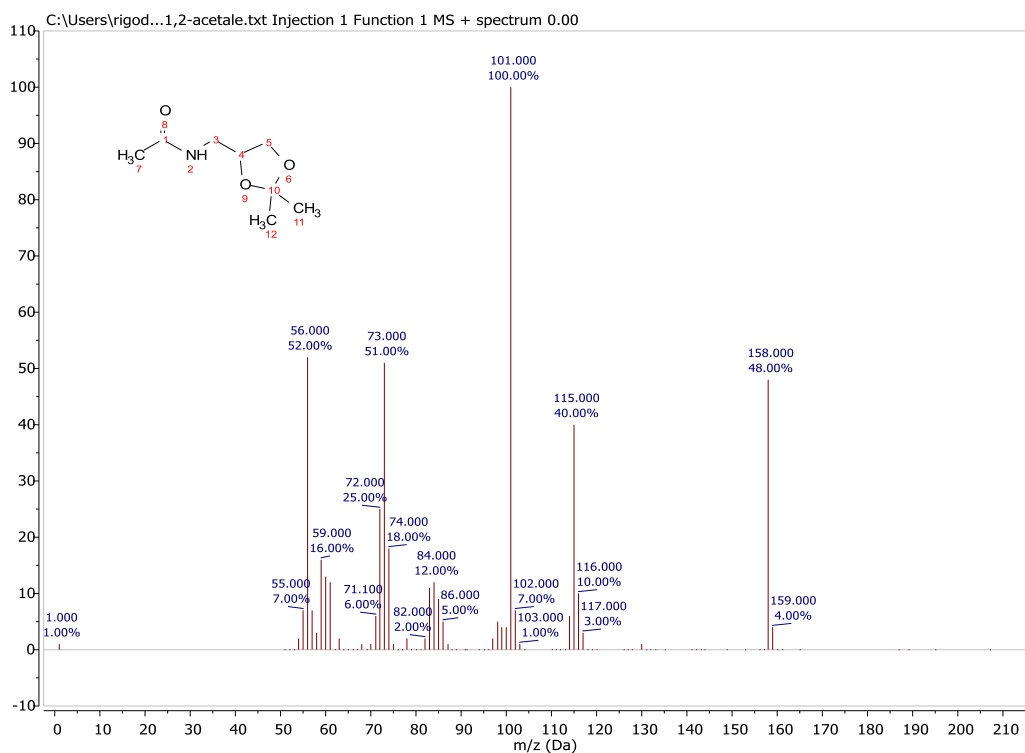
Figure A.2.3.9. *MS spectrum (70eV) of compound **1b***

GC/MS (relative intensity, 70 eV) *m/z*: 158 (48), 115 (40), 101 (100), 73 (51), 56 (52).

N-(2,2-dimethyl-1,3-dioxan-5-yl)acetamide, 2b
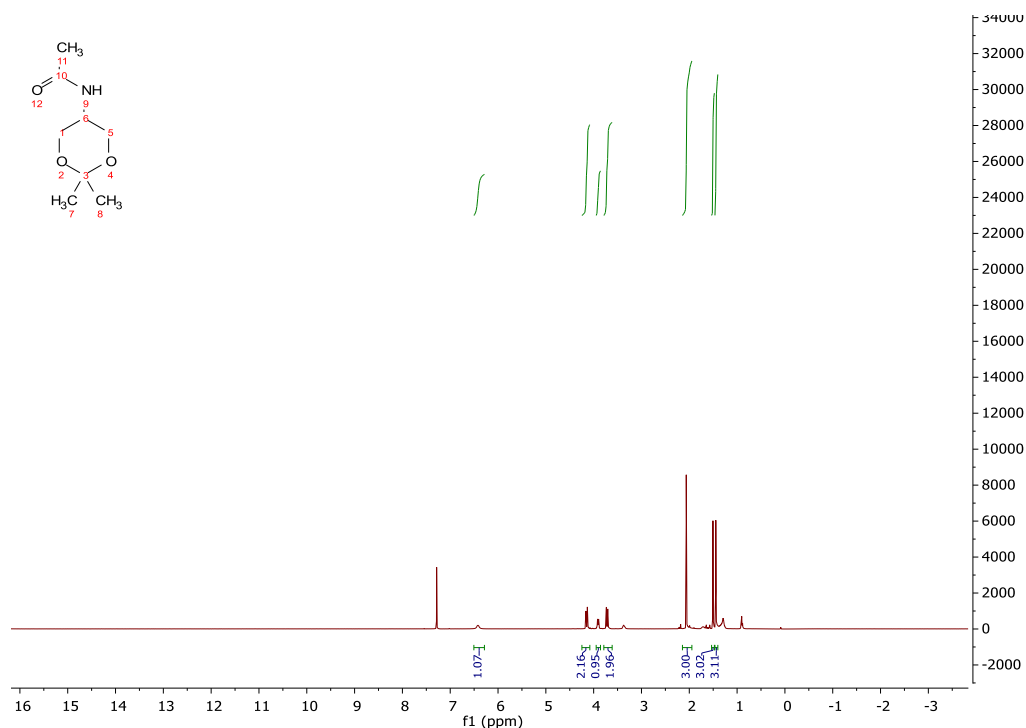
Figure A.2.3.10. *^{1}H NMR of compound **2b** in CDCl$_3$*

^{1}H NMR (400 MHz, 298 K, CDCl$_3$) δ: 6.5 (m, 1H), 4.10 (m, 2H), 3.97 (m, 1H), 3.72 (m, 2H), 2.04 (s, 3H), 1.46 (s, 3H), 1.43 (s, 3H).
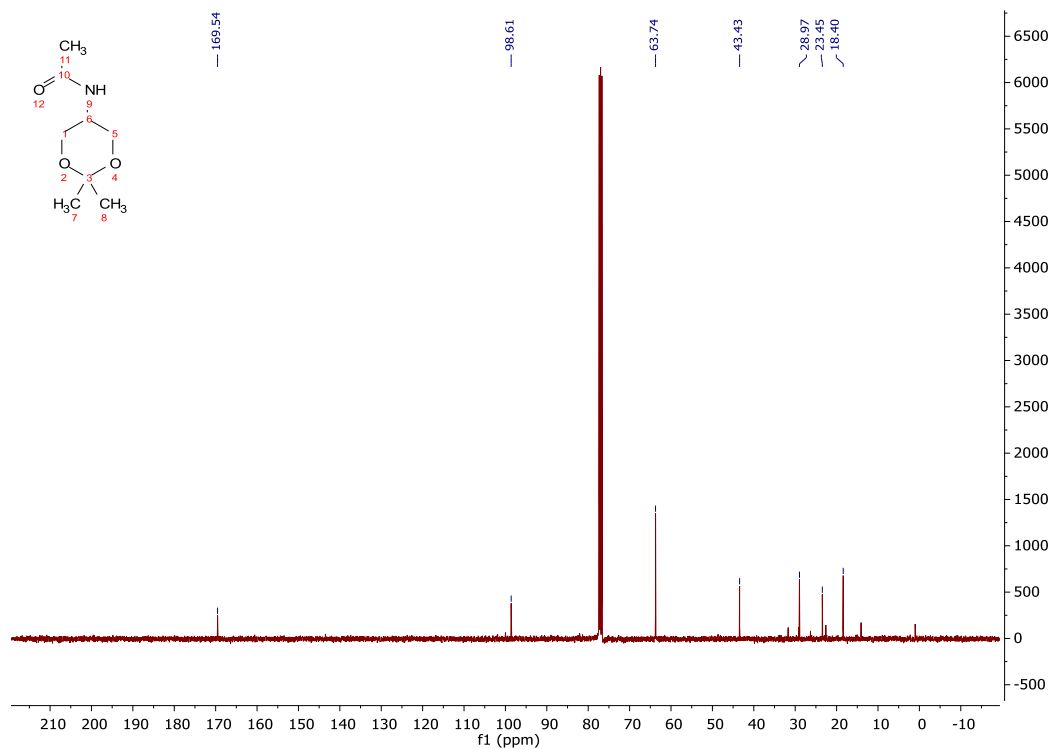
Figure A.2.3.11. ^{13}C NMR of compound **2b** in CDCl$_3$

^{13}C{H} NMR (101 MHz, 298 K, CDCl$_3$) δ: 169.54, 98.61, 63.74, 43.43, 28.97, 23.45, 18.40.
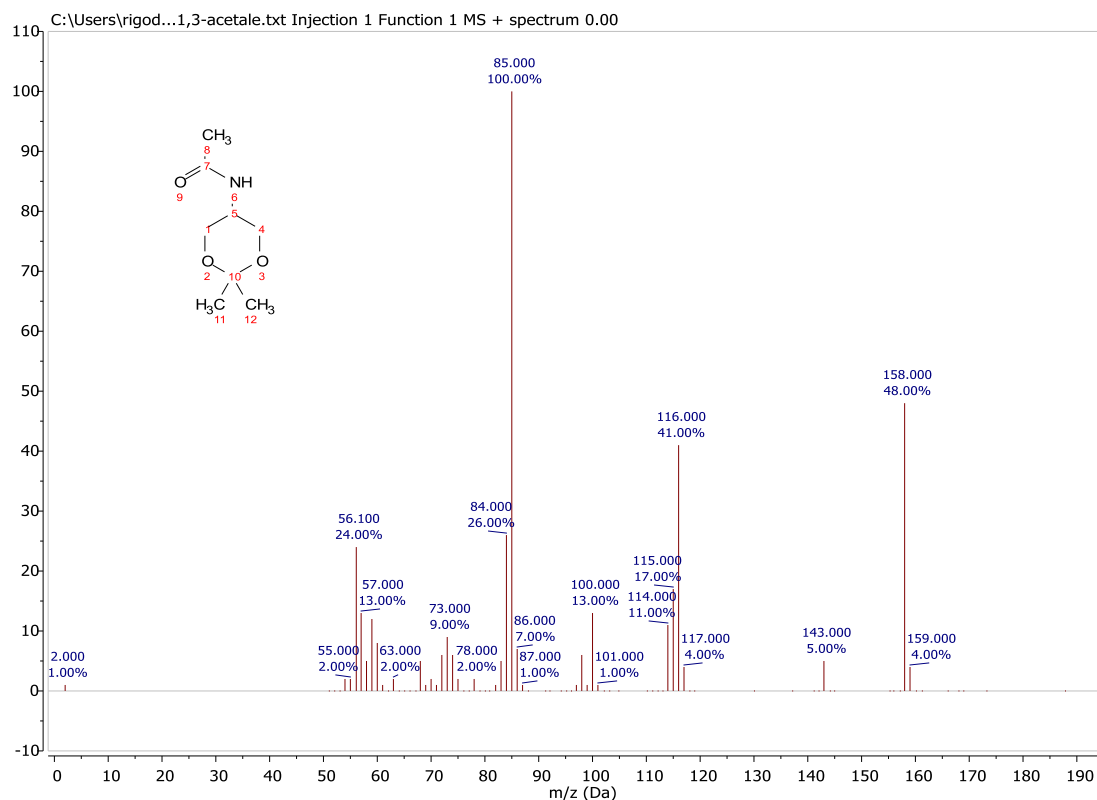
Figure A.2.3.12. MS spectrum (70eV) of compound **2b**

GC/MS (relative intensity, 70 eV) *m/z*: 158 (48), 116 (41), 100 (13), 85 (100), 56 (24).

Appendix A.4 – Chapter 4

A.4 CO_2 insertion into terminal epoxides

2a: 4-phenyl-1,3-dioxolan-2-one (styrene carbonate)
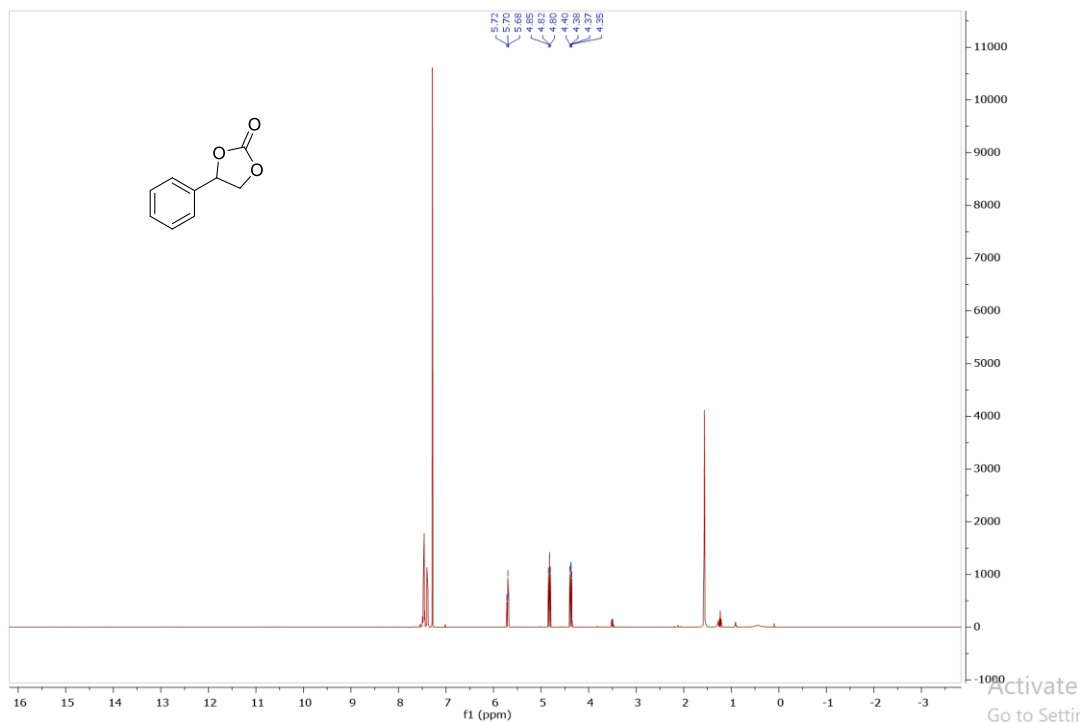
Figure A.4.1. ^1H NMR of product **2a** (400 MHz, 298 K, CDCl$_3$)

δ (ppm): 7.51-7.35 (m, 5H), 5.70 (t, 1H), 4.82 (dd, 1H), 4.37 (dd, 1H).
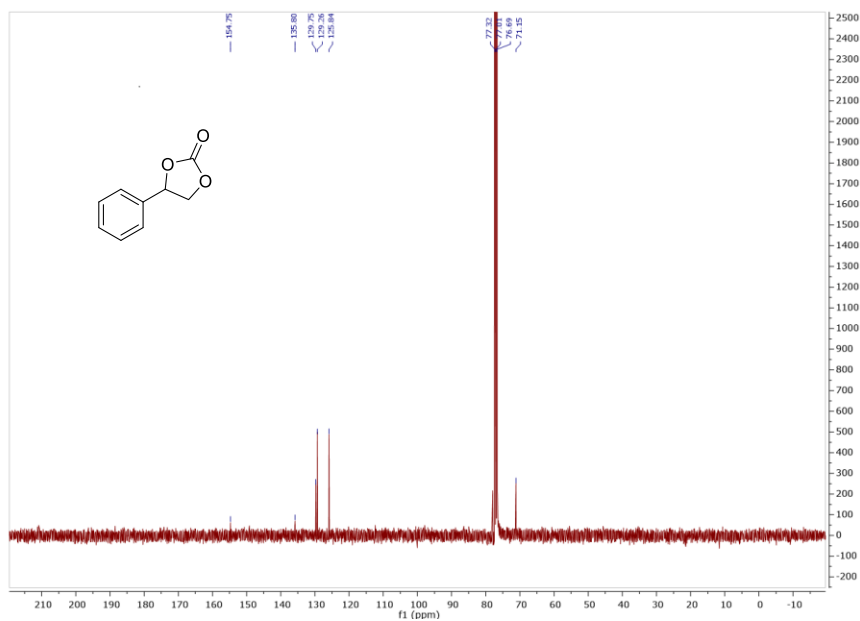
Figure A.4.1. ^{13}C NMR of product **2a** (100 MHz, 298 K, CDCl$_3$)

δ (ppm): 154.7, 135.8, 129.7, 129.2, 125.8, 77.3, 77.0, 76.6, 71.1.
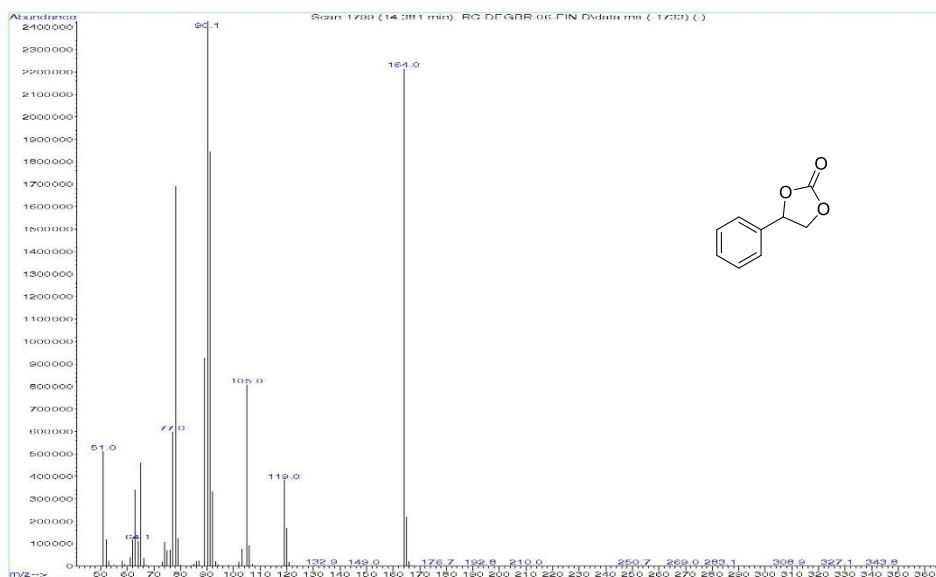
Figure A.4.3. *MS spectrum of product **2a** (EI, 70 eV)*

m/z (70 eV): 166 (M^{+2},1); 164 (M$^+$,91); 119(16); 92 (14); 91 (76); 90 (100); 89 (38); 78 (70); 77 (25); 65 (19); 63 (14); 51 (21).

2b: 4-ethyl-1,3-dioxolan-2-one (butylene carbonate)
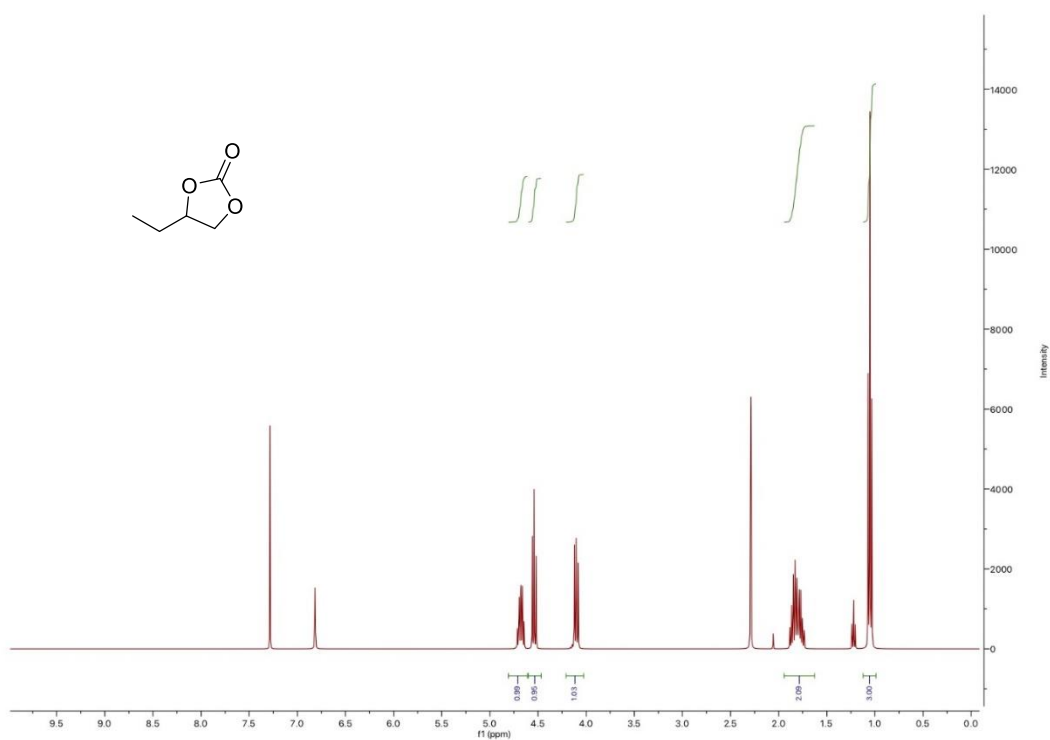
Figure A.4.12. *^{1}H NMR of product **2b** (400 MHz, 298 K, CDCl$_3$)*

δ (ppm): 4.86-4.58 (dd, 1H), 4.60-4.39 (t, 1H), 4.23-4.00 (dd, 1H), 1.93-1.70 (m, 2H), 1.18-0.84 (t, 3H). The peaks at 6.82 ppm and 2.30 ppm are relative to mesitylene used as internal standard.

269
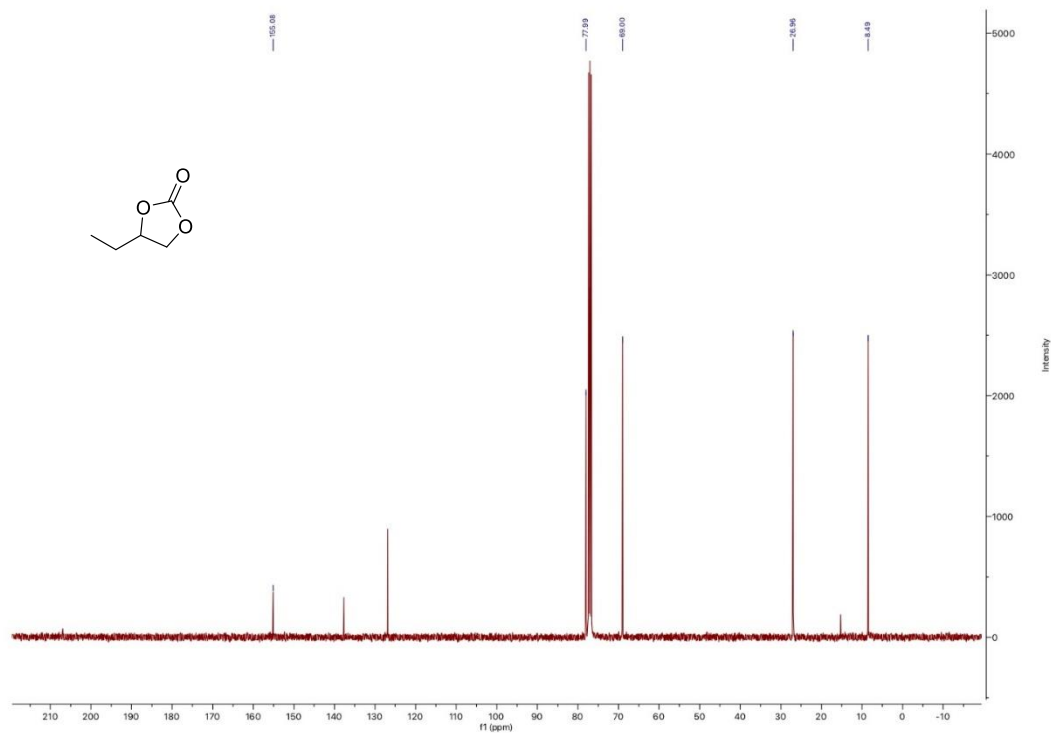
Figure A.4.13. *¹³C NMR of product **2b** (100 MHz, 298 K, CDCl₃)*

δ (ppm): 155.08, 77.99, 69.00, 26.96, 8.49.
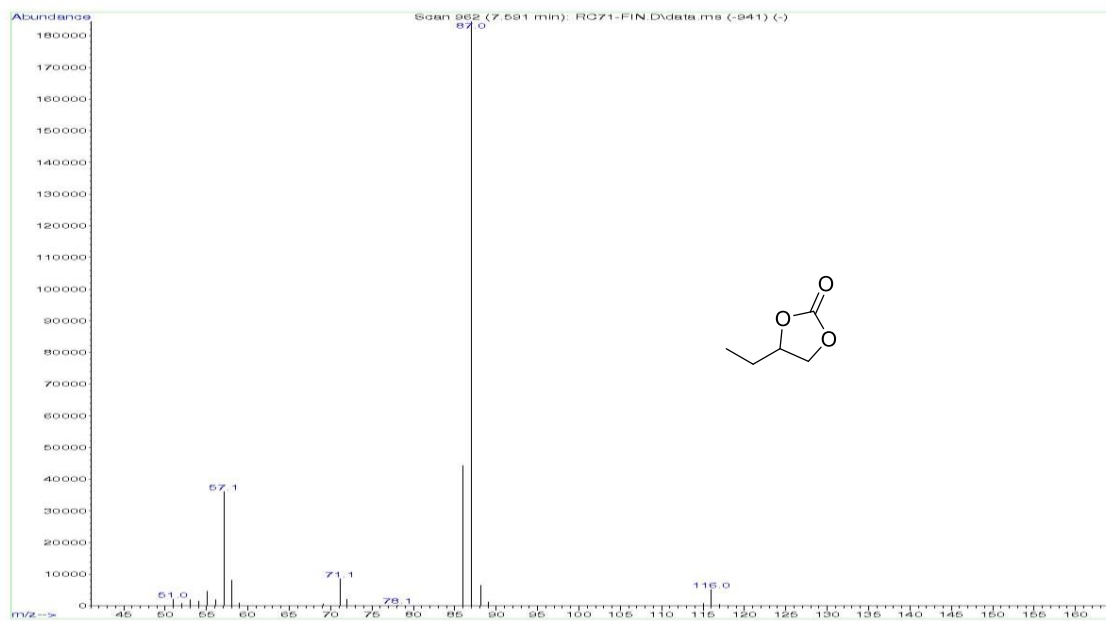
Figure A.4.14. *MS spectrum of product **2b** (EI, 70 V)*

m/z (70 eV): 116 (M⁺,3); 87 (100); 86 (24); 57 (20).

2c: 4-butyl-1,3-dioxolan-2-one (hexylene carbonate)
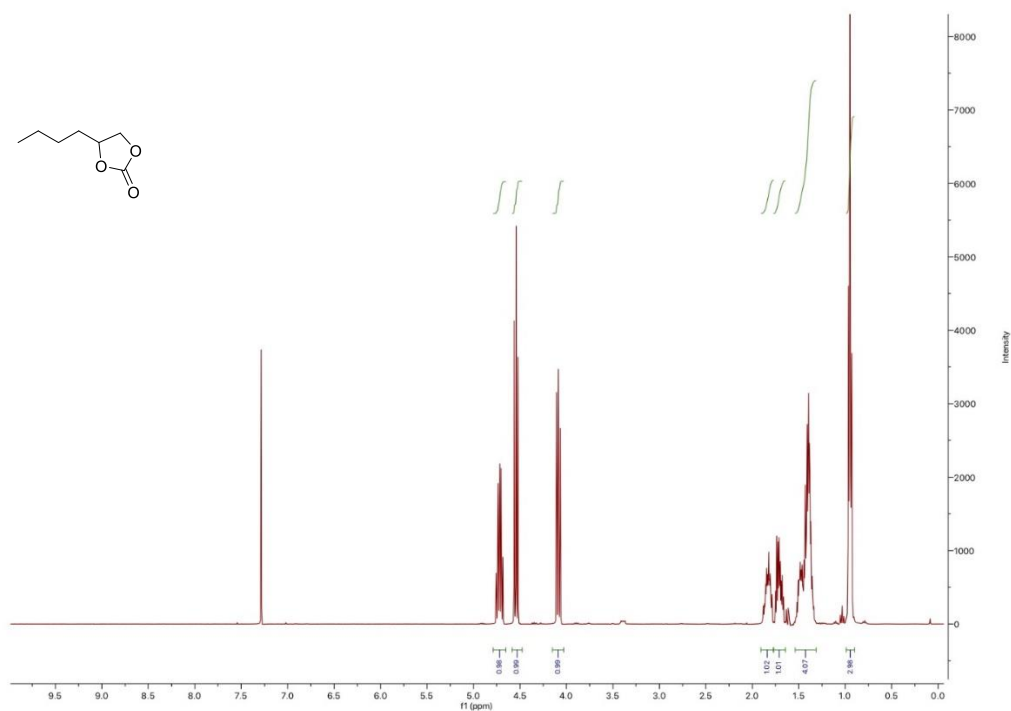
Figure A.4.9. *^{1}H NMR of product **2c** (400 MHz, 298 K, CDCl$_3$)*

δ (ppm): 4.80-4.65 (m, 1H), 4.61-4.48 (dd, 1H), 4.13-4.03 (dd, 1H), 1.92-1.76 (m, 1H), 1.77-1.64 (m, 1H), 1.55-1.30 (m, 4H), 1.00-0.89 (t, 3H).
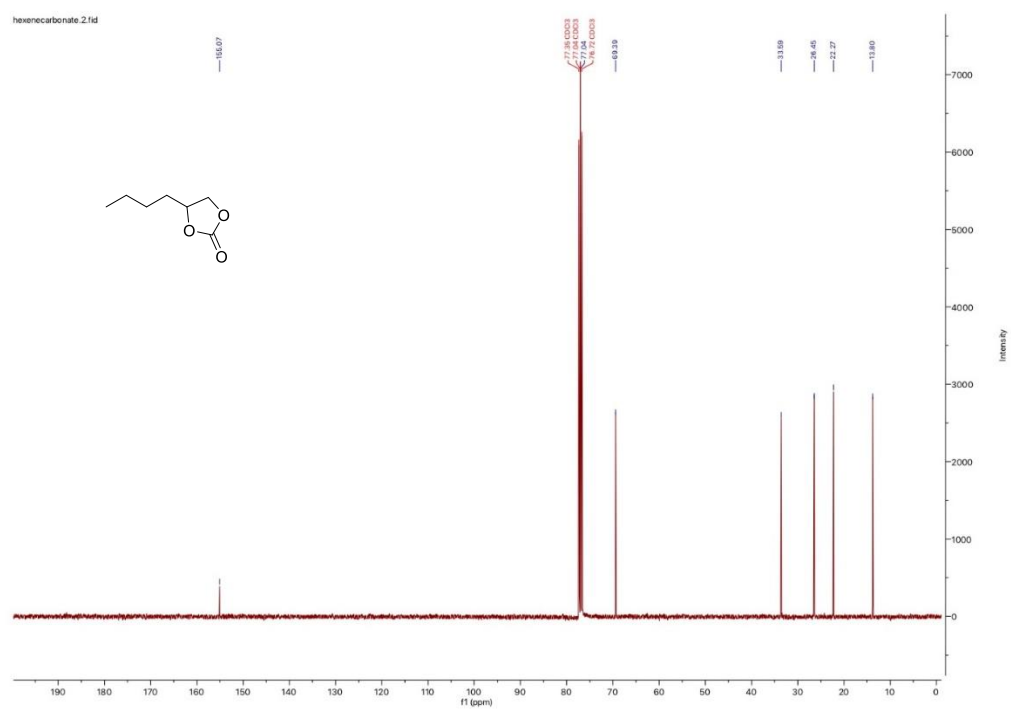
Figure A.4.10. *^{13}C NMR of product **2c** (100 MHz, 298 K, CDCl$_3$)*

δ (ppm): 155.07, 77.04, 69.39, 33.59, 26.45, 22.27, 13.80.
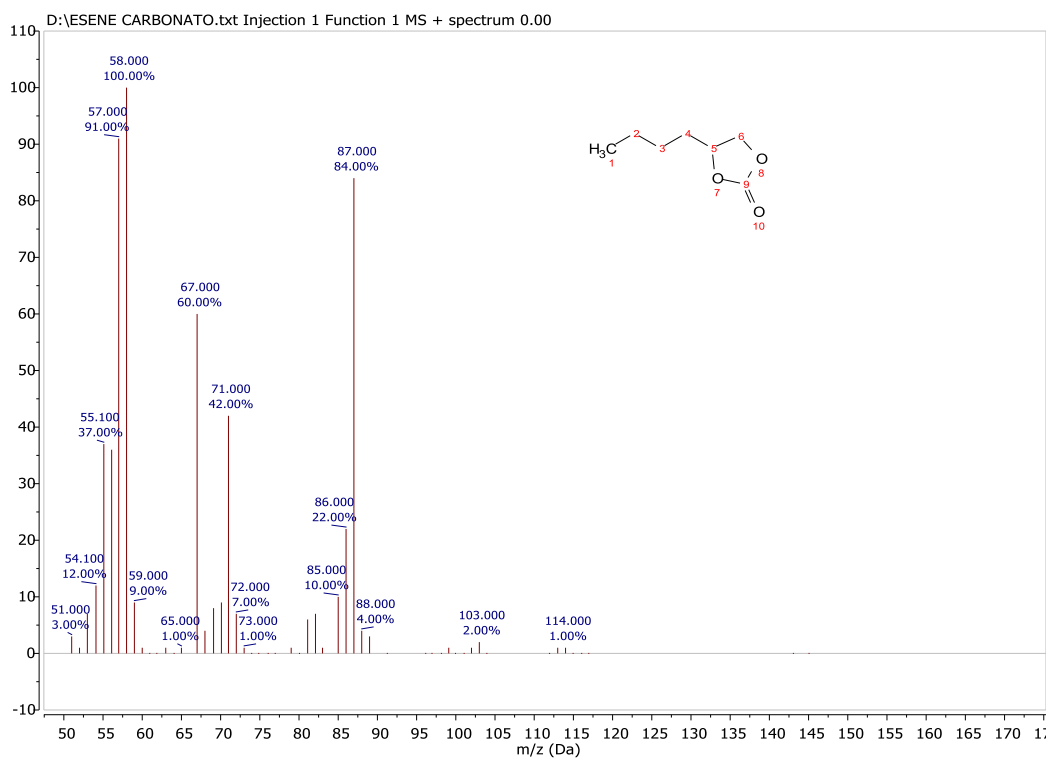
Figure A.4.11. MS spectrum of product 2c (EI, 70 V)

m/z (70 eV): 114 (1), 87 (84), 71 (42), 67 (70), 58 (100), 57 (91), 55 (37).

2d: 4-octyl-1,3-dioxolan-2-one (decene carbonate)
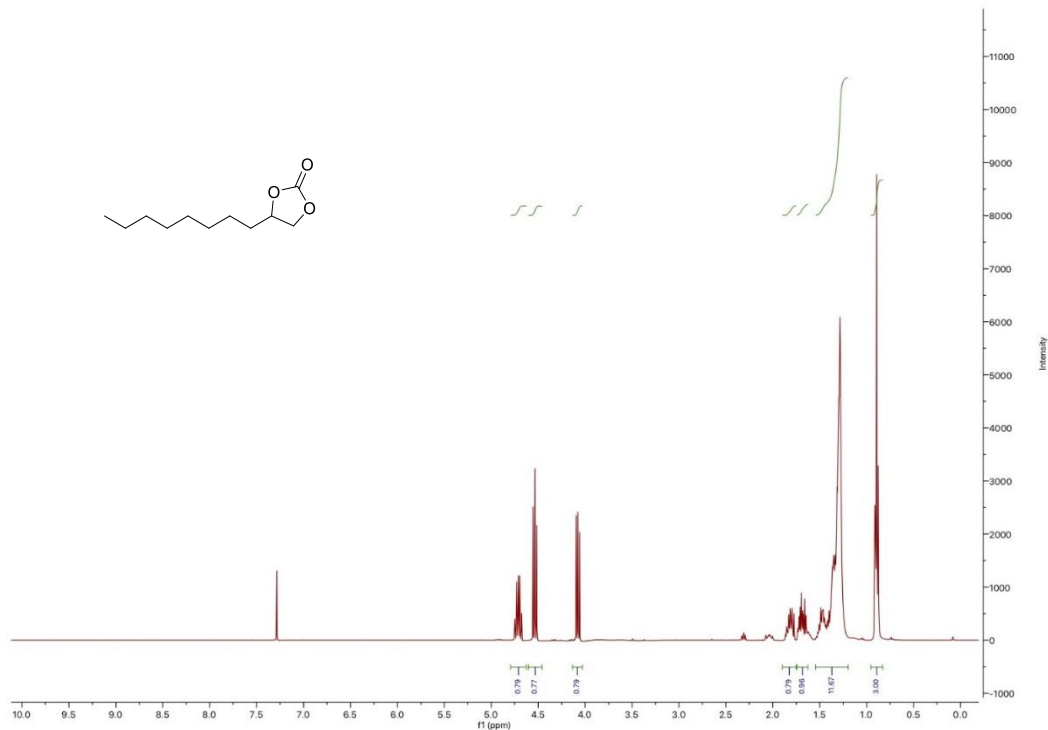
Figure A.4.15. ^{1}*H NMR of product* **2d** *(400 MHz, 298 K, CDCl$_3$)*

δ (ppm): 4.81-4.64 (m, 1H), 4.59-4.46 (dd, 1H), 4.16-3.97 (dd, 1H), 1.90-1.75 (m, 1H), 1.75-1.60 (m, 1H), 1.55-1.16 (m, 12H), 1.02-0.74 (m, 3H).
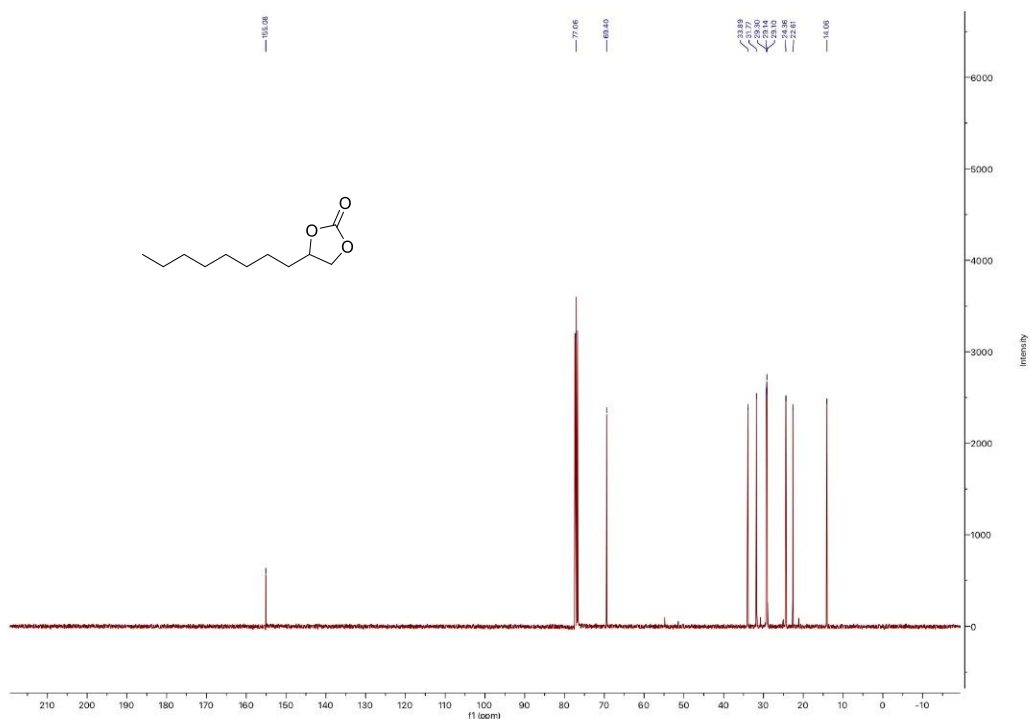
Figure A.4.16. ^{13}C NMR of product **2d** (100 MHz, 298 K, CDCl$_3$)

δ (ppm): 155.08, 77.06, 69.40, 33.89, 31.77, 29.30, 29.14, 29.10, 24.36, 22.61, 14.06.
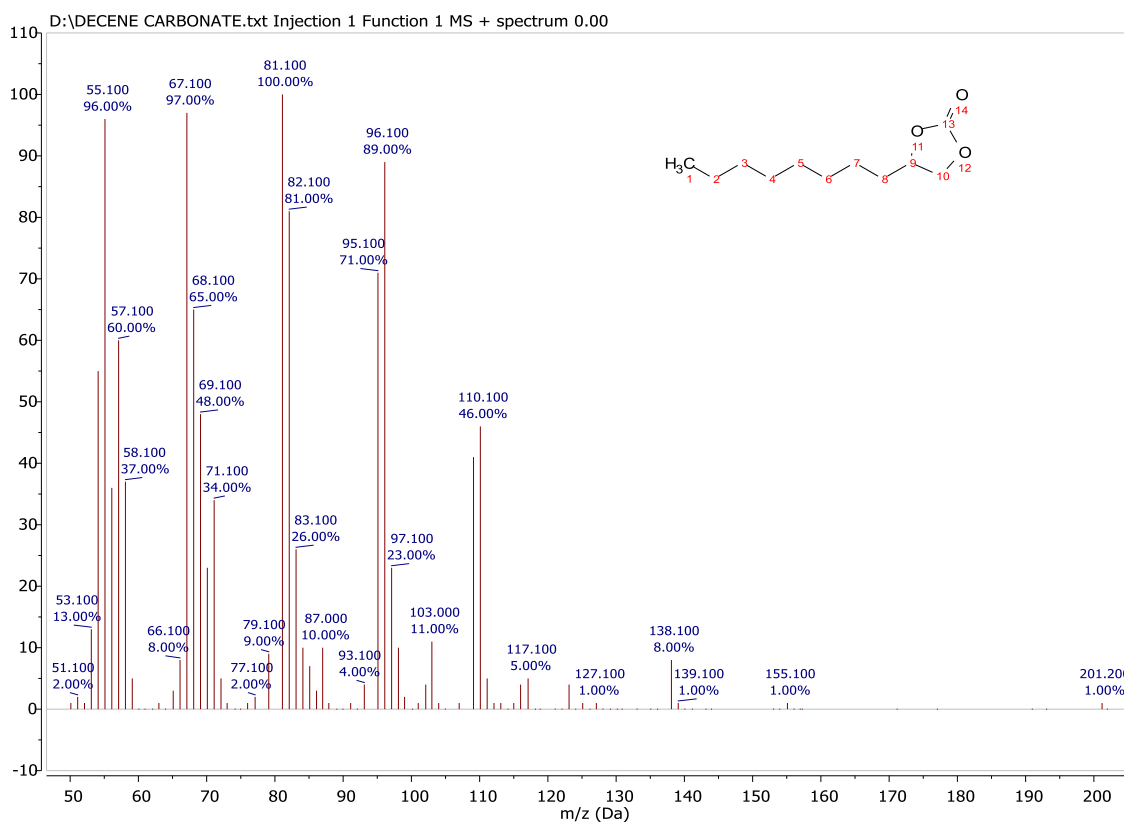
Figure A.4.17. MS spectrum of product **2d** (EI, 70 V)

m/z (70 eV): 201 (MH$^+$, 1), 110 (46), 96 (89), 81 (100), 67 (97), 55 (96).

2e: 4-(butoxymethyl)-1,3-dioxolan-2-one (butyl glycidyl carbonate)

Figure A.4.3. ^{1}H NMR of product **2e** (400 MHz, 289 K, CDCl$_3$)

δ (ppm): 4.84-4.79 (m, 1H), 4.51 (dd, 1H), 4.41 (dd, 1H), 3.69 (dd, 1H), 3.63 (dd, 1H), 3.54 (t, 2H), 1.65-1.52 (m, 2H), 1.46-1.31 (m, 2H), 0.94 (t, 3H).

Figure A.4.4. ^{13}C NMR of product **2e** (100 MHz, 289 K, CDCl$_3$)

δ (ppm): 154.9, 75.0, 71.9, 69.6, 66.3, 31.5, 19.1, 13.8.
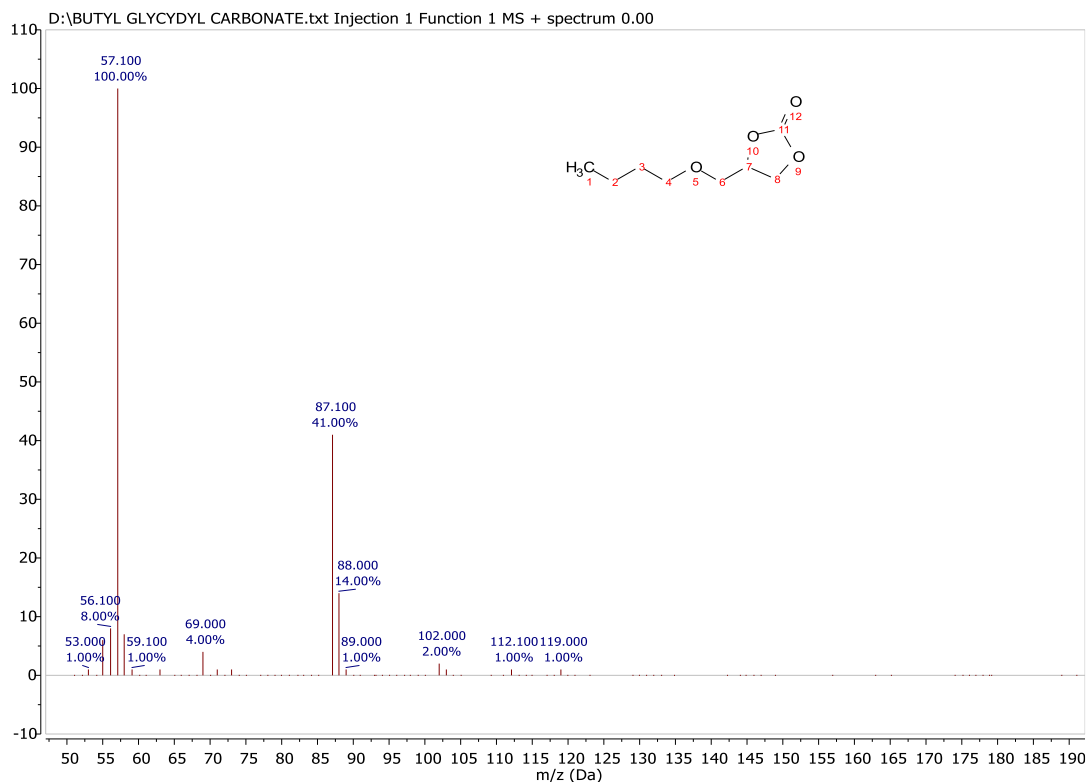
Figure A.4.5. *MS spectrum of product **2e** (EI, 70 eV)*

m/z (70 eV): 119 (1), 87 (41), 69 (4), 57 (100).

2f: 4-(phenoxymethyl)-1,3-dioxolan-2-one (phenyl glycidyl carbonate)
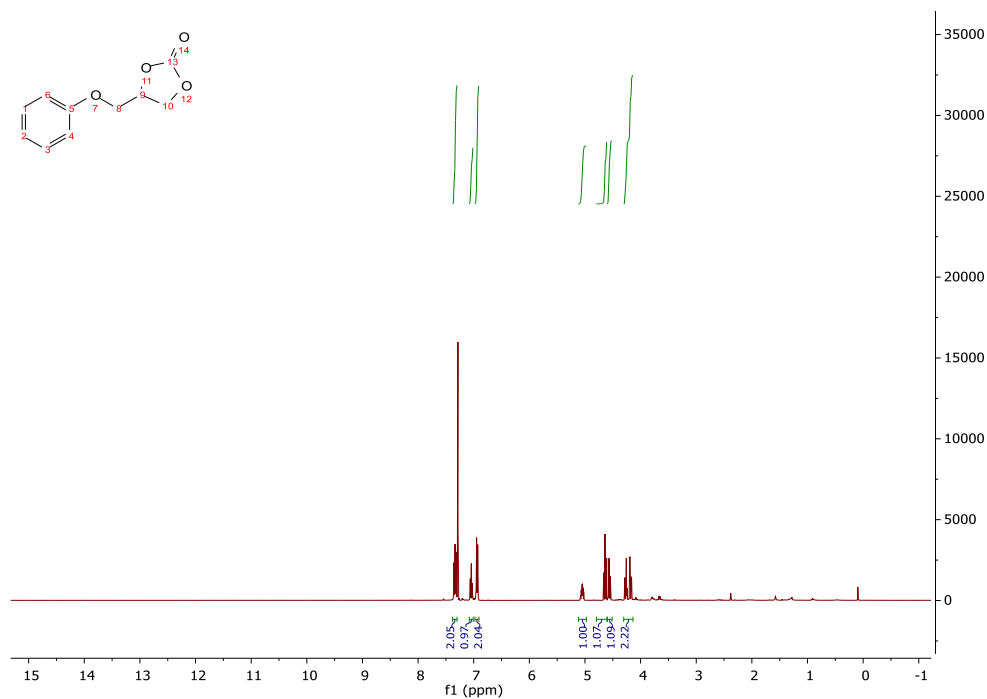
Figure A.4.6. *^{1}H NMR spectrum of product **2e** (400 MHz, 298 K, CDCl$_3$)*

δ (ppm): 7.34 (m, 2H), 7.04 (m, 1H), 6.94 (m, 2H), 5.09-5.01 (m, 1H), 4.68-4.52 (m, 2H), 4.30-4.16 (m, 2H).

275
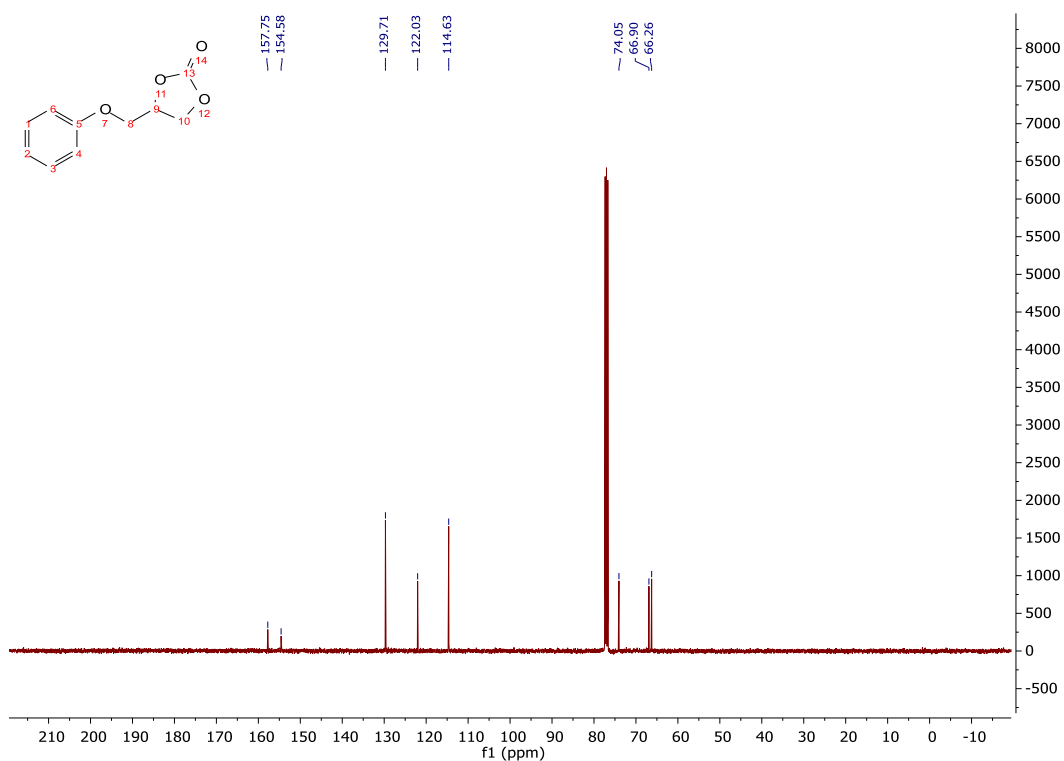
Figure A.4.7. *^{13}C NMR spectrum of product **2e** (100 MHz, 298 K, CDCl$_3$)*

δ (ppm): 157.75, 154.58, 129.71, 122.03, 114.63, 74.05, 66.90, 66.26.
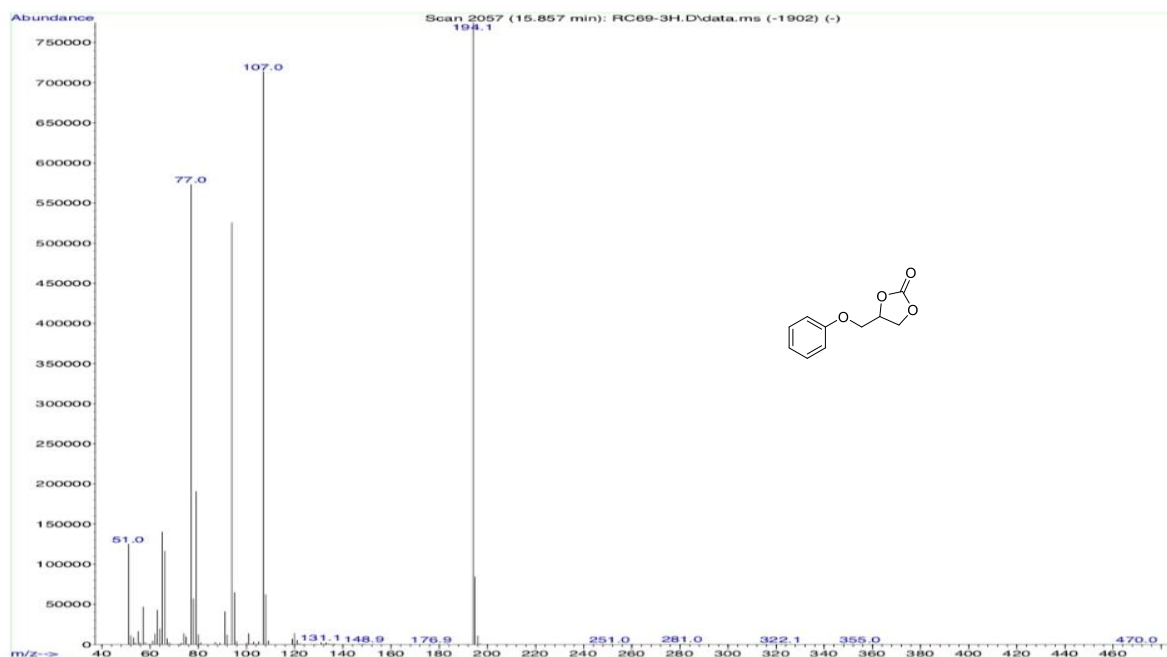
Figure A.4.8. *MS spectrum of product **2e** (EI, 70 V)*

m/z (70 eV): 196 (MH$_2^+$,1); 195(M^{+1},11); 194 (M$^+$,100);107 (92); 95 (8); 94 (68); 79 (25); 77 (74); 66 (15); 65 (18); 63 (6); 51 (16).

276

2g: 4,4'-((butane-1,4-diylbis(oxy))bis(methylene))bis(1,3-dioxolan-2-one)
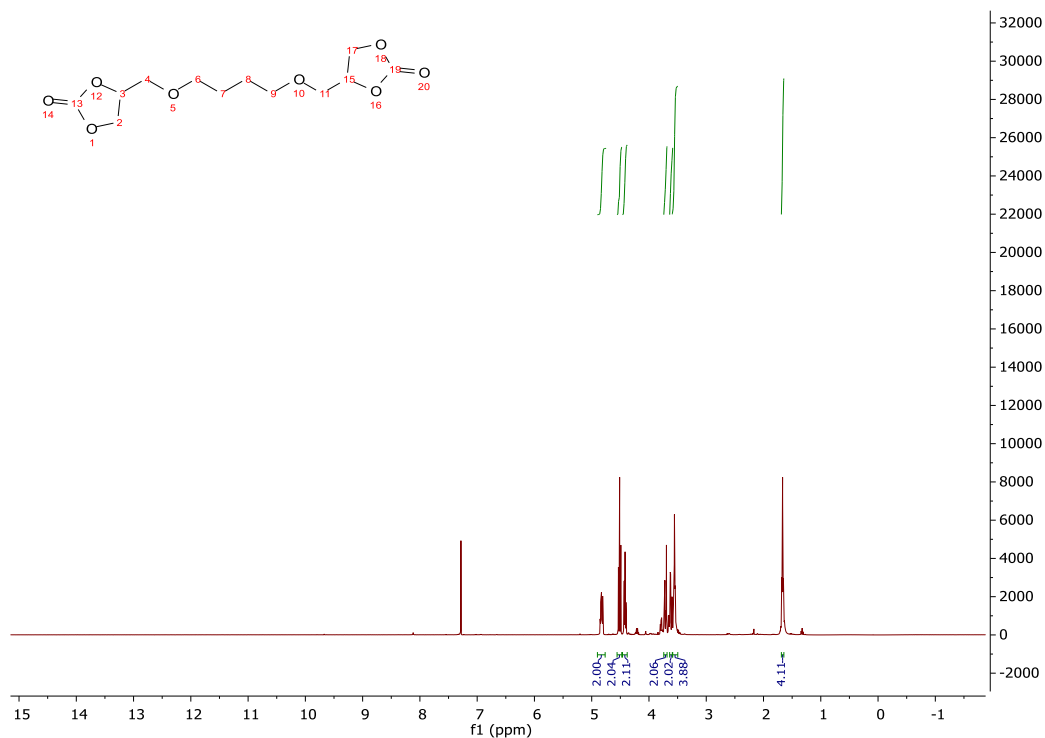
Figure A.4.18. ^1H NMR of product **2g** (400 MHz, 298 K, CDCl$_3$)

δ (ppm): 4.85-4.80 (m, 2H), 4.50 (t, 2H), 4.40 (m, 2H), 3.70 (m, 2H), 3.60 (m, 2H), 3.55 (m, 4H), 1.65 (m, 4H).
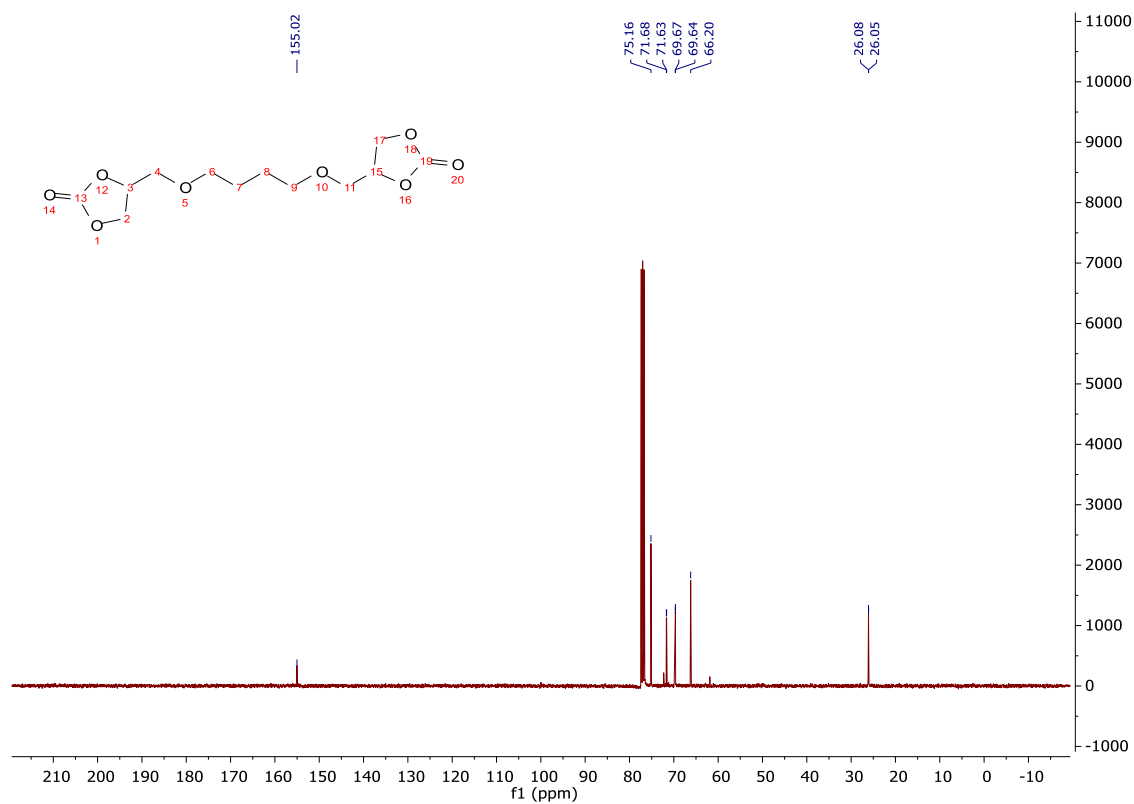
Figure A.4.19. ^{13}C NMR of product **2g** (100 MHz, 298 K, CDCl$_3$)

δ (ppm): 155.02, 75.16, 71.68, 71.63, 69.67, 69.64, 66.20, 26.08, 26.05.

277
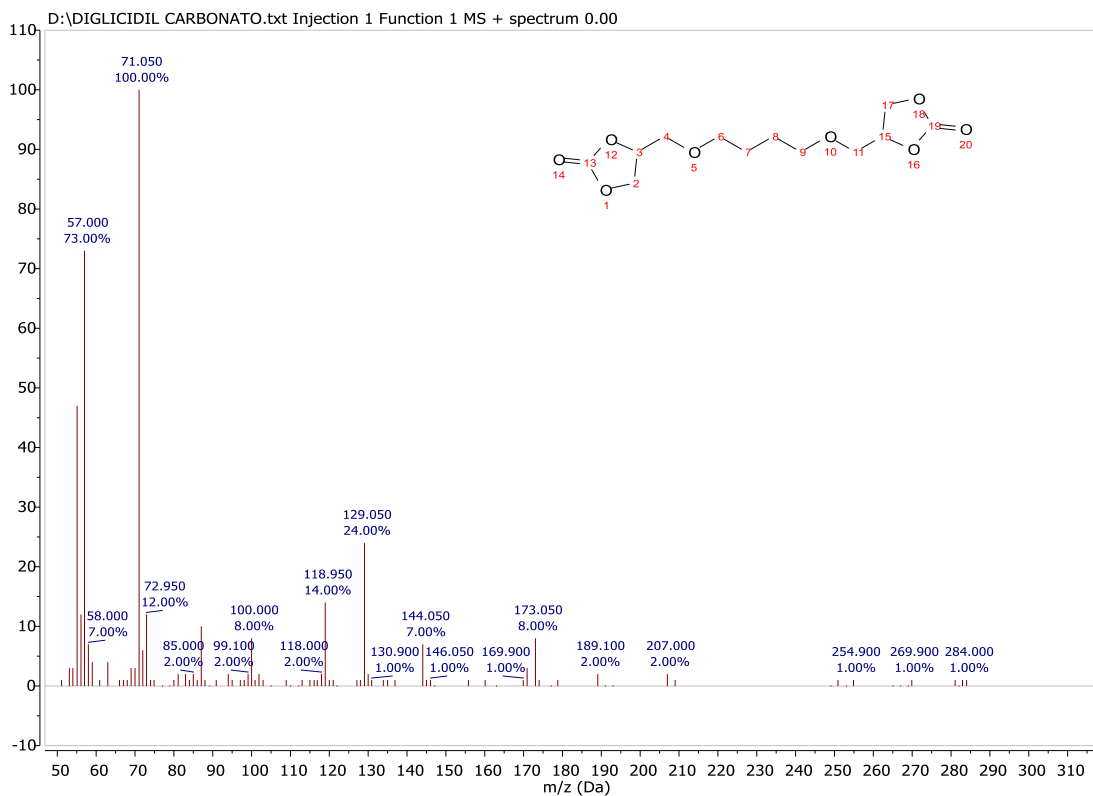
Figure A.4.20. *MS spectra of product **2g** (EI, 70 V).*

m/z (70 eV): 173 (8), 129 (24), 119 (14), 71 (100), 57 (73).

Appendix A.5 – Chapter 5

A.5 Diversified upgrading of 5-hydroxymethylfurfural (HMF)

2: (5-formylfuran-2-yl)methyl acetate, HMF acetate (AMF)
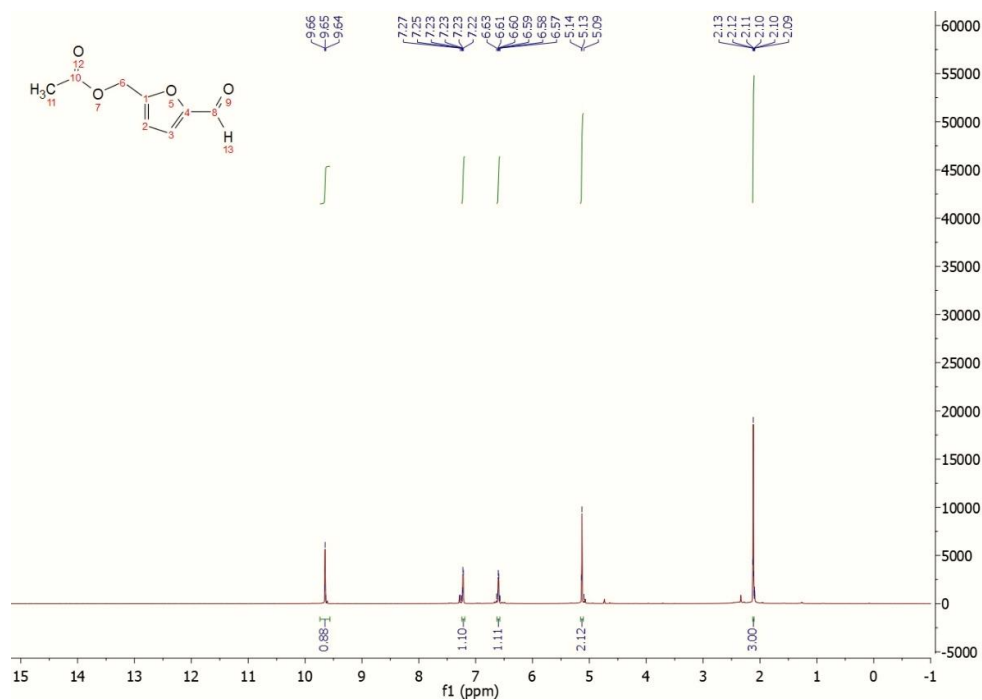
Figure A.5.1. ^1H NMR of product **2** (400 MHz, 298 K, CDCl$_3$)

δ (ppm): 9.65 (s, 1H), 7.25 (d, 1H), 6.60 (d, 1H), 5.13 (s, 2H), 2.2 (s, 3H).
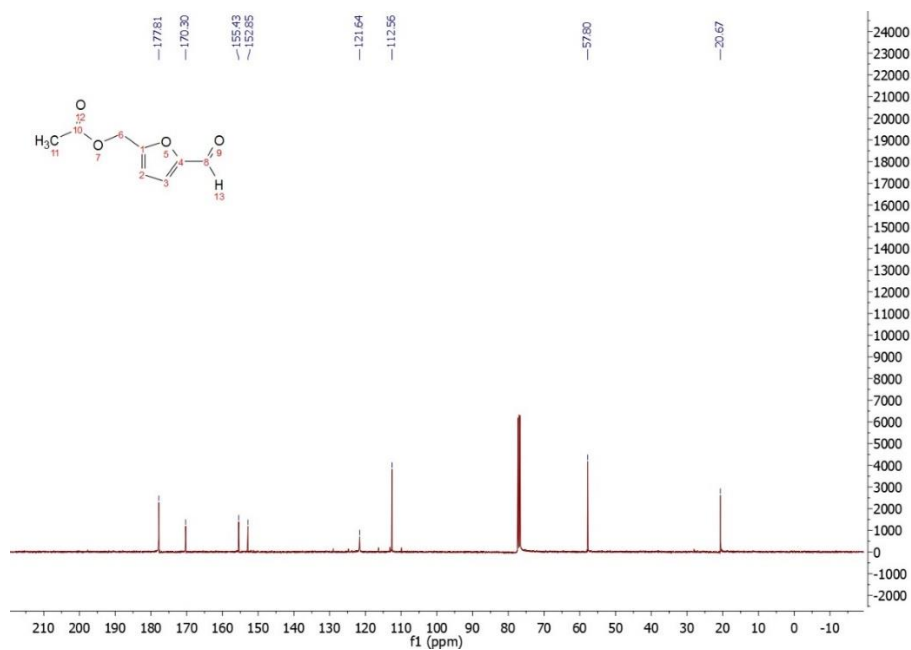
Figure A.5.2. ^{13}C NMR of product **2** (100 MHz, 298 K, CDCl$_3$)

δ (ppm): 177.81, 170.30, 155.43, 152.85, 121.64, 112.56, 57.80, 20.67.

Figure A.5.3. MS spectrum of compound **2** (EI, 70 eV)
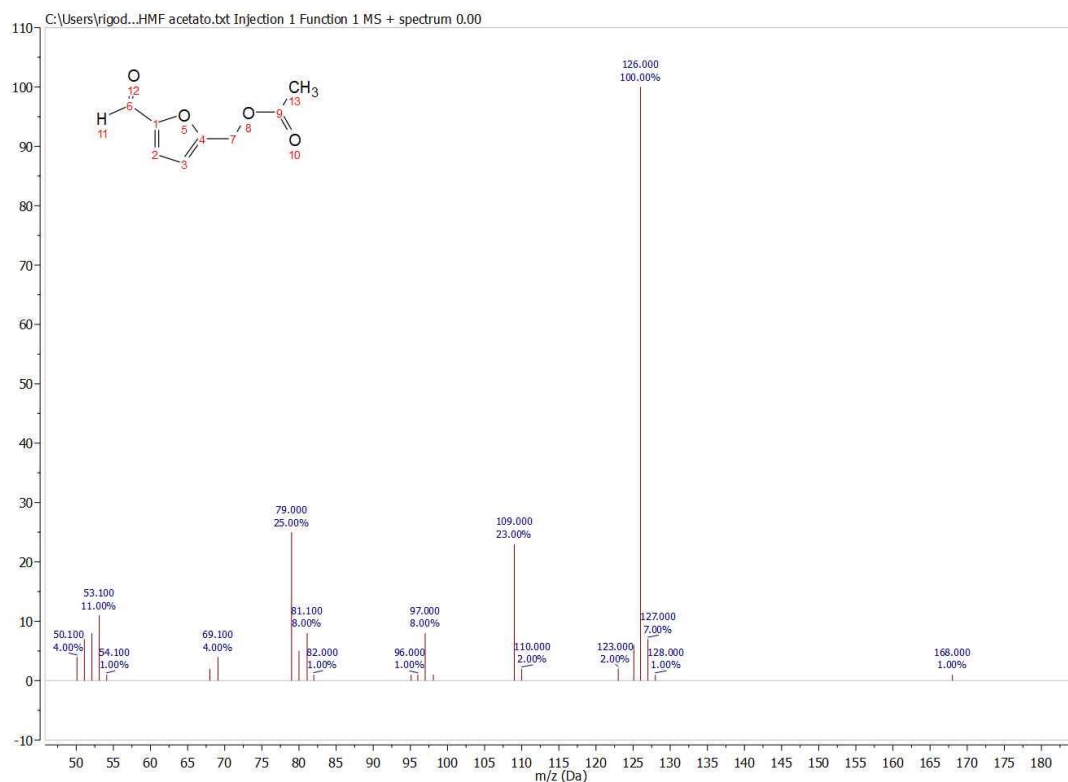
m/z (70 eV): 168 (M⁺, 1), 126 (100), 109 (23), 79 (25), 53 (11).

3a: (E)-(5-(3-oxobut-1-en-1-yl)furan-2-yl)methyl acetate

Figure A.5.4. ¹H NMR of product **3a** (400 MHz, 298 K, CDCl₃)
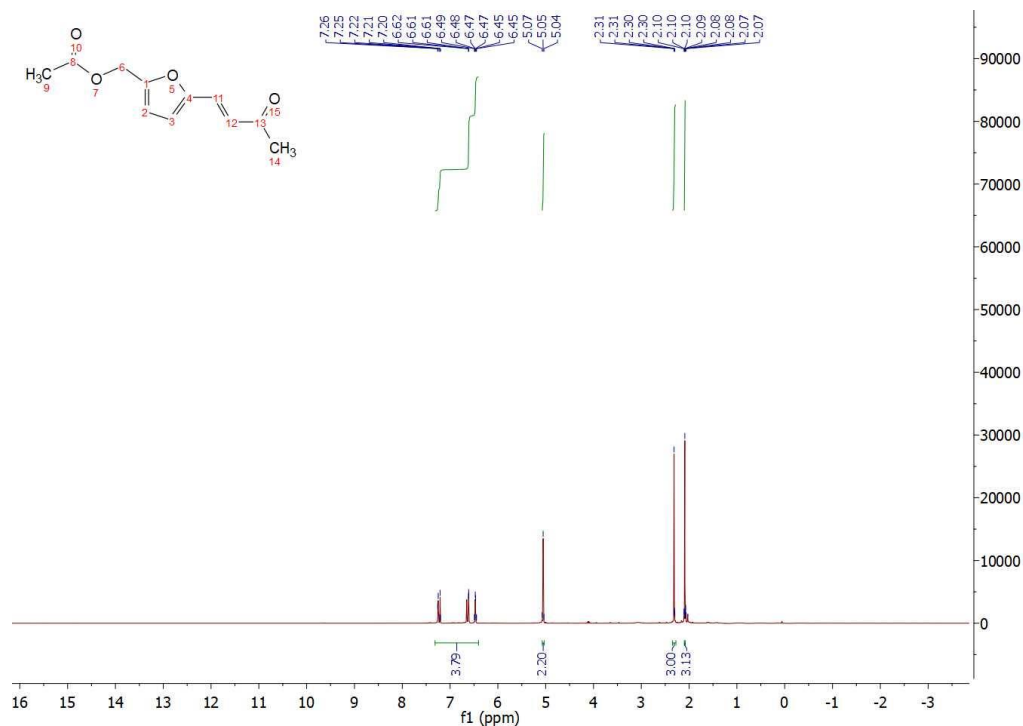
δ (ppm): 7.35-6.5 (m, 4H), 5.05 (s, 2H), 2.3 (s, 3H), 2.05 (s, 3H).
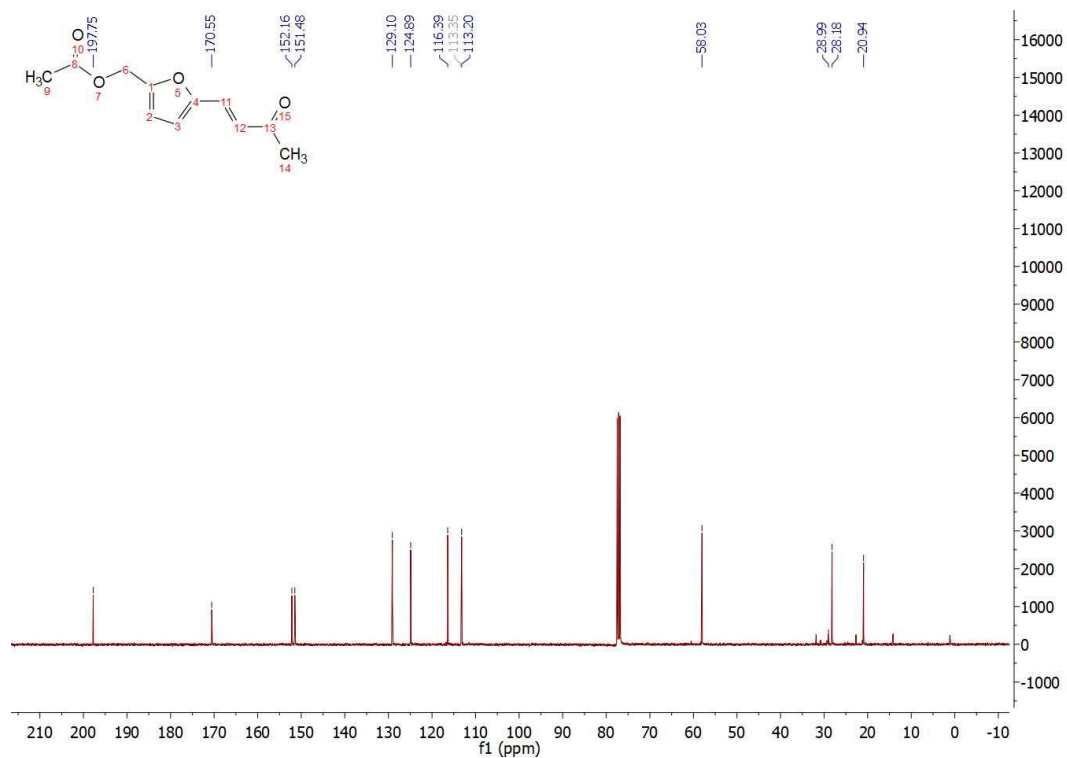
Figure A.5.5. *¹³C NMR of product **3a** (100 MHz, 298 K, CDCl₃)*

δ (ppm): 197.75, 170.55, 152.16, 151.48, 129.10, 124.89, 116.39, 113.20, 58.03, 28.99, 20.94.
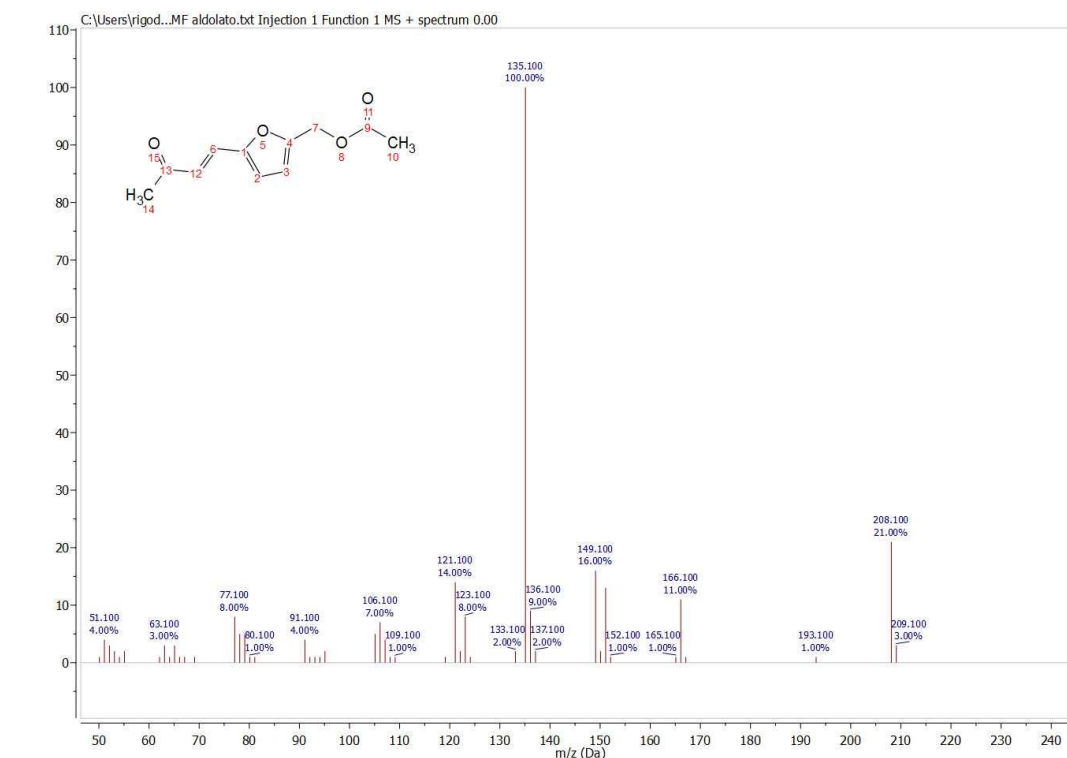
Figure A.5.6. *MS spectrum of compound **3a** (EI, 70 eV)*

m/z (70 eV): 204 (M⁺, 21), 166 (11), 149 (16), 135 (100), 121 (14), 106 (7), 77 (8), 55 (4).

3b: ((E)-4-(5-(hydroxymethyl)furan-2-yl)but-3-en-2-one)

Compound **3b** was isolated after the reaction of HMF (0.5 mmol), iPAc (1.5 equivs.) and acetone (16 equivs.) carried out at 30°C for 15 h in the presence of Cs_2CO_3 (10 mol%) as a catalyst. Product **3b** was obtained in a 12% yield by FCC of the reaction mixture (Stationary phase: SiO_2; eluent: Et_2O).
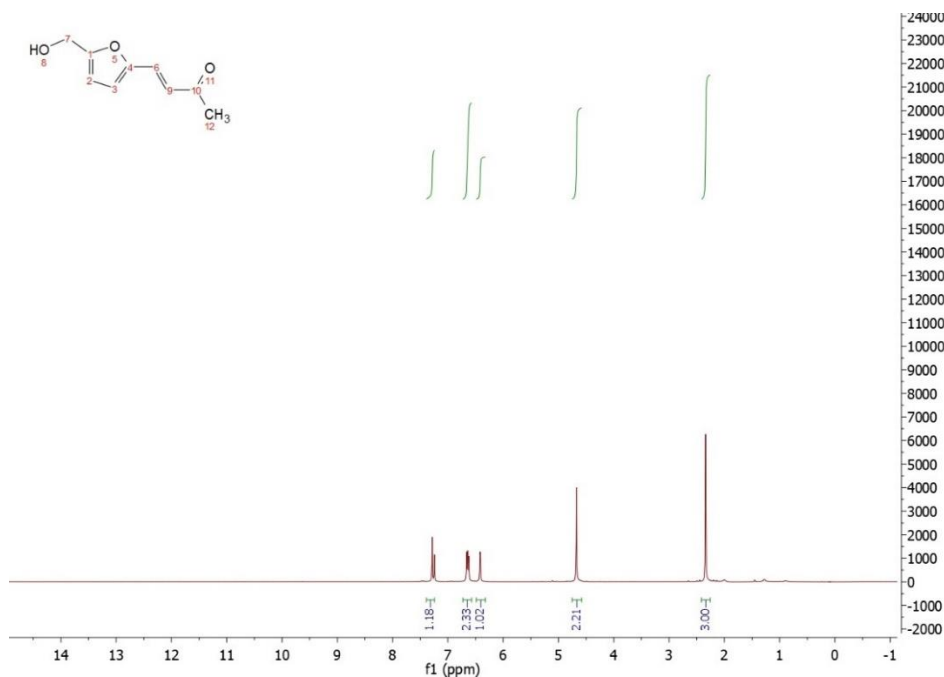
Figure A.5.7. *^{1}H NMR of product **3b** (400 MHz, 298 K, CDCl$_3$)*

δ (ppm): 7.28 (s, 1H), 6.65 (t, 2H), 6.40 (s, 1H), 4.68 (s, 2H), 2.34 (s, 3H).
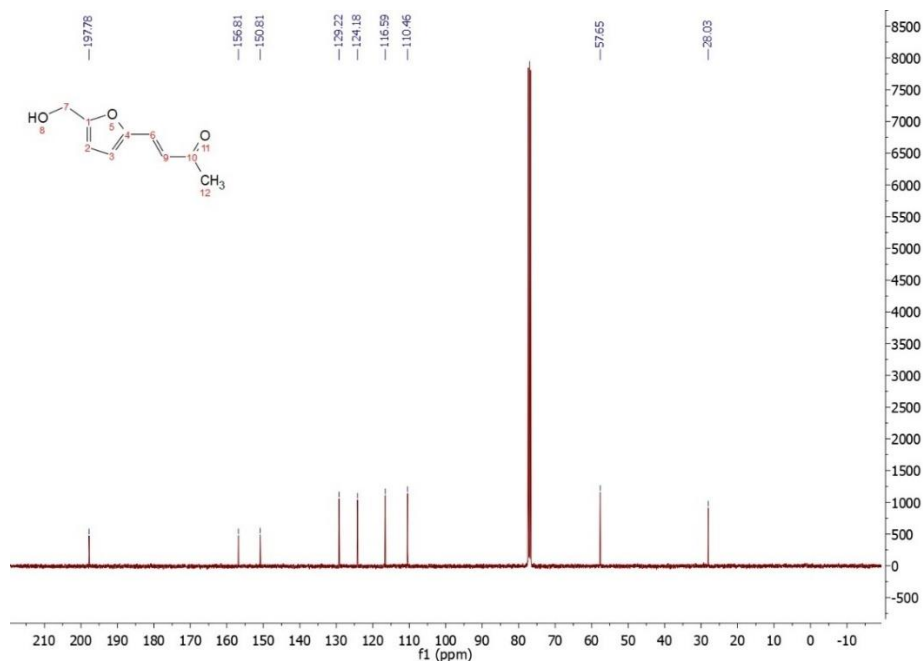
Figure A.5.8. *^{13}C NMR of product **3b** (100 MHz, 298 K, CDCl$_3$)*

δ (ppm): 197.78, 156.81, 150.81, 129.22, 124.18, 116.59, 110.46, 57.65, 28.03.

Figure A.5.9. MS spectrum of compound **3b** (EI, 70 eV)
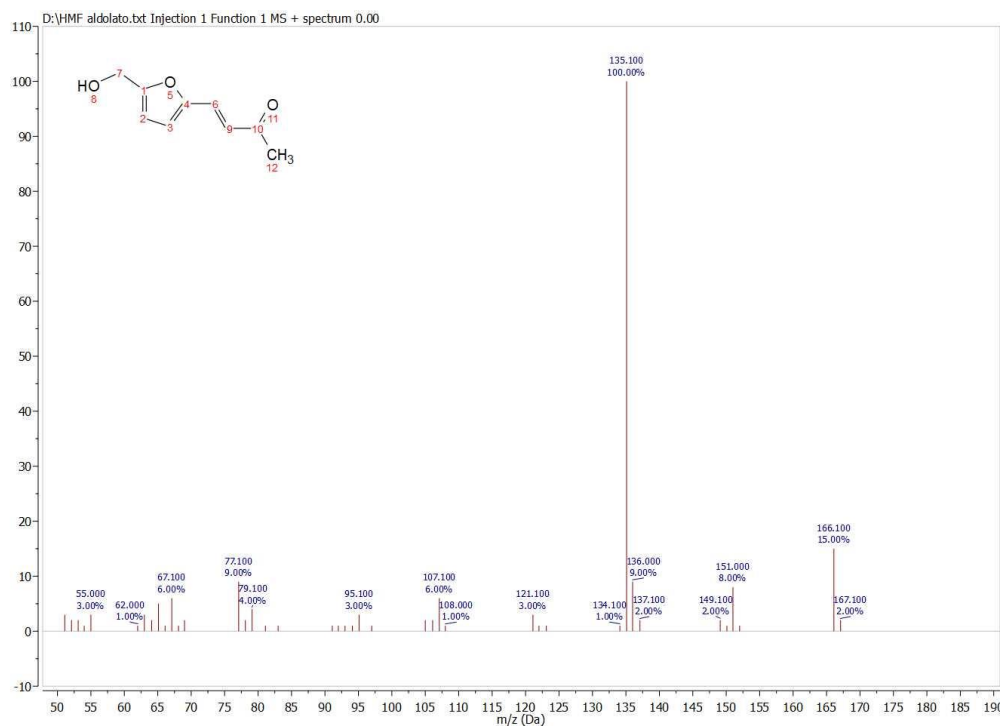
m/z (70 eV): 166 (M$^+$, 1), 151 (8), 135 (100), 107 (6), 77 (9), 55 (3).

3c: (E)-(5-(3-oxobut-1-en-1-yl)furan-2-yl)methyl carbonate

Figure A.5.10. ^{1}H NMR of product **3c** (400 MHz, 298 K, CDCl$_3$)
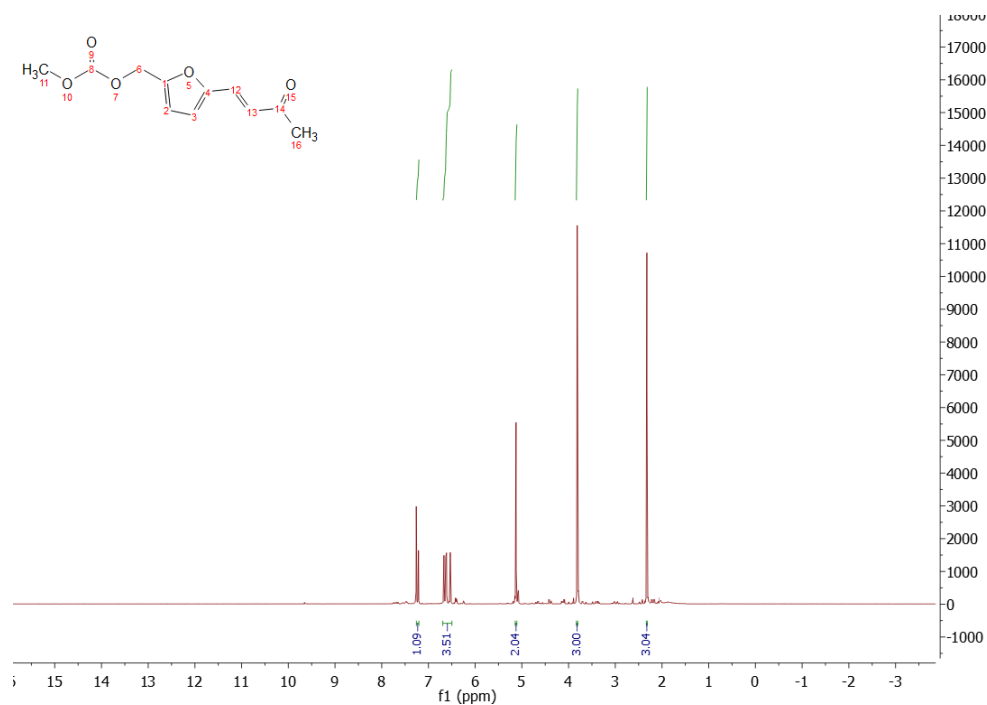
δ (ppm): 7.25 (d, 1H), 6.55 (m, 3H), 5.05 (s, 2H), 3.85 (s, 3H), 2.3 (s, 3H).

283
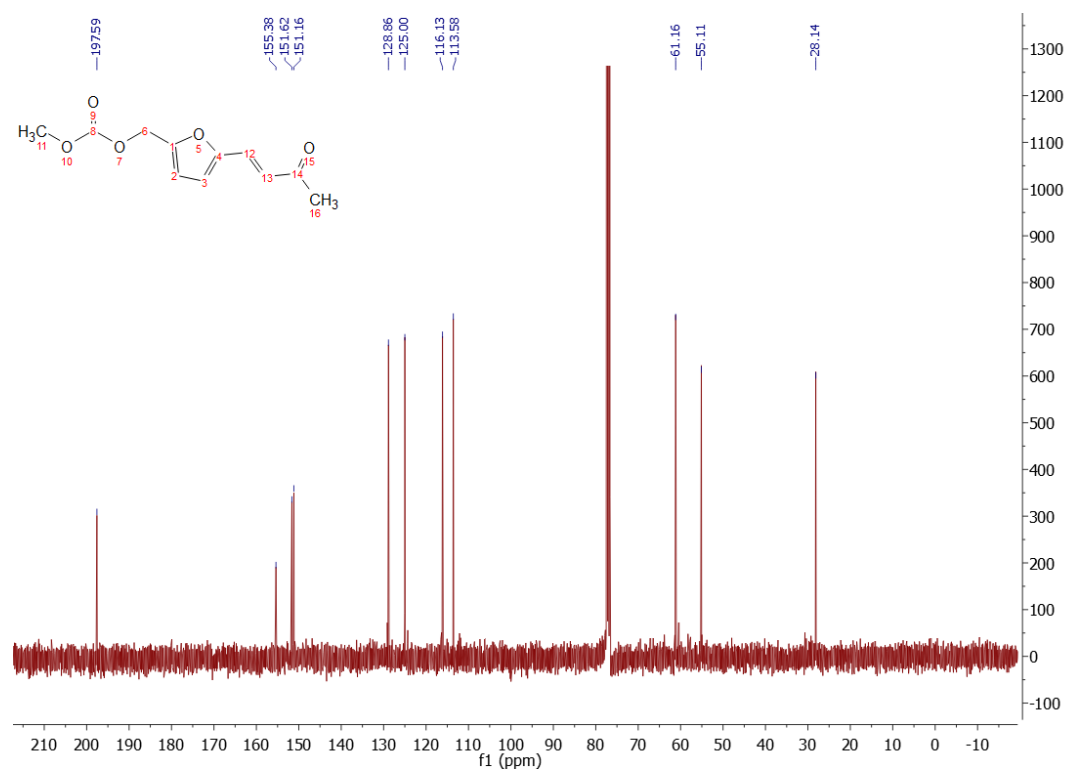
Figure A.5.11. ^{13}C NMR of product **3c** (100 MHz, 298 K, CDCl$_3$)

δ (ppm): 197.59, 155.38, 151.62, 151.16, 128.86, 125.00, 116.13, 113.58, 61.16, 55.11, 28.14.
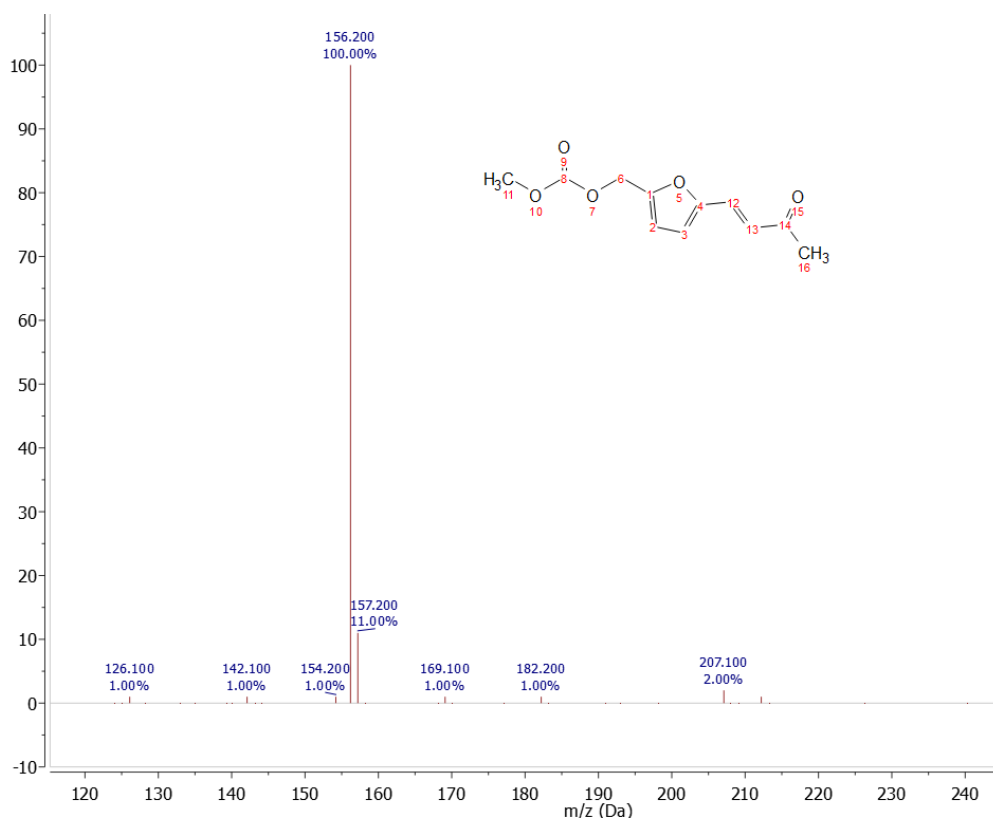
Figure A.5.12. MS spectrum of compound **3c** (EI, 70 eV)

m/z (70 eV): 207 (2), 182 (1), 169 (1), 156 (100), 142 (1), 126 (1).

4: (5-formylfuran-2-yl)methyl carbonate, HMF carbonate (HMFC)
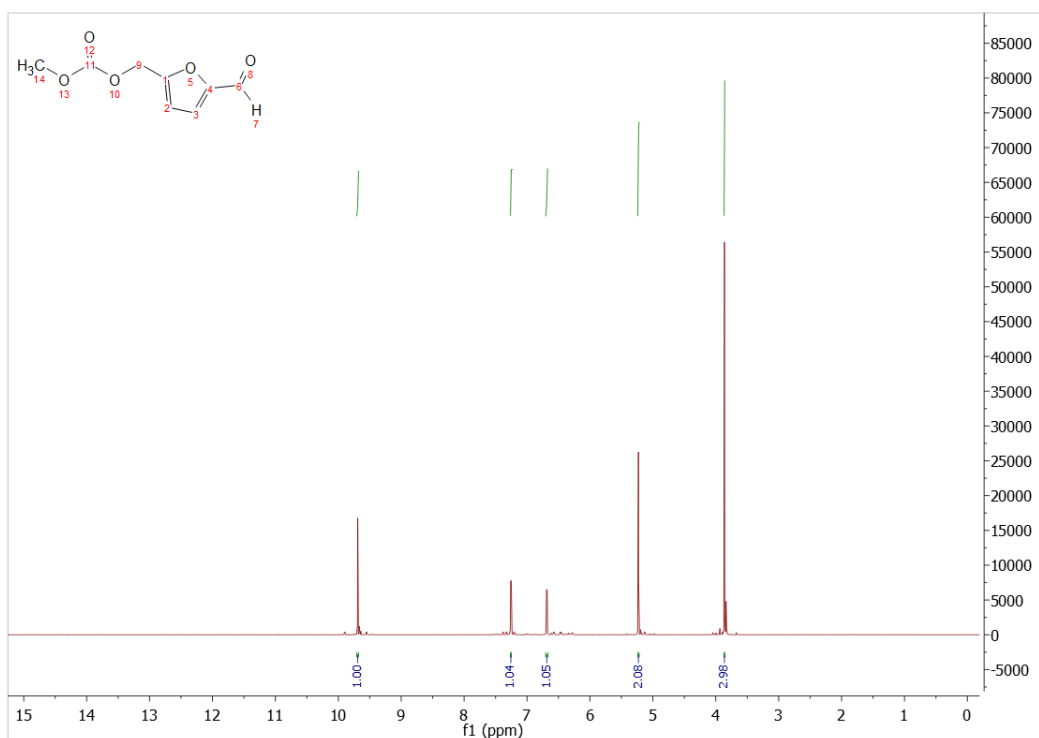
Figure A.5.13. ^{1}H NMR of product **4** (400 MHz, 298 K, CDCl$_3$)

δ (ppm): 9.69 (s, 1H), 7.25 (s, 1H), 6.68 (s, 1H), 5.23 (s, 2H), 3.86 (s, 3H).
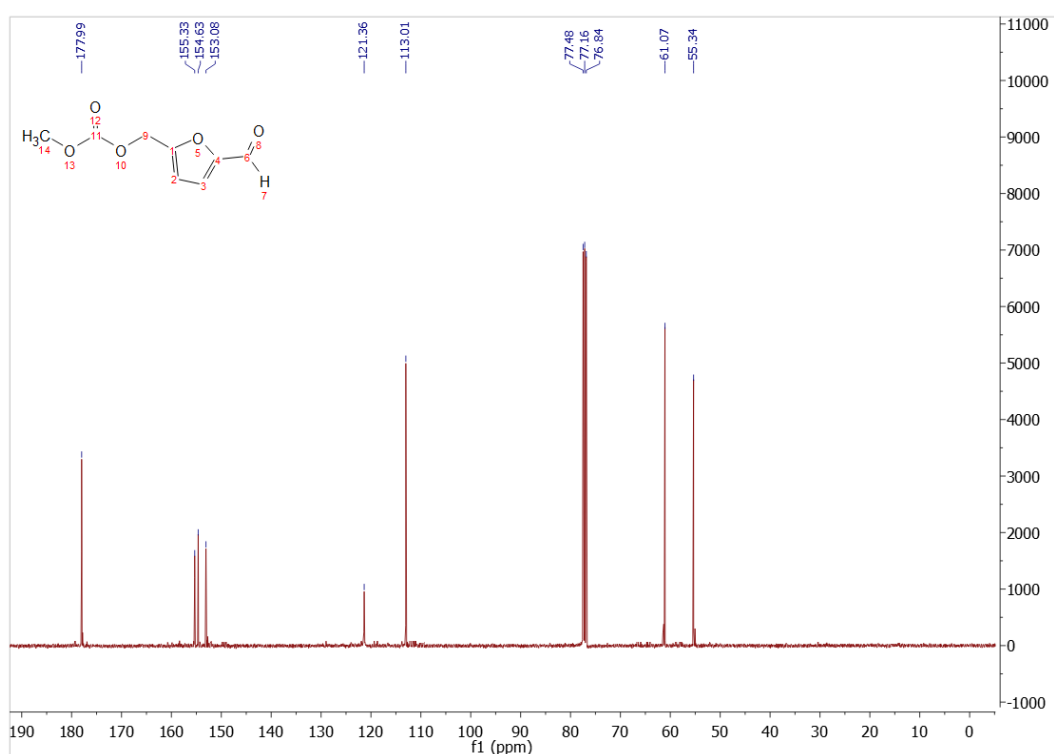
Figure A.5.14. ^{13}C NMR of product **4** (100 MHz, 298 K, CDCl$_3$)

δ (ppm): 177.99, 155.33, 154.63, 153.08, 121.36, 113.01, 61.07, 55.34.
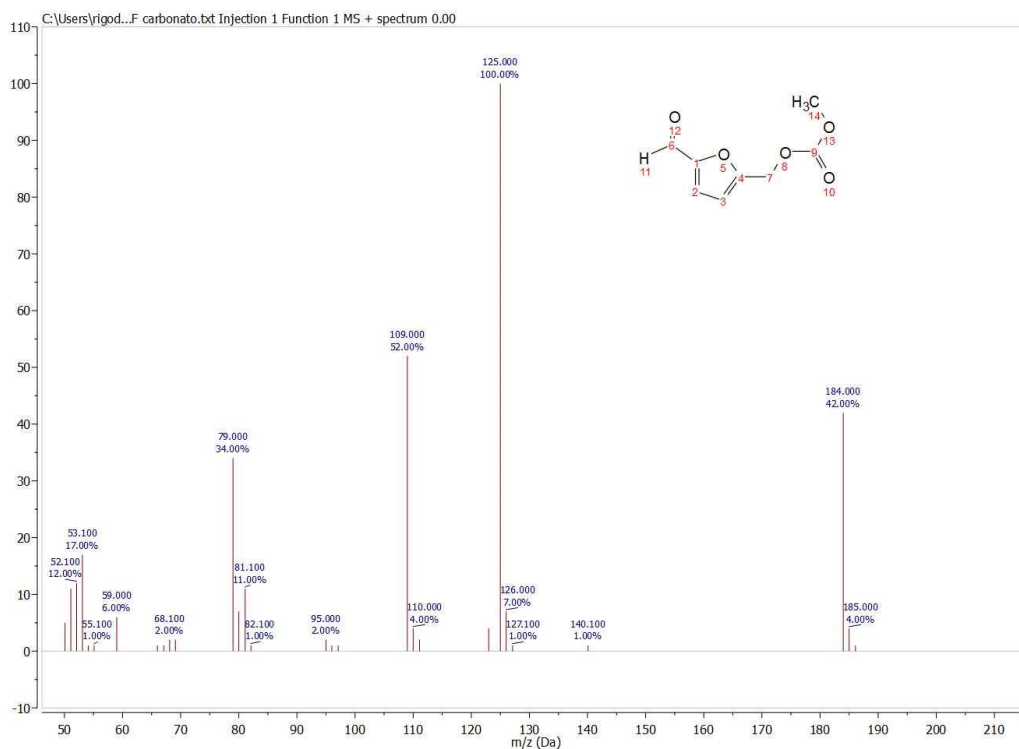
Figure A.5.15. *MS spectrum of compound **4** (EI, 70 eV)*

m/z (70 eV): 184 (M⁺, 42), 125 (100), 109 (52), 79 (34), 55 (17).

5a: 2-(((5-(hydroxymethyl)furan-2-yl)methyl)amino)ethan-1-ol
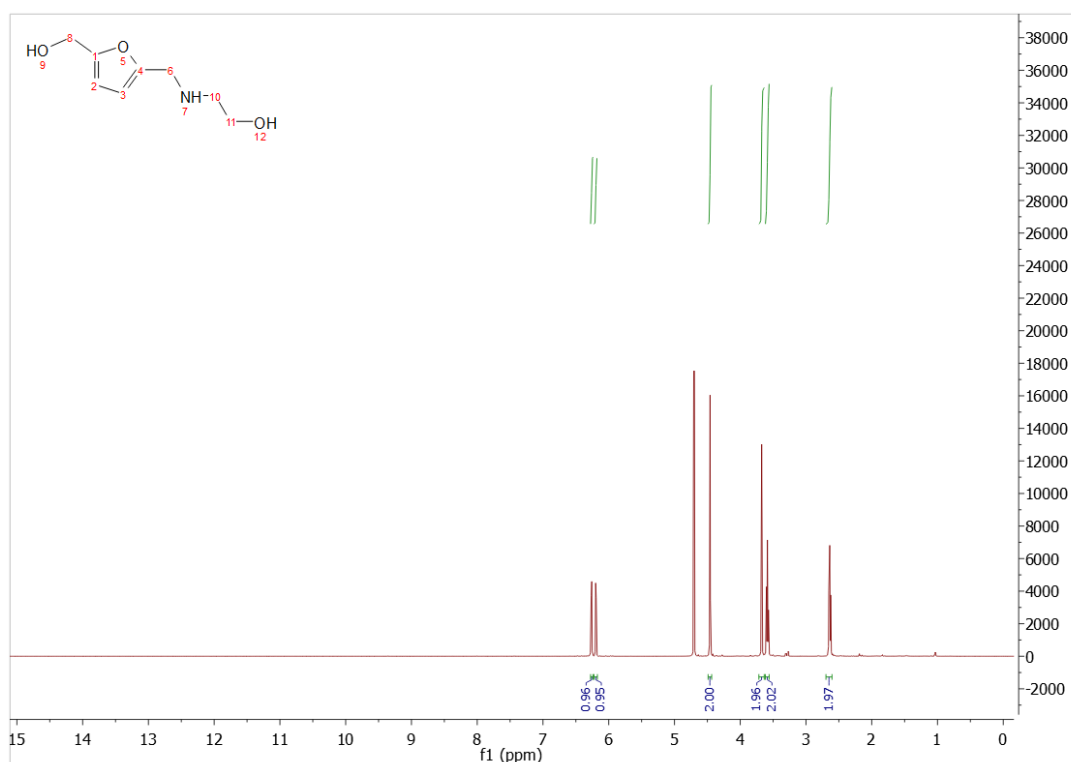
Figure A.5.16. *¹H NMR of product **5a** (400 MHz, 298 K, D₂O)*

δ (ppm): 6.26 (d, *J* = 3.2 Hz, 1H), 6.20 (s, 1H), 4.46 (s, 2H), 3.67 (s, 2H), 3.59 (s, 1H), 2.64 (s, 1H).

286
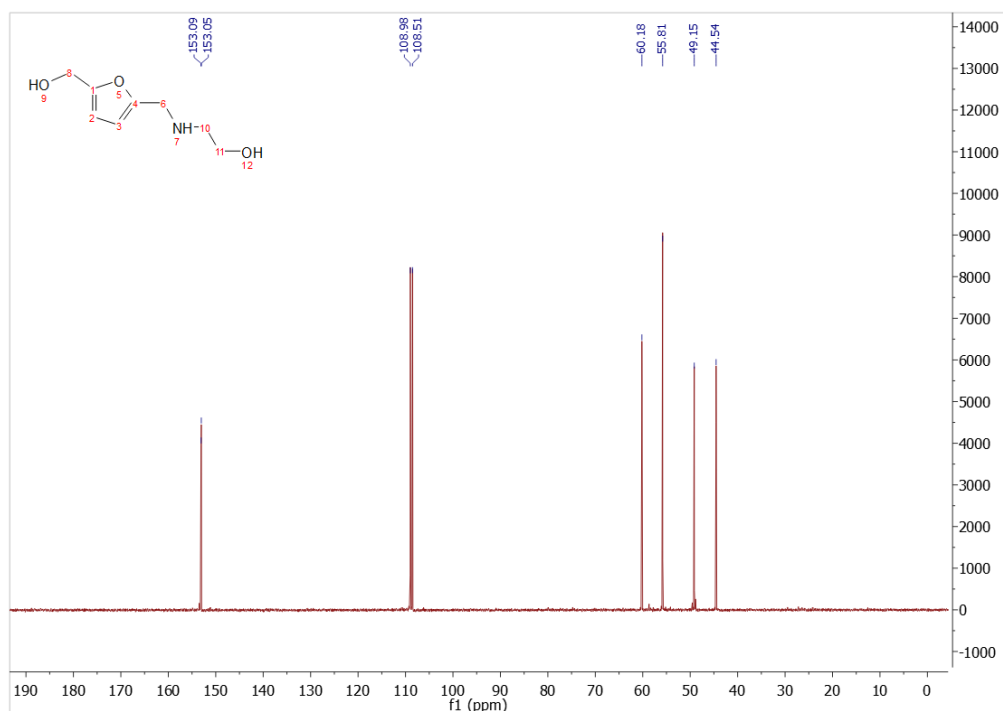
Figure A.5.17. ^{13}C NMR of product **5a** (100 MHz, 298 K, D₂O)

δ (ppm): 153.09, 153.05, 108.98, 108.51, 60.18, 55.81, 49.15, 44.54

Since compound **5a** was not detectable by GC-MS, its MS spectrum is not reported.

5b: 3-(((5-(hydroxymethyl)furan-2-yl)methyl)amino)propan-1-ol
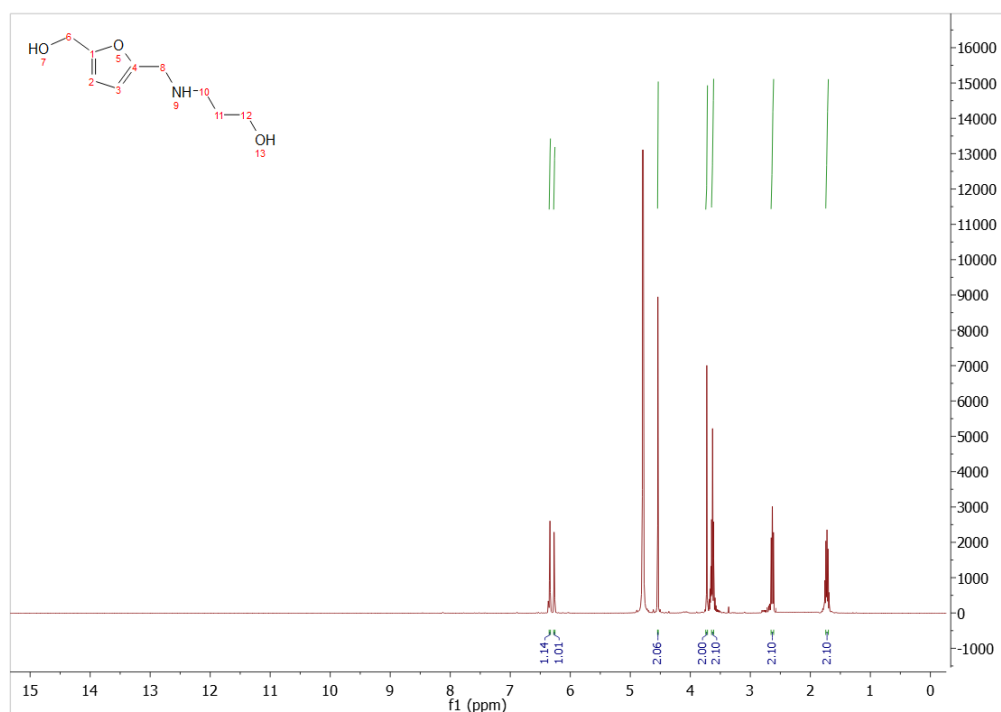
Figure A.5.18. ^1H NMR of product **5b** (400 MHz, 298 K, D₂O)

δ (ppm): 6.34 (d, 1H), 6.27 (d, 1H), 4.54 (s, 2H), 3.73 (s, 2H), 3.63 (m, 2H), 2.63 (m, 2H), 1.72 (m, 2H).
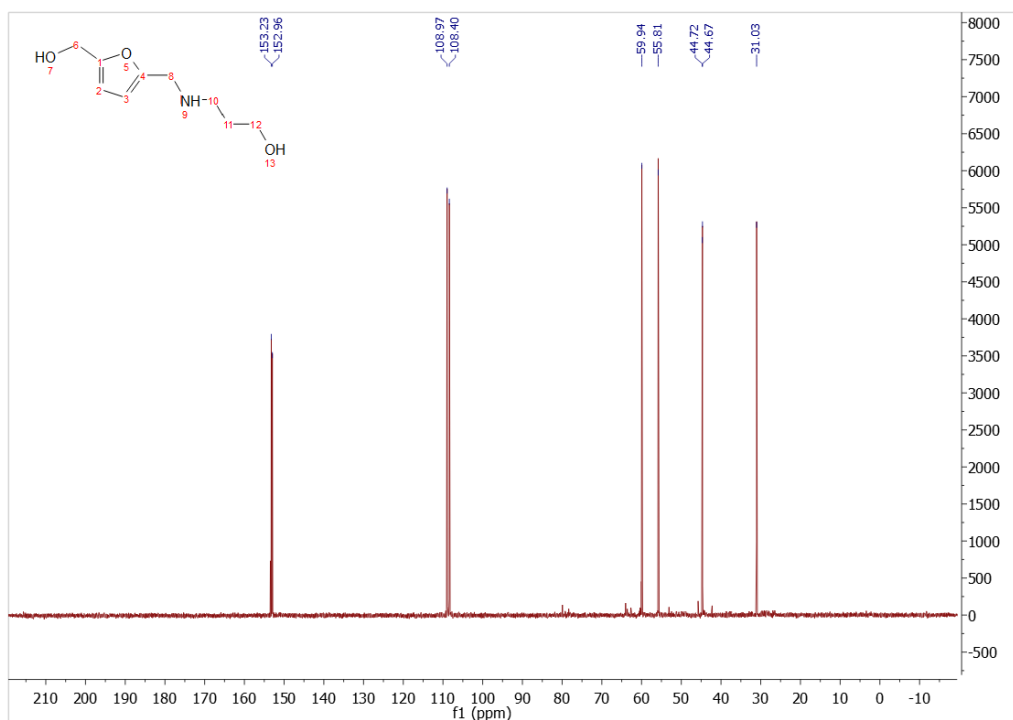
Figure A.5.19. ^{13}C NMR of product **5b** (100 MHz, 298 K, D$_2$O)

δ (ppm): 153.23, 152.96, 108.97, 108.40, 59.94, 55.81, 44.72, 44.67, 31.03.

Since compound **5b** was not detectable by GC-MS, its MS spectrum is not reported.

5c: 3-(((5-(hydroxymethyl)furan-2-yl)methyl)amino)propane-1,2-diol
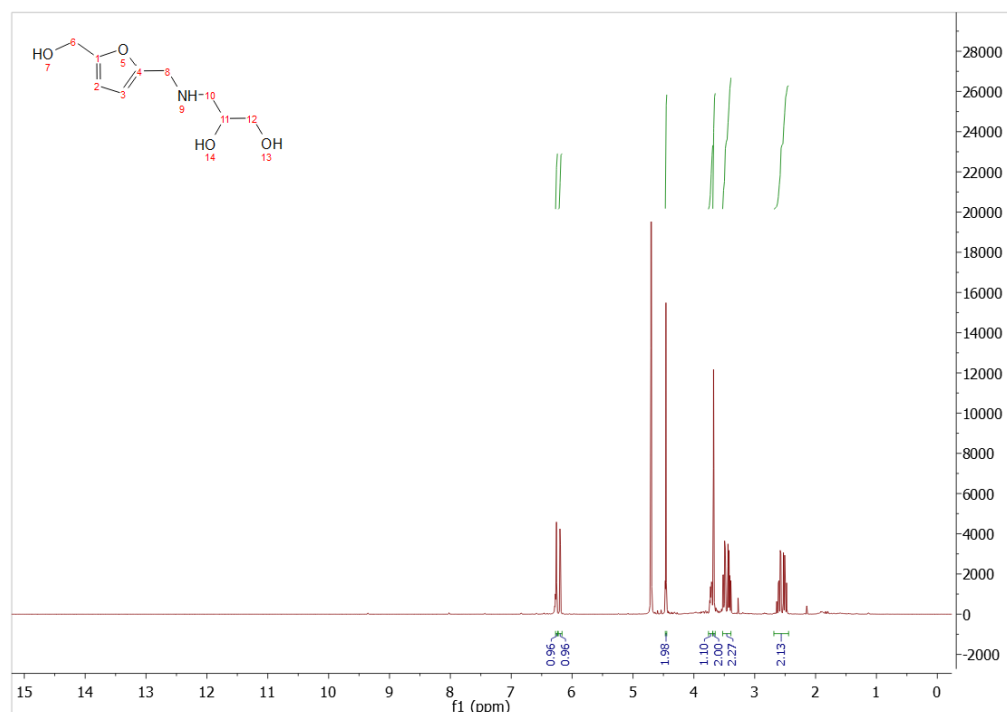
Figure A.5.20. ^1H NMR of product **5c** (400 MHz, 298 K, D$_2$O)

δ (ppm): 6.26 (d, 1H), 6.20 (d, 1H), 4.46 (s, 2H), 3.71 (m, 1H), 3.68 (s, 2H), 3.49 (m, 2H), 2.58 (m, 2H).

288
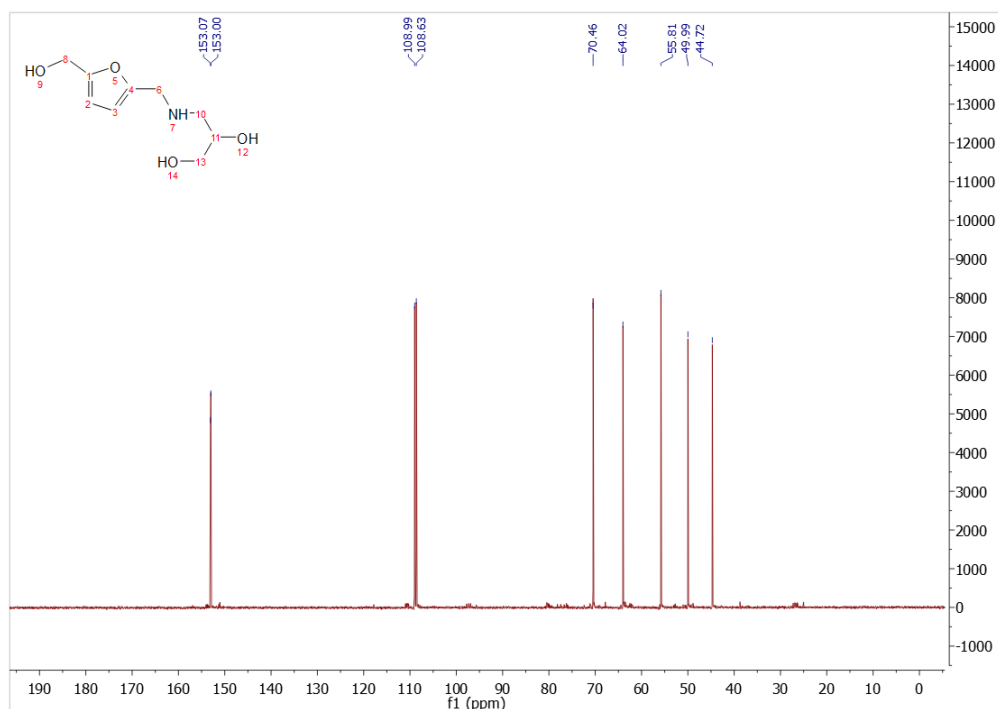
Figure A.5.21. ^{13}C NMR of product **5c** (100 MHz, 298 K, D$_2$O)

δ (ppm): 153.07, 153.00, 108.99, 108.63, 70.46, 64.02, 55.81, 49.99, 44.72.

Since compound **5c** was not detectable by GC-MS, its MS spectrum is not reported.

5d: 2-(((5-(hydroxymethyl)furan-2-yl)methyl)amino)propane-1,3-diol
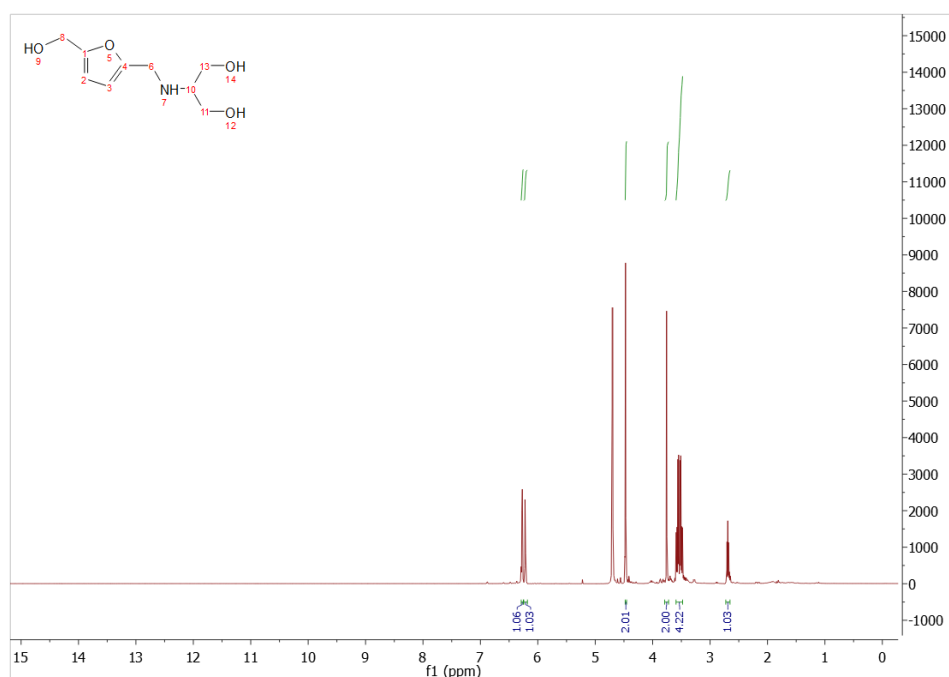
Figure A.5.22. ^1H NMR of product **5d** (400 MHz, 298 K, D$_2$O)

δ (ppm): 6.27 (d, 1H), 6.22 (d, 1H), 4.47 (s, 2H), 3.76 (s, 2H), 3.55 (m, 4H), 2.69 (m, 1H).
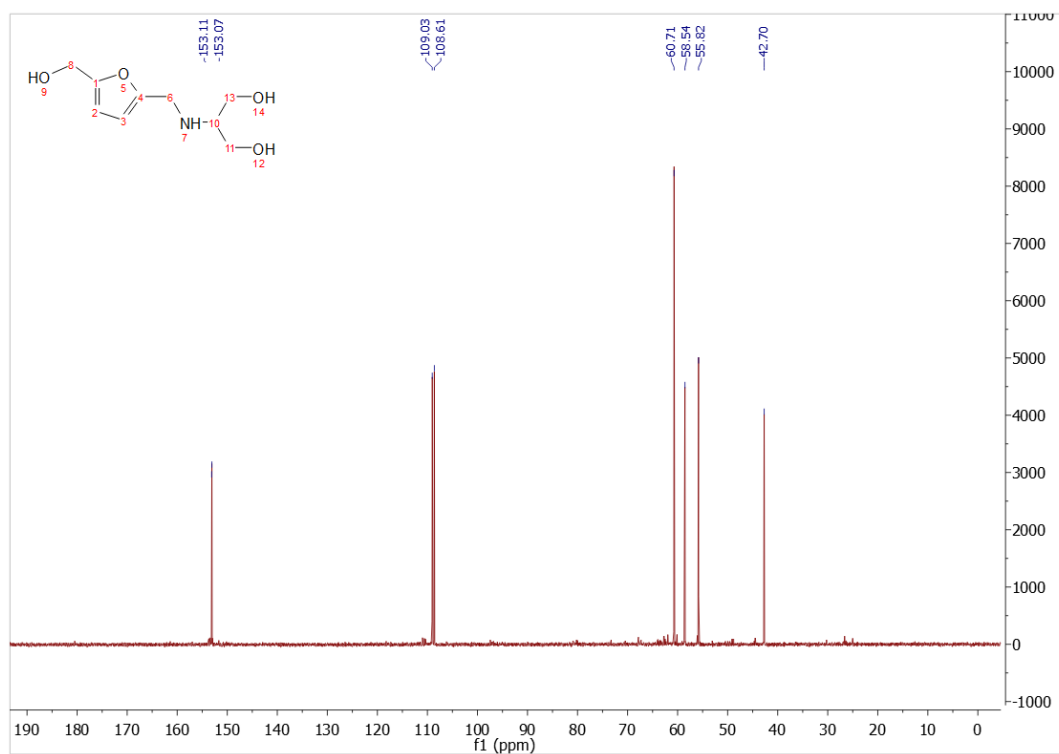
Figure A.5.23. *^{13}C NMR of product **5d** (100 MHz, 298 K, D_2O)*

δ (ppm): 153.11, 153.07, 109.03, 108.61, 60.71, 58.54, 55.82, 42.70.

Since compound **5d** was not detectable by GC-MS, its MS spectrum is not reported.

6a: (5-vinylfuran-2-yl)methanol
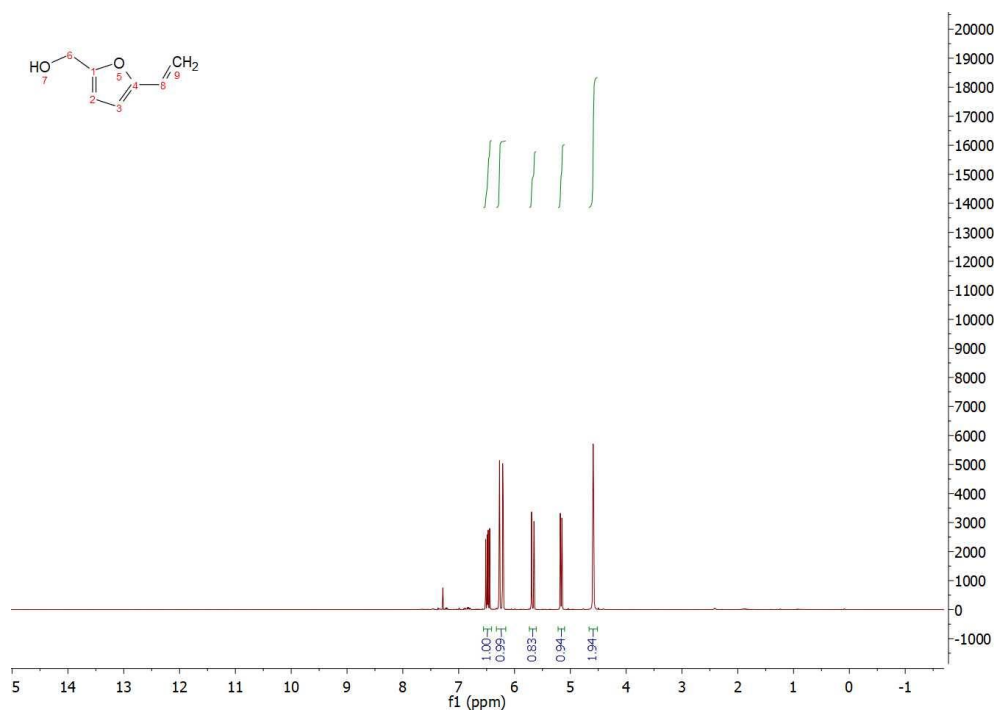
Figure A.5.24. *^{1}H NMR of product **6a** (400 MHz, 298 K, $CDCl_3$)*

δ (ppm): 6.50 (q, 1H), 6.25 (dd, 1H), 5.68 (d, 1H), 5.15 (d, 1H), 4.60 (s, 1H).
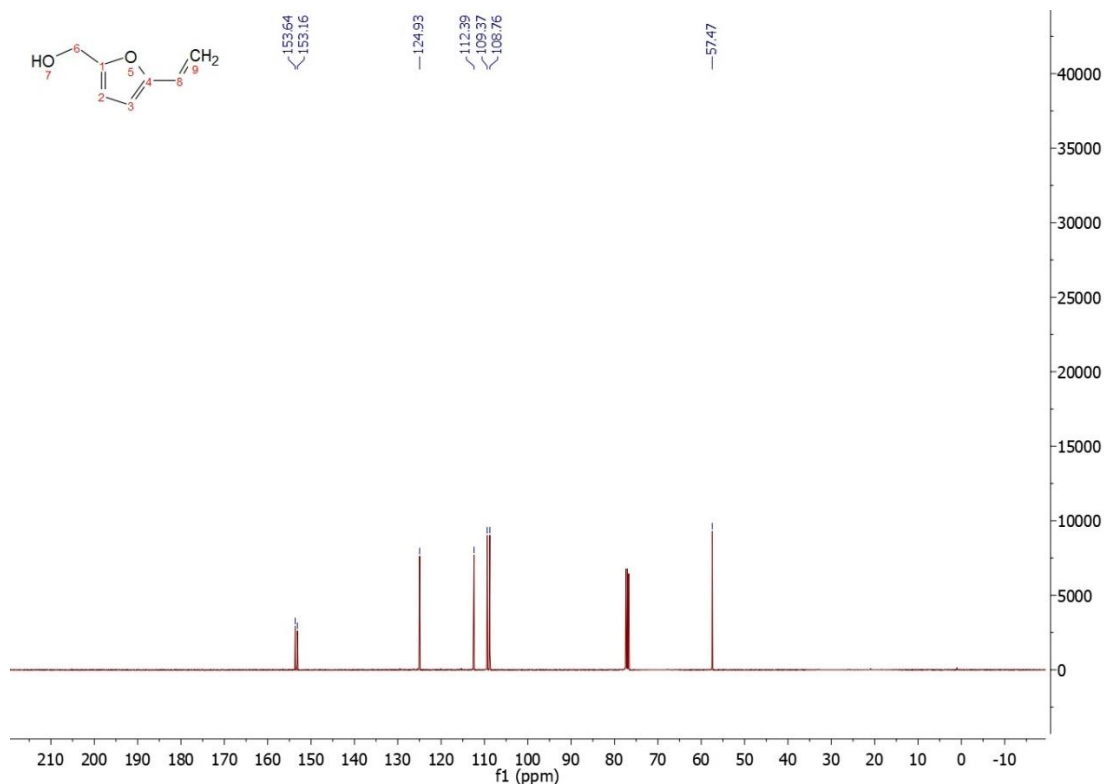
Figure A.5.25. ^{13}C NMR of product **6a** (100 MHz, 298 K, CDCl₃)

δ (ppm): 153.64, 153.16, 124.93, 112.39, 109.37, 108.76, 57.47.
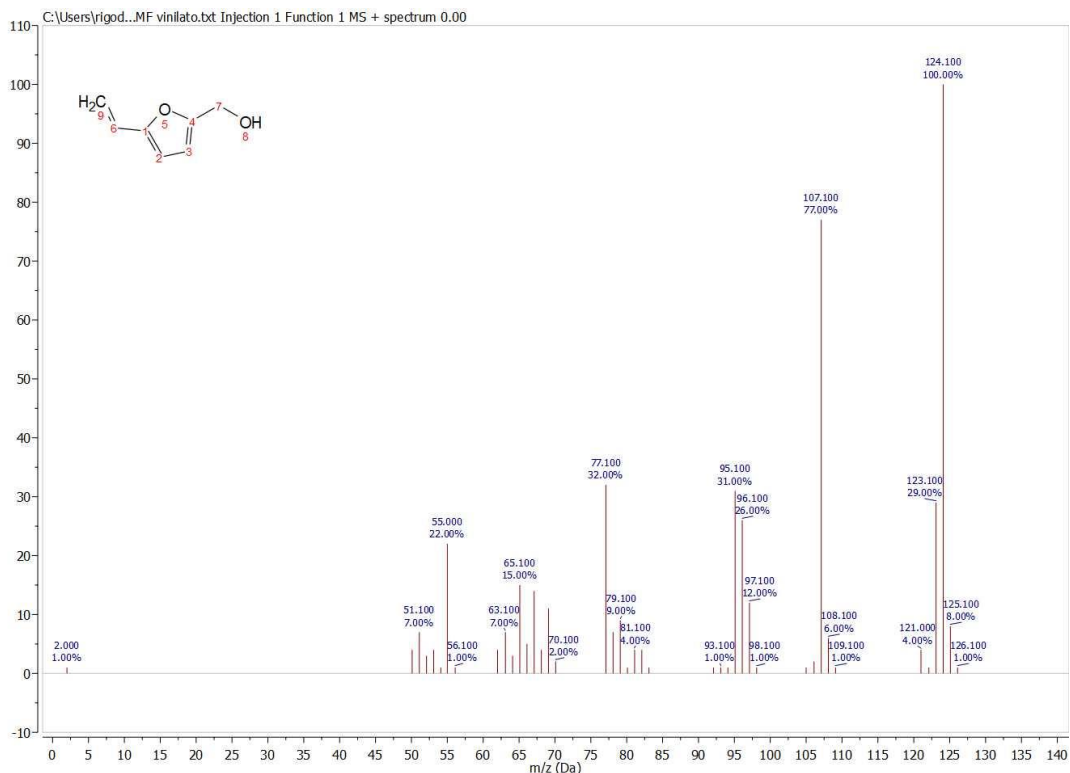
Figure A.5.26. MS spectrum of compound **6a** (EI, 70 eV)

m/z (70 eV): 124 (M⁺, 100), 107 (77), 95 (31), 77 (32), 55 (22).

Figure A.5.27. *¹H NMR of product **6b** (400 MHz, 298 K, CDCl₃)*
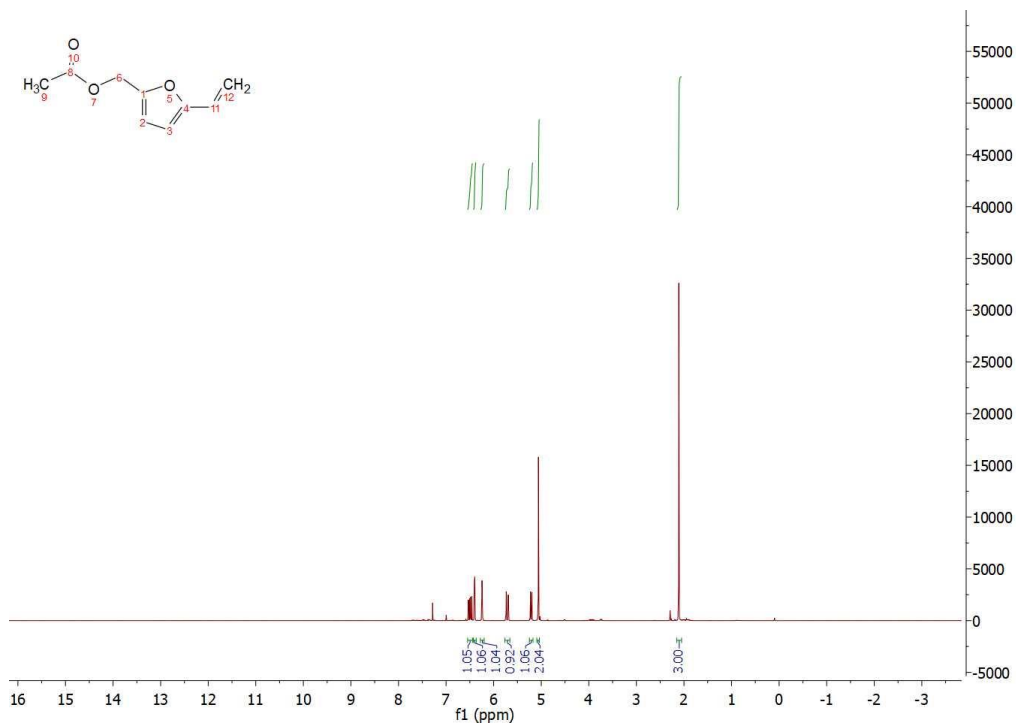
δ (ppm): 6.50 (q, 1H), 6.40 (d, 1H), 6.25 (d, 1H), 5.70 (d, 1H), 5.20 (d, 1H), 5.06 (s, 2H), 2.10 (s, 3H).

Figure A.5.28. *¹³C NMR of product **6b** (100 MHz, 298 K, CDCl₃)*
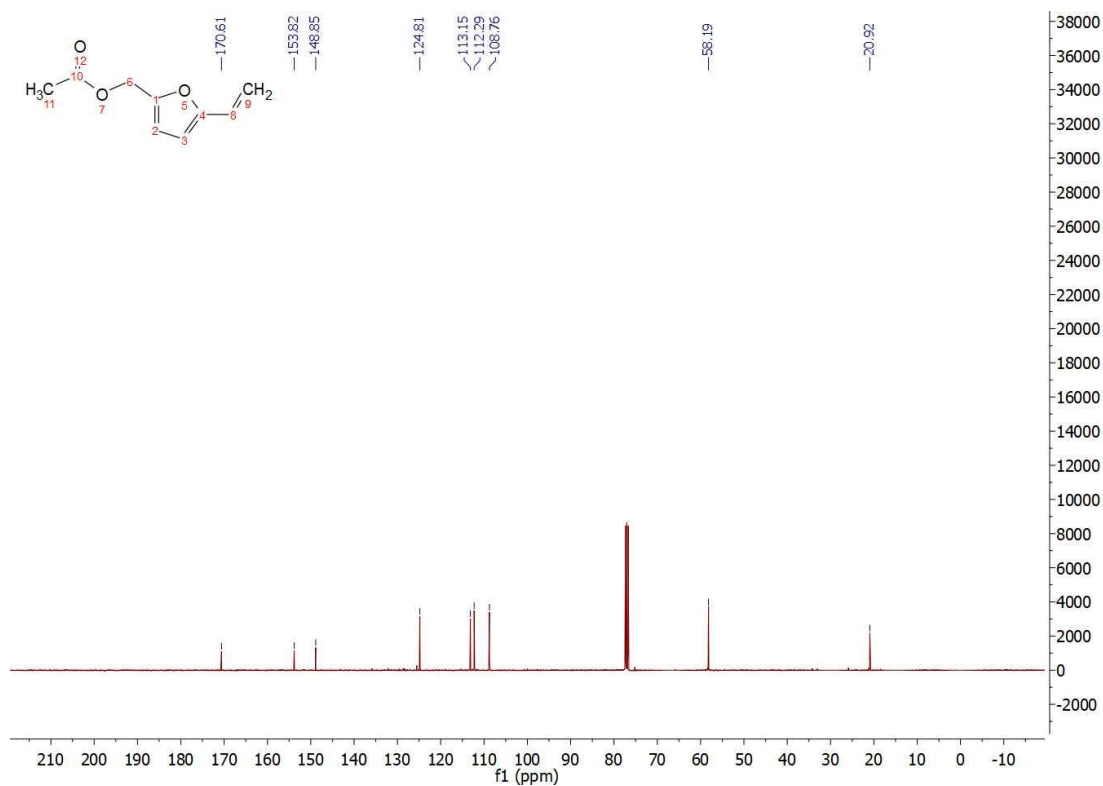
δ (ppm): 170.61, 153.82, 148.85, 124.81, 113.15, 112.29, 108.76, 58.19, 20.92.
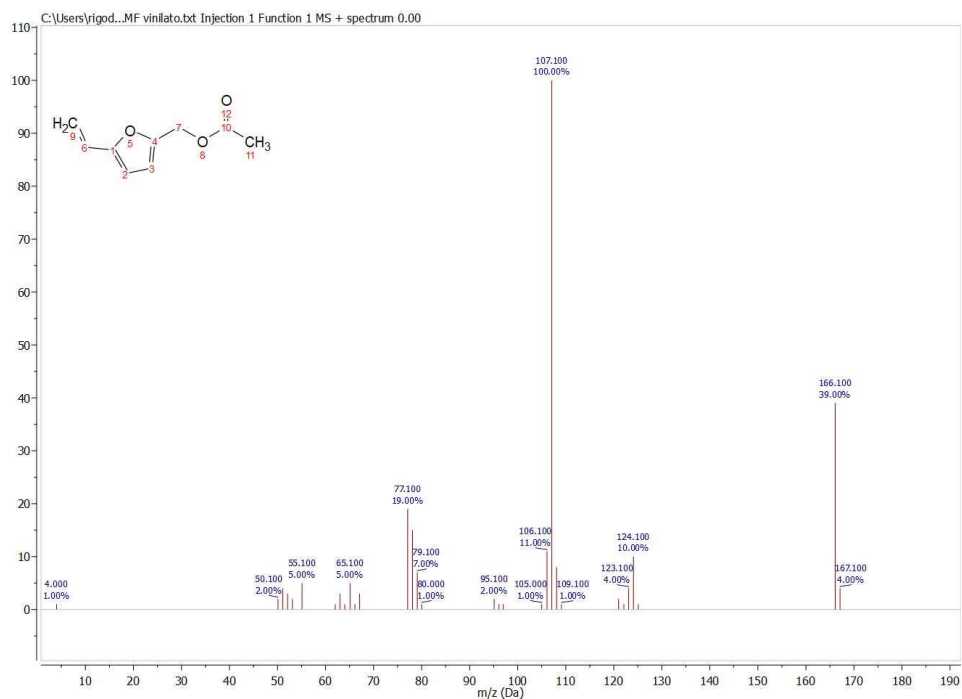
Figure A.5.29. *MS spectrum of compound **6b** (EI, 70 eV)*

m/z (70 eV): 166 (M⁺, 39), 124 (10), 107 (100), 77 (19), 55 (5).

6c: methyl ((5-vinylfuran-2-yl)methyl) carbonate
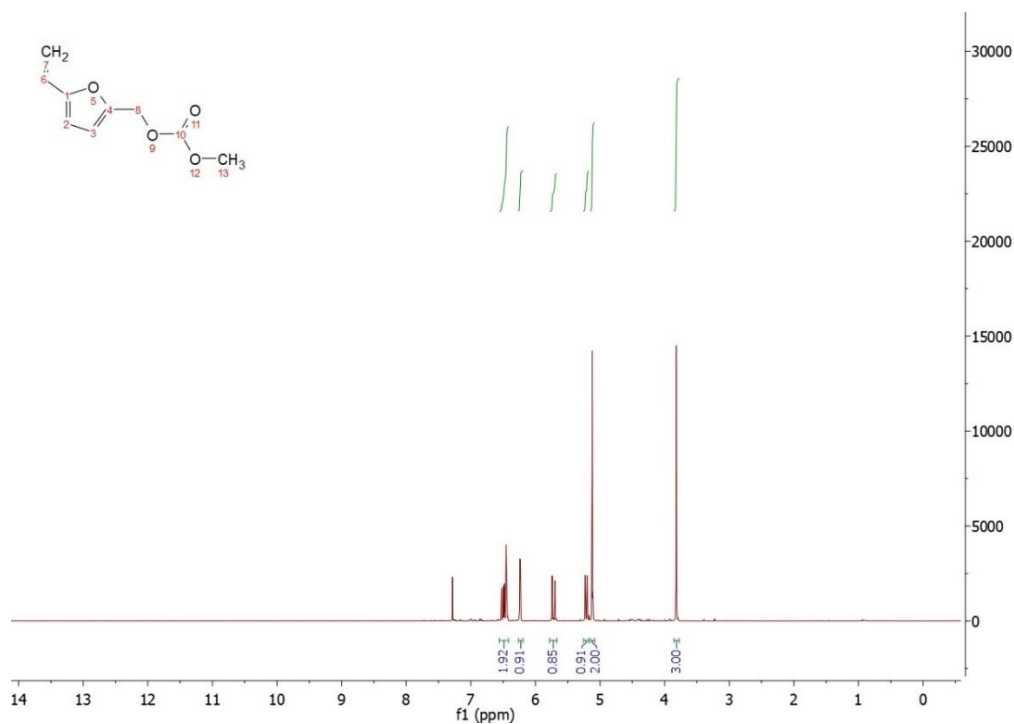
Figure A.5.30. *¹H NMR of product **6c** (400 MHz, 298 K, CDCl₃)*

δ (ppm): 6.50 (q, 1H), 6.48 (d, 1H), 6.25 (d, 1H), 5.75-5.69 (d, 1H), 5.2 (d, 1H), 5.12 (s, 2H), 3.82 (s, 3H).
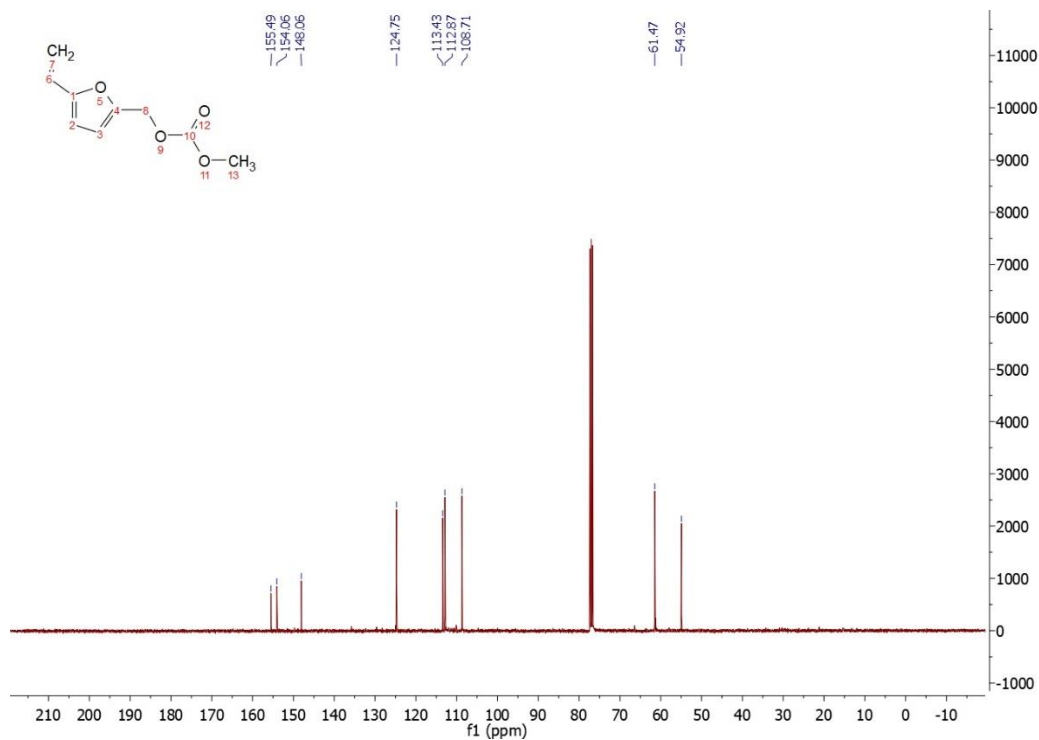
Figure A.5.31. ^{13}C NMR of product **6c** (100 MHz, 298 K, CDCl₃)

δ (ppm): 155.49, 154.06, 148.06, 124.75, 113.43, 112.87, 108.71, 61.47, 54.92.
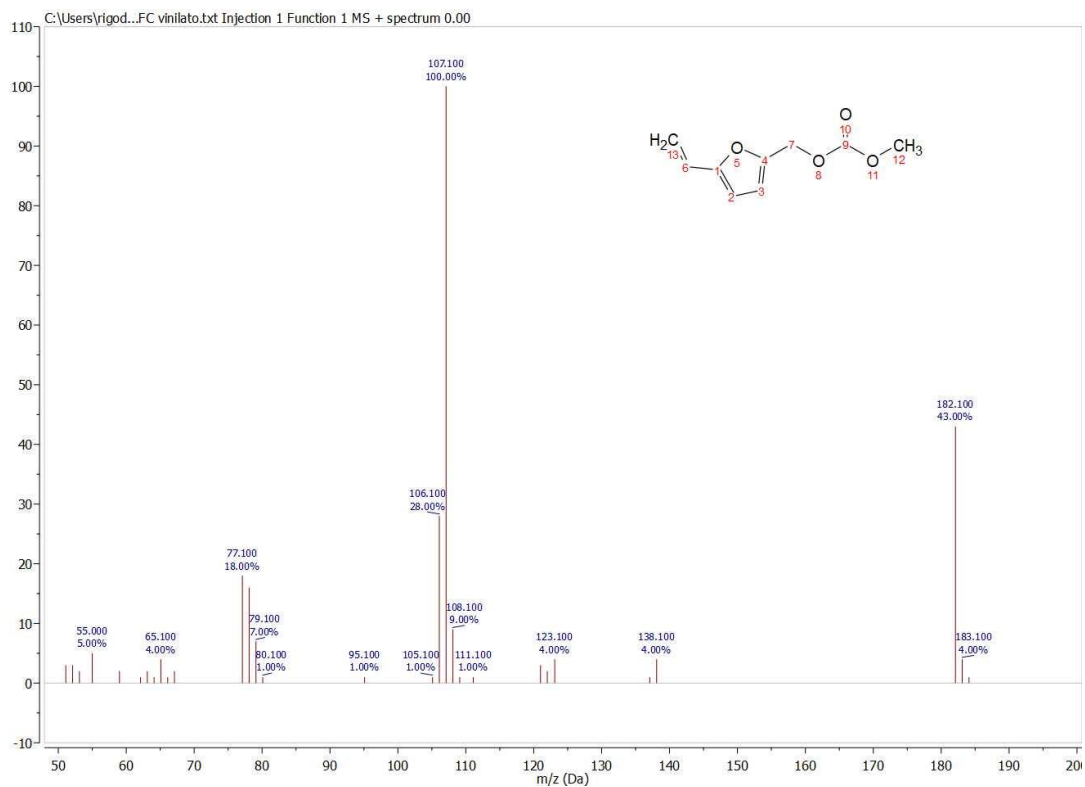
Figure A.5.32. MS spectrum of compound **6c** (EI, 70 eV)

m/z (70 eV): 182 (M⁺, 43), 107 (100), 77 (18), 55 (5).

Appendix A.6 – Chapter 6

A.6   A new family of renewable thermosets: Kraft lignin polyadipates

Synthesis of the C₆-Cross Linking Mixture

A mixture of adipic acid (5 g, 34.2 mmol), IPA (10 equiv, 34.25 g), and H_2SO_4 (0.8 mol%, 26.7 mg, 0.27 mmol) for 6 h at 97 °C (b.p. of IPA). Once the reaction was complete, the excess of IPA and other volatile co-products were removed by distillation under vacuum (40 °C, 5 mbar. The residual products mixture was analyzed by ^{1}H NMR, ^{13}C NMR, ^{1}H ^{13}C HMBC, and high-resolution mass spectrometry.
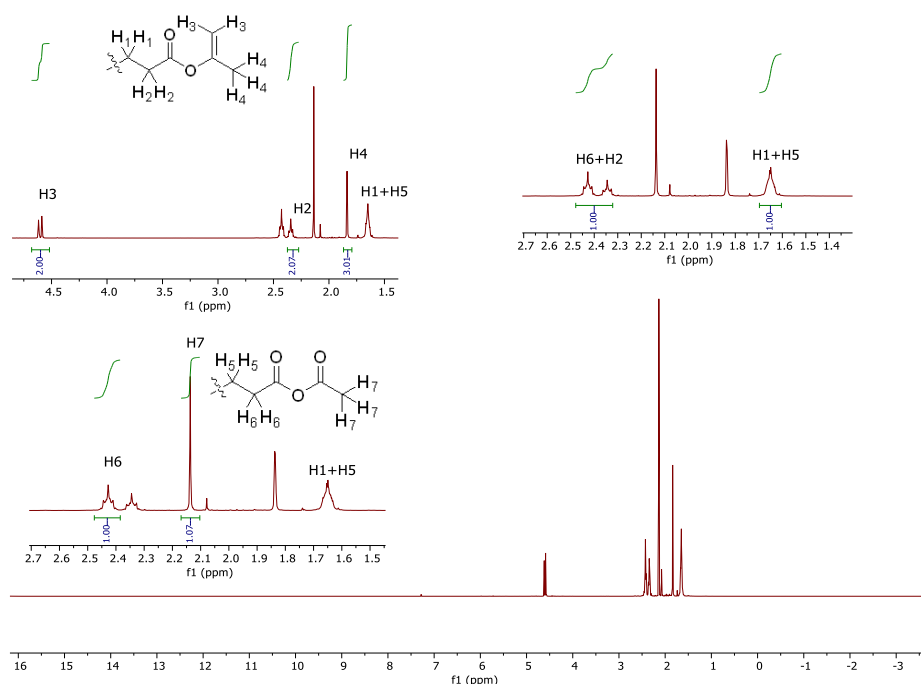
Figure A.6.1. ^{1}H NMR spectrum of C₆-CLM (400 MHz, 298 K, CDCl₃)
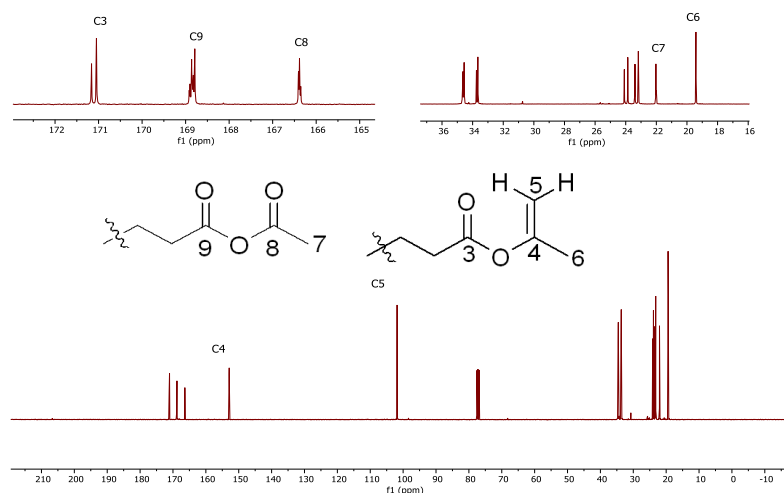
Figure A.6.2. ^{13}C NMR spectrum of C₆-CLM (100 MHz, 298 K, CDCl₃)

295
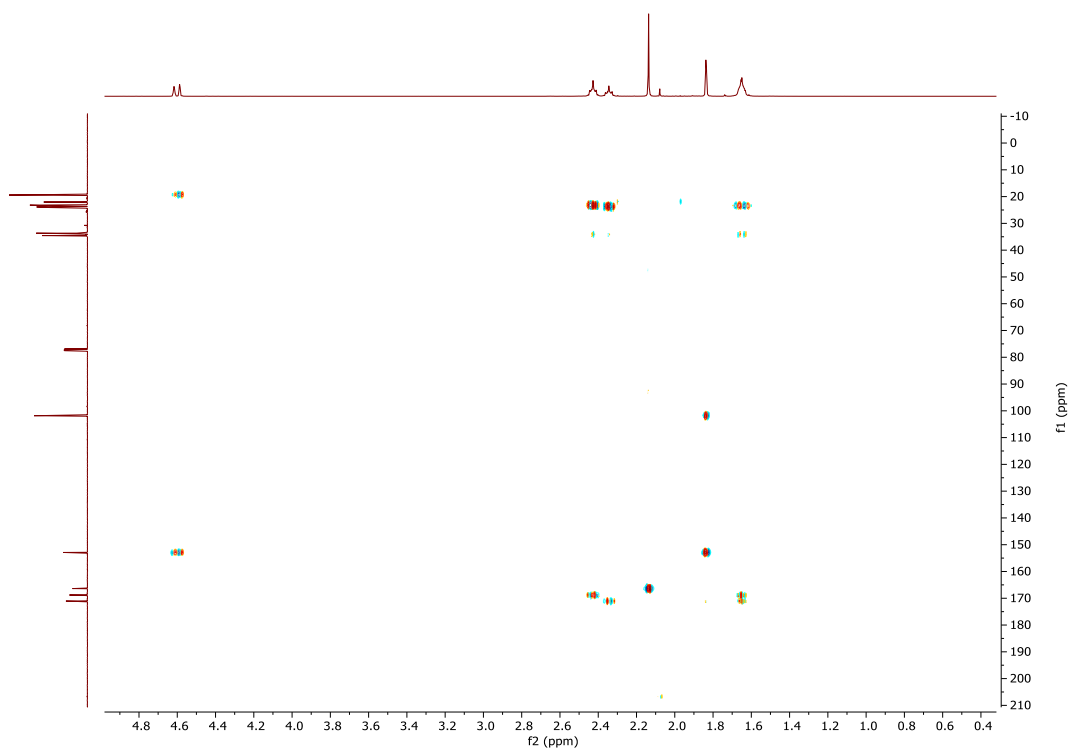
Figure A.6.3. ^1H ^{13}C HMBC spectrum of C_6-CLM (298 K, CDCl$_3$)
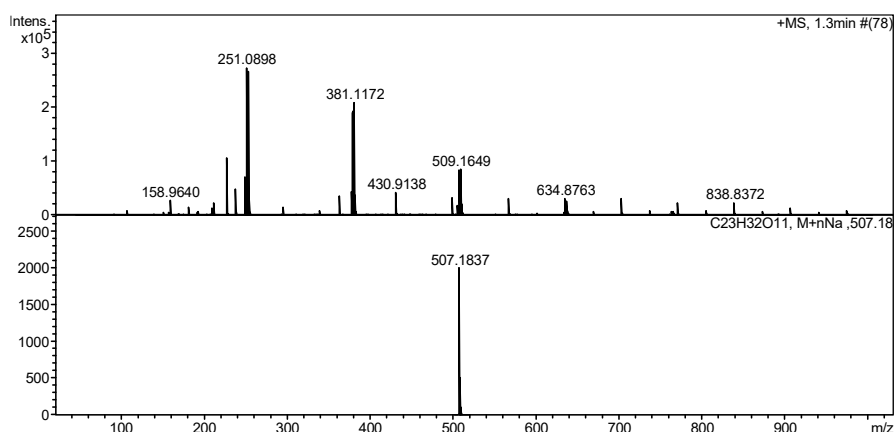
Figure A.6.4. HR-MS spectrum of C_6-CLM.

Chemical characterization of C$_6$-CLM

The multiplet centered at 2.51 were assigned to the α-protons of the anhydrides $(A_{anhydride})$ and the multiplet centered at 2.44 ppm were assigned to the α-protons of the isopropenyl groups $(A_{isopropenyl})$. Thus, the amount of anhydride and isopropenyl groups in equiv/g were calculated as follows using toluene as the internal standard $(A_{toluene})$ is the area of the aliphatic protons (-CH$_3$) of toluene at 2.23 ppm.

Eq. A.6.1
$$(equiv/g)_{anhydride} = \frac{\left[\left(\frac{1}{2}\cdot A_{anhydride}\right)/\left(\frac{1}{3}\cdot A_{toluene}\right)\right]/mol_{toluene}}{g_{mixture}}$$

Eq. A.6.2
$$(equiv/g)_{isopropenyl} = \frac{\left[\left(\frac{1}{2}\cdot A_{isopropenyl}\right)/\left(\frac{1}{3}\cdot A_{toluene}\right)\right]/mol_{toluene}}{g_{mixture}}$$

$mol_{toluene}$ refers to the moles of toluene weighted into the NMR tube and $g_{mixture}$ refers to the mass of CLM weighted into the NMR tube.
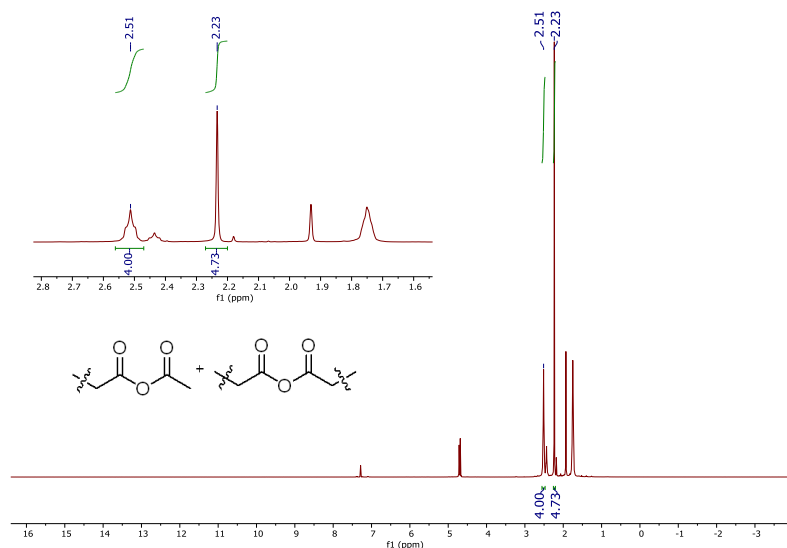
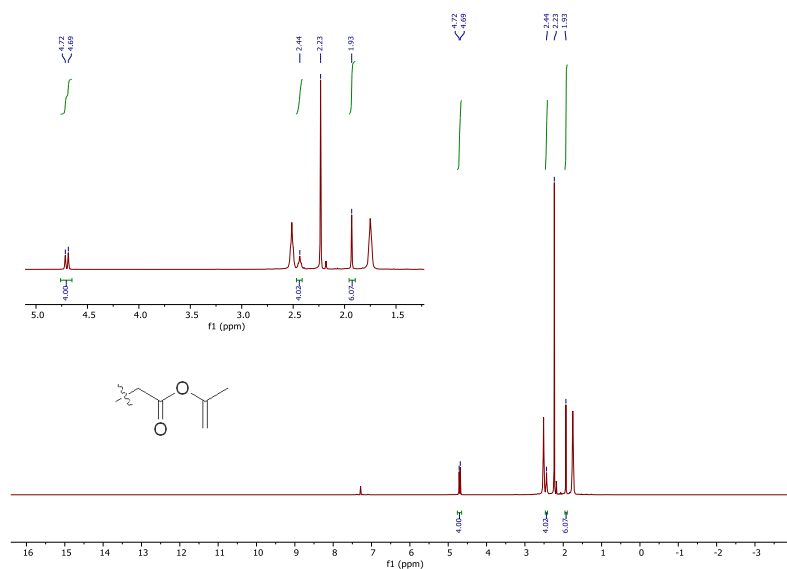***Figure A.6.5.*** *^{1}H NMR spectrum of C_6-CLM reporting the integration of anhydrides*

Figure A.6.6. *^{1}H NMR spectrum of C_6-CLM reporting the integration of isopropenyl groups*

Real-time analysis of the reaction for the C_6-CLM preparation

A mixture of adipic acid (5 g, 34.2 mmol) and IPA (10 equiv, 34.25 g) was set to react under H_2SO_4 catalysis (0.8 mol%, 26.7 mg, 0.27 mmol) for 24 h at 97 °C. The mixture was sampled at a given time interval (10 min to 24 h). Each sample was treated as follows: the excess IPA and other by-products were removed under vacuum (40 °C, 5 mbar) and the residual mixture was analyzed by ^{1}H NMR. After 6 h, the reaction reached the thermodynamic equilibrium and the distribution of the products did not change.
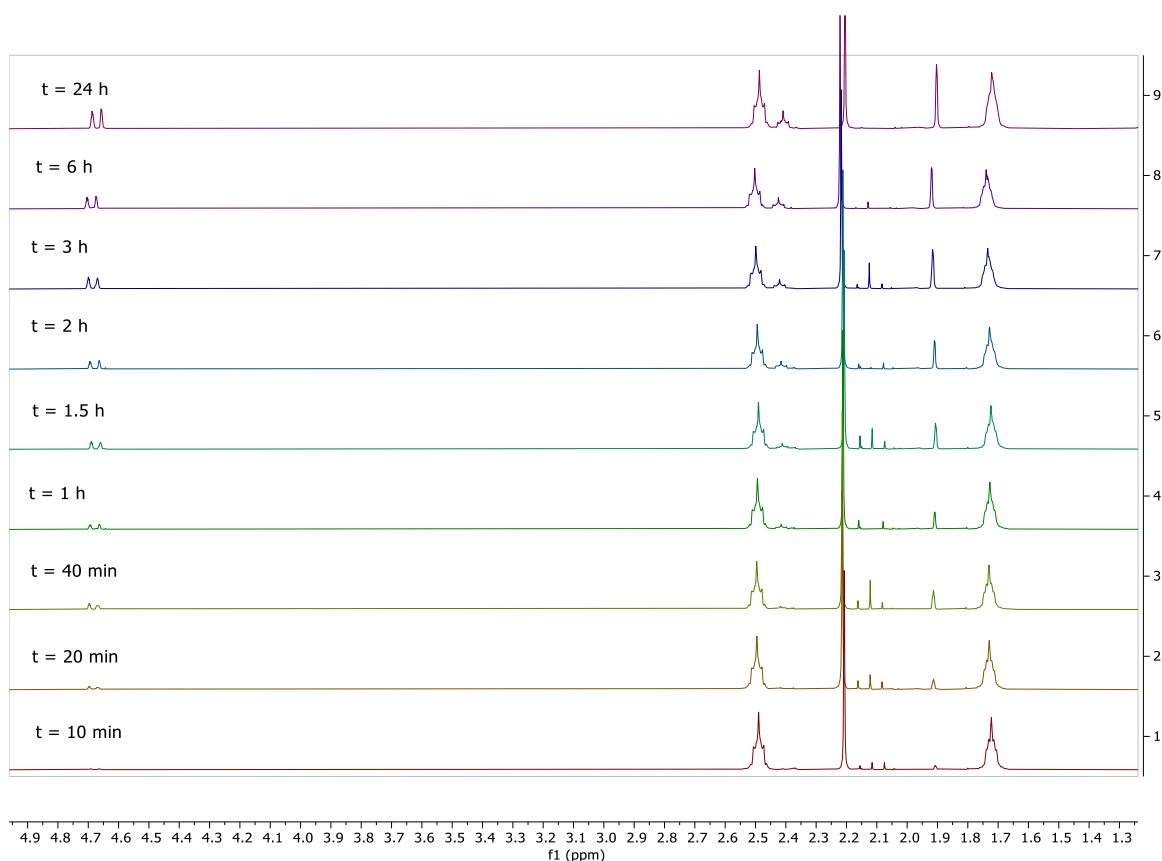
Figure A.6.7. ^1H *NMR spectrum in CDCl$_3$ of the C$_6$-CLM mixture in the time range 10 min-24 h*

Synthesis of Lignoboost Kraft lignin polyadipate (KLPA)

Softwood Lignoboost Kraft lignin (KL) bearing 6.5 mmol/g of free hydroxyl groups[1] was dried at 60 °C overnight before utilization and stored under vacuum. KL (30 g) and C$_6$-CLM (19.5 g) were mixed in an equimolar amount to lignin hydroxyl groups. A homogeneous solid primer was obtained by letting the CLM soak onto the KL. The resulting dark brown powder was then heated to 100 °C for 10 min when the KL started reacting with the CLM to yield a viscous homogenous liquid, the masterbatch. The masterbatch was poured, while still warm, into a PTFE rectangular mold between two flat surfaces and heated at 100 °C for 16 h under pressure to achieve the crosslinking while maintaining the shape. After the reaction completion, a Kraft lignin *poly*-adipate in a form of a dark brown rigid solid was obtained.

Figure A.6.8. KLPA tensile samples 70 mm x 15 mm x 1.2 mm (left), cylinder Ø 70 mm x 40 mm (center) and disc Ø 70 mm x 1.2 mm (right)

KL polyesters tensile properties

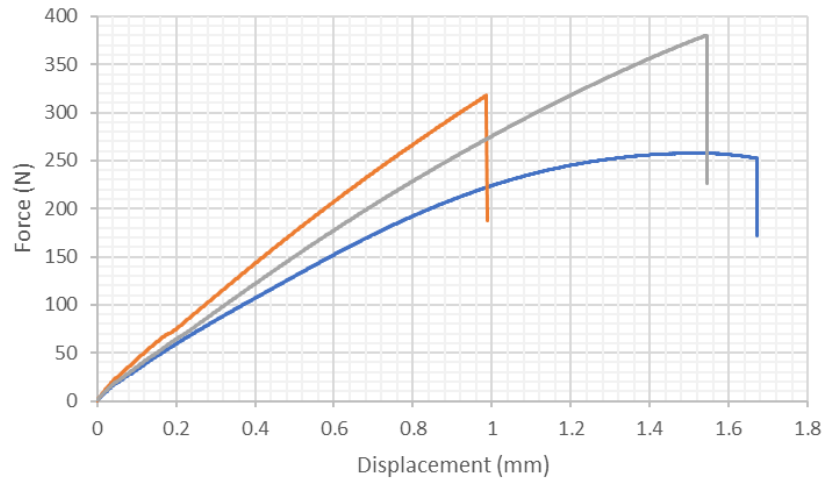***Figure A.6.9.*** *KL:CLM 1:1*

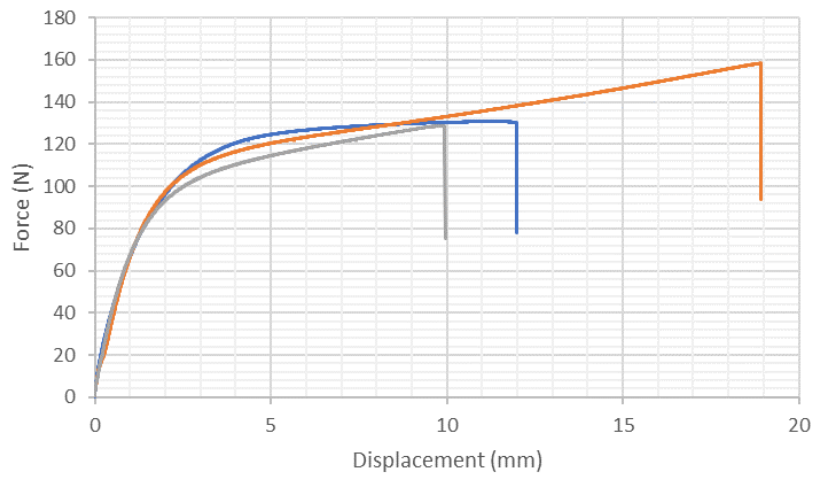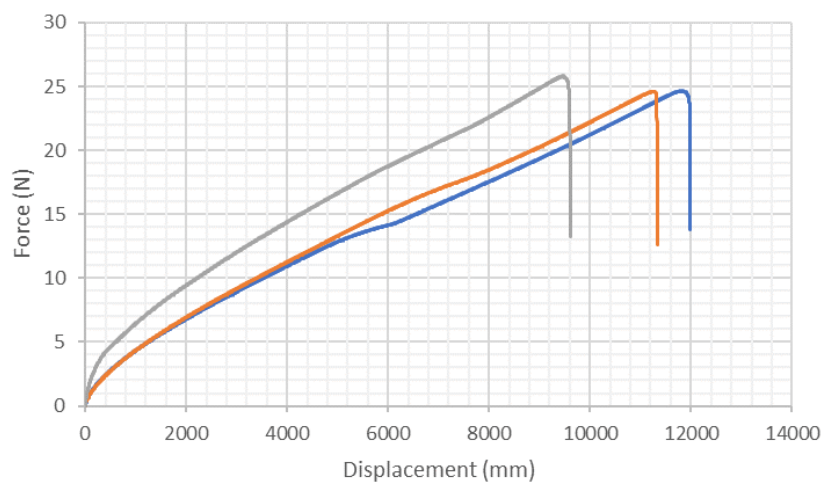***Figure A.6.10***. *KL:CLM 1:1.5*

Figure A.6.11. *KL:CLM 1:2*

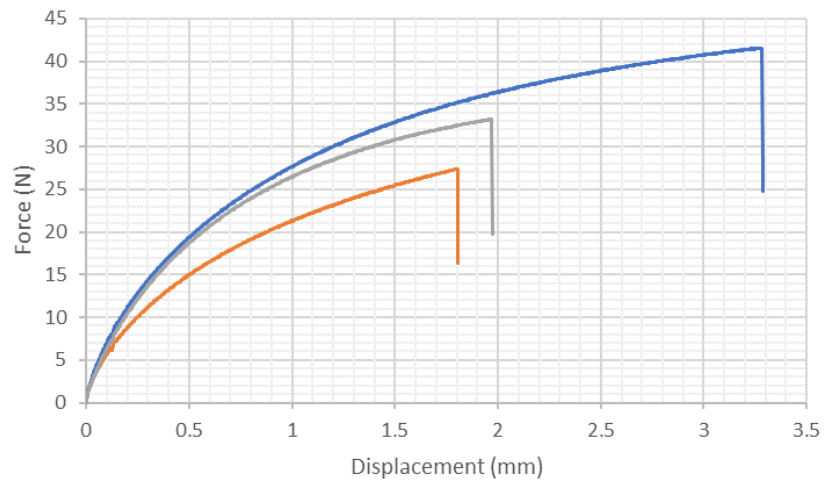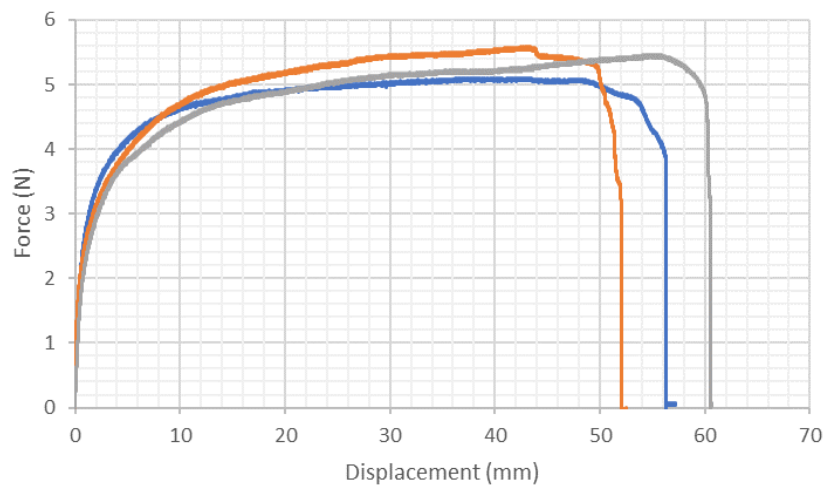***Figure A.6.12.*** *KL:CLM 1:1 with 10 wt% of glycerol*

Figure A.6.13. *KL:CLM 1:1 with 20 wt% of glycerol*